NELSON GONÇALO MORTÁGUA GOMES

ISOLATION, CHARACTERIZATION AND BIOLOGICAL ACTIVITY EVALUATION OF BIOACTIVE COMPOUNDS FROM MARINE SPONGE-ASSOCIATED FUNGI

Tese de Candidatura ao grau de Doutor em Ciências Biomédicas submetida ao Instituto de Ciências Biomédicas Abel Salazar da Universidade do Porto.

Orientador – Professor Doutor Anake Kijjoa

Professor Catedrático

Instituto de Ciências Biomédicas Abel Salazar da Universidade do Porto.

The experimental work of this thesis has been carried out in the Departamento de Química, Instituto de Ciências Biomédicas Abel Salazar (ICBAS), Universidade do Porto.

The candidate performed this work with a doctoral fellowship (SFRH/BD/65671/2009) supported by FCT (Fundação para a Ciência e a Tecnologia) supported by the European Social Fund (ESF).

This work was also partially funded by the Project MARBIOTECH (reference NORTE-07-0124-FED ER-000047) within the SR&TD Integrated Program MARVALOR—Building research and innovation capacity for improved management and valorization of marine resources, supported by the Programa Operacional Regional do Norte (ON.2—O Novo Norte) and by the European Regional Development.

Author:

Nelson Gonçalo Mortágua Gomes

goncalomortagua@hotmail.com

+351 912 039 663

PhD Thesis in Biomedical Sciences

Title: Isolation, Characterization and Biological Activity Evaluation of Bioactive Compounds from Marine Sponge-Associated Fungi

Supervisor:

Professor Doutor Anake Kijjoa

ankijjoa@icbas.up.pt

Instituto de Ciências Biomédicas Abel Salazar da Universidade do Porto

March 2014

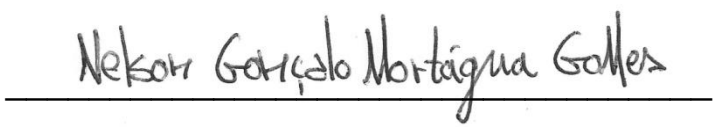

AUTHOR'S DECLARATION

Under the terms of the nº2, alínea a, do artigo 31º do Decreto-Lei nº230/2009, the author hereby declared that he has afforded a major contribution to the conceptual design and technical execution of the work, interpretation of the results and manuscript preparation of the original articles included in this thesis. Under the terms of the referred Decree-Law, the author hereby declared that the following original articles/communications were prepared in the scope of this thesis.

LIST OF PUBLICATIONS/COMMUNICATIONS

PUBLICATIONS

Articles in International Peer-Reviewed Journals

Original Research

Gomes, N.M., Dethoup, T., Singburaudom, N., Gales, L., Silva, A.M.S, Kijjoa, A. (**2012**). Eurocristatine, a new diketopiperazine dimer from the marine sponge-associated fungus *Eurotium cristatum*. *Phytochemistry Letters* 5(4), 717–720.

Eamvijarn, A., **Gomes, N.M.**, Dethoup, T., Buaruang, J., Manoch, L., Silva, A., Pedro, M., Marini, I., Roussis, V., Kijjoa, A. (**2013**). Bioactive meroditerpenes and indole alkaloids from the soil fungus *Neosartorya fischeri* (KUFC 6344), and the marine-derived fungi *Neosartorya laciniosa* (KUFC 7896) and *Neosartorya tsunodae* (KUFC 9213). *Tetrahedron* 69(40), 8583–8591.

Gomes, N.M., Bessa, L.J., Buttachon, S., Costa, P.M., Buaruang, J., Dethoup, T., Silva, A.M.S., Kijjoa, A. (**2014**). Antibacterial and Antibiofilm Activities of Tryptoquivalines and Meroditerpenes Isolated from the Marine-Derived Fungi *Neosartorya paulistensis*, *N. laciniosa*, *N. tsunodae*, and the Soil Fungi *N. fischeri* and *N. siamensis*. *Marine Drugs* 12(2), 822-839.

Book Chapters

Theoretical Background

Gomes, N.M., Buttachon, S., Kijjoa, A. Meroterpenoids from Marine Microorganisms: Potential Scaffolds for New Chemotherapy Leads. In: *Anticancer Drugs from Marine Origins* (Ed. Kim, S.-K.) (*Accepted*).

COMMUNICATIONS

Posters

Gomes, N.G.M., Dethoup, T., Gales, L., Silva, A.M.S., Kijjoa, A. Bioactive Secondary Metabolites from the Marine Sponge-Associated Fungus *Eurotium cristatum*. *2nd International Symposium of Modern Medicine, Traditional Chinese Medicine and Uighur Medicine and 12th National Symposium of Integrative Medicine in Prevention and Treatment of Respiratory Diseases*. Urumqi, China, September 15-20, **2012**.

Gomes, N.G.M., Dethoup, T., Gales, L., Silva, A.M.S., Kijjoa, A. Bioactive Secondary Metabolites from Marine Sponge-Associated Fungi Collected from the Gulf of Thailand. *14th International Symposium on Marine Natural Products & 8th European Conference on Marine Natural Products*. La Toja, Galicia, Spain, September 15-20, **2013**.

INDEX

AKNOWLEDGMENTS…….. xxi
ABSTRACT…… xxv
RESUMO…….. xxvii
LIST OF ABBREVIATIONS…….…… xxix
STATEMENT OF THE OBJECTIVES……. xxxv

Chapter I. Introduction……..... 1
1.1. General Introduction……. 3
1.1.1. Natural Products: An Established and Continuing Source of Novel Drug Leads……... 3
1.2. Ocean as an Unlimited Source for Novel Drugs……..... 5
1.2.1. Clinical Pipeline of Marine Pharmaceuticals……..... 7
1.2.2. Statistical Perspective on Marine Natural Products Research..... 13
1.2.3. Marine Microbial Consortia as the True Metabolic Source of Bioactive Metabolites…… 15
1.2.4. Marine Natural Products Research and the "*Supply Problem*".... 16
1.3. The Potential of Marine Microbial Diversity……..... 18
1.3.1. Marine Microorganisms as a Source of Novel Drug Candidates. 19
1.3.2. Marine Microorganisms: Cultivating the Uncultured and Activating Silent Clusters……... 21
1.4. Fungi from Marine Habitats as Producers of Relevant Bioactive Secondary Metabolites……. 22
1.4.1. Definition of Marine Fungi and Taxonomy……... 24
1.4.2. Distribution of Marine-Derived Fungi and Chemical Studies…… 25
1.4.3. Marine Sponge-Associated Fungi – A Promising Source of Bioactive Secondary Metabolites…… 27
1.4.4. Biologically Active Metabolites of Marine Sponge-Associated Fungi in Preclinical Development…… 29

Chapter II. Chemistry of the Genera *Emericella*, *Eurotium* and *Neosartorya*..... 33

2.1. An Overview of Secondary Metabolites…….. 35

2.2. The Genus *Emericella*…….. 36

2.2.1. *Emericella aurantio-brunnea*…….. 38

2.2.2. *Emericella desertorum*…… 38

2.2.3. *Emericella falconensis*…… 39

2.2.4. *Emericella foveolata*…… 40

2.2.5. *Emericella heterothallica*……. 41

2.2.6. *Emericella nidulans*……. 41

2.2.7. *Emericella purpurea*…… 42

2.2.8. *Emericella quadrilineata*……. 42

2.2.9. *Emericella rugulosa*……. 44

2.2.10. *Emericella striata*……..... 44

2.2.11. *Emericella unguis*…….. 45

2.2.12. *Emericella variecolor*……. 46

2.2.13. Unspecified *Emericella* species……..... 48

2.3. The Genus *Eurotium*……. 51

2.3.1. *Eurotium chevalieri*…….. 51

2.3.2. *Eurotium cristatum*……..... 51

2.3.3. *Eurotium herbariorum*…… 52

2.3.4. *Eurotium repens*……..... 53

2.3.5. *Eurotium rubrum*..... 54

2.4. The Genus *Neosartorya*……... 55

2.4.1. *Neosartorya fischeri*……. 56

2.4.2. *Neosartorya glabra*…….. 58

2.4.3. *Neosartorya pseufischeri*……..... 59

2.4.4. *Neosartorya quadricincta*……..... 60

2.4.5. *Neosartorya siamensis*……..... 60

2.4.6. *Neosartorya tsunodae*…… … 61

2.4.7. Unspecified *Neosartorya* species…….. 62

Chapter III. Results and Discussion……..... 63

3.1. Chemical Investigation of the Marine Derived Fungi…….... 65

3.1.1. Structure Elucidation of Triterpenoid Steroids……. 68

*3.1.1.1. Ergosterol (**EV1**)*…… 68

*3.1.1.2. Ergosterol peroxide (**EV2**)*……..... 73

3.1.2. Structure Elucidation of Orcinol and 1*H*-Indole-3-carboxylic acid……..... 77

*3.1.2.1. Orcinol (**EV3**)*…….. 77

*3.1.2.2. 1H-Indole-3-carboxylic acid (**EV4**)*…….. 78

3.1.3. Structure Elucidation of Anthraquinones…….. 81

*3.1.3.1. Erythroglaucin (**EC1**)*……. 81

*3.1.3.2. Physcion (**EC2**)* ……. 84

*3.1.3.3. Catenarin (**EC3**)* ……..... 87

*3.1.3.4. Emodin (**EC4**)* ……..... 90

*3.1.3.5. Questin (**EC5**)* ……..... 95

3.1.4. Structure Elucidation of Diketopiperazine Derivatives……..... 100

*3.1.4.1. cyclo-(L-Tryptophyl-L-phenylalanyl) (**EV5**)*……..... 100

*3.1.4.2. Neoechinulin A (**EC8**)* …….. 104

*3.1.4.3. Neoechinulin E (**EC9**)* …….. 110

*3.1.4.4. Neoechinulin (**EC7**)* …….. 113

*3.1.4.5. Echinulin (**EC6**)* ……. 116

*3.1.4.6. Eurocristatine (**EC10**)* ……..... 121

3.1.5. Structure Elucidation of Meroditerpenes…….. 127

*3.1.5.1. Chevalone B (**NL1**)* ……..... 127

*3.1.5.2. Aszonapyrone A (**NL2**)*……..... 133

*3.1.5.3. Aszonapyrone B (**NL3**)* ……..... 136

*3.1.5.4. Sartorypyrone C (**NP1**)* ……..... 139

3.1.6. Structure Elucidation of Quinazolinone Alkaloids……..... 145

*3.1.6.1. 4(3H)-Quinazolinone (**NP4**)* …… 145

*3.1.6.2. 3'-(4-Oxoquinazolin-3-yl)spiro[1H-indole-3,5'-oxolane]-2,2'-dione (**NP5/NL5**)* ……. 147

*3.1.6.3. Tryptoquivaline L (**NP2/NL4**)* …….. 151

*3.1.6.4. Tryptoquivaline H (**NP3**)* …….. 157

*3.1.6.5. Tryptoquivaline F (**NP6**)* …….. 162
*3.1.6.6. Tryptoquivaline T (**NL6**)* …….. 166
3.2. Biological Activity Evaluation of the Isolated Fungal Secondary Metabolites…….. 174
3.2.1. Antifungal and Antibacterial Activity Evaluation…….. 174
3.2.2. Cytotoxic Activity Evaluation……. 175
3.2.3. Antibacterial and Antibiofilm Activity Evaluation…… 176

Chapter IV. Materials and Methods…… 183
4.1. General Experimental Procedures…….... 185
4.2. Isolation and Identification of the Biological Material……. 186
4.2.1. *Emericella variecolor* KUFC 7092……. 186
4.2.2. *Eurotium cristatum* KUFC 7356……. 187
4.2.3. *Neosartorya laciniosa* KUFC 7896……..... 188
4.2.4. *Neosartorya paulistensis* KUFC 7897……..... 189
4.3. Extraction and Isolation of Metabolites……..... 191
4.3.1. *Emericella variecolor* KUFC 7092……..... 191
4.3.2. *Eurotium cristatum* KUFC 7356……. 192
4.3.3. *Neosartorya laciniosa* KUFC 7896……..... 194
4.3.4. *Neosartorya paulistensis* KUFC 7897……..... 195
4.4. Physical Characteristics and Spectroscopic Data……..... 197
4.5. X-Ray Crystallographic Analysis of EC10 and NL3…….. 199
4.6. Biological Activity Assays……..... 200
4.6.1. Cytotoxic Activity Bioassays……..... 200
4.6.1.1. Samples…….. 200
4.6.1.2. Cell cultures……..…… 200
4.6.1.3. Cell growth inhibitory assay……. 200
4.6.2. Antifungal Activity Bioassays……. 201
4.6.3. Antibacterial Activity Bioassays……. 202
4.6.3.1. Bacterial Strains……. 202
4.6.3.2. Determination of Minimum Inhibitory and Bactericidal Concentrations…….…….... 202
4.6.3.3. Synergistic Studies……..... 203

4.6.3.4. Antibiofilm Activity Assay……. 204

Chapter V. Conclusion…….... 207

REFERENCES……..... 213

APPENDICES……..... 265

Appendix I. NMR Spectra of the Isolated Compounds……..... 267

Appendix II. Gomes, N.M., Dethoup, T., Singburaudom, N., Gales, L., Silva, A.M.S, Kijjoa, A. (2012). Eurocristatine, a new diketopiperazine dimer from the marine sponge-associated fungus *Eurotium cristatum*. *Phytochemistry Letters*, 5(4) 717–720……. 295

Appendix III. Eamvijarn, A., Gomes, N.M., Dethoup, T.,Buaruang, J., Manoch, L., Silva, A., Pedro, M., Marini, I., Roussis, V., Kijjoa, A. (2013). Bioactive meroditerpenes and indole alkaloids from the soil fungus *Neosartorya fischeri* (KUFC 6344), and the marine-derived fungi *Neosartorya laciniosa* (KUFC 7896) and *Neosartorya tsunodae* (KUFC 9213). *Tetrahedron* 69(40), 8583–8591……. 301

Appendix IV. Gomes, N.M., Bessa, L.J., Buttachon, S., Costa, P.M., Buaruang, J., Dethoup, T., Silva, A.M.S., Kijjoa, A. (2014). Antibacterial and Antibiofilm Activities of Tryptoquivalines and Meroditerpenes Isolated from the Marine-Derived Fungi *Neosartorya paulistensis*, *N. laciniosa*, *N. tsunodae*, and the Soil Fungi *N. fischeri* and *N. siamensis*. *Marine Drugs* 12(2), 822-839……... 313

Appendix IV. Gomes, N.M., Buttachon, S., Kijjoa, A. Meroterpenoids from Marine Microorganisms: Potential Scaffolds for New Chemotherapy Leads. In: *Anticancer Drugs from Marine Origins* (Ed. Kim, S.-K.) (*Accepted*)……. 333

FIGURES INDEX

Figure 1. Some examples of natural drug leads approved for use in Medicine……..... 4
Figure 2. The structure of didemnin B (**7**)…….... 7
Figure 3a. Marine natural products or derivatives thereof approved for use by FDA or EMA……..…….. 11
Figure 3b. Marine natural products or derivatives thereof approved for use by FDA or EMA……..…….. 12
Figure 4. Temporal trend in the number of novel products obtained from marine organisms……..…….. 13
Figure 5. Temporal trends in the number of novel compounds isolated from different marine organisms between 1985 and 2008…… 14
Figure 6. Pie charts showing **A**: the collected sources of the twenty-one marine-derived or marine-inspired agents in the clinic or clinical trial, and **B**: the same agents with their demonstrated or predicted metabolic sources……..... 15
Figure 7. Chemical structures of novel drug candidates produced by marine microorganisms……..…… 20
Figure 8. Structures of cyanosafracin B (**24**) and the hemisynthesis product trabectedin (**14**)…….…….. 21
Figure 9. Examples of fungal-derived drugs currently used in therapeutics…….. 23
Figure 10. The structures of cephalosporin C (**30**) and siccayne (**31**)….. 25
Figure 11. New compounds from marine-derived fungi, according to year of publication……..... 26
Figure 12. New compounds from marine-derived fungi until mid-2010, divided by sources of the fungal strains……... 27
Figure 13. The number of distinct fungal genera based on the marine source……..... 28
Figure 14. Examples of marine sponge-derived fungi compounds with potential for preclinical development…… 30

Figure 15. Structures of echinocandin B (**40**) and semi-synthetic derivative anidulafungin (**41**)…….. 37
Figure 16. New constituents of *E. aurantio-brunnea*……. 38
Figure 17. New constituents of *E. desertorum* strain CBS 653.73……. 39
Figure 18. New constituents of *E. falconensis* strain NHL 2999……. 40
Figure 19. Structure of secoemestrin (**71**)…….. 40
Figure 20. New constituents of *E. heterothallica*……... 41
Figure 21. Structures of arugosins G (**78**) and H (**79**)…….. 42
Figure 22. New constituents of *E. purpurea* strain IFO 30849…… 43
Figure 23. New constituents of *E. quadrilineata*…… 43
Figure 24. New constituents of *E. rugulosa*……..... 44
Figure 25. New constituents of *E. striata* strain 80-NE-22…….. 45
Figure 26. New constituents of *E. unguis*..... 46
Figure 27. New constituents of *E. variecolor*…….. 48
Figure 28. New constituents of *Emericella* sp. HK-ZJ…….. 49
Figure 29. Structures of emericellamides A (**129**) and B (**130**)……... 49
Figure 30. New constituents of *Emericella* sp. AST 0036……..... 50
Figure 31. New xanthones of *Emericella* sp. 25379 strain ……. 50
Figure 32. New constituents of *E. chevalieri* EuCO1……..... 52
Figure 33. Structures of cristatumins A-E (**145-149**)……. 53
Figure 34. New benzyl derivatives of *E. repens* (UM-031509)……..... 54
Figure 35. New constituents of *E. rubrum*…….. 55
Figure 36. New constituents of *N. fischeri*…….. 57
Figure 37. New constituents of *N. glabra*……..... 58
Figure 38. New constituents of *N. pseudofischeri*……. 59
Figure 39. Structure of PF1223 (**188**)…….. 60
Figure 40. New constituents of *N. siamensis* KUFC 6349……... 61
Figure 41. Structure of sartorypyrone B (**196**)……..... 61
Figure 42. New constituents of unspecified *Neosartorya* species…….. 62
Figure 43. Constituents of *Emericella variecolor* KUFC 7092……. 65
Figure 44. Constituents of *Eurotium cristatum* KUFC 7356……. 66
Figure 45. Constituents of *Neosartorya laciniosa* KUFC 7896……..... 67
Figure 46. Constituents of *Neosartorya paulistensis* KUFC 7897…….. 67

Figure 47. Structure of ergosterol (**EV1**)…… 73
Figure 48. Structure of ergosterol peroxide (**EV2**)……. 75
Figure 49. Structure of orcinol (**EV3**)……... 78
Figure 50. Structure of 1*H*-indole-3-carboxylic acid (**EV4**)…….. 80
Figure 51. Structure of erythroglaucin (**EC1**)…….. 84
Figure 52. Structure of physcion (**EC2**)……... 86
Figure 53. Structure of catenarin (**EC3**)…….. 89
Figure 54. Structure of emodin (**EC4**)…….. 92
Figure 55. Structure of questin (**EC5**)…….. 98
Figure 56. Structure of cyclo-(L-tryptophyl-L-phenylalanil) (**EV5**)……... 104
Figure 57. Structure of neoechinulin A (**EC8**)…… 108
Figure 58. Structure of neoechinulin E (**EC9**)…… 112
Figure 59. Structure of neoechinulin (**EC7**)…… 116
Figure 60. Structure of echinulin (**EC6**)……... 120
Figure 61. Structure of eurocristatine (**EC10**)……. 124
Figure 62. ORTEP view of **EC10**…….. 125
Figure 63. Diketopiperazine dimers related to eurocristatine (**EC10**)…… 126
Figure 64. Structure of chevalone B (**NL1**)……. 132
Figure 65. Structure of aszonapyrone A (**NL2**)…….. 136
Figure 66. ORTEP view of **NL3**…… 139
Figure 67. Structure of aszonapyrone B (**NL3**)…….. 139
Figure 68. Structure of sartorypyrone C (**NP1**)…….. 142
Figure 69. Structures of aszonapyrones A (**NL2**) and B (**NL3**), sartorypyrones A-C (**177**, **196** and **NP1**) and chevalones A-C (**139-141**)……...……... 144
Figure 70. Structure of 4(3*H*)-quinazolinone (**NP4**)…….. 147
Figure 71. Structure of 3'-(4-oxoquinazolin-3-yl)spiro[1*H*-indole-3,5'-oxolane]-2,2'-dione (**NP5/NL5**)…….. 151
Figure 72. Structure of tryptoquivaline L (**NP2/NL4**)……. 157
Figure 73. Structure of tryptoquivaline H (**NP3**)……. 161
Figure 74. Structure of tryptoquivaline F (**NP6**)…… 165
Figure 75. Structure of tryptoquivaline T (**NL6**)…….. 170

Figure 76. Structures of the compounds tested for antifungal and antibacterial activities…….. 174
Figure 77. Structures of the compounds tested for *in vitro* cytotoxic activity against human cancer cell lines…….. 175
Figure 78. Structures of the compounds tested for antibacterial and antibiofilm activities…….. 177
Figure 79. Biomass quantification of biofilms of Gram-positive bacteria formed in the presence of concentrations ranging from 2x MIC to 1/4 MIC of aszonapyrone A (**NL2**)……... 180
Figure 80. Evaluation of *S. aureus* ATCC 25953 biofilm formation. Live/dead viability staining images after 24h. Control (**A**); Biofilm formation in the presence of the MIC (**B**) and in the presence of 1/2 of the MIC (**C**) of aszonapyrone A (**NL2**)…….. 181
Figure 81. Structures of the meroditerpenes tested for antibacterial activity……..... 182
Figure 82. *Clatria reinwardti* (**a**). *E. variecolor* KUFC 7092. Colony on MEA with 70% sea water after 14 days (**b**). Conidiophores and conidia (**c**). SEM image of ascospores (**d**, **e**)…… 186
Figure 83. *Mycale* sp. (**a**). *E. cristatum* KUFC 7356. Colony on PDA with 70% sea water after 14 days (**b**). Conidiophores and conidia (**c**). SEM image of ascospores (**d**, **e**)……. 187
Figure 84. Diseased-coral (*Porites lutea*)…… 188
Figure 85. *N. laciniosa* KUFC 7896. Colonies incubated for 14 days at 28ºC on CZA (**a**), CYA (**b**) and MEA (**c**) media. Ascomata (**d**), Conidia (**e**). SEM image of ascospores (**f**)……. 189
Figure 86. *Chondrilla australiensis* (**a**). *N. paulistensis* KUFC 7897. Colony on PDA with 70% sea water after 14 days (**b**). Ascomata (**c**). Conidia (**d**). SEM image of ascospores (**d**, **e**)……. 190

TABLES INDEX

Table 1. Marine pharmaceuticals: Current pipeline…….. 9
Table 2. ^{1}H and ^{13}C NMR data ($CDCl_3$, 300.13 and 75.47 MHz) of **EV1**……..... 68
Table 3. ^{1}H and ^{13}C NMR data (DMSO-d_6, 500.13 and 125.77 MHz) of **EV2**……..... 74
Table 4. ^{1}H and ^{13}C NMR data ($CDCl_3$, 300.13 and 75.47 MHz) of **EV3**... 77
Table 5. ^{1}H and ^{13}C NMR data (DMSO-d_6, 500.13 and 125.77 MHz) of **EV4**……. 79
Table 6. ^{1}H and ^{13}C NMR data ($CDCl_3$, 500.13 and 125.77 MHz) of **EC1**. 82
Table 7. ^{1}H and ^{13}C NMR data ($CDCl_3$, 500.13 and 125.77 MHz) of **EC2**. 85
Table 8. ^{1}H and ^{13}C NMR data (DMSO-d_6, 300.13 and 75.47 MHz) of **EC3**……..... 88
Table 9. ^{1}H and ^{13}C NMR data (DMSO-d_6, 500.13 and 125.77 MHz) of **EC4**……..... 90
Table 10. ^{1}H and ^{13}C NMR data (DMSO-d_6, 300.13 and 75.47 MHz) of **EC5**……..... 96
Table 11. ^{1}H and ^{13}C NMR data (DMSO-d_6, 300.13 and 75.47 MHz) of **EV5**……... 100
Table 12. ^{1}H and ^{13}C NMR data (DMSO-d_6, 300.13 and 75.47 MHz) of **EC8**……..... 105
Table 13. ^{1}H and ^{13}C NMR data (DMSO-d_6, 300.13 and 75.47 MHz) of **EC9**……..... 110
Table 14. ^{1}H and ^{13}C NMR data (DMSO-d_6, 300.13 and 75.47 MHz) of **EC7**……..... 114
Table 15. Comparison of ^{1}H and ^{13}C NMR data (DMSO-d_6, 300.13 and 75.47 MHz) of **EC7** and **EC9**…… 115
Table 16. Comparison of ^{1}H and ^{13}C NMR data (300.13 and 75.47 MHz) of **EC6** ($CDCl_3$) and **EC8** (DMSO-d_6)…… 117
Table 17. ^{1}H and ^{13}C NMR data (DMSO-d_6, 300.13 and 75.47 MHz) of **EC10**……..... 121
Table 18. ^{1}H and ^{13}C NMR data ($CDCl_3$, 300.13 and 75.47 MHz) of **NL1**. 128

Table 19. ^{1}H and ^{13}C NMR data (DMSO-d_6, 300.13 and 75.47 MHz) of **NL2**..... 133
Table 20. ^{1}H and ^{13}C NMR data (DMSO-d_6, 300.13 and 75.47 MHz, T = 45 ºC) of **NL3**..... 137
Table 21. Comparison of the ^{1}H and ^{13}C NMR data (DMSO-d_6, 300.13 and 75.47 MHz) of **NL2** and **NL3**..... 138
Table 22. ^{1}H and ^{13}C NMR data (DMSO-d_6, 300.13 and 75.47 MHz) of **NP1**..... 140
Table 23. ^{1}H and ^{13}C NMR data (DMSO-d_6, 500.13 and 125.77 MHz) of .**NP4**..... 145
Table 24. ^{1}H and ^{13}C NMR data (DMSO-d_6, 300.13 and 75.47 MHz) of **NP5/NL5**..... 148
Table 25. ^{1}H and ^{13}C NMR data (DMSO-d_6, 300.13 and 75.47 MHz) of **NP2/NL4**..... 152
Table 26. ^{1}H and ^{13}C NMR data (DMSO-d_6, 300.13 and 75.47 MHz) of **NP3**..... 158
Table 27. ^{1}H and ^{13}C NMR data (DMSO-d_6, 300.13 and 75.47 MHz) of **NP6**..... 163
Table 28. ^{1}H and ^{13}C NMR data (DMSO-d_6, 300.13 and 75.47 MHz) of **NL6**..... 167
Table 29. Growth inhibitory effect of diketopiperazine alkaloids **EC7-EC10** and meroditerpenes **NL2** and **NL3**..... 176
Table 30. Antibacterial activity, expressed in µg/mL of compounds **NP1-NP6** and **NL2-NL6** against reference strains (**a**) and of **NL2** against multidrug-resistant isolates (**b**)..... 177
Table 31. Antibacterial efficacy of combined effect of antibiotics with compounds **NP1-NP6** and **NL2-NL6** (15 µg/disc) against three multidrug-resistant isolates, using the disc diffusion method..... 178
Table 32. FIC Index results obtained with aszonapyrone A (**NL2**) and antibiotic combinations by checkerboard method..... 179

SCHEMES INDEX

Scheme 1. Schematic diagram of the research process…… **xxxv**

Scheme 2. Biosynthetic pathway of the anthraquinones **EC1-EC5**……. 99

Scheme 3. Proposed biosynthetic pathway for eurocristatine (**EC10**)……. 127

Scheme 4. Proposed biosynthetic pathway for sartorypyrone C (**NP1**), aszonapyrones A (**NL2**) and B (**NL3**) and chevalone B (**NL1**)…….. 143

Scheme 5. Biosynthetic pathways for 3-(4-oxoquinazolin-3-yl)spiro[1*H*-indole-3,5-oxolane]-2,2'-dione (**NP5/NL5**) and tryptoquivalines L (**NP2/NL4**), H (**NP3**) and F (**NP6**)…… 171

ACKNOWLEDGMENTS

I would like to acknowledge some people without whom this work would not have been made possible.

I wish to express my deep gratitude and admiration to Professor Dr. Anake Kijjoa, my supervisor, mentor and friend, for his unwavering support, constant encouragement but mainly for his supervision, characterized by seriousness and accuracy. I have nothing else than to be proud and considered to be an enormous privilege to have performed this study under his supervision.

My sincere thanks to Professor Dr. Madalena Pinto, Head of Department of the Departamento de Química Orgânica, Faculdade de Farmácia, Universidade do Porto, CEQUIMED – Centro de Química Medicinal da Universidade do Porto, for providing logistical support.

I am indebt to Professor Dr. Artur Silva, Departamento de Química, Universidade de Aveiro, for the ^{1}H and ^{13}C NMR measurements, and to Dr. Mick Lee, Department of Chemistry, Leicester University, UK, for HRMS measurements. Special thanks are given to Professor Dr. Luís Gales, Instituto de Ciências Biomédicas Abel Salazar (ICBAS), Universidade do Porto, for the X-ray crystallography analysis.

I am deeply indebt to Professor Dr. Tida Dethoup and Professor Dr. Leka Manoch, from the Department of Plant Pathology, Kasetsart University, Bangkok, Thailand, and to Mr. Jamrearn Buaruang, Division of Environmental Science, Faculty of Science, Ramkhamhaeng University, Bangkok, Thailand, for collection, isolation, identification and culture of the marine fungi, as well as preparation of the extracts.

Also a thankful word for Professor Dr. Paulo Costa, Instituto de Ciências Biomédicas Abel Salazar (ICBAS), Universidade do Porto, and Dr. Lucinda Bessa, CIIMAR – Centro Interdisciplinar de Investigação Marinha e Ambiental,

Universidade do Porto, for performing the antibacterial and antibiofilm assays, to to Professor Dr. Madalena Pedro, CEQUIMED – Centro de Química Medicinal da Universidade do Porto and Instituto Superior de Ciências da Saúde do Norte (CESPU), for the cytotoxic activity assays, and to Professor Dr. Eugénia Pinto, CEQUIMED – Centro de Química Medicinal da Universidade do Porto, Faculdade de Farmácia, Universidade do Porto, for antifungal assays.

A very special thanks goes to Mrs. Júlia Bessa not only for her technical assistance, but also for the constant encouragement and friendship. My sincere thanks goes also to Ms. Sara Cravo, Ms. Sonia Pereira and Mrs. Isabel for their technical assistance.

Special thanks to my neighbor and friend, Professor Dr. Augusto Faustino for introducing me to Professor Dr. Anake Kijjoa.

A sincere and eternal thank to my lab mates Amnat, Ângela, Chadaporn, Clayton, Decha, Ioulia, Madalena, Renato, Suradet, Sutsawat and Tida for all the shared knowledge, for providing an amazing working atmosphere, and above all for their friendship.

I would like also to express my gratitude to my hometown friends Anaís, Ricardo, Roberto and Tânia and to my long time friends André, Daniel and Francisco from being always there when I need.

A kind and eternal thank to my brother Luís, to my sister-in-law Cláudia, and to my nephews, Kiko and Bá, for all the love and support during these four years. An additional special thank to my brother Luís, for the eternal encouragement and for being not only a brother, but also a father and a friend.

I would like to express my gratitude to my parents whom words cannot describe their existence. Thanks to my father Nelson, for providing me all the support (including financial when needed) to achieve my goals, for his encouragement, and for all the sacrifices to make my life better.

Finally, I would like to thank to my mother Elisabete, not only for all the support, patience and love, but essentially from her constant fighting attitude against all the unfair life adversities, that always inspired me. Mom, this thesis is dedicated to you.

ABSTRACT

The marine environment is a tremendous source of biologically active metabolites, representing a valuable source with great potential for the development of pharmaceuticals. Marine-derived fungi are known to produce structurally unique secondary metabolites, and since the beginning of the 1990s, a sharp and exponential increase in the number of reported relevant biologically active metabolites occurred.

The aim of this study was to isolate and evaluate the biological activity of secondary metabolites produced by marine derived-fungi collected from the Gulf of Thailand. To achieve this aim, three marine sponge-associated fungi, *Emericella variecolor* KUFC 7092, *Eurotium cristatum* KUFC 7356 and *Neosartorya paulistensis* KUFC 7897, and the diseased coral-derived fungus *Neosartorya laciniosa* KUFC 7896, were investigated.

Chemical investigation of the ethyl acetate extract of the culture of *E. variecolor* KUFC 7092, isolated from the marine sponge *Clathria reinwardti*, resulted in the isolation of five known compounds, ergosterol, ergosterol peroxide, orcinol, 1*H*-indole-3-carboxylic acid and cyclo-(L-tryptophyl-L-phenylalanyl).

A new diketopiperazine dimer, eurocristatine, was isolated in addition to nine known metabolites including the anthraquinones erythroglaucin, physcion, catenarin, emodin and questin, and the diketopiperazine alkaloids echinulin, neoechinulin, neoechinulin A and neoechinulin E, from the ethyl acetate extract of the culture of the sponge-associated fungus *E. cristatum* KUFC 7356. The diketopiperazine derivatives, including the new diketopiperazine dimer, were evaluated for their *in vitro* growth inhibitory activity against MCF-7 (breast adenocarcinoma), NCI-H-460 (non-small lung cancer) and A375-C5 (melanoma) cell lines, and the results showed that they were inactive against the three cell lines. Both anthraquinones and diketopiperazine alkaloids were also evaluated for their antifungal activity against the human pathogenic fungi *Candida albicans*, *Aspergillus fumigatus* and *Trichophyton rubrum*, as well as for their antibacterial

activity against the human pathogenic bacteria *Staphylococcus aureus*, *Escherichia coli* and *Pseudomonas aeruginosa*, but no antimicrobial activity was registered.

The ethyl acetate extract of the culture of the diseased coral-derived fungus *N. laciniosa* KUFC 7896 furnished a new tryptoquivaline analogue, tryptoquivaline T, in addition to the previously described tryptoquivaline L, 3'-(4-oxoquinazolin-3-yl)spiro[1*H*-indole-3,5'-oxolane]-2,2'-dione, and the meroditerpenes chevalone B, and aszonapyrones A and B. Aszonapyrones A and B were also evaluated for their *in vitro* growth inhibitory activity against MCF-7, NCI-H-460 and A375-C5 cell lines. Aszonapyrone A displayed strong growth inhibitory activity against the three cell lines with GI_{50} values of 13.6 ± 0.9 µM, 11.6 ± 1.5 µM and 10.2 ± 1.2 µM, for MCF-7, NCI-H-460 and A375-C5, respectively, while aszonapyrone B was inactive at the highest concentration tested (150 µM)

Chemical investigation of the ethyl acetate extract of the culture of the marine sponge-associated fungus *N. paulistensis* KUFC 7897, resulted in isolation of a new aszonapyrone analogue which we have named sartorypyrone C, in addition to five known metabolites including tryptoquivalines L, H, F, 3′-(4-oxoquinazolin-3-yl)spiro[1*H*-indole-3,5′-oxolane]-2,2′-dione and 4(3*H*)-quinazolinone.

In addition to the metabolites isolated from *N. paulistensis* KUFC 7897, tryptoquivaline T and aszonapyrones A and B isolated from *N. laciniosa* KUFC 7896, were also tested for their antibacterial activity against four reference strains (*Staphylococcus aureus*, *Bacillus subtilis*, *Escherichia coli* and *Pseudomonas aeruginosa*), as well as the environmental multidrug-resistant isolates. Only aszonapyrone A exhibited significant antibacterial activity as well as synergism with antibiotics against the Gram-positive multidrug-resistant strains. Additionally, aszonapyrone A was also found to inhibit the biofilm formation in both reference strains and multi-drug resistant isolates.

RESUMO

O ambiente marinho é um importante reservatório de metabolitos bioactivos, representando uma fonte valiosa e com enorme potencial para a descoberta e desenvolvimento de novos fármacos. Os fungos marinhos são conhecidos por produzirem metabolitos secundários com estruturas químicas únicas e, desde o início dos anos 90 houve um aumento acentuado e exponencial no número de metabolitos com atividade biológica relevante.

Os objetivos deste estudo foram o isolamento e avaliação da atividade biológica de metabolitos secundários produzidos por fungos marinhos coletados no Golfo da Tailândia. Para esse efeito foram investigados três fungos associados com esponjas marinhas, *Emericella variecolor* KUFC 7092, *Eurotium cristatum* KUFC 7356 e *Neosartorya paulistensis* KUFC 7897, bem como um fungo associado com um coral infetado, *Neosartorya laciniosa* KUFC 7896.

O estudo químico do extrato de acetato de etilo da cultura de *E. variecolor* KUFC 7092, isolado da esponja marinha *Clathria reinwardti*, resultou no isolamento de cinco compostos conhecidos, ergosterol, peróxido de ergosterol, orcinol, ácido 1*H*-indole-3-carboxílico e ciclo-(L-triptofil-L-fenilalanil).

Um novo dímero de dicetopiperazina, eurocristatine, foi isolado além de nove metabolitos conhecidos incluindo as antraquinonas eritroglaucina, fisciona, catenarina, emodina e questina, e os alcaloides dicetopiperazínicos equinulina, neoequinulina, neoequinulina A e neoequinulina E, do extrato de acetato de etilo da cultura de *E. cristatum* KUFC 7356 isolado de uma esponja marinha. Foi efetuada a avaliação *in vitro* da atividade citotóxica dos derivados dicetopiperazínicos, incluindo o novo dímero dicetopiperazínico, sobre as linhas celulares MCF-7 (adenocarcinoma da mama), NCI-H-460 (cancro de pulmão de não-pequenas células) e A375-C5 (melanoma), tendo-se verificado que todos os compostos testados foram inativos nas três linhas celulares. Foi também avaliada a atividade antifúngica das antraquinonas e dos alcaloides dicetopiperazínicos contra os fungos patogénicos para o humano, *Candida albicans*, *Aspergillus*

fumigatus e *Trichophyton rubrum*, assim como a sua atividade antibacteriana contra as bactérias patogénicas para o humano, *Staphylococcus aureus*, *Escherichia coli* e *Pseudomonas aeruginosa*, mas não se verificou qualquer atividade antimicrobiana.

Do extrato de acetato de etilo da cultura de *N. laciniosa* KUFC 7896, isolado de um coral infetado, foi isolado um novo análogo da triptoquivalina, triptoquivalina T, além de triptoquivalina L, 3'-(4-oxoquinazolin-3-il)espiro[1*H*-indole-3,5'-oxolano]-2,2'-diona, e os meroditerpenos chevalona B, e as aszonapironas A e B. Efetuou-se a avaliação da atividade citotóxica *in vitro* das aszonapironas A e B contra as linhas celulares MCF-7, NCI-H-460 e A375-C5. A aszonapirona A exibiu forte atividade nas três linhas celulares com valores de IC_{50} de 13.6 ± 0.9 μM, 11.6 ± 1.5 μM and 10.2 ± 1.2 μM, para MCF-7, NCI-H-460 and A375-C5 respetivamente, enquanto a aszonapirona B foi inativa na maior concentração testada (150 μM).

O estudo químico do extrato de acetato de etilo da cultura de *N. paulistensis* KUFC 7897 isolado de uma esponja marinha, resultou no isolamento da sartorypirona C, um novo análogo das aszonapironas, além de cinco compostos conhecidos incluindo as triptoquivalinas L, H e F, 3'-(4-oxoquinazolin-3-il)espiro[1*H*-indole-3,5'-oxolano]-2,2'-diona e 4(3*H*)-quinazolinona.

Além dos metabolitos isolados da cultura *N. paulistensis* KUFC 7897, os compostos triptoquivalina L e aszonapironas A e B, isolados da cultura *N. laciniosa* KUFC 7896, foram também avaliados pela sua atividade antibacteriana em quatro estirpes-referência (*Staphylococcus aureus*, *Bacillus subtilis*, *Escherichia coli* e *Pseudomonas aeruginosa*), assim como em estirpes multi-resistentes contra fármacos isoladas do meio ambiente. Apenas a aszonapirona A apresentou atividade antibacteriana significativa assim como sinergismo com antibióticos contra as estirpes Gram-positivas multi-resistentes a fármacos. Adicionalmente, verificou-se que a aszonapirona A também causou inibição na formação de biofilme nas estirpes-referência, assim como nas estirpes multi-resistentes a fármacos.

LIST OF ABBREVIATIONS

[^{3}H]EBOB	[^{3}H]Ethynylbicycloorthobenzoate
[M+H$^+$]	Pseudo-molecular ion (Positive ion mode)
$[\alpha]^{20}_D$	Specific optical rotation at 20 ºC for D (sodium) line
$[\alpha]^{25}_D$	Specific optical rotation at 25 ºC for D (sodium) line
®	Register or Trademark
Å	Angstrom
Ac	Acetyl
Ac_2O	Acetic anhydride
ADC	Antibody Drug Conjugate
Akt	Protein kinase B
AMP	Ampicillin
amu	Atomic mass unit
Ara-A	Arabino furanosyladenine
Ara-C	Arabinosyl cytosine
ASK-1	Apoptosis Signal-regulating Kinase 1
ATCC	American Type Culture Collection
Bcl-2	B-cell lymphoma 2
BIC	Biofilm Inhibitory Concentration
brd	Broad doublet
brs	Broad singlet
C/EBPβ	CCAAT-Enhancer-binding protein β
Calcd.	Calculated
cAMP	Cyclic adenosine monophosphate
CCDC	Cambrige Crystallographic Data Centre
CCR5	C-C Chemokine Receptor type 5
$CDCl_3$	Deuterated chloroform
CDP	Cyclodipeptide Synthase
CFU	Colony-Forming Unit
CH_2Cl_2	Dichloromethane
$CHCl_3$	Chloroform
CIP	Ciprofloxacin

CLSI	Clinical Laboratory Standards Institute
CO_2	Carbon dioxide
CoA	Coenzyme A
ConA	Concanavalin A
COSY	Correlated Spectroscopy
COX-2	Cyclooxygenase 2
CREB	cAMP Response Element-Binding protein
CTX	Cefotaxime
CXCR4	Chemokine (C-X-C) receptor
CYA	Czapek Yeast Autolysate Agar
CZA	Czapek's Agar
dd	Double doublet
ddd	Double double doublet
DEPT	Distortionless Enhancement by Polarization Transfer
DHA	Docosahexaenoic Acid
DMSO	Dimethylsulfoxide
DMSO-d_6	Deuterated dimethylsulfoxide
DNA	Deoxyribonucleic Acid
DPPH	2,2-Diphenylpicrylhydrazyl
dt	Double triplet
E	Erythromycin
EMA	European Medicines Agency
EPA	Eicosapentaenoic Acid
ERCC1	Excision Repair Cross-Complementation group 1
ERα	Estrogen Receptor α
ESI	Electrospray Ionization
EtOAc	Ethyl acetate
EU	European Union
FBS	Fetal Bovine Serum
FDA	Food and Drug Administration
FGFR2	Fibroblast Growth Factor Receptor 2
FIC	Fractional Inhibitory Concentration
g	Gram

GABA	Gamma-aminobutyric acid
GC	Gas Chromatography
GI_{50}	Half maximal growth inhibitory concentration
H_2O	Water
hACAT	Cultured Human Keratinocyte
HeLa	Henrietta Lacks
HMBC	Heteronuclear Multiple Bond Correlation
HRMS	High Resolution Mass Spectrometry
HSQC	Heteronuclear Single Quantum Coherence
HSV	Herpes simplex Virus
HUVEC	Human Umbilical Vein Endothelial Cells
Hz	Hertz
IC_{50}	Half maximal inhibitory concentration
ICAM-1	Intercellular Adhesion Molecule 1
ICTF	International Commission on the Taxonomy of Fungi
IgG	Immunoglobulin G
IL-1β	Interleukin 1β
IL-6	Interleukin 6
iNOS	Inducible Nitric Oxide Synthase
IR	Infrared
J	Coupling constant in Hz
JNK	Jun N-terminal Kinase
KDR/Flk-1	Fetal Liver Kinase 1
KUFC	Kasetsart University Fungal Culture
LC	Liquid Chromatography
Lp-PLA_2	Lipoprotein-associated phospholipase A_2
LPS	Lipopolysaccharide
m	Multiplet
m/z	Mass per charge
MAO	Monoamine Oxidase
MAPK	Mitogen-Activated Protein Kinase
MBC	Minimum Bactericidal Concentration
Me	Methyl

Me_2CO	Acetone
MEA	Malt Extract Agar
MeOH	Methanol
MetAP2	Methionine aminopeptidase-2
MH	Mueller-Hinton Agar
MHB	Mueller-Hinton Broth
MHz	Mega hertz
MIC	Minimum Inhibitory Concentration
MIP	Macrophage Inflammatory Protein
MKK6	Mitogen-activated protein kinase kinase 6
MKK7	Mitogen-activated protein kinase kinase 7
mm	Millimeter
MMAE	Monomethyl Auristatin E
MMAF	Monomethyl Auristatin F
MMP-2	Matrix Metalloproteinase 2
MMP-9	Matrix Metalloproteinase 9
MOPS	3-(N-morpholino)propanesulfonic acid
mp	Melting point in ºC
MPP^+	1-Methyl-4-phenylpyridinium
MRSA	Methicillin-resistant *Staphylococcus aureus*
MS	Mass Spectrometry
NA	Not Available
Na_2SO_4	Sodium sulfate
NAD(P)H	Nicotinamide Adenine Dinucleotide Phosphate
$NaHCO_3$	Sodium bicarbonate
NCE	New Chemical Entities
NCI	National Cancer Institute
NF-κB	Nuclear factor kappa-light-chain-enhancer of activated B cells
NK-1	Human Neurokinin Receptor 1
nm	Nanometer
NMR	Nuclear Magnetic Resonance
NO	Nitric oxide
NOESY	Nuclear Overhauser Effect Spectroscopy

NRPS	Nonribossomal Peptide Synthetase
NSCLC	Non-Small Cell Lung Cancer
ºC	Celsius degrees
OD_{595}	Optical Density at 595 nm
ORTEP	Oak Ridge Thermal Ellipsoid Plot
OX	Oxacillin
PBS	Phosphate Buffered Saline
pcPTase	Polycyclic polyketide prenyltransferase
PEPCK	Phosphoenolpyruvate carboxykinase
PGE_2	Prostaglandin E2
P-gp	P-glycoprotein 1
PKCα	Protein Kinase C α
PTLC	Preparative Thin Layer Chromatography
PTP1B	Protein-Tyrosine Phosphatase 1B
Py	Pyridine
q	Quartet
QToF	Quantum Time of Flight
RAPD	Random Amplified Polymorphic DNA
ROS	Reactive Oxygen Species
RPMI	Roswell Park Memorial Institute
s	Singlet
S	Streptomycin
SAR	Structure-Activity Relationship
SEM	Scanning Electron Microscope
SEM	Standard error of the mean
Si gel	Silica gel
SP	Substance P
sp.	Species (singular)
spp.	Species (plural)
SRB	Sulforhodamine B
SSF	Solid State Fermentation
t	Triplet
TGF-β1	Transforming Growth Factor β1

TLC	Thin Layer Chromatography
TNF-α	Tumor Necrosis Factor α
TSB	Tryptic Soy Broth
UPLC	Ultra Performance Liquid Chromatography
US	United States
UV	Ultraviolet
VA	Vancomycin
VEGF	Vascular Endothelial Growth Factor
VRE	Vancomycin-resistant *Enterococcus*
δ	Chemical shift value in ppm
ε	Molar absorptivity (molar extinction coefficient)
ΣFIC	FIC index

STATEMENT OF THE OBJECTIVES

The main objective of the present study is to investigate the secondary metabolites produced by cultures of the marine sponge and coral-associated fungi for evaluation of their anticancer, antibacterial and antifungal activities. As our group has been focusing mainly on the constituents of the genus *Neosartorya*, investigation of the secondary metabolites of the marine-derived *Neosartorya* species will allow us to compare the chemical profiles of the marine strains with their terrestrial counterparts. Besides, this comparative study will provide an additional tool, useful for a taxonomic characterization of the genus, through a chemotaxonomic analysis (Frisvad *et al*., 2008).

To achieve these objectives, the work was divided according to Scheme 1:

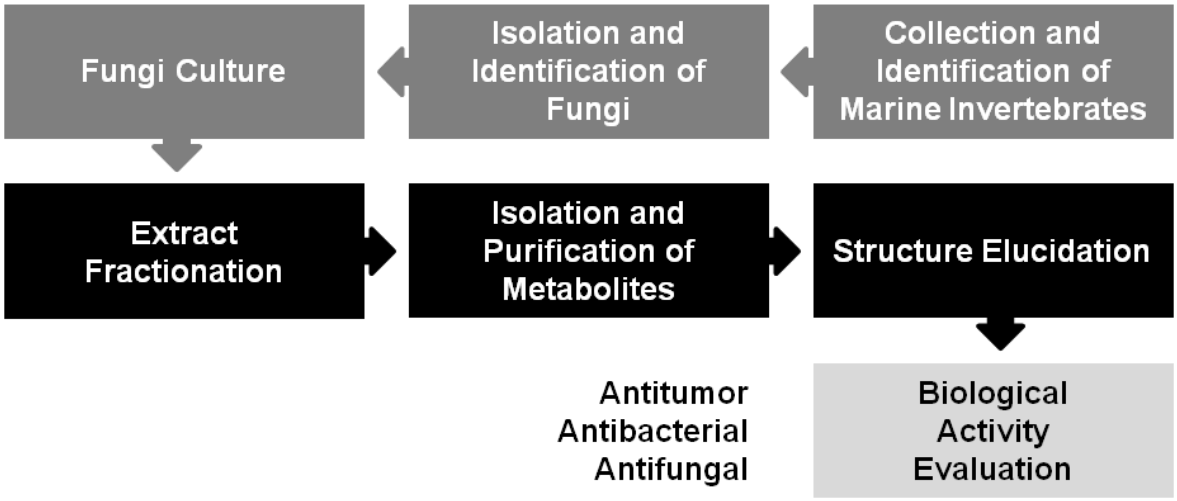

Scheme 1. Schematic diagram of the research process.

I. Collection, Isolation, Identification and Culture of the Marine Fungi

The marine sponges and coral were collected by scuba diving in the Gulf of Thailand and the Andaman Sea.

Identification of the fungi was based on macro- and microscopic characteristics observed under light and scanning electron microscopes (SEM) as

well as with molecular data such as DNA GC content and RAPD (random amplified polymorphic DNA) fingerprint (Glass and Donaldson, 1995).

II. Isolation and Identification of the Secondary Metabolites

The crude ethyl extracts of the culture of the marine fungi were fractionated by column chromatography, and the purification of the metabolites from the column fractions was carried out by PTLC, and/or crystallization. The structures of the pure compounds were established by 1D and 2D NMR spectral analysis (^{1}H, ^{13}C, DEPT 90º and 135º, COSY, HSQC, HMBC, NOESY), HRMS, IR, UV, and X-ray crystallography when the compounds exist in crystalline form.

III. Biological Activity Evaluation

a) Screening of antitumor activity: The effects of the compounds on the growth of human tumor cell lines were evaluated according to the procedure adopted by the National Cancer Institute (NCI, US) in the "*In vitro* Anticancer Drug Discovery Screen" using the protein-binding dye sulforhodamine B to assess cell growth (Skehan *et al*., 1990).

b) Screening of antifungal activity: The compounds were evaluated for their growth inhibitory effects against yeasts, filamentous fungi and filamentous dermatophytes by a dilution method (Wayne, 2002a; 2002b).

c) Screening of antibacterial activity: The compounds were tested for their antibacterial activity against human pathogenic bacteria (including multidrug-resistant isolates) (Johnson *et al*., 2002; Odds, 2003; Wayne, 2011).

CHAPTER I
INTRODUCTION

1.1. General Introduction

Since ancient times, Nature played a major role as the main source of medicinal extracts used, as well as the source of several natural products that led to the development of various drugs currently used for the treatment of a wide spectrum of diseases. Based on empirical knowledge, natural product extracts, mainly plant-derived, have formed the basis of traditional medicine systems. However, it was only in the 20th century that research focused on the identification and characterization of the compounds responsible for the medicinal properties. The urgent need of new therapeutic alternatives, mainly for the treatment of cancer and infectious diseases, as well as the new chemical entities (NCE) decline in drug development pipelines, led to the rekindling of interest in "*rediscovering natural products*" focusing in alternative sources such as the oceans. It is clear that Nature will continue to be a major source of new structural leads (Cragg and Newman, 2013).

Berkowitz's comment in Rouhi's report clearly states the potential and essential role of natural products in therapeutics: "*We would not have the top-selling drug class today, the statins; the whole field of angiotensin antagonists and angiotensin converting-enzyme inhibitors; the whole area of immuno-suppressives; nor most of the anticancer and antibacterial drugs. Imagine all of those drugs not being available to physicians or patients today."* (Rouhi, 2003).

1.1.1. Natural Products: An Established and Continuing Source of Novel Drug Leads

Despite the millenary use of natural medicinal products, research concerning the isolation and use of pure substances in therapeutics dates from the post-Industrial Revolution period in the 19th century. The emergence of natural products clearly reached its climax in the last century, with the discovery of several drugs covering a wide range of diseases (Cragg and Newman, 2013).

The discovery of penicillin G (**1**) (Figure 1) from the filamentous fungus *Penicillium notatum* by Fleming in the late 1920s, and the observation of the broad

therapeutic use of this agent in the 1940s, was a landmark discovery that ushered in a new Era in medicine, "*The Golden Age of Antibiotics*", and promoted the intensive investigation of Nature as a source of novel bioactive agents (Walsh, 2004). The opium poppy (*Papaver somniferum*) is another classic and valuable example being the source of papaverine (**2**) (Figure 1), which formed the basis for the antihypertensive agent verapamil. However this plant is better known as a source of the opiate analgesic alkaloid morphine (**3**) (Figure 1).

Most of the cholesterol lowering agents (statins) are synthetic analogues derived from the fungal metabolites mevastatin (**4**) (Figure 1), isolated from *Penicillium citrinum* (Endo *et al*., 1976), as well as lovastatin (**5**) (Figure 1) isolated from *Monascus ruber* and *Aspergillus terreus* (Buckland *et al*., 1989; Negishi *et al*., 1986). Two lipid-regulating drugs of this class, atorvastatin and simvastatin, feature prominently in the top ten drugs by cost, led by Lipitor® (atorvastatin) with an annual sale reaching 7.2 billion US dollars in 2010, only in the US (Kleinrock, 2011).

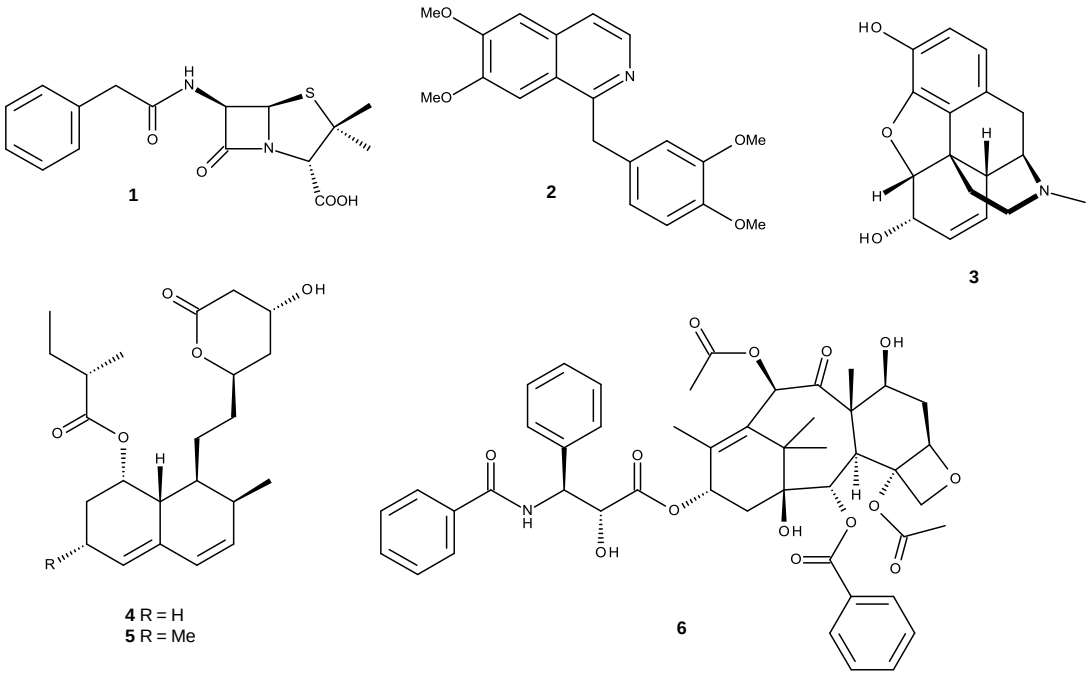

Figure 1. Some examples of natural drug leads approved for use in Medicine.

Paclitaxel (**6**) (Taxol®) (Figure 1), the exciting plant-derived chemotherapy drug was originally isolated from the Pacific yew tree *Taxus brevifolia*. The discovery in 1979 of its mode of action, through promotion of the assembly of tubulin into microtubules by Schiff and Horwitz and its report in 1980 (Schiff and Horwitz, 1980), was a key milestone in the lengthy development process, being approved for clinical use against ovarian cancer in 1992 and against breast cancer in 1994. Recently, a new semi-synthetic derivative, cabazitaxel (Jevtana®) developed by Sanofi-Aventis, was approved by the FDA for the treatment of hormone-refractory prostate cancer (http://www.cancer.gov/cancertopics/druginfo/fda-cabazitaxel, accessed on 24th November 2013).

During the last century, natural products research led to the development of several drugs currently used in Medicine against a wide range of diseases. In fact, the most recent survey by Newman and Cragg (2012) analyzing the sources of new drugs over the period 01/1981 – 12/2010, indicates that while 66% of the 1073 small molecule NCEs are formally synthetic, only 36% can be classified as truly synthetic or devoid of natural inspiration. Furthermore, when considering disease categories, for the 1073 small molecules, 69% of anti-infectives and 75% of anticancer drugs introduced into the market can be traced back as naturally derived or inspired.

The role of natural sources in the finding of novel drug leads is unquestionable and since there are still many unexplored resources from Nature, an enormous chance for finding new or less investigated organisms, and thereby new lead structures still exists (Aly *et al*., 2011; Hill, 2013).

1.2. Ocean as an Unlimited Source for Novel Drugs

Comprising almost three quarters of the Earth's surface, oceans represent a rich source of both biological and chemical diversity, containing nearby 200 000 catalogued species, representing only ~9% from the estimated value of 2.2 million of species dwelling in ocean depths (Mora *et al*., 2011). Some marine habitats are known to be particularly numerous in species, especially tropical marine reefs,

which represent one of the most diverse ecosystems encountered on Earth, comparable in diversity to tropical rain forests.

Marine organisms growing in a unique and stressful habitat can develop the ability to produce unusual and structurally complex secondary metabolites. In the marine environment, where a different environment results in a different transcriptome, proteosome, and finally a different metabolome which allows an organism to survive, one can speculate that different secondary metabolites might be the result of special requirements to adapt to such an extreme environment (Firn and Jones, 2000). Almost all forms of life in the marine environment have been investigated for their natural products content, representing a valuable source of novel compounds with great potential as pharmaceuticals, nutritional supplements, cosmetics, agrochemicals and enzymes, many of them with a strong potential market value (Blunt *et al*., 2013; Kijjoa and Sawangwong, 2004).

Bioactive marine natural products can be defined as biologically active products, including primary and secondary metabolites, from marine sources and despite the increasing interest in marine primary metabolites such as lipids, enzymes and complex heteropolysaccharides, the main focus and potential rely on the secondary metabolites. Over 22 000 structurally diverse marine metabolites have been isolated and characterized over the last fifty years. (Blunt *et al*., 2013; Hu *et al*., 2011). Main areas of research on marine natural products are devoted to the discovery of new anticancer and antimicrobial drugs, somehow related to the severe mortality and morbidity related to cancer, as well as the increasing drug resistant bacterial pathogens (Blunt *et al*., 2013; Hill, 2013; Mayer *et al*., 2013). However, the study of marine natural products so far has not only allowed the development of new drug leads, but also the identification of new molecular targets for therapeutic intervention (Amador *et al*., 2003).

Drug discovery from marine sources seems to have benefited from a renaissance in the past ten years, which was made possible by new developments in analytical technology, spectroscopy and high-throughput screening (Molinski, 2010). Additionally, the recognized potential from marine environment led to significant efforts to isolate and identify new marine-derived natural products over the last decade by collaboration of both pharmaceutical companies and academic institutions, accompanied by funding supports from governmental agencies (Bórrensen *et al*., 2010).

In 2010, the global market for marine biotechnology products and processes was estimated in €2.8 billion with a cumulative annual growth rate of 4-5 %. Less conservative estimates predicted an annual growth in the sector of even up to 10-12 % in the following years, considering the huge potential and high expectations for further development of this sector at a global scale (Bórrensen *et al*., 2010).

The annual reviews on marine natural products by Blunt *et al*. (2013 and previous reviews) as well as the MarinLit database (http://www.rsc.org/Publishing/CurrentAwareness/MarinLit.asp), established in 1970's by Blunt and Munro and recently acquired by the Royal Society of Chemistry, clearly states the unequivocal potential of marine organisms as sources of novel drug leads, and an overview of the impressive variety of marine-derived compounds.

1.2.1. Clinical Pipeline of Marine Pharmaceuticals

The first described marine natural product to enter clinical trials as an antineoplastic agent was didemnin B (**7**) (Figure 2), a cyclic depsipeptide isolated from the tunicate *Tridemnum solidum* (Rinehart Jr. *et al*., 1981).

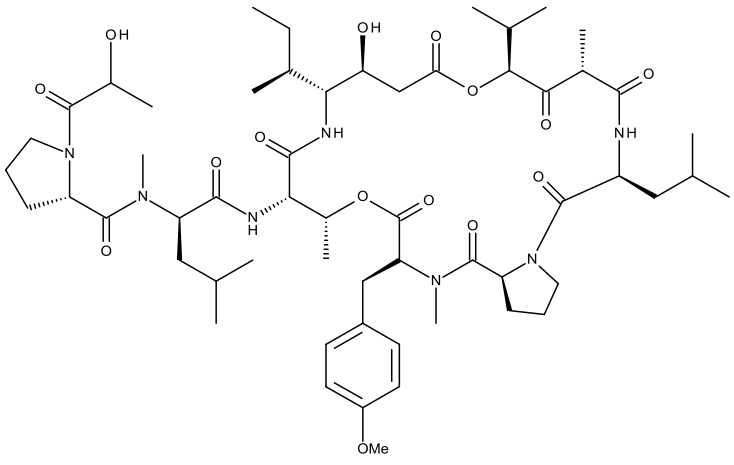

7

Figure 2. Structure of didemnin B (**7**).

The compound displayed good antitumor activity against B16 melanoma, and moderate activity against M5076 sarcoma and P388 leukemia cell lines, as well as good antiviral and potent immunosuppressive activities (Chun *et al*., 1986). Although the Phase II clinical trials against kidney adenocarcinoma, advanced epithelial ovarian cancer, and metastatic breast cancer have been concluded, didemnin B (**7**) exhibited high toxicity and no further trials were held (Nuijen *et al*., 2000).

Marine clinical pharmaceutical pipeline (Table 1) currently consists of seven FDA approved drugs (Figures 3a and 3b) and ten compounds in Phase I, II and III of clinical development (http://marinepharmacology.midwestern.edu/ accessed on 18th October 2013).

Cytarabine (Ara-C, arabinosyl cytosine) (**8**) (Figure 3a) is a synthetic pyrimidine nucleoside which was developed from spongothymidine (**9**) (Figure 3a), originally isolated from the Caribbean sponge *Tethya crypta* (Bergmann and Feeney, 1951). The compound is a cytotoxic agent which, when converted intracellularly to cytosine arabinoside triphosphate, competes with the physiologic substrate deoxycytidine triphosphate, resulting in both inhibition of DNA polymerase and DNA synthesis. Cytarabine (**8**) became the first marine-derived drug that received a FDA approval in 1969, and is currently available as either conventional cytarabine (Cytosar-U®) or liposomal formulations (Depocyt®). Conventional cytarabine (Cytosar-U®) is for treatment of acute lymphocytic leukemia, acute myelocytic leukemia and blast crisis phase of chronic myelogenous leukemia and meningeal leukemia, while liposomal cytarabone (Depocyt®) is indicated for intrathecal treatment of lymphomatous meningitis (Absalon and Smith, 2009; Thomas, 2009; http://www.cancer.gov/cancertopics/druginfo/cytarabine accessed on 3rd 2013). Vidarabine (Ara-A, arabino furanosyladenine) (**10**) (Figure 3a) is a synthetic purine nucleoside, developed from the nucleoside spongouridine (**11**) (Figure 3a), also isolated from the same sponge (Bergmann and Feeney, 1951). Although its antiviral mechanism of action has not been established, vidarabine (**10**) appears to interfere with the early steps of viral DNA synthesis.

Table 1. Marine pharmaceuticals: Current pipeline (http://marinepharmacology.midwestern.edu/ accessed on 18th October 2013)

Clinical status	Compound name (Trademark)	Marine organism[a]	Chemical class	Disease area	C / I[b]
FDA EMA Approved	Cytarabine (Cytosar-U®)	Sponge	Nucleoside	Cancer	1
	Vidarabine (Vira-A®)	Sponge	Nucleoside	Antiviral	NA
	Ziconotide (Prialt®)	Cone snail	Peptide	Pain	2
	Eribulin mesylate (Halaven®)	Sponge	Macrolide	Cancer	3
	Omega-3-acid ethyl esters (Lovaza®)	Fish	ω-3 fatty acids	Hyper--triglyceridemia	4
	Trabectedin (ET-743) (Yondelis®)	Tunicate	Alkaloid	Cancer	5
	Brentuximab vedotin (Adcentris®)	Mollusk cyanobacterium	ADC (MMAE)	Cancer	6
Phase III	Plitidepsin (Aplidin®)	Tunicate	Depsipeptide	Cancer	5
Phase II	DMXBA	Worm	Alkaloid	Schizophrenia	7
	PM00104 (Zalypsis®)	Mollusk	Alkaloid	Cancer	5
	PM01183	Tunicate	Alkaloid	Cancer	5
	CDX-011	Mollusc cyanobacterium	ADC (MMAE)	Cancer	8
Phase I	Marizomib (Salinosporamide A)	Bacterium	β-lactone-γ-lactam	Cancer	9
	PM060184	Sponge	Polyketide	Cancer	5
	Bryostatin	Bryozoan	Macrolide lactone	Cancer	10
	SGN-75	Mollusk cyanobacterium	ADC (MMAF)	Cancer	6
	ASG-5ME	Mollusk cyanobacterium	ADC (MMAE)	Cancer	6

[a]The marine pharmaceuticals pipeline consists of natural products, analogs or derivatives of compounds produced by this marine organism.

[b]C / I (Company or Institution): 1 Bedford Laboratories; 2 Azurpharma; 3 Eisai Inc; 4 GlaxoSmithKline; 5 Pharmamar; 6 Seattle Genetics; 7 University of Colorado Health Sciences Center; 8 Celldex Therapeutics; 9 Phase I Clinical Trial sponsored by Triphase Research and Development Corporation; 10 National Cancer Institute.

Abbreviations: FDA: Food and Drug Administration; **EMA:** European Medicines Agency; **NA:** Not available; **ADC:** Antibody drug conjugate; **MMAE:** Monomethyl auristatin E; **MMAF:** Monomethyl auristatin F.

Vidarabine (Vira-A®) received the FDA approval in 1976 and is currently used as a 3% opththalmic ointment for the treatment of acute keratoconjunctivitis, recurrent epithelial keratitis caused by herpes simplex virus type 1 and 2, and superficial keratitis caused by herpes simplex virus that has not responded to topical idoxuridine (Herplex®) (Martindale, 2012).

Ziconotide (**12**) (Figure 3a) (Prialt®) is the synthetic equivalent of a naturally occurring 25-amino acid peptide, ω-conotoxin MVIIA (**13**) (Figure 3a), originally isolated from the venom of the fish-hunting marine snail *Conus magus* (Olivera, 2000). Ziconotide (**12**) is a potent analgesic with a completely novel mechanism of action (Bingham *et al*., 2010), reversibly blocking N-type calcium channels located on primary nociceptive afferent nerves in the superficial layers of the dorsal horn of the spinal cord. Binding of ziconotide (**12**) to presynaptic N-type calcium channels reduces the release of excitatory neurotransmitter from the primary afferent nerve terminals (McGivern, 2006). Ziconotide (**12**) received the FDA approval in 2004, and is currently used for the management of severe chronic pain in patients with cancer or AIDS for whom intrathecal therapy is warranted and who are intolerant or refractory to other treatments such as systemic analgesics, adjunctive therapies or morphine (Pope and Deer, 2013; Rauck *et al*., 2009; Staats *et al*., 2004).

In 2001, trabectedin (**14**) (Figure 3a) (Yondelis®), also known as ecteinascidin-743 (ET-743), a tetrahydroisoquinolone alkaloid originally extracted from the tunicate *Ecteinascidia turbinata,* was developed by PharmaMar (Rinehart *et al*., 1990, 1991; Wright *et al*., 1990). Although the mechanism of action is not fully understood, it is well known that trabectedin (**14**) binds by a covalent reversible bond to the DNA minor groove (Zewail-Foote and Hurley, 2001). Yondelis® was approved in EU for the treatment of soft tissue sarcoma (Verweij, 2009), and later for the treatment of relapsed platinum-sensitive ovarian cancer (Yap *et al*., 2009).

Halichondrin B (**15**) (Figure 3a), a polyether macrolide originally isolated from the marine sponge *Halichondria okadai* in the late 1980s, displayed potent anticancer activity in preclinical animal models (Fodstad *et al*., 1996; Hirata and Uemura 1986). Eribulin mesylate (**16**) (Figure 3a), a synthetic analog of halichondrin B (**15**), developed by Esai Pharmaceuticals, is a non-taxane microtubule inhibitor currently used in US, EU and Asia, under the trade name

Halaven® for the treatment of metastatic breast cancer after two or more chemotherapy regimens for metastatic disease (Martindale, 2012).

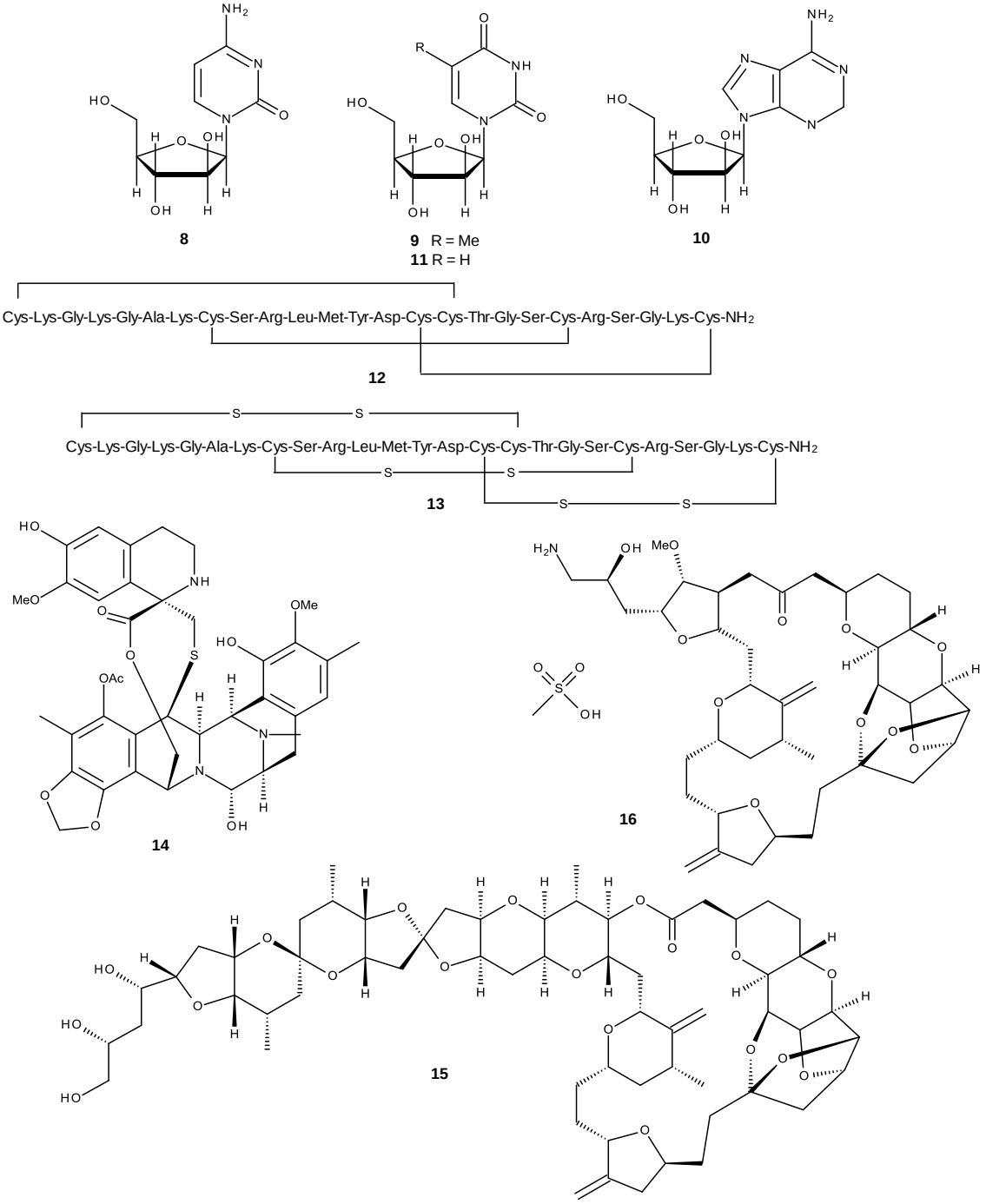

Figure 3a. Marine natural products or derivatives thereof approved for use by FDA or EMA.

Lovaza®, a highly purified and concentrated ω-3 polyunsaturated fatty acids preparation obtained from fish oils mainly comprised of EPA (20:5(n-3)) (**17**) and DHA (22:6(n-3)) (**18**) (Figure 3b), was approved in 2004 by FDA as an adjunct to diet in adults with high triglyceride levels (≥500 mg/dL) (Koski, 2008). It was commercialized in EU under the tradename Omacor®, and is also used in coronary arteriosclerosis, familial combined hyperlipidemia as well as for secondary prevention after myocardial infarction (Martindale, 2012).

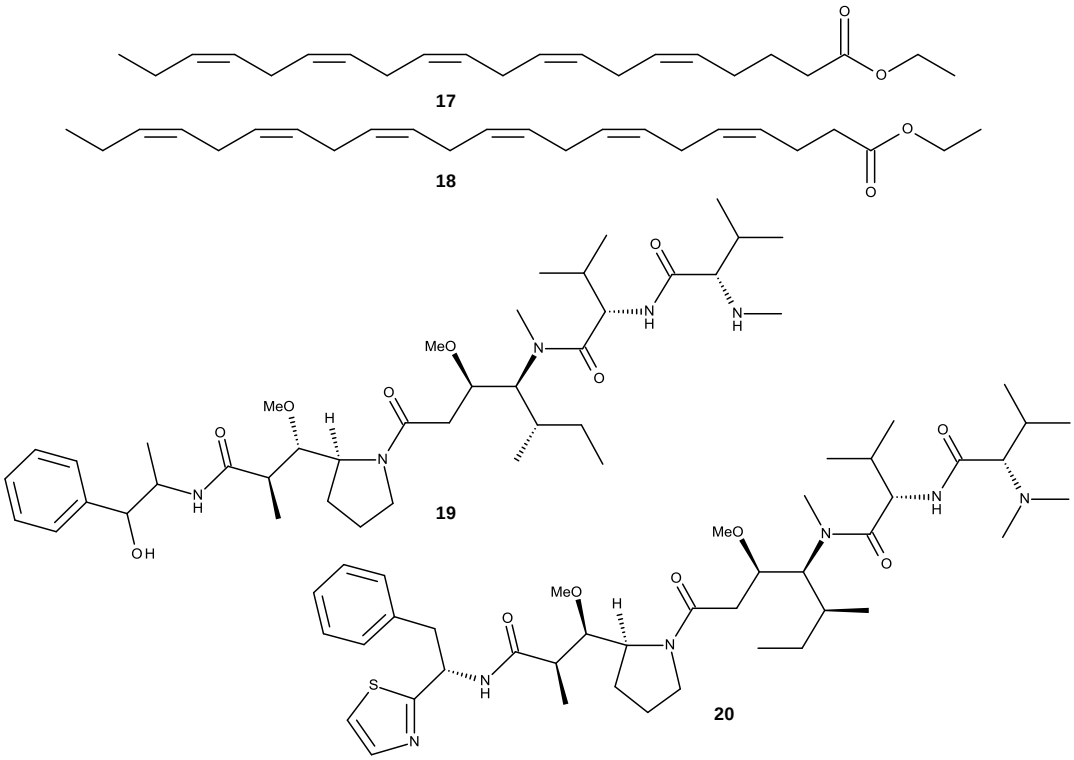

Figure 3b. Marine natural products or derivatives thereof approved for use by FDA or EMA.

Brentuximab vedotin is a CD30-directed antibody-drug conjugate (ADC) consisting of three components: the chimeric IgG1 antibody cAC10 which is specific for human CD30, the microtubule disrupting agent monomethyl auristatin E (**19**) (Figure 3b) (MMAE), and a protease-cleavable linker that covalently attaches MMAE (**19**) to cAC10. The microtubule disrupting agent MMAE (**19**) binds to tubulin, disrupting the microtubule network which leads to cell cycle arrest

and apoptotic death of the cells (Watanabe *et al*., 2007). Brentuximab vedotin (Adcentris®) was approved by FDA for the treatment of anaplastic large T-cell systemic malignant lymphoma and Hodgkin's disease (Martindale, 2012). MMAE (**19**) is a synthetic analog of dolastatin 10 (**20**) (Figure 3b) originally isolated from the sea hare *Dolabella auricularia*, and recently from a marine cyanobacterium *Symploca* sp. (Luesch *et al*., 2001).

It is expected that the number of candidates to enter clinical trials in a near future is vast. Only referring to the period from 2009 to 2011, the preclinical pharmaceutical pipeline consists of over 250 marine compounds that will enrich the marine clinical pharmaceutical pipeline with novel lead compounds (Mayer *et al*., 2013). Despite some limitations, the current success rate of discovery from the marine world, namely seven clinically approved drugs from 22 000, is significantly better than the industry average (Gerwick and Moore, 2012).

1.2.2. Statistical Perspective on Marine Natural Products Research

Over 22 000 structurally diverse marine metabolites have been isolated and characterized over the last five decades, with 1152 new compounds only for the year 2011 (Blunt *et al*., 2013).

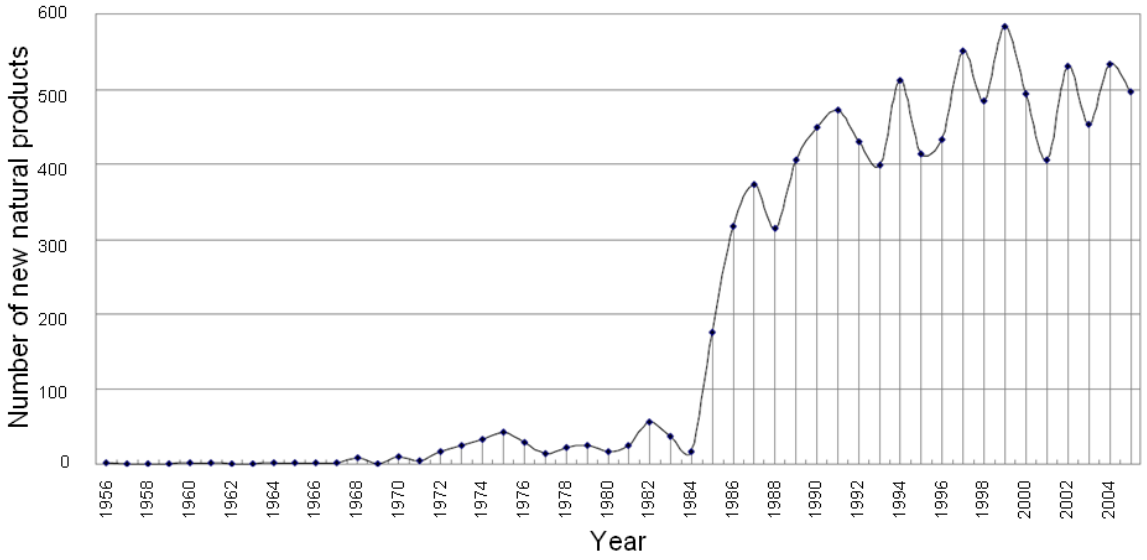

Figure 4. Temporal trend in the number of novel products obtained from marine organisms (Hu *et al*., 2011).

Before the 1980s, marine natural products discovered annually were less than 100, however there was an outstanding development since the mid-1980s (Figure 4), coincident with the development and progress of structure elucidation techniques (Hu *et al*., 2011).

Regarding to its source, majority of novel compounds from marine organisms, approximately 75% were isolated from invertebrates mainly from the phyla Porifera (mostly sponges) but also from Coelenterate phyla (mostly coral) (Figure 5). Additionally, algae and microorganisms are also major sources of novel metabolites, with a special focus on microorganisms due to the increasing focus from marine natural product chemists (Hu *et al*., 2011). In contrast to macroorganisms, microorganisms represent promising natural product sources due to the feasible and sustainable production of large quantities of secondary metabolites with reasonable cost, by large-scale cultivation and fermentation of the source organisms (Waites *et al*., 2001; Xiong *et al*., 2013).

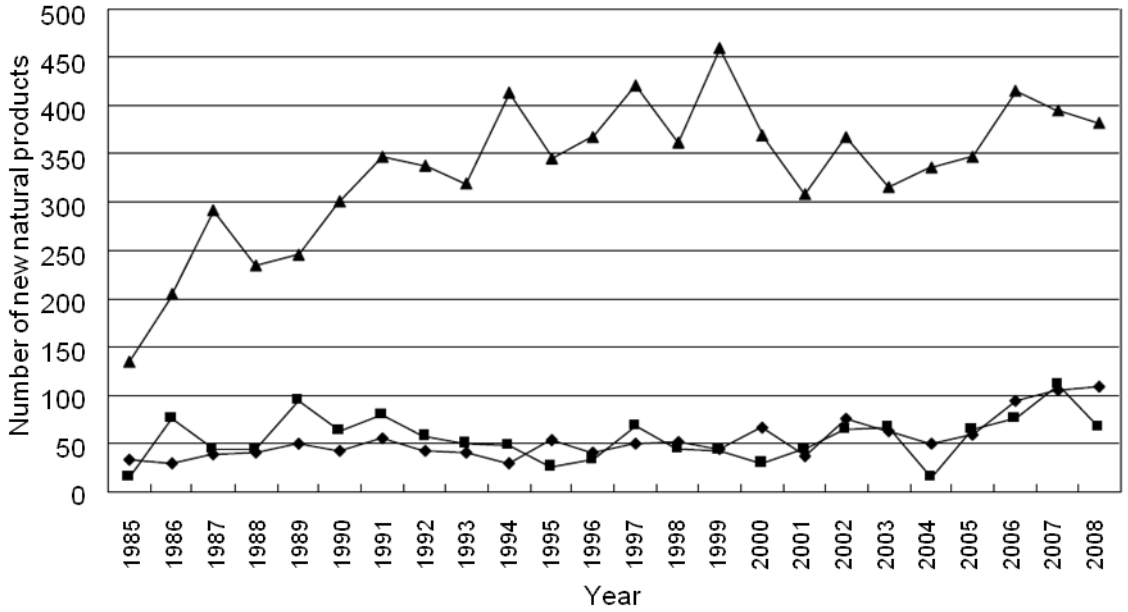

Figure 5. Temporal trends in the number of novel compounds isolated from different marine organisms between 1985 and 2008. ▲ Marine invertebrate; ■ Marine algae;◆ Marine microorganisms (including phytoplankton) (Hu *et al*., 2011)

1.2.3. Marine Microbial Consortia as the True Metabolic Source of Bioactive Metabolites

The symbiotic microbial consortia also prove to be a source of bioactive compounds with pharmaceutical potential, and there is a growing recognition that marine invertebrates and marine plants surface are usually populated with enormous quantities of associated or symbiotic microorganisms (Gerwick and Fenner, 2013).

According to Gerwick and Fenner (2013), at the end of the year 2012, there were twenty-one marine derived or marine-inspired agents in the clinic or clinical trials (outdated data). Pie chart **A** (Figure 6) summarizes the collected sources of organisms that have yielded these agents, and reveals that marine invertebrates are the richest collected source (18 of 21, 86%).

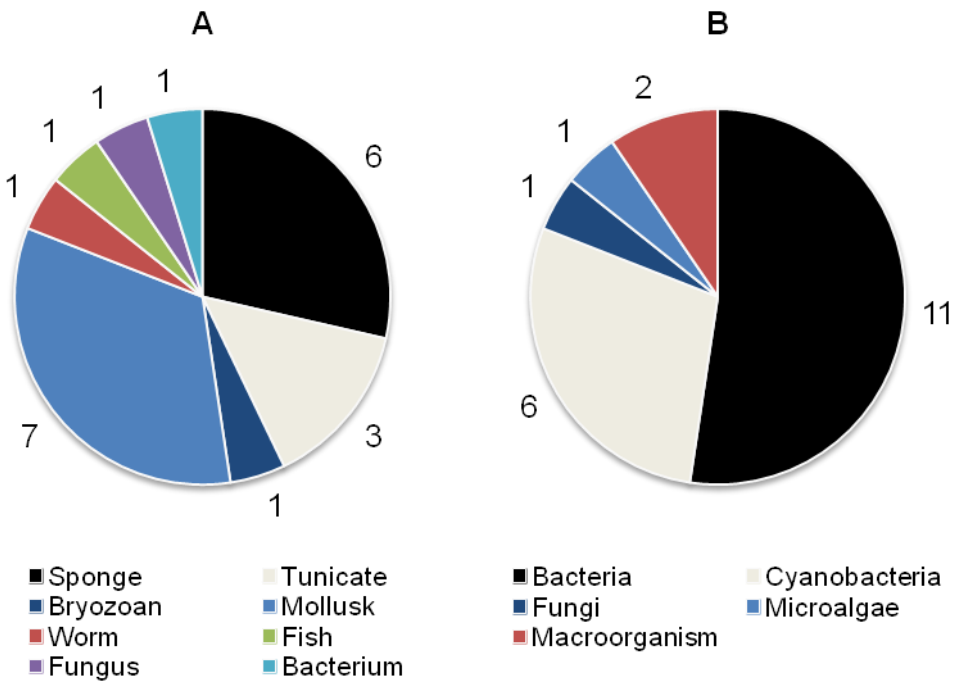

Figure 6. Pie charts showing **A:** the collected sources of the twenty-one marine-derived or marine-inspired agents in the clinic or clinical trial, and **B:** the same agents with their demonstrated or predicted metabolic sources (Gerwick and Fenner, 2013).

However, there are strong evidences that some promising marine natural compounds in clinical trials, as well as some approved marine-derived agents supposedly produced by invertebrates, are in fact metabolic products of their associated microorganisms or derived from a diet of prokaryotic microorganisms (Gerwick and Fenner, 2013; Gerwick and Moore, 2012; Haefner, 2003; Simmons *et al*., 2008). For example, dolastatin 10 (**20**) (Figure 3b) which was first reported as a metabolite of the Indian Ocean sea hare *Dolabella auricularia* (Pettit *et al*., 1987), was later found to be produced by the gastropod's diet cyanobacteria of the genera *Simploca* and *Lyngbya* (Luesch *et al*., 2001; Williamson *et al*., 2000).

Another example refers to a recent report by Rath and co-workers on metagenomic sequencing of total DNA from *Ecteinascidia turbinata* and associated microorganisms, suggesting that the individual genes responsible for trabectedin (**14**) (Figure 3a) production has microbial origin from the associated-γ-proteobacterium *Candidatus Endoecteinascidia frumentensis* (Rath *et al*., 2011). As noted above, the collected source has oftentimes been shown or is strongly suspected of harboring or feeding upon microorganisms that are the actual producers of the bioactive agent. Analysis of pie chart **B** (Figure 6), displaying the actual or suspected metabolic source of the twenty-one marine derived or marine-inspired agents in the clinic or clinical trials by the time of the end of 2012, reveals that marine microbes are the real metabolic jewels of the world's oceans, accounting for 90% of the twenty-one marine derived agents in clinical trials and approved pharmaceutical agents by the end of 2012 (Gerwick and Fenner, 2013).

The realization that microbes are the true metabolic sources of several relevant bioactive compounds raised hope of obtaining a sustainable and less limited supply of compounds for testing and drug development.

1.2.4. Marine Natural Products Research and the "*Supply Problem*"

The fact that virtually no marine natural product can so far be found on the shelves of pharmacies is certainly not due to a limited chemical diversity of marine organisms. The last fifty years of research on marine natural products led to the development of seven agents that have entered the clinic as approved drugs, plus

a substantial number of candidates progressing through the development process. However, despite the success stories, several factors contribute to the lack of the development in the area of marine pharmaceuticals. Biologically active natural products are often produced in relatively small amounts, and often by rare animals whose natural populations cannot sustain the extensive collections required for clinical trials. Insufficient quantities of material to allow for study completion, difficulties of retrieving a sustained and reliable harvest of a marine organism, limited amounts of compounds for pre-clinical development, and difficulties in culturing marine organisms, are limiting factors that need to be overcome (Bhadury *et al*., 2006). To overcome such limitations, several approaches can be used like the chemical synthesis, mass cultivation of the producer organisms, or through genomic engineering, but the large scale production of metabolites with potential clinical relevance to meet the demand for clinical trials and drug development, continues to be a major challenge.

Despite the vast number of examples of successfully synthesized natural products with medicinal relevance (Nicolaou *et al*., 2012), not always chemical synthesis may be a solution due to the economically non viable approach. Trabectedin (ecteinascidin-743) (**14**) and halichondrin B (**15**) (Figure 3a) examples demonstrate that some marine natural products have such complex structures leading to high costs associated with their chemical synthesis (Cuevas *et al*., 2000). A notable exception is ziconotide (**12**) (Figure 3a), which due to its peptide nature can be obtained in virtually unlimited amount through synthesis (Olivera, 2000).

Mariculture of macroorganims is another alternative mean for the production of large amounts of metabolites, but rarely can be considered to be cost-effective. The first example of mass cultivation of sponge species for pharmaceutical purposes was the large-scale culture of *Lissodendoryx* sp. to obtain sufficient amount of halichondrin B (**15**) (Figure 3a) for clinical trials. From one metric ton of the sponge, only *ca.* 300 mg of a mixture of two halichondrin analogues could be obtained (Hart *et al*., 2000). Even with a more favorable ratio of compound production vs. biomass, to obtain approximately 1 g of trabectedin (**14**) (Figure 3a), close to one metric ton (wet weight) of *Ecteinascidia turbinata* has to be collected and extracted, which is economically unfeasible (Mendola, 2000).

Organisms that could easily be cultured in large amounts would thus be ideal. Such organisms might well be marine microorganisms.

1.3. The Potential of Marine Microbial Diversity

Whereas in the last decades the focus in marine natural product research was mainly on macroorganisms such as sponges, sea weeds and others, nowadays it is clearly evident that microorganisms from the marine habitat are equally rich sources of novel constituents, and often the true metabolic producers of bioactive metabolites whose production was originally attributed to a macroorganism (Gerwick and Fenner, 2013; Gerwick and Moore, 2012; Haefner, 2003; Simmons *et al*., 2008). Additionally, microorganisms are far more accessible through sustainable production by fermentation than many marine macroorganisms that usually have to be collected from limited wild stocks (Proksch *et al*., 2010). These two main factors reveal that microbes are truly the treasure troves of new marine pharmaceuticals.

As microorganisms occupy almost every niche on Earth, scientists speculate that each drop of water taken from the ocean will contain microbial species unknown to humans in a ratio 9:1 (Colwell, 2002). To maximize the chemical diversity available from marine microbes, other sources like the deep-ocean and geothermal vents are becoming the focus of considerable interest from natural product research chemists (Bhatnagar and Kim, 2010; Pettit, 2011). In fact, diverse bioactive secondary metabolites have been reported from cultured extreme-tolerant microorganisms, extremophiles, and deep-sea microbes. Due to the extreme physical and chemical conditions at deep-sea, hydrothermal vents sites conditions are constantly fluctuating, representing a nearly inexhaustible source of genomic innovation (Pettit, 2011).

Although numerous natural products have been identified from marine microorganisms during the last decades, it is obvious that a plethora of compounds still await discovery. This assumption results not only from the fact that only a small number of microorganisms have been cultivated and discovered yet but also from recent genome sequencing projects (Brakhage and Schroeckh, 2011).

1.3.1. Marine Microorganims as a Source of Novel Drug Candidates

Microorganisms are a prolific source of structurally diverse bioactive metabolites and have yielded some of the most important products of the pharmaceutical industry, including antibiotics and blockbuster medicines with tremendous economic importance. These include antibacterial agents such as the penicillins and cephalosporins, aminoglycosides and tetracyclines, immunosuppressive agents, cholesterol lowering agents such as mevastatin and lovastatin, and antihelmintic and antiparasitic drugs such as ivermectins. These tremendous successful stories of drug discovery from microorganisms, revolutionized the therapy concepts, pushing the academia and pharmaceutical industry to develop programs on natural product discovery, emphasized on marine microbial fermentation based technologies (Debbab *et al*., 2010).

Current marine clinical pharmaceutical pipeline includes one microbial metabolite in phase I of clinical trials, but several drug leads from marine microbiota in pre-clinical development are expected to advance clinical development to be pharmaceutically relevant drugs (Bhatnagar and Kim, 2010; Gerwick and Fenner, 2013; Newman and Hill, 2006).

Salinosporamide A (NPI-0052) (**21**) (Figure 7), a β-lactone produced by fermentation cultures of *Salinispora tropica*, is a powerful 20S proteasome inhibitor and one of the most promising candidates in chemotherapy (Feling *et al*., 2003). Nereus Pharmaceuticals has licensed this compound under the name Marizomib®, which is now in Phase I clinical trials as a single agent in patients with advanced solid tumors, and also in combination with vorinostat, a histone deacetylase inhibitor, for the treatment of advanced pancreatic carcinoma, non-small cell lung carcinoma and melanoma (Hamlin *et al*., 2009; Potts *et al*., 2011). Interestingly, *S. tropica* belongs to the recently described and exclusively marine genus of Streptomycete bacteria known as *Salinispora*, of which three species are recognized and all inhabit marine sediments. From over 100 cultivated *Salinispora* spp. strains, more than 80% inhibited human tumor cell growth, and 35% showed antibacterial properties toward a wide range of drug-resistant human pathogens,

representing one of the most recent and promising sources for novel drug leads (Fenical and Jensen, 2006).

Plinabulin (NPI-2358) (**22**) (Figure 7) is a potent and selective tumor vascular disrupting agent, and one of over 200 synthetic analogues in the series that were prepared following the discovery of the parent compound phenylahistidin (also known as halimide) (**23**) (Figure 7). Phenylahistidin (**23**) was isolated from cultures of the marine alga-derived fungus *Aspergillus ustus*, and displayed potent cytotoxic activity toward human cancer cell lines and tubulin polymerization inhibition (Kanoh *et al*., 1997; 1999). Two phase I trials have been reported, as a single agent in patients with advanced solid tumors or lymphomas (Mita *et al*., 2010), or in combination with docetaxel in patients with non-smal cell lung cancer (NSCLS) (Millward *et al*., 2012). The favorable results led to a phase II ADVANCE clinical trial of plinabulin (**22**) in combination with docetaxel in patients with NSCLS, that was recently completed, but no further information was provided (http://clinicaltrials.gov/show/NCT00630110 accessed on 18th October 2013).

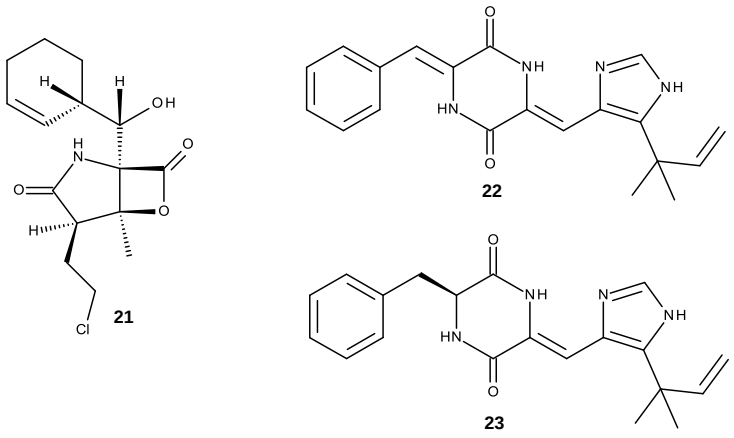

Figure 7. Chemical structures of novel drug candidates produced by marine microorganisms.

Finally, the most recent and exciting discovery is seriniquinone, produced by a unique marine bacterium of the genus *Serinicoccus*, recovered from shallow marine sediments. *In vitro* screening in the NCI 60 cell line panel showed pronounced selectivity toward all melanoma cell lines tested, particularly hostile to a dangerous form of metastatic melanoma. Seriniquinone has a unique way of

inducing apoptosis, targeting the recently discovered protein dermcidin, overexpressed in melanoma, activating apoptosis and the induction of autophagocytosis leading to efficient cell death (Fenical *et al*., 2013).

1.3.2. Marine Microorganisms: Cultivating the Uncultured and Activating Silent Clusters

Until recently, the inability to cultivate most naturally occurring microorganisms has severely limited the exploration of the potential of both terrestrial and marine microbes. In fact, it has been estimated that much less than 1% of microorganisms seen microscopically have been cultured. However, marine microorganisms low culturability may reflect the artificial conditions inherent in most culture media, e.g., the lack of specific nutrient required for growth. Energy sources, nutrients and proper physicochemical conditions are necessary for microbial growth, and culture mimicking the natural environment is critical to recover the uncultivated microorganisms (Kjer *et al*., 2010; Zengler *et al*., 2002).

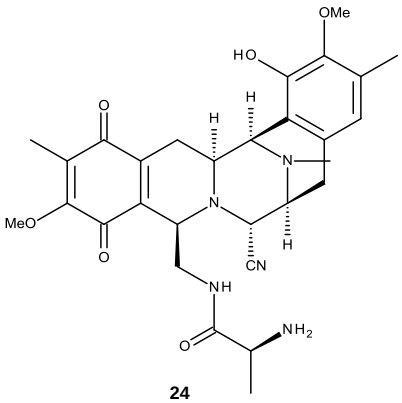

24

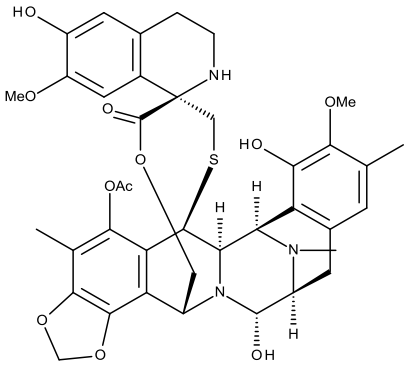

14

Figure 8. Structures of cyanosafracin B (**24**) and the hemisynthesis product trabectedin (**14**).

Alternatively, these compounds could be produced in bulk, by total or semisynthetic pathways, through fermentation technologies. A widely known example is the production of trabectedin (**14**) (Figure 8). Due to the supply

problem and high costs associated with chemical synthesis, this drug is produced by hemisynthesis starting from cyanosafracin B (**24**) (Figure 8), a fermentation product of the terrestrially-derived bacterium *Pseudomonas fluorescens* (Cuevas *et al*., 2000). Fermentation processes have gained considerable relevance for commercial production of relevant metabolites like trabectedin (Demain, 2000).

On the other hand, Solid State Fermentation (SSF) became quite popular and is widely used for the production of bioactive secondary metabolites from fungi (Hölker *et al*., 2004).

Recent advances in molecular biology of fungal secondary metabolism may offer a better insight into how biogenetic gene clusters are regulated and whether their expression is affected by culture conditions and environmental changes, allowing the optimization of secondary metabolites production under laboratory conditions (Fox and Howlett, 2008; Yu and Keller, 2005). Additionally, combinatorial biosynthesis involving introduction of biosynthetic gene clusters into microorganisms, is a powerful and recent tool allowing the synthesis of novel metabolites, due to the effect of new enzymes on the metabolic pathways. Genomic technologies provide a unique opportunity not only to produce pharmacologically relevant compounds, thus overcoming the supplying issue, but also to explore further the potential of marine microorganisms to generate new and potentially useful chemicals (Firn and Jones, 2000). Currently, the main challenge is not the cultivation of potentially relevant microorganisms in the laboratory, but the perception that the majority of the secondary metabolite biosynthesis gene clusters are silent under standard laboratory conditions, thus not allowing the expression of silent gene clusters and the consecutive production of new potentially natural products (Hertweck, 2009).

1.4. Fungi from Marine Habitats as Producers of Relevant Bioactive Secondary Metabolites

Besides blockbuster drugs from fungal origin such as the cholesterol biosynthesis inhibitors (statins) and β-lactam antibiotics, there are several further examples of drugs approved for clinical use such as the immunosuppressant drugs mycophenolate mofetil (**25**) (CellCept®) and cyclosporine A (**26**) (Restasis® /

Sandimmune®), the alkaloid ergotamine (**27**) (Migranal® / Ergomar®) still used for migraine treatment, and the widely used antibiotics terpenoid fusidic acid (**28**) (Fucidin® / Fucithalmic®) and griseofulvin (**29**) (Grivulfin® / Fulvicin-U/F®) (Figure 9) (Aly *et al*., 2011).

In the meantime, world's bestselling anticancer drug paclitaxel (Taxol®) (**6**) (Figure 1), initially isolated from the plant *Taxus brevifolia*, was found to be a biosynthetic product of several endophytic fungi like *Taxomyces andreanae* (Stierle *et al*., 1993) and *Pestalotiopsis microspora* (Li *et al*., 1998). More recently other endophytic fungi were shown to also produce camptothecin (Puri *et al*., 2005) and anticancer drugs precursor podophyllotoxin (Amna *et al*., 2006; Eyberger *et al*., 2006). This reason contributed to the increasing recognition of fungal secondary metabolites as an auspicious resource for new drug leads, especially in the cancer area (Greve *et al*., 2010).

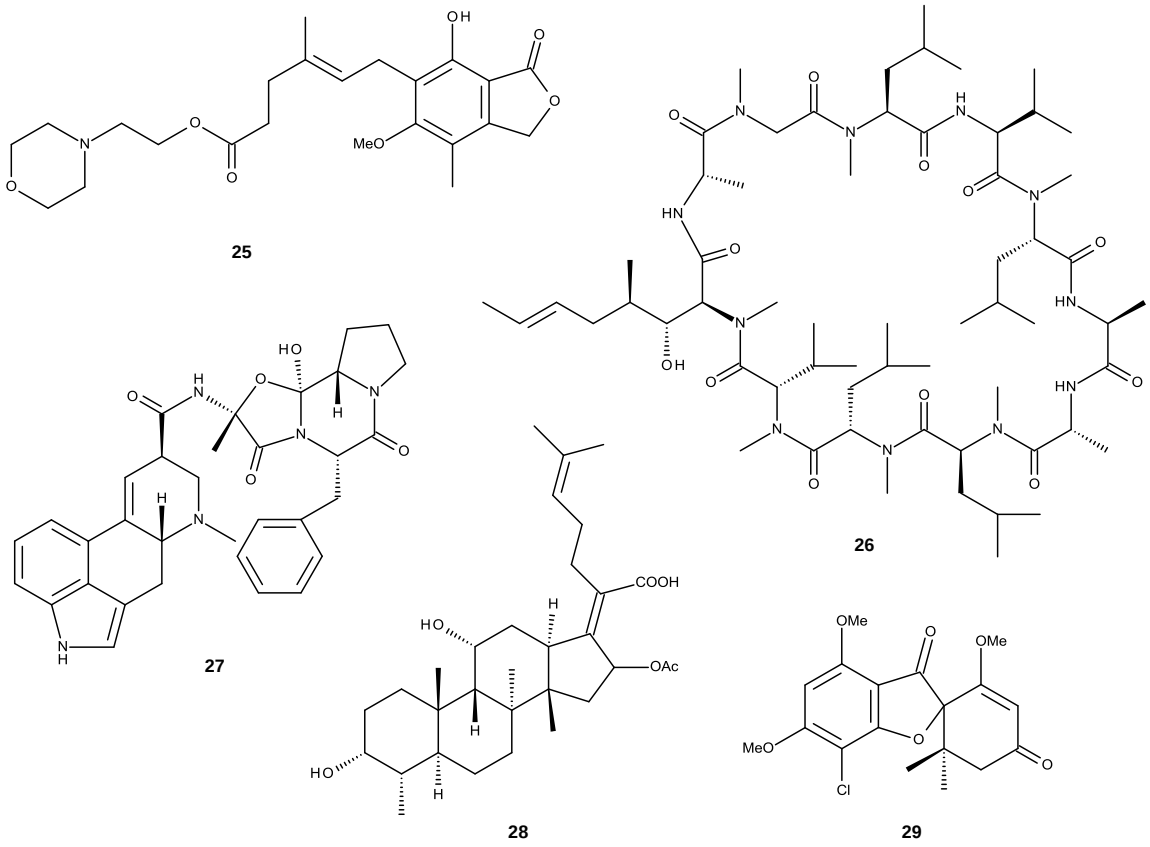

Figure 9. Examples of fungal-derived drugs currently used in therapeutics.

The early years of drug discovery from microfungi revolutionized medicine, with metabolites mainly isolated from soil samples, however the reduced hit-rate of novel compounds led to the study of alternative sources, mainly from marine habitats (Bugni and Ireland, 2004; Rateb and Ebel., 2011; Saleem *et al*., 2007)

1.4.1. Definition of Marine Fungi and Taxonomy

The origin of marine fungal strains has been the subject of controversy, limiting the definition of "*marine fungi*". According to Kohlmeyer "*classic*" definition, fungi growing in the sea can be grouped into obligate and facultative marine fungi. "*Obligate marine fungi*" are those "*that grow and sporulate exclusively in a marine or estuarine habitat*" while "*facultative marine fungi*" are defined as "*fungi from freshwater or terrestrial areas also able to grow in the natural marine environment*". Additionally, based on the germination ability, it has been suggested that indigenous marine species should be separated from non-indigenous species, often referred to as "*contaminants*" or "*transients*", *i.e.* terrestrial or freshwater species that are dormant in marine habitats (Kohlmeyer and Kohlmeyer, 1979).

Oceans are the source of an amazing biological diversity, regarding to marine fungi, with various estimates being proposed for the number of species, depending on whether the taxa are obligate or facultative. The final estimated number points to 10 000 species of marine fungi, 537 already described as obligate marine fungi (Jones, 2011).

Literature surveys showed that the most deeply studied marine fungal strains belong to genera that are ubiquitous in the terrestrial environment such as *Aspergillus*, *Penicillium*, *Cladosporium*, *Phoma* and *Fusarium*, being *Aspergillus* genus the main contributor as source of bioactive secondary metabolites from marine fungi (Lee *et al*., 2013). Although most metabolites from marine fungi are closely related to metabolites from their terrestrial counterparts, there are some unique examples indicating that marine strains may possess biosynthetic capabilities which differ in some aspects from those of terrestrial fungi (Bianabi and Laatsch, 1998). Lack of reports and the fact that many obligate marine fungi species are slow-growing and therefore, not convenient for standard chemical and biological screening methods, leads to a limited contribution to the overall number

of metabolites reported (Bugni and Ireland, 2004; Rateb and Ebel, 2011; Saleem *et al*., 2007).

1.4.2. Distribution of Marine-Derived Fungi and Chemical Studies

Marine fungi are known to produce structurally unique secondary metabolites due to the adaptation to a very distinct set of environmental pressures from marine environment (Bhadury *et al*., 2006,). Mechanisms of fungal antagonism and defense often include the production of biologically active metabolites by one species that exert effects on potential competitors and/or predators, being often hypothesized that some of their metabolic capabilities may be influenced by selection pressures exerted by other organisms (Gloer, 1995).

However, only recently marine-derived fungi have received attention from Natural Products chemists, and until the 1990s studies reporting chemistry from marine fungi were rare, with only fifteen metabolites being discovered until 1992 (Fenical and Jensen, 1993). First report of a bioactive marine fungal metabolite dates back to the 1940s with the identification of cephalosporin C (**30**) (Figure 10) from *Acremonium chrysogenum*, and siccayne (**31**) (Figure 10) was most likely the first antibiotic reported from an obligate marine fungus *Halocyphina villosa* in 1981 (Kupka *et al*., 1981), although it was known to be produced by the terrestrial mitosporic fungus *Helminthosporium siccans* (Ishibashi *et al*., 1968).

Since the beginning of the 1990s, a sharp and exponential increase in the number of reported structures from marine-derived fungi occurred, and this trend continues nowadays, supposedly far from reaching its climax.

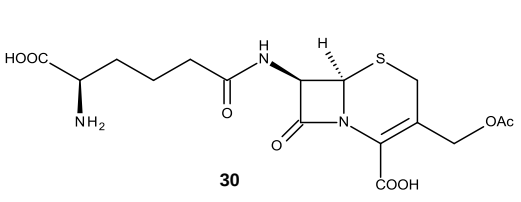

30

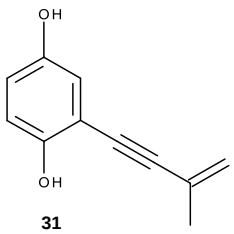

31

Figure 10. The structures of cephalosporin C (**30**) and siccayne (**31**).

Three main review papers covering the reports since the beginning until mid-2010 allow a general overview on the potential of marine fungi as a source of new bioactive compounds (Bugni and Ireland, 2004; Rateb and Ebel, 2011; Saleem *et al*., 2007). The general overview from Saleem *et al*. (2007) covering the period 2000-2005, clearly lacks a large number of reported metabolites, thus not being considered for statistical purposes. According to Bugni and Ireland (2004), from the beginning until 2002, only 272 new structures have been reported, while in 2009 alone more than two thirds of this figure was reached, being predicted that the total number of new natural products from marine fungi was superior to 1000 by the mid-2010 (Figure 11) (Rateb and Ebel, 2011). Algae and sponges are the top-ranking sources of marine fungal diversity, expressed in the number of new structures reported, while corals account for only 3% of the total compounds in literature (Figure 12).

Despite the notable increase in isolates from sediments, especially from the deep sea, almost two thirds of all new compounds derived from isolates from living matter, stating the enormous potential of symbiotic fungal consortia as an exciting target for drug discovery (Rateb and Ebel, 2011).

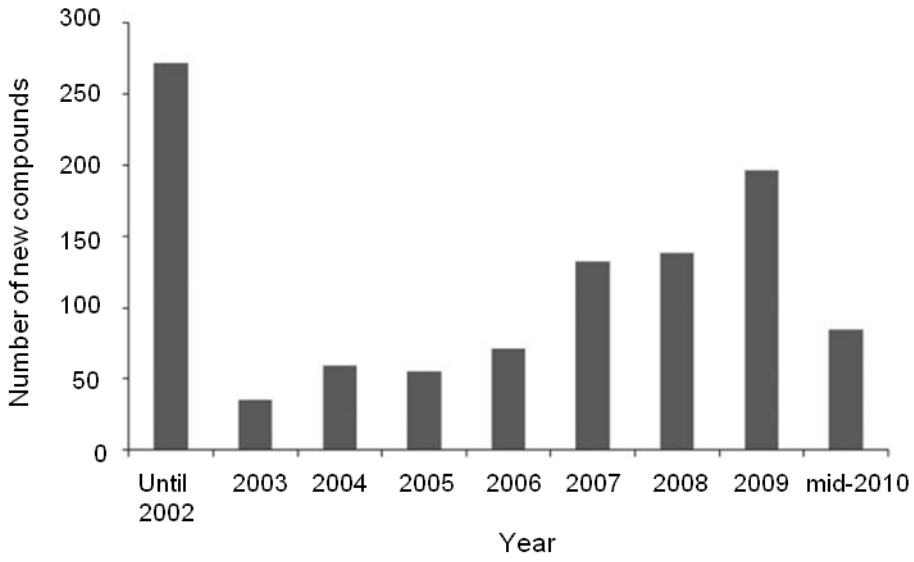

Figure 11. New compounds from marine-derived fungi, according to year of publication (Rateb and Ebel, 2011).

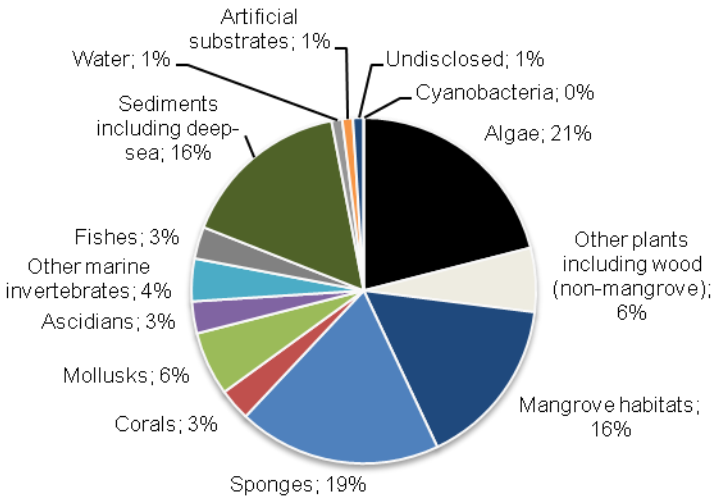

Figure 12. New compounds from marine-derived fungi until mid-2010, divided by sources of the fungal strains (Rateb and Ebel, 2011).

1.4.3. Marine Sponge-Associated Fungi – A Promising Source of Bioactive Secondary Metabolites

Over the past years, marine invertebrates mainly sponges, became the dominant source of novel bioactive metabolites (Hu *et al*., 2011). When compared to other marine invertebrates, the phylum Porifera seems to possess a wide range of biosynthetic capabilities, being the focus of much recent interest due to the formation of close associations with a wide variety of microorganisms, often correlated with the richness of biologically active secondary metabolites (Taylor *et al*., 2007; Wang *et al*., 2013).

Marine sponges are hosts for a large community of microorganisms, including bacteria and fungi, which can comprise as much as 40% of the sponge tissue volume, allowing nutrient acquisition, stabilization of sponge skeleton, processing of metabolic waste and, secondary metabolite production (Taylor *et al*., 2007; Thomas *et al*., 2010). Soft-bodied organisms like sponges, lack obvious structural defense mechanisms, and thus rely on chemical defense by production of secondary metabolites, often from associated microflora (Debbab *et al*., 2012; Taylor *et al*., 2007; Wang *et al*., 2013). As an example, *Oscillatoria spongeliae*, a cyanobacterial symbiont of *Dysidea herbacea*, is proven to be the producer of

antimicrobial polybrominated biphenyl ethers which might keep the sponge free of other bacteria (Unson *et al*., 1994).

Marine sponges have been demonstrated to represent one of the richest sources of fungal diversity. Several cultivation-based studies with marine sponges have shown a vast biological diversity, yielding the greatest taxonomic diversity in comparison with other marine sources (Figure 13) (Bugni and Ireland, 2004).

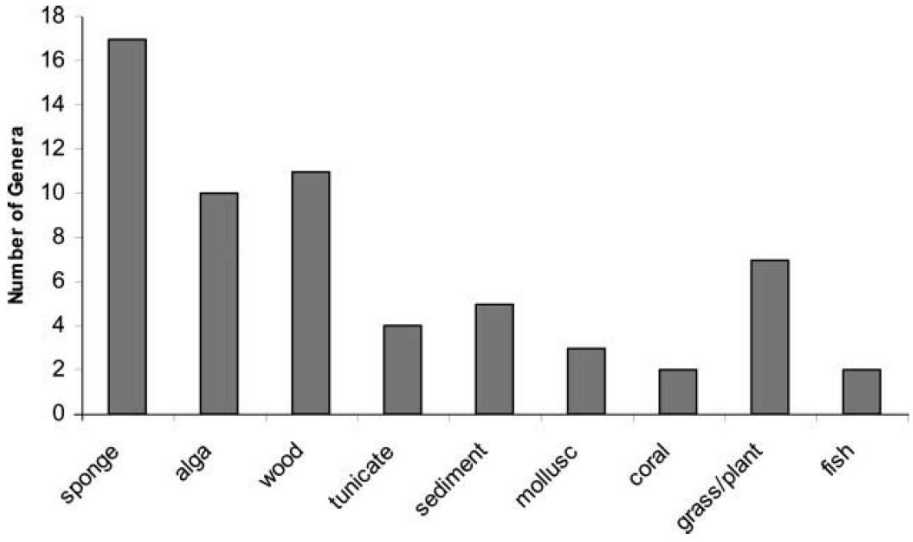

Figure 13. The number of distinct fungal genera based on the marine source (Bugni and Ireland, 2004).

For some given species of sponges, analogously to sponge-associated bacteria, some of the marine-derived strains appear to be unique and at least partially sponge specific and fairly stable in both space and time (Hentschel *et al*., 2002; Taylor *et al*., 2007). However, opposite to bacteria, it seems that many of the isolated fungi from sponges are of suspected terrestrial origin, due to the similarity to typical terrestrial strains. Interestingly of 681 fungal strains isolated from sixteen sponges worldwide, most belonged to *Aspergillus* and *Penicillium* genera, ubiquitous in terrestrial habitats (Höller *et al*., 2000).

The isolation of several metabolites from terrestrial microorganisms originally reported from marine sponges, also supports and provides experimental evidence to this hypothesis, however unlike bacteria, so far there is no report on

fungi as source of any natural product previously ascribed to a marine sponge (König *et al*., 2006; Thomas *et al*., 2010).

A plausible and widely accepted explanation for the fact that many of the fungi isolated from sponges belong to genera ubiquitous from terrestrial habitats, is that fungal spores may be washed into the sea and sequestered by sponges through filter feeding and retained in the inhalant canals. Furthermore, so far there is no evidence indicating that fungi actively grow inside sponges suggesting that their presence is in fact limited to spores. However, many of the compounds reported from marine isolates of the genera *Aspergillus* or *Penicilium* are often remarkably different from those of terrestrial counterparts suggesting that at least, on a biosynthetic level, many sponge-associated fungi are distinguished from their terrestrial analogues (Proksch *et al*., 2010).

1.4.4. Biologically Active Metabolites from Marine Sponge-Associated Fungi in Preclinical Development

Despite the absence of marine fungal metabolites in the current marine clinical pharmaceutical pipeline, marine sponge-associated fungi are known for being an excellent reservoir of bioactive metabolites with potent activities covering a wide range of biological functions (Bugni and Ireland, 2004; Rateb and Ebel, 2011; Saleem *et al*., 2007). The previously referred phenylahistidin (**23**) (Figure 7), the lead structure of plinabulin (**22**) (Figure 7) whose phase II clinical trials have been recently completed, is the most important representative of marine fungal-derived natural products so far.

The first metabolite reported from a sponge-associated fungus is the polyketide trichoharzin (**32**) (Figure 14), which was isolated from an imperfect fungus *Trichoderma harzianum* Rifai isolated from a marine sponge *Mycale cecilia* (Kobayashi *et al*., 1993). Interestingly, the trichoharzin analog, deoxynortrichoharzin (**33**) (Figure14) was also obtained from the sponge derived-fungus *Paecilomyces* cf. *javanica* (Rahbaek *et al.,* 1998).

Sorbicillactone A (**34**) (Figure 14), an alkaloid possessing a unique bicyclic lactone structure isolated from the sponge *Ircinia fasciculata*-associated fungus *Penicillium chrysogenum*, is known to have antiviral and neuroprotective

properties (Bringmann *et al*., 2005; 2007). Owing to its highly selective cytostatic activity against murine leukemic lymphoblasts, this compound has been recently qualified for human trials. The heterodimer asperazine (**35**), isolated from the saltwater culture of the Caribbean *Hyrtios* sponge-associated *Aspergillus niger*, also displayed significant differential cytotoxicity against a mouse leukemia cell line (L1210) (Varoglu *et al*., 1997).

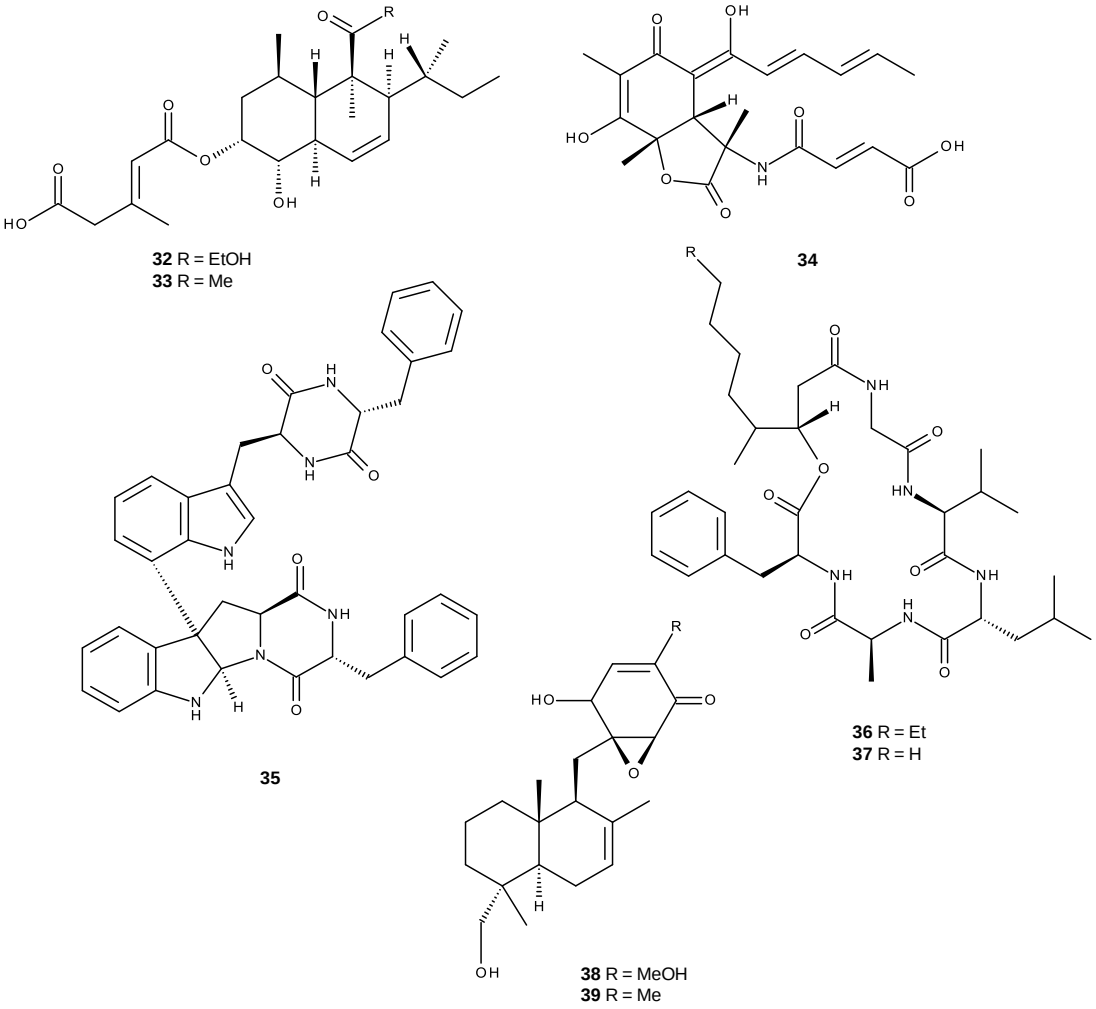

Figure 14. Examples of marine sponge-derived fungi compounds with potential for preclinical development.

Moreover, scopularides A (**36**) and B (**37**) (Figure 14), natural cyclodepsipeptides isolated from the marine sponge-derived fungus *Scopulariopsis brevicaulis* were recently patented due to their potent inhibitory

activity against several tumor cell lines, including pancreatic and colon tumor cell lines (Yu *et al*., 2008). The fungus *Paraconiothyrium* cf *sporulosum*, isolated from the Caribbean marine sponge *Ectyplasia perox*, was found to produce a new class of sesquiterpene epoxycyclohexenones with an unprecedented distinctive substitution and oxidation patters (Mohamed *et al*., 2009). Strikingly, epoxyphomalin A (**38**) (Figure 14) displayed not only remarkable cytotoxicity at nanomolar concentrations, but also an intriguing activity profile in COMPARE analyses that did not correlate with those of reference anticancer agents, suggesting a different mode of action from that of the reference compounds. Furthermore, it was also found that incubation of purified human 20S proteasome with epoxyphomalins A (**38**) and B (**39**) (Figure 14) led to a dose-dependent inhibition of chymotrypsin-, caspase-, and trypsin-like proteasome activities, indicating a potent inhibition of 20S proteasome. Consequently, epoxyphomalins could be considered as new promising chemotherapeutic alternatives for the treatment of several tumors, due to their capacity to inhibit the proteasome (Mohamed *et al*., 2010).

There is a vast number of bioactive marine sponge-derived fungal metabolites with a wide set of bioactivities, and many of them are potential candidates for preclinical development (Blunt *et al*., 2013; Proksch *et* al., 2010; Rateb and Ebel, 2011; Thomas *et al*., 2010; Xiong *et al*., 2013).

Thus, sponge-fungal association is a potential chemical and ecological phenomenon which provides sustainable resource for developing novel pharmaceutical leads for a promising and rational target in drug discovery.

CHAPTER II

CHEMISTRY OF THE GENERA *EMERICELLA*, *EUROTIUM* AND *NEOSARTORYA*

Four marine-derived fungi selected for chemical investigation in this thesis belong to three distinct genera, namely *Emericella* (*Emericella variecolor* KUFC 7092), *Eurotium* (*Eurotium cristatum* KUFC 7356) and *Neosartorya* (*Neosartorya paulistensis* KUFC 7897 and *N. laciniosa* KUFC 7896).

The four fungal species are the sexual counterparts of the genus *Aspergillus*, a relevant and efficient saprophytic genus widely found in diverse environments, including Oceans. *Aspergillus* genus consists of several hundred highly aerobic mold species and has been the target of several studies mainly due to several human pathogenic species responsible for infections leading to a high rate of morbidity and mortality, but also due to the relevant economic impact, mainly in developing countries, associated with the destructive effect in agriculture. On the other hand, this genus includes several species widely used in the food and beverage industry, being classified as a biotechnological "*cell factory*" (Gibbons and Rokas, 2013). Additionally, the genus *Aspergillus* was the source of several drugs currently used in therapeutics as referred previously, having revolutionized Medicine, yielding several blockbuster drugs and drug leads of enormous potential (Aly *et al*., 2011).

The biotechnological potential of *Aspergillus* relies not only on economic relevance of microbial fermentations, but also on the genomic diversity leading to the production of several bioactive metabolites, classifying the genus as an attractive and valuable source for drug discovery, which is the main focus of the present study (Lee *et al*., 2013). Also the fact that ascomycetous fungi can be grown easily in culture and their teleomorphic states induced in the laboratory, led to the selection of these genera as a target for chemical and biological studies.

2.1. An Overview of Secondary Metabolites

Contrary to *Aspergillus* genus, only a few species of teleomorphs have been investigated for their secondary metabolites and associated biological activities. However, the number of bioactive compounds reported so far is exponentially increasing, both the previously reported from other species and novel chemical structures. Due to the highly specific profiles of secondary metabolites, especially from *Aspergillus* and *Penicillium* teleomorphs, it is not

surprising the isolation of several common extrolites produced by a limited number of fungal species from the same genus.

The distinct morphological features from fungal sexual stages allowed a dual nomenclature permitting separate names for anamorphs of fungi with a pleomorphic life-cycle, causing several equivoques regarding the correct and unequivocal taxonomic classification of several species. The increased number of mycologists recognizing the urgent need of a transition to a single-name nomenclatural system for fungi, resulted in the preparation of "*Amsterdam Declaration on Fungal Nomenclature*", agreed under the auspices of the International Commission on the Taxonomy of Fungi (ICTF) during the symposium "*One Fungus = One Name*" held in Amsterdam in April 2011 (Hawksworth *et al*., 2011a; 2011b). The discontinuance of the dual nomenclature system was later approved and adopted in the 18th International Botanical Congress in Melbourne in July 2011, and the Vienna edition of the "*International Code of Botanical Nomenclature*" has been replaced by the "*The International Code of Nomenclature for algae, fungi, and plants (The Melbourne Code)*" published in December 2012. According to the "*Melbourne Code*", after 1 January 2013 one fungus can only have one name (Hawksworth, 2011a; 2011b; McNeill *et al*., 2011).

The following literature review will focus strictly on the teleomorphs from the genera *Emericella*, *Eurotium* and *Neosartorya*, following the taxonomic classification of the species adopted by the authors by the date of the publication, not necessarily adopting "*Melbourne Code*" recent recommendations. Despite the chemotaxonomic importance of secondary metabolites, the aim of this review is not to give an extensive and exhaustive report of all the secondary metabolites isolated from the referred genera. Instead, an overview on novel secondary metabolites and their associated bioactivities will be presented as an insight on the potential of the selected species for the isolation of novel bioactive secondary metabolites.

2.2. The Genus *Emericella*

The genus *Emericella* was described by Berkeley (1857) based on *E. variecolor* Berk. & Broome, and comprises thirty-four species, corresponding to the

sexual state of *Aspergillus* species, notably the *A. nidulans* group among others. The genus *Emericella* comprises a well-studied group of secondary metabolite-rich fungi that are of concern in food and feed processing and storage, because of many sterigmatocystin producing species. Additionally, the genus was proved to be a prolific source of relevant bioactive metabolites with *E. nidulans* being the source of echinocandin B (**40**) (Figure 15), the starting molecule for the semi-synthetic antifungal anidulafungin (Eraxistm®) (**41**) (Figure 15) approved for the treatment of candidiasis of the esophagus and disseminated candidiasis, intra-abdominal and peritonitis (Hof and Dietz, 2009; Martindale, 2012).

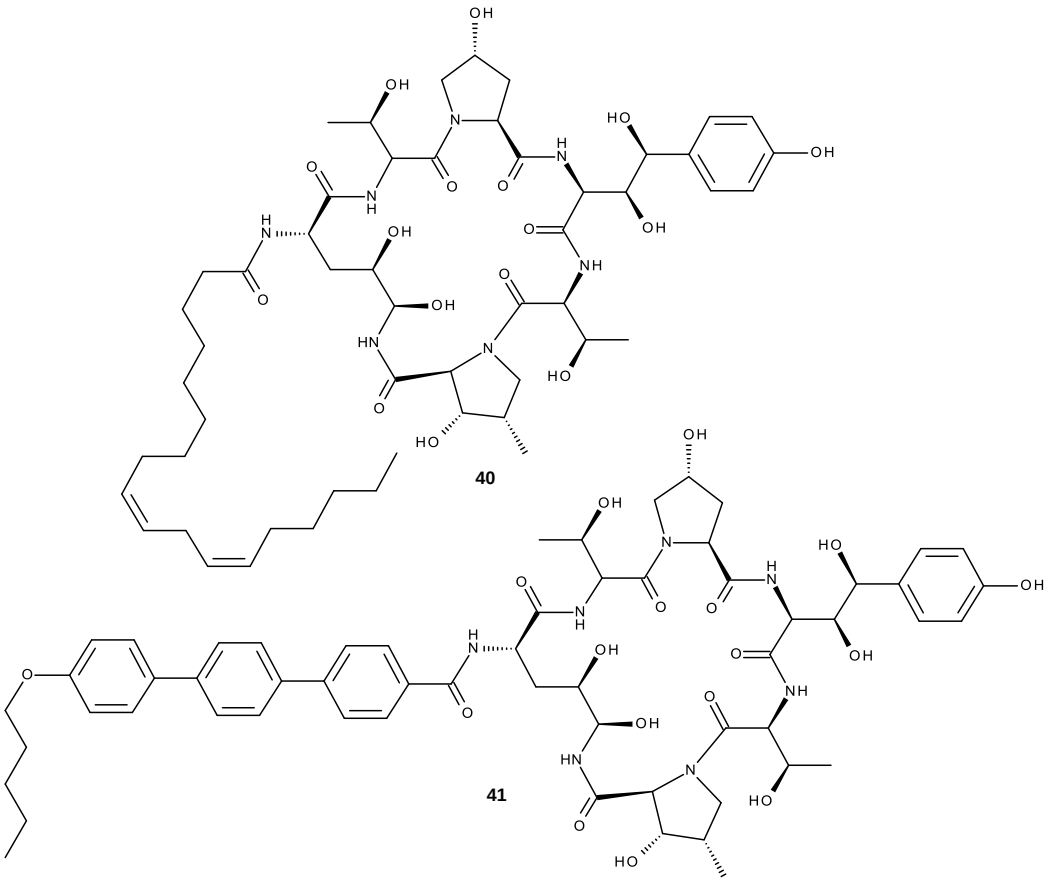

Figure 15. Structures of echinocandin B (**40**) and semi-synthetic derivative anidulafungin (**41**)**.**

2.2.1. *Emericella aurantio-brunnea*

Bioassay guided fractionation of the bioactive extract of the. *E. aurantio-brunnea* strain yielded four new variecolin analogues, emericolins A-D (**42-45**) (Figure 16). Despite the extract activity competing with macrophage inflammatory protein (MIP)-1α for binding to human CCR5, none of the variecolin analogues displayed activity in the CCR5 assay (Yoganathan *et al*., 2004). Two additional sesterterpenes related to variecolin, variecoacetals A and B (**46, 47**) were reported by Fujimoto *et al*. (2000) as well as the new sesquiterpenetriol diester emeremophiline (**48**) (Figure 16), from the EtOAc extract of *E. aurantio-brunnea* IFM42008. Both variecoacetals A and B (**46, 47**), as well as emeromophiline (**48**) displayed moderate immunosuppressive activity.

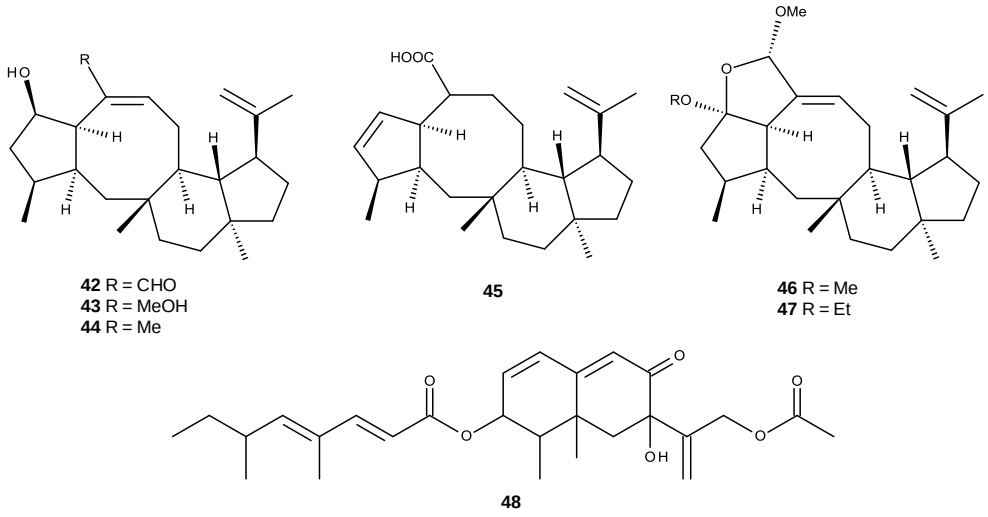

Figure 16. New constituents of *E. aurantio-brunnea*.

2.2.2. *Emericella desertorum*

Three new bicoumarins, desertorins A-C (**49-51**) (Figure 17) were isolated from the chloroform extract of the mycelia of *E. desertorum* strain CBS 653.73, collected from desert soils in Egypt (Nozawa *et al*., 1987a). Later, the two new indoloditerpenes emindoles DA (**52**) and DB (**53**) (Figure 17) were also isolated from the same strain (Nozawa *et al*., 1988).

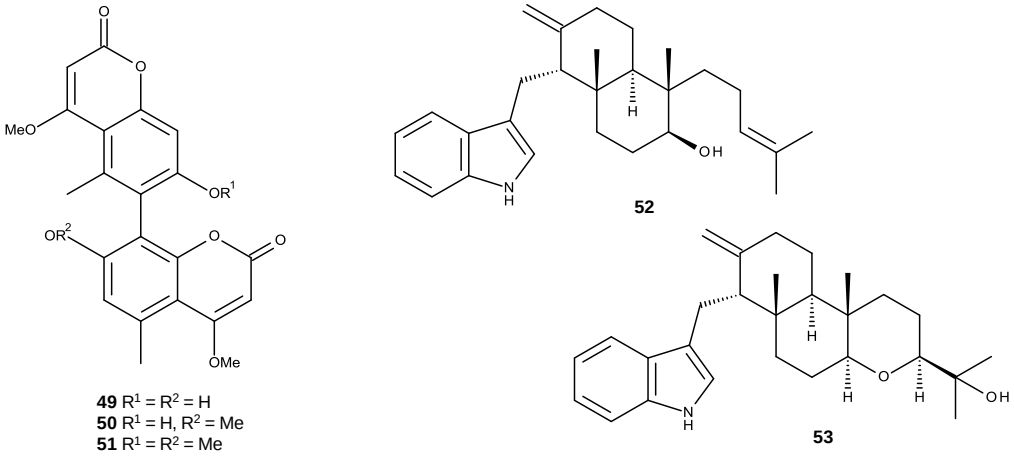

Figure 17. New constituents of *E. desertorum* strain CBS 653.73.

2.2.3. *Emericella falconensis*

Azaphilone derivatives falconensins A-N (**54-67**) and a new azaphilone, monomethyldihydromitorubrin (**68**) (Figure 18), were reported from *E. falconensis* strain NHL 2999 isolated from Venezuelan soil (Itabashi *et al*., 1992; 1993; 1996; Ogasawara and Kawai, 1998). Despite the lack of antibacterial activity, falconensins A-C (**54-56**) displayed an inhibitory effect on 12-O-tetradecanoylphorbol 13-acetate-induced inflammatory ear edema in mice (Yasuhara *et al*., 1994).

From the same strain, the two new cyclopentenone pigments falconensones A (**69**) and B (**70**) (Figure 18) were later isolated (Ogasawara *et al*., 1997). Falconensone A (**69**) and its synthetic derivatives caused inhibition of cell growth and induction of differentiation in human promyelocytic leukemia cell line HL60, suggesting eventual clinical potential as an antiproliferative agent for leukemia treatment (Takahashi *et al*., 1998). Additionally, falconensone A (**69**) and its derivatives also appear to be effective antioxidants (Takahashi *et al*., 2000).

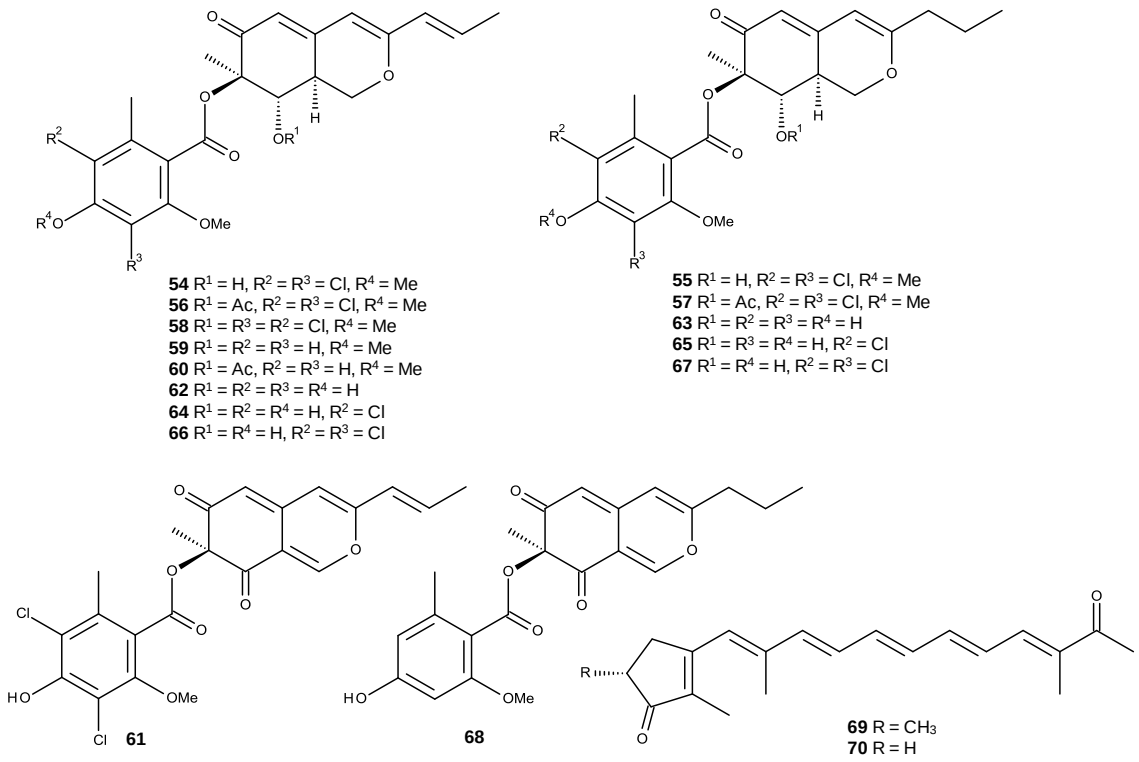

Figure 18. New constituents of *E. falconensis* strain NHL 2999.

2.2.4. *Emericella foveolata*

A new member of the epitetrathiodiketopiperazine family, secoemestrin C (**71**) (Figure 19), related to the macrocyclic antifungal dithiodiketopiperazine emestrin (**97**) (Figure 25) previously isolated from other *Emericella* species, was isolated from *E. foveolata* strain IFO 30559 (Ooike *et al*., 1997).

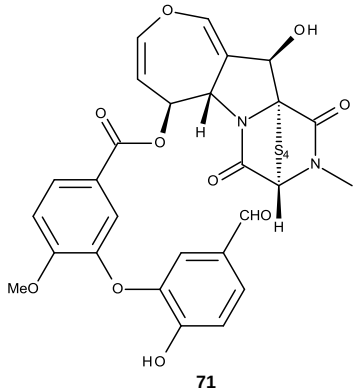

Figure 19. Structure of secoemestrin C (**71**)**.**

2.2.5. *Emericella heterothallica*

From the chloroform extract of the mycelia of the fungus *E. heterothallica* strain ATCC 16824, the pyrazinone emeheterone (**72**) along with a new thiodiketopiperazine emethacin A (**73**) (Figure 20) were isolated (Kawahara *et al*., 1988a; 1989a). Later, four novel epipolythiodiketopiperazines, emethallicins A-D (**74-77**) (Figure 20), were reported from the same strain as well as from the additional ATCC 16847 strain. Emethallicins A-D (**74-77**) displayed potent inhibitory activities upon compound 48/80-induced histamine release from mast cells, and were also shown to be potent 5-lipoxygenase inhibitors (Kawahara *et al*., 1989b; 1990).

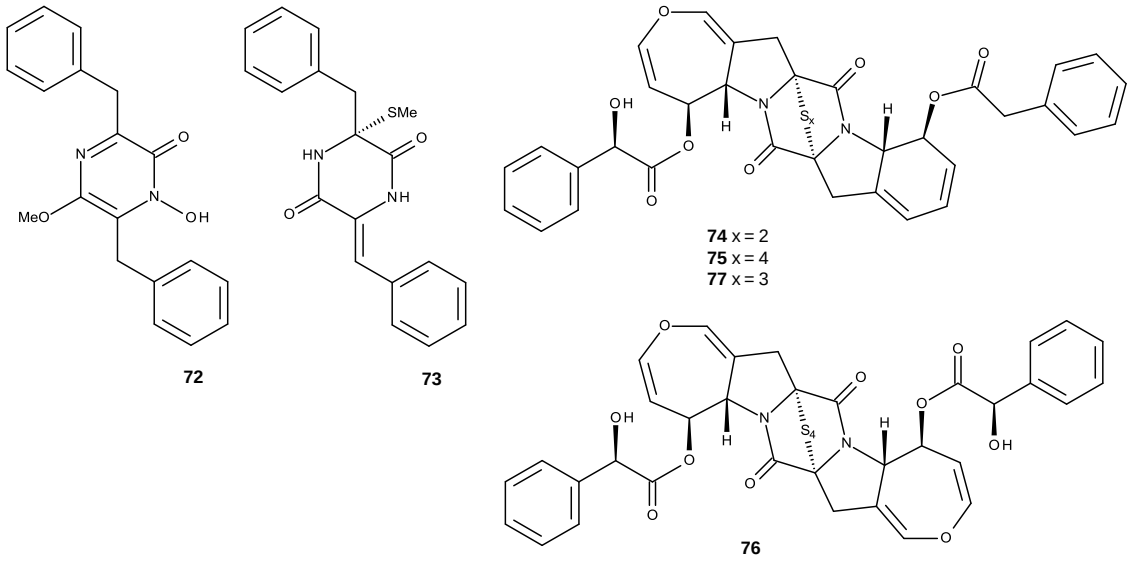

Figure 20. New constituents of *E. heterothallica*.

2.2.6. *Emericella nidulans*

The marine-derived fungus *E. nidulans* var. *acristata* which was isolated as an endophyte from a green alga collected around Sardinia, was found to produce two new arugosins G (**78**) and H (**79**) (Figure 21). Contrary to additional arugosins, also isolated from the same extract, arugosins G (**78**) and H (**79**) did not exhibit antitumor activity in a wide panel of 36 human tumor cell lines (Kralj *et ai*., 2006).

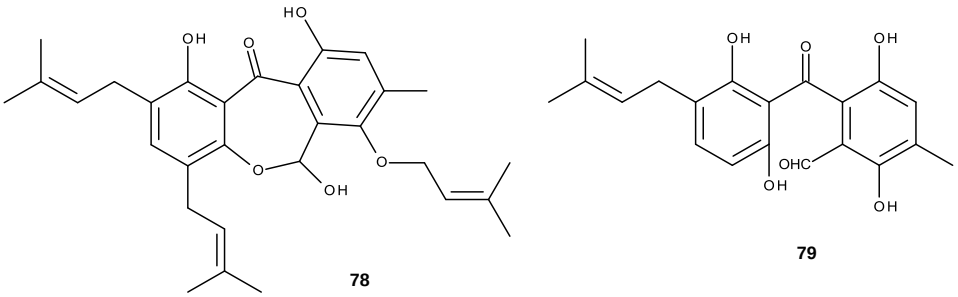

Figure 21. Structures of arugosins G (**78**) and H (**79**).

2.2.7. *Emericella purpurea*

Two new sesterterpenes variecolol (**80**) and variecolactone (**81**) (Figure 22) were identified as metabolites of the fungus *E. purpurea* strain IFO 30849 (Takahashi *et al*., 1999). The same extract yielded three new yellow pigments epurpurins A-C (**82-84**) and three new indoloditerpenes emindole PA, PB and PC (**85-87**) (Figure 22) (Hosoe *et al*., 2006; Takahashi *et al*., 1996).

2.2.8. *Emericella quadrilineata*

In a screening study of immunomodulatory fungal constituents, Fujimoto *et al.* (2006) reported the isolation of the new xanthone (4*S*,4a*R*,9a*R*)-4a-carbomethoxy-1,4,4a,9a-tetrahydro-4,8-dihydroxy-6-methylxanthone (**88**) and the new furanone 9-hydroxymicroperfuranone (**89**) (Figure 23), from the EtOAc extract of *E. quadrilineata* IFM42027. Despite the immunosuppressive activity of the extract, none of the new compounds were showed to be active (Fujimoto *et al*., 2006).

Recently, a new echinocandin analog, echinocandin E (**90**) (Figure 23) was identified from a strain of *E. quadrilineata*. Echinocandin E (**90**) was determined to be less potent (IC_{50} = 1.5 µm) against *Candida albicans* than echinocandin B (**40**) (Figure 15) (IC_{50} = 0.27 µm) (Cruz *et al*., 2012).

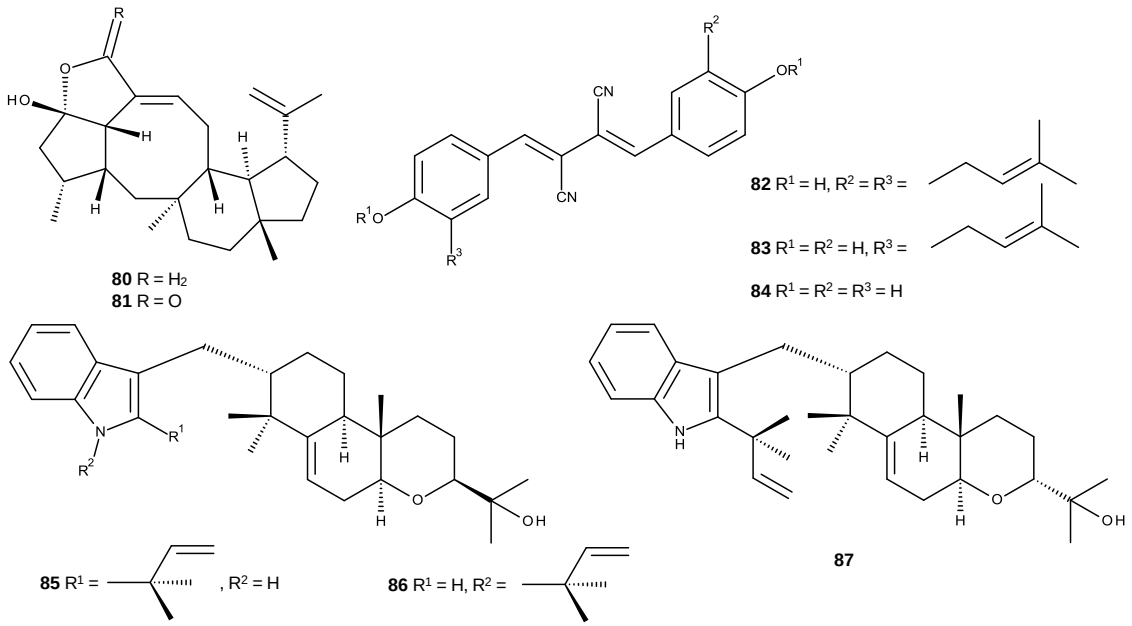

Figure 22. New constituents of *E. purpurea* strain IFO 30849.

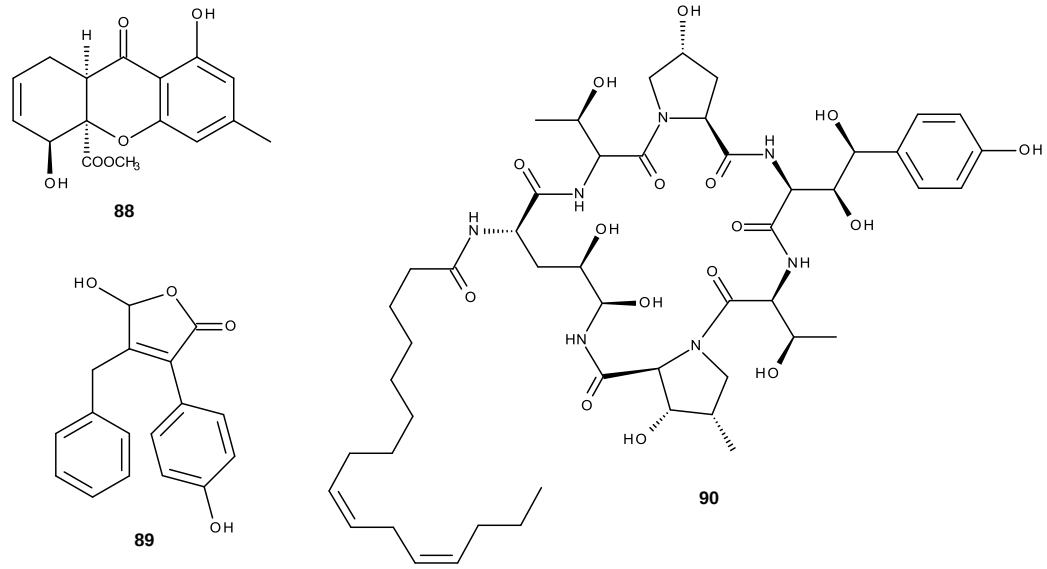

Figure 23. New constituents of *E. quadrilineata.*

2.2.9. *Emericella rugulosa*

New prenylated xanthones, reguloxanthones A-C (**91-93**), 14-methoxytajixanthone (**94**), and tajixanthone ethanoate (**95**) (Figure 24) were isolated from the fungus *E. rugulosa*, along with several known xanthones. Additionally, regulosone (**96**) (Figure 24) was also isolated from *E. rugulosa* and exhibited the *in vitro* antimalarial activity against *Plasmodium falciparum*, antimycobacterial activity, as well as strong cytotoxic activity against BC1, KB, and NCI-H187 cancer cell lines (Moosophon *et al*., 2009).

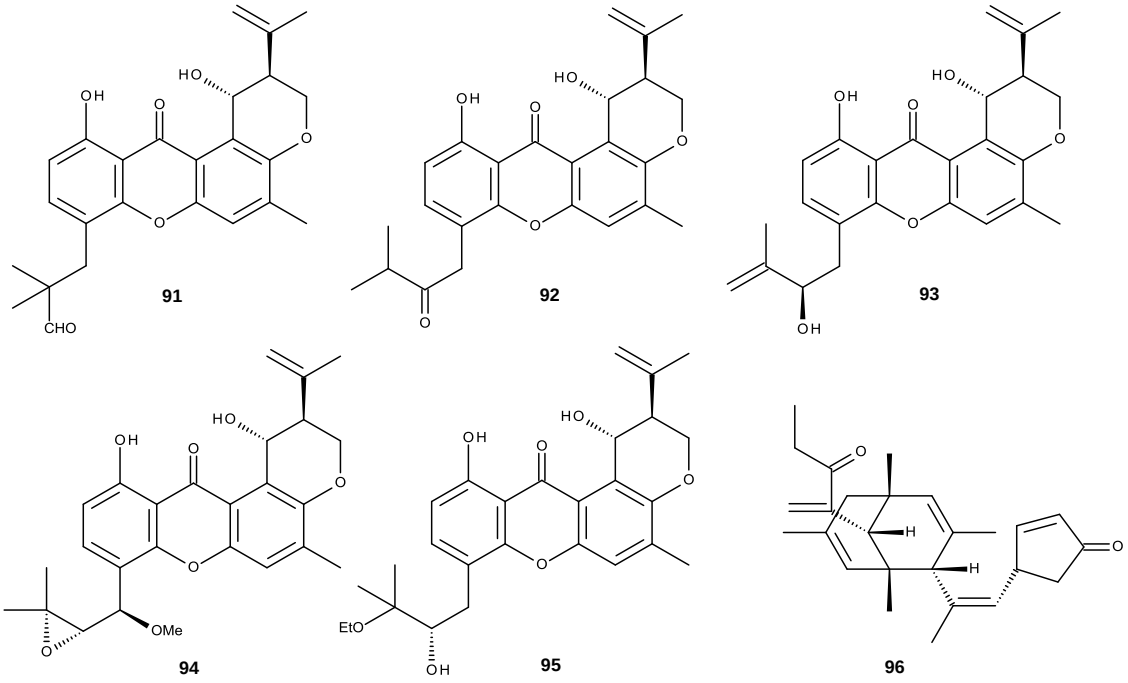

Figure 24. New constituents of *E. rugulosa*.

2.2.10. *Emericella striata*

Chemical analysis of *E. striata* strain 80-NE-22 resulted in the isolation of emestrin (**97**), emestrin B (**98**) and related dethiodiketopiperazine derivatives lacking polysulfide internal bond, namely aurantioemestrin (**99**) and dethiosecoemestrin (**100**) (Figure 25) (Kawahara *et al.,* 1986; Nozawa *et al*., 1987b; Seya *et al*., 1985; 1986a; 1986b).

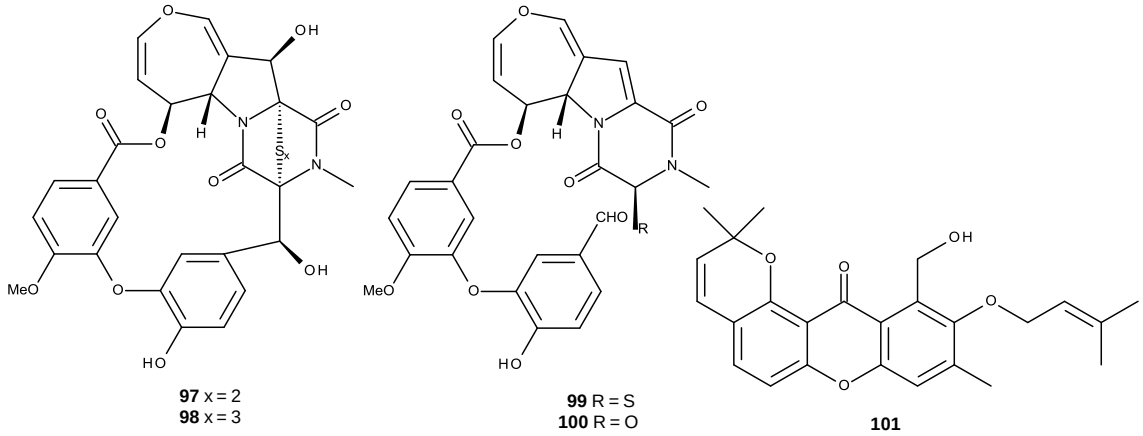

Figure 25. New constituents of *E. striata* strain 80-NE-22.

Both emestrin (**97**) and emestrin B (**98**) were found to possess antibacterial activity against *Escherichia coli* and *Bacillus subtilis*, while dethiosecoemestrin (**100**) was active against *E.coli* (Seya *et al.,* 1986b; Nozawa *et al*., 1987b). Additionally, emestrin (**97**) displayed also antifungal activity, inhibiting the growth of *Gibberella zeae* and *Penicillium expansum* (Seya *et al*., 1986a). Recently, emestrin (**97**) was also isolated from *E. nidulans* MFW39, isolated from marine ascidia, and was found to exhibit relevant cytotoxicity against T47D, HepG2, C28, and HeLa cell lines (Nursid *et al*., 2011). Also from *E. striata* strain 80-NE-22, the new xanthone cycloisoemericellin (**101**) was later reported (Figure 25) along with the known arugosins (Kawahara *et al*., 1988b).

2.2.11. *Emericella unguis*

E. unguis strain IFM 42017 was found to produce four new depsidones, emeguisins A-C (**102-104**) and 2-chlorounguinol (**105**), along with the new phthalide 3-ethyl-5,7-dihydroxy-3,6-dimethylphthalide (**106**) (Figure 26). Although the EtOAc extract of this fungus was found to have monoamine oxidase (MAO) inhibitory activity, the isolated depsidones displayed only a moderate activity. Additionally, emeguisin A (**102**) was found to inhibit the growth of *Bacillus subtilis* (Kawahara *et al*., 1988c; 1988d).

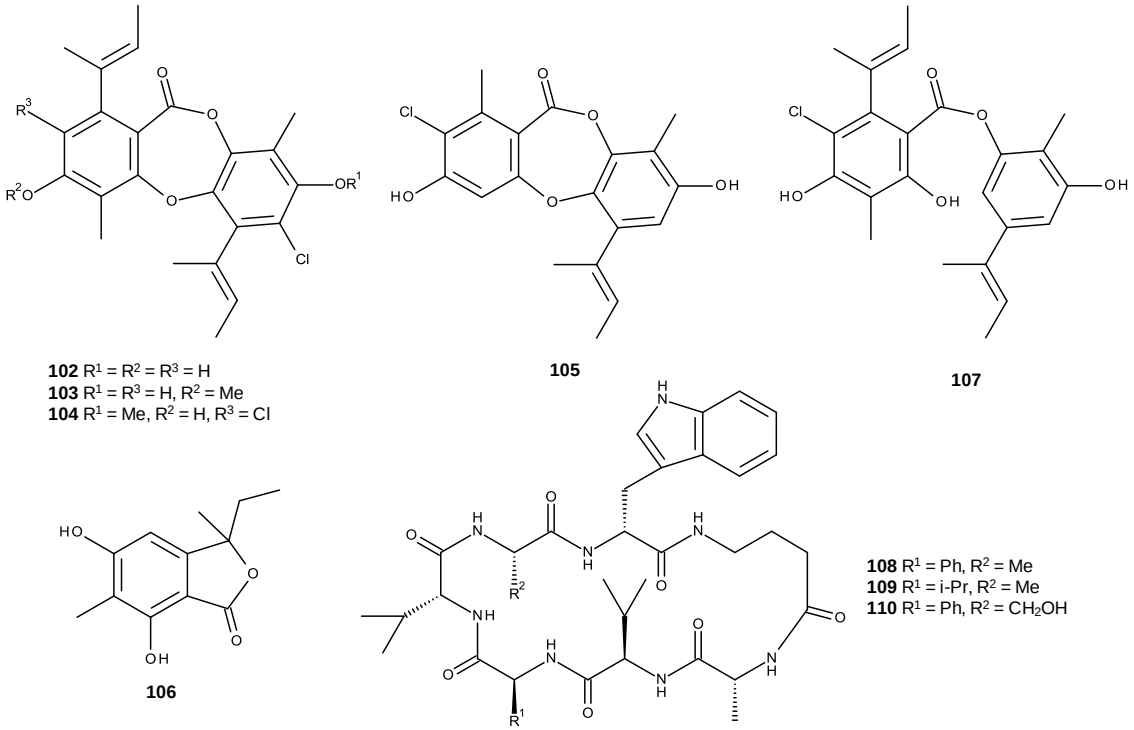

Figure 26. New constituents of *E. unguis*.

Later, the new emerguisins-related depside guisinol (**107**) (Figure 26) was reported from a marine isolate originated from the jellyfish *Stomolophus meleagris* collected in the Paria Bay, Venezuela, by Nielsen *et al*. (1999). Guisinol (**107**) exhibited antibacterial activity against *Staphylococcus aureus*. Unguisins A-C (**108-110**) (Figure 26), the first cyclic heptapeptides with GABA incorporated in the ring, were also isolated from the same extract. Unguisin A (**108**) and B (**109**) were found to exhibit moderate antibacterial activity against *S. aureus* and *Vibrio parahaemolyticus* (Malmström, 1999; Malmström *et al*., 2002a).

2.2.12. *E. variecolor*

E. variecolor, the perfect state of *Aspergillus variecolor* (syn. *A. stellatus*) is one of the most studied species from the genus *Emericella*. It was found to produce a variety of secondary metabolites, including prenylated xanthones, sesterterpenes and meroterpenoids.

Emervaridione (**111**) and varioxiranediol (**112**) (Figure 27) were isolated from the EtOAc extract of an endophytic *E. variecolor* (Liangsakul *et al*., 2011). The marine *E. variecolor* strain M75-2, isolated from a Caribbean sponge, was found to produce three new terrein derivatives, varitriol (**113**), varioxirane (**114**) and dihydroterrein (**115**), along with the new xanthone varixanthone (**116**) (Figure 27). Varitriol (**113**) was tested in the NCI 60-cell line *in vitro* panel, and was found to exhibit strong cytotoxic activity against several cancer cell lines, with remarkable potency toward renal cancer cell line RXF 393 (GI_{50} = 0.163 µM) and breast cancer cell line T-47D (GI_{50} = 0.210 µM). While varixanthone (**116**) displayed potent antimicrobial activity against *Escherichia coli*, *Proteus* sp. and *Bacillus subtilis*, with a minimal inhibitory concentration (MIC) value of 12.5 µg/mL (Malmström *et al*., 2002b).

Another marine sponge-derived strain isolated from the marine sponge *Haliclona valliculata* collected in Elba, Italy, yielded the new prenylated xanthone isoemericellin (**117**) and a new anthraquinone evariquinone (**118**) (Figure 27). Evariquinone (**118**) exhibited strong antiproliferative activity towards KB and NCI-H460 cells at a concentration of 3.16 µg/mL (Bringmann *et al*., 2003).

Two new sesterterpenes, 6-*epi*-ophiobolin G (**119**) and 6-*epi*-ophiobolin N (**120**) (Figure 27), along with six previously reported ophiobolins, were isolated by Wei *et al*. (2004) from the EtOAc extract of *E. variecolor* GF10 which was isolated from a marine sediment collected in Gokasyo Gulf, Japan. All ophiobolins, including 6-*epi*-ophiobolin G (**119**) and 6-*epi*-ophiobolin N (**120**) displayed cytotoxic activity against neuroblastoma cell line Neuro 2A (Wei *et al*., 2004). Later, a new polyketide, shimalactone A (**121**) (Figure 27) was discovered from the same extract, and was shown to induce neuritogenesis in neuroblastoma cell line Neuro 2A at 10 µg/mL (Wei *et al*., 2005). The toxic metabolite asteltoxine (**122**) (Figure 27) was isolated from the moldy rice artificially infected with *E. variecolor* NHL 2881 (Maebaxashi *et al*., 1983).

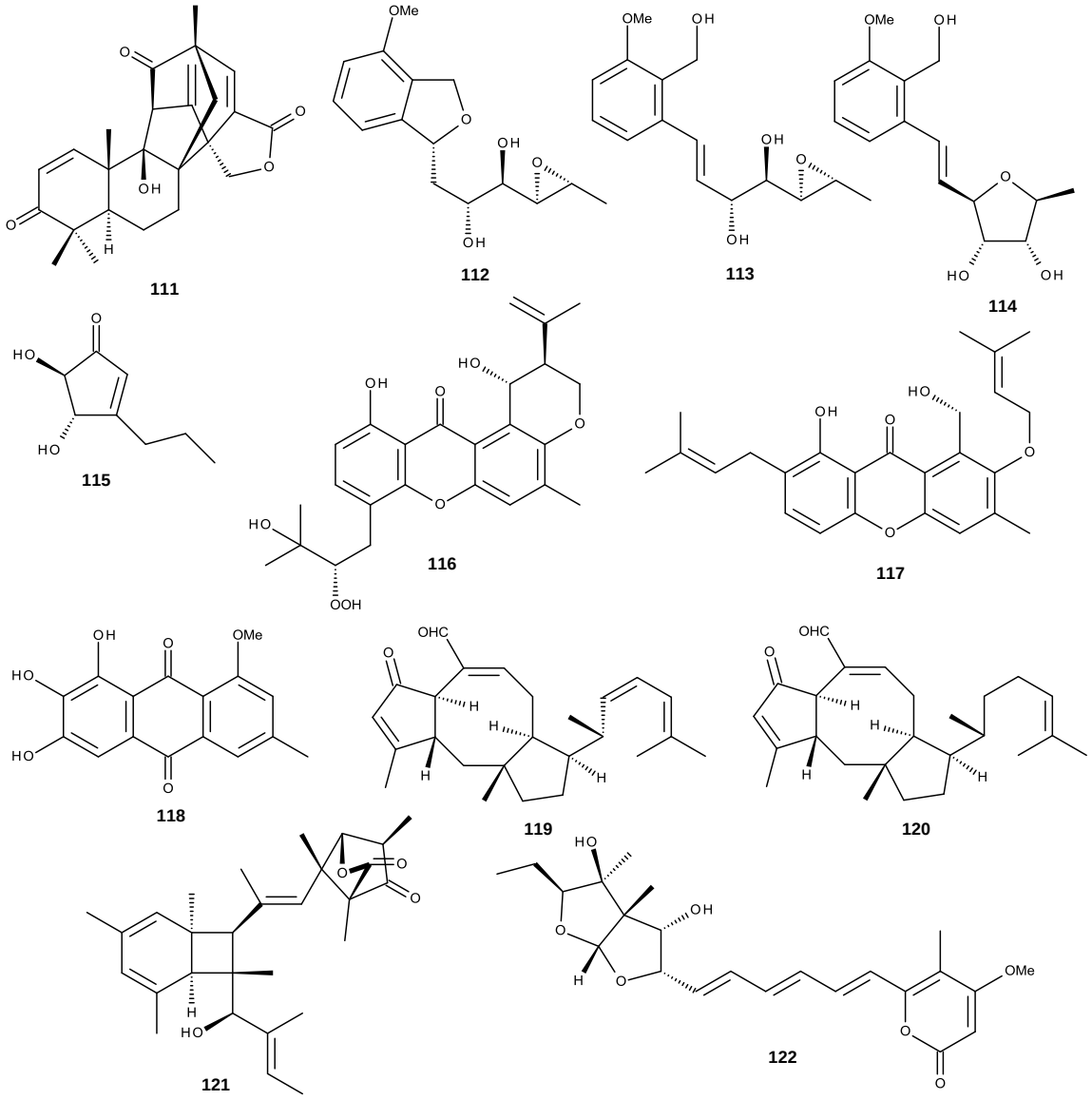

Figure 27. New constituents of *E. variecolor*.

2.2.13. Unspecified *Emericella* species

Bioassay guided-fractionation of the endophytic *Emericella* sp. HK-ZJ, isolated from the mangrove plant *Aegiceras corniculatum*, resulted in the discovery of six new isoindolone derivatives, emerimidines A (**123**) and B (**124**), and the meroterpenoids emeriphenolicins A-D (**125-128**) (Figure 28). Only emerimidines A (**123**) and B (**124**) showed moderate *in vitro* antiviral activity against H_1N_1, with IC_{50} values of 42.07 μg/mL and 62.05 μg/mL, respectively (Zhang *et al*., 2011).

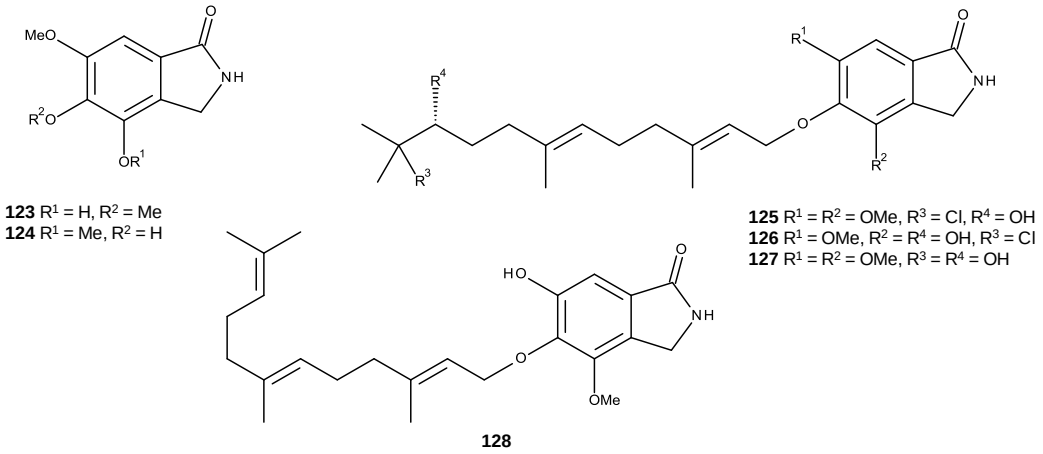

Figure 28. New constituents of *Emericella* sp. HK-ZJ.

Competing co-culture of the marine-derived fungus *Emericella* sp. (strain CNL-665) with the marine actinomycete *Salinispora arenicola*, yielded two new cyclic depsipeptides, emericellamides A (**129**) and B (**130**) (Figure 29), both of which displayed modest antibacterial activity against methicillin-resistant *Staphylococcus aureus* (MRSA) (Oh *et al*., 2007).

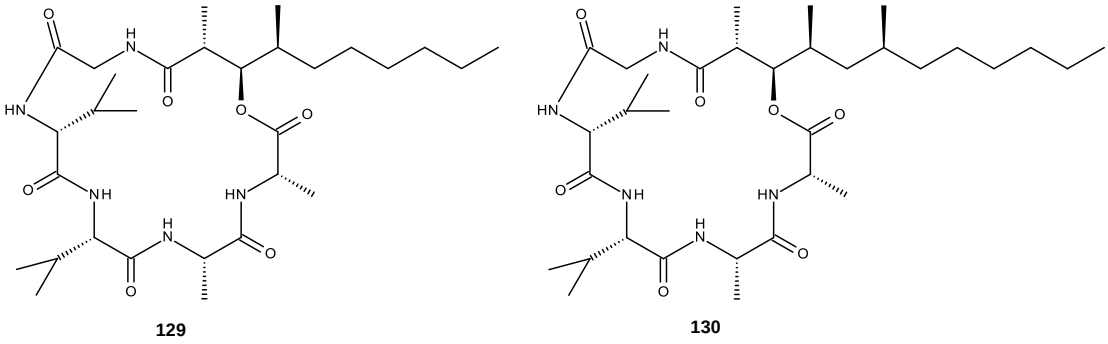

Figure 29. Structures of emericellamides A (**129**) and B (**130**).

Recently, Xu *et al*. (2013a) reported the isolation of the new epitetrathiodiketopiperazine secoemestrin D (**136**), along with five new sesterterpenoids with an unprecedented carbon skeleton, emericellenes A-E (**131-135**) (Figure 30), from the endophytic fungal strain *Emericella* sp. AST0036, isolated from a leaf of *Astragalus lentiginosus*. Secoemestrin D (**136**) exhibited strong cytotoxic activity against six cancer cell lines with apparent selectivity to

human glioma (SF-268) and metastatic breast adenocarcinoma (MDA-MB-231) cell lines.

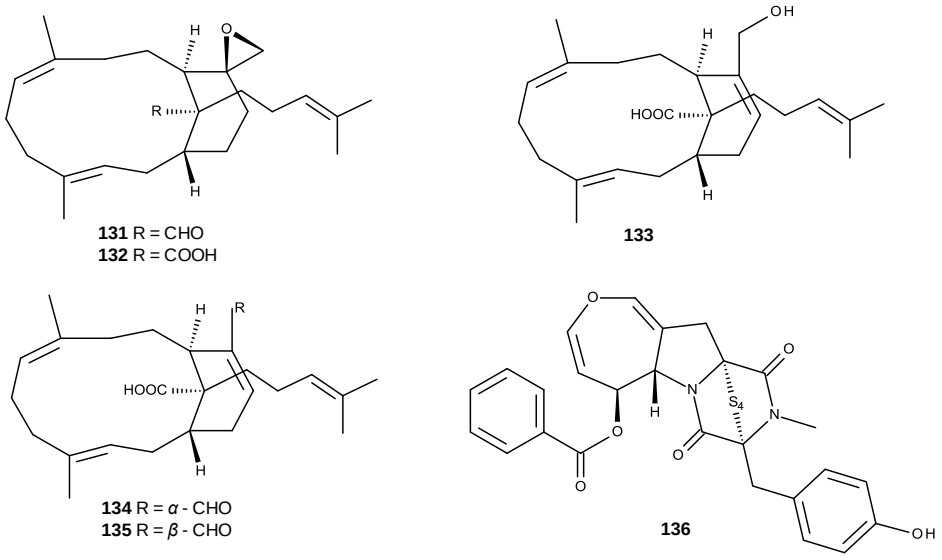

Figure 30. New constituents of *Emericella* sp. AST0036.

The strain 25379 of *Emericella* sp., isolated from the surface of a coral collected at Marietas Islands, Mexico, produced the new xanthones 15-chlorotajixanthone hydrate (**137**) and 14-methoxytajixanthone (**138**) (Figure 31). Both compounds inhibited the activation of the calmodulin-sensitive cAMP phosphodiesterase, with 14-methoxytajixanthone (**138**) displaying comparable effect with that of chlorpromazine (Figueroa *et al*., 2009).

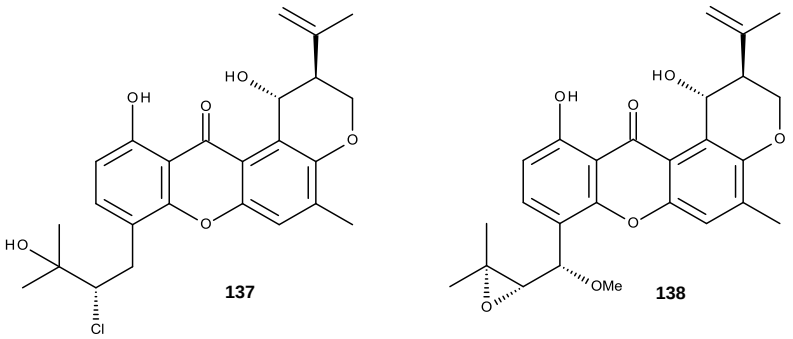

Figure 31. New xanthones of *Emericella* sp. 25379 strain.

2.3. The Genus *Eurotium*

Eurotium species are the sexual states of *Aspergillus* species, notably the *A. glaucus* group among others which is closely related to *Emericella*, and are also widely found in the environment (Geiser, 2009). Some *Eurotium* species have been used for manufacturing the traditional Japanese fermented food "*dried bonito*" (katsuobushi) and "*karebushi*" (Miyake *et al*., 2010).

Although only a few species of *Eurotium* have been investigated for their bioactive secondary metabolites, there are already some recent reports on the isolation of numerous types of compounds, such as alkaloids, phenolic compounds and anthraquinones.

2.3.1. *Eurotium chevalieri*

The strain *E. chevalieri* EuCO1 collected from rhizosphere soil at Surathani Province, Thailand was found to produce five new meroditerpenoids, chevalones A-D (**139-142**) and aszonapyrone B (**143**), as well as the new sesquiterpene alkaloid eurochevalierine (**144**) (Figure 32). Chevalone D (**142**) and eurochevalierine (**144**) exhibited antimalarial activity against *Plasmodium falciparum* with IC_{50} values of 3.1 and 3.4 µg/mL, while chevalone C (**141**) displayed strong antibacterial activity against *Mycobacterium tuberculosis*, with a MIC value of 6.3 µg/mL. Additionally, chevalones B-D (**140-142**) and eurochevalierine (**144**) were found to be cytotoxic against BC1, KB and NCI-H187 cancer cell lines, with IC_{50} values ranging from 2.9 to 9.8 µg/mL (Kanokmedhakul *et al*., 2011).

2.3.2. *Eurotium cristatum*

Three new diketopiperazine indole alkaloids and a new diketopiperazine dimer, cristatumins A-D (**145-148**) (Figure 33) have been reported from the culture extract of the endophytic fungus *E. cristatum* EN-220, which was isolated from the marine alga *Sargassum thunbergii*. While cristatumin A (**145**) exhibited potent

inhibitory activity against *Escherichia coli* and *Staphylococcus aureus*, cristatumin B (**146**) displayed moderate lethal activity against brine shrimp (*Artemia salina*) (Du *et al*., 2012).

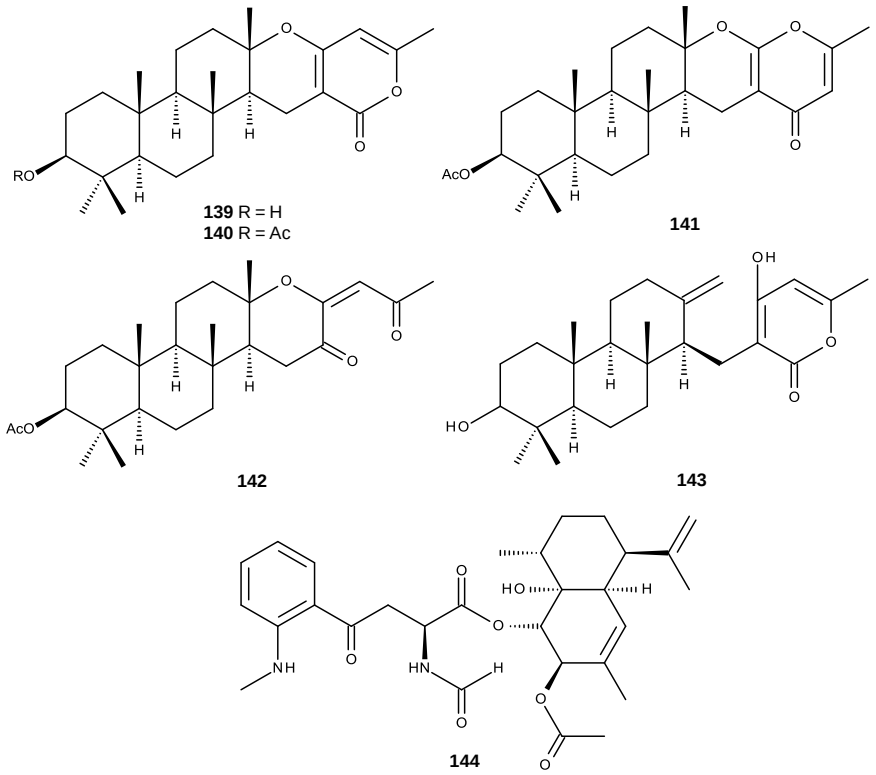

Figure 32. New constituents of *E. chevalieri* EuCO1.

2.3.3. *Eurotium herbariourum*

A new diketopiperazine dimer, cristatumin E (**149**) (Figure 33), was recently isolated from a marine alga-associated *E. herbariorum* strain HT-2. Cristatumin E (**149**) was found to be moderately cytotoxic against K562 tumor cell line with an IC_{50} value of 8.3 μM, however it displayed weak antibacterial activity against *Enterobacter aerogenes* and *Escherichia coli* (Li *et al*., 2013a).

2.3.4. *Eurotium repens*

Benzyl derivatives have frequently been reported from several *Eurotium* species. Two new additional benzyl derivatives, (*E*)-2-(hept-1-enyl)-3-(hydroxymethyl)-5-(3-methylbut-2-enyl)benzene-1,4-diol (**150**) and (*E*)-4-(hept-1-enyl)-7-(3-methylbut-2-enyl)-2,3-dihydrobenzofuran-2,5-diol (**151**) (Figure 34) have been isolated from the fungus *E. repens* (UM-031509), along with several known benzyl derivatives.

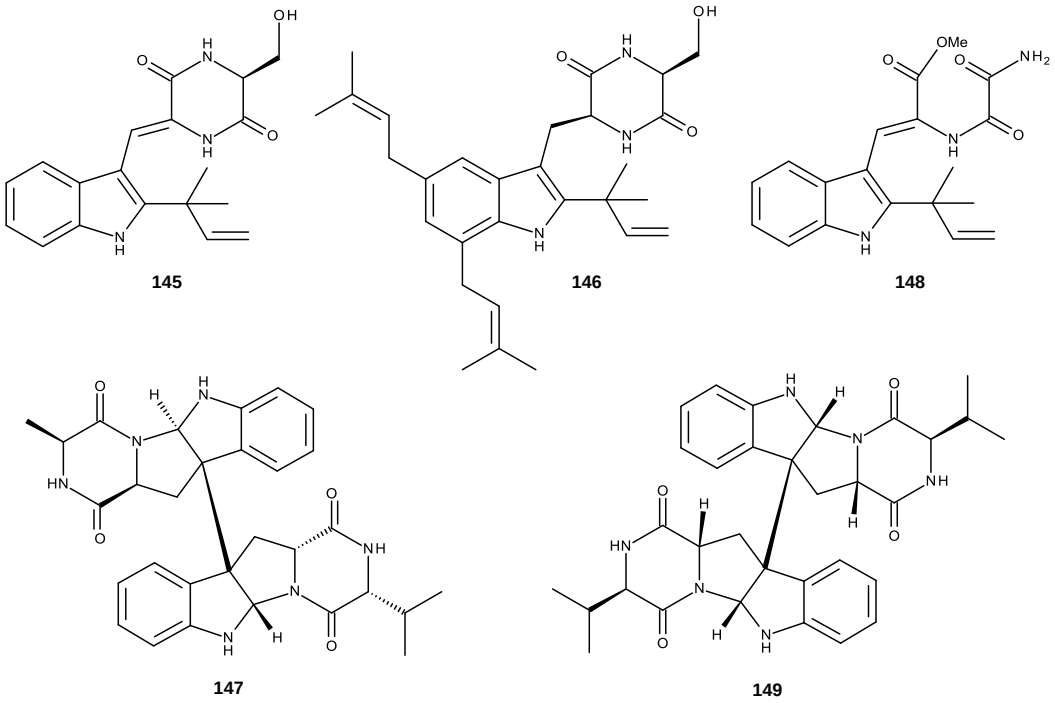

Figure 33. Structures of cristatumins A-E (**145-149**).

Compound **150** showed good binding affinity for human opioid or cannabinoid receptors (Gao *et al*., 2011a). It also exhibited antimicrobial activity against *Staphylococcus aureus* and *Candida glabrata*, and moderate antimalarial activity against chloroquine-sensitive and –resistant *Plasmodium falciparum* (Gao *et al*., 2012).

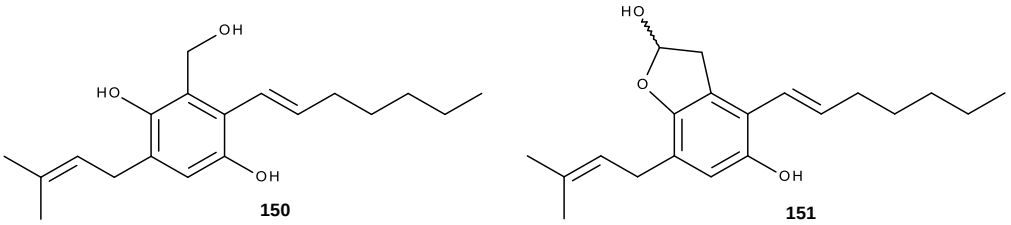

Figure 34. New benzyl derivatives of *E. repens* (UM-031509).

2.3.5. *Eurotium rubrum*

Chemical analysis of the endophytic fungus *E. rubrum*, isolated from the inner tissue of stems of the mangrove plant *Hibiscus tiliaceus* collected from Hainan Island (China), resulted in isolation of four new benzaldehyde derivatives, eurotirumin (**152**), 2-(2',3-epoxy-1'-heptenyl)-6-hydroxy-5-(3''-methyl-2''-butenyl)benzaldehyde (**153**), (*E*)-6-hydroxy-7-(3-methyl-2-butenyl)-2-(3-oxobut-1-enyl)chroman-5-carbaldehyde (**154**) and 2-(1',5'-heptadienyl)-3,6-dihydroxy-5-(3''-methyl-2''-butenyl)benzaldehyde (**155**) (Figure 35) (Li *et al*., 2008a). From the same extract, eurorubrin (**156**) and four new anthraquinone derivatives, 2-*O*-methyl-9-dehydroxyeurotinone (**157**), 2-*O*-methyl-4-*O*-(α-D-ribofuranosyl)-9-dehydroxyeurotinone (**158**)**,** 9-dehydroxyeurotinone, (**160**) and the anthraquinone glycoside 3-*O*-(α-D-ribofuranosyl)-questin (**159**) were also isolated (Figure 35). All compounds were evaluated for their radical scavenging properties by using DPPH radical scavenging assay, and only eurorubrin (**156**) showed strong activity with IC_{50} value of 44.0 μM (Li *et al*., 2009a). Additionally, 9-dehydroxyeurotinone (**160**) exhibited moderate cytotoxic activity against SW1990 cancer cell line, and weak antibacterial activity against *Escherichia coli* (Yan *et al*., 2012). This extract was also shown to be the source of new diketopiperazine alkaloids, namely 12-demethyl-12-oxo-eurotechinulin (**161**), dehydroechinulin (**162**), and dehydrovariecolorin L (**163**) (Figure 35). Among the three new alkaloids, only 12-demethyl-12-oxo-eurotechinulin (**161**) exhibited moderate cytotoxic activity against a single cancer cell line (SMMC-7721) (Li *et al*., 2008b; Yan *et al*., 2012).

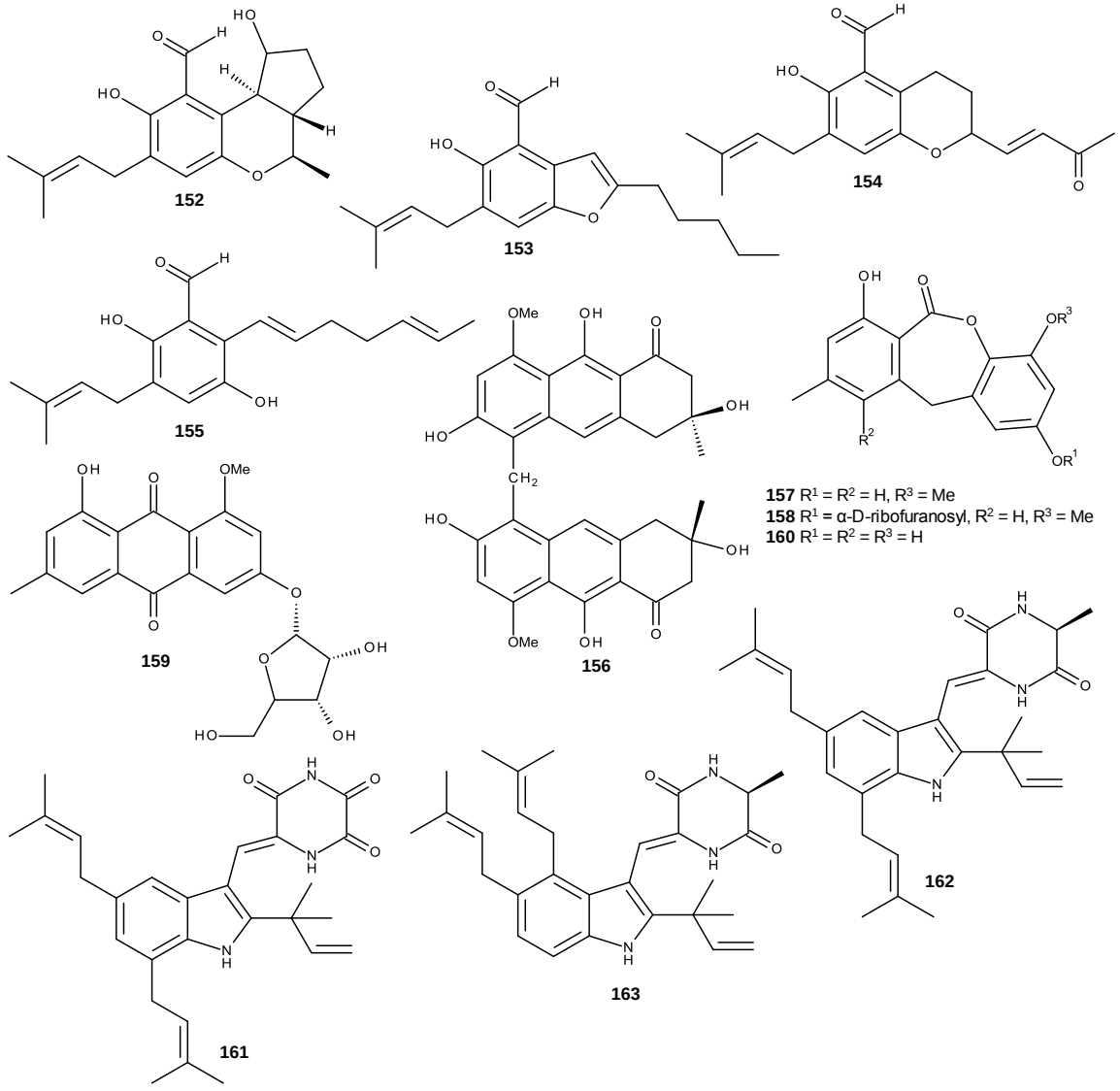

Figure 35. New constituents of *E. rubrum*.

2.4. The Genus *Neosartorya*

Neosartorya species are the teleomorphic state of *Aspergillus* section *Fumigati*. While the *Aspergillus* species only produce conidiospores, *Neosartorya* species produce both a sexual state, with ascospores, and an asexual state with conidiospores (Frisvad *et al*., 2009). *Neosartorya* includes several species which are important because they can be pathogenic or allergic to man, causing food spoilage and production of mycotoxins. However, *Neosartorya* species became

also an attractive source for the purpose of drug discovery due to the production of several interesting bioactive secondary metabolites (Hong *et al*., 2008).

2.4.1. *Neosartorya fischeri*

A culture of *N. fischeri* (SC4) isolated from a plant rhizosphere collected near We Fung Chi Cascade, Taiwan, was found to produce three new quinazolone indole alkaloids, fiscalins A-C (**164-166**) (Figure 36), all causing inhibition of radiolabeled substance P (SP) ligand to the human neurokinin (NK-1) receptor with *Ki* values of 57, 174 and 68 µM, respectively (Wong *et al*., 1992).

From the strain IFO9857 of *N. fischeri* var. *glabra*, researchers from Nippon Kayaku Co. Ltd., reported the isolation of three potent antifungal metabolites, NK372135 A-C (**167-169**) (Figure 36). These compounds, especially NK372135 C (**169**), exhibited potent antifungal activity against *Candida albicans* with an IC_{50} value of 0.27 µg/mL (Morino *et al*., 1994).

The strain IFM52672 produced two new cyclopentanone derivatives, isoterrein (**170**) and terrein (**171**) (Wakana *et al*., 2006), while fischeacid (**172**) and fischexanthone (**173**) (Figure 36) were reported from a marine-derived *N. fischeri* strain 1008F1 (Tan *et al*., 2012).

The activation of the polycyclic polyketide prenyltransferase (pcPTase) in transformant T2 *N. fischeri* culture induced the production of the new metabolite neosartoricin (**174**) (Figure 36) which exhibited *in vitro* antiproliferative activity on anti-CD3/CD28-activated murine spleenic T-cells with an IC_{50} value of 2.99 µM. Interestingly, the LC/MS analysis of the transformant T2 extract indicated the production of multiple new metabolites that are not found in wild strains of *N. fischeri* (Chooi *et al*., 2013).

Chemical investigation of a *N. fischeri* strain isolated from the river Vah sediments in Slovakia, led to the isolation of a new yellow pigment named neosartorin (**175**) (Proksa *et al*., 1998). Recently, Eamvijarn *et al*., (2013) reported the isolation of the 5-hydroxyl analogue of aszonalenin (**176**), as well as a new meroditerpene named sartorypyrone A (**177**) (Figure 36) from the culture of the soil fungus *N. fischeri* KUFC 6344. While sartorypyrone A (**177**) displayed strong growth inhibitory activity against MCF-7 (breast adenocarcinoma), NCI-H460 (non-

small cell lung cancer) and A375-C5 (melanoma) cell lines, with GI_{50} values ranging from 17.8 ± 7.4 to 25.0 ± 2.4 μM , 1-formyl-5-hydroxyaszonalenin (**176**) exhibited only weak inhibitory activity (Eamvijarn *et al*., 2013).

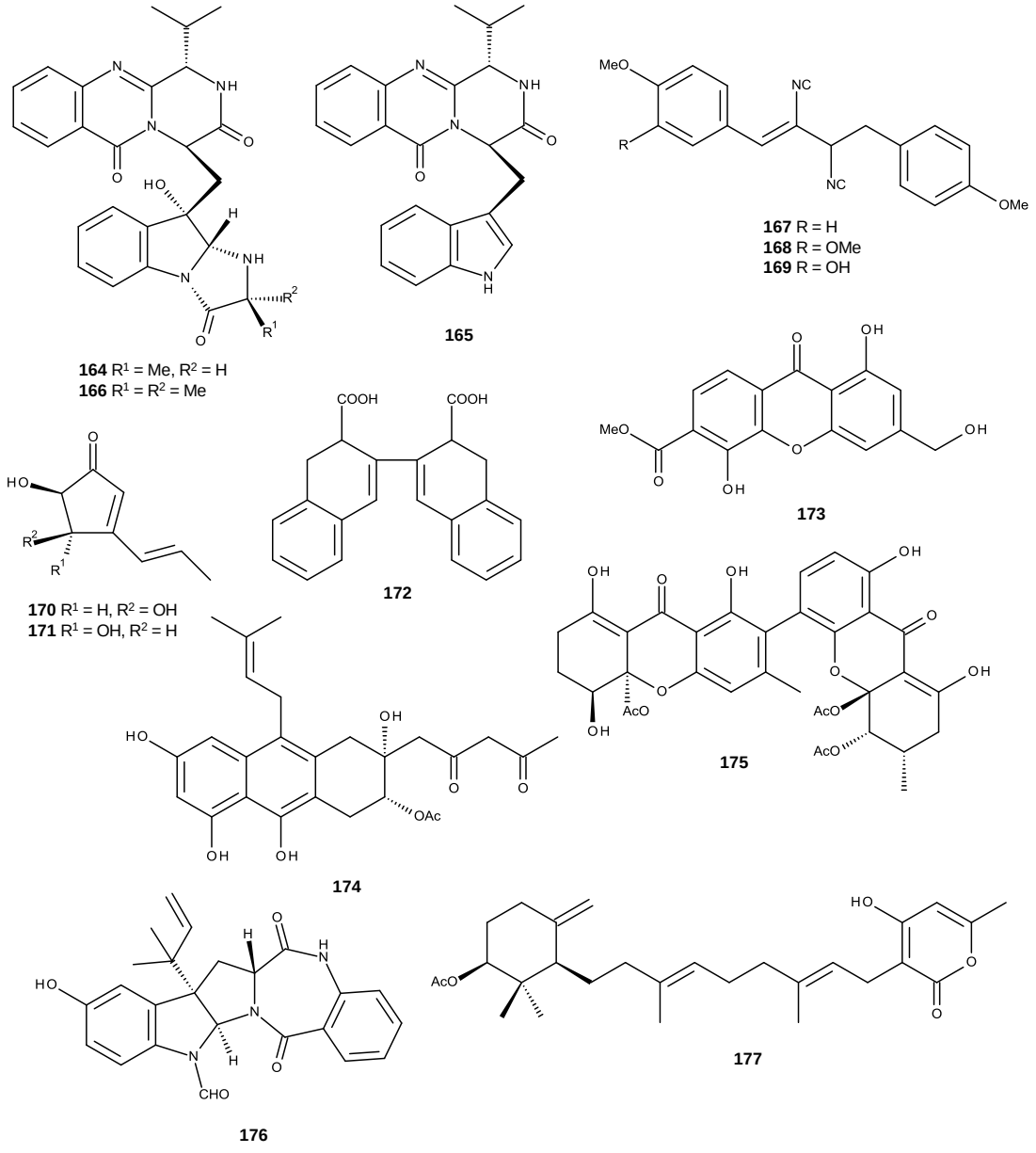

Figure 36. New constituents of *N. fischeri*.

2.4.2. *Neosartorya glabra*

Three new bicyclic lactones, glabramycins A-C (**178-180**) (Figure 37) were obtained from the soil *N. glabra* strain MF7030, F-155,700, using an antisense strategy. When tested against a panel of pathogenic bacteria, the three glabramycins exhibited antibacterial activity however, glabramycin C (**180**) showed pronounced activity against *Streptococcus pneumoniae*, and modest antibacterial activity against *Staphylococcus aureus* with MIC values of 2 and 16 µg/mL, respectively (Jayasuriya *et al*., 2009).

Three new reverse prenylated indole alkaloids, sartoryglabrins A-C (**181-183**) (Figure 37) have been reported by Kijjoa *et al*. (2011) from an unidentified strain of *N. glabra* obtained from an agricultural soil at Chonburi Province, Thailand. All the compounds exhibited strong to moderate *in vitro* growth inhibitory activity on MCF-7 cancer cell line with GI_{50} values ranging from 27.0 ± 0.57 to 53.0 ± 4.7 µM.

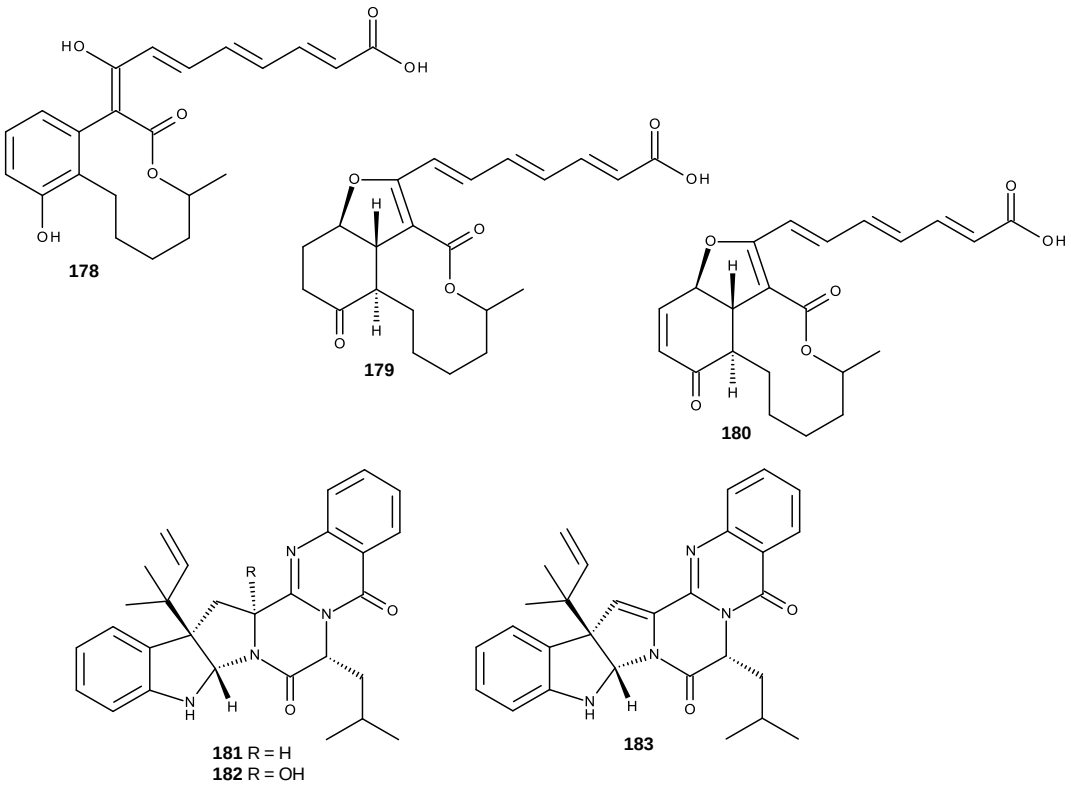

Figure 37. New constituents of *N. glabra*.

2.4.3. *Neosartorya pseudofischeri*

Chemical investigation of a collection of *N. pseudofischeri* KUFC 6422 from agricultural soil collected in Thailand, led to the isolation of 3-hydroxy-5-methylphenyl 2,4-dihydroxy-6-methylbenzoate (**184**), 3,8-diacetyl-4-(3-methoxy-4,5-methylenedioxy)benzyl-7-phenyl-6-oxa-3,8-diazabicyclo[3.2.1]octane (**185a** and **185b**) and a new quinazolinone-containing indole alkaloid pseudofischerine (**186**) (Figure 38) (Eamvijarn *et al*., 2012). Another strain of *N. pseudofischeri* (CBS 404.67) was found to produce a new cytotoxic pyrroloindole sesquiterpenoid, named fischerindoline (**187**) (Figure 38), that exhibited moderate *in vitro* growth inhibitory activity against six human and mouse cancer cell lines (Masi *et al*., 2013).

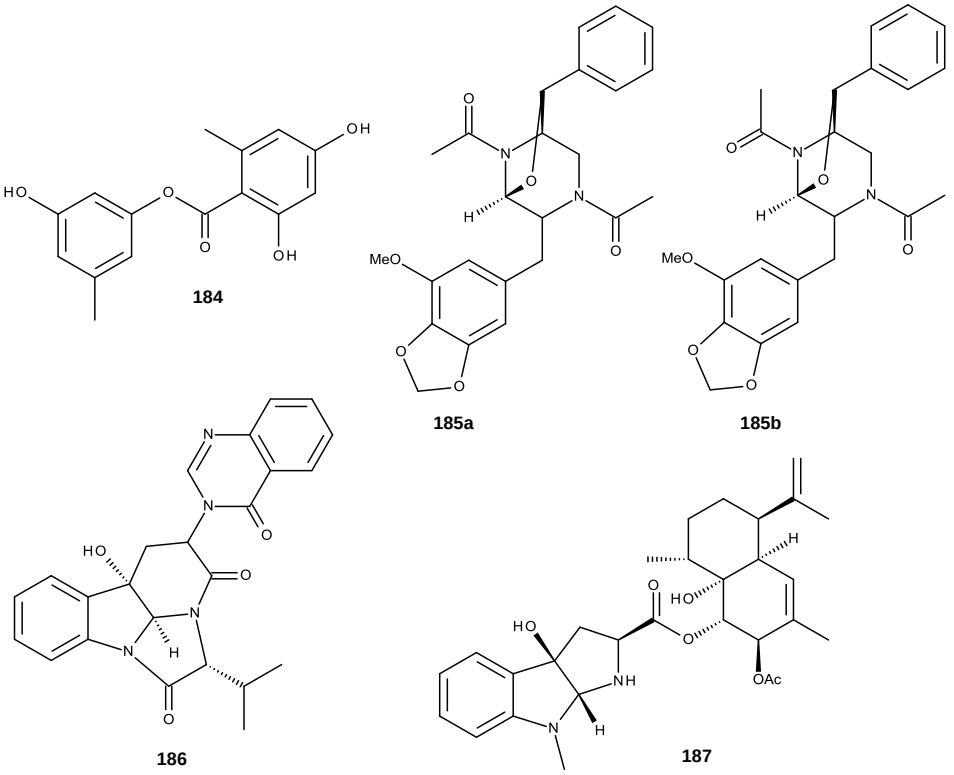

Figure 38. New constituents of *N. pseudofischeri*.

2.4.4. *Neosartorya quadricincta*

A new prenylated dihydroisocoumarin derivative, PF1223 (**188**) (Figure 39), was reported from the culture of *N. quadricincta* strain PF1223.

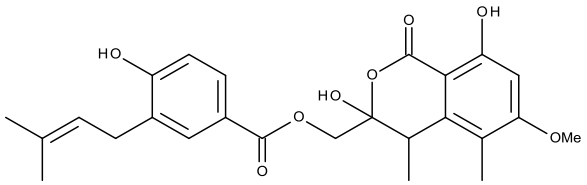

188

Figure 39. Structure of PF1223 (**188**).

PF1223 (**188**) inhibited [^{3}H]ethynylbicycloorthobenzoate ([^{3}H]EBOB) binding by 65% at the concentration of 2.2 µM, exhibiting binding activity for the insect GABA receptor and proving to be a lead compound for the development of novel insecticides (Ozoe *et al*., 2004).

2.4.5. *Neosartorya siamensis*

The EtOAc extract of the culture of the new specie *N. siamensis* KUFC 6349 collected from forest soil at Samaesarn Island, Chonburi Province (Thailand), yielded two new quinazolinone derivatives, tryptoquivaline O (**189**) and 3'-(4-oxoquinazolin-3-yl)spiro[1H-indole-3,5'-oxolane]-2,2'-dione (**190**), four new fiscalin analogues, *epi*-fiscalin C (**191**), *epi*-fiscalin A (**192**), neofiscalin A (**193**) and, *epi*-neofiscalin A (**194**), as well as the new indoloazepinone derivative, sartorymensin (**195**) (Figure 40). Sartorymensin (**195**) exhibited moderate *in vitro* growth inhibitory activity on the human U373 and Hs683 glioblastoma, the A549 non-small cell lung cancer, the MCF-7 breast cancer and the SKMEL-28 melanoma cell lines, with IC_{50} values ranging from 39 to 73 µM (Buttachon *et al*., 2012).

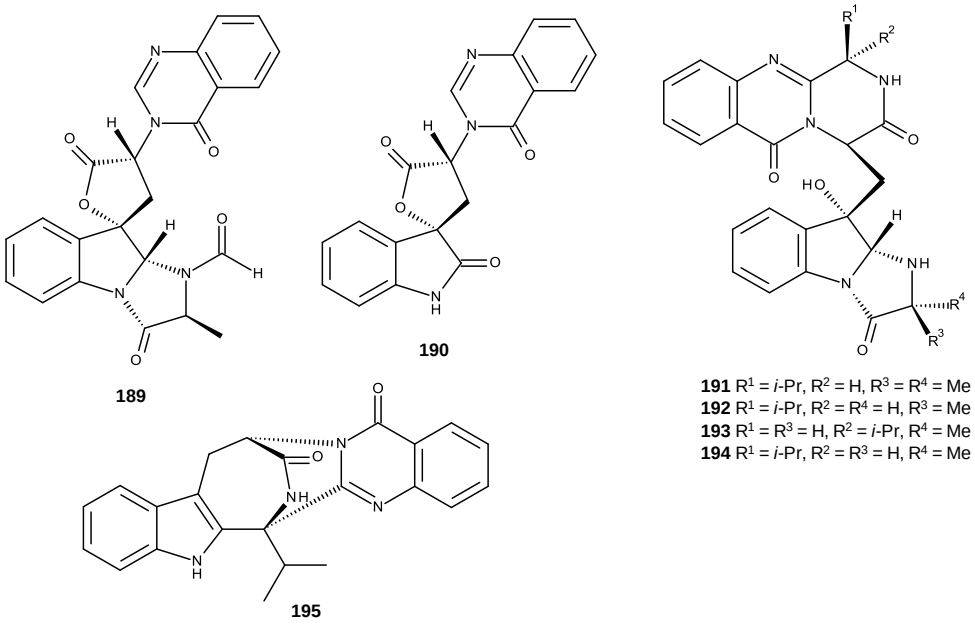

Figure 40. New constituents of *N. siamensis* KUFC 6349.

2.4.6. *Neosartorya tsunodae*

The only report on the chemical investigation of *N. tsunodae* was recently published by Kijjoa's group. The marine sponge-associated fungus *N. tsunodae* KUFC 9213, yielded sartorypyrone B (**196**) (Figure 41), a new analogue of chevalone C. Sartorypyrone B (**196**) displayed strong growth inhibitory activity against MCF-7, NCI-H460 and A375-C5 cancer cell lines with GI_{50} values of 17.8 ± 7.4, 20.5 ± 2.4 and 25.0 ± 4.4 μM, respectively (Eamvijarn *et al*., 2013).

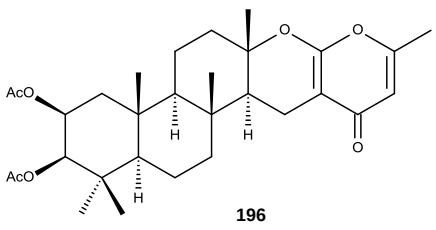

Figure 41. Structure of sartorypyrone B (**196**).

2.4.7. Unspecified *Neosartorya* species

Chemical investigation of an unspecified *Neosartorya* sp. from soil sample led to the isolation of a novel angiogenesis inhibitor, azaspirene (**197**) (Figure 42). Azaspirene (**197**) completely inhibited VEGF (vascular endothelial growth factor) induced cell migration in human umbilical vein endothelial cells (HUVECs) at the concentration of 27.1 μM, without significant cell toxicity (Asami *et al*., 2002). Further studies showed that the anti-angiogenic activity was associated with the suppression of Raf-1 activation (Asami *et al*., 2008). Another endothelial-cell growth inhibitor RK-805 (6-oxo-6-deoxyfumagillol) (**198**) was later isolated from the same culture. Additionally, RK-805 (**198**) also selectively inhibited methionine aminopeptidase-2 (MetAP2), supporting the potential of the compound for the development of new angiogenesis inhibitors (Asami *et al*., 2004).

Marine-derived *Neosartorya* sp. HN-M-3, collected from marine mud in the intertidal zone of Hainan Province (China), was found to produce four new tryptoquivaline analogues, tryptoquivalines P-S (**199-202**) (Figure 42) (Sun *et al*., 2012; Xu *et al*., 2013b).

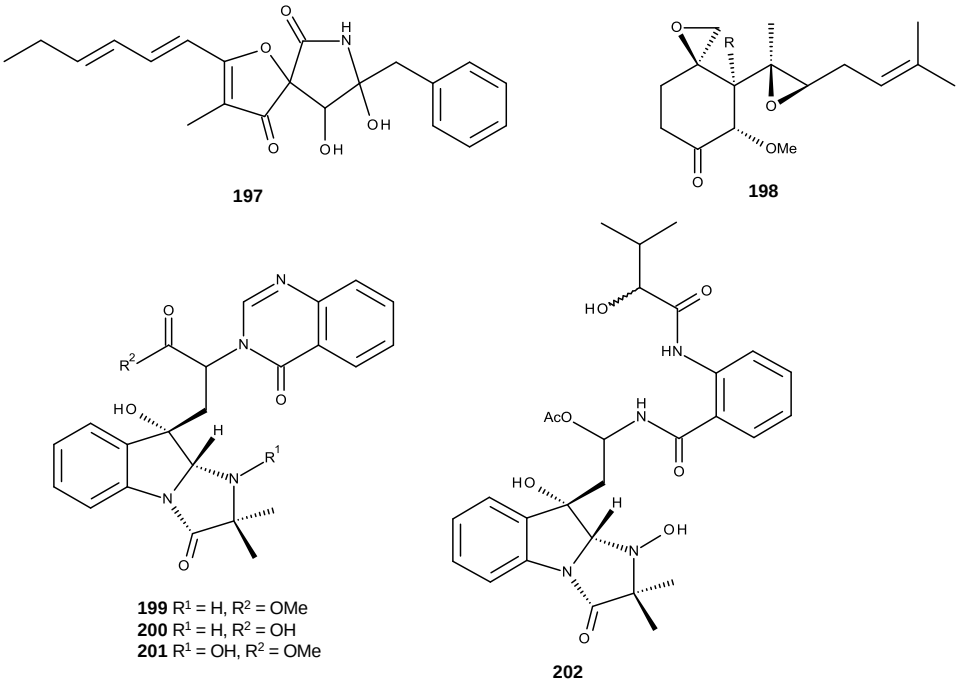

Figure 42. New constituents of unspecified *Neosartorya* species.

CHAPTER III
RESULTS AND DISCUSSION

3.1. Chemical Investigation of the Marine Derived Fungi

Chemical investigation of the marine sponge-associated fungus *Emericella variecolor* KUFC 7092, resulted in isolation of ergosterol (**EV1**), ergosterol peroxide (**EV2**), orcinol (**EV3**), 1*H*-indole-3-carboxylic acid (**EV4**) and cyclo-(L-tryptophyl-L-phenylalanyl) (**EV5**) (Figure 43).

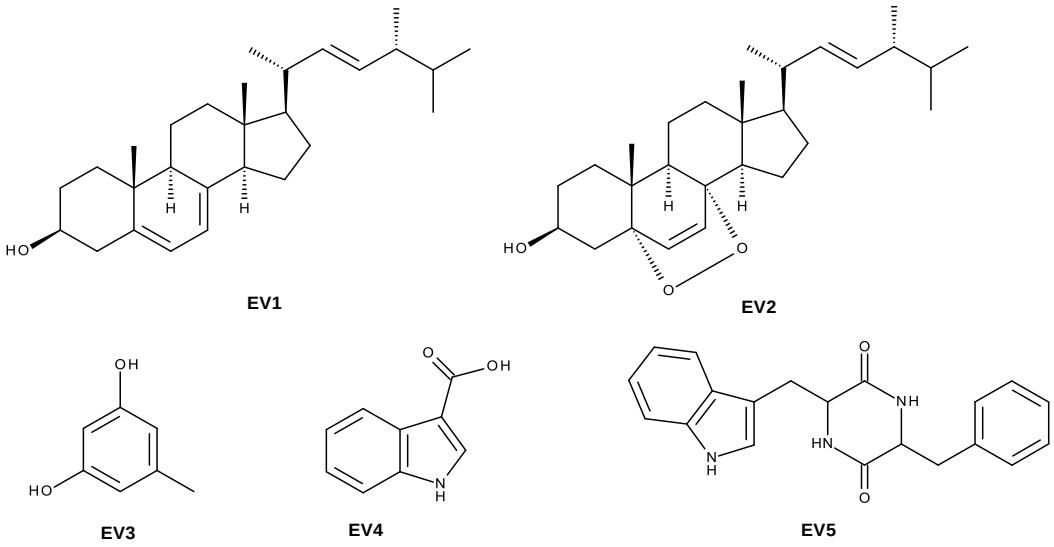

Figure 43. Constituents of *Emericella variecolor* KUFC 7092.

The EtOAc extract of the marine sponge-derived fungus *Eurotium cristatum* KUFC 7356 furnished five known anthraquinones (**EC1-EC5**), four previously reported indolopolyketopiperazine alkaloids (**EC6-EC9**) and a new diketopiperazine dimer (**EC10**) (Figure 44).

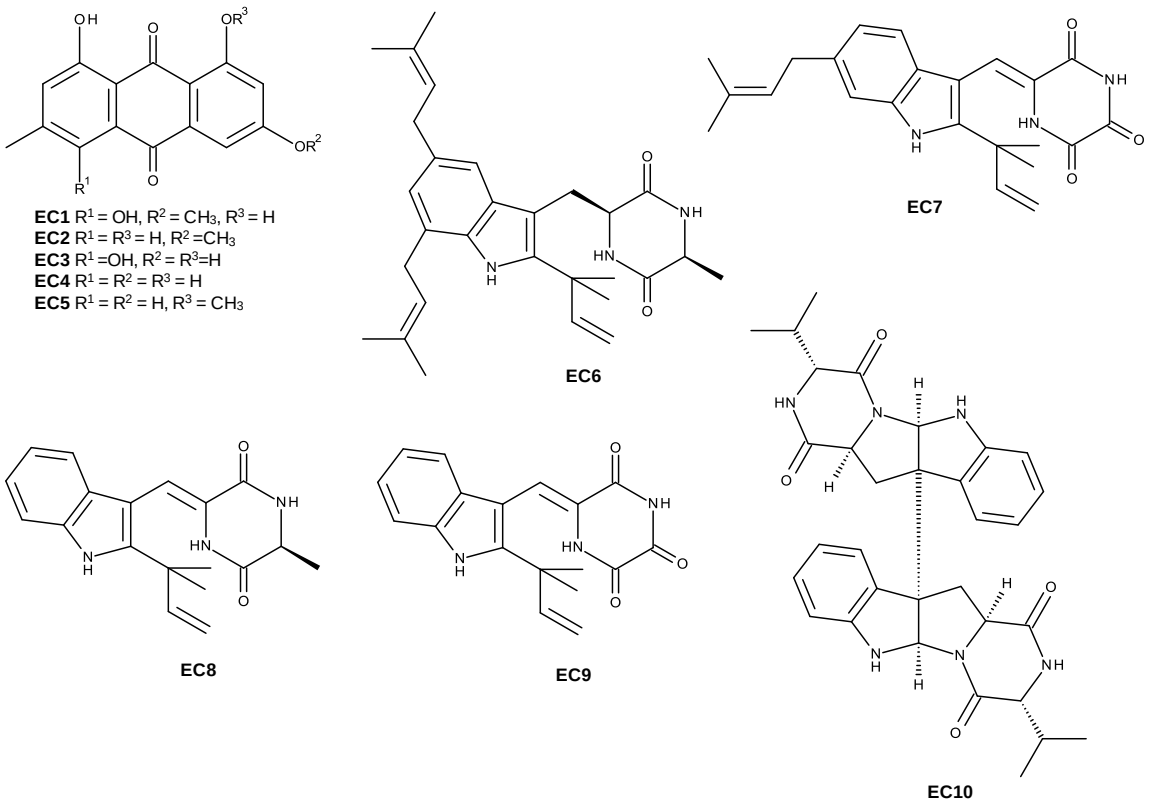

Figure 44. Constituents of *Eurotium cristatum* KUFC 7356.

Two marine-derived *Neosartorya* species were investigated namely, the diseased coral-derived *N. laciniosa* KUFC 7896 and the marine sponge associated *N. paulistensis* KUFC 7897.

From the EtOAc extract of the culture of *N. laciniosa* KUFC 7896, a new tryptoquivaline analogue, tryptoquivaline T **(NL6)** , was isolated, in addition to five known metabolites including the meroditerpenes chevalone B **(NL1)**, aszonapyrones A **(NL2)** and B **(NL3)**, tryptoquivaline L **(NL4)** and 3'-(4-oxoquinazolin-3-yl)spiro[1*H*-indole-3,5'-oxolane]-2, 2'-dione **(NL5)** (Figure 45).

Examination of the EtOAc extract of the culture of *N. paulistensis* KUFC 7897 yielded a new aszonapyrone analogue, sartorypyrone C (**NP1**), in addition to five previously reported metabolites including tryptoquivalines L (**NP2**), H (**NP3**) and F (**NP6**), 4(3*H*)-quinazolinone **(NP4)** and 3'-(4-oxoquinazolin-3-yl)spiro[1*H*-indole-3,5'-oxolane]-2, 2'-dione **(NP5)** (Figure 46).

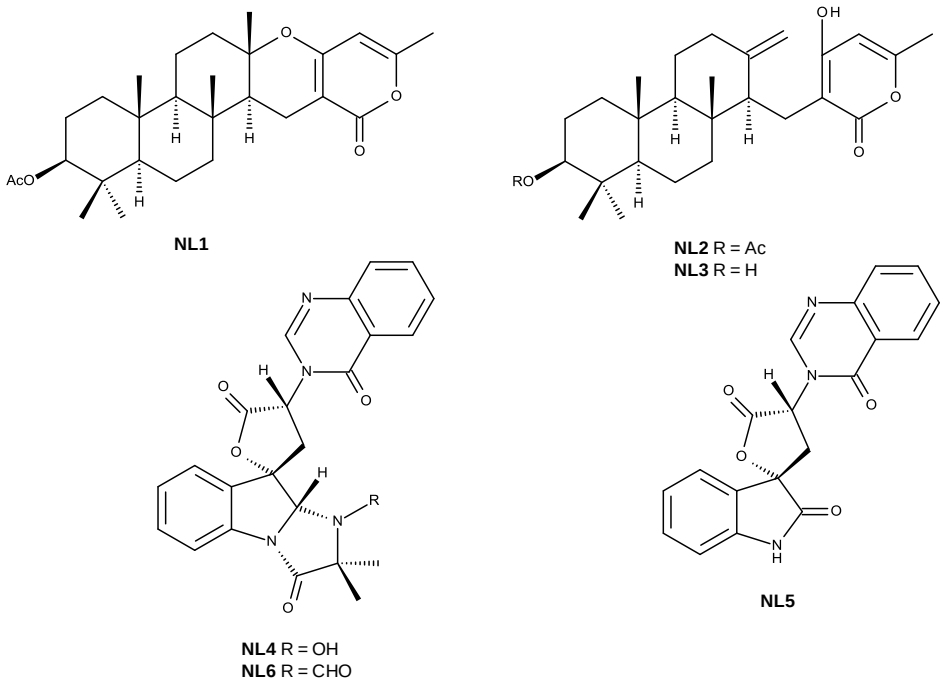

Figure 45. Constituents of *Neosartorya laciniosa* KUFC 7896.

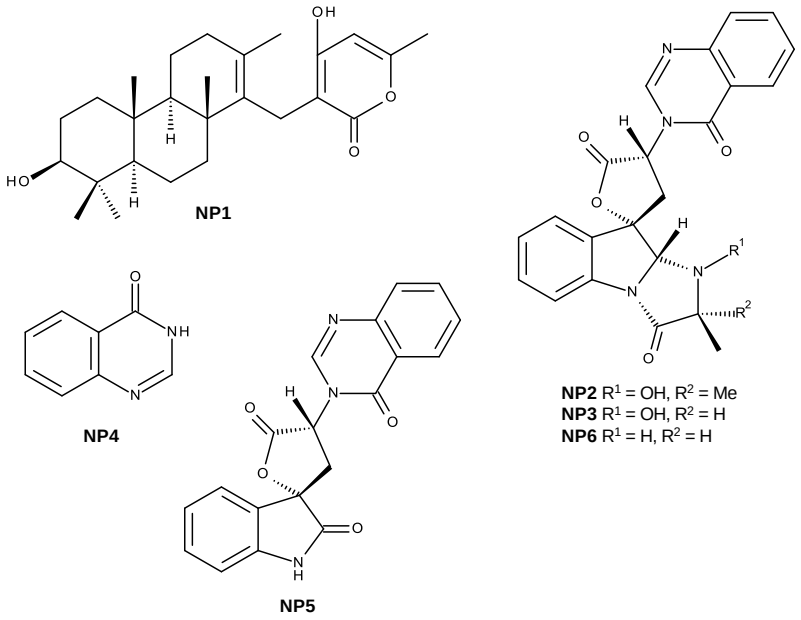

Figure 46. Constituents of *Neosartorya paulistensis* KUFC 7897.

3.1.1. Structure Elucidation of Triterpenoid Steroids

3.1.1.1. Ergosterol (EV1)

EV1 was isolated as white amorphous solid. The ^{13}C NMR, DEPT and HSQC spectra (Table 2) revealed the presence of two quaternary sp^2 (δ_C 141.3, 139.7), four methine sp^2 (δ_C 135.5, 131.9, 119.5, 116.3), two quaternary sp^3 (δ_C 42.0, 37.0), seven methine sp^3 (δ_C 70.3, 55.7, 54.5, 46.2, 42.8, 40.4, 33.0), seven methylene sp^3 (δ_C 40.7, 39.0, 38.3, 31.9, 29.5, 28.3, 23.0) and six methyl (δ_C 21.1, 19.9, 19.6, 17.6, 16.2, 12.0) carbons.

Table 2. ^1H and ^{13}C NMR data ($CDCl_3$, 300.13 and 75.47 MHz) of **EV1**.

Position	δ_C, type	δ_H, mult. (*J* in Hz)	COSY	HMBC
1α	38.3, CH_2	1.29, *m*	H-2a	C-3
β		2.01, *m*	H-2b	---
2a	31.9, CH_2	2.01, *m*	H-1α	---
b		1.51, *m*	H-1β, 3	---
3	70.3, CH	3.63, *m*	H-2b, 4a, 4b	---
4a	40.7, CH_2	2.44, *m*	H-3, 4b, 6	C-2, 3, 5, 6, 10
b		2.28, *m*	H-3, 4a, 6	---
5	139.7, C	---	---	---
6	119.5, CH	5.57, *dd* (5.6, 2.3)	H-4a, 4b, 7	C-4, 8, 10
7	116.3, CH	5.38, *m*	H-6, 14	C-5, 9, 14
8	141.3, C	---	---	---
9	46.2, CH	1.96, *m*	---	C-5
10	37.0, C	---	---	---
11a	23.0, CH_2	1.69, *m*	H-11b, 12a	---
b		1.33, *m*	H-11a, 12b	---
12a	39.0, CH_2	2.04, *m*	H-11a, 12b	C-14
b		1.24, *m*	H-11b, 12a	C-18
13	42.0, C	---	---	---
14	54.5, CH	2.02, *m*	H-7	C-9, 13, 17
15	28.3, CH_2	1.74, *m*	H-16b	---
16a	29.5, CH_2	1.76, *m*	---	---
b		1.29, *m*	H-15	---
17	55.7, CH	1.26, *m*	H-20	C-12, 13, 14, 15, 16, 20, 21
18	12.0, CH_3	0.63, *s*	---	C-12, 13, 14, 17
19	16.2, CH_3	0.94, *s*	---	C-1, 5, 9, 10
20	40.4, CH	2.03, *m*	H-17, 21, 22	C-13
21	21.1, CH_3	1.04, *d* (6.7)	H-20	C-17, 20, 22, 23
22	135.5, CH	5.16, *dd* (15.0, 7.5)	H-20, 23	C-20, 22, 24
23	131.9, CH	5.23, *dd* (15.0, 7.0)	H-22, 24	C-20, 22, 24, 25, 28
24	42.8, CH	1.82, *m*	H-23, 25, 28	C-22, 23, 25, 26/27
25	33.0, CH	1.48, *m*	H-24, 26/27	C-22, 23, 26/27
26/27	19.9, CH_3	0.84, *d* (6.7)	H-25	C-24, 25, 26/27
	19.6, CH_3.	0.82, *d* (6.7)	H-25	C-24, 25, 26/27
28	17.6, CH_3	0.92, *d* (6.7)	H-24	C-23, 24, 25

The presence of six sp^2 carbons (δ_C 141.3, 139.7, 135.5, 131.9, 119.5 and 116.3), together with the four olefinic protons at δ_H 5.57, *dd* (*J* = 5.6, 2.3 Hz), 5.38, *m*, 5.23, *dd* (*J* = 15.0, 7.0 Hz) and 5.16, *dd* (*J* = 15.0, 7.5 Hz), suggested the existence of three double bonds in the molecule. The COSY spectrum (Table 2) showed that the proton at δ_H 5.16, *dd* (*J* = 15.0, 7.5 Hz; δ_C 135.5) was coupled to the proton at δ_H 5.23, *dd* (*J* = 15.0, 7.0 Hz; δ_C 131.9), suggesting that they belong to a *trans* substituted double bond. The COSY spectrum also displayed correlations between the olefinic proton at δ_H 5.23, *dd* (*J* = 15.0, 7.0 Hz) and the methine proton at δ_H 1.82, *m* (δ_C 42.8). In turn, the multiplet of the methine proton at δ_H 1.82 gave cross peaks to the signals of the methine proton at δ_H 1.48, *m* (δ_C 33.0) and the doublet of the methyl protons at δ_H 0.92 (*J* = 6.7 Hz; δ_C 17.6), whereas the multiplet of the methine proton at δ_H 1.48 (δ_C 33.0) also gave cross peaks with the two methyl doublets at δ_H 0.84 (*J* = 6.7 Hz; δ_C 19.9) and δ_H 0.82 (*J* = 6.7 Hz; δ_C 19.6). These correlations suggested the presence of the coupling system of:

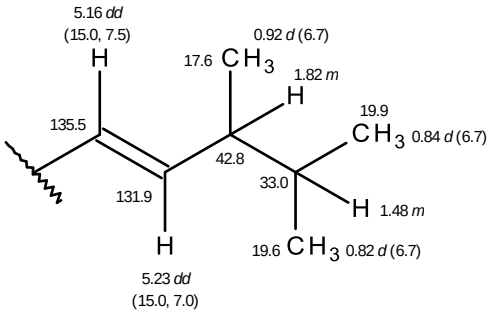

On the other hand, the olefinic proton at δ_H 5.16, *dd* (*J* = 15.0, 7.5 Hz; δ_C 135.5) gave cross peaks to the multiplet of the methine proton at δ_H 2.03 (δ_C 40.4) which, in turn, gave cross peaks to the methyl doublet at δ_H 1.04 (*J* = 6.7 Hz; δ_C 21.1) as well as the multiplet of the methine proton at δ_H 1.26 (δ_C 55.7), suggesting the presence of the coupling system of 2,5,6-trimethyl-3-hepten-2-yl (**A**).

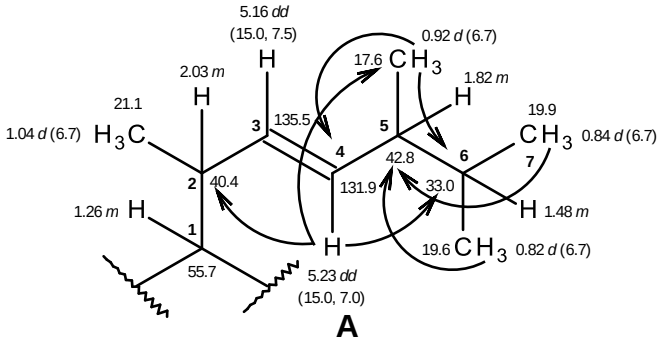

A

The HMBC correlations (Table 2) of the methyl protons at δ_H 0.92, *d* (*J* = 6.7 Hz; δ_C 17.6) to the carbons at δ_C 131.9, 42.8 and 33.0; of the methyl protons at δ_H 0.84, *d* (*J* = 6.7 Hz; δ_C 19.9) and δ_H 0.82, *d* (*J* = 6.7 Hz; δ_C 19.6) to the carbon at δ_C 42.8; of the olefinic proton at δ_H 5.23, *dd* (*J* = 15.0, 7.0 Hz; δ_C 131.9) to the carbons at δ_C 40.4, 33.0 and 17.6, and of the methyl protons at δ_H 1.04, *d* (*J* = 6.7 Hz; δ_C 21.1) to the olefinic carbon at δ_C 135.5 and the methine carbon at δ_C 55.7, confirmed this structure.

Another portion of the molecule comprised two methyl groups (δ_H 0.94, *s*; δ_C 16.2 and δ_H 0.63, *s*; δ_C 12.0) on quaternary carbons, two tetrasubstituted double bonds (δ_C 141.3, 139.7, 119.5, 116.3; δ_H 5.57, *dd*, *J* = 5.6, 2.3 Hz and 5.38, *m*), one oxymethine carbon (δ_C 70.3; δ_H 3.63, *m*), three methine carbons (δ_C 55.7, 54.5 and 46.2), seven methylene carbons (δ_C 40.7, 39.0, 38.3, 31.9, 29.5, 28.3, 23.0) and two quaternary carbons (δ_C 42.0 and 37.0). The COSY spectrum displayed strong cross peak between the signals of the olefinic protons at δ_H 5.57, *dd* (*J* = 5.6, 2.3 Hz; δ_C 119.5) and δ_H 5.38, *m* (δ_C 116.3) as well as weak cross peaks between the signal of the olefinic proton at δ_H 5.57, *dd* (*J* = 5.6, 2.3 Hz; δ_C 119.5) and the signals of the methylene protons at δ_H 2.44, *m* and 2.28, *m* (δ_C 40.7). In turn, these methylene protons also showed correlations with the oxymethine proton at δ_H 3.63, *m* (δ_C 70.3). The HMBC spectrum showed cross peaks of the multiplet of the olefinic proton at δ_H 5.38 (δ_C 116.3) to the quaternary sp^2 carbon δ_C 139.7 and the methine sp^3 carbon at δ_C 46.2; of the signal of the olefinic proton at δ_H 5.57, *dd* (*J* = 5.6, 2.3 Hz; δ_C 119.5) to the quaternary carbon at δ_C 141.3 and the quaternary sp^3 carbon at δ_C 37.0; of the signals of the methylene protons at δ_H 2.44, *m* and 2.28, *m* (δ_C 40.7) to the methine sp^2 carbon at δ_C 119.5 and the methylene carbon at δ_C 31.9, and of the methyl singlet at δ_H 0.94 (δ_C 16.2) to the quaternary sp^3 carbon at δ_C 37.0, the quaternary sp^2 carbon

at δ_C 139.7, the methine sp^3 carbon at δ_C 46.2 and the methylene carbon at δ_C 38.3. These correlations suggested the existence of the 6,7-substituted 4a-methyl-1,2,3,4,4a,5-hexahydronaphthalen-2-ol moiety.

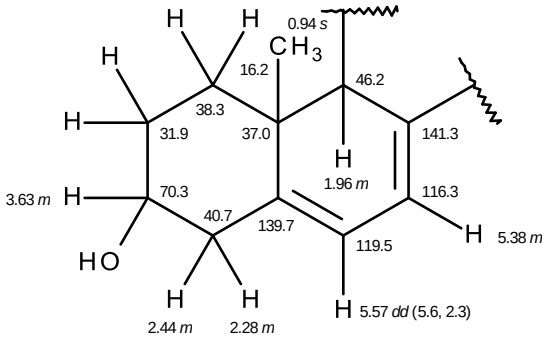

Moreover, the HMBC spectrum also displayed cross peaks of the multiplet of the olefinic proton at δ_H 5.38 (δ_C 116.3) and the methyl singlet at δ_H 0.63 (δ_C 12.0) to the methine sp^3 carbon at δ_C 54.5. Furthermore, the methyl singlet at δ_H 0.63 (δ_C 12.0) gave HMBC cross peaks with the quaternary carbon at δ_C 42.0, the methine sp^3 carbon at δ_C 55.7 and the methylene carbon at δ_C 39.0, the signal of the methine proton at δ_H 2.02, *m* (δ_C 54.5) gave cross peaks to the methine sp^3 carbons at δ_C 46.2 and δ_C 55.7, and to the quaternary sp^3 carbon at δ_C 42.0, and the signal of the methine proton at δ_H 1.26, *m* (δ_C 55.7) gave cross peaks to the methylene carbons at δ_C 39.0, 29.5 and 28.3, the methine carbon at δ_C 54.5, and the quaternary carbon at δ_C 42.0. Consequently the hexahydronaphthalene moiety was fused with the octahydro-1H-indene moiety through the olefinic carbon at δ_C 141.3 and the methine carbon at δ_C 46.2, forming thus a tetracyclic skeleton of androstane (**B**).

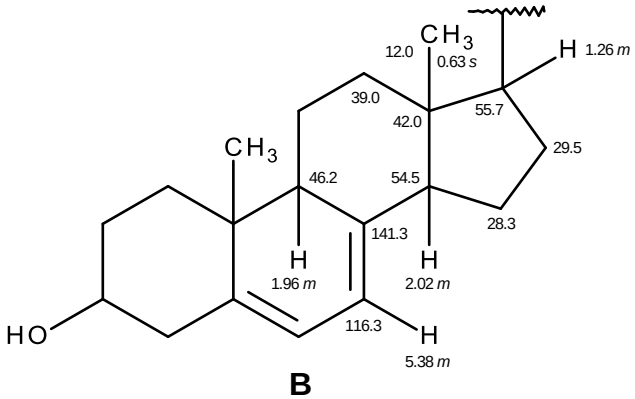

B

Since the COSY spectrum exhibited correlation between the proton signal at δ_H 2.03, *m* (δ_C 40.4) of fragment **A** and the proton signal at δ_H 1.26, *m* (δ_C 55.7) of fragment **B**, it was clear that these two fragments were connected through the methine carbons at δ_C 40.4 of the former and at δ_C 55.7 of the latter. This was supported by the HMBC correlations of the methyl singlet at δ_H 1.04, *d* (*J* = 6.7; δ_C 21.1) to the methine carbon at δ_C 55.7, as well as of the methine proton at δ_H 1.26, *m* (δ_C 55.7) to the methine carbon at δ_C 40.4, and the methyl carbon at δ_C 21.1. Therefore the complete structure of **EV1** was:

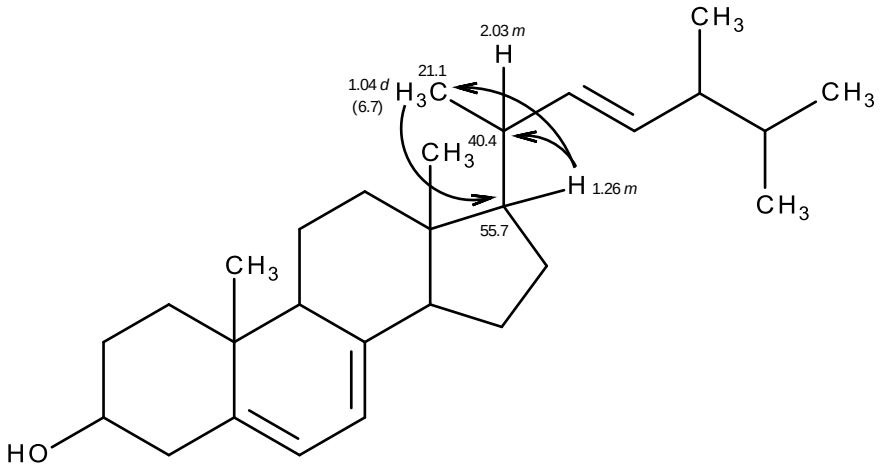

Literature survey revealed that the structure of **EV1** corresponded to ergosterol (Figure 47), a fungal sterol widely reported from many fungal species such as *Aspergillus fumigatus* (Alcazar-Fuoli *et al*., 2008), *Pleurotus ostreatus* (Ramos-Ligonio *et al*., 2012), and from various strains of *Emericella* spp., namely *E. striata* (Kawahara *et al*., 1988b), *E. unguis* (Kawahara *et al*., 1998c) as well as from other strains of *E. variecolor* (Liangsakul *et al*., 2011; Malmström *et al*., 2002b). The ^{1}H and ^{13}C NMR data of **EV 1** were compatible with those of ergosterol reported by Tuckey *et al*. (2012).

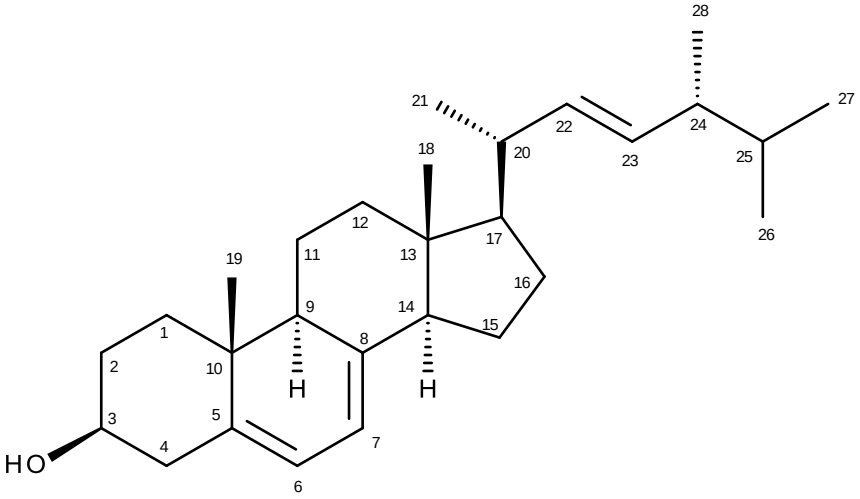

Figure 47. Structure of ergosterol (**EV1**).

3.1.1.2. Ergosterol peroxide (EV2)

EV2 was isolated as colorless needles, and the general features of its ^{1}H and ^{13}C NMR spectra (Table 3) closely resembled those of **EV1**. The ^{13}C NMR spectrum of **EV2** also displayed twenty-eight carbon signals, which can be categorized through DEPT and HSQC spectra, as four methine sp^2 (δ_C 135.6, 135.2, 131.5, 130.2), four quaternary sp^3 (δ_C 81.4, 78.4, 44.0, 36.5), seven methine sp^3 (δ_C 64.6, 55.4, 51.2, 50.8, 42.0, 39.9, 32.5), seven methylene sp^3 (δ_C 38.7, 36.9, 34.5, 29.9, 28.3, 22.8, 20.2) and six methyl (δ_C 20.7, 19.8, 19.5, 17.9, 17.3, 12.6) carbons.

Like **EV1**, **EV2** also contained the 2,5,6-trimethyl-3-hepten-2-yl moiety which was confirmed by the COSY and HMBC correlations (Table 3).

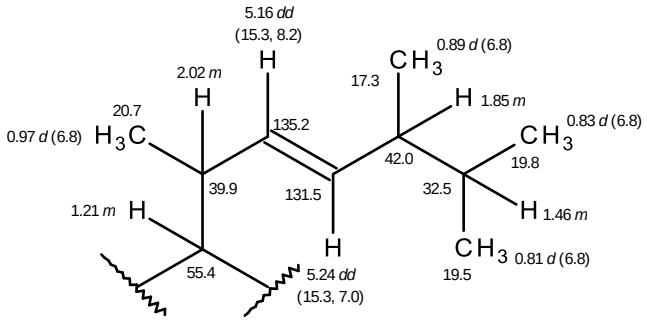

Contrary to **EV1**, the ^{1}H and ^{13}C NMR spectra revealed the presence of one *cis* double bond (δ_C 135.6; δ_H 6.23, *d*, *J* = 8.5 Hz and δ_C 130.2; δ_H 6.44, *d*, *J* = 8.5 Hz) and two oxygenated quaternary sp^3 carbons at δ_C 81.4 and δ_C 78.4, instead of two conjugated double bonds, in the androstane moiety. The signal of the olefinic proton at δ_H 6.23, *d* (*J* = 8.5 Hz; δ_C 135.6) displayed HMBC cross peaks to the carbons at δ_C 36.9, 81.4 and 78.4, while the signal of the olefinic proton at δ_H 6.44, *d* (*J* = 8.5 Hz; δ_C 130.2) gave HMBC cross peaks to the carbons at δ_C 81.4 and 50.8, suggesting that the double bond was located on C-6/C-7, whereas C-5 and C-8 were oxygenated.

Table 3. ^{1}H and ^{13}C NMR data (DMSO-d_6, 500.13 and 125.77 MHz) of **EV2**.

Position	δ_C, type	δ_H, mult. (*J* in Hz)	COSY	HMBC
1α	34.5, CH_2	1.71, *dd* (13.5, 3.2)	H-2a, 2b	---
β		1.61. *m*	H-2a	C-3, 10
2a	29.9, CH_2	1.65, *m*	H-1α, 1β, H-2b	---
b		1.38, *m*	H-1α, 2a, 3	---
3	64.6, CH	3.57, *m*	H-2b, 4	---
4	36.9, CH_2	1.83, *m*	H-3	C-2, 3, 5, 6, 10
5	81.4, C	---	---	---
6	135.6, CH	6.23, *d* (8.5)	H-7	C-4, 5, 8
7	130.2, CH	6.44, *d* (8.5)	H-6	C-5, 8, 9
8	78.4, C	---	---	---
9	50.8, CH	1.32, *m*	---	C-1, 7, 8
10	36.5, C	---	---	---
11a	22.8, CH_2	1.48, *m*	H-11b, 12a, 12b	---
b		1.13, *m*	H-11a, 12a	---
12a	38.7, CH_2	1.88, *m*	H-11a, 11b, 12b	---
b		1.18, *m*	H-11a, 12a	---
13	44.0, C	---	---	---
14	51.2, CH	1.44, *m*	---	C-8, 16
15a	28.3, CH_2	1.66, *m*	H-15b, 16	---
b		1.23, *m*	H-15a	---
16	20.2, CH_2	1.39, *m*	H-15a	---
17	55.4, CH	1.21, *m*	H-20, 22	C-13, 15, 18, 20
18	12.6, CH_3	0.77, *s*	---	C-12, 13, 14, 17
19	17.9, CH_3	0.79, *s*	---	C-5, 9, 10
20	39.9, CH	2.02, *m*	H-17, 21, 22	---
21	20.7, CH_3	0.97, *d* (6.8)	H-20	C-17, 20, 22
22	135.2, CH	5.16, *dd* (15,3, 8.2)	H-17, 20, 23	C-20, 24
23	131.5, CH	5.24, *dd* (15.3, 7.0)	H-22, 24	C-20, 24
24	42.0, CH	1.85, *m*	H-23, 25, 28	C-25, 26, 27, 28
25	32.5, CH	1.46, *m*	H-24, 26/27	C-23, 24, 26/27
26/27	19.8, CH_3	0.83, *d* (6.8)	H-25, 26/27	C-24, 25, 26/27
	19.5, CH_3	0.81, *d* (6.8)	H-25, 26/27	C-24, 25, 26/27
28	17.3, CH_3	0.89, *d* (6.8)	H-24	C-23, 24, 25
OH-3	---	4.63, *brs*	---	---

This was corroborated by the HMBC correlation of the methyl singlet at δ_H 0.79 (δ_C 17.9) to the oxygenated quaternary carbon at δ_C 81.4 (C-5). Taking together the NMR data, it was possible to conclude that the structure of **EV2** was:

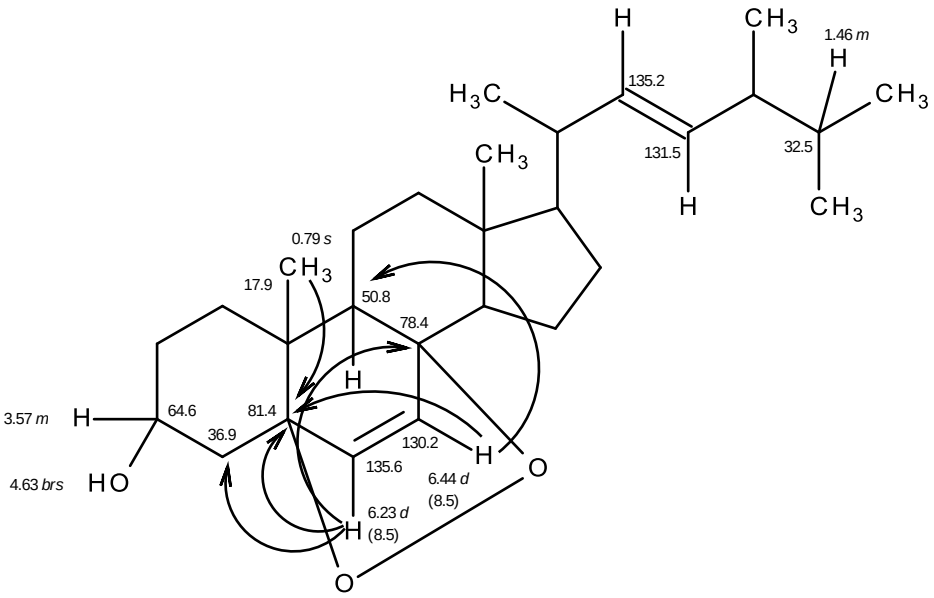

The ^{1}H and ^{13}C NMR chemical shift values of **EV2** are compatible with those reported for ergosterol peroxide (Figure 48) by Kim *et al*. (1997).

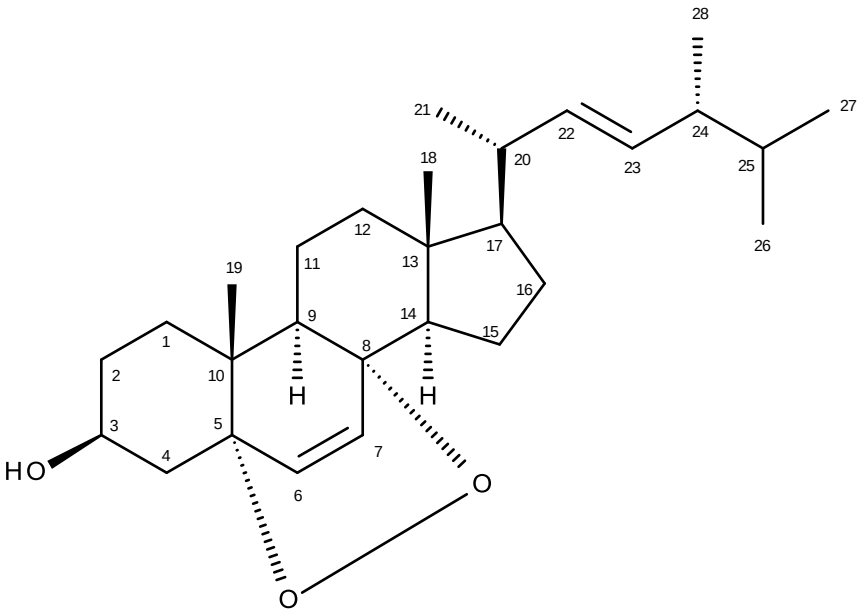

Figure 48. Structure of ergosterol peroxide (**EV2**).

Ergosterol (**EV1**) and ergosterol peroxide (**EV2**) belong to the subclass of modified triterpenoid steroids, which include several widely known drugs such as corticosteroids and cardioactive glycosides, several biological and physiologically relevant hormones, as well as phytosterols. Isolation of ergosterol and ergosterol peroxide from the extract of *E. variecolor* KUFC 7092 was not surprising since ergosterol is the predominant fungal sterol, representing approximately 70% of the sterols present in fungi. As a component of fungal membranes, ergosterol is involved in several biological functions such as membrane fluidity regulation, activity and distribution of integral proteins and control of the cellular cycle (Bard *et al*., 1993). Analogously, isolation of ergosterol peroxide is not unexpected since it has been reported as the H_2O_2-dependent enzymatic oxidation product of ergosterol (Bates *et al*., 1976).

Despite their wide distribution, both fungal steroids have been a focus of several reports regarding to their therapeutic potential. Apart from being the major precursor for the synthesis of vitamin D_2 (Holick, 2003), there are a number of reports on biologically active properties of ergosterol as well as of ergosterol peroxide.

Both ergosterol and its peroxide were reported as anti-inflammatory agents, suppressing LPS-induced inflammation in RAW 246.7 macrophages through the inhibition of NF-κB and C/EBPβ, as well as phosphorylation of MAPK's (Kobori *et al*., 2007). Kuo *et al*. (2011) have found that the anti-inflammatory action of ergosterol was also associated with the inhibition of COX-2 expression. In the previous study by Kobori *et al*. (2007), ergosterol peroxide was found to display growth inhibitory activity against colorectal adenocarcinoma HT29 cells, presumably as a result of the accumulation of ROS. In spite of the fact that antitumor molecular mechanisms of ergosterol and ergosterol peroxide are not clarified yet, there are several reports on their cytotoxic activity against a wide spectrum of cancer cell lines. While ergosterol displayed growth inhibitory activity against MCF-7 (breast adenocarcinoma) cell line (Subbiah and Abplanalp, 2003) and an inhibitory effect on rat urinary bladder carcinogenesis (Yazawa *et al*., 2000), ergosterol peroxide was shown to be cytotoxic against human hepatocellular carcinoma Hep 3B (Chen *et al*., 2009a) and human multiple myeloma U266 cells (Rhee *et al*., 2012), and against human gastric tumor (SNU-1), human hepatoma (SNU-354), human colorectal tumor (SNU-C4) and murine

sarcoma-180 cell lines (Nam *et al*., 2001). Additionally, ergosterol peroxide also exhibited inhibitory effect against androgen-sensitive (LNCaP) and –insensitive (DU-145) human prostate cancer cells at micromolar concentrations (Russo *et al*., 2010), as well as against several chemoresistant tumor cells (Wu *et al*., 2012). Interestingly, while ergosterol acts as a modulator of the cholesterol regulatory effect in cell cycle progression in human cells (Suárez *et al*., 2002), its peroxide displayed the anti-atherosclerotic activity, through the ihbition of hACAT-1 and Lp-PLA_2 (Kim *et al*., 2005). The biological properties of ergosterol peroxide include also antibacterial (Duarte *et al*., 2007) and trypanocidal activity (Ramos-Lignorio *et al*., 2012) against *Mycobacterium tuberculosis* and *Trypanosoma cruzi*, respectively, as well as renal fibrosis preventive effect (Zhu *et al*., 2013).

3.1.2. Structure Elucidation of Orcinol and 1*H*-Indole-3-carboxylic acid

3.1.2.1. Orcinol (EV3)

EV3 was isolated as colorless mass. The ^{13}C NMR, DEPT and HSQC spectra (Table 4) revealed the presence of three quaternary sp^2 (δ_C 157.8, 156.3, 141.0), three methine sp^2 (δ_C 112.1, 111.3, 103.4) and one methyl (δ_C 21.4) carbon. The ^1H NMR spectrum revealed the presence of three *meta*-coupled aromatic protons at δ_H 6.19, *dd*, *J* = 2.0, 2.0 Hz (δ_C 103.4), δ_C 6.30, *d*, *J* = 2.0 Hz, 2H (δ_C 112.1 and 111.3), and the aromatic methyl protons at δ_H 2.13, *s* (δ_C 21.4) (Table 4).

Table 4. ^1H and ^{13}C NMR data ($CDCl_3$, 300.13 and 75.47 MHz) of **EV3**.

Position	δ_C, type	δ_H, mult. (*J* in Hz)	HMBC
1	157.8, C	---	---
2	103.4, CH	6.19, *dd* (2.0, 2.0)	C-1, 3, 4, 6
3	156.3, C	---	---
4	112.1, CH	6.30, *d* (2.0)	C-2, 3, 6, 7
5	141.0, C	---	---
6	111.3, CH	6.30, *d* (2.0)	C-1, 2, 4, 7
7	21.4, CH_3	2.13, *s*	C-4, 5, 6

The low frequencies of the aromatic protons, together with high frequencies of the quaternary sp^2 carbons (δ_C 157.8 and 156.3) suggested the 1,3,5-

trissubstituted methylphenol. The HMBC spectrum (Table 4) showed cross peaks of the methyl singlet at δ_H 2.13 (δ_C 21.4) to the carbon at δ_C 141.0, 112.1 and 111.3; of the doublet at δ_H 6.30 (*J* = 2.0 Hz) to the carbons at δ_C 156.3, 112.1, 111.3, 103.4 and 21.4; and of the double doublet at δ_H 6.19 (*J* = 2.0, 2.0 Hz; δ_C 103.4) to the carbon at δ_C 157.8, 156.3, 112.1 and 111.3, thus suggesting the structure of **EV3** as 5-methylbenzene 1,3-diol.

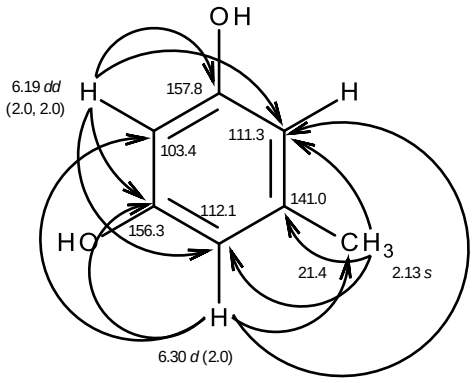

The ^{1}H and ^{13}C NMR data of **EV3** were in agreement with those reported for orcinol (Figure 49) by Gavin and Tabacchi (1975). Orcinol (**EV3**) has been also reported from the lichens *Evernia prunasti* (L.) A_{RCH} (Nomura *et al*., 2012) and *Parmotrema grayana* and was found to have antioxidant activity (Thadhani *et al*., 2011).

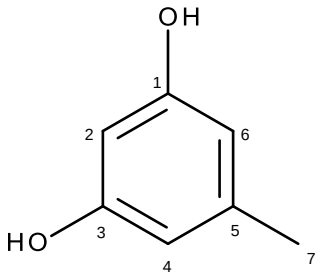

Figure 49. Structure of orcinol (**EV3**).

3.1.2.2. 1*H*-Indole-3-carboxylic acid (EV4)

EV4 was isolated as white amorphous solid. The ^{13}C NMR, DEPT and HSQC spectra (Table 5) revealed the presence of four quaternary sp^2 (δ_C 165.9,

136.4, 126.0, 107.3) and five methine sp^2 (δ_C 132.3, 122.1, 121.0, 120.6, 112.2) carbons.

Table 5. ^{1}H and ^{13}C NMR data (DMSO-d_6, 500.13 and 125.77 MHz) of **EV4**.

Position	δ_C, type	δ_H, mult. (*J* in Hz)	COSY	HMBC
2	132.3, CH	8.00, *s*	---	C-3, 8, 9
3	107.3, C	---	---	---
4	120.6, CH	8.00, *d* (7.6)	H-5	C-3, 6, 8
5	121.0, CH	7.15, *ddd* (7.6, 7.6, 1.3)	H-4, 6	C-7, 9
6	122.1, CH	7.19, *ddd* (7.6, 7.6, 1.3)	H-5, 7	C-4, 8
7	112.2, CH	7.46, *d* (7.6)	H-6	C-5, 9
8	136.4, C	---	---	---
9	126.0, C	---	---	---
10	165.9, CO	---	---	---
NH	---	11.81, *s*	---	---
OH	---	11.95, *brs*	---	---

The ^{1}H NMR spectrum (Table 5) displayed two doublets at δ_H 8.00 (*J* = 7.6 Hz) and δ_H 7.46 (*J* = 7.6 Hz), two double double doublets at δ_H 7.19 (*J* = 7.6, 7.6, 1.3 Hz) and δ_H 7.15 (*J* = 7.6, 7.6, 1.3 Hz), two singlets at δ_H 8.00 and 11.81, besides a broad singlet at δ_H 11.95.

The COSY spectrum (Table 5) exhibited cross peaks of the doublet at δ_H 8.0 (*J* = 7.6 Hz) to the double double doublet at δ_H 7.15 (*J* = 7.6, 7.6, 1.3 Hz), and of the doublet at δ_H 7.46 (*J* = 7.6 Hz) to the double double doublet at δ_H 7.19 (*J* = 7.6, 7.6, 1.3 Hz). In turn, the two double double doublets at δ_H 7.15 (*J* = 7.6, 7.6, 1.3 Hz) and 7.19 (*J* = 7.6, 7.6, 1.3 Hz) were correlated with each other, as well as with the doublets at δ_H 8.00 (*J* = 7.6 Hz) and 7.46 (*J* = 7.6 Hz), respectively, suggesting the presence of a 1,2-disubstituted benzene ring (**A**). This was confirmed by the correlations displayed by the HMBC spectrum (Table 5) which showed cross peaks of the doublet at δ_H 7.46 (*J* = 7.6 Hz; δ_C 112.2) to the sp^2 methine carbon at δ_C 121.0 and the sp^2 quaternary carbon at δ_C 126.0, and of the doublet at δ_H 8.0 (*J* = 7.6 Hz; 120.6) to the sp^2 methine carbon at δ_C 122.1 and the sp^2 quaternary carbon at δ_C 136.4.

Furthermore, the HMBC spectrum also exhibited cross peaks of the doublet at δ_H 8.00 (*J* = 7.6 Hz; δ_C 120.6) to the quaternary sp^2 carbon at δ_C 107.3, and of the singlet at δ_H 8.00 (δ_C 132.3) to the quaternary sp^2 carbons at δ_C 107.3 and 126.0, suggesting that one of the substituents of the 1,2-dissubstituted benzene ring was an ethenyl fragment (**B**). Since the singlet at δ_H 8.00 (δ_C 132.3) also

showed the HMBC cross peak to quaternary sp^2 carbon at δ_C 136.4, the cyclic nature of the substituents on the carbons at δ_C 126.0 and 136.4 was suggested (**B**). Moreover, the chemical shift value of the substituted aromatic carbon at δ_C 136.4 and of the olefinic carbon at δ_C 132.3 (δ_H 8.00, *s*) were characteristics of the nitrogen bearing sp^2 carbons.

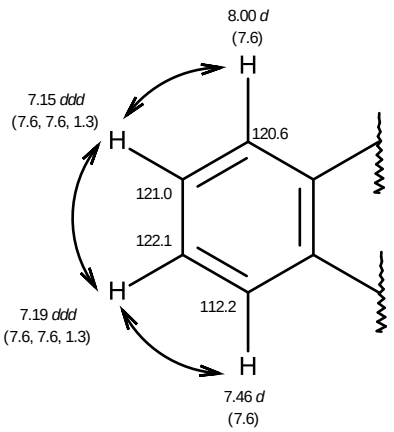

A

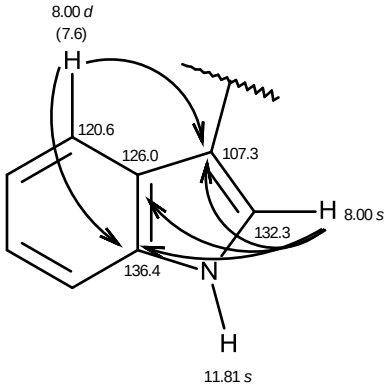

B

Since the ^{1}H NMR spectrum displayed a singlet at δ_H 11.81, the presence of the 2,3-dihydro-1*H*-indole rings system was proposed. That the substituent on C-3 (δ_C 107.3) of the indole moiety was the carboxyl group was supported by the presence of the carbon at δ_C 165.9, characteristic of the conjugated carbonyl, and a broad singlet at δ_H 11.95 in the ^{1}H NMR spectrum. This hypothesis was also supported by a low chemical shift value of C-3 (δ_C 107.3) which is characteristic of the sp^2 carbon with the electron withdrawing substituent. Consequently the structure of **EV4** was proposed as:

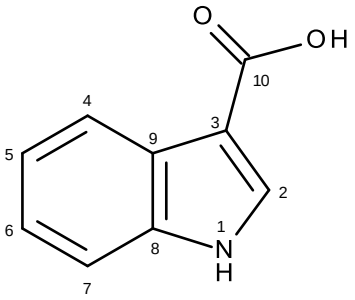

Figure 50. Structure of 1*H*-indole-3-carboxylic acid (**EV4**).

Literature survey revealed that the structure of **EV4** corresponded to the monoindole alkaloid 1*H*-indole-3-carboxylic acid (Figure 50) (Wang *et al*., 2012) previously reported not only from fungi (Wu *et al*., 2013) but also from several other sources such as *Streptomyces* sp. (Kavitha *et al*., 2010, Shaaban *et al*., 2008), plant pathogens (Tan *et al*., 2004) and marine sponges (Wang *et al*., 2012). 1*H*-Indole-3-carboxylic acid proved to be a promising antimicrobial agent, displaying good antibacterial activity not only against the Gram-positive bacteria *Staphylococcus aureus* and *Staphylococcus epidermis*, but also against the Gram-negative *Escherichia coli* and *Xanthomonas campestris*. Additionally, the monoindole alkaloid exhibited also good antifungal activity against dermatophytes such as *Candida albicans* and *Epidermophyton flocosum*, as well as strong growth inhibitory activity against *Fusarium oxysporum* (Kavitha *et al*., 2010).

3.1.3. Structure Elucidation of Anthraquinones

3.1.3.1. Erythroglaucin (EC1)

EC1 was isolated as red needles. The ^{1}H NMR spectrum (Table 6) exhibited the signals of three hydrogen-bonded hydroxyl groups at δ_H 13.75, *s*, 12.46, *s* and 12.38, *s*, in addition to three doublets of the aromatic protons at δ_H 7.41 (*J* = 2.5 Hz), 7.14 (*J* = 0.8 Hz) and 6.71 (*J* = 2.5 Hz), and a methyl doublet at 2.36 (*J* = 0.8 Hz). The ^{13}C NMR spectrum (Table 6) displayed sixteen carbon signals which, through DEPT (90º and 135º) and HSQC spectra (Table 6), were categorized into two conjugated ketone carbonyls (δ_C 188.9, 186.5), nine quaternary sp^2 (δ_C 166.4, 165.2, 157.9, 157.2, 140.7, 135.1, 111.8, 110.6, 110.5), three methine sp^2 (δ_C 129.3, 105.4, 106.9), one methoxy (δ_C 56.2) and one methyl (δ_C 16.5) carbons.

The COSY spectrum (Table 6) showed correlations between the *meta*-coupled aromatic protons at δ_H 6.71, *d* (*J* = 2.5 Hz; δ_C 106.9) and δ_H 7.41, *d* (*J* = 2.5 Hz; δ_C 105.4) on the one hand, and between the aromatic proton at δ_H 7.14, *d* (*J* = 0.8 Hz; δ_C 129.3) and the methyl protons at δ_H 2.36, *d* (*J* = 0.8 Hz; δ_C 16.5) on the other hand, suggesting the presence of one 1,2,3,4,6-pentasubstituted and one 1,2,3,5-tetrasubstituted benzene rings in the molecule.

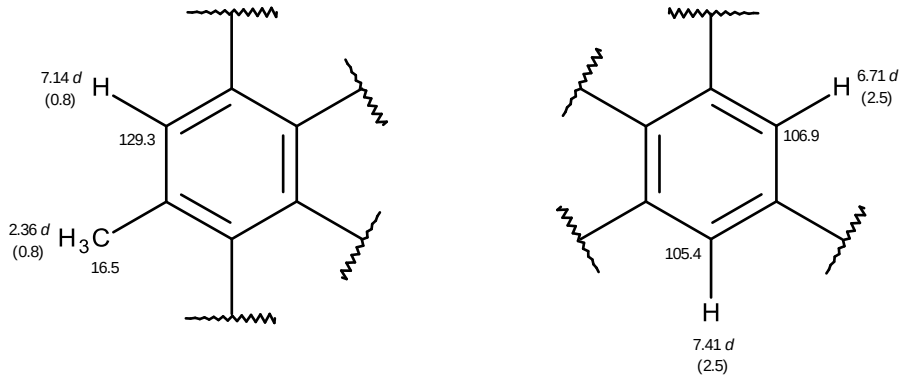

Table 6. ^{1}H and ^{13}C NMR data ($CDCl_3$, 500.13 and 125.77 MHz) of **EC1**.

Position	δ_C, type	δ_H, mult. (*J* in Hz)	COSY	HMBC
1	157.2, C	---	---	---
2	129.3, CH	7.14, *d* (0.8)	H-11	C-4, 9a, 11
3	140.7, C	---	---	---
4	157.9, C	---	---	---
4a	111.8, C	---	---	---
5	105.4, CH	7.41, *d* (2.5)	H-7	C-7, 8a, 10
6	166.4, C	---	---	---
7	106.9, CH	6.71, *d* (2.5)	H-5	C-5, 8, 8a
8	165.2, C	---	---	---
8a	110.5, C	---	---	---
9	188.9, CO	---	---	---
9a	110.6, C	---	---	---
10	186.5, CO	---	---	---
10a	135.1, C	---	---	---
11	16.5, CH_3	2.36, *d* (0.8)	H-2	C-2, 3, 4
OCH_3-6	56.2, CH_3	3.95, *s*	---	C-6
OH-1	---	12.38, *s*	---	C-1, 2, 9a
OH-4	---	13.75, *s*	---	C-3, 4, 4a
OH-8	---	12.46, *s*	---	C-7, 8, 8a

The HMBC spectrum (Table 6) showed correlations of the hydrogen-bonded hydroxyl proton at δ_H 12.38, s to the carbons at δ_C 157.2, 129.3, and 110.6, of another hydrogen-bonded hydroxyl proton at δ_H 13.75, *s*, to the carbons at δ_C 157.9, 140.7 and 111.8, of the methyl protons at δ_H 2.36, *d* (*J* = 0.8 Hz; δ_C 16.5) to the carbons at δ_C 140.7, 129.3 and 157.9, as well as of the aromatic proton at δ_H 7.14, *d* (*J* = 0.8 Hz; δ_C 129.3) to the carbons at δ_C 110.6 and 157.9, suggesting that the 1,2,3,4,6-pentasubstituted benzene was part of the system shown below:

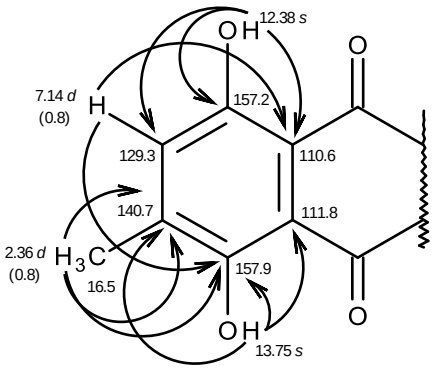

That three of the substituents of the 1,2,3,5-tetrasubstituted benzene ring were hydroxyl, methoxy and the carbonyl groups was substantiated by the HMBC correlations of the aromatic proton at δ_H 6.71, *d* (*J* = 2.5 Hz; δ_C 106.9) to the carbons at δ_C 110.5 and 105.4, of the aromatic proton at δ_H 7.41, *d* (*J* = 2.5 Hz; δ_C 105.4) to the carbons at δ_C 186.5, 110.5 and 106.9, of the hydrogen-bonded hydroxyl proton at δ_H 12.46, *s* to the carbons at δ_C 165.2, 106.9 and 110.5, and of the methoxy proton at δ_H 3.95, *s* (δ_C 56.2) to the carbon at δ_C 166.4.

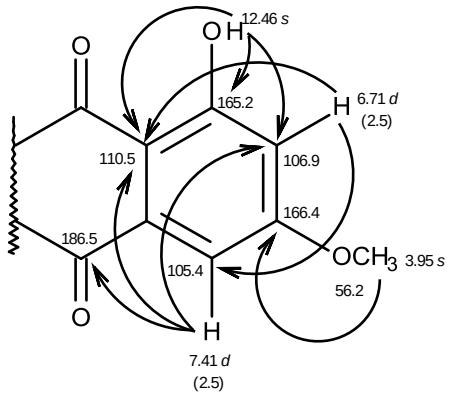

Combining these two partial structures led to the structure of **EC1** as 1,4,8-trihydroxy-6-methoxy-3-methylanthracene-9,10-dione. The NMR data of **EC1** were compatible with those reported for erythroglaucin (Figure 51), the anthraquinone isolated from different species of the genus *Eurotium* (Anke *et al*., 1980). Erythroglaucin has not only been reported as a metabolic product from different genus of microfungi, namely *Alternaria* (Andersen *et al*., 2008; Suemitsu *et al*., 1977), but also from macrofungi (Beattie *et al*., 2010) and several lichens of different genera (Manojlović *et al*., 2000; Sochting and Frödén, 2002).

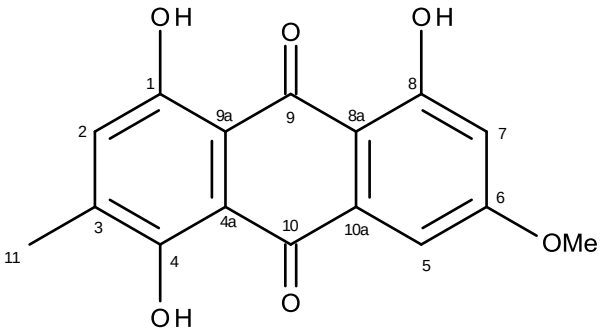

Figure 51. Structure of erythroglaucin (**EC1**).

Regarding to its biological properties, this anthraquinone was reported to have antibacterial activity against *Pseudomonas fluorescens* and *Pseudomonas glicinea*, and antifungal activity against human pathogenic fungi including *Aspergillus niger*, *Doratomyces stemonitis*, *Penicillium verucosum* and *Trichoderma viride* (Manojlović *et al*., 2000). Interestingly, erythroglaucin was found to cause DNA cleavage through photo-induced production of ROS (Rajendran *et al*., 2004). It displayed also moderate radical-scavenging activity against DPPH (Wang *et al*., 2006). Erythroglaucin was shown to display structure-uncoupling activity using rat liver mitochondria (Betina and Kuzela, 1987), as well as iron-chelating capability (Engstrom *et al*., 1982).

3.1.3.2. Physcion (EC2)

EC2 was isolated as orange needles, and the general features of its ^{1}H and ^{13}C NMR spectra closely resembled those of **EC1**. However, the ^{1}H NMR spectrum (Table 7) revealed the presence of two hydrogen-bonded hydroxyl groups at δ_H 12.13, *s* and δ_H 12.33, *s*, four aromatic protons at δ_H 6.69, *d* (*J* = 2.5 Hz), 7.09, *d* (*J* = 0.8 Hz), 7.38, *d* (*J* = 2.5 Hz) and 7.64, *d* (*J* = 0.8 Hz), one methoxy group (δ_H 3.94, *s*) and one aromatic methyl group (δ_H 2.46, *s*). The ^{13}C NMR spectrum (Table 7) displayed also sixteen carbon signals which were categorized, according to DEPT (90º and 135º) and HSQC (Table 7), as two ketone carbonyls (δ_C 195.9, 182.1), eight quaternary sp^2 (δ_C 166.5, 165.2, 162.5, 148.5, 135.2, 133.2, 114.0, 110.3), four methine sp^2 (δ_C 125.5, 121.3, 108.2,

106.8), one methoxy (δ_C 56.1) and one methyl (δ_C 22.2) carbon, suggesting the anthraquinone nucleus.

Table 7. ^{1}H and ^{13}C NMR data ($CDCl_3$, 500.13 and 125.77 MHz) of **EC2**.

Position	δ_C, type	δ_H, mult. (*J* in Hz)	HMBC
1	162.5, C	---	---
2	125.5, CH	7.09, *d* (0.8)	C-4, 9a, 11
3	148.5, C	---	---
4	121.3, CH	7.64, *d* (0.8)	C-2, 9a, 10, 11
4a	133.2, C	---	---
5	108.2, CH	7.38, *d* (2.5)	C-7, 8a, 10
6	166.5, C	---	---
7	106.8, CH	6.69, *d* (2.5)	C-5, 8, 8a
8	165.2, C	---	---
8a	110.3, C	---	---
9	195.9, CO	---	---
9a	114.0, C	---	---
10	182.1, CO	---	---
10a	135.2, C	---	---
11	22.2, CH_3	2.46, *s*	C-2, 3, 4
OCH_3-6	56.1, CH_3	3.94, *s*	C-6
OH-1	---	12.13, *s*	C-1, 2, 9a
OH-4	---	---	---
OH-8	---	12.33, *s*	C-7, 8, 8a

That one of the 1,2,3,5-tetrasubstituted benzene rings was a 1-hydroxy-3-methoxybenzene ring of the anthraquinone was corroborated not only by the chemical shift values of the aromatic protons and their corresponding carbons (δ_H 6.69, *d*, *J* = 2.5 Hz; δ_C 106.8 / δ_H 7.38, *d*, *J* = 2.5 Hz; δ_C 108.2) and the hydrogen-bonded hydroxyl group at δ_H 12.33, *s*, but also by the HMBC correlations of the hydroxyl proton at δ_H 12.33, *s* to the carbons at δ_C 165.2, 110.3 and 106.8, of the aromatic proton at δ_H 6.69, *d* (*J* = 2.5 Hz; δ_C 106.8) to the carbon at δ_C 165.2, 108.2 and 110.3, and of the aromatic proton at δ_H 7.38, *d* (*J* = 2.5 Hz; δ_C 108.2) to the carbons at δ_C 110.3 and 106.8 and to the carbonyl carbon at δ_C 182.1. That another part of the anthraquinone was a 1-hydroxy-3-methylbenzene was supported by the presence of the hydrogen-bonded hydroxyl proton at δ_H 12.13, *s*, which gave HMBC correlations to the carbons at δ_C 162.5, 125.5 and 114.0, and the methyl singlet at δ_H 2.46 (δ_C 22.2) which, in turn, gave HMBC correlations to the carbons at δ_C 148.5, 125.5, and 121.3, as well as the HMBC correlations of the doublet of the aromatic proton at δ_H 7.64 (*J* = 0.8 Hz; δ_C 121.3) to the carbonyl at

δ_C 182.1, the methyl carbon at δ_C 22.2, and the aromatic carbons at δ_C 125.5 and 114.0.

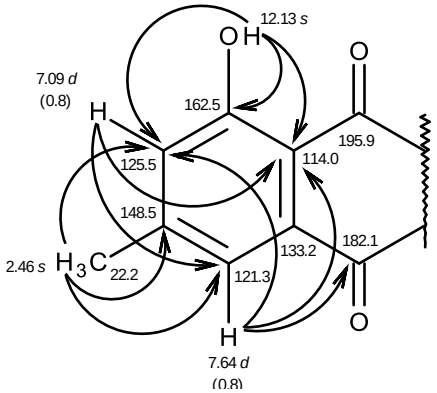

Thus the structure of **EC2** was proposed as 1,8-dihydroxy-6-methoxy-3-methylanthracene-9,10-dione. The ^{1}H and ^{13}C NMR data of **EC2** was compatible with those of physcion (Figure 52), the pigment isolated from several species of the genus *Eurotium* (Anke *et al*., 1980).

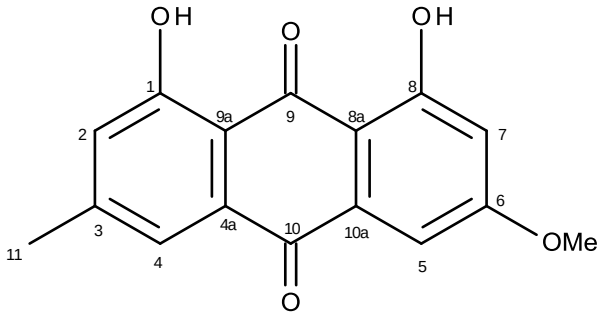

Figure 52. Structure of physcion (**EC2**).

Physcion was reported not only from different fungal species, mainly from *Aspergillus* (Li *et al*., 2014; Yang *et al*., 2013a) and *Microsporum* genera (Wijesekara *et al*., 2014), and from lichens (Bačkorová *et al*., 2012), but also as a pigment from several plant species, especially from the genus *Rheum* (Agarwal *et al*., 2000; Choi *et al*., 2013; Feng *et al*., 2013), *Cassia* (Jain *et al*, 2013; Kim *et al*., 2004) and *Polygonum* (Leu *et al*., 2008; Qiu *et al*., 2013).

The biological activities of physcion are vast and cover a wide range of potentially useful therapeutic properties. Like erythroglaucin, physcion exhibited strong to moderate antifungal activity not only against the human pathogenic fungi *Candida albicans*, *Cryptococcus neoformans* and *Trichophyton mentagrophytes* (Agarwal *et al*., 2000), but also against plant pathogenic fungi such as *Botrytis cinerea*, *Erysiphe graminis*, *Phytophthera infestans* and *Rhizoctomia solani* (Kim *et al*., 2004). Recently, the antiproliferative properties of physcion were reported. It displayed inhibitory activity against human cervical carcinoma HeLa cells by causing apoptosis with formation of intracellular free radicals like ROS, as well as through the regulation of Bcl-2 and Bax expression, and activation of caspase-3 pathway (Wijisekara *et al*., 2014). Additionally, the compound exhibited also *in vitro* cytotoxic activity against the human cancer cell lines A375 (malignant skin melanoma), Hep2 (epidermoid laryngeal carcinoma) and U937 (lymphoma). Anti-inflammatory properties of physcion were also reported in the same study, presumably due to the inhibition of the expression of iNOS protein (Gosh *et al*., 2010). In other recent study, physcion was classified as a potentially usefull agent for diabetic nephropathy treatment, due to its inhibitory activity on the secretion of IL-6 in high-glucose-induced mesangial cells, and by causing significant decrease on the production of collagen IV and fibronectin (Yang *et al*., 2013a). Furthermore, the suppression of IL-1β and protein expression of ICAM-1 and caspase-3 were associated with physcion protective effects against cerebral injury (Zhang *et al*., 2005). However, the most interesting biological property of physcion refers to its potent tyrosinase inhibitory activity which together with the great percutaneous absorption classified the compound as a potentially useful skin-whitening agent (Leu *et al*., 2008). Physcion also exhibited iron-chelating capability (Engstrom *et al*., 1982).

3.1.3.3. Catenarin (EC3)

EC3 was isolated as dark orange amorphous solid. The ^{1}H and ^{13}C NMR data (Table 8) closely resembled those of **EC1**, except for the lack of the methoxy substituent, suggesting a similar structure to that of **EC1**. The ^{13}C NMR and HSQC spectra (Table 8) revealed the presence of fifteen carbon signals, which were categorized as two hydrogen bonded ketone carbonyls (δ_C 187.5, 186.3), nine

quaternary sp^2 (δ_C 166.4, 164.6, 156.7, 156.0, 139.6, 134.7, 111.6, 110.2, 108.7), three methine sp^2 (δ_C 129.2, 108.8, 108.3) and one methyl (δ_C 15.9) carbon. The ^{1}H NMR spectrum (Table 8) revealed the presence of three hydrogen-bonded hydroxyl protons at δ_H 13.17, *brs* and at δ_H 12.16 *brs* (2OH), three aromatic protons at δ_H 7.23, *s*, 7.10, *d* (*J* = 2.4 Hz), 6.53, *d* (*J* = 2.4 Hz) and one aromatic methyl group at δ_H 2.24, *s*.

Table 8. ^{1}H and ^{13}C NMR data (DMSO-d_6, 300.13 and 75.47 MHz) of **EC3**.

Position	δ_C, type	δ_H, mult. (*J* in Hz)	HMBC
1	156.0, C	---	---
2	129.2, CH	7.23, *s*	C-4, 9a, 11
3	139.6, C	---	---
4	156.7, C	---	---
4a	111.6, C	---	---
5	108.8, CH	7.10, *d* (2.4)	C-7, 8a, 10
6	166.4, C	---	
7	108.3, CH	6.53, *d* (2.4)	C-5, 8, 8a
8	164.6, C	---	---
8a	108.7, C	---	---
9	187.5, CO	---	---
9a	110.2, C	---	---
10	186.3, CO	---	---
10a	134.7, C	---	---
11	15.9, CH_3	2.24, *s*	C-2, 3, 4
OH-1	---	12.16, *brs*	---
OH-4	---	13.17, *brs*	---
OH-6	---	ND	---
OH-8	---	12.16, *brs*	---

ND Not detected

The HMBC spectrum (Table 8) displayed correlations of the aromatic proton at δ_H 7.23, *s* (δ_C 129.2) to the carbons at δ_C 156.7, 110.2, 15.9, and of the methyl protons at δ_H 2.24, *s* (δ_C 15.9) to the carbons at δ_C 156.7, 139.6 and 129.2, confirming the existence of the 1,4-dihydroxy-5-methyl benzene moiety analogously to **EC1**. In turn, the HMBC cross peaks of the doublet of the proton at δ_H 7.10 (*J* = 2.4 Hz; δ_C 108.8) to the carbons at δ_C 186.3, 108.7, 108.3, as well as of the doublet at δ_H 6.53 (*J* = 2.4 Hz; δ_C 108.3) to the carbons at δ_C 164.6, 108.8 and 108.7, determined a 1,5-dihydroxybenzene ring structure.

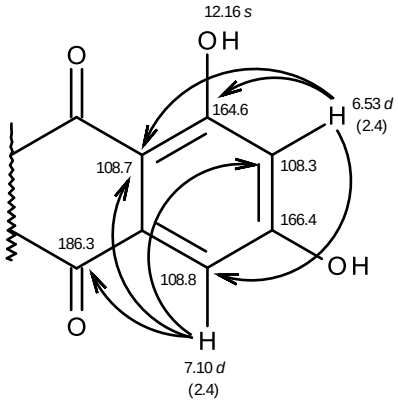

Combination of the two partial structures led to the structure of **EC3** as 1,4,6,8-tetrahydroxy-3-methylanthracene-9,10-dione. The ^{1}H and ^{13}C NMR data of **EC3** are compatible with those reported for catenarin (Figure 53), the anthraquinone isolated from *Eurotium cristatum* (Anke *et al*., 1980).

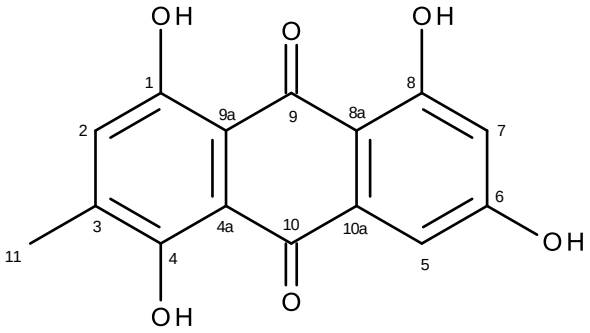

Figure 53. Structure of catenarin (**EC3**).

Like erythroglaucin and physcion, catenarin was also identified as a metabolic product of several fungal species of the genus *Eurotium* (Anke *et al*., 1980; Du *et al*., 2008). Catenarin was originally isolated from several species of the plant pathogenic fungi of the genus *Helminthosporium* (Raistrick *et al*., 1933; 1934) and later from other plant pathogens such as *Pyrenophora tritici-repentis* (Wakuliński *et al*., 2003) and *Talaromyces stipitatus* (van Eijk, 1973), as well as from the shrub *Ventilago leiocarpa* Benth. (Lin *et al*., 2001).

Catenarin also exhibited antibacterial activity namely against the Gram-positive bacteria *Aureobacterium liquefaciens*, *Arthrobacter globiformis*, *Bacillus brevis*, *Bacillus circulans*, *Bacillus subtilis* and *Curtobacterium plantarum*, as well

as antifungal activity against *Epicoccum nigrum* (Wakuliński *et al*., 2003). Catenarin was found to prevent type 1 diabetes in non-obese diabetic mice through a strong suppressive effect on leukocyte migration, which involved the inactivation of the MKK6/p38 and MKK7/JNK signaling cascades and the reduction of calcium influx in the CCR5 and CXCR4 pathways in T cells (Shen *et al*., 2012).

3.1.3.4. Emodin (EC4)

EC4 was isolated as yellow amorphous solid and its ^{1}H and ^{13}C NMR data (Table 9) closely resembled those of **EC2**. However, the ^{1}H and ^{13}C NMR spectra of **EC4** did not exhibit the signal of a methoxy group. The ^{13}C NMR spectrum displayed fifteen carbon signals which were categorized, according to DEPT (90º and 135º) and HSQC (Table 9), as two ketone carbonyls (δ_C 189.6, 181.4), eight quaternary sp^2 (δ_C 165.8, 164.6, 161.4, 148.2, 135.0, 132.8, 113.3, 108.8), four methine sp^2 (δ_C 124.1, 120.5, 108.9, 107.9) and one methyl (δ_C 21.5) carbons. The ^{1}H NMR spectrum (Table 9) displayed two pairs of *meta*-coupled aromatic protons at δ_H 7.45, *d* (*J* = 1.2 Hz) / 7.14, *d* (*J* = 1.2 Hz), and at 7.08, *d* (*J* = 2.4 Hz) / 6.56, *d* (*J* = 2.4 Hz), as well as one aromatic methyl group at δ_H 2.39, *s*.

Table 9. ^{1}H and ^{13}C NMR data (DMSO-d_6, 500.13 and 125.77 MHz) of **EC4**.

Position	δ_C, type	δ_H, mult. (*J* in Hz)	HMBC
1	161.4, C	---	---
2	124.1, CH	7.14, *d* (1.2)	C-1, 4, 9a, 11
3	148.2, C	---	---
4	120.5, CH	7.45, *d* (1.2)	C-2, 9a, 10, 11
4a	132.8, C	---	---
5	108.9, CH	7.08, *d* (2.4)	C-6, 7, 8a, 10
6	165.8, C	---	---
7	107.9, CH	6.56, *d* (2.4)	C-5, 8, 8a
8	164.6, C	---	---
8a	108.8, C	---	---
9	189.6, CO	---	---
9a	113.3, C	---	---
10	181.4, CO	---	---
10a	135.0, C	---	---
11	21.5, CH_3	2.39, *s*	C-2, 3, 4
OH-1		12.00, *brs*	---
OH-6		ND	---
OH-8		12.00, *brs*	---

ND Not detected

The chemical shift values of the two *meta*-coupled aromatic protons at δ_H 7.08, *d* (*J* = 2.4 Hz; δ_C 108.9) and 6.56, *d* (*J* = 2.4 Hz; δ_C 107.9), and the HMBC correlations (Table 9) of the unshielded aromatic proton at δ_H 7.08, *d* (*J* = 2.4 Hz; δ_C 108.9) to the non-hydrogen bonded carbonyl at δ_C 181.4 and to the carbons at δ_C 165.8, 108.8, 107.9, and of the shielded aromatic proton at δ_H 6.56, *d* (*J* = 2.4 Hz; δ_C 107.9) to the carbons at δ_C 164.6, 108.9, 108.8, revealed the existence of the 6,8-dihydroxybenzene ring of the anthraquinone.

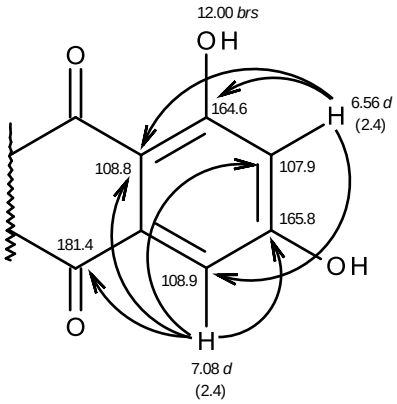

The existence of the 1-hydroxy-5-methyl benzene moiety of the anthraquinone was corroborated by the HMBC cross peaks of the doublet at δ_H 7.45 (*J* = 1.2 Hz; δ_C 120.5) to the non-hydrogen bonded carbonyl carbon at δ_C 181.4 and the carbons at δ_C 124.1, 113.3, 21.5, of the doublet at δ_H 7.14 (*J* = 1.2 Hz; δ_C 124.1) to the carbons at δ_C 161.4, 120.5, 113.3, 21.5, as well as of the methyl singlet at δ_H 2.39 (δ_C 21.5) to the carbons at δ_C 148.2, 124.1 and 120.5.

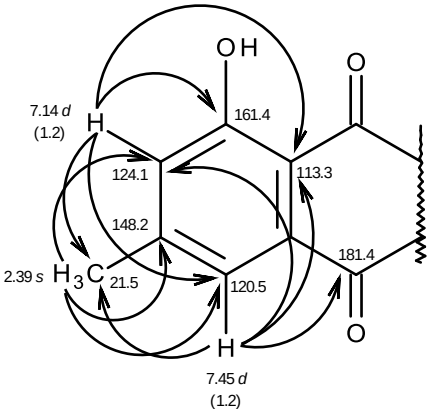

Therefore, the structure of **EC4** was proposed as 1,6,8-trihydroxy-3-methylanthracene-9,10-dione, or commonly known as emodin (Figure 54). The ^{1}H and ^{13}C NMR data of **EC4**, as well as its physical constants were compatible with those of the anthraquinone emodin, reported earlier from several species of the lichens of the genus *Xanthoria* (Manojlović *et al*., 2000).

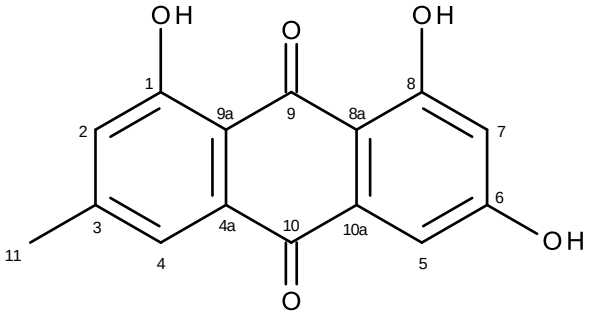

Figure 54. Structure of emodin (**EC4**).

Despite its isolation from the fungi of the genus *Eurotium* (Anke *et al*., 1980), emodin has been widely reported from several plant genera including *Cassia* (Kim *et al*., 2004; Lee *et al*., 2010), *Frangula* (Kremer *et al*., 2012) and *Polygonum* (Hsiang and Ho, 2008; Kuo *et al*., 1997; Leu *et al*, 2008), and as a major constituent of rhubarb, *Rheum palmatum* L. (Chen *et al*., 2002; 2010a; Choi *et al*., 2013).

Emodin is the most extensively studied anthraquinone which displayed a vast number of pharmacological properties such as antitumor, immunosuppressive, antimicrobial, anti-inflammatory and antidiabetic. Literature survey reveals several reports on its cytotoxic activity against several human cancer cell lines through several different mechanisms (Hsu and Chung, 2012). Emodin exhibited antiproliferative effect against Raji, HeLa, Calu-1 Wish, Vero, SW620 and K562 cell lines (Choi *et al*., 2007; Kuo *et al*., 1997; Lin *et al*.,2001), with a notable antitumor effect in human leukemia K562 cell line, both *in vitro* and *in vivo*, leading to a significant decrease of tumor volume and weight in nude mice inoculated with K562 cells (Chun-Guang *et al*., 2010). However, the majority of reports refer to the anticancer potential of emodin against human pancreatic and liver cancer cell lines. Emodin demonstrated antiproliferative and antimetastatic

effect on human pancreatic cancer cell line SW 1999 (Liu *et al*., 2011a) and induced Panc-1 cells apoptosis through the decline of the mitochondrial membrane potential (Liu *et al*., 2012). Furthermore, it also potentiated the antitumor effects of gemcitabine in human pancreatic cancer cell line SW 1999, which was related to the downregulation of NF-κB, leading to an enhancement on the effect of gemcitabine and overcoming resistance (Liu *et al*., 2011b). Interestingly, emodin displayed the synergistic property of overcoming chemoresistance in several cancer cell lines, significantly enhancing the DNA damage caused by oxaliplatin and inducing oxaliplatin resistance reversal in hepatocellular carcinoma HepG2 cells, through the inhibition of ERCC1 expression by the FGFR2/ERK1/2 signaling pathway (Chen *et al*., 2013). Notably, emodin was reported to display antiproliferative activity against other human liver cancer cells such as SK-HEP-1, Bel-7402 and PLC/PRF/5, through several complementary mechanisms including the activation of caspase-8 and -9, p53 and p21 upregulation, NF-κB downregulation, and intracellular ROS production (Shieh *et al*., 2004; Yu *et al*., 2013). Emodin was also proved to be an effective apoptosis inducer in human promyeloleukemic HL-60 and in C6 glioma cells through the activation of the caspase-3 cascade (Chen *et al*., 2002; Kuo *et al*., 2009), and the antiproliferative activity against prostate cancer cell lines LNCaP and PC-3, as well as against the human lung (A549) and bone (MG-63) cell lines, also seems to be partially dependent on the generation of ROS (Masaldan and Iyer, 2014). The antimetastatic activity was also observed in prostate DU 145 and lung A549 cancer cell lines by downregulation of the expression of the chemokine receptor CXCR4 (Ok *et al*., 2012). Zhang *et al*. (1999) reported that emodin was a potent tyrosine kinase inhibitor and repressed cellular transformation and metastasis in breast cancer cells (Zhang *et al*., 1999; Zhang and Hung, 1996). Recently, the antiproliferative effect on breast cancer cell lines was reported as being associated with the downregulation of the estrogen receptor α (ERα) protein levels, thereby suppressing ERα transcriptional activation in MCF-7 and MDA-MB-453 cell lines (Huang *et al*., 2013). These findings led us to hypothesize that the *in vitro* anticancer activity of the crude extract of *Eurotium cristatum* KUFC 7356 against MCF-7 cancer cell line (Almeida *et al*., 2010) may be in part derived from emodin cytotoxic activity. Additionally, emodin was found to inhibit the migration and invasion in human tongue cancer SCC-4 cells through the inhibition of gene

expression of MMP-9 and MMP-2 (Chen *et al*., 2010a) and by inducing DNA damage and inhibiting DNA repair gene expression (Chen *et al*., 2010b). Recently, emodin was also classified as a potential new therapeutic drug for head and neck squamous cell carcinoma cancer due to its *in vivo* inhibitory activity of *TWIST1*-induced invasions, and inhibition of the β-catenin and Akt pathways (Way *et al*., 2014). Immunosuppressive properties of emodin have also been reported demonstrating a helpful effect for the modulation of immune suppression and induction of immune tolerance through the inhibition of the differentiation and maturation of dendritic cells and increased production of $CD4^+CD25^+$ T cells (Zhang *et al*., 2012). Emodin immunosuppressive properties were confirmed by the immunosuppressive effect mediated through the generation of hydrogen peroxide from semiquinone and regulation by arachidonic acid metabolites (Huang *et al*., 1992), and the *in vivo* effect alleviating acute rejection following liver transplantation in rats as prolonging liver allograft survival (Tong *et al*., 2011). Administration of emodin against LPS-induced mouse mastitis revealed a protective effect against LPS-induced mammary gland injury and inflammatory cell infiltration by decreasing the transcriptional production of proinflammatory cytokines TNF-α, IL-6 and IL-1β (Li *et al*., 2013b). The anti-inflammatory properties of emodin were also observed in other *in vivo* models, displaying an effective anti-inflammatory response in collagen-induced arthritic mice through the inhibition of the NF-κB pathway and subsequent MMP production (Hwang *et al*., 2013) as well as a significant reduction of oedema volume in carrageenan-induced rat-paw model through iNOS inhibition (Gosh *et al*., 2010). Recently, the *in vitro* anti-inflammatory activity of emodin on LPS-induced RAW264.7 macrophages was also reported, supposedly due to the inhibition of P-gp function caused by the decreased expression of COX-2 protein through the MAPK/AP1 pathway (Choi *et al*., 2013). Emodin revealed also therapeutic potential in the prevention or treatment of glucose-induced structural and functional abnormalities, due to the amelioration of glucose-induced TGF-β1 and matrix synthesis in human peritoneal mesothelial cells by inhibiting PKCα activation and phosphorylation of CREB (Chan *et al*., 2003). Furthermore, emodin exhibited potent and selective *in vitro* and *in vivo* inhibitory activity against 11β-hydroxysteroid dehydrogenase type 1, and its oral administration in diet-induced obese mice antagonized insulin resistance and lowered blood glucose and hepatic PEPCK (Feng *et al*., 2010; Liu

et al., 2009). Recently, it was also reported to cause a significant decrease of collagen IV and fibronectin production (Yang *et al*., 2013a), revealing a potential use not only in diabetic nephropathy but also generally in metabolic syndrome or type 2 diabetes. Its potential in the treatment of progressive renal diseases was also confirmed by the amelioration of renal failure in nephrectomized rats treated with emodin, due to the suppression of IL-1β induced mesangial cells proliferation (Wang *et al*., 2007). The potent *in vivo* anti-angiogenic effect through the inhibitory function toward VEGF-A –induced angiogenesis by blocking receptor-2 (KDR/Flk-1) phosphorylation (Kwak *et al*., 2006) as well as the *in vitro* anticoagulation effect of emodin-eluting biodegradable polymer coating stents (Pan *et al*., 2010), turn emodin as an interesting candidate for the development of alternative drugs for the treatment of cardiovascular diseases. When administered orally in IgE-sensitized mice, emodin exhibited anti-allergic activity, suppressing IgE-mediated anaphylactic reaction and mast cell activation (Lu *et al*., 2011). Emodin was also demonstrated to be a potential candidate for the development of antipigmentation agents due to its inhibition of phosphorylation of Kit and other transmembrane tyrosine kinases, and subsequent melanin synthesis (Lee *et al*., 2010). Emodin exhibited antimicrobial activity against several human pathogenic fungi and bacteria such as *Aspergillus niger*, *Doratomyces stemonitis*, *Trichoderma viride* and *Penicillium verucosum*, and against the bacteria *Pseudomonas fluorescens*, *Pseudomonas glicinea*, *Pseudomonas phaseolicola* (Manojlović *et al*., 2000), *Streptococcus iniae* (Nakano *et al*., 2012) and *Helicobacter pylori* strains SS1 and ATCC 43504 (Chen *et al*., 2009b), respectively. Emodin displayed also antiviral activity against herpes simplex virus (HSV) type 1, through the inhibition of HSV-1 UL12 alkaline nuclease (Hsiang and Ho, 2008).

3.1.3.5. Questin (EC5)

EC5 was isolated as orange-yellow amorphous solid and its ^{1}H and ^{13}C NMR spectra (Table 10) were very similar to those of **EC2**. The ^{1}H spectrum (Table 10) displayed the signals of one hydrogen-bonded hydroxyl proton at δ_H 13.24, *s*, two pairs of *meta*-coupled aromatic protons at δ_H 7.42, *d* (*J* = 1.6 Hz) / 7.12, *d* (*J* = 1.6 Hz), and at δ_H 7.20, *d* (*J* = 2.3 Hz) / 6.84, *d* (*J* = 2.3 Hz), one methoxy group at δ_H 3.90, *s* and one methyl group at δ_H 2.39, *s*. The ^{13}C NMR,

DEPT and HSQC spectra (Table 10) revealed the presence of one hydrogen-bonded carbonyl (δ_C 186.3), one non hydrogen-bonded carbonyl (δ_C 182.3), eight quaternary sp^2 (δ_C 164.4, 163.4, 161.7, 146.6, 136.8, 132.0, 114.4, 112.6), four methine sp^2 (δ_C 124.2, 119.1, 106.9, 104.9), one methoxy (δ_C 56.3) and one methyl (δ_C 21.4) carbon.

Table 10. ^{1}H and ^{13}C NMR data (DMSO-d_6, 300.13 and 75.47 MHz) of **EC5**.

Position	δ_C, type	δ_H, mult. (*J* in Hz)	HMBC
1	161.7, C	---	---
2	124.2, CH	7.12, *d* (1.6)	C-4, 9a, 11
3	146.6, C	---	---
4	119.1, CH	7.42, *d* (1.6)	C-2, 9a, 10, 11
4a	132.0, C	---	---
5	106.9, CH	7.20, *d* (2.3)	C-7, 8a, 10
6	164.4, C	---	---
7	104.9, CH	6.84, *d* (2.3)	C-5, 6, 8a
8	163.4, C	---	---
8a	112.6, C	---	---
9	186.3, CO	---	---
9a	114.4, C	---	---
10	182.3, CO	---	---
10a	136.8, C	---	---
11	21.4, CH_3	2.39, *s*	C-2, 3, 4
OCH_3-8	56.3, CH_3	3.90, *s*	C-8
OH-1	---	13.24, *s*	---
OH-6	---	ND	---

ND Not detected

The chemical shift values of the *meta*-coupled protons (and their corresponding carbons) at δ_H 7.42, *d* (*J* = 1.6 Hz; δ_C 119.1) and 7.12, *d* (*J* = 1.6 Hz; δ_C 124.2), and the aromatic methyl protons at δ_H 2.39, *s* (δ_C 21.4) were similar to those of the 1-hydroxy-3-methylphenyl portion of **EC2**. This was corroborated by the HMBC correlations of the aromatic proton at δ_H 7.42, *d* (*J* = 1.6 Hz; δ_C 119.1) to the carbonyl carbon at δ_C 182.3, and the carbons at δ_C 124.2, 114.4, 21.4, of the aromatic proton at δ_H 7.12, *d* (*J* = 1.6 Hz; δ_C 124.2) to the carbons at δ_C 119.1, 114.4, 21.4, and of the methyl protons at δ_H 2.39, *s* (δ_C 21.4) to the carbons at δ_C 146.6, 124.2 and 119.1.

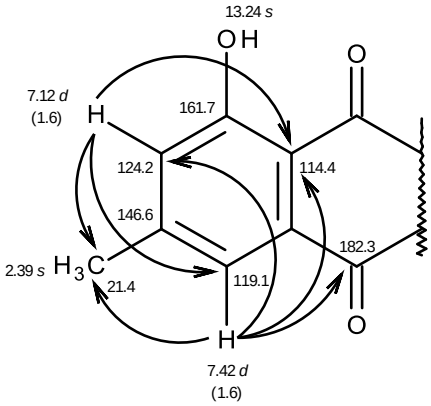

That another part of the anthraquinone was 6-hydroxy-8-methoxyphenyl instead of 8-hydroxy-6-methoxyphenyl as in **EC2** was supported by the presence of only one hydrogen-bonded hydroxyl group, as well as by the HMBC correlations of the aromatic proton at δ_H 7.20, *d* (*J* = 2.3 Hz; δ_C 106.9) to the carbons at δ_C 182.3, 112.6, 104.9, of the aromatic proton at δ_H 6.84, *d* (*J* = 2.3 Hz; δ_C 104.9) to the carbons at δ_C 164.4, 112.6, 106.9, as well as of the methoxy protons at δ_H 3.90, *s* (δ_C 56.3) to the carbon at δ_C 163.4.

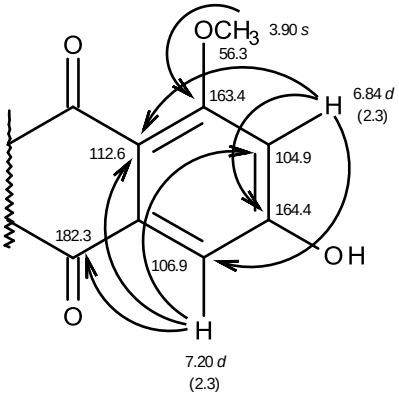

Consequently, the structure of **EC5** was established as 1,6-dihydroxy-8-methoxy-3-methyl-9,10-anthracene-9,10-dione, commonly known as questin (Figure 55) (Fujimoto *et al*., 1999).

Like erythroglaucin, physcion, catenarin and emodin, questin has been also previously reported from several species of *Eurotium* (Anke *et al*., 1980; Slack *et al*, 2009), as well as from plants belonging to the genera *Cassia* (Hyun *et al*., 2009) and *Polygonum* (Choi *et al*., 2007).

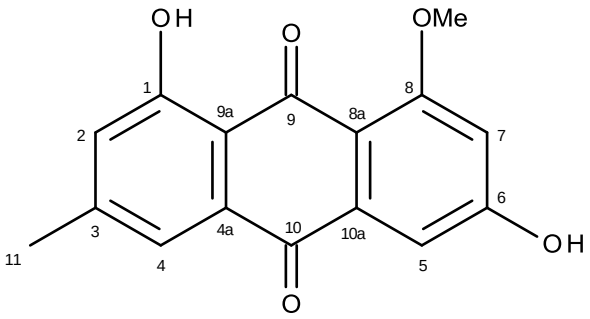

Figure 55. Structure of questin (**EC5**).

Like emodin, questin also displayed high immunosuppressive activity against Con A (T cells) and LPS-induced (B cells) proliferation of mouse splenic lymphocytes (Fujimoto *et al*., 1999). Questin was also proved to be cytotoxic against human colon cancer cell SW620 and exhibited inhibitory activity against Cdc25 B (Choi *et al*., 2007).

Anthraquinones are aromatic polyketides produced by repetitive Claisen condensations of an acyl CoA starting unit with malonyl-CoA elongations units. Biosynthesis of erythroglaucin (**EC1**), physcion (**EC2**), catenarin (**EC3**), emodin (**EC4**) and questin (**EC5**) is shown in Scheme 2 (Dewick, 2009).

Anthraquinones are commonly isolated from plants of the Polygonaceae family, e.g., the genus *Rheum* and *Polygonum* (Choi *et al*., 2007; 2013; Feng *et al*., 2013; Hsiang and Ho, 2008; Kuo *et al*., 1997; Leu *et al*., 2008; Qiu *et al*., 2013), however they have been also reported from several fungal species of the genus *Eurotium* (Anke *et al*., 1980; Du *et al*., 2008; Li *et al*., 2009a; Slack *et al*., 2009). Although erythroglaucin, physcion and catenarin have been previously reported from *E. cristatum* (Almeida *et al*., 2010; Anke *et al*., 1980), this study reports the presence of emodin and questin for the first time from this species (Gomes *et al*., 2012).

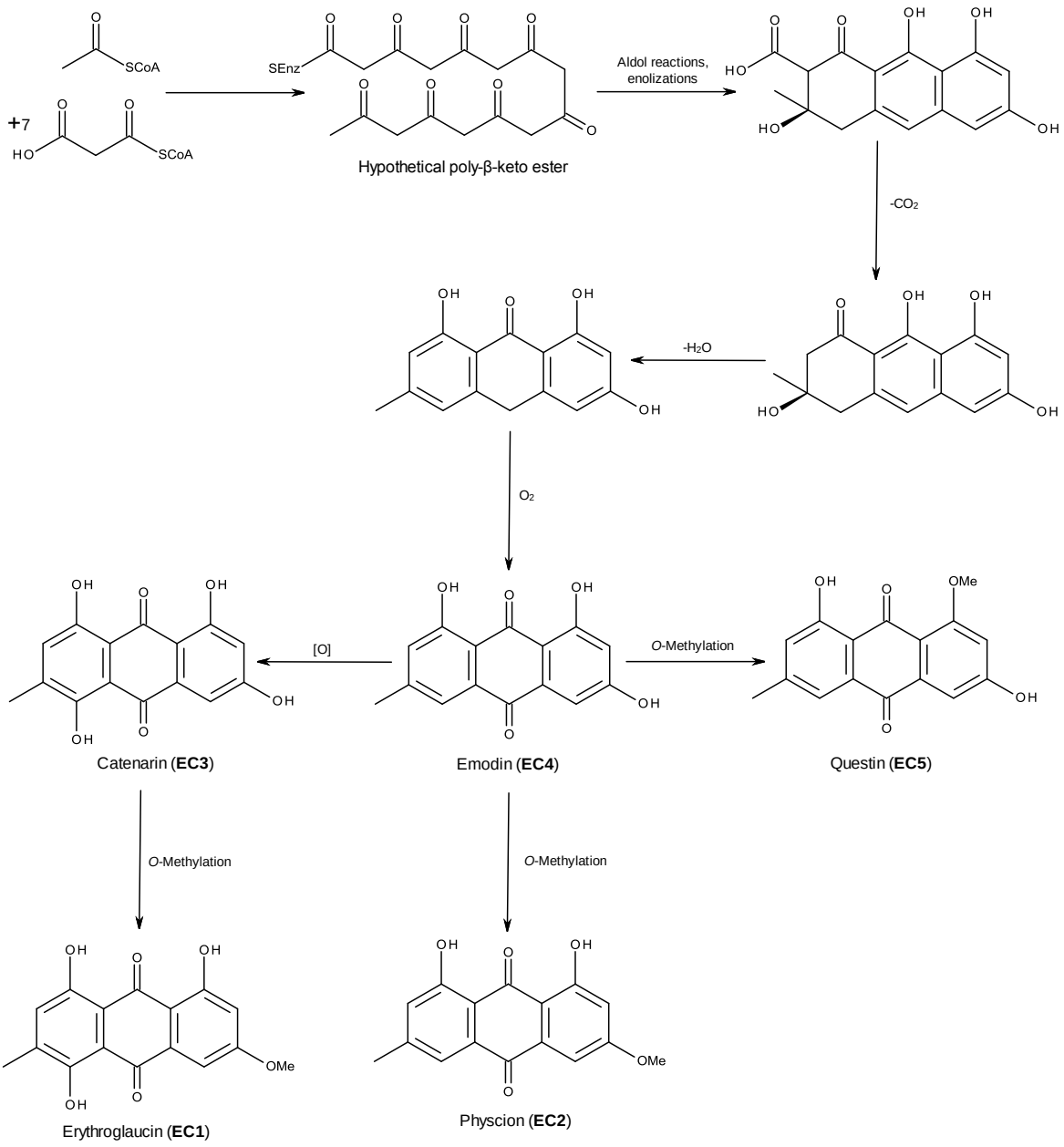

Scheme 2. Biosynthetic pathway of the anthraquinones **EC1-EC5**.

3.1.4. Structure Elucidation of Diketopiperazine Derivatives

3.1.4.1. cyclo-(L-Tryptophyl-L-phenylalanyl) (EV5)

EV5 was isolated as white solid. The ^{13}C NMR, DEPT and HSQC spectra (Table 11) revealed the presence of six quaternary sp^2 (δ_C 166.9, 166.2, 136.5, 136.1, 127.6, 108.8), ten methine sp^2 (δ_C 129.7, 129.7, 128.1, 128.1, 126.4, 124.5, 121.0, 118.8, 118.5, 111.4), two methine sp^3 (δ_C 55.6, 55.3) and two methylene sp^3 (δ_C 39.7, 29.7) carbons.

Table 11. ^1H and ^{13}C NMR data (DMSO-d_6, 300.13 and 75.47 MHz) of **EV5**.

Position	δ_C, type	δ_H, mult. (*J* in Hz)	COSY	HMBC
1	---	10.9, *s*	---	C-3, 8, 9
2	124.5, CH	6.94, *s*	---	C-3, 8, 9
3	108.8, C	---	---	---
4	118.8, CH	7.47, *d* (7.5)	H-5	C-3, 6, 8
5	118.5, CH	6.97, *dd* (7.5, 7.5)	H-4, 6	C-7, 9
6	121.0, CH	7.06, *dd* (7.5, 7.5)	H-5, 7	C-4, 8
7	111.4, CH	7.31, *d* (7.5)	H-6	C-5, 9
8	136.1, C	---	---	---
9	127.6, C	---	---	---
10a	29.7, CH_2	2.78, *dd* (14.4, 4.3)	H-10b, 11	C-2, 3, 11, 16
b		2.50, *dd* (14.4, 5.9)	H-10a, 11	C-2, 3, 11, 16
11	55.3, CH	3.96, *m*	H-10, 12	C-16
12	---	7.94, *d* (2.3)	H-11	C-14, 16
13	166.2, CO	---	---	---
14	55.6, CH	3.83, *m*	H-15, 17	C-13
15	---	7.73, *d* (2.3)	H-14	C-11, 13
16	166.9, CO	---	---	---
17a	39.7, CH_2	2.43, *dd* (13.4, 4.6)	H-14, 17b	C-13, 14, 18, 19, 23
b		1.80, *dd* (13.4, 7.1)	H-14, 17a	C-13, 14, 18, 19, 23
18	136.5, C	---	---	---
19	129.7, CH	6.68, *d* (6.9)	H-20	C-17, 21
20	128.1, CH	7.17, *m*	H-19, 21	C-18, 22
21	126.4, CH	7.17, *m*	H-20, 22	C-19, 23
22	128.1, CH	7.17, *m*	H-21, 23	C-18, 20
23	129.7, CH	6.67, *d* (6.9)	H-22	C-17, 21

The ^1H NMR spectrum in combination with the HSQC spectrum (Table 11), displayed the signals of four aromatic protons at δ_H 7.47, *d*, *J* = 7.5 Hz (δ_C 118.8), 6.97, *dd*, *J* = 7.5, 7.5 Hz (δ_C 118.5), 7.06, *dd*, *J* = 7.5, 7.5 Hz (δ_C 121.0), and 7.31, *d*, *J* = 7.5 Hz (δ_C 111.4). The COSY spectrum (Table 11) showed cross peaks of the doublet at δ_H 7.47 (*J* = 7.5 Hz) to the double doublet at δ_H 6.97 (*J* = 7.5, 7.5

Hz), as well as of the doublet at δ_H 7.31 (*J* = 7.5 Hz) to the double doublet at δ_H 7.06 (*J* = 7.5, 7.5 Hz), with the coupling constant values indicating an *ortho*-coupling between the two pairs of protons. Furthermore, the two double doublets at δ_H 6.97 (*J* = 7.5, 7.5 Hz) and δ_H 7.06 (*J* = 7.5, 7.5 Hz) were correlated with each other indicating the presence of a 1,2-disubstituted benzene ring. Analogously to **EV4**, the HMBC cross peaks of the methine singlet at δ_H 6.94 (δ_C 124.5) to the quaternary sp^2 carbon at δ_C 136.1 and 127.6, of the doublet at δ_H 7.47 (*J* = 7.5 Hz; δ_C 118.8) to δ_C 108.8 and δ_C 136.1, and of the doublet at δ_H 7.31 (*J* = 7.5 Hz; δ_C 111.4) to δ_C 127.6, revealed the presence of a 2,3-dihydro-1*H*-indole moiety (**A**).

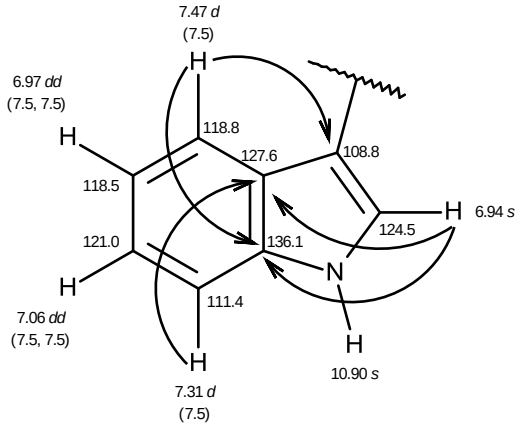

A

The ^{1}H NMR spectrum also displayed the signals of additional five aromatic protons at δ_H 6.68, *d*, *J* = 6.9 Hz, δ_H 7.17, *m*, δ_H 7.17, *m*, δ_H 7.17, *m* and δ_H 6.67,*d*, *J* = 6.9 Hz, which, in combination with the HSQC spectrum, were assigned to the monosubstituted benzene ring (**B**). This was supported by the COSY cross peaks of the two doublets at δ_H 6.68 (*J* = 6.9 Hz; δ_C 129.7) and δ_H 6.67 (*J* = 6.9 Hz; δ_C 129.7) to a multiplet at δ_H 7.17, as well as by the HMBC cross peaks of the doublets at δ_H 6.68 (*J* = 6.9 Hz; δ_C 129.7) and δ_H 6.67 (*J* = 6.9 Hz; δ_C 129.7) to the carbon at δ_C 126.4, and of the multiplet at δ_H 7.17 to the carbons at δ_C 129.7 and 136.5.

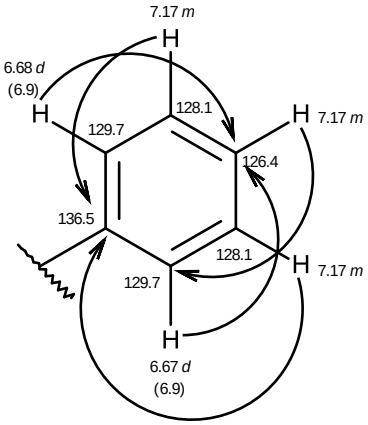

B

The ^{1}H NMR spectrum, in conjunction with the HSQC spectrum, also exhibited two pairs of methylene proton at δ_H 2.50, *dd* (*J* = 14.4, 5.9 Hz; δ_C 29.7) / 2.78, *dd* (*J* = 14.4, 4.3 Hz; δ_C 29.7) and δ_H 1.80, *dd* (*J* = 13.4, 7.1 Hz; δ_C 39.7) / 2.43, *dd* (*J* = 13.4, 4.6 Hz; δ_C 39.7), two multiplets of methine protons at δ_H 3.96 (δ_C 55.3) and δ_H 3.83 (δ_C 55.6), as well as two doublets at δ_H 7.94 (*J* = 2.3 Hz) and δ_H 7.73 (*J* = 2.3 Hz). As the latter doublets did not display HSQC cross peaks, they were assumed to be nitrogen-bearing protons.

The COSY spectrum revealed the presence of two coupling systems, one of which comprising the two double doublets at δ_H 2.50 (*J* = 14.4, 5.9 Hz; δ_C 29.7) and 2.78 (*J* = 14.4, 4.3 Hz; δ_C 29.7), the multiplet at 3.96 (δ_C 55.3) and the doublet at δ_H 7.94 (*J* = 2.3 Hz), and another of the double doublets at δ_H 1.80 (*J* = 13.4, 7.1 Hz; δ_C 39.7) and 2.43 (*J* = 13.4, 4.6 Hz; δ_C 39.7), the multiplet at δ_H 3.83 (δ_C 55.6) and the doublet at δ_H 7.73 (*J* = 2.3 Hz). Since the HMBC spectrum exhibited cross peaks of the doublet at 7.94 (*J* = 2.3 Hz) to the methine carbon at δ_C 55.6 and the quaternary carbon at δ_C 166.9, and of the doublet at δ_H 7.73 (*J* = 2.3 Hz) to the methine carbon at δ_C 55.3 and the quaternary carbon at δ_C 166.2, the two coupling systems should be in a cyclic form. Furthermore, the methylene proton at δ_H 2.78, *dd* (*J* = 14.4, 4.3 Hz; δ_C 29.7) also showed HMBC correlations to the methine carbon at δ_C 55.3 and the quaternary carbon at δ_C 166.9, while the methylene proton at δ_H 2.43, *dd* (*J* = 13.4, 4.6 Hz; δ_C 39.7) exhibited HMBC correlations to the methine carbon at δ_C 55.6 and the quaternary carbon at δ_C 166.2. The correlation pattern and the ^{1}H and ^{13}C chemical shift values were characteristic of the disubstituted 1,4-diketopiperazine ring (**C**).

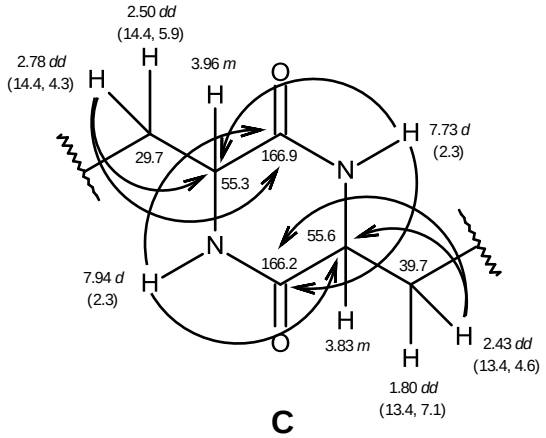

C

That the 1,4-diketopiperazine ring was linked to the 2,3-dihydro-1*H*-indole moiety (**A**) through the methylene carbon at δ_C 29.7, and with the phenyl ring (**B**) through the methylene carbon at δ_C 39.7, was supported by the HMBC correlations of the methylene proton at δ_H 2.78, *dd* (*J* = 14.4, 4.3 Hz; δ_C 29.7) and 2.50, *dd* (*J* = 14.4, 5.9 Hz; δ_C 29.7) to the olefinic carbons at δ_C 108.8 and 124.5, as well as of the aromatic protons at δ_H 6.68, *d* (*J* = 6.9 Hz; δ_C 129.7) and δ_H 6.67, *d* (*J* = 6.9 Hz; δ_C 129.7) to the methylene carbon at δ_C 39.7.

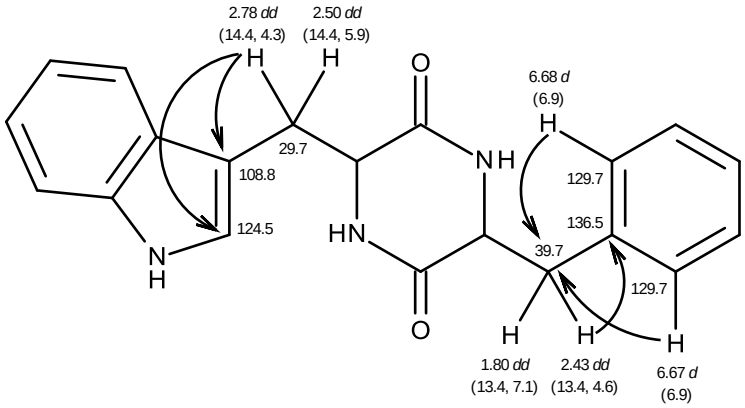

Therefore, the structure of **EV5** was proposed as 3-benzyl-6-(1*H*-indol-3 ylmethyl)piperazine-2,5-dione. The ^{1}H and ^{13}C NMR data of **EV5** were in agreement with those reported for cyclo-(L-tryptophyl-L-phenylalanyl) (Figure 56) by Kimura *et al*. (1996). This cyclic peptide was reported from both *Penicillium* (Kimura *et al*., 1996) and *Aspergillus* spp. (Chu *et al*., 2011), and recently from the Gram-negative bacterium *Comamonas testosterone* (Kumar *et al*., 2013).

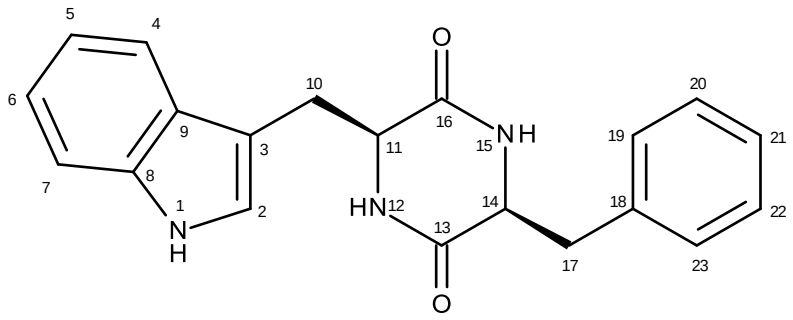

Figure 56. Structure of cyclo-(L-tryptophyl-L-phenylalanyl) (**EV5**).

Cyclo-(L-tryptophyl-L-phenylalanyl) was shown to exhibit antibacterial activity against ten human pathogenic bacteria with a significantly good activity against the Gram-negative bacteria *Vibrio cholera* and *Salmonella typhi*, proving to be more effective than the standard antibiotics ciprofloxacin and ampicillin. Additionally, it displayed also good antifungal activity against plant pathogenic fungi, with a significantly potent activity against *Fusarium oxysporum* and *Rhizoctonia solani* (Kumar *et al*., 2013). Its antiproliferative properties were reported by Ding *et al*. (2008), as moderate growth inhibitor of thirty-seven human tumor cell lines, with an average IC_{50} value of 3.3 µg/mL.

3.1.4.2. Neoechinulin A (EC8)

EC8 was isolated as dark red solid and its ^{1}H and ^{13}C NMR data (Table 12) were similar to those of **EV5**. The ^{13}C NMR (Table 12) spectrum revealed the presence of two amide carbonyls (δ_C 166.0, 159.0), six methine sp^2 (δ_C 144.7, 120.6, 119.3, 118.5, 111.5, 110.2), five quaternary sp^2 (δ_C 143.8, 134.9, 125.6, 124.5, 102.8), one methylene sp^2 (δ_C 111.4), one methine sp^3 (δ_C 50.6), one quaternary sp^3 (δ_C ~39.0) and three methyl (δ_C 27.3, 27.3, 19.8) carbons.

The ^{1}H NMR and HSQC spectra (Table 12) exhibited the presence of four aromatic protons at δ_H 7.43, *dd* (*J* = 7.3, 1.2 Hz; δ_C 111.5), 7.20, *d* (*J* = 7.3 Hz; δ_C 118.5), 7.08, *ddd* (*J* = 7.3, 7.3, 1.2 Hz; δ_C 120.6) and 7.02, *ddd* (*J* = 7.3, 7.3, 1.2 Hz; δ_C 119.3). The COSY spectrum (Table 12) revealed cross peaks between the doublet at δ_H 7.20 (*J* = 7.3 Hz) and the double double doublet at δ_H 7.02 (*J* = 7.3, 7.3, 1.2 Hz), between the double doublet at δ_H 7.43 (*J* = 7.3, 1.2 Hz) and the double double doublet at δ_H 7.08 (*J* = 7.3, 7.3, 1.2 Hz), and between the double

double doublet at δ_H 7.08 (*J* = 7.3, 7.3, 1.2 Hz) and the double double doublet at δ_H 7.02 (*J* = 7.3, 7.3, 1.2 Hz), thus suggesting the presence of a 1,2-disubstituted benzene ring.

Table 12. ^{1}H and ^{13}C NMR data (DMSO-d_6, 300.13 and 75.47 MHz) of **EC8**.

Position	δ_C, type	δ_H, mult. (*J* in Hz)	COSY	HMBC
1	---	10.95, *s*	H-5	C-2, 3, 3a, 7a
2	143.8, C	---	---	---
3	102.8, C	---	---	---
3a	125.6, C	---	---	---
4	118.5, CH	7.20, *d* (7.3)	H-5	C-3, 6, 7a
5	119.3, CH	7.02, *ddd* (7.3, 7.3, 1.2)	H-4, 6	C-3a, 7
6	120.6, CH	7.08, *ddd* (7.3, 7.3, 1.2)	H-5, 7	C-4, 7a
7	111.5, CH	7.43, *dd* (7.3, 1.2)	H-6	C-3a, 5
7a	134.9, C	---	---	---
8	110.2, CH	6.96, *s*	---	C-2, 3a, 10, 13
9	124.5, C	---	---	---
10	159.0, CO	---	---	---
11	---	8.35, *d* (1.7)	H-12	C-9, 13
12	50.6, CH	4.14, *dd* (6.9, 1.7)	H-11, 20	C-13, 20
13	166.0, CO	---	---	---
14	---	8.27, *brs*	---	C-10, 12, 13
15	~39.0, C	---	---	---
16	144.7, CH	6.08, *dd* (17.3, 10.4)	H-17a, 17b	C-2, 15, 18, 19
17a	111.4, CH_2	5.05, *d* (17.3)	H-16, 17b	C-15, 16
b		5.06, *d* (10.4)	H-16, 17a	C-15, 16
18	27.3, CH_3	1.51, *s*	---	C-2, 15, 16, 19
19	27.3, CH_3	1.51, *s*	---	C-2, 15, 16, 18
20	19.8, CH_3	1.45, *d* (6.9)	H-12	C-12, 13

The HMBC spectrum (Table 12) exhibited correlations of the aromatic proton at δ_H 7.20, *d* (*J* = 7.3 Hz; δ_C 118.5) to the carbons at δ_C 120.6 and 134.9, of the aromatic proton at δ_H 7.02, *ddd* (*J* = 7.3, 7.3, 1.2 Hz; δ_C 119.3) to the carbons at δ_C 125.6 and 111.5, of the aromatic proton at δ_H 7.08, *ddd* (*J* = 7.3, 7.3, 1.2 Hz; δ_C 120.6) to the carbons at δ_C 134.9 and 118.5, and of the aromatic proton at δ_H 7.43, *dd* (*J* = 7.3, 1.2 Hz; δ_C 111.5) to the carbons at δ_C 119.3 and 125.6, thus confirming the 1,2-disubstituted benzene moiety. Since the HMBC spectrum also showed cross peaks of the doublet at δ_H 7.20, *d* (*J* = 7.3 Hz; δ_C 118.5) to the quaternary sp^2 carbon at δ_C 102.8, and of the singlet at δ_H 10.95 to the quaternary sp^2 carbons at δ_C 102.8, 143.8 and the aromatic carbons at δ_C 134.9 and 125.6, the presence of the 2,3-disubstituted 2,3-dihydro-*1H*-indole moiety was proposed.

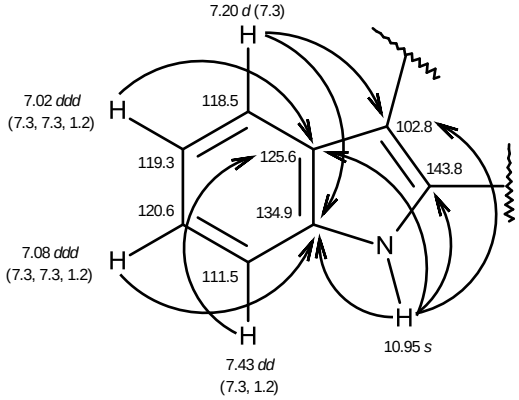

Furthermore, the COSY spectrum also revealed couplings of the olefinic proton at δ_H 6.08, *dd* (*J* = 17.3, 10.4 Hz; δ_C 144.7) to the methylene sp^2 protons at δ_H 5.05, *d* (*J* = 17.3 Hz; δ_C 111.4) and 5.06, *d* (*J* = 10.4 Hz; δ_C 111.4). Since the HMBC spectrum displayed correlations of the olefinic proton at δ_H 6.08, *dd* (*J* = 17.3, 10.4 Hz; δ_C 144.7) to the quaternary sp^3 carbon at δ_C ~39.0 and the methyl carbons at δ_C 27.3, of the methylene protons at δ_H 5.05, *d* (*J* = 17.3 Hz; δ_C 111.4) and 5.06, *d* (*J* = 10.4 Hz; δ_C 111.4) to the carbons at δ_C 144.7 and 39.0, and of the methyl protons at δ_H 1.51, *s* (δ_C 27.3) to the carbons at δ_C ~39.0 and 144.7, the presence of a 1-methylbuten-3-yl moiety was confirmed.

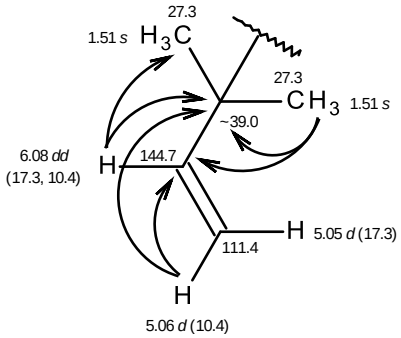

That the 1-methylbuten-3-yl moiety was attached to C-2 (δ_C 143.8) of the indole ring system was supported by the HMBC correlations of the methyl protons at δ_H 1.51, *s*, and the olefinic proton at δ_H 6.08, *dd* (*J* = 17.3, 10.4 Hz; δ_C 144.7) to the quaternary sp^2 carbon at δ_C 143.8:

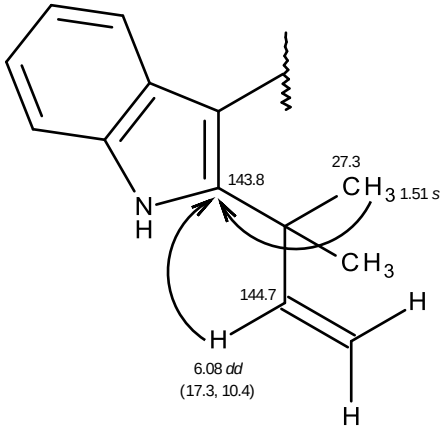

The COSY spectrum also revealed the continuous coupling system of the doublet at δ_H 8.35 (*J* = 1.7 Hz), the double doublet at δ_H 4.14 (*J* = 6.9, 1.7 Hz; δ_C 50.6) and the methyl doublet at δ_H 1.45 (*J* = 6.9 Hz; δ_C 19.8). On the other hand, the doublet at δ_H 8.35 (*J* = 1.7 Hz) exhibited the HMBC cross peaks to the quaternary sp^2 carbon at δ_C 124.5 and the carbonyl at δ_C 166.0, while the broad singlet at δ_H 8.27 gave HMBC cross peaks to the carbons at δ_C 159.0 and 50.6. Since the singlet of the olefinic proton at δ_H 6.96 (δ_C 110.2) showed also cross peaks to the carbonyls at δ_C 166.0 and 159.0, the presence of 1,4-diketopiperazine with substituents on C-2 (δ_C 124.5) and C-5 (δ_C 50.6), was confirmed.

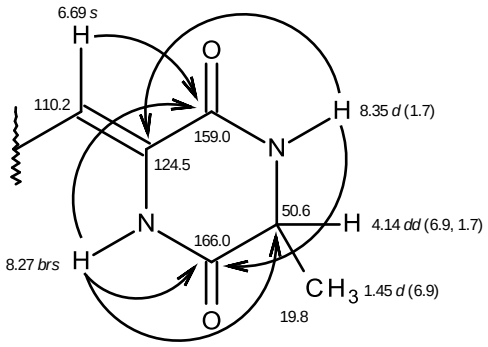

Finally, the HMBC cross peak of the singlet at δ_H 6.96 (δ_C 110.2) to the carbons of the indole ring system at δ_C 143.8 and 125.6 confirmed the attachment of the substituted 1,4-diketopiperazine moiety to 2,3-dihydro-*1H*-indole portion through the carbon at δ_C 110.2 of the former and the carbon at δ_C 102.8 of the latter.

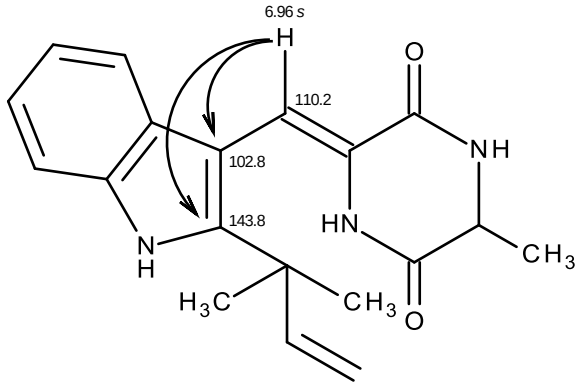

Therefore, the structure of **EC8** was proposed as (3*Z*)-3-[[2-(1,1-dimethylallyl)-1*H*-indol-3-yl]methylene]-6-methyl-piperazine-2,5 dione which is commonly known as neoechinulin A (Figure 57) (Li *et al*., 2004).

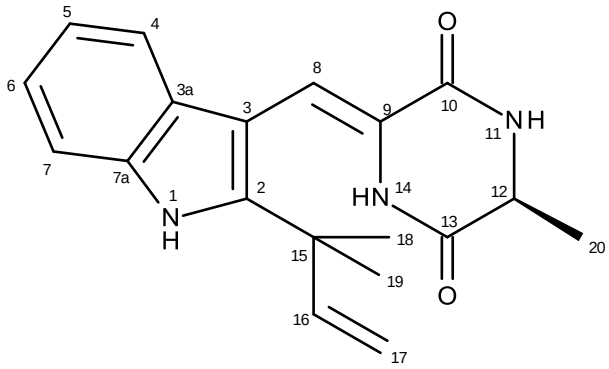

Figure 57. Structure of neoechinulin A (**EC8**).

Neoechinulin A has been widely reported from several species of fungi, both from marine and terrestrial environments, essentially from species of the genus *Aspergillus* (Dossena *et al*., 1974; Li *et al*., 2004; Marchelli *et al*., 1977; Nagasawa *et al*., 1975; Yagi and Do, 1999) and *Eurotium* (Du *et al*., 2012; Kim *et al*., 2013; Li *et al*., 2008b; Slack *et al*., 2009). Interestingly, most of the *Aspergillus* spp. reported to produce neoechinulin A, refer to *Eurotium* anamorphs. Additionally, the diketopiperazine alkaloid was also found to be a metabolic product of several marine derived species of the genus *Chaetomium* (Wang *et* al., 2006), *Microsporum* (Dewapriya *et al*., 2013; Wijesekara *et al*., 2014) and

Penicillium (Zhou *et al*., 2010), as well as from the higher plants *Bridelia ferruginea* (Pettit *et al*., 2008) and *Cyrtomium fortumei* (Yang *et al*., 2013b).

Neoechinulin A was reported as a potential candidate for the development of new drugs for the treatment of neurodegenerative diseases like Parkinson and Alzheimer's disease. Neoechinulin A can protect neuronal PC12 cells from cytotoxicity due to oxidative / nitrosative stress induced by the superoxide / nitric oxide co-generator 3-morpholinosydronimine (SIN-1), inducing activation of caspase-3-like proteases and by elevating the cellular reserve capacity for NAD(P)H generation (Akashi *et al*., 2012; Kimoto *et al*., 2007; Kuramochi *et al*., 2008; Maruyama *et al*., 2004). Subsequent studies revealed that neoechinulin A can also protect PC12 cells from the Parkinson disease-inducing neurotoxins MPP^+ and rotenone (Akashi *et al*., 2011; Kajimura *et al*., 2008). Interestingly, a SAR study performed to examine the cytoprotective activity of neoechinulin A and several synthetic derivatives, against cytotoxicity induced by SIN-1 in NGF-differentiated PC12 cells, revealed that the C-8/C-9 double bond plays a key role in the cytoprotective activity (Aoki *et al*., 2010). Recently, neoechinulin A revealed potential to be developed as a modulator of neuro-inflammatory process in Alzheimer's disease due to its anti-inflammatory activity, presumably dependent on the regulation of p38 and ASK-1 kinases, and nuclear translocation of the NF-κB p65 and p50 subunits (Dewapriya *et al*., 2013). The anti-inflammatory effect was also observed in LPS-stimulated RAW 264.7 macrophages through the inhibition of the NF-κB and p38 MAPK pathways. Additionally, neoechinulin A also markedly suppressed the production of NO and PGE_2 and the expression of iNOS and COX-2 (Kim *et al*., 2013). In other recent study, neoechinulin A antiproliferative effect against human cervical carcinoma HeLa cells has been tested. It was found to exhibit significant cytotoxic activity by inducing cell apoptosis in association with the activation of the expression of caspase family enzymes and p53, followed by Bax and Bcl-2 regulation (Wijisekara *et al*., 2014). Neoechinulin A also displayed significant radical scavenging activity against DPPH, having higher antioxidant activity than α-tocopherol, and its UV-A protecting activity being more effective than the sunscreen oxybenzone (Li *et al*., 2004; Yagi and Do, 1999).

3.1.4.3. Neoechinulin E (EC9)

EC9 was isolated as an orange-red solid. The ^{13}C NMR (Table 13) displayed signals for eighteen carbons, which were categorized as two amide carbonyls (δ_C 160.5, 152.3), six quaternary sp^2 (δ_C 157.3, 145.6, 135.2, 126.1, 123.4, 103.8), six methine sp^2 (δ_C 144.9, 121.1, 119.8, 119.7, 116.0, 111.6), one methylene sp^2 (δ_C 112.0), one quaternary sp^3 (δ_C ~39.0) and two methyl (δ_C 27.7, 27.7) carbons. The ^1H and ^{13}C NMR spectra of **EC9** (Table 13) closely resembled those of **EC8**, except for the lack of one methine (δ_H 4.14, *dd*, *J* = 6.9, 1.7 Hz; δ_C 50.6) and one methyl (δ_H 1.45, *d*, *J* = 6.9 Hz; δ_C 19.8), and the presence of the additional quaternary sp^2 carbon at δ_C 157.3.

Table 13. ^1H and ^{13}C NMR data (DMSO-d_6, 300.13 and 75.47 MHz) of **EC9**.

Position	δ_C, type	δ_H, mult. (*J* in Hz)	COSY	HMBC
1	---	11.23, *s*	---	C-2, 3, 3a
2	145.6, C	---	---	---
3	103.8, C	---	---	---
3a	126.1, C	---	---	---
4	119.7, CH	7.43, *d* (7.6)	H-5	C-6, 7a
5	119.8, CH	7.02, *dd* (7.6, 7.6)	H-4, 6	C-3a, 7
6	121.1, CH	7.11, *dd* (7.6, 7.6)	H-5, 7	C-4, 7a
7	111.6, CH	7.43, *d* (7.6)	H-6	C-3a, 5
7a	135.2, C	---	---	---
8	116.0, CH	7.19, *d* (1.0)	---	C-2, 3a, 10
9	123.4, C	---	---	---
10	160.5, CO	---	---	---
11	---	11.97, *brs*	---	---
12	157.3, C	---	---	---
13	152.3, CO	---	---	---
14	---	9.85, *brs*	---	C-10, 12
15	~39.0, C	---	---	---
16	144.9, CH	6.07, *dd* (17.5, 10.6)	H-17a, 17b	---
17a	112.0, CH_2	5.06, *d* (17.5)	H-16	C-15, 16
b		5.08, *d* (10.6)	H-16	C-15, 16
18	27.7, CH_3	1.48, *s*	---	C-2, 15, 16, 19
19	27.7, CH_3	1.48, *s*	---	C-2, 15, 16, 18

The ^1H NMR and HSQC spectra (Table 13) exhibited the signals of four aromatic protons at δ_H 7.43, *d* (*J* = 7.6 Hz, 2H; δ_C 119.7 and 111.6), 7.11, *dd* (*J* = 7.6, 7.6 Hz; δ_C 121.1) and 7.02, *dd* (*J* = 7.6, 7.6 Hz; δ_C 119.8) which, through the COSY correlations, revealed the presence of a 1,2-disubstituted benzene ring, similar to that of **EC8**. Furthermore, the singlet at δ_H 11.23, which gave HMBC cross peaks to the carbon of the benzene ring at δ_C 126.1 and the substituted olefinic carbons at δ_C 103.8 and 145.6, suggested that the 1,2-disubstituted

benzene ring is part of the 2,3-dihydro-*1H*-indole ring system. Similar to **EC8**, the presence of the 1-methylbuten-3-yl fragment was evidenced by the coupling of the two doublets at δ_H 5.06 (*J* = 17.5 Hz; δ_C 112.0) and 5.08 (*J* = 10.6 Hz; δ_C 112.0) to the double doublet at δ_H 6.07 (*J* = 17.5, 10.6 Hz; δ_C 144.9), as well as the presence of the two methyl groups at δ_H 1.48, s (δ_C 27.7). Like **EC8**, the 1-methylbuten-3-yl on C-2 (δ_C 145.6) of the indole ring was substantiated by the HMBC cross peak between the singlet of the methyl protons at δ_H 1.48 (δ_C 27.7) and the carbon at δ_C 145.6 of the indole moiety.

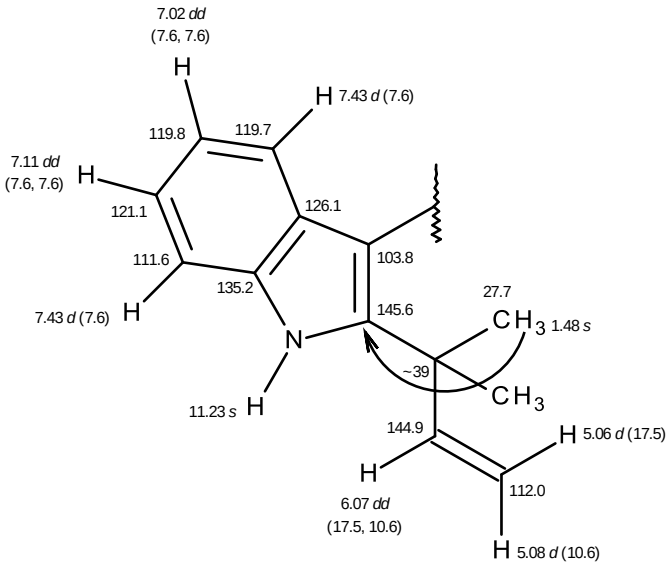

Contrary to **EC8**, the olefinic proton of a trisubstituted double bond and the broad singlets of the amide hydrogens appeared at higher frequencies (δ_H 7.19, *J* = 1.0 Hz; δ_C 116.0) / (δ_H 9.85; δ_H 11.97, respectively). Interestingly, the broad singlet at δ_H 9.85 showed HMBC cross peaks to the quaternary carbons at δ_C 160.5 and 157.3, while the broad singlet at δ_H 11.97 did not exhibit any cross peaks. Similar to **EC8**, the doublet of the olefinic proton at δ_H 7.19 (*J* = 1.0 Hz; δ_C 116.0) exhibited HMBC cross peaks to the carbons at δ_C 126.1 and 145.6 of the 2,3-dihydro-*1H*-indole moiety, in addition to the quaternary sp^2 carbon at δ_C 160.5. Considering the chemical shift value of the carbons and protons, as well as the HMBC correlations, this portion of **EC9** must be:

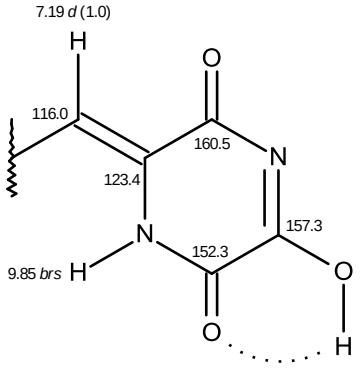

Thus, the structure of **EC9** was proposed as:

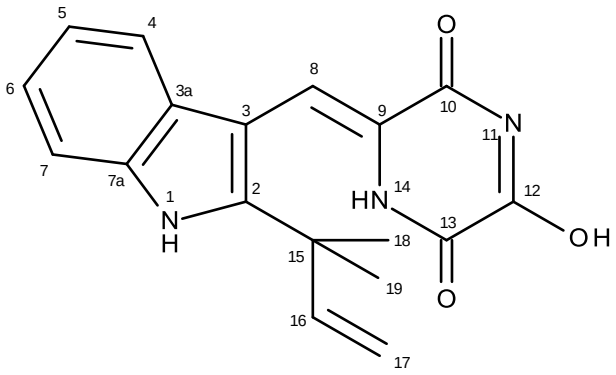

Figure 58. Structure of the enol form of neoechinulin E (**EC9**).

After a literature search, it was found that neoechinulin E, the prenylated indolopiperazine derivative, isolated from *Aspergillus amstelodami* (Marchelli *et al*., 1977) presented the same ^{1}H and ^{13}C data as that of **EC9**. However, the structure of neoechinulin E was reported as:

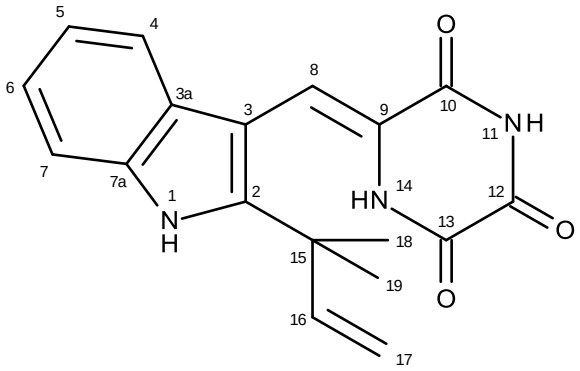

It is important to note that the structure of **EC9** and neoechinulin E are tautomers, which **EC9** represents an enol form (Figure 58).

Contrary to neoechinulin A, neoechinulin E has not widely been reported. Except for its identification from the fungi *Aspergillus amstelodami* and the plant *Cyrtomium fortumei*, (Marchelli *et al*., 1977 and Yang *et al*., 2013b respectively), neoechinulin E was reported so far, from the genus *Eurotium* (Li *et al*., 2008b; Slack *et al*., 2009).

To the best of our knowledge, the only reported biological property of neoechinulin E refers to its strong radical scavenging activity against DPPH (Li *et al*., 2008b).

3.1.4.4. Neoechinulin (EC7)

EC7 was isolated as a purple solid. The ^{13}C NMR (Table 14) displayed twenty-three carbon signals which were categorized, according to HSQC and DEPT (135º and 90º), as ten quaternary sp^2 (δ_C 160.5, 157.3, 152.3, 145.3, 135.5, 134.4, 131.1, 124.2, 123.0, 103.6), six methine sp^2 (δ_C 145.0, 124.1, 120.8, 119.6, 116.2, 110.6), one methylene sp^2 (δ_C 111.9), one quaternary sp^3 (δ_C ~39.0), one methylene sp^3 (δ_C 33.8) and four methyl (δ_C 27.7, 27.7, 25.6, 17.7) carbons.

The ^{13}C NMR spectrum (Table 14) was very similar to that of **EC9** except for the presence of additional two methyl carbons at δ_C 17.7 and 25.6, one methylene sp^3 at δ_C 33.8, one methine sp^2 at δ_C 124.1 and one quaternary sp^2 at δ_C 131.1. The COSY spectrum (Table 14) displayed correlations of the olefinic proton at δ_H 5.35, *t* (*J* = 7.4 Hz; δ_C 124.1) to the methylene protons at δ_H 3.39, *d* (*J* = 7.4 Hz, 2H; δ_C 33.8) and the methyl protons at δ_H 1.73, s ($2CH_3$, δ_C 17.7 and 25.6), suggesting that the additional five carbons was 3-methyl-2-butenyl moiety.

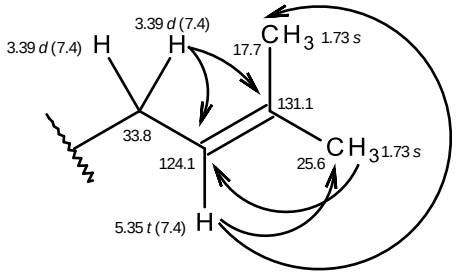

This was confirmed by the HMBC cross peaks of the doublet of the methylene protons at δ_H 3.39 (*J* = 7.4 Hz, 2H; δ_C 33.8) to the methine sp^2 carbon at δ_C 124.1 and the quaternary sp^2 carbon at δ_C 131.1, of the triplet at δ_H 5.35 (*J* = 7.4 Hz; δ_C 124.1) to the methyl carbons at δ_C 17.7 and 25.6, and of the singlet at δ_H 1.73 ($2CH_3$, δ_C 17.7 and 25.6) to the quaternary sp^2 carbon at δ_C 131.1 and the methine sp^2 carbon at δ_C 124.1.

Table 14. ^1H and ^{13}C NMR data (DMSO-*d*$_6$, 300.13 and 75.47 MHz) of **EC7**.

Position	δ_C, type	δ_H, mult. (*J* in Hz)	COSY	HMBC
1	---	11.11, *s*	---	C-2, 3, 3a
2	145.3, C	---	---	---
3	103.6, C	---	---	---
3a	124.2, C	---	---	---
4	119.6, CH	7.34, *d* (8.1)	H-5	C-3, 6, 7a
5	120.8, CH	6.87, *d* (8.1)	H-4, 20	C-3a, 7, 20
6	134.4, C	---	---	---
7	110.6, CH	7.21, *s*	H-20	C-3a, 5, 20
7a	135.5, C	---	---	---
8	116.2, CH	7.19, *s*	---	C-2, 3a, 10
9	123.0, C	---	---	---
10	160.5, CO	---	---	---
11	---	11.98, *brs*	---	C-9, 13
12	157.3, CO	---	---	---
13	152.3, CO	---	---	---
14	---	9.77, *brs*	---	C-10
15	~39.0, C	---	---	---
16	145.0, CH	6.07, *dd* (17.3, 10.5)	H-17a, 17b	C-15, 18, 19
17a	111.9, CH_2	5.06, *d* (17.3)	H-16, 17b	C-15, 16
b		5.09, *d* (10.5)	H-17, 17a	C-15, 16
18	27.7, CH_3	1.48, *s*	---	C-2, 16, 19
19	27.7, CH_3	1.48, *s*	---	C-2, 16, 18
20	33.8, CH_2	3.39, *d* (7.4)	H-21	C-5, 6, 7, 21, 22
21	124.1, CH	5.35, *t* (7.4)	H-20, 23, 24	C-23, 24
22	131.1, C	---	---	---
23	17.7, CH_3	1.73, *s*	H-21	C-21, 22, 24
24	25.6, CH_3	1.73, *s*	H-21	C-21, 22, 23

Unlike the ^1H NMR spectrum of **EC9**, the ^1H NMR spectrum (Table 14) of **EC7** displayed three aromatic protons at δ_H 7.34, *d* (*J* = 8.1 Hz; δ_C 119.6), δ_H 7.21, *s* (δ_C 110.6) and δ_H 6.87, *d* (*J* = 8.1 Hz; δ_H 120.8), suggesting the presence of a substituent on C-5 or C-6 of the benzene ring of the 2,3-dihydro-*1H*-indole portion. Since the doublet at δ_H 7.34 (*J* = 8.1 Hz; δ_C 119.6) gave HMBC cross peaks to the carbons at δ_C 103.6 and 135.5, which were assigned to C-3 and C-7a of the indole portion, and also to the quaternary sp^2 carbon at δ_C 134.4, the substituent was on C-6 (δ_C 134.4) of the benzene ring. That the substituent on C-6 (δ_C 134.4) was the

3-methyl-2-butenyl group was supported by the HMBC cross peaks of the doublet at δ_H 6.87 (*J* = 8.1 Hz; δ_C 120.8) and the singlet at δ_H 7.21 (δ_C 110.6) to the methylene carbon signal at δ_C 33.8, as well as of the doublet at δ_H 3.39 (*J* = 7.4 Hz; δ_C 33.8) to the aromatic carbons at δ_C 120.8 and 110.6.

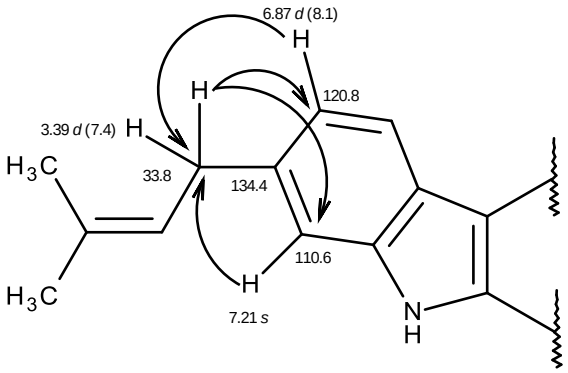

Table 15. Comparison of ^{1}H and ^{13}C NMR data (DMSO-d_6, 300.13 and 75.47 MHz) of **EC7** and **EC9**.

Position	**EC7**		**EC9**	
	δ_C, type	δ_H, mult. (*J* in Hz)	δ_C, type	δ_H, mult. (*J* in Hz)
1	---	11.11, *s*	---	11.23, *s*
2	145.3, C	---	145.6, C	---
3	103.6, C	---	103.8, C	---
3a	124.2, C	---	126.1, C	---
4	119.6, CH	7.34, *d* (8.1)	119.7, CH	7.43, *d* (7.6)
5	120.8, CH	6.87, *d* (8.1)	119.8, CH	7.02, *dd* (7.6, 7.6)
6	134.4, C	---	121.1, CH	7.11, *dd* (7.6, 7.6)
7	110.6, CH	7.21, *s*	111.6, CH	7.43, *d* (7.6)
7a	135.5, C		135.2, C	---
8	116.2, CH	7.19, *s*	116.0, CH	7.19, *d* (1.0)
9	123.0, C	---	123.4, C	---
10	160.5, CO	---	160.5, CO	---
11	---	11.98, *brs*	---	11.97, *brs*
12	157.3, CO	---	157.3, C	---
13	152.3, CO	---	152.3, CO	---
14	---	9.77, *brs*	---	9.85, *brs*
15	~39.0, C	---	~39.0, C	---
16	145.0, CH	6.07, *dd* (17.3, 10.5)	144.9, CH	6.07, *dd* (17.5, 10.6)
17a	111.9, CH_2	5.06, *d* (17.3)	112.0, CH_2	5.06, *d* (17.5)
b		5.09, *d* (10.5)		5.08, *d* (10.6)
18	27.7, CH_3	1.48, *s*	27.7, CH_3	1.48, *s*
19	27.7, CH_3	1.48, *s*	27.7, CH_3	1.48, *s*
20	33.8, CH_2	3.39, *d* (7.4)	---	---
21	124.1, CH	5.35, *t* (7.4)	---	---
22	131.7, C	---	---	---
23	17.7, CH_3	1.73, *s*	---	---
24	25.6, CH_3	1.73, *s*	---	---

The rest of the ^{13}C and ^{1}H signals were very similar to those of **EC9** (Table 15).

Therefore, **EC7** corresponded to **EC9** with a prenyl group on C-6 (δ_C 134.4). The structure established for **EC7** corresponded to neoechinulin (Figure 59), a prenylated indolopiperazine derivative previously reported from the fungi *Aspergillus amstelodami* (Marchelli *et al*., 1977) and *Aspergillus ruber* (Nagasawa *et al*., 1975).

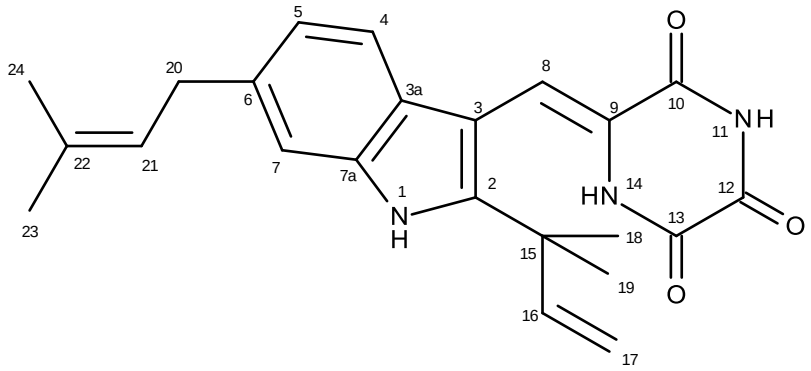

Figure 59. Structure of neoechinulin (**EC7**).

3.1.4.5. Echinulin (EC6)

EC6 was isolated as white amorphous solid. The ^{13}C NMR spectrum (Table 16) revealed the presence of two amide carbonyls (δ_C 168.7, 167.9), five methine sp^2 (δ_C 145.7, 124.5, 122.8, 122.8, 115.1), eight quaternary sp^2 (δ_C 141.3, 133.8, 132.9, 132.2, 131.5, 129.0, 123.4, 104.1), one methylene sp^2 (δ_C 112.3), two methine sp^3 (δ_C 54.6, 50.7), one quaternary sp^3 (δ_C 38.9), three methylene sp^3 (δ_C 34.6, 31.3, 29.5) and seven methyl (δ_C 27.9, 27.8, 25.8, 25.7, 19.8, 17.9, 17.9) carbons.

The ^{1}H NMR spectrum (Table 16) displayed signals of one amine proton at δ_H 8.08, *s*, two aromatic protons at δ_H 7.16, *s* and 6.83, *s*, two amide protons at δ_H 6.80, *brs* and 5.74, *brs*, five olefinic protons at δ_H 6.13, *dd* (*J* = 17.5, 10.6 Hz), 5.43, *t* (*J* = 6.1 Hz), 5.39, *m*, 5.19, *d* (*J* = 17.5 Hz) and 5.18, *d* (*J* = 10.6), two methine protons at δ_H 4.43, *d* (*J* = 10.0 Hz) and 4.12, *m*, six methylene protons at δ_H 3.67, *dd* (*J* = 14.7, 2.9 Hz), 3.56, *d* (*J* = 6.1 Hz; 2H), 3.42, *d* (*J* = 6.8 Hz; 2H)

and 3.21, *dd* (*J* = 14.7, 11.7 Hz) and seven methyl groups at δ_H 1.89, *s*, 1.83, *s*, 1.77, *s* (6H), 1.57, *d* (*J* = 7.3 Hz) and 1.54, *s* (6H).

Table 16. Comparison of the ^{1}H and ^{13}C NMR data (300.13 and 75.47 MHz) of **EC6** ($CDCl_3$) and **EC8** (DMSO-d_6).

Position	**EC6**		**EC8**	
	δ_C, type	δ_H, mult. (*J* in Hz)	δ_C, type	δ_H, mult. (*J* in Hz)
1	---	8.08, *s*	---	10.95, *s*
2	141.3, C	---	143.8, C	---
3	104.1, C	---	102.8, C	---
3a	129.0, C	---	125.6, C	---
4	115.1, CH	7.16, *s*	118.5, CH	7.20, *d* (7.3)
5	133.8, C	---	119.3, CH	7.02, *ddd* (7.3, 7.3, 1.2)
6	122.8, CH	6.83, *s*	120.6, CH	7.08, *ddd* (7.3, 7.3, 1.2)
7	123.4, C	---	111.5, CH	7.43, *dd* (7.3, 1.2)
7a	132.2, C	---	134.9, C	---
8a	29.5, CH_2	3.21, *dd* (14.7, 11.7)	110.2, CH	6.96, *s*
b		3.67, *dd* (14.7, 2.9)		
9	54.6, CH	4.43, *d* (10.0)	124.5, C	---
10	168.7, CO	---	159.0, CO	---
11	---	6.80, *brs*	---	8.35, *d* (1.7)
12	50.7, CH	4.12, *m*	50.6, CH	4.14, *dd* (6.9, 1.7)
13	167.9, CO	---	166.0, CO	---
14	---	5.74, *brs*	---	8.27, *brs*
15	38.9, C	---	~39.0, C	---
16	145.7, CH	6.13, *dd* (17.5, 10.6)	144.7, CH	6.08, *dd* (17.3, 10.4)
17a	112.3, CH_2	5.19, *d* (17.5)	111.4, CH_2	5.05, *d* (17.3)
b		5.18, *d* (10.6)		5.06, *d* (10.4)
18	27.9, CH_3	1.54, *s*	27.7, CH_3	1.51, *s*
19	27.8, CH_3	1.54, *s*	27.7, CH_3	1.51, *s*
20	34.6, CH_2	3.42, *d* (6.8)	19.8, CH_3	1.45, *d* (6.9)
21	124.5, CH	5.39, *m*	---	---
22	131.5, C	---	---	---
23	17.9, CH_3	1.77, *s*	---	---
24	25.8, CH_3	1.77, *s*	---	---
25	31.3, CH_2	3.56, *d* (6.1)	---	---
26	122.8, CH	5.43, *t* (6.1)	---	---
27	132.9, C	---	---	---
28	17.9, CH_3	1.89, *s*	---	---
29	25.7, CH_3	1.83, *s*	---	---
30	19.8, CH_3	1.57, *d* (7.3)	---	---

Analysis of the ^{1}H and ^{13}C NMR spectra of **EC6** revealed that, except for the substituted benzene ring, another part of the molecule was similar to that of **EC8** differing only in the single bond on C-8/C-9 in the former, instead of the double bond in the latter.

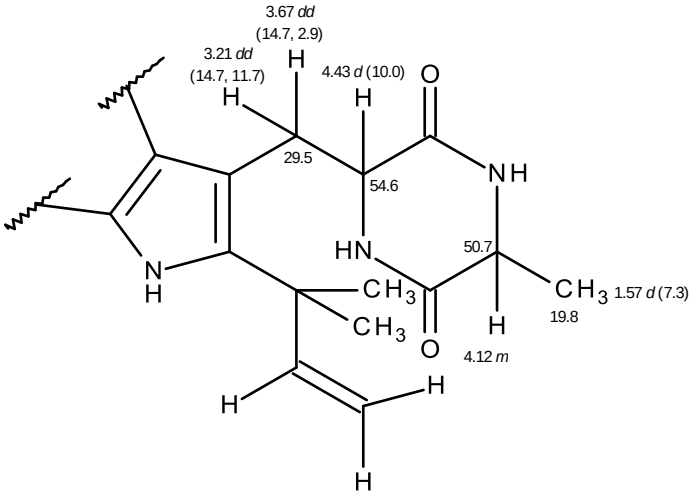

In contrast to **EC8**, the ^{1}H NMR spectrum displayed only two singlets of the aromatic protons at δ_H 7.16 and 6.83, suggesting that they were in the *meta* position of the benzene ring of the 2,3-dihydro-*1H*-indole portion. Furthermore, the ^{13}C NMR spectrum revealed additional carbons comprising two pairs of methyl (δ_C 17.9, 2CH_3 / δ_C 25.7, 25.8), two methine sp^2 (δ_C 122.8, 124.5), two quaternary sp^2 (δ_C 131.5, 132.9) and two methylene sp^3 (δ_C 31.3, 34.6) carbons which, in combination with the presence of the methyl singlets at δ_H 1.89, 1.83 and 1.77 (6H), a triplet at δ_H 5.43 (*J* = 6.1 Hz), a multiplet at δ_H 5.39, and two doublets at δ_H 3.42 (*J* = 6.8 Hz) and 3.56 (*J* = 6.1 Hz), confirmed the existence of another two prenyl groups in the molecule. Consequently, the benzene ring of the indole portion of **EC6** bares two prenyl substituents either on C-5 and C-7, or C-4 and C-6.

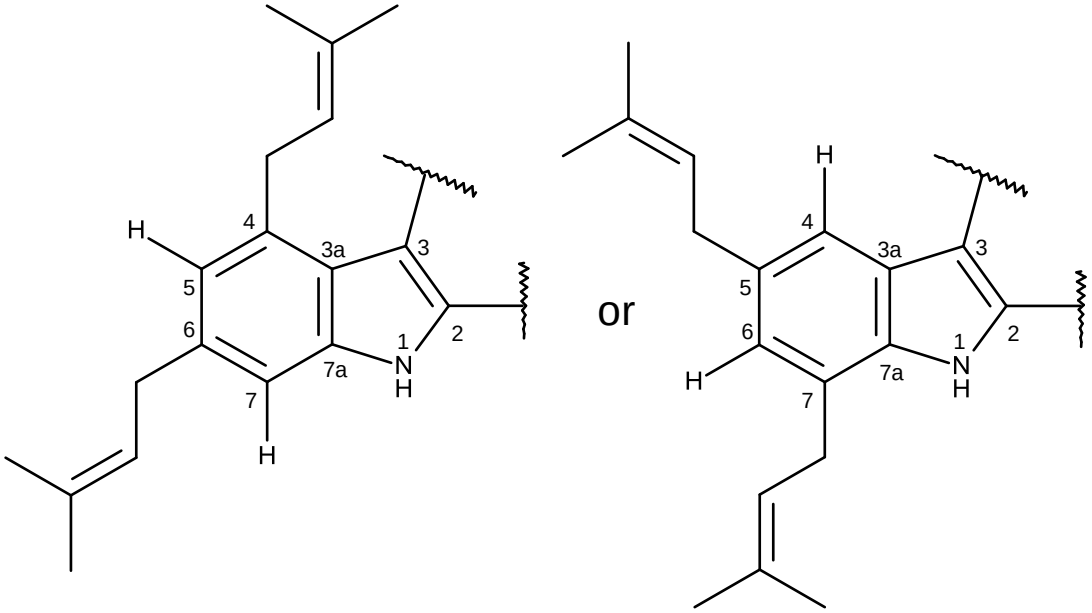

Since the chemical shift values of the aromatic protons of **EC6** (δ_H 7.16, *s* and 6.83, *s*) were more similar to those of H-4 (δ_H 7.20) and H-6 (δ_H 7.08) than those of H-5 (δ_H 7.02) and C-7 (δ_H 7.43) of **EC8**, the two prenyl substituents were placed on C-5 (δ_C 133.8) and C-7 (δ_C 123.4) of the benzene ring of the 2,3-dihydro-*1H*-indole moiety. Therefore **EC6** was identified as echinulin (Figure 60). In fact, echinulin was previously reported from the culture of the same fungus by Almeida *et al*. (2010) and later by Du *et al*. (2012).

Echinulin is a common prenylated indolopiperazine derivative, first isolated from *Aspergillus amstelodami* in 1961 by Birch *et al*., and later from various sources such as its teleomorph *Eurotium amstelodami* (Slack *et al*., 2009), as well as from several other species from the genus *Eurotium* (Butinar *et al*., 2005; Gao *et al*., 2011a; Li *et al*., 2008b; Podojil *et al*., 1979; Smetanina *et al*.,2007; Sohn *et al*., 2013). Echinulin was also identified from cultures of different fungal species such as *Aspergillus variecolor* (Wang *et al*., 2007) and *Penicillium griseofulvum* (Zhou *et al*., 2010), as well as from different plants of Anacardiaceae, Cucurbitaceae and Orchidaceae families (Talapatra *et al*., 2001; Zhao *et al*., 1991).

Echinulin displayed *in vitro* inhibitory activity with an IC_{50} value of 29.4 µM against PTP1B, a potential drug target for the treatment of type 2 diabetes and obesity (Sohn *et al*., 2013).

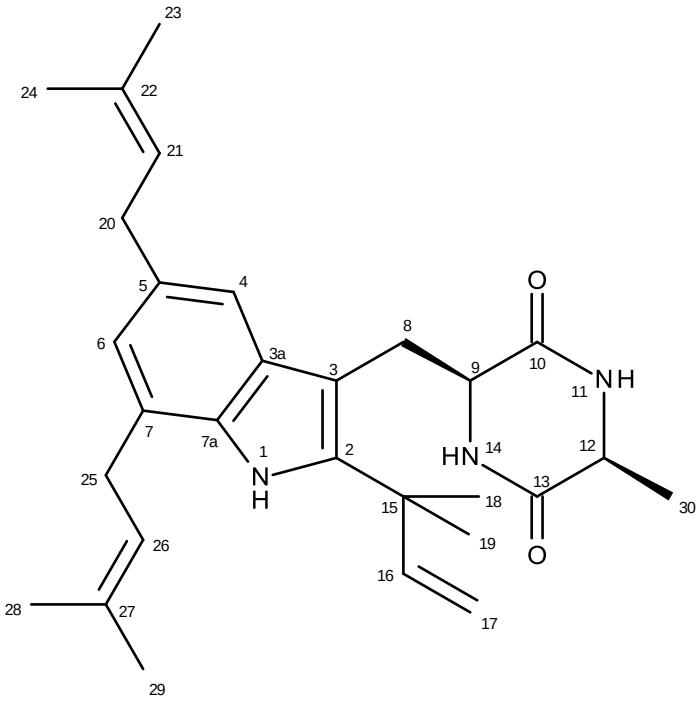

Figure 60. Structure of echinulin (**EC6**).

Similarly to the anthraquinones **EC1-EC5** isolated and those reported in literature, also the polyprenylated indole diketopiperazine alkaloids echinulin, neoechinulin, neoechinulin A and E, belong to the characteristic metabolic profile from *Eurotium* genus. Despite the reports on the isolation of the diketopiperazine derivatives from some plants (Pettit *et al*., 2008; Talapatra *et al*., 2001; Yang *et al*., 2013a; Zhao *et al*., 1991) and other fungi (Dewapriya *et al*., 2013; Wang *et al*., 2006; 2007; Wijesekara *et al*., 2014; Zhou *et al*., 2010), most reports refer to echinulin, neoechinulin, neoechinulin A and E as metabolic products from *Eurotium* species (Almeida *et al*., 2010; Birch *et al*., 1961; Du *et al*., 2012; Kim *et al*., 2013; Li *et al*., 2008b; Slack *et al*., 2009) was well as from their anamorphs, specially from *Aspergillus amstelodami* (Marchelli *et al*., 1977).

With exception to echinulin, previously reported by Almeida *et al*. (2010), and neoechinulin A by Du *et al*. (2012), this was the first report on the isolation of the diprenylated triketopiperazine alkaloid neoechinulin from *Eurotium* species, thus classifying it as a possible new extrolite for this genus, and an additional tool

for taxonomic identification (Gomes *et al*., 2012). Additionally, neoechinulin E was also identified for the first time from *E. cristatum* species (Gomes *et al*., 2012).

3.1.4.6. Eurocristatine (EC10)

A new diketopiperazine dimer (**EC10**), which we named eurocristatine, was also isolated from *E. cristatum* KUFC 7356, in addition to the known metabolites (**EC1-EC9**).

EC10 was isolated as white crystals and its IR spectrum showed absorption bands for amine (3450 cm^{-1}), aromatic (3190 cm^{-1}) and carbonyls (1662 cm^{-1}) groups. The ^{13}C NMR, DEPT and HSQC spectra (Table 17) revealed the presence of sixteen carbon signals which can be categorized as two amide carbonyls (δ_C 168.4, 167.5), two quaternary sp^2 (δ_C 149.1, 130.4), four methine sp^2 (δ_C 128.7, 124.4, 117.9, 108.9), one quaternary sp^3 (δ_C 59.7), four methine sp^3 (δ_C 78.8, 62.3, 55.7, 32.0), one methylene sp^3 (δ_C 37.3) and two methyl (δ_C 19.0, 18.0) carbons. However, the (+)-HR-ESIMS exhibited the *m/z* 569.2905 $[M+H]^+$, which corresponded to the molecular formula $C_{32}H_{36}N_6O_4$, implying that each carbon signal must correspond to two carbon atoms.

Table 17. ^1H and ^{13}C NMR data (DMSO-d_6, 300.13 and 75.47 MHz) of **EC10**.

P[a]	δ_C, type	δ_H, mult. (*J* in Hz)	COSY	HMBC	NOESY
1	---	6.74, *brs*	H-2	C-2, 3, 4, 9	H-2
2	78.8, CH	4.90, *brs*	H-1	---	H-1, 11
3	59.7, C	---	---	---	---
4	130.4, C	---	---	---	---
5	124.4, CH	7.39, *d* (7.5)	H-2	C-3, 7, 9	H-6, 12β
6	117.9, CH	6.63, *dd* (7.5, 7.5)	H-5, 7	C-4, 8	---
7	128.7, CH	7.02, *dd* (7.5, 7.5)	H-6, 8	C-5, 9	---
8	108.9, CH	6.60, *d* (7.5)	H-7	C-4, 6	---
9	149.1, C	---	---	---	---
11	55.7, CH	4.12, *t* (9.0)	H-12α, 12β	C-12, 13	H-2, 17, 18, 19
12α	37.3, CH_2	2.39, *dd* (14.0, 9.5)	H-11, 12β	C-3, 4, 11, 13	H-12β
12β		3.14, *dd* (14.0, 9.5)	H-11, 12α	C-3, 4, 11, 13	H-5, 12α
13	168.4, CO	---	---	---	---
14	---	8.27, *d* (4.2)	H-15	C-11, 13, 15, 16	H-17, 18, 19
15	62.3, CH	3.39, *t* (5.0)	H-14, 17	C-13, 16, 17, 18, 19	---
16	167.5, CO	---	---	---	---
17	32.0, CH	1.94, *m*	H-15, 18, 19	C-15, 16, 18, 19	H-11, 18, 19
18	19.0, CH_3	0.80, *d* (6.7)	H-17	C-15, 18, 19	H-17, 19
19	18.0, CH_3	0.69, *d* (6.7)	H-17	C-15, 18, 19	H-17, 18

P[a] Position

The coupling system of the aromatic protons at δ_H 7.39, *d* (*J* = 7.5 Hz; δ_C 124.4), 6.63, *dd* (*J* = 7.5, 7.5 Hz; δ_C 117.9), 7.02, *dd* (*J* = 7.5, 7.5 Hz; δ_C 128.7) and 6.60, *d* (*J* = 7.5 Hz; δ_C 108.9) observed in the COSY spectrum (Table 17), revealed the presence of one 1,2-disubstituted benzene ring. This was confirmed by the HMBC cross peaks of the doublet at δ_H 7.39 (*J* = 7.5 Hz; δ_C 124.4) to the carbons at δ_C 128.7 and 149.1, of the double doublet at 6.63 (*J* = 7.5, 7.5 Hz; δ_C 117.9) to the carbons at δ_C 108.9 and 130.4, of the double doublet at δ_H 7.02 (*J* = 7.5, 7.5 Hz; δ_C 128.7) to the carbons at δ_C 124.4 and 149.1, and of the doublet at δ_H 6.60 (*J* = 7.5 Hz; δ_C 108.9) to the carbons at δ_C 117.9 and 130.4. Moreover, the doublet at δ_H 7.39 (*J* = 7.5 Hz; δ_C 124.4) also showed HMBC cross peaks to the quaternary sp^3 carbon at δ_C 59.7, while the broad singlet at δ_H 6.74, which did not show cross peaks with any carbon in the HSQC spectrum, displayed HMBC cross peaks to the aromatic carbons at δ_C 130.4 and 149.1 as well as to the quaternary sp^3 carbon at δ_C 59.7 and the methine sp^3 carbon at δ_C 78.8. These correlations suggested the presence of the 2,3,3-trisubstituted-2,3-dihydro-*1H*-indole portion.

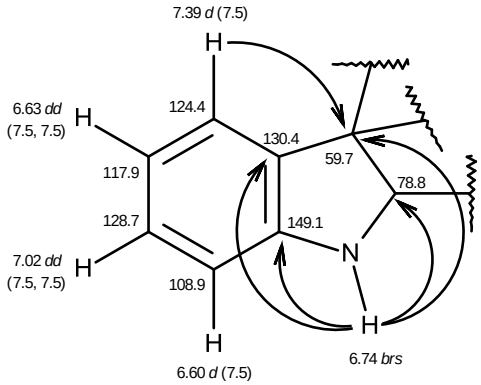

The COSY spectrum showed that another part of the molecule consisted of three coupling systems, i.e., of the methylene protons at δ_H 2.39, *dd* (*J* = 14.0, 9.5 Hz; δ_C 37.3) and 3.14, *dd* (*J* = 14.0, 9.5 Hz; δ_C 37.3) to the methine proton at δ_H 4.12, *t* (*J* = 9.0 Hz; δ_C 55.7), of the amide proton at δ_H 8.27, *d* (*J* = 4.2 Hz) to the methine proton at δ_H 3.39, *t* (*J* = 5.0 Hz; δ_C 62.3) and of the methine proton at δ_H 3.39, *t* (*J* = 5.0 Hz; δ_C 62.3) to the methine proton at δ_H 1.94, *m* (δ_C 32.0), and of the methine proton at δ_H 1.94, *m* (δ_C 32.0) to the methyl protons at δ_H 0.80, *d* (*J* = 6.7 Hz; δ_C 19.0) and 0.69, *d* (*J* = 6.7 Hz; δ_C 18.0). The HMBC spectrum showed cross peaks of the doublet of the amide proton at δ_H 8.27 (*J* = 4.2 Hz) to the

methine carbon signals at δ_C 55.7, 62.3 and the amide carbonyl carbons at δ_C 167.5 and 168.4, indicating that another portion of the molecule was a 1,4-diketopiperazine system. Additionally, the HMBC cross peaks of the doublet of the amide proton at δ_H 8.27 (*J* = 4.2 Hz) to the methine carbon at δ_C 62.3, of the triplet at δ_H 3.39 (*J* = 5.0 Hz; δ_C 62.3) to the carbon at δ_C 32.0 and to the methyl carbons at δ_C 19.0 and 18.0, and of the multiplet of the methine proton at δ_H 1.94 (δ_C 32.0) to the amide carbonyl carbon at δ_C 167.5, to the methine carbon at δ_C 62.3 and methyl carbons at δ_C 19.0 and 18.0, indicated that the isopropyl moiety was placed on C-15 (δ_C 62.3) of the diketopiperazine ring.

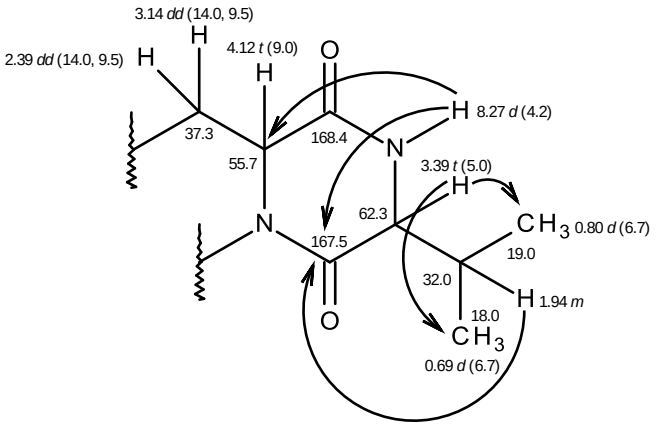

That the 1,4-diketopiperazine ring moiety was linked to the indole ring system through C-2 (δ_C 78.8) of the latter and N-10 of the former, and through the methylene group on C-3 (δ_C 59.7) of the latter and C-11 (δ_C 55.7) of the former, was evidenced by correlations between the methine proton at δ_H 4.12, *t* (*J* = 9.0 Hz; δ_C 55.7) and the signals of the methylene protons at δ_H 3.14, *dd* and 2.39, *dd* (*J* = 14.0, 9.5 Hz; δ_C 37.3), as well as the HMBC correlations of the methylene proton at δ_H 2.39, *dd* (*J* = 14.0; 9.5 Hz; δ_C 37.3) to the carbons at δ_C 59.7, 130.4 and 168.4.

The cross peaks observed in the NOESY spectrum between the signals at δ_H 4.90, *brs* / 4.12, *t* (*J* = 9.0 Hz) and δ_H 4.12, *t* (*J* = 9.0 Hz) / 1.94, *m*, δ_H 4.12, *t* (*J* = 9.0 Hz) / 0.80, *d* (*J* = 6.7 Hz), δ_H 4.12, *t* (*J* = 9.0 Hz) / 0.69, *d* (*J* = 6.7 Hz), suggested that the isopropyl substituent was α oriented.

Taking altogether the NMR data, the partial structure **A** ($C_{16}H_{18}N_3O_2$) was proposed.

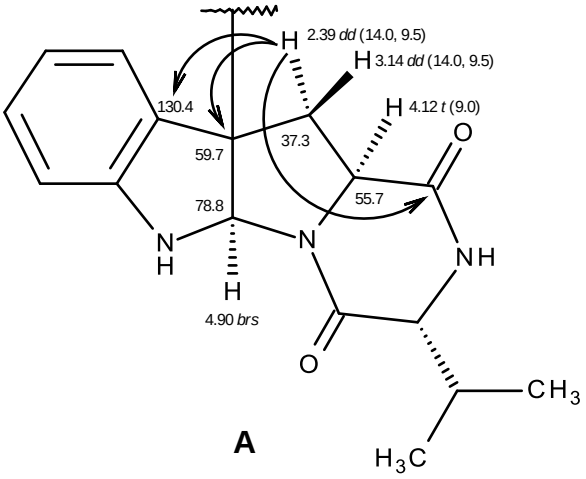

A

Since the (+)-HR-ESIMS gave the molecular formula $C_{32}H_{36}N_6O_4$, the complete structure of eurocristatine (**EC10**) (Figure 61) must comprise two **A** units connected to each other through the carbon at δ_C 59.7.

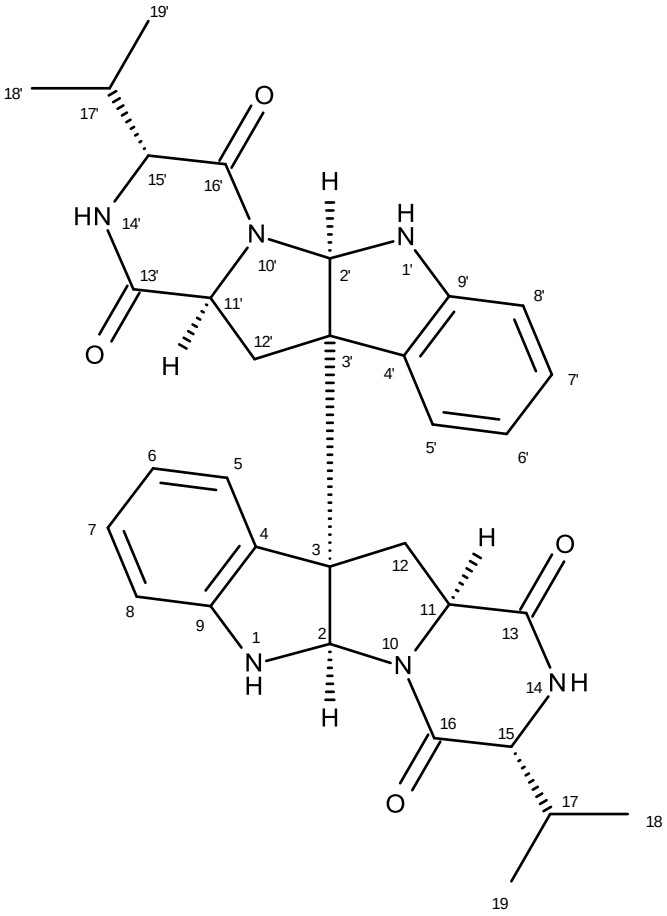

Figure 61. Structure of eurocristatine (**EC10**).

Final proof of the structure and stereochemistry assigned to **EC10** was provided by an X-ray analysis which established the absolute configuration of C-2/2', C-3/3', C-11/11' and C-15/15', respectively as 2/2'*R*, 3/3'*S*, 11/11'*S* and 15/15'*R*. The result depicted in the ORTEP view shown in Figure 62 also revealed the symmetrical nature of eurocristatine (**EC10**).

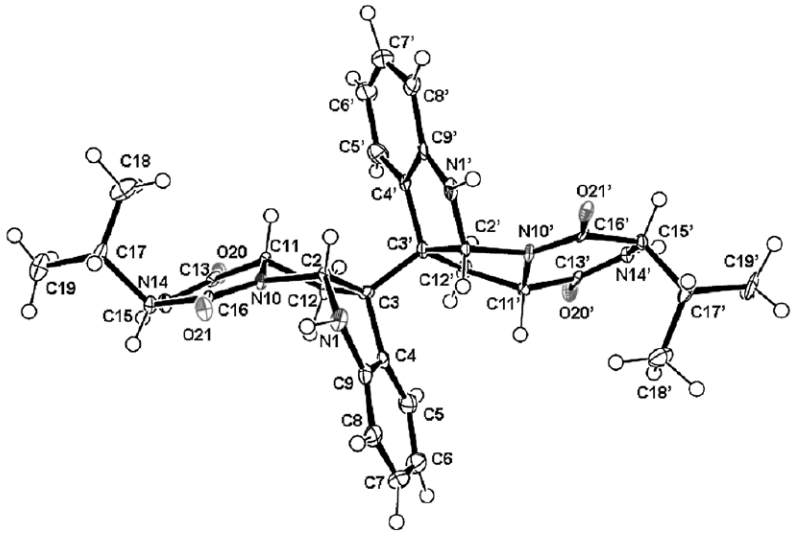

Figure 62. ORTEP view of **EC10**.

Although several diketopiperazine dimers have been previously reported from many fungal sources, and especially from *Aspergillus* species (Barrow *et al*., 1993; Barrow and Sedlock, 1994; Cai *et al*., 2012; Ding *et al*., 2008; Li *et al*., 2009b; Ovenden *et al*., 2004; Raju *et al*., 2009; Son *et al*., 1999; Takahashi *et al*., 1994; 1995a; 1995b; Varoglu *et al*., 1997; Yamada *et al*., 2002), eurocristatine (**EC10**) represents the first diketopiperazine dimer isolated from the genus *Eurotium*.

Recently, two diketopiperazine dimers whose structures closely resemble to eurocristatine (**EC10**), were reported from two distinct marine algal-derived strains of *Eurotium* sp. (Figure 63). Interestingly, the unsymmetrical dimer cristatumin D (**148**) was also isolated from a strain of *E. cristatum* EN-220 isolated from the marine alga *Sargassum thunbergii* (Du *et al*., 2012), whereas cristatumin E (**149**) the stereoisomer of eurocristatine (**EC10**), was isolated from the algicolous *Eurotium herbariorum* HT-2 (Li *et al*., 2013a).

Innumerable natural products bearing the 2,5-diketopiperazine ring with a wide spectrum of therapeutically relevant bioactivities have been isolated to date. Diketopiperazines, also known as piperazine-2,5-diones, are the simplest cyclodipeptides found in Nature, derived from different amino acids and one or more isoprene units, being also found as degradation products of polypeptides. This class of bioactive secondary metabolites is produced by several organisms such as fungi, bacteria, plants and even mammals, being often found alone or embedded in larger and more complex architectures. Natural diketopiperazines are biosynthetically assembled by nonribosomal peptide synthetases (NRPSs) and cyclodipeptide synthases (CDPs), with a structural diversity achieved through choice of amino acid precursors and enzyme-catalyzed reactions like dimerizations (Cornacchia *et al*., 2012; Martins and Carvalho, 2007).

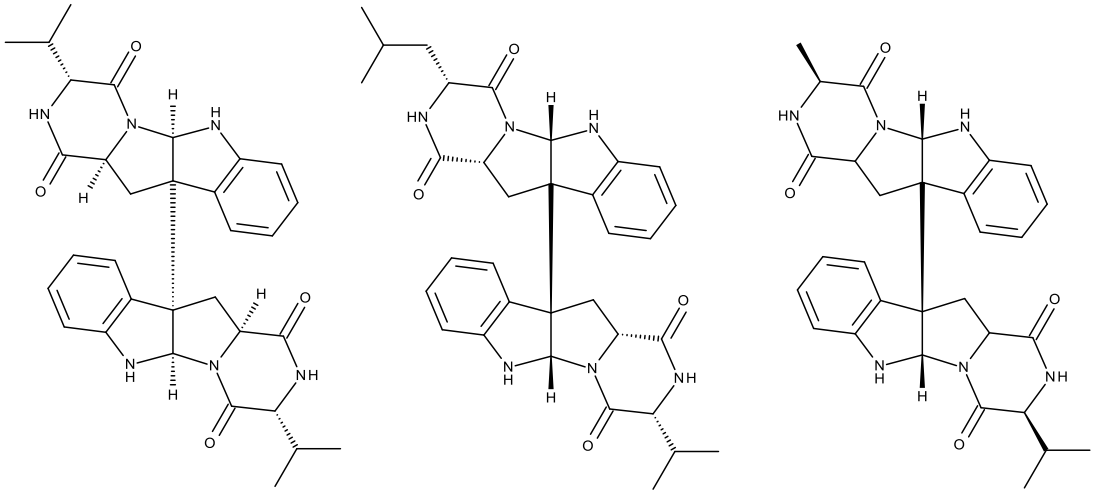

Figure 63. Diketopiperazine dimers related to eurocristatine **(EC10)**.

While cyclo-(L-tryptophyl-L-phenylalanyl) (**EV5**) derives from a simple cyclization of L-tryptophan and L-phenylalanine, echinulin (**EC6**) and its analogs correspond to tri-, di- (**EC7**) or mono- (**EC8-9**) prenylated derivatives of a cyclic dipeptide consisting of L-tryptophan and L-alanine. Eurocristatine (**EC10**) is a dimerized cyclic dipeptide derived from two molecules of L-tryptophan and two molecules of L-valine. Despite the limited number of reports concerning the biosynthesis of dimerized cyclodipeptides, recently a plausible and unifying

hypothesis was proposed for the biosynthetic pathway of dimeric diketopiperazines joined through C3/C3' bond (Kim *et al*., 2009). Thus the structure of eurocristatine (**EC10**) suggests that it was derived from a common biosynthetic pathway proposed in Scheme 3.

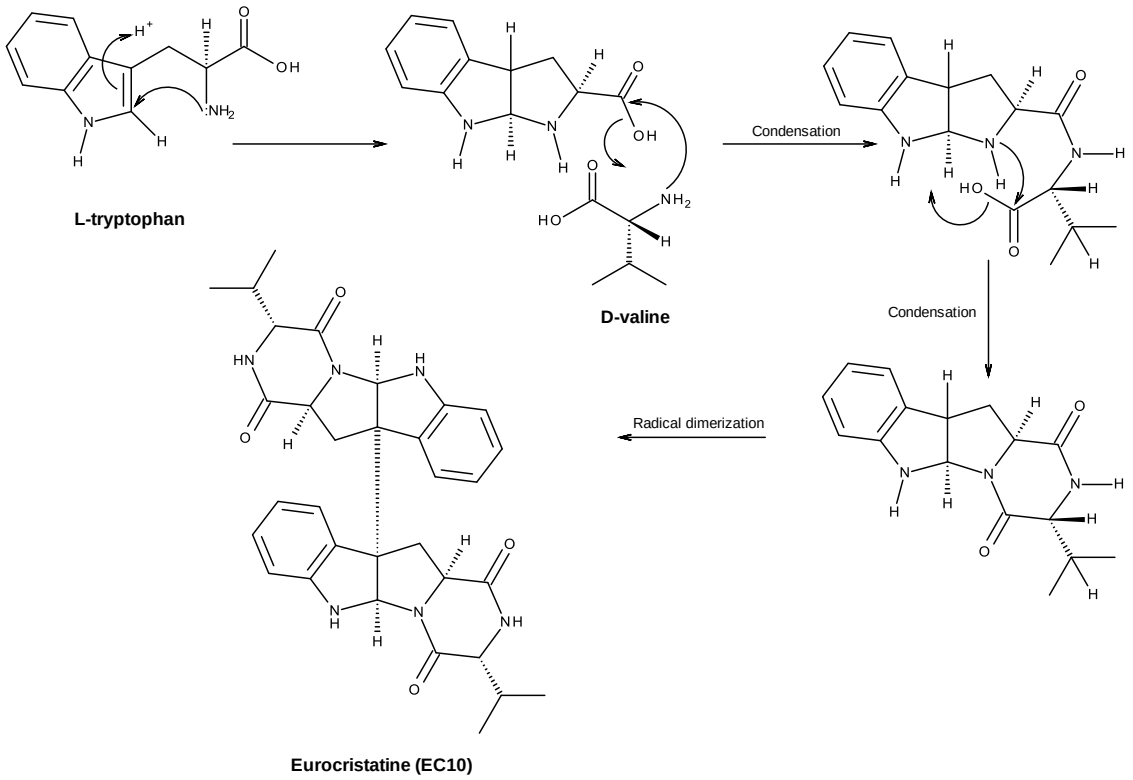

Scheme 3. Proposed biosynthetic pathway for eurocristatine (**EC10**).

3.1.5. Structure Elucidation of Meroditerpenes

3.1.5.1. Chevalone B (NL1)

NL1 was isolated as colorless crystal and its molecular formula $C_{28}H_{40}O_5$ was established on the basis of the (+)-HR-ESIMS *m/z* 457.2949 $[M+H]^+$ (calculated 457.2954), indicating nine degrees of unsaturation. The IR spectrum showed absorption bands for ester (1702 cm^{-1}), conjugated ketone (1585 cm^{-1}) and olefinic (1585 cm^{-1}) groups.

The ^{13}C NMR, DEPT and HSQC spectra (Table 18) revealed the presence of one ester carbonyl (δ_C 170.9), one conjugated ester carbonyl (δ_C 165.3), three

quaternary sp^2 (δ_C 163.2, 159.7, 97.7), one methine sp^2 (δ_C 100.6), four methine sp^3 (δ_C 80.6, 60.1, 55.4, 51.8), four quaternary sp^3 (δ_C 80.4, 37.3, 37.1, 36.9), seven methylene sp^3 (δ_C 40.8, 40.1, 37.9, 23.4, 18.6, 17.7, 16.7) and seven methyl (δ_C 27.8, 21.2, 20.4, 19.7, 16.4, 16.2, 16.0) carbons.

Table 18. ^1H and ^{13}C NMR data ($CDCl_3$, 300.13 and 75.47 MHz) of **NL1**.

Position	δ_C, type	δ_H, mult. (*J* in Hz)	COSY	HMBC
1α	37.9, CH_2	1.73, *m*	H1β	C-2, 3, 5
β		1.07, *m*	H-1α	---
2	23.4, CH_2	1.68, *m*	H-3	C-3
3	80.6, CH	4.46, *dd* (11.0, 5.1)	H-2	C-1, 2, 22, 23, CO (Ac-3)
4	37.3, C	---	---	---
5	55.4, CH	0.88, *m*	H-6α, 6β	---
6α	17.7, CH_2	1.57, *m*	H-5	---
β		1.46, *m*	H-5	---
7α	40.8, CH_2	1.86 *dt* (12.8, 4.8)	H-7β	C-5, 8, 9
β		1.04, *m*	H-7α	---
8	36.9, C	---	---	---
9	60.1, CH	0.93, *dd* (12.4, 2.0)	H-11β	---
10	37.1, C	---	---	---
11α	18.6, CH_2	1.70, *m*	H-11β, 12α	---
β		1.35, *dd* (12.4, 3.2)	H-9, 11α, 12α	---
12α	40.1, CH_2	2.06, *dd* (12.0, 4.3)	H-11α, 11β, 12β	C-9, 14
β		1.59, *dd* (12.0, 3.2)	H-12α	---
13	80.4, C	---	---	---
14	51.8, CH	1.46, *dd* (12.8, 4.8)	H-15α, 15β	C-7, 9, 12, 13,
15α	16.7, CH_2	2.43, *dd* (16.9, 4.8)	H-14, 15β	C-13, 14, 16, 17, 21
β		2.17, *dd* (16.9, 12.0)	H-14, 15α	C-8, 14, 16
16	97.7, C	---	---	---
17	163.2, C	---	---	---
18	100.6, CH	5.69, *s*	H-20	C-16, 17, 19, 20
19	159.7, C	---	---	---
20	19.7, CH_3	2.18, *s*	H-18	C-18, 19
21	165.3, CO	---	---	---
22	27.8, CH_3	0.86, *s*	---	C-3, 4, 5, 23
23	16.0, CH_3	0.89, *s*	---	C-3, 4, 5, 22
24	16.2, CH_3	0.88, *s*	---	C-1, 5, 9, 10
25	16.4, CH_3	0.87, *s*	---	C-7, 8, 9, 14
26	20.4, CH_3	1.20, *s*	---	C-12, 13, 14
Ac-3	170.9, CO	---	---	---
	21.2, CH_3	2.05, *s*	---	CO (Ac-3)

The ^1H NMR spectrum, in conjunction with the HSQC spectrum (Table 18), displayed the signals of one olefinic proton at δ_H 5.69, *s*, one oxymethine proton at δ_H 4.46, *dd* (*J* = 11.0, 5.1 Hz), three methine protons at 1.46, *dd* (*J* = 12.8, 4.8 Hz), 0.93, *dd* (*J* = 12.4, 2.0 Hz) and 0.88, *m*, and seven methyl groups at δ_H 2.18, *s*, 2.05, *s*, 1.20, *s*, 0.89, *s*, 0.88, *s*, 0.87, *s* and 0.86, *s*.

While the COSY spectrum (Table 18) displayed the cross peak of the oxymethine proton signal at δ_H 4.46, *dd* (*J* = 11.0, 5.1 Hz) to the signals of the methylene protons at δ_H 1.68, *m* (2H; δ_C 23.4), the HMBC spectrum (Table 18) displayed correlations of the oxymethine proton at δ_H 4.46, *dd* (*J* = 11.0, 5.1 Hz; δ_C 80.6) and of the methyl protons at δ_H 2.05, *s* (δ_C 21.2) to the carbonyl carbon at δ_C 170.9, indicating the presence of the acetoxyl group on the oxymethine carbon (δ_C 80.6). Furthermore, the HMBC cross peaks of the signal of the oxymethine proton at δ_H 4.46, *dd* (*J* = 11.0, 5.1 Hz; δ_C 80.6) to the methyl carbons at δ_C 27.8 and 16.0, and to the methylene sp^3 carbons at δ_C 37.9 and 23.4, and of the signals of the methyl protons at δ_H 0.86, *s* (δ_C 27.8) and 0.89, *s* (δ_C 16.0) to the oxymethine carbon at δ_C 80.6, the quaternary sp^3 carbon at δ_C 37.3 and the methine sp^3 carbon at δ_C 55.4, suggested the existence of the fragment **A**.

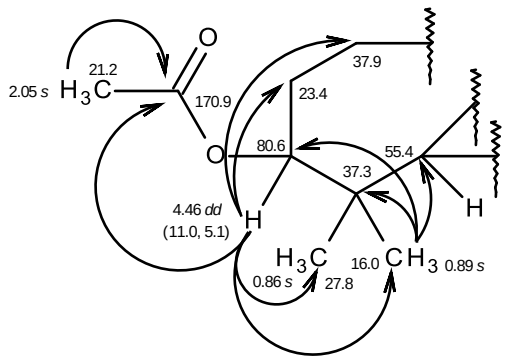

A

Additionally, the HMBC correlations of the methyl protons at δ_H 0.88, *s* (δ_C 16.2) to the methine sp^3 carbons at δ_C 60.1 and 55.4, the methylene sp^3 carbon at δ_C 37.9, and of the methyl protons at δ_H 0.87, *s* (δ_C 16.4) to the carbons at δ_C 60.1, 40.8 and 36.9, suggested the existence of a 2-acetoxy-5,6-disubstituted-1,1,4a,6-tetramethyldecalin fragment (**B**).

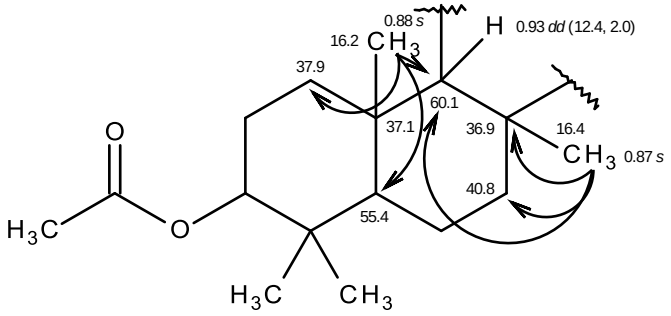

B

Moreover, the methyl singlet at δ_H 0.87 (δ_C 16.4) also gave cross peak to the methine sp^3 carbon at δ_C 51.8, which, in turn showed HMBC cross peak to the methyl singlet at δ_H 1.20 (δ_C 20.4). Since the methyl singlet at δ_H 1.20 (δ_C 20.4) also displayed HMBC cross peaks to the oxyquaternary carbon at δ_C 80.4 and the methylene carbon at δ_C 40.1, the perhydrophenanthrene skeleton was suggested. This was supported by the HMBC correlations of the methylene proton at δ_H 2.06, *dd* (*J* = 12.0, 4.3 Hz; δ_C 40.1) to the methine sp^3 carbons at δ_C 60.1, 51.8, and of the methine proton at δ_H 1.46, *dd* (*J* = 12.8, 4.8 Hz; δ_C 51.8) to the carbons at δ_C 80.4, 60.1 and 40.1. Since the COSY spectrum displayed correlations of the methine proton at δ_H 1.46, *dd* (*J* = 12.8, 4.8 Hz; δ_C 51.8) to the methylene protons at δ_H 2.43, *dd* (*J* = 16.9, 4.8 Hz; δ_C 16.7) and 2.17, *dd* (*J* = 16.9, 12.0 Hz; δ_C 16.7), the methylene group (δ_C 16.7) was connected to the methine carbon at δ_C 51.8. The HMBC cross peaks of the methylene protons at δ_H 2.43, *dd* (*J* = 16.9, 4.8 Hz; δ_C 16.7) and 2.17, *dd* (*J* = 16.9, 12.0 Hz; δ_C 16.7) to the carbons at δ_C 80.4 and 51.8 confirmed the presence of fragment **C**.

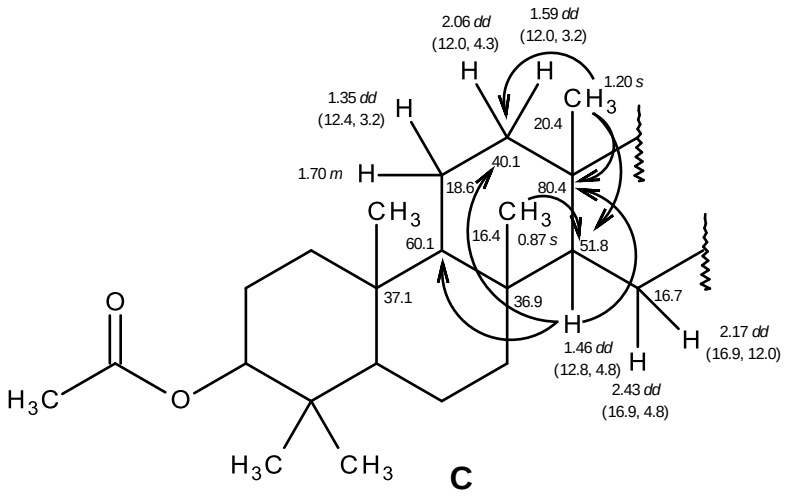

C

Another portion of the molecule consists of the olefinic proton at δ_H 5.69, *s* (δ_C 100.6) and the methyl protons at δ_H 2.18, *s* (δ_C 19.7), which showed cross peak to each other in the COSY spectrum, suggesting an allylic coupling. This was also confirmed by the HMBC cross peak between the singlet at δ_H 5.69 (δ_C 100.6) to the methyl carbon at δ_C 19.7. Since the HBMC spectrum displayed cross peaks of the singlet of the olefinic proton at δ_H 5.69 (δ_C 100.6) to the sp^2 carbons at δ_C 163.2, 159.7, 97.7, this portion must contain two double bonds. The HMBC spectrum also displayed cross peaks of the methyl singlet at δ_H 2.18 (δ_C 19.7) to the quaternary sp^2 carbon at δ_C 159.7 and the methine sp^2 carbon at δ_C 100.6. This correlation pattern, together with the presence of a quaternary sp^2 carbon at 165.3, suggested that this portion of the molecule should correspond to 6-methyl-2*H*-pyran-1-one (**D**).

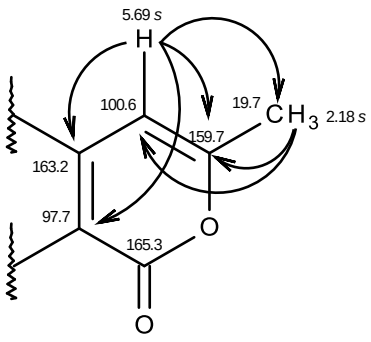

D

That the perhydrophenanthrene portion (fragment **C**) was connected to the 6-methyl-2*H*-pyran-1-one portion (fragment **D**) through an ethereal bridge, was substantiated by the HMBC cross peaks of the signals of the methylene protons at δ_H 2.43, *dd* (*J* = 16.9, 4.8 Hz; δ_C 16.7) and 2.17, *dd* (*J* = 16.9, 12.0 Hz; δ_C 16.7) to the carbonyl carbon at δ_C 165.3 and the quaternary sp^2 carbons at δ_C 163.2 and 97.7 of the 6-methyl-2*H*-pyran-1-one ring. Thus, the structure of **NL1** was established as:

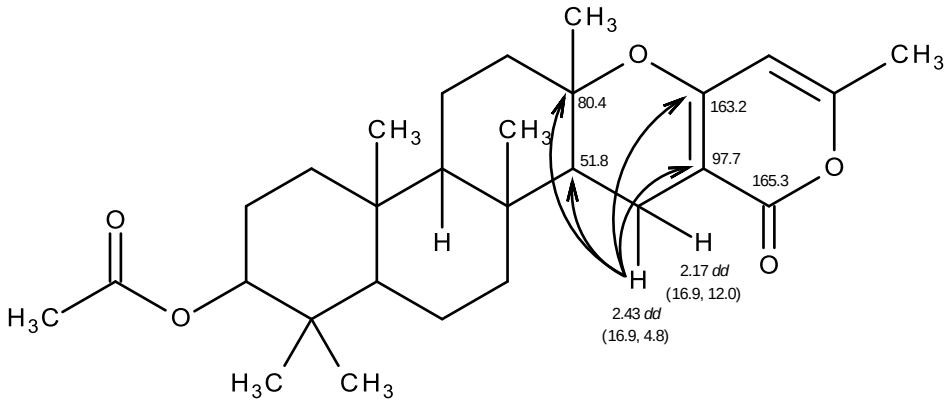

Since the oxymethine proton (H-3) appeared as a double doublet at δ_H 4.46 (*J* = 11.0, 5.1 Hz), the position of the acetoxyl group on C-3 (δ_C 80.6) was β-oriented (Kojima and Hogura, 1989).

Literature survey revealed that **NL1** corresponded to chevalone B (Figure 64), a meroditerpene isolated from the culture of fungus *Eurotium chevalieri* (Kanokmedhakul *et al*., 2011).

Chevalone B was reported to exhibit strong cytotoxicity against human epidermoid carcinoma (KB) and human small cell lung cancer (NCI-H187) cell lines with IC_{50} values of 2.9 and 3.9 µg/mL (Kanokmedhakul *et al*., 2011).

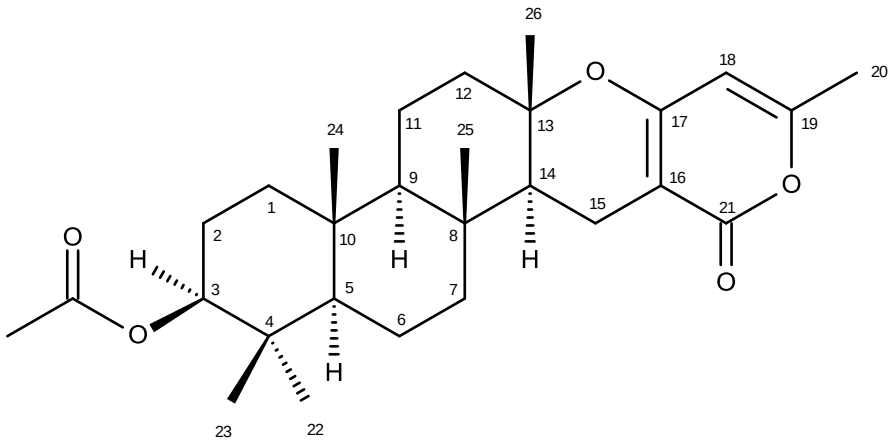

Figure 64. Structure of chevalone B (**NL1**).

3.1.5.2. Aszonapyrone A (NL2)

NL2 was also isolated as colorless crystal and its (+)-HR-ESIMS *m/z* 457.2954 $[M+H]^+$ (calculated for $C_{28}H_{41}O_5$) indicated that it had the same molecular formula ($C_{28}H_{40}O_5$) and degree of unsaturation as **NL1**. The ^1H and ^{13}C NMR spectra of **NL2** (Table 19) resembled those of **NL1**, expect for the presence of the exocyclic methylene group (δ_H 4.83, *s* and 4.60, *s*; δ_C 106.4 and δ_C 148.3) instead of the methyl group on the oxyquaternary carbon (δ_H 1.20, *s*; δ_C 20.4) of **NL1**, and a broad singlet of the hydroxyl group at δ_H 11.18.

Table 19. ^1H and ^{13}C NMR data (DMSO-d_6, 300.13 and 75.47 MHz) of **NL2**.

Position	δ_C, type	δ_H, mult. (*J* in Hz)	COSY	HMBC
1α	37.6, CH_2	1.64, *brd* (11.2)	H-1β	C-3, 5
β		1.00, *m*	H-1α	C-24
2	22.9, CH_2	1.62, *m*	H-3	---
3	79.9, CH	4.39, *dd* (10.1, 5.9)	H-2	C-1, 22, 23, Ac-3
4	37.4, C	---	---	---
5	54.7, CH	0.92, *d* (9.5)	H-6β	---
6α	18.4, CH_2	1.54, *m*	---	---
β		1.40, *m*	H-5	---
7α	39.5, CH_2	1.85, *m*	H-7β	C-5, 9
β		1.38, *m*	H-7α	C-25
8	37.4, C	---	---	---
9	59.1, CH	1.06, *d* (12.2)	H-11α	---
10	36.9, C	---	---	---
11α	23.4, CH_2	1.24, *m*	H-9	---
β		1.57, *m*	---	---
12α	37.7, CH_2	2.50, *brs*	---	C-14
β		1.80, *m*	---	C-9, 13
13	148.3, C	---	---	---
14	53.0, CH	2.44, *d* (2.9)	H-15α, 15β	C-7,13, 16, 25
15α	18.3, CH_2	2.46, *dd* (14.4, 2.9)	H-14, 15β	C-13, 14, 16, 17, 21
β		2.30, *d* (14.4)	H-14, 15α	C-13, 14, 16, 17, 21
16	101.0, C	---	---	---
17	164.7, C	---	---	---
18	99.9, CH	5.92, *s*	H-20	C-16, 17, 19, 20
19	159.5, C	---	---	---
20	19.2, CH_3	2.11, *s*	H-18	C-18, 19
21	164.8, CO	---	---	---
22	27.7, CH_3	0.83, *s*	---	C-3, 4, 5, 23
23	16.0, CH_3	0.81, *s*	---	C-3, 4, 5, 22
24	16.4, CH_3	0.80, *s*	---	C-1, 5, 9
25	14.9, CH_3	0.69, *s*	---	C-7, 9, 14
26a	106.4, CH_2	4.83, *s*	H-14, H-26b	C-12, 14
b		4.60, *s*	H-26a	C-12, 14
Ac-3	170.1, CO	---	---	---
	21.0, CH_3	2.00, *s*	---	CO (Ac-3)
OH-17	---	11.18, *brs*	---	---

The existence of the 2-acetoxy-5,6-disubstituted-1,1,4a,6-tetramethyldecalin fragment was evidenced by the HMBC correlations (Table 19) of the oxymethine proton at δ_H 4.39, *dd* (*J* = 10.1, 5.9 Hz; δ_C 79.9) to the acetoxy carbonyl carbon at δ_C 170.1, the methylene carbon at δ_C 37.6, and the methyl carbons at δ_C 27.7 and 16.0, of the methyl protons at δ_H 2.00, *s* (δ_C 21.0) to the carbonyl carbon at δ_C 170.1, of the methyl protons at δ_H 0.83, *s* (δ_C 27.7) and 0.81, *s* (δ_C 16.0) to the methine sp^3 carbons at δ_C 79.9 and 54.7, and the quaternary sp^3 carbon at δ_C 37.4, of the methyl protons at δ_H 0.80, *s* (δ_C 16.4) to the methine sp^3 carbons at δ_C 59.1 and 54.7, and the methylene carbon at δ_C 37.6, and of the methyl protons at δ_H 0.69, *s* (δ_C 14.9) to the methine sp^3 carbons at δ_C 59.1 and 53.0, and the methylene carbon at δ_C 39.5. As the HMBC spectrum displayed cross peaks of the methylene proton singlets at δ_H 4.83 (δ_C 106.4) and 4.60 (δ_C 106.4) to the methylene carbon at δ_C 37.7 and the methine carbon at δ_C 53.0, the exocyclic methylene group was on C-13 (δ_C 148.3).

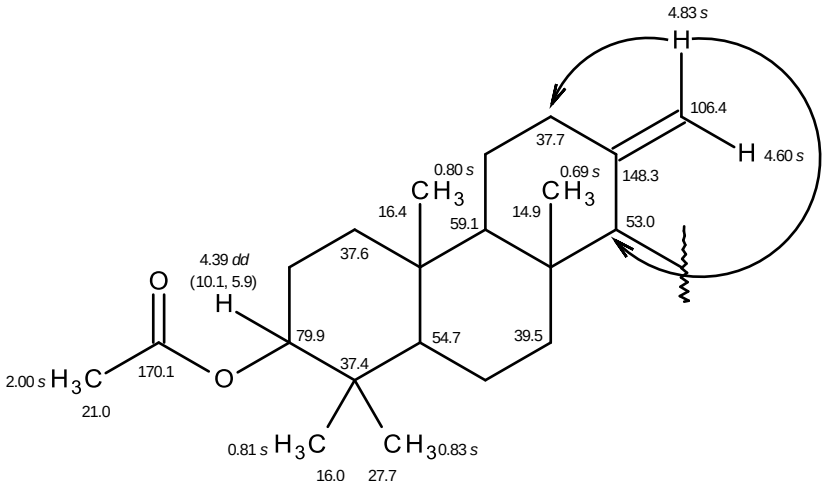

Similar to **NL1**, the nonterpenoid moiety of **NL2** was also the 6-methyl-2*H*-pyran-1-one as evidenced by the allylic coupling of the olefinic proton at δ_H 5.92, *s* (δ_C 99.9) to the methyl protons at δ_H 2.11, *s* (δ_C 19.2) observed in the COSY spectrum (Table 19), as well as by the HMBC cross peaks of the singlet of the olefinic proton at δ_H 5.92 (δ_C 99.9) to the olefinic carbons at δ_C 164.7, 159.5, 101.0 and the methyl carbon at δ_C 19.2, and of the methyl singlet at δ_H 2.11 (δ_C 19.2) to the olefinic carbons at δ_C 159.5 and 99.9. Since the ^{1}H NMR spectrum displayed a broad singlet at δ_H 11.18, it was suggested that the hydroxyl group was on the olefinic carbon at δ_C 164.7. This hypothesis was supported by the chemical shift

value of the hydroxyl proton at δ_H 11.18, *brs*, characteristic of the enolic hydroxyl group, as well as the absence of oxyquaternary carbon at δ_C 80.4.

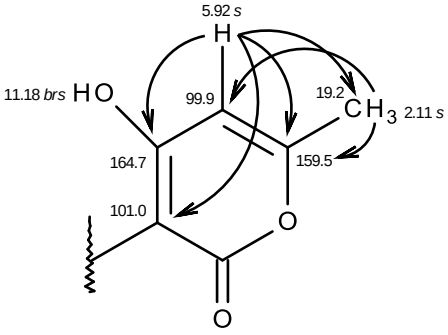

Like **NL1**, the perhydrophenanthrene and the 6-methyl-2*H*-pyran-1-one portions were connected through the methylene group (δ_H 2.46, *dd*, *J* = 14.4, 2.9 Hz; δ_C 18.3) of the former and the quaternary sp^2 carbon at δ_H 101.0 of the latter, as evidenced by the HMBC cross peaks of the double doublet of the methylene proton at 2.46 (*J* = 14.4, 2.9 Hz; δ_C 18.3) to the carbons at δ_C 101.0, 164.7 and 164.8.

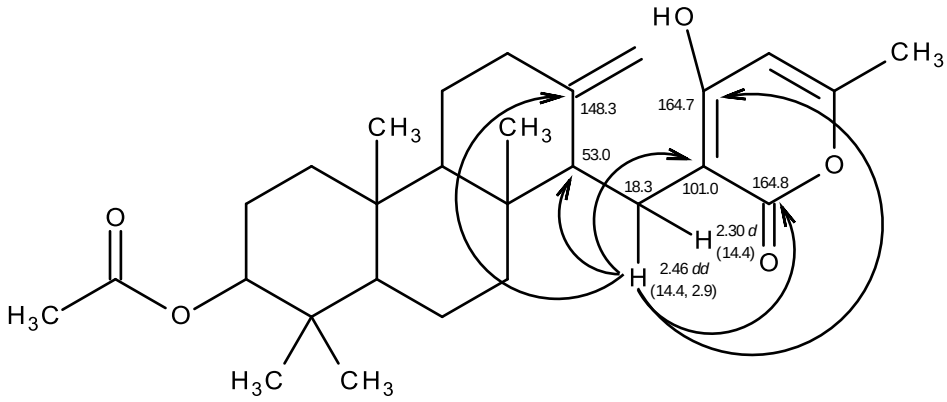

Thus, the structure of **NL2** was established as [8- [(4-hydroxy-6-methyl -2-oxo-pyran-3-yl) methyl] - 1,1,4a,8a – tetramethyl – 7 – methylene - 2,3,4,4b,5,6,8,9,10,10a-decahydrophenanthren-2-yl] acetate, which corresponds to the meroditerpene aszonapyrone A (Figure 65), originally isolated from the fungus *Aspergillus zonatus* by Kimura *et al*. (1982), and recently from the fungus *Eurotium chevalieri* (Kanokmedhakul *et al*., 2011).

Aszonapyrone A was found to exhibit antibacterial activity against *Staphylococcus aureus* 209P and *S. aureus* res. with the MIC value of 6.3 µg/mL (Kimura *et al*., 1982).

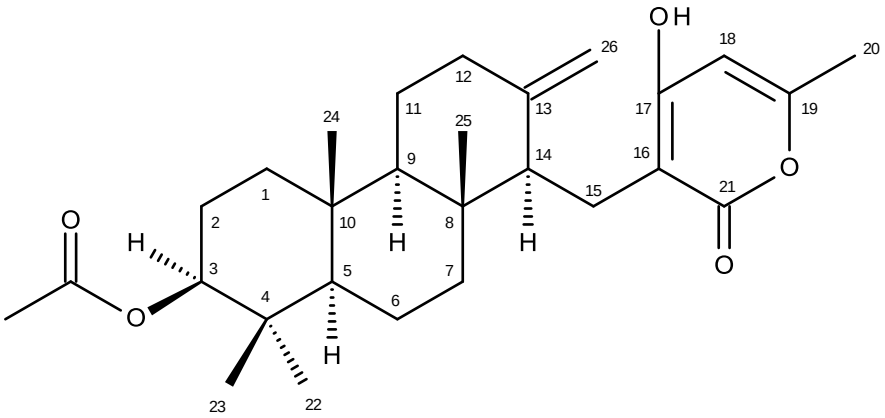

Figure 65. Structure of aszonapyrone A (**NL2**).

3.1.5.3. Aszonapyrone B (NL3)

NL3 was also isolated as colorless crystal. The ^{1}H and ^{13}C NMR spectra of **NL3** (Table 20) closely resembled those of **NL2**, except for the lack of the acetoxyl group (δ_H 2.00, *s*; δ_C 21.0 / δ_C 170.1). The ^{13}C NMR, DEPT and HSQC spectra (Table 20) revealed the presence of one conjugated ester carbonyl (δ_C 164.7), four quaternary sp^2 (δ_C 164.5, 158.8, 148.3, 100.9), one methylene sp^2 (δ_C 105.9), one methine sp^2 (δ_C 99.9), four methine sp^3 (δ_C 80.0, 59.4, 54.8, 52.9), seven methylene sp^3 (δ_C 39.9, 38.1, 37.4, 27.0, 22.7, 18.3, 18.3), three quaternary sp^3 (δ_C 39.9, 37.4, 36.9) and five methyl (δ_C 29.9, 18.9, 15.8, 15.4, 14.7) carbons. The presence of the hydroxyl group on C-3 (δ_C 80.0) of the diterpenoid moiety was confirmed by a multiplet at δ_H 3.10 in the ^{1}H NMR spectrum and the corresponding oxymethine carbon at δ_C 80.0, as well as the higher chemical shift value of C-2 (δ_C 27.0) than that in **NL1** and **NL2**.

The rest of the ^{1}H and ^{13}C signals were very similar to those of **NL2** (Table 20).

Table 20. ^{1}H and ^{13}C NMR data (DMSO-d_6, 300.13 and 75.47 MHz, T = 45 ºC) of **NL3**.

Position	δ_C, type	δ_H, mult. (*J* in Hz)	COSY	HMBC
1α	38.1, CH_2	1.65, *m*	H-1β	---
β		0.95, *m*	H-1α	---
2	27.0, CH_2	1.50, *m*	H-3	---
3	80.0, CH	3.10, *m*	H-2	---
4	37.4, C	---	---	---
5	54.8, CH	0.80, *m*	H-6β	---
6α	18.3, CH_2	1.60, *m*	---	---
β		1.39, *m*	H-5	---
7	38.7, CH_2	1.65, *m*	---	---
8	39.9, C	---	---	---
9	59.4, CH	1.02, *m*	H-11	---
10	36.9, C	---	---	---
11	22.7, CH_2	1.61, *m*	H-9	---
12	39.9, CH_2	2.50, *m*	---	---
13	148.3, C	---	---	---
14	52.9, CH	2.47, *m*	---	C-12, 16
15α	18.3, CH_2	2.50, *m*	H-15β	C-13, 21
β		2.30, *m*	H-15α	C-13, 14, 16, 21
16	100.9, C	---	---	---
17	164.5, C	---	---	---
18	99.9, CH	5.90, *s*	H-20	C-16, 19, 20
19	158.8, C	---	---	---
20	18.9, CH_3	2.10, *s*	H-18	---
21	164.7, CO	---	---	---
22	29.9, CH_3	0.92, *s*	---	C-3, 4, 5, 23
23	15.4, CH_3	0.69, *s*	---	C-3, 4, 5, 22
24	15.8, CH_3	0.78, *s*	---	C-1, 5, 9, 10
25	14.7, CH_3	0.71, *s*	---	C-8, 9, 13
26a	105.9, CH_2	4.82, *s*	H-26b	C-12, 14
b		4.60, *s*	H-26a	C-12, 14

Thus, the structure of **NL3** was established as the deacetyl analogue of **NL2**, which corresponded to aszonapyrone B (Figure 67), also isolated from *Eurotium chevalieri* (Kanokmedhakul *et al*., 2011).

Table 21. Comparison of the ^{1}H and ^{13}C NMR data (DMSO-d_6, 300.13 and 75.47 MHz) of **NL2** and **NL3**.

Position	**NL2**		**NL3**	
	δ_C, type	δ_H, mult. (*J* in Hz)	δ_C, type	δ_H, mult. (*J* in Hz)
1α	37.6, CH_2	1.64, *brd* (11.2)	38.1, CH_2	1.65, *m*
β		1.00, *m*		0.95, *m*
2	22.9, CH_2	1.62, *m*	27.0, CH_2	1.50, *m*
3	79.9, CH	4.39, *dd* (10.1, 5.9)	80.0, CH	3.10, *m*
4	37.4, C	---	37.4, C	---
5	54.7, CH	0.92, *d* (9.5)	54.8, CH	0.80, *m*
6α	18.4, CH_2	1.54, *m*	18.3, CH_2	1.60, *m*
β		1.40, *m*		1.39, *m*
7α	39.5, CH_2	1.85, *m*	38.7, CH_2	1.65, *m*
β		1.38, *m*		
8	37.4, C	---	39.9, C	---
9	59.1, CH	1.06, *d* (12.2)	59.4, CH	1.02, *m*
10	36.9, C	---	36.9, C	---
11α	23.4, CH_2	1.24, *m*	22.7, CH_2	1.61, *m*
β		1.57, *m*		
12α	37.7, CH_2	2.50, *brs*	39.9, CH_2	2.50, *m*
β		1.80, *m*		
13	148.3, C	---	148.3, C	---
14	53.0, CH	2.44, *brd* (2.9)	52.9, CH	2.47, *m*
15α	18.3, CH_2	2.46, *dd* (14.4, 2.9)	18.3, CH_2	2.50, *m*
β		2.30, *d* (11.8)		2.30, *m*
16	101.0, C	---	100.9, C	---
17	164.7, C	---	164.5, C	---
18	99.9, CH	5.92, *s*	99.9, CH	5.90, *s*
19	159.5, C	---	158.8, C	---
20	19.2, CH_3	2.11, *s*	18.9, CH_3	2.10, *s*
21	164.8, CO	---	164.7, CO	---
22	27.7, CH_3	0.83, *s*	29.9, CH_3	0.92, *s*
23	16.0, CH_3	0.81, *s*	15.4, CH_3	0.69, *s*
24	16.4, CH_3	0.80, *s*	15.8, CH_3	0.78, *s*
25	14.9, CH_3	0.69, *s*	14.7, CH_3	0.71, *s*
26a	106.4, CH_2	4.83, *s*	105.9, CH_2	4.82, *s*
b		4.60, *s*		4.60, *s*
Ac-3	170.1, CO	---		
	21.0, CH_3	2.00, *s*		
OH-17	---	11.18, *brs*		

Since **NL3** was obtained in suitable crystal for the X-ray diffraction, its crystal structure was determined. X-ray analysis confirmed the proposed structure and the absolute configuration of the stereogenic carbons (C-3*S*, C-8*S* and C-10*R*) as previously proposed by Kanokmedhakul *et al.* (2011). The ORTEP view of **NL3** is shown in Figure 66.

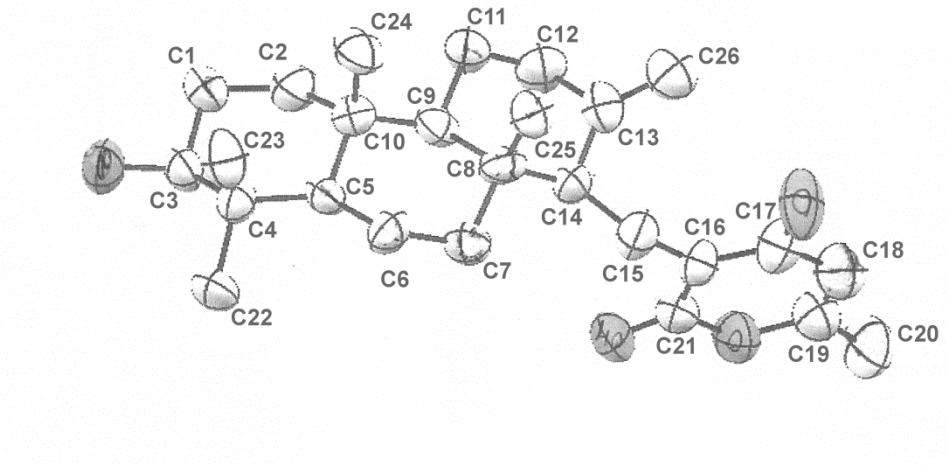

Figure 66. ORTEP view of **NL3**.

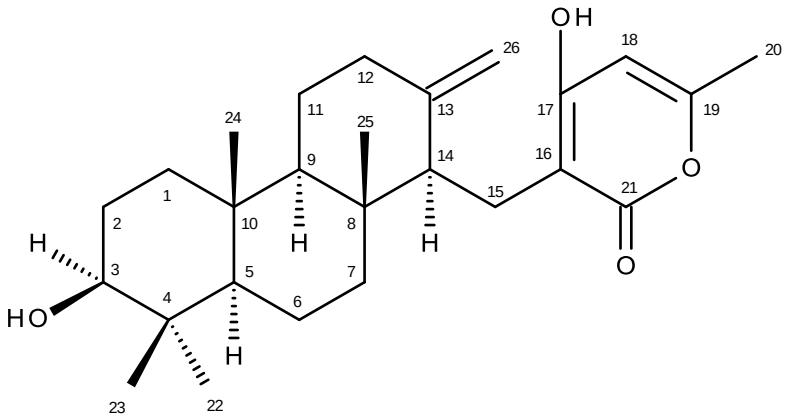

Figure 67. Structure of aszonapyrone B (**NL3**).

3.1.5.4. Sartorypyrone C (NP1)

NP1 was isolated as white solid and its molecular formula $C_{26}H_{38}O_4$ was established on the basis of the (+)-HR-ESIMS *m/z* 415.2836 $[M+H]^+$ (calculated 415.2848), indicating eight degrees of unsaturation. The IR spectrum showed absorption bands for hydroxyl (3445 cm^{-1}), conjugated ester carbonyl (1668 cm^{-1}) and olefin (1649, 1636 cm^{-1}) groups. The general features of the ^1H and ^{13}C NMR spectra of **NP1** (Table 22) closely resembled those of **NL3.** The ^{13}C NMR, DEPT and HSQC spectra (Table 22) exhibited the signals of six quaternary sp^2 (δ_C 164.6, 164.3, 159.3, 136.6, 126.2. 101.4), one methine sp^2 (δ_C 99.9), three quaternary sp^3 (δ_C 38.8, 38.4 and 36.8), one oxymethine sp^3 (δ_C 76.9), two

methine sp^3 (δ_C 56.0, 54.8), seven methylene sp^3 (δ_C 38.0, 37.9, 34.2, 22.1, 21.7, 18.2, 17.7), and six methyl (δ_C 28.1, 21.2, 20.3, 19.2, 16.3 and 15.7) carbons. However, contrary to the ^{13}C NMR spectrum of **NL3**, the ^{13}C NMR spectrum of **NP1** displayed a tetrasubstituted double bond (δ_C 126.2 and 136.6) and a sp^2 methyl group (δ_H 1.55, *s*; δ_C 20.3) instead of the exocyclic methylene group.

The ^1H NMR spectrum together with the HSQC spectrum (Table 22), displayed the signals of an olefinic proton at δ_H 5.90, *s*, methylene protons at δ_H 3.02, *brs*, one oxymethine proton at δ_H 2.97, *m*, two methine protons at δ_H 0.97, *brd* (*J* = 11.4 Hz) and 0.67, *brd* (*J* = 9.6 Hz), and six methyl groups at δ_H 2.12, *s*, 1.55, *s*, 0.89, *s*, 0.86, *s*, 0.77, *s*, and 0.66, *s*.

Table 22. ^1H and ^{13}C NMR data (DMSO-d_6, 300.13 and 75.47 MHz) of **NP1**

Position	δ_C, type	δ_H, mult. (*J* in Hz)	COSY	HMBC
1	37.9, CH_2	1.65, *m*	H-2	---
2	21.7, CH_2	1.46, *m*	H-1, 3	---
3	76.9, CH	2.97, *m*	H-2	---
4	38.4, C	---	---	---
5	54.8, CH	0.67, *brd* (9.6)	H-6	---
6	17.7, CH_2	1.35, *m*	H-5, 7	---
7	38.0, CH_2	1.96, *m*	H-6	---
8	38.8, C	---	---	---
9	56.0, CH	0.97, *brd* (11.4)	H-11	C-24
10	36.8, C	---	---	---
11	18.2, CH_2	1.46, *m*	H-9, 12	---
12	34.2, CH_2	1.94, *m*	H-11	---
13	126.2, C	---	---	---
14	136.6, C	---	---	---
15	22.1, CH_2	3.02, *brs*	---	C-8, 13, 14, 16, 17, 21
16	101.4, C	---	---	---
17	164.3, C	---	---	---
18	99.9, CH	5.90, *s*	H-20	C-16, 17, 19, 20
19	159.3, C	---	---	---
20	19.2, CH_3	2.12, *s*	H-18	C-18, 19
21	164.6, C	---	---	---
22	28.1, CH_3	0.86, *s*	---	C-3, 4, 5, 23
23	15.7, CH_3	0.66, *s*	---	C-3, 4, 5, 22
24	16.3, CH_3	0.77, *s*	---	C-1, 5, 9, 10
25	21.2, CH_3	0.89, *s*	---	C-8, 9, 14
26	20.3, CH_3	1.55, *s*	---	C-12, 13, 14

The HMBC correlations (Table 22) of the methyl protons at δ_H 0.86, *s* (δ_C 28.1) and 0.66, *s* (δ_C 15.7) to the carbons at δ_C 76.9, 54.8, 38.4, of the methyl protons at δ_H 0.77, *s* (δ_C 16.3) to the carbons at δ_C 56.0, 54.8, 37.9 and 36.8, and of the methyl protons at δ_H 0.89, *s* (δ_C 21.2) to the carbons at δ_C 136.6, 56.0 and 38.8, confirmed the presence of the tetramethylperhydrophenanthrene moiety.

Moreover, the HMBC cross peaks of the singlet of the methyl protons at δ_H 1.55 (δ_C 20.3) to the tetrasubstituted olefinic carbons at δ_C 136.6 and 126.2, and the methylene carbon at δ_C 34.2, of the singlet of the methyl protons at δ_H 0.89 (δ_C 21.2) to the olefinic carbon at δ_C 136.6, of the methylene protons at δ_H 3.02, *brs* (2H; δ_C 22.1) to the olefinic carbons at δ_C 136.6 and 126.2 confirmed the presence of the methyl group at C-13 (δ_C 126.2).

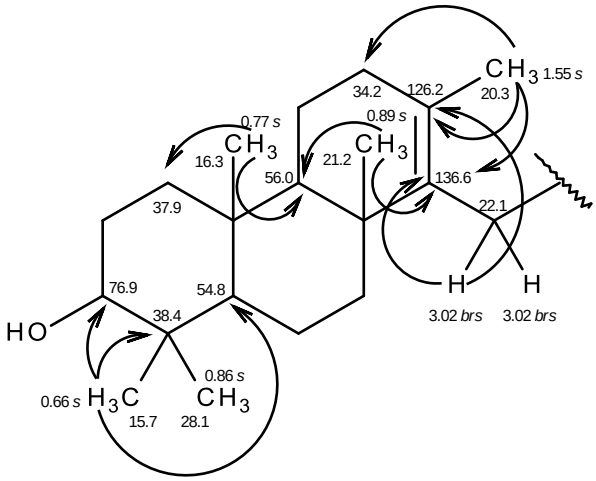

The existence of the same 4-hydroxy-6-methyl-2*H*-pyran-2-one was evidenced by the singlets of the olefinic proton at δ_H 5.90 and the methyl protons at δ_H 2.12 in the ^{1}H NMR spectrum as well as by the HMBC cross peaks of the singlet at δ_H 5.90, *s* (δ_C 99.9) to the carbons at δ_C 164.3, 159.3, 101.4, 19.2, and of the methyl singlet at δ_H 2.12 (δ_C 19.2) to the carbons at δ_C 159.3 and 99.9. In the same manner, the HMBC cross peaks of the broad singlet at δ_H 3.02 of the methylene protons (δ_C 22.1) to the tetrasubstituted olefinic carbons at δ_C 136.6 and 126.2 of the perhydrophenanthrene portion and to the carbons at δ_C 164.6, 164.3 and 101.4 of the 4-hydroxy-6-methyl-2*H*-pyran-2-one portion, confirmed that the two portions were connected through this methylene carbon (δ_C 22.1).

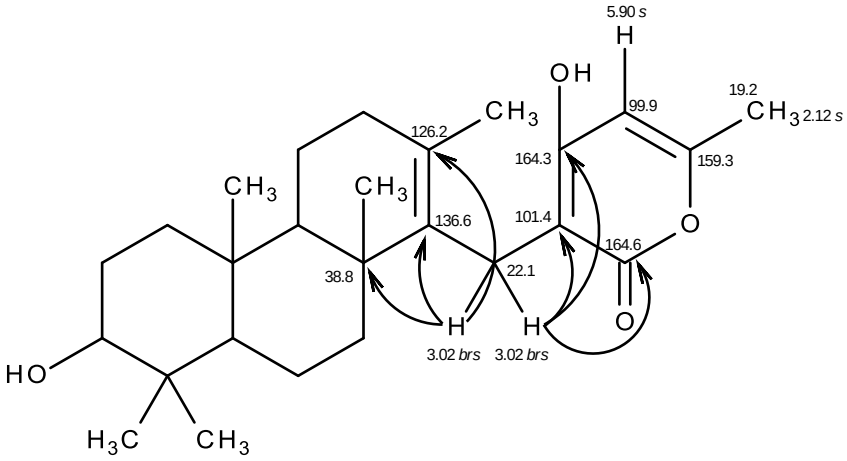

Finally, the stereochemistry of the hydroxyl group on C-3 (δ_C 76.9) was β as supported by the chemical shift value (δ_C 15.7) of the C-4 axial methyl (CH_3-23) which suffered a γ-*gauche* interaction (Mahato and Kundu,1994).

Thus the structure of **NP1** is established as 3-[[(4aR,4bR,7S,8aR,10aR)-7-hydroxy-2,4b,8,8,10a-pentamethyl-4,4a,5,6,7,8a,9,10-octahydro-3H-phenanthren-1-yl]methyl]-4-hydroxy-6-methyl-pyran-2-one. Literature survey revealed that **NP1** is a new analogue of aszonapyrones which we have named sartorypyrone C (Figure 68).

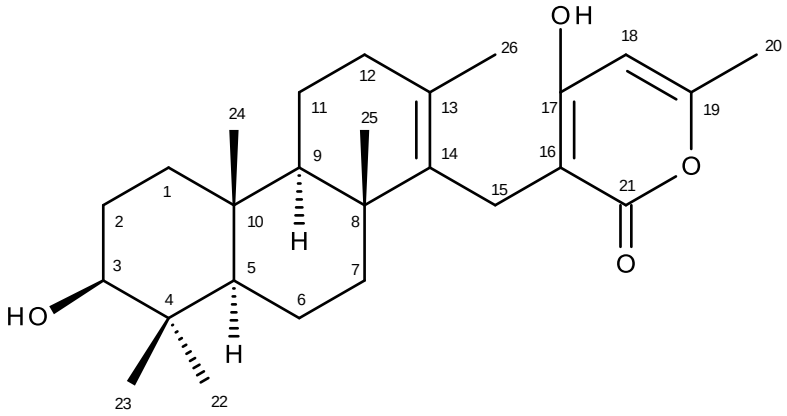

Figure 68. Structure of sartorypyrone C (**NP1**).

Terpenoid moieties can be appended to such diverse molecules such as ribosomal and non-ribosomal peptides, phenazines, pyrroles, however predominantly polyketides, leading to a class of secondary metabolites commonly known as meroterpenoids.

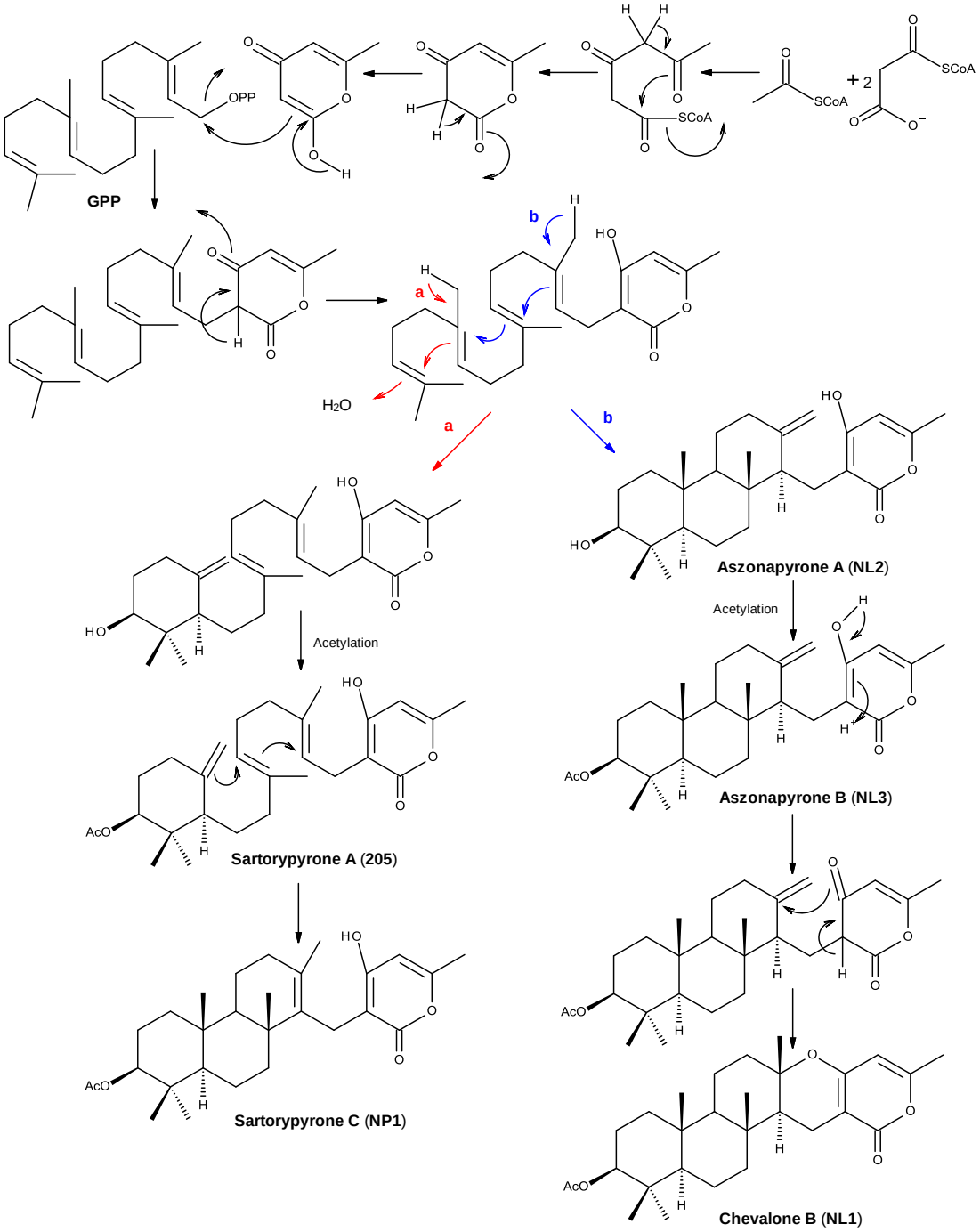

Scheme 4. Proposed biosynthetic pathway for sartorypyrone C (**NP1**), aszonapyrones A (**NL2**) and B (**NL3**) and chevalone B (**NL1**).

Isolation of the new monocyclic meroditerpene sartorypyrone A (**177**) from the culture of the soil fungus *Neosartorya fischeri* KUFC 6344, as well as the isolation of sartorypyrone B (**196**) from the marine sponge-associated *Neosartorya tsunodae* KUFC 9213 by our research group (Eamvijarn *et al*., 2013), allowed the establishment of an hypothetical biosynthetic pathway leading to the formation of sartorypyrone C (**NP1**), chevalone B (**NL1**), and aszonapyrones A (**NL2**) and B (**NL3**) (Scheme 4).

Despite the general occurrence of meroterpenenes from higher plants and marine organisms, this class of metabolites is most often isolated from fungi (Geris and Simpson, 2009). A number of diterpenes containing a α- or β-pyrone ring has been reported as a preponderant group of fungal secondary metabolites (Geris and Simpson, 2009). The proposed metabolic pathways (Scheme 4) clearly evidence the structural similarity of aszonapyrones A (**NL2**) and B (**NL3**), sartorypyrones A-C (**177**, **196** and **NP1**) and chevalones A-C (**139-141**) (Figure 69).

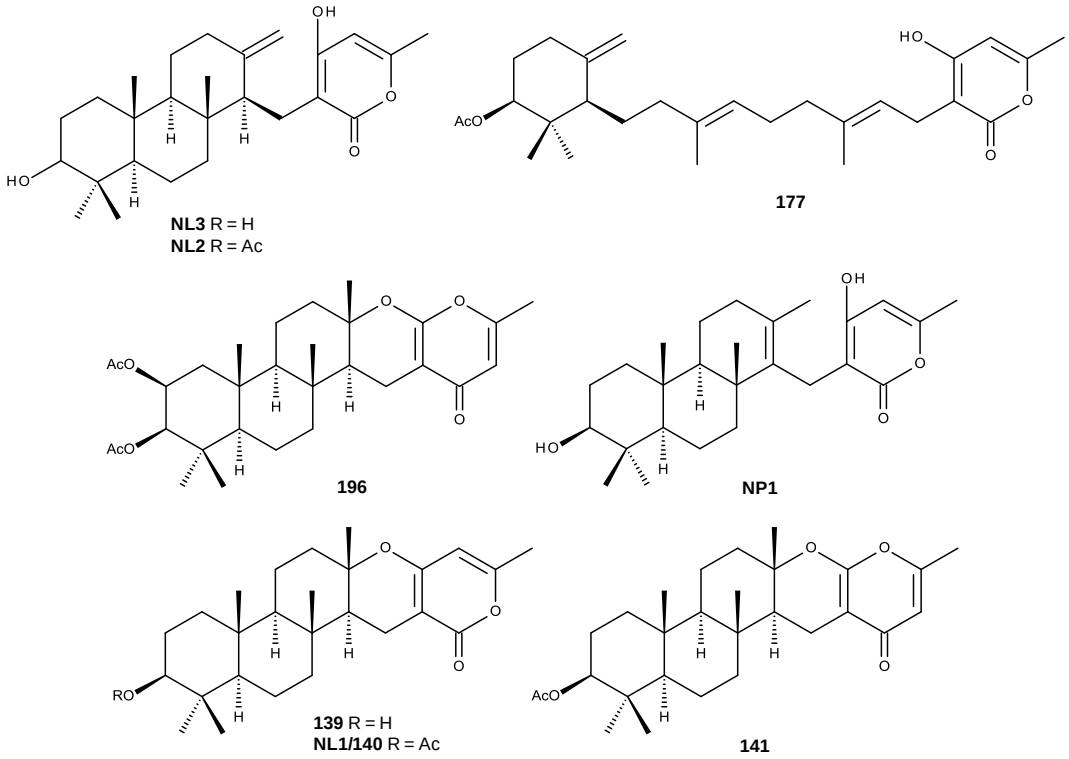

Figure 69. Structures of aszonapyrones A (**NL2**) and B (**NL3**), sartorypyrones A-C (**177, 196** and **NP1**) and chevalones A-C (**139-141**).

Despite the isolation of aszonapyrone A from a culture of *Aspergillus zonatus* (Kimura *et al*., 1982) and from *Eurotium chevalieri* (Kanokmedhakul *et al*., 2011), as well as the isolation of chevalones A-C also from *E. chevalieri* (Kanokmedhakul *et al*., 2011), it is apparent that this subclass of meroditerpenes belong to a new extrolite profile from some species of *Neosartorya*. This finding is supported by the isolation of sartorypyrone C from *N. paulistensis* KUFC 7897 (Gomes *et al*., 2014), chevalone B and aszonapyrones A and B from *N. laciniosa* KUFC 7896 (Eamvijarn *et al*., 2013), as well as by the isolation of sartorypyrone A and aszonapyrone A from *N. fischeri* KUFC 6344, sartorypyrone B from *N. tsunodae* KUFC 9213 (Eamvijarn *et al*., 2013), and chevalones B and C from *N. siamensis* KUFC 6349 (Gomes *et al*., 2014).

3.1.6. Structure Elucidation of Quinazolinone Alkaloids

3.1.6.1. 4(3*H*)-Quinazolinone (NP4)

NP4 was isolated as colorless crystal. The ^{13}C NMR, DEPT and HSQC spectra (Table 23) displayed signals of three quaternary sp^2 (δ_C 160.7, 148.8, 122.6) and five methine sp^2 (δ_C 145.4, 134.3, 127.2, 126.8, 125.8) carbons.

The ^{1}H NMR spectrum (Table 23) displayed a broad singlet at δ_H 12.27, apparently belonging to the amine/amide proton, a singlet of an imine proton at δ_H 8.10, one double doublet at δ_H 8.13 (*J* = 7.7, 1.2 Hz), two double double doublets at δ_H 7.82 (*J* = 7.7, 7.7, 1.2 Hz) and 7.53 (*J* = 7.7, 7.7, 1.2 Hz) and one doublet at δ_H 7.67 (*J* = 7.7 Hz).

Table 23. ^{1}H and ^{13}C NMR data (DMSO-d_6, 500.13 and 125.77 MHz) of **NP4**.

Position	δ_C, type	δ_H, mult. (*J* in Hz)	COSY	HMBC
2	145.4, CH	8.10, *s*	---	---
4	160.7, CO	---	---	---
5	122.6, C	---	---	---
6	125.8, CH	8.13, *dd* (7.7, 1.2)	H-7	C-4, 8, 10
7	126.8, CH	7.53, *ddd* (7.7, 7.7, 1.2)	H-6, 8	C-5, 9
8	134.3, CH	7.82, *ddd* (7.7, 7.7, 1.2)	H-7, 9	C-6, 10
9	127.2, CH	7.67, *d* (7.7)	H-8	C-5, 7
10	148.8, C	---	---	---
NH-3	---	12.27, *brs*	---	---

The COSY spectrum (Table 23) displayed correlations between the double doublet at δ_H 8.13 (*J* = 7.7, 1.2 Hz) and the double double doublet at δ_H 7.53 (*J* = 7.7, 7.7, 1.2 Hz), as well as between the doublet at δ_H 7.67 (*J* = 7.7 Hz) and the double double doublet at δ_H 7.82 (*J* = 7.7, 7.7, 1.2 Hz) indicating an *ortho*-coupling between the two pairs of protons. Furthermore, the two double double doublets at δ_H 7.53 (*J* = 7.7, 7.7, 1.2 Hz) and 7.82 (*J* = 7.7, 7.7, 1.2 Hz) were correlated with each other, indicating the presence of a 1,2-disubstituted benzene ring. This was confirmed by the HMBC cross peaks of the double doublet at δ_H 8.13 (*J* = 7.7, 1.2 Hz; δ_C 125.8) to the carbons at δ_C 148.8 and 134.3, of the double double doublet at δ_H 7.53 (*J* = 7.7, 7.7, 1.2 Hz; δ_C 126.8) to the carbons at δ_C 127.2 and 122.6, of the double double doublet at δ_H 7.82 (*J* = 7.7, 7.7, 1.2 Hz; δ_C 134.3) to the carbons at δ_C 148.8 and 125.8, and of the doublet at δ_H 7.67 (*J* = 7.7 Hz; δ_C 127.2) to the carbons at δ_C 126.8 and 122.6.

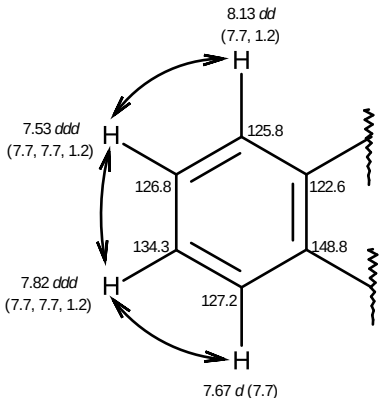

The HMBC spectrum (Table 23) also revealed the correlation of the aromatic proton at δ_H 8.13, *dd* (*J* = 7.7, 1.2 Hz; δ_C 125.8) to the quaternary sp^2 carbon at δ_C 160.7.

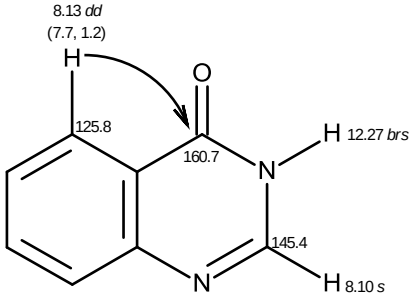

Taking altogether the ^{1}H and ^{13}C NMR data, the structure of **NP4** was proposed as 4(*3H*)-quinazolinone (Figure 70). The structure was confirmed by comparison of its ^{1}H and ^{13}C NMR data with those provided by NMR Shift Database website (http://nmrshiftdb.nmr.uni-koeln.de/portal/js_pane/P-Results/nmrshiftdbaction/showDetailsFromHome/molNumber/20050524;jsessionid=B74F40CF04748F5C14DE27712653152A?&tab=1_0#spectrum20096536 accessed on 11th March 2013). Literature survey revealed that **NP4** is a new natural product. However, its derivatives have been widely reported from various biological sources (Mhaske and Argade, 2006)

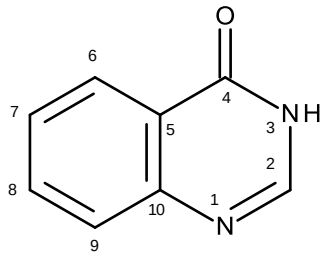

Figure 70. Structure of 4(*3H*)-quinazolinone (**NP4**).

3.1.6.2. 3'- (4-Oxoquinazolin-3-yl) spiro [1*H*-indole-3,5'-oxolane] - 2,2'-dione (NP5/NL5)

NP5/NL5 was isolated as white solid and its molecular formula $C_{19}H_{13}N_3O_4$ was established based on the (+)-HR-ESIMS *m/z* 348.0968 $[M+H]^+$ peak, indicating fifteen degrees of unsaturation. The ^{13}C NMR, DEPT and HSQC spectra (Table 24) revealed the presence of seven quaternary sp^2 (δ_C 175.4, 171.9, 159.8, 147.8, 142.7, 126.4, 121.4), nine methine sp^2 (δ_C 147.8, 135.1, 131.6, 127.7, 127.4, 126.1, 125.3, 123.1, 110.7), one quaternary sp^3 (δ_C 80.9), one methine sp^3 (δ_C 56.5) and one methylene sp^3 (δ_C 33.4) carbon.

The ^{1}H NMR spectrum (Table 24) displayed signals for eight aromatic protons at δ_H 8.23, *d* (*J* = 7.6 Hz), 7.92, *dd* (*J* = 7.6, 7.6 Hz), 7.76, *d* (*J* = 7.6 Hz), 7.66, *d* (*J* = 7.6 Hz), 7.63, *dd* (*J* = 7.6, 7.6 Hz), 7.41, *dd* (*J* = 7.6, 7.6 Hz), 7.18, *dd* (*J* = 7.6, 7.6 Hz) and 6.96, *d* (*J* = 7.6 Hz), suggesting the existence of two aromatic rings. The COSY spectrum (Table 24) exhibited cross peaks of the doublet at δ_H 7.66 (*J* = 7.6 Hz) to the double doublet at δ_H 7.18 (*J* = 7.6, 7.6 Hz) and of the

doublet at δ_H 6.96 (*J* = 7.6 Hz) to the double doublet at δ_H 7.41 (*J* = 7.6, 7.6 Hz), as well as between the double doublets at δ_H 7.18 (*J* = 7.6, 7.6 Hz) and 7.41 (*J* = 7.6, 7.6 Hz) indicating the presence of a 1,2-disubstituted benzene ring.

Table 24. ^{1}H and ^{13}C NMR data (DMSO-d_6, 300.13 and 75.47 MHz) of **NP5/NL5**.

Position	δ_C, type	δ_H, mult. (*J* in Hz)	COSY	HMBC
2	175.4, CO	---	---	---
3	80.9, C	---	---	---
3a	126.4, C	---	---	---
4	125.3, CH	7.66, *d* (7.6)	H-5	C-3, 6, 7a
5	123.1, CH	7.18, *dd* (7.6, 7.6)	H-4, 6	C-3a, 7
6	131.6, CH	7.41, *dd* (7.6, 7.6)	H-5, 7	C-7a, 4
7	110.7, CH	6.96, *d* (7.6)	H-6	C-3a, 5
7a	142.7, C	---	---	---
2’	171.9, CO	---	---	---
3’	56.5, CH	5.67, *t* (10.0)	H-4’	C-2’, 2’’,4’, 4’’
4’	33.4, CH_2	3.01, *d* (10.0)	H-3’	C-2, 2’, 3, 3a, 3’
2’’	147.8, CH	8.63, *s*	---	C-3’, 4’’, 8’’a
4’’	159.8, CO	---	---	---
4’’a	121.4, C	---	---	---
5’’	126.1, CH	8.23, *d* (7.6)	H-6’’	C-4’’, 7’’, 8’’a
6’’	127.7, CH	7.63, *dd* (7.6, 7.6)	H-5’’, 7’’	C-4’’a, 8’’
7’’	135.1, CH	7.92, *dd* (7.6, 7.6)	H-6’’, 8’’	C-5’’, 8’’a
8’’	127.4, CH	7.76, *d* (7.6)	H-7’’	C-4’’a, 6’’, 8’’a
8’’a	147.7, C	---	---	---
NH-1		10.92, *s*	---	C-2, 3, 3a, 7a

This was confirmed by the HMBC cross peaks of the doublet at δ_H 7.66 (*J* = 7.6 Hz; δ_C 125.3) to the carbon at 142.7, and of the doublet at δ_H 6.96 (*J* = 7.6 Hz; δ_C 110.7) to the quaternary sp^2 carbon at δ_C 126.4. Moreover, the HMBC spectrum (Table 24) also showed cross peaks of the singlet at δ_H 10.92, which showed no HSQC correlation, to the quaternary carbons of the aromatic ring at δ_C 126.4 and 142.7, as well as to the oxygen bearing quaternary sp^3 carbon at δ_C 80.9 and the carbonyl carbon at δ_C 175.4, suggesting that the 1,2-disubstituted benzene ring was part of a 3-disubstituted 1*H*-indolin-2-one portion. This was also supported by the HMBC correlation between the aromatic proton at δ_H 7.66 (*J* = 7.6 Hz; δ_C 125.3) to the oxyquaternary carbon at δ_C 80.9.

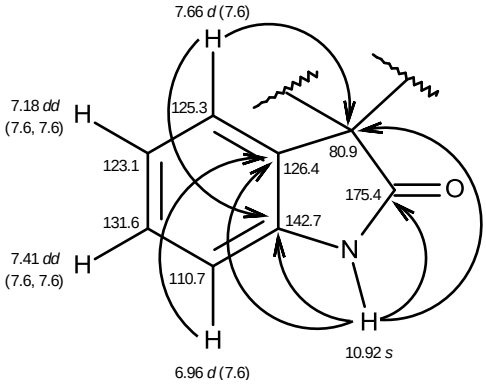

The COSY spectrum also showed another coupling system consisting of the triplet at δ_H 5.67 (J = 10.0 Hz, δ_C 56.5) and the doublet at δ_H 3.01 (2H, J = 10.0 Hz, δ_C 33.4). Further analysis of the HMBC spectrum revealed cross peaks of the doublet at δ_H 3.01 (2H, J = 10.0 Hz; δ_C 33.4) to the carbonyl carbon at δ_C 175.4, the aromatic carbon at δ_C 126.4 and the oxyquaternary carbon at δ_C 80.9 of the indolinone fragment, as well as of the triplet of the methine proton δ_H 5.67 (J = 10.0 Hz; δ_C 56.5) to the carbonyl carbon at δ_C 171.9 and the methylene carbon at δ_C 33.4. These correlations suggested the attachment of a spirolactone ring at C-3 (δ_C 80.9) of the indolinone ring.

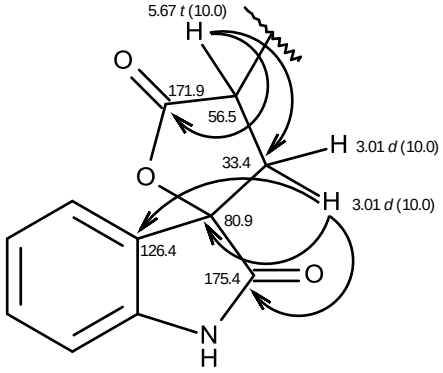

Another portion of the molecule also consists of the 1,2-disubstituted benzene ring which was evidenced by the cross peaks of the doublet at δ_H 8.23 (J = 7.6 Hz) to the double doublet at δ_H 7.63 (J = 7.6, 7.6 Hz), of the doublet at δ_H 7.76 (J = 7.6 Hz) to the double doublet at δ_H 7.92 (J = 7.6, 7.6 Hz), as well as between the double doublets at δ_H 7.63 (J = 7.6, 7.6 Hz) and δ_H 7.92 (J = 7.6, 7.6 Hz) in the COSY spectrum. Moreover, the HMBC cross peaks of the doublet at δ_H 8.23 (J = 7.6 Hz; δ_C 126.1) to the quaternary sp^2 carbons at δ_C 159.8 and 147.7, of

the doublet at δ_H 7.76 (J = 7.6 Hz; δ_C 127.4) to the quaternary sp^2 carbons at δ_C 147.7 and 121.4, as well as of the singlet at δ_H 8.63 (δ_C 147.8) to the carbons at δ_C 159.8 and 147.7, suggested that the 1,2-disubstituted benzene ring was part of a *N*-substituted quinazolin-4-one fragment.

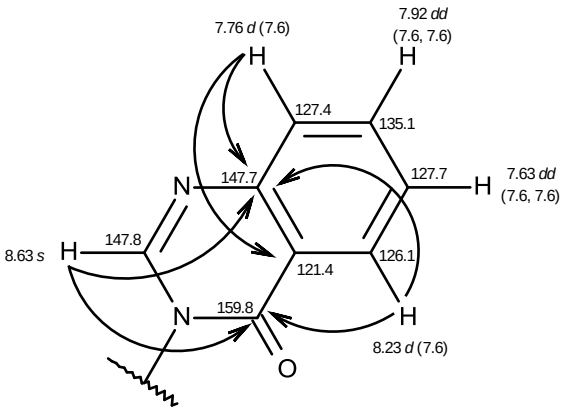

That the spiro[indoline-3,5'-tetrahydrofuran]-2,2'-dione fragment was connected to the quinazolin-4-one moiety through the methine carbon at δ_C 56.5 of the former and the amide nitrogen atom of the latter, was substantiated by the HMBC cross peaks of the triplet of the methine proton at δ_H 5.67 (J = 10.0 Hz; δ_C 56.5) to the carbons at δ_C 159.8 and 147.8 from the quinazolinone moiety, as well as of the singlet of methine proton at δ_H 8.63, *s* (δ_C 147.8) to the methine carbon at δ_C 56.5.

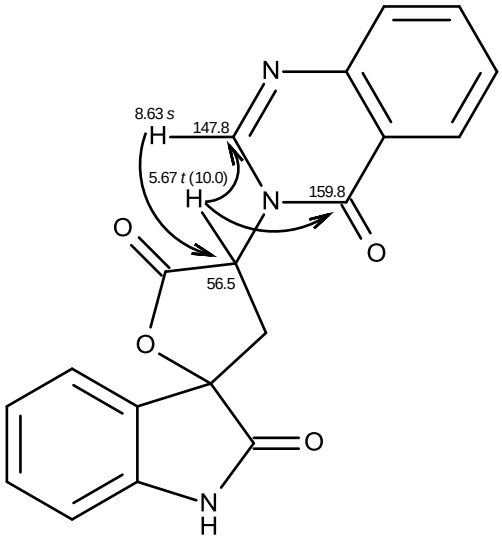

Thus, the structure of **NP5/NL5** was established as 3'-(4-oxoquinazolin-3-yl)spiro[1*H*-indole-3,5'-oxolane]-2, 2'-dione (Figure 71). Furthermore, the NOESY spectrum displayed a correlation between the signals of the methine proton at δ_H 5.67, *t* (*J* = 10.0 Hz; δ_C 56.5) and the imine proton at δ_H 8.63, *s* (δ_C 147.8).

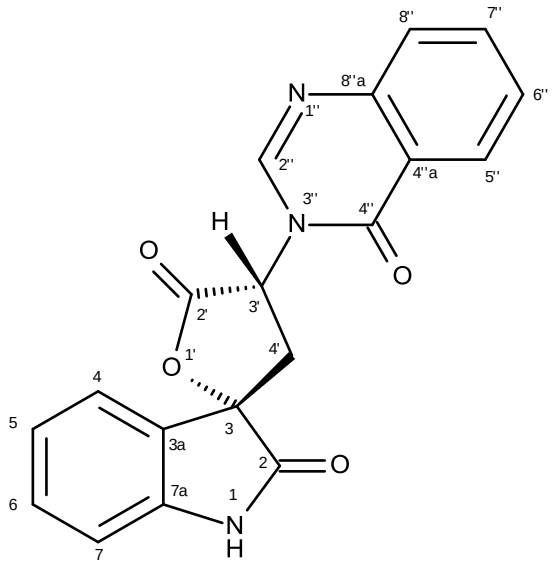

Figure 71. Structure of 3'-(4-oxoquinazolin-3-yl)spiro[1*H*-indole-3,5'-oxolane]-2, 2'-dione (**NP5/NL5**).

The ^{1}H and ^{13}C NMR and other physical data including the optical rotation of **NP5/NL5** ($[\alpha]^{20}_{D}$ = +19.7) were in agreement with those reported for 3'-(4-oxoquinazolin-3-yl) spiro [1*H*-indole-3,5'-oxolane]- 2,2'-dione, the indoloquinazolinone alkaloid previously isolated from the soil fungus *Neosartorya siamensis* KUFC 6349 by Buttachon *et al*. (2012).

3.1.6.3. Tryptoquivaline L (NP2/NL4)

NP2/NL4 was isolated as colorless crystal and exhibited the (+)-HR-ESIMS $[M+H]^+$ peak at *m/z* 433.1509 corresponding to $C_{23}H_{21}N_4O_5$, indicating sixteen degrees of unsaturation. The ^{13}C NMR, DEPT and HSQC spectra (Table 25) revealed the presence of seven quaternary sp^2 (δ_C 171.3, 170.8, 159.8, 147.6, 138.3, 132.4, 121.4), nine methine sp^2 (δ_C 147.6, 135.1, 131.8, 127.7, 127.4,

126.2, 126.1, 125.4, 114.8), four quaternary sp^2 (δ_C 147.6, 138.3, 132.4, 121.4), two methine sp^3 (δ_C 86.2, 56.9), two quaternary sp^3 (δ_C 83.5, 70.4), one methylene sp^3 (δ_C 34.5) and two methyl (δ_C 22.8, 16.4) carbons.

Table 25. ^{1}H and ^{13}C NMR data (DMSO-*d*$_6$, 300.13 and 75.47 MHz) of **NP2/NL4**.

Position	δ_C, type	δ_H, mult. (*J* in Hz)	COSY	HMBC
2	86.2, CH	5.25, *s*	---	C-3,13, 14, 15
3	83.5, C	---	---	---
4	132.4, C	---	---	---
5	126.1, CH	7.83, *d* (7.3)	H-6	C-7, 9
6	125.4, CH	7.36, *ddd* (7.3, 7.3, 1.1)	H-5, 7	C-4, 8
7	131.8, CH	7.54, *dd* (7.3, 7.3)	H-6, 8	C-5, 9
8	114.8, CH	7.51, *d* (7.3)	H-7	C-4, 6
9	138.3, C	---	---	---
11	170.8, CO	---	---	---
12	56.9, CH	5.59, *t* (10.0)	H-13α, 13β	C-11, 13, 18, 26
13α	34.5, CH_2	3.07, *dd* (13.1, 9.3)	H-12, 13β	C-2, 11, 12
β		3.45, *dd* (13.1, 11.9)	H-12, 13α	C-2, 3, 4, 12
14	171.3, CO	---	---	---
15	70.4, C	---	---	---
18	159.8, CO	---	---	---
19	121.4, C	---	---	---
20	126.2, CH	8.25, *d* (7.7)	H-21, 22	C-18, 22, 24
21	127.7, CH	7.64, *dd* (7.7, 7.7)	H-20, 22	C-19, 23
22	135.1, CH	7.93, *ddd* (7.7, 7.7, 1.2)	H-20, 21, 23	C-20, 24
23	127.4, CH	7.77, *d* (7.7)	H-22	C-19, 21
24	147.6, C	---	---	---
26	147.6, CH	8.57, *s*	---	C-12, 18, 19, 24
27	16.4, CH_3	1.36, *s*	---	C-14, 15, 28
28	22.8, CH_3	1.26, *s*	---	C-14, 15, 27
OH	---	8.81, *s*	---	C-2, 15

The ^{1}H NMR spectrum (Table 25) was similar to that of **NP5/NL5** exhibiting the signals of eight aromatic protons at δ_H 8.25, *d* (*J* = 7.7 Hz), 7.93, *ddd* (*J* = 7.7, 7.7, 1.2 Hz), 7.83, *d* (*J* = 7.3 Hz), 7.77, *d* (*J* = 7.7 Hz), 7.64, *dd* (*J* = 7.7, 7.7 Hz), 7.36, *ddd* (*J* = 7.3, 7.3, 1.1 Hz), 7.54, *dd* (*J* = 7.3, 7.3 Hz) and 7.51, *d* (*J* = 7.3 Hz), a triplet of one methine proton at δ_H 5.59 (*J* = 10.0 Hz) and a singlet of one methine proton at δ_H 5.25, two methylene protons at δ_H 3.45, *dd* (*J* = 13.1, 11.9 Hz) and 3.07, *dd* (*J* = 13.1, 9.3 Hz), a singlet of the imine proton at δ_H 8.57, besides a singlet of the hydroxyl/amine proton at δ_H 8.81, and two methyl singlets at δ_H 1.36 and 1.26.

Like **NP5/NL5**, the presence of a 1,2-disubstituted benzene ring was evidenced by the COSY cross peaks of the doublet at δ_H 7.83 (*J* = 7.3 Hz) to the

double double doublet at δ_H 7.36 (*J* = 7.3, 7.3, 1.1 Hz), of the doublet at δ_H 7.51 (*J* = 7.3 Hz) to the double doublet at δ_H 7.54 (*J* = 7.3, 7.3 Hz), and also by the double double doublet at δ_H 7.36 (*J* = 7.3, 7.3, 1.1 Hz) and the double doublet at 7.54 (*J* = 7.3, 7.3 Hz) . Additionally, the HMBC cross peaks of the doublet at δ_H 7.83 (*J* = 7.3 Hz; δ_C 126.1) to the quaternary sp^2 carbon at δ_C 138.3, the double double doublet at δ_H 7.36 (*J* = 7.3, 7.3, 1.1 Hz; δ_C 125.4) to the quaternary sp^2 carbon at δ_C 132.4, the double doublet at δ_H 7.54 (*J* = 7.3, 7.3 Hz; δ_C 131.8) to the quaternary sp^2 carbon at δ_C 138.3, the doublet at δ_H 7.51 (*J* = 7.3 Hz; δ_C 114.8) to the quaternary sp^2 carbon at δ_C 132.4, confirmed the presence of the 1,2-disubstituted benzene ring. Since the singlet at δ_H 5.25 (δ_C 86.2) gave cross peak to the oxyquaternary sp^3 carbon at δ_C 83.5, the presence of a 2,3-dihydro-1*H*-indole was suggested.

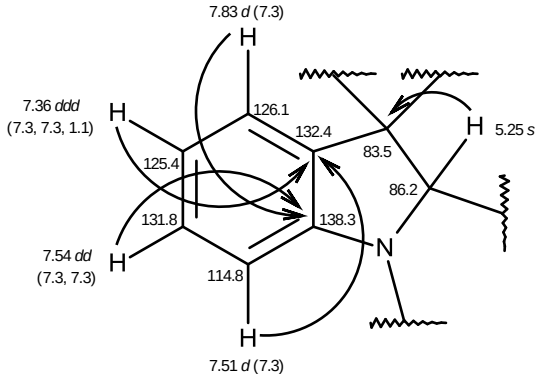

Similar to **NP5/NL5**, the COSY spectrum showed the coupling of the methylene protons at δ_H 3.07, *dd* (*J* = 13.1, 9.3 Hz) and 3.45, *dd* (*J* = 13.1, 11.9 Hz) to the methine proton at δ_H 5.59, *t* (*J* = 10.0 Hz), suggesting the existence of a five-membered spirolactone substituent at C-3 (δ_C 83.5). This was confirmed by the HMBC correlations of the methine proton at δ_H 5.25, *s* (δ_C 86.2) to the methylene carbon at δ_C 34.5 and the quaternary sp^2 carbon at δ_C 171.3, of the methylene proton at δ_H 3.45, *dd* (*J* = 13.1, 11.9 Hz; δ_C 34.5) to the carbons at δ_C 83.5, 86.2 and 132.4 of the indole moiety, and the methine sp^3 carbon at δ_C 56.9, of the methylene proton at δ_H 3.07, *dd* (*J* = 13.1, 9.3 Hz; δ_C 34.5) to the methine carbon at 86.2 of the indole moiety, the methine sp^3 carbon at δ_C 56.9, and the carbonyl carbon at δ_C 170.8, as well as of the methine proton at δ_H 5.59, *t* (*J* = 10.0 Hz; δ_C 56.9) to the methylene carbon at δ_C 34.5 and the carbonyl carbon at δ_C 170.8.

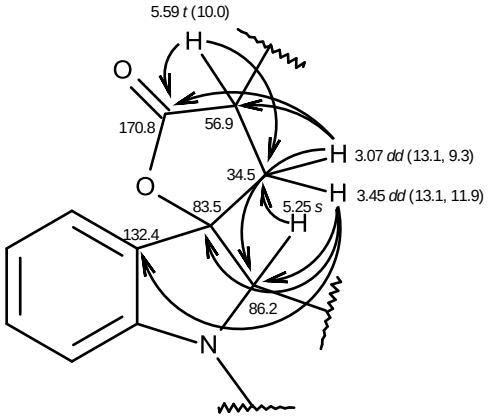

Further analysis of the HMBC spectrum revealed that the singlet at δ_H 5.25 (δ_C 86.2) of the 2,3-dihydro-1*H*-indole portion also gave cross peaks to the quaternary carbon at δ_C 70.4 and the carbonyl carbon at δ_C 171.3, while the two methyl singlets at δ_H 1.26 (δ_C 22.8) and δ_H 1.36 (δ_C 16.4) also gave cross peaks to the quaternary carbon at δ_C 70.4 and the carbonyl carbon at δ_C 171.3. These correlations led to the conclusion that the carbonyl carbon at δ_C 171.3 was connected to the nitrogen of the indole ring and thus suggesting the presence of a *6-5-5-gem*-dimethylimidazoindolone ring. Moreover, since the singlet at δ_H 8.81 gave cross peaks to the quaternary carbon at δ_C 70.4 and the methine carbon at δ_C 86.2, the hydroxyl group was placed on the nitrogen of the imidazolone ring.

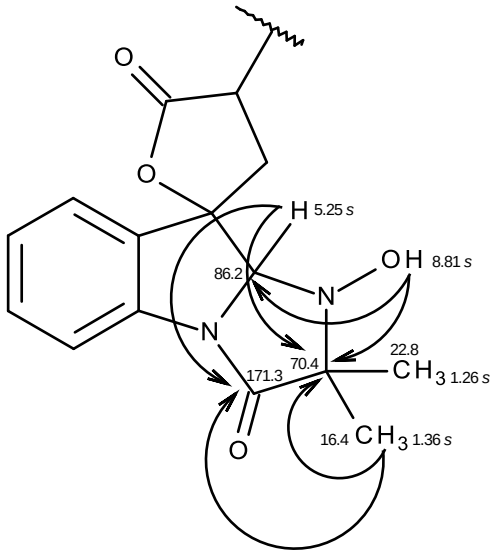

That the aromatic protons at δ_H 8.25, *d* (*J* = 7.7 Hz), 7.64, *dd* (*J* = 7.7, 7.7 Hz), 7.93, *ddd* (*J* = 7.7, 7.7, 1.2 Hz) and 7.77, *d* (*J* = 7.7 Hz) belonged to another 1,2-disubstituted benzene ring was supported by the cross peaks between the doublet at δ_H 8.25 (*J* = 7.7 Hz) and the double doublet at δ_H 7.64 (*J* = 7.7, 7.7 Hz), between the doublet at δ_H 7.77 (*J* = 7.7 Hz) and the double double doublet at δ_H 7.93 (*J* = 7.7, 7.7, 1.2 Hz) as well as the cross peaks between the double doublet at δ_H 7.64 (*J* = 7.7, 7.7 Hz) and the double double doublet at δ_H 7.93 (*J* = 7.7, 7.7, 1.2 Hz) observed in the COSY spectrum. This was confirmed by the HMBC cross peaks of the double doublet at δ_H 7.64 (*J* = 7.7, 7.7 Hz; δ_C 127.7) to the quaternary sp^2 carbon at δ_C 121.4, and of the double double doublet at δ_H 7.93 (*J* = 7.7, 7.7, 1.2 Hz; δ_C 135.1) to the quaternary sp^2 carbon at δ_C 147.6. Since the doublet at δ_H 8.25 (*J* = 7.7 Hz; δ_C 126.2) and the singlet at δ_H 8.57 (δ_C 147.6) showed HMBC cross peaks to the quaternary sp^2 carbons at δ_C 159.8 and 147.6, the second 1,2-disubstituted benzene ring was part of a *N*-substituted quinazolin-4-one moiety.

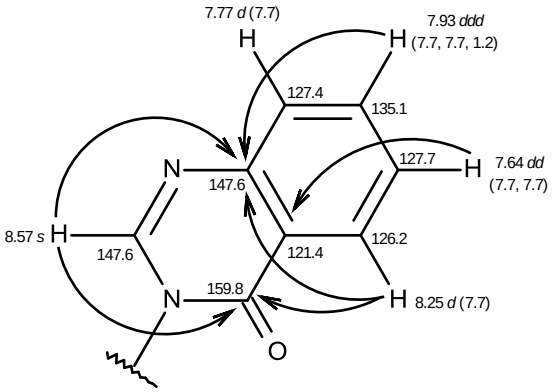

That the quinazolinone moiety was connected to the *6-5-5-gem*-dimethylimidazoindolone ring system via the five-membered spirolactone was evidenced by the HMBC correlations of the methine proton at δ_H 5.59, *t* (*J* = 10.0 Hz; δ_C 56.9) to the carbonyl carbon at δ_C 159.8 and the methine sp^2 carbon at δ_C 147.6 of the quinazolinone ring, as well as of the imine proton at δ_H 8.57, *s* (δ_C 147.6) to the methine sp^3 carbon at δ_C 56.9 of the spirolactone ring.

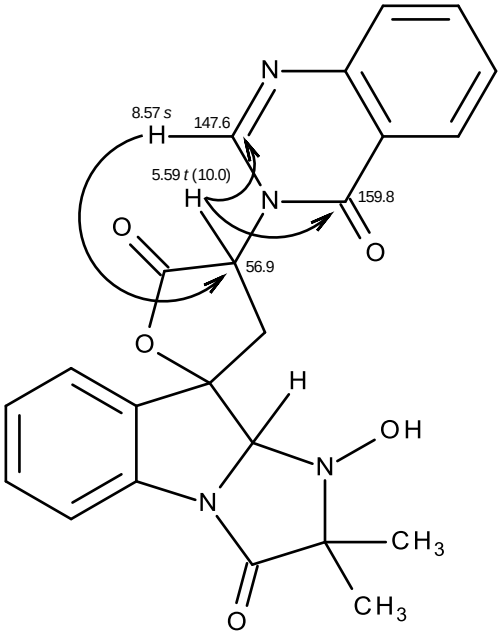

In order to determine the stereochemistry of **NP2/NL4**, the NOESY experiment was carried out. The NOESY spectrum exhibited correlations between the signals of the singlet at δ_H 5.25 and the signals of the protons at δ_H 8.81, *s* (N-OH), 3.07, *dd* (*J* = 13.1, 9.3 Hz), and 1.36, *s*, as well as between the signals of the imine proton at δ_H 8.57, *s* and the proton at δ_H 5.59, *t* (*J* = 10.0 Hz), indicating that the methine proton at δ_H 5.25, *s* and the methyl protons at δ_H 1.36, *s* are on the same side, and that the methine proton at δ_H 5.25, *s* is β-oriented.

The ^{1}H and ^{13}C NMR data and the optical rotation of **NP2/NL4** ($[\alpha]^{20}_{D}$ = -30.5) were in agreement with those of tryptoquivaline L (Figure 72) previously reported from *Neosartorya siamensis* KUFC 6349 (Buttachon *et al*., 2012).

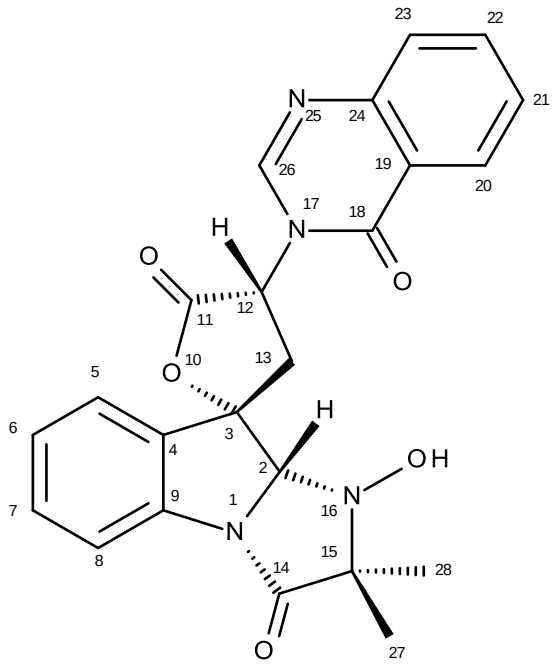

Figure 72. Structure of tryptoquivaline L (**NP2/NL4**).

3.1.6.4. Tryptoquivaline H (NP3)

NP3 was also isolated as white solid and its molecular formula $C_{22}H_{18}N_4O_5$ was established on the basis of the (+)-HR-ESIMS *m/z* 419.13496 $[M+H]^+$, indicating sixteen degrees of unsaturation. The general features of the ^1H and ^{13}C NMR spectra (Table 26) of **NP3** were very similar to those of **NP2/NL4**.

The ^{13}C NMR, DEPT and HSQC spectra (Table 26) displayed signals of seven quaternary sp^2 (δ_C 170.6, 169.9, 159.8, 147.5, 138.2, 132.4, 121.4), nine methine sp^2 (δ_C 147.6, 135.1, 131.9, 127.6, 127.4, 126.1, 126.0, 125.5, 114.9), three methine sp^3 (δ_C 88.6, 67.3, 56.9), one quaternary sp^3 (δ_C 83.7), one methylene sp^3 (δ_C 33.8) and one methyl (δ_C 10.6) carbon.

The ^1H NMR spectrum, in conjunction with the HSQC spectra (Table 26), displayed two singlets of one proton each at δ_H 8.79 and δ_H 8.55, besides the signals of eight aromatic protons at δ_H 8.24, *dd* (*J* = 7.7, 1.3 Hz), 7.93, *ddd* (*J* = 7.7, 7.7, 1.3 Hz), 7.81, *d* (*J* = 7.5 Hz), 7.77, *d* (*J* = 7.7 Hz), 7.64, *dd* (*J* = 7.7, 7.7 Hz), 7.54, *ddd* (*J* = 7.5, 7.5, 1.0 Hz), 7.51, *d* (*J* = 7.5 Hz) and 7.37, *ddd* (*J* = 7.5, 7.5, 1.0 Hz), three methine protons at δ_H 5.58, *t* (*J* = 10.0 Hz), 5.43, *s* and 4.01, *q* (*J* = 7.0 Hz), two methylene protons at δ_H 3.46, *dd* (*J* = 13.1, 11.0 Hz) and 3.04, *dd* (*J* = 13.1, 9.3 Hz), and one methyl doublet at δ_H 1.44 (*J* = 7.1 Hz).

Table 26. ^{1}H and ^{13}C NMR data (DMSO-d_6, 300.13 and 75.47 MHz) of **NP3**.

Position	δ_C, type	δ_H, mult. (*J* in Hz)	COSY	HMBC
2	88.6, CH	5.43, *s*	---	C-3,13, 14, 15
3	83.7, C	---	---	---
4	132.4, C	---	---	---
5	126.0, CH	7.81, *d* (7.5)	H-6	C-3, 7, 9
6	125.5, CH	7.37, *ddd* (7.5, 7.5, 1.0)	H-5, 7	C-4, 8
7	131.9, CH	7.54, *ddd* (7.5, 7.5, 1.0)	H-6, 8	C-5, 9
8	114.9, CH	7.51, *d* (7.5)	H-7	C-4, 6
9	138.2, C	---	---	---
11	170.6, CO	---	---	---
12	56.9, CH	5.58, *t* (10.0)	H-13α, 13β	C-3, 11, 18, 26
13α	33.8, CH_2	3.04, *dd* (13.1, 9.3)	H-12, 13β	C-2, 4, 11
β		3.46, *dd* (13.1, 11.0)	H-12, 13α	C-2, 3, 4, 12
14	169.9, CO	---	---	---
15	67.3, CH	4.01, *q* (7.0)	H-27	C-2, 14, 27
18	159.8, CO	---	---	---
19	121.4, C	---	---	---
20	126.1, CH	8.24, *dd* (7.7, 1.3)	H-21	C-18, 22, 24
21	127.6, CH	7.64, *dd* (7.7, 7.7)	H-20, 22	C-19, 23
22	135.1, CH	7.93, *ddd* (7.7, 7.7, 1.3)	H-21, 23	C-20, 24
23	127.4, CH	7.77, *d* (7.7)	H-22	C-19, 21
24	147.5, C	---	---	---
26	147.6, CH	8.55, *s*	---	C-12, 18, 19, 24
27	10.6, CH_3	1.44, *d* (7.1)	H-15	C-14, 15
OH	---	8.79, *s*	---	C-2, 15

The presence of the 2,3-dihydro-1*H*-indole ring system connected to the spirolactone ring on C-3, as was in **NP2/NL4**, was confirmed by the cross peaks of the double double doublet at δ_H 7.37 (*J* = 7.5, 7.5, 1.0 Hz; δ_C 125.5) to the doublet at δ_H 7.81 (*J* = 7.5 Hz; δ_C 126.0) and the double double doublet at δ_H 7.54 (*J* = 7.5, 7.5, 1.0 Hz; δ_C 131.9), of the doublet at δ_H 7.51 (*J* = 7.5 Hz; δ_C 114.9) to the double double doublet at δ_H 7.54 (*J* = 7.5, 7.5, 1.0 Hz; δ_C 131.9), and of the triplet at δ_H 5.58 (*J* = 10.0 Hz; δ_C 56.9) to the two double doublets of the methylene protons at δ_H 3.04 (*J* = 13.1, 9.3 Hz; δ_C 33.8) and 3.46 (*J* = 13.1, 11.0 Hz; δ_C 33.8) in the COSY spectrum (Table 26), as well as by the HMBC cross peaks of the singlet at δ_H 5.43 (δ_C 88.6) to the carbons at δ_C 83.7 and 33.8, of the triplet at δ_H 5.58 (*J* = 10.0 Hz; δ_C 56.9) to the carbons at δ_C 83.7 and 170.6, and of the double doublets δ_H 3.46 (*J* = 13.1, 11.0 Hz; δ_C 33.8) and 3.04 (*J* = 13.1, 9.3 Hz; δ_C 33.8) to the carbons at δ_C 83.7, 88.6, 56.9 and 170.6.

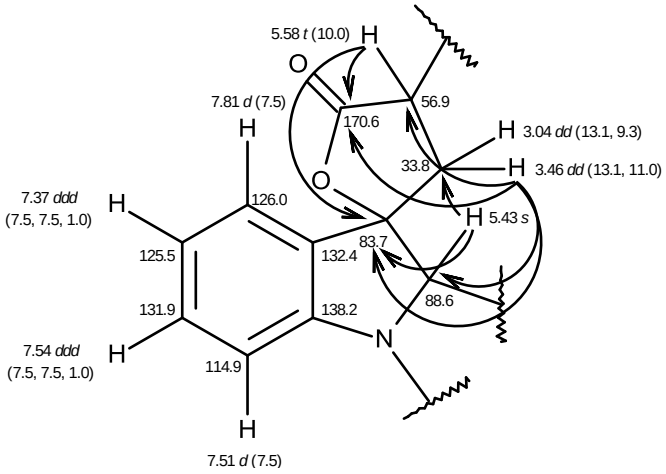

The presence of the *6-5-5*-methylimidazoindoline ring system was based on the cross peaks between the methyl doublet at δ_H 1.44 (J = 7.1 Hz) and the methine quartet at δ_H 4.01 (J = 7.0 Hz), in the COSY spectrum, as well as by the HMBC cross peaks of the methyl doublet at δ_H 1.44 (J = 7.1 Hz; δ_C 10.6) to the methine carbon at δ_C 67.3 and the carbonyl carbon at δ_C 169.9, of the methine quartet at δ_H 4.01 (J = 7.0 Hz; δ_C 67.3) to the methine carbon at δ_C 88.6, the carbonyl carbon at δ_C 169.9 and the methyl carbon at δ_C 10.6, as well as of the methine singlet at δ_H 5.43 (δ_C 88.6) to the carbonyl carbon at δ_C 169.9 and the methine carbon at δ_C 67.3. Since the HMBC spectrum showed cross peaks of the singlet at δ_H 8.79 to the methine sp^3 carbons at δ_C 88.6 and 67.3, the hydroxyl group (δ_H 8.79, *s*) was on the nitrogen of the imidazolone ring.

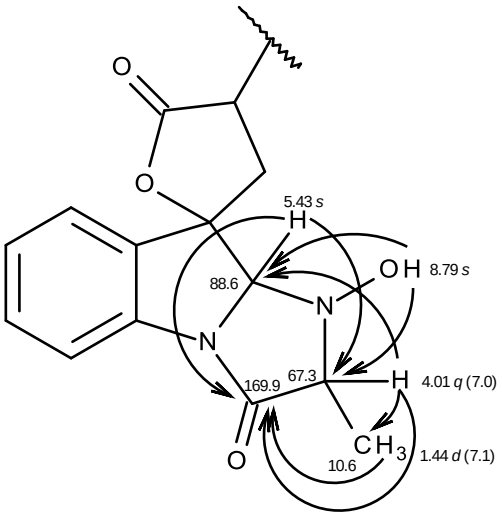

The COSY spectrum also displayed cross peaks for the aromatic protons at δ_H 8.24, *dd* (*J* = 7.7, 1.3 Hz), 7.93, *ddd* (*J* = 7.7, 7.7, 1.3 Hz), 7.77, *d* (*J* = 7.7 Hz) and 7.64, *dd* (*J* = 7.7, 7.7 Hz), evidencing the coupling system of another 1,2-disubstituted benzene ring. Analogously to **NP2/NL4** and **NP5/NL5**, the HMBC cross peaks of the double doublet at δ_H 8.24 (*J* = 7.7, 1.3 Hz; δ_C 126.1) to the quaternary sp^2 carbons at δ_C 159.8 and 147.5, of the doublet at δ_H 7.77 (*J* = 7.7 Hz; δ_C 127.4) to the quaternary sp^2 carbon at δ_C 121.4, as well as of the singlet of the methine proton at δ_H 8.55 (δ_C 147.6) to the quaternary sp^2 carbons at δ_C 159.8, 147.5 and 121.4, provided an unequivocal evidence of the existence of the *N*-substituted quinazolin-4-one ring system.

.

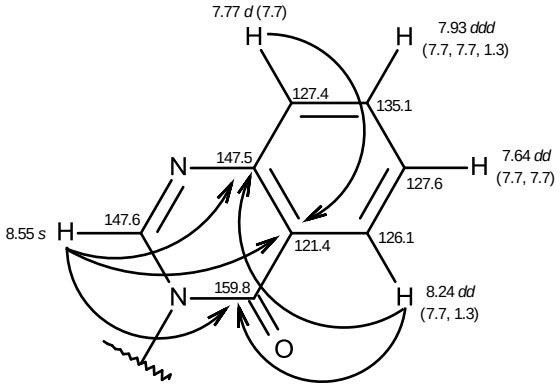

As in **NP2/NL4**, the *6-5-5*-methylimidazoindoline ring system was connected to the quinazolinone moiety through the methine carbon at δ_C 56.9 of the five-membered spirolactone ring and the amide nitrogen of the quinazolinone ring, as evidenced by the HMBC cross peaks of the triplet at δ_H 5.58, *t* (*J* = 10.0 Hz; δ_C 56.9) to the imine carbon at δ_C 147.6 and the carbonyl carbon at δ_C 159.8.

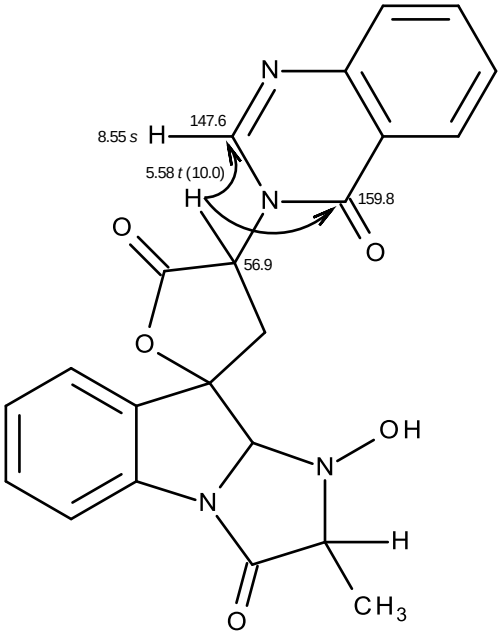

Since the NOESY spectrum exhibited the correlation between the methine proton at δ_H 5.43, *s* (δ_C 88.6) and the methyl protons at δ_H 1.44, *d* (*J* = 7.1 Hz; δ_C 10.6), the methyl group and this methine proton are on the same side of the imidazoindolone moiety.

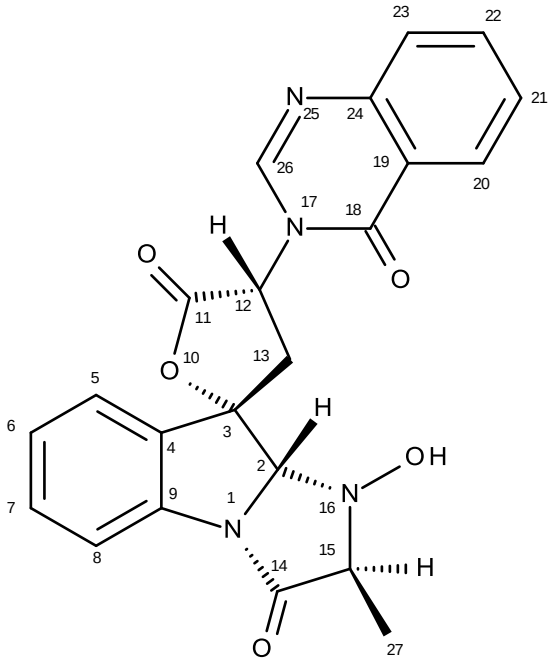

Figure 73. Structure of tryptoquivaline H (**NP3**).

Thus, the structure corresponds to that of tryptoquivaline H (Figure 73), a tryptoquivaline analogue previously reported from *Neosartorya siamensis* KUFC 6349 (Buttachon *et al*., 2012).

3.1.6.5. Tryptoquivaline F (NP6)

NP6 was also isolated as white solid, and its molecular formula $C_{22}H_{18}N_4O_4$, established on the basis of the (+)-HR-ESIMS m/z 403.1399 $[M+H]^+$, was 16 amu less than that of **NP3**, implying that its molecular formula is one oxygen atom less that of **NP3**. Analysis of the ^1H, ^{13}C NMR, COSY, HSQC, and HMBC spectra (Table 27) revealed a close similarity between the structures of **NP6** and **NP3.** The ^{13}C NMR, DEPT and HSQC spectra (Table 27) displayed signals of seven quaternary sp^2 (δ_C 176.9, 170.8, 159.7, 147.6, 140.9, 131.9, 121.4), nine methine sp^2 (δ_C 147.6, 135.1, 131.7, 127.7, 127.4, 126.2, 126.0, 125.5, 117.1), one quaternary sp^3 (δ_C 86.3), three methine sp^3 (δ_C 84.6, 59.5, 57.0), one methylene sp^3 (δ_C 31.0) and one methyl (δ_C 17.6) carbon.

The ^1H NMR spectrum (Table 27) displayed the signals of eight aromatic protons at δ_H 8.22, *d* (*J* = 7.7 Hz), 7.90, *dd* (*J* = 7.7, 7.7 Hz), 7.76, *d* (*J* = 7.7 Hz), 7.69, *d* (*J* = 7.5 Hz), 7.63, *dd* (*J* = 7.7, 7.7 Hz), 7.57, *dd* (*J* = 7.5, 7.5 Hz), 7.47, *d* (*J* = 7.5 Hz) and 7.39, *dd* (*J* = 7.5, 7.5 Hz), and the COSY spectrum (Table 27) revealed the coupling systems of two 1,2-disubstituted benzene rings as in **NP2/NL4** and **NP3**. Like **NP3**, the ^1H NMR spectrum (Table 27) showed a singlet of the olefinic proton at δ_H 8.55, a triplet and a doublet of the methine protons at δ_H 5.66 (*J* = 9.7 Hz) and 5.50 (*J* = 8.5 Hz) respectively, a multiplet and a double doublet of the methylene protons at δ_H 3.44 and 2.88 (*J* = 12.0, 9.4 Hz) respectively, the quartet of the methine proton at δ_H 3.63 (*J* = 6.6 Hz) and the doublet of the methyl protons at δ_H 1.39 (*J* = 6.8 Hz). However, the triplet at δ_H 3.90 (*J* = 7.0 Hz), which did not show any HSQC correlation, was present instead of the singlet of the N-OH proton (δ_H 8.79).

Table 27. ^{1}H and ^{13}C NMR data (DMSO-d_6, 300.13 and 75.47 MHz) of **NP6**.

Position	δ_C, type	δ_H, mult. (*J* in Hz)	COSY	HMBC
2	84.6, CH	5.50, *d* (8.5)	---	C-3, 14
3	86.3, C	---	---	---
4	131.9, C	---	---	---
5	125.5, CH	7.69, *d* (7.5)	H-6	C-3, 7, 9
6	126.0, CH	7.39, *dd* (7.5, 7.5)	H-5, 7	C-4, 8
7	131.7, CH	7.57, *dd* (7.5, 7.5)	H-6, 8	C-5, 9
8	117.1, CH	7.47, *d* (7.5)	H-7	C-4, 6
9	140.9, C	---	---	---
11	170.8, CO	---	---	---
12	57.0, CH	5.66, *t* (9.7)	H-13α, 13β	C-11, 18
13α	31.0, CH_2	2.88, *dd* (12.0, 9.4)	H-12, 13β	C-11
β		3.44, *m*	H-12, 13α	---
14	176.9, CO	---	---	---
15	59.5, CH	3.63, *q* (6.6)	NH, H-27	---
18	159.7, CO	---	---	---
19	121.4, C	---	---	---
20	126.2, CH	8.22, *d* (7.7)	H-21	C-18, 22, 24
21	127.7, CH	7.63, *dd* (7.7, 7.7)	H-20, 22	C-19, 23
22	135.1, CH	7.90, *dd* (7.7, 7.7)	H-21, 23	C-20, 24
23	127.4, CH	7.76, *d* (7.7)	H-22	C-19, 21
24	147.6, C	---	---	---
26	147.6, CH	8.55, *s*	---	C-12, 18, 24
27	17.6, CH_3	1.39, *d* (6.8)	H-15	C-14, 15
NH	---	3.90, *t* (7.0)	H-2, 15	---

While the HMBC correlations of the aromatic proton at δ_H 7.69, *d* (*J* = 7.5; δ_C 125.5) to the quaternary carbons at δ_C 140.9 and 86.3, the aromatic proton at δ_H 7.47, *d* (*J* = 7.5 Hz; δ_C 117.1) to the quaternary sp^2 carbon at δ_C 131.9, and the methine proton at δ_H 5.50, *d* (*J* = 8.5 Hz; δ_C 84.6) to the quaternary sp^3 carbon at δ_C 86.3 indicated that one of the 1,2-disubstituted benzene rings was part of a 2,3-dihydro-1*H*-indole moiety (**A**), the HMBC correlations between the aromatic proton at δ_H 8.22, (*J* = 7.7 Hz; δ_C 126.2) and the quaternary sp^2 carbons at δ_C 159.7 and 147.6, the aromatic proton at δ_H 7.76, d (*J* = 7.7 Hz; δ_C 127.4) and the quaternary sp^2 carbon at δ_C 121.4, and between the methine proton at δ_H 8.55, s (δ_C 147.6) and the quaternary sp^2 carbons at δ_C 159.7 and 147.6, revealed the existence of the *N*-substituted quinazolin-4-one ring (**B**), as in **NP2/NL4** and **NP3**.

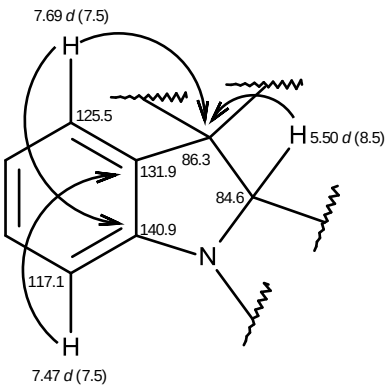

A

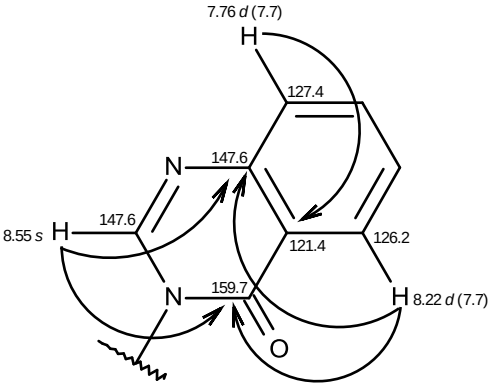

B

The HMBC cross peaks (**C**) of the methine proton at δ_H 5.50, *d* (*J* = 8.5 Hz; δ_C 84.6) to the amide carbonyl at δ_C 176.9, and of the methyl protons at δ_H 1.39, *d* (*J* = 6.8 Hz; δ_C 17.6) to the carbonyl carbon at δ_C 176.9 and the methine carbon at δ_C 59.5 confirmed the presence of the *6-5-5*-methylimidazoindolone ring. The COSY spectrum displayed correlations (**D**) between the proton at δ_H 3.90, *t* (*J* = 7.0 Hz) and the methine protons at δ_H 5.50, *d* (*J* = 8.5 Hz) and 3.63, *q* (*J* = 6.6 Hz), suggesting that the N16-OH group of **NP2/NL4** and **NP3** was replaced by N16-H in **NP6**.

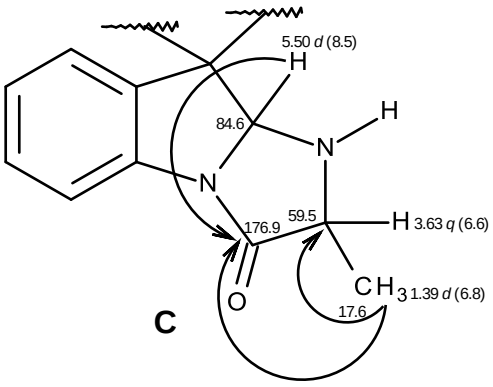

C

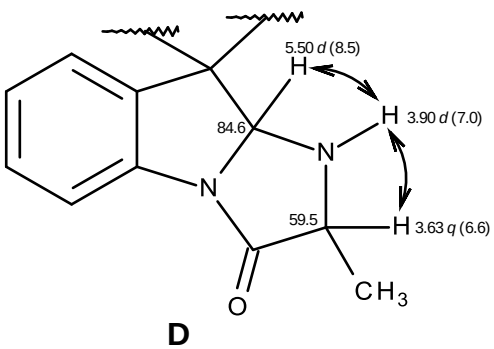

D

The connection of the imidazoindolone ring to the quinazolinone ring via the five-membered spirolactone ring was confirmed by the HMBC correlations of the methine proton at δ_H 5.66, *t* (*J* = 9.7 Hz; δ_C 57.0) to the carbonyl carbons at δ_C 170.8 and 159.7, and of the imine proton at δ_H 8.55, *s* (δ_C 147.6) to the methine sp^3 carbon at δ_C 57.0.

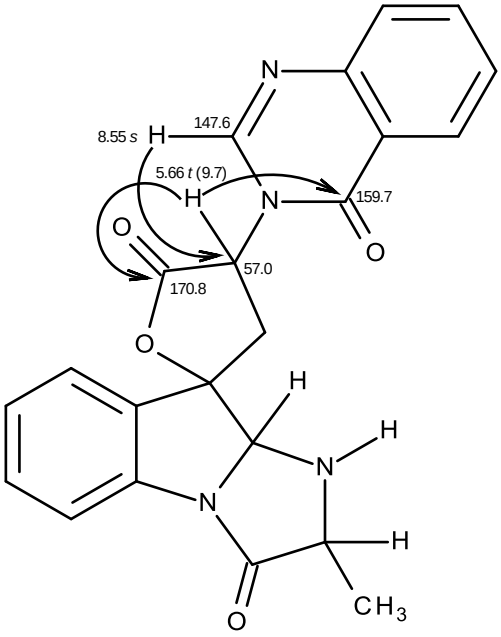

Analogously to **NP2/NL4** and **NP3**, the NOESY spectrum exhibited correlations between the signals of the proton at δ_H 5.50, *d* (*J* = 8.5 Hz) and the methyl protons at δ_H 1.39, *d* (*J* = 6.8 Hz), as well as between the signals of the methine proton at δ_H 5.66, *t* (*J* = 9.7 Hz) and the methine proton at δ_H 8.55, *s*.

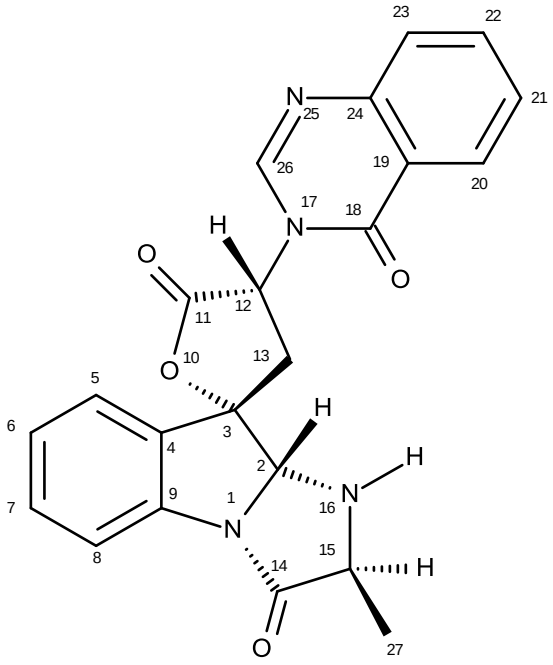

Figure 74. Structure of tryptoquivaline F (**NP6**).

Consequently, the structure of **NP6** was established as tryptoquivaline F (Figure 74), the deoxy analog of tryptoquivaline H (**NP3**). The ^{1}H and ^{13}C NMR data, as well as the optical rotation ($[\alpha]^{20}_{D}$ = -120.0) of **NP6** were in agreement with those reported for tryptoquivaline F, a tryptoquivaline derivative isolated also from *Neosartorya siamensis* KUFC 6349 (Buttachon *et al*., 2012).

3.1.6.6. Tryptoquivaline T (NL6)

NL6 was isolated as white solid (mp. 258-260 ºC), and its molecular formula $C_{24}H_{20}N_4O_5$ was established on the basis of the (+)-HR-ESIMS *m/z* 445.1512 $[M+H]^+$, indicating seventeen degrees of unsaturation. The IR spectrum showed absorption bands for aromatic (3010, 1582, 1450 cm^{-1}) and carbonyls of ester/amide groups (1700 cm^{-1}). The general features of the ^{1}H and ^{13}C spectra (Table 28) of **NL6** closely resembled those of **NP2/NL4**. The ^{13}C NMR, DEPT and HSQC spectra (Table 28) revealed three amide/ester carbonyls (δ_C 172.5, 171.1 and 160.0), one *N*-formyl (δ_C 162.3), four quaternary sp^2 (δ_C 147.8, 138.4, 133.5, 121.4), nine methine sp^2 (δ_C 148.1, 135.1, 131.8, 127.6, 127.4, 126.8, 126.7, 126.2, 116.4), two quaternary sp^3 (δ_C 84.2 and 64.1), two methine sp^3 (δ_C 81.0 and 57.7), one methylene sp^3 (δ_C 33.8) and two methyl (δ_C 26.6 and 25.5) carbons.

The ^{1}H NMR spectrum (Table 28) displayed the signals of one olefinic proton at δ_H 8.62, *s*, eight aromatic protons at δ_H 8.26, *dd* (*J* = 8.0, 1.0 Hz), 8.04, *dd* (*J* = 8.0, 1.0 Hz), 7.93, *ddd* (*J* = 8.0, 8.0, 1.0 Hz), 7.76, *d* (*J* = 8.0 Hz), 7.63, *ddd* (*J* = 8.0, 8.0, 1.0 Hz), 7.61, *ddd* (*J* = 8.0, 8.0, 1.0 Hz), 7.56, *dd* (*J* = 8.0, 1.0 Hz) and 7.46, *ddd* (*J* = 8.0, 8.0, 1.0 Hz), two methine protons at δ_H 6.10, *s* and 5.47, *dd* (*J* = 10.7, 8.6 Hz), two methylene protons at δ_H 3.40, *dd* (*J* = 14.0, 10.7 Hz) and 3.30, *dd* (*J* = 14.0, 8.6 Hz), and the protons of two methyl groups at δ_H 1.72, *s* and 1.55, *s*, besides a doublet at δ_H 8.73 (*J* = 0.9 Hz).

Table 28. ^{1}H and ^{13}C NMR data (DMSO-d_6, 300.13 and 75.47 MHz) of **NL6**.

Position	δ_C, type	δ_H, mult. (*J* in Hz)	COSY	HMBC
2	81.0, CH	6.10, *s*	H-29	C-3,13, 14
3	84.2, C	---	---	---
4	133.5, C	---	---	---
5	126.8, CH	8.04, *dd* (8.0, 1.0)	H-6	C-3, 7, 9
6	126.7, CH	7.46, *ddd* (8.0, 8.0, 1.0)	H-5	C-4, 8
7	131.8, CH	7.61, *ddd* (8.0, 8.0, 1.0)	H-6, 8	C-5, 9
8	116.4, CH	7.56, *dd* (8.0, 1.0)	H-7	C-4, 6
9	138.4, C	---	---	---
11	171.1, CO	---	---	---
12	57.7, CH	5.47, *dd* (10.7, 8.6)	H-13	C-11, 18
13α	33.8, CH_2	3.30, *dd* (14.0, 8.6)	H-12, 13β	C-2, 3, 4
β		3.40, *dd* (14.0, 10.7)	H-12, 13α	C-2, 3, 4
14	172.5, CO	---	---	---
15	64.1, C	---	---	---
18	160.0, CO	---	---	---
19	121.4, C	---	---	---
20	126.2, CH	8.26, *dd* (8.0, 1.0)	H-21	C-18, 22, 24
21	127.6, CH	7.63, *ddd* (8.0, 8.0, 1.0)	H-20, 22	C-19, 23
22	135.1, CH	7.93, *ddd* (8.0, 8.0, 1.0)	H-21, 23	C-20, 24
23	127.4, CH	7.76, *d* (8.0)	H-22	C-19, 21
24	147.8, C	---	---	---
26	148.1, CH	8.62, *s*	---	C-12, 18, 24
27	26.6, CH_3	1.72, *s*	---	C-14, 15, 28
28	25.5, CH_3	1.55, *s*	---	C-14, 15, 27
29	162.3, CO	8.73, *d* (0.9)	H-2	C-2

The coupling system of the aromatic protons at δ_H 8.04, *dd* (*J* = 8.0, 1.0 Hz), 7.46, *ddd* (*J* = 8.0, 8.0, 1.0 Hz), 7.61, *ddd* (*J* = 8.0, 8.0, 1.0 Hz) and 7.56, *dd* (*J* = 8.0, 1.0 Hz), which was evidenced by the COSY spectrum (Table 28), together with the HMBC correlations (Table 28) of the aromatic proton at δ_H 8.04, *dd* (*J* = 8.0, 1.0 Hz; δ_C 126.8) to the quaternary carbons at δ_C 84.2 and 138.4, of the aromatic proton at δ_H 7.56, *dd* (*J* = 8.0, 1.0 Hz; δ_C 116.4) to the quaternary sp^2 carbon at δ_C 133.5, of the methine proton at δ_H 6.10, *s* (δ_C 81.0) to the quaternary carbons at δ_C 84.2 and 172.5, and of the methyl protons at δ_H 1.72, *s* (δ_C 26.6) and 1.55, *s* (δ_C 25.5) to the quaternary carbon at δ_C 64.1 and the carbonyl carbon at δ_C 172.5, indicated the presence of the *6-5-5-gem*-dimethylimidazoindolone ring system. The presence of the doublet at δ_H 8.73 (*J* = 0.9 Hz), which gave the HSQC cross peak to the carbon at δ_C 162.3, indicated the presence of the aldehyde group. Since this doublet displayed HMBC cross peak to the methine carbon at δ_C 81.0, the formyl group was on the nitrogen atom of the imidazolone ring.

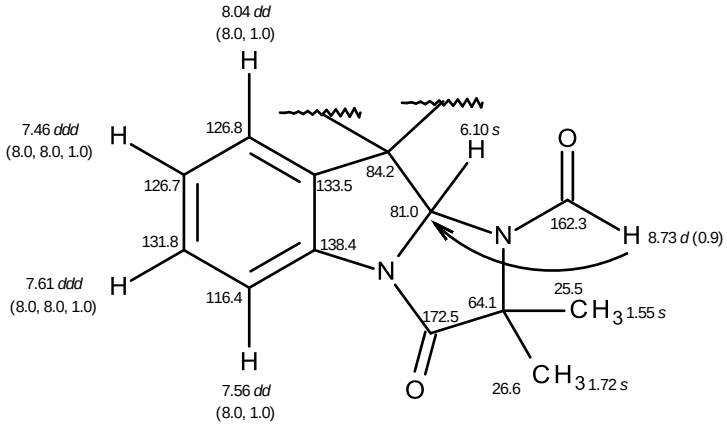

The COSY spectrum also revealed another coupling system of the aromatic protons at δ_H 8.26, *dd* (*J* = 8.0, 1.0 Hz), 7.63, *ddd* (*J* = 8.0, 8.0, 1.0 Hz), 7.93, *ddd* (*J* = 8.0, 8.0, 1.0 Hz) and 7.76, *d* (*J* = 8.0 Hz), of the 1,2-disubstituted benzene ring which, through the HMBC correlations of the aromatic proton at δ_H 8.26, *dd* (*J* = 8.0, 1.0 Hz; δ_C 126.2) to the quaternary sp^2 carbons at δ_C 160.0 and 147.8, of the aromatic proton at δ_H 7.76, *d* (*J* = 8.0 Hz; δ_C 127.4) to the quaternary sp^2 carbon at δ_C 121.4, and of the methine proton at δ_H 8.62, *s* (δ_C 148.1) to the quaternary sp^2 carbons at δ_C 160.0 and 147.8, confirmed the presence of the same *N*-substituted quinazolin-4-one moiety as in **NP2/NL4**.

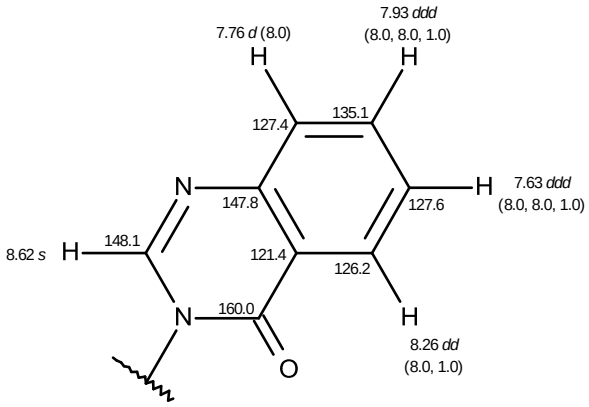

The HMBC correlations of the methylene protons at δ_H 3.30, *dd* (*J* = 14.0, 8.6 Hz; δ_C 33.8) and 3.40, *dd* (*J* = 14.0, 10.7 Hz; δ_C 33.8) to the carbons at δ_C 81.0, 84.2 and 133.5 of the indole moiety, of the methine proton at δ_H 5.47, dd (*J* = 10.7, 8.6 Hz; δ_C 57.7) to the carbonyl carbons at δ_C 171.1 and 160.0, as well as of the methine proton at δ_H 8.62, s (δ_C 148.1) to the methine carbon at δ_C 57.7, confirmed that the *N*-substituted quinazolin-4-one and *6-5-5-gem*-

dimethylimidazoindolone fragments were connected via the five-membered spirolactone as in **NP2/NL4, NP3** and **NP6**.

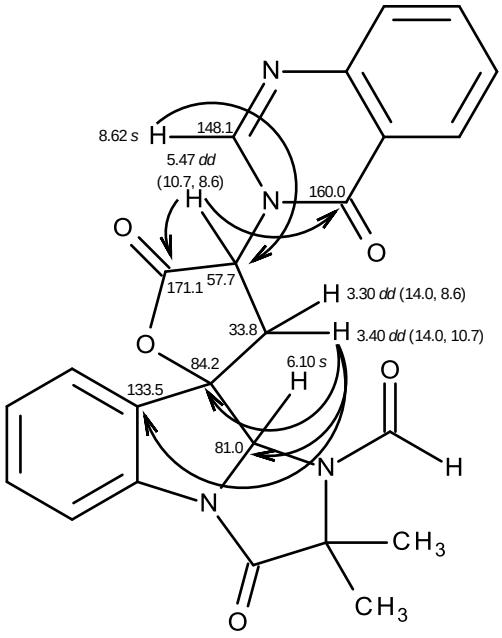

The only difference between the structures of **NL6** and **NP2/NL4** is the presence of the formyl group on N-16 of the *gem*-dimethyl imidazoindole moiety in the former and a hydroxyl group in the latter. On the other hand, the structure of **NL6** differs from that of tryptoquivaline O, which was previously isolated from *Neosartorya siamensis* KUFC 6349 (Buttachon *et al.*, 2012), in that there are two methyl groups on C-15 (δ_C 64.1) of the imidazoindole ring in the former instead of one methyl group in the latter.

Since the chemical shift values of the protons at δ_H 6.10, *s* and 5.47, *dd* (*J* = 10.7, 8.6 Hz) of **NL6** are similar of those of the corresponding protons of tryptoquivaline O, we assume that the stereochemistry of **NL6** is the same as that of tryptoquivaline O, *i.e.*, C-2*S*, C-3*S* and C-12*R*. This assumption was also supported by the negative value of the rotation ($[\alpha]_D^{25}$ = - 83.3) of **NL6**. Thus, **NL6** is a new tryptoquivaline analogue which we have named tryptoquivaline T (Figure 75).

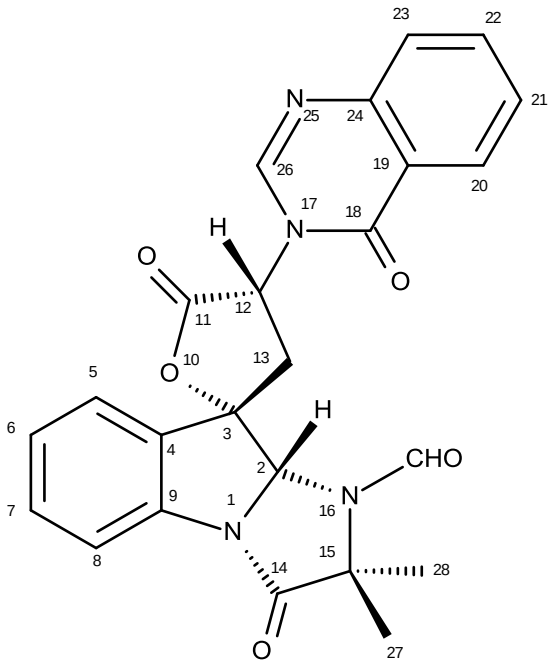

Figure 75. Structure of tryptoquivaline T (**NL6**).

The biosynthetic pathway for the isolated tryptoquivalines, which are characterized by quinazolinone ring connected to a *6-5-5*-imidazoindolone ring system via a five-membered spirolactone, still remains uncharacterized. So, we proposed the biosynthetic pathways (Scheme 5) of these compounds, based on the previous study by Gao *et al*. (2011b). The skeleton of tryptoquivalines is originated from L-tryptophan which undergoes epimerization to yield D-tryptophan. Condensation of D-tryptophan with anthranillic acid and one biological equivalent of formaldehyde give the indoline quinazolinone derivative. Epoxidation of the indole moiety and subsequent opening of the epoxide ring yields the hydroxy iminium intermediate followed by lactonization to form the spirolactone ring. Condensation with 2-aminobutiric acid (Pathway a) leads to the formation of the *gem*-dimethyl group in *6-5-5*-imidazoindolone ring present in tryptoquivaline L, while the methyl group in tryptoquivalines F and H derives from the condensation with L-alanine (Pathway b).

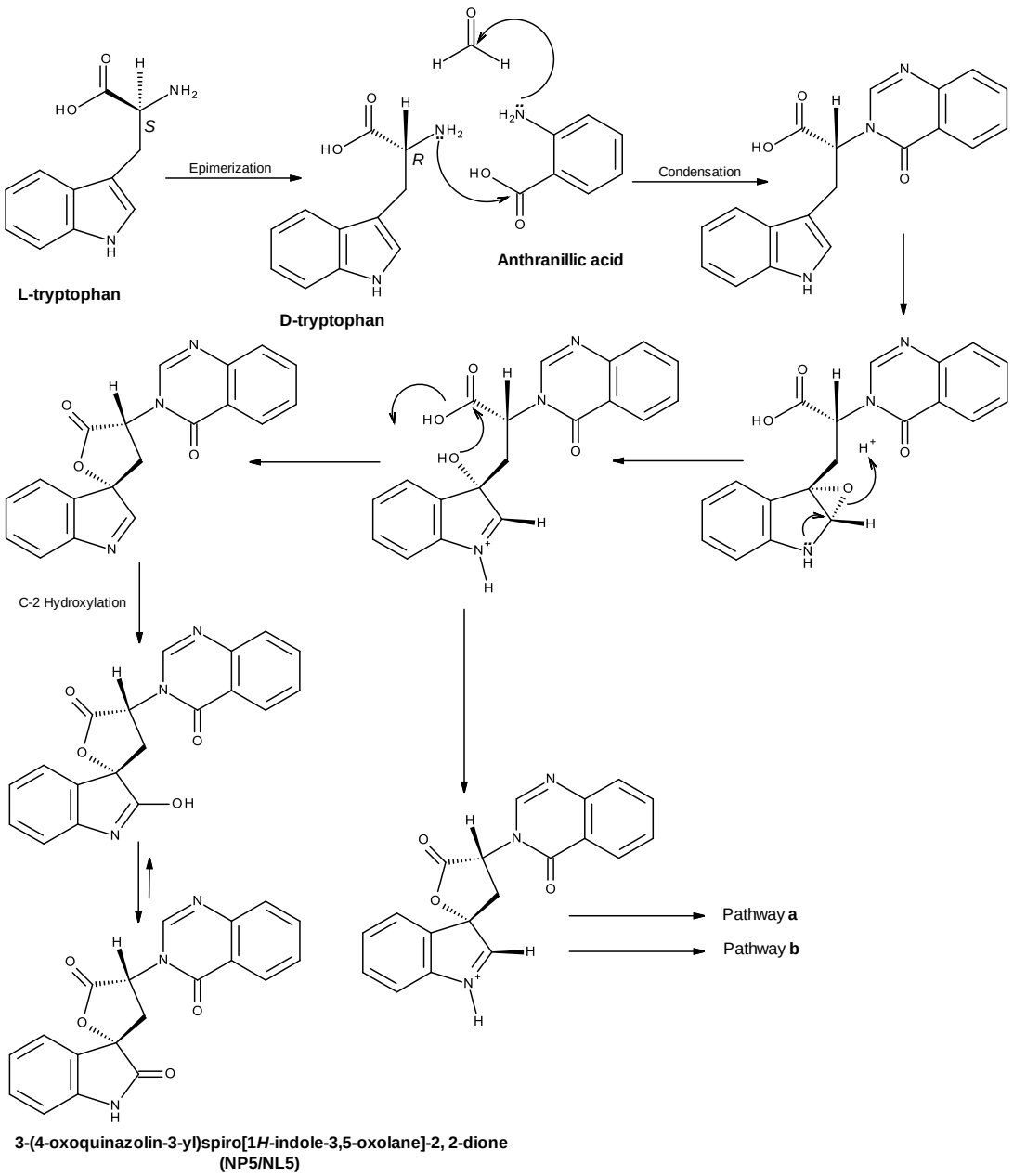

Scheme 5. Biosynthetic pathways for 3-(4-oxoquinazolin-3-yl)spiro[1*H*-indole-3,5-oxolane]-2,2'-dione (**NP5/NL5**) and tryptoquivalines L (**NP2/NL4**), H (**NP3**) and F (**NP6**).

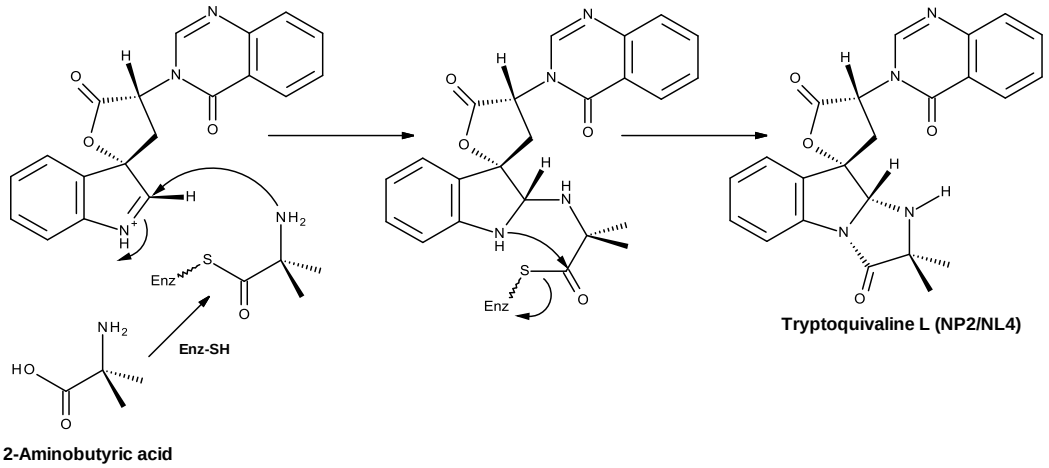

Pathway a

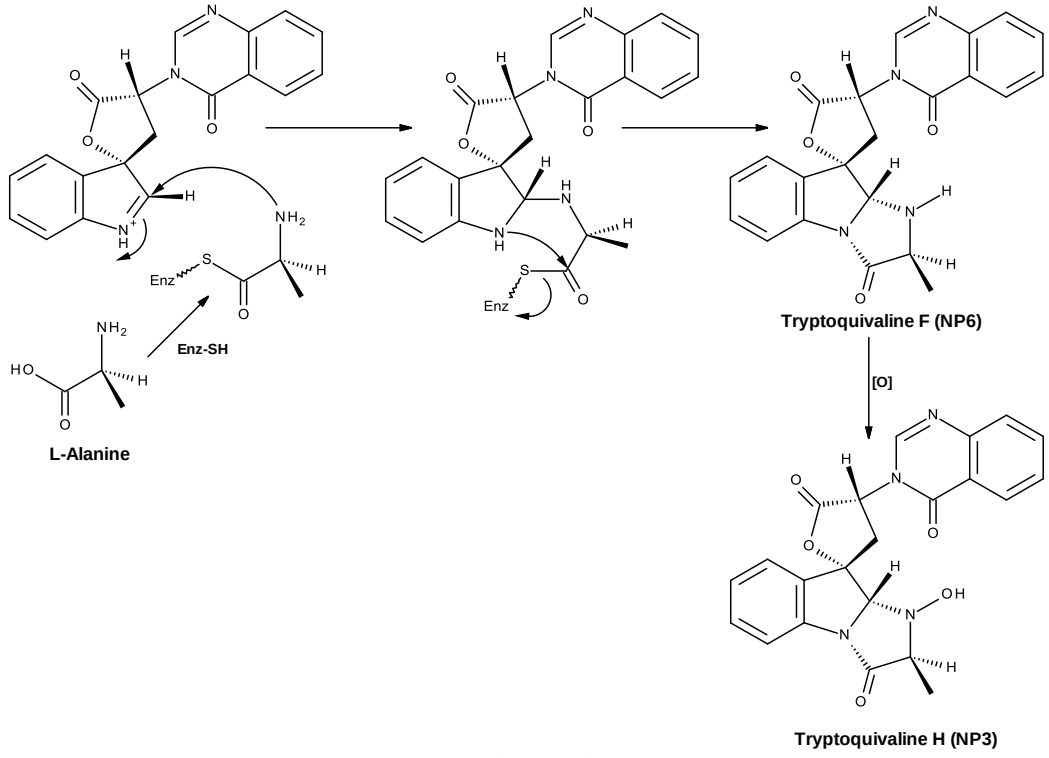

Pathway b

Scheme 5 (cont). Biosynthetic pathways for 3-(4-oxoquinazolin-3-yl)spiro[1*H*-indole-3,5-oxolane]-2,2'-dione (**NP5/NL5**) and tryptoquivalines L (**NP2/NL4**), H (**NP3**) and F (**NP6**).

So far, tryptoquivaline family of alkaloids was found to be produced exclusively by fungi, being identified from *Aspergillus* species such as *A. clavatus* (Büchi *et al*., 1977; Clardy *et al*, 1975), *A. fumigatus* (Yamazaki *et al*., 1976; 1977; 1978; 1979), from a marine unidentified *Aspergillus* strain (Zhou *et al*., 2013) as well as from *Corynascus setosus* (Fujimoto *et al*., 1996).

Despite the isolation of tryptoquivalines L, H and F from the cultures of *A. fumigatus* (Yamazaki *et al*., 1977; 1978) and *Neosartorya siamensis* KUFC 6349 (Buttachon *et al*., 2012), this is the first report on the isolation of tryptoquivalines L, H and F from *N. paulistensis*, as well as the isolation of tryptoquivaline L and the new tryptoquivaline T from *N. laciniosa* (Gomes *et al*., 2014).

Analogously to the meroditerpenes isolated from *N. paulistensis* KUFC *7897* and *N. laciniosa* KUFC 7896, as well as from other *Neosartorya* species, tryptoquivalines are also suggested as specific extrolites from some *Neosartorya* species, which can be used as a supplement to morphological and genetic taxonomic studies (Samson *et al*., 2007). The taxonomic study on the genus *Neosartorya* by Samson *et al*. (2007) led to the identification of tryptoquivaline-like and tryptoquivalone-like extrolites from several species such as *N. aureola*, *N. fischeri*, *N. laciniosa*, *N. udagawae* and *N. warcupii*. Furthermore, besides the isolation of tryptoquivalines O from *N. siamensis* KUFC 6349 (Buttachon *et al*., 2012), the new tryptoquivalines P, Q, R and S were also isolated from the marine-derived fungus *Neosartorya* sp. HN-M-3 (Sun *et al*., 2012; Xu *et al*., 2013b).

Consequently, the isolation of tryptoquivalines L, H, F from the *Neosartorya* species we have investigated, can provide an additional tool for the identification of the species *N. paulistensis* and *N. laciniosa*, as well as tryptoquivaline T, a new extrolite which could be useful for the chemotaxonomic identification of other species from *Neosartorya* genus.

3.2. Biological Activity Evaluation of the Isolated Fungal Secondary Metabolites

Some of isolated compounds from the investigated fungal extracts were tested in three main biological assays: antifungal, antibacterial and cytotoxic activities against human cancer cell lines.

3.2.1. Antifungal and Antibacterial Activities Evaluation

The anthraquinones, erythroglaucin (**EC1**), physcion (**EC2**), catenarin (**EC3**) and emodin (**EC4**), as well as the diketopiperazine alkaloids, echinulin (**EC6**), neoechinulin (**EC7**), neoechinulins A (**EC8**) and E (**EC9**), and eurocristatine (**EC10**) (Figure 76) isolated from *E. cristatum* KUFC 7356 EtOAc extract, were tested for antifungal and antibacterial activities evaluation.

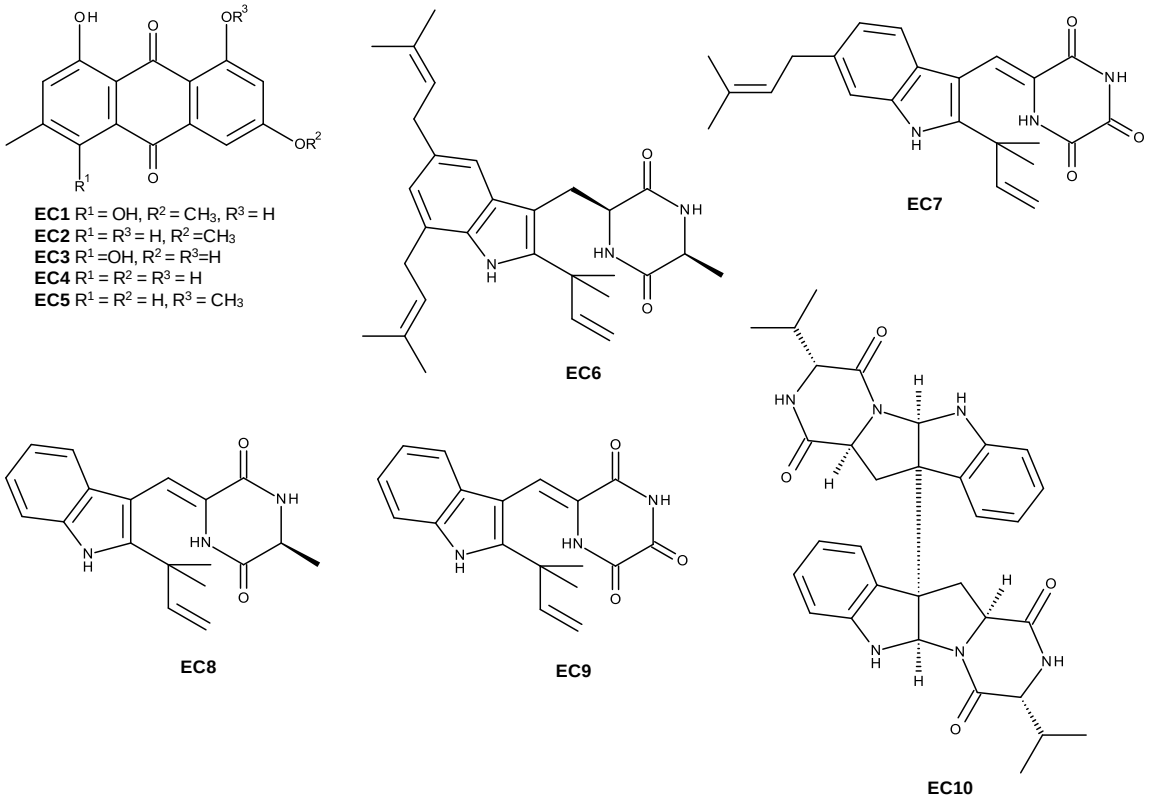

Figure 76. Structures of the compounds tested for antifungal and antibacterial activities.

Metabolites were tested for their antifungal activity against yeast (*Candida albicans*), filamentous fungus (*Aspergillus fumigatus*) and dermatophyte (*Trichophyton rubrum*) strains, and antibacterial activity against *Staphylococcus aureus*, *Escherichia coli* and *Pseudomonas aeruginosa*, according to the procedure described by Wattanadilok *et al*. (2007), specified in Materials and Methods (*see 4.6.2. Antifungal Activity Bioassays*). However, none of the compounds exhibited antifungal activity (Gomes *et al*., 2012).

3.2.2. Cytotoxic Activity Evaluation

The diketopiperazine alkaloids, neoechinulin (**EC7**), neoechinulins A (**EC8**) and E (**EC9**) and eurocristatine (**EC10**) isolated from *E. cristatum* KUFC 7356, and the meroditerpenes aszonapyrones A (**NL2**) and B (**NL3**), isolated from *N. laciniosa* KUFC 7896 extract (Figure 77) were tested for their *in vitro* growth inhibitory effect against three human tumor cell lines MCF-7 (breast adenocarcinoma), NCI-H460 (non-small cell lung cancer) and A375-C5 (melanoma) by the protein binding dye SRB method (*see Chapter IV Materials and Methods, 4.6.1. Cytotoxic Activity Bioassays*).

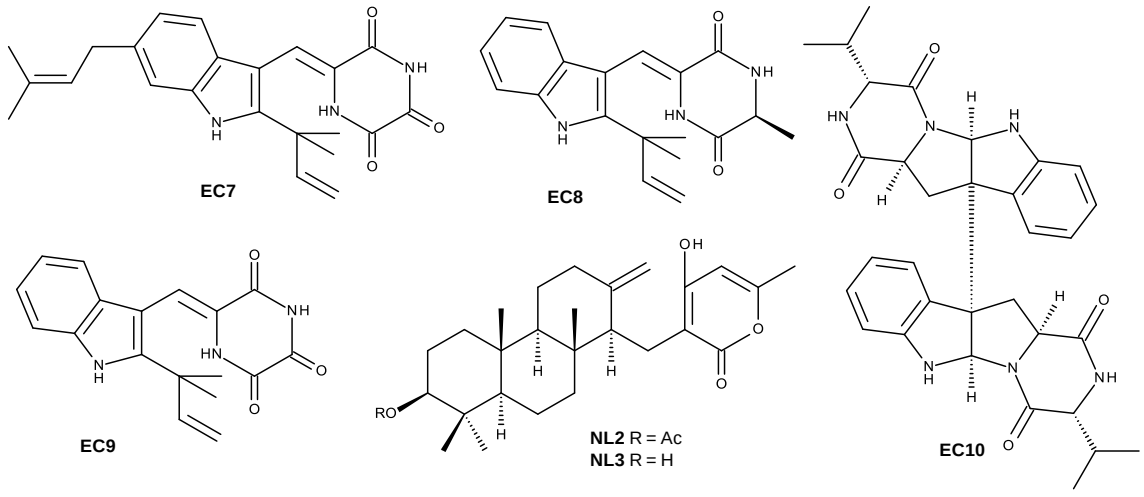

Figure 77. Structures of the compounds tested for *in vitro* cytotoxic activity against human cancer cell lines.

None of the diketopiperazine alkaloids (**EC7-10**) displayed growth inhibitory activity on the three human tumor cell lines (Gomes *et al*., 2012). However, the meroditerpene aszonapyrone A (**NL2**) showed strong growth inhibitory activity against the three cell lines, with GI_{50} = 13.6 ± 0.9 µM, 11.6 ± 1.5 µM and 10.2 ± 1.2 µM, for MCF-7, NCI-H460 and A375-C5, respectively, while aszonapyrone B (**NL3**), whose structure corresponds to 3-deacetyl aszonapyrone A, was inactive at the highest concentration tested (150 µM) (Table 29) (Eamvijarn *et al*., 2013).

Table 29. Growth inhibitory effect of diketopiperazine alkaloids **EC7-EC10** and meroditerpenes **NL2** and **NL3**

Compounds	GI_{50} (µM)		
	MCF-7	NCI-H460	A375-C5
EC7	> 150	> 150	> 150
EC8	> 150	> 150	> 150
EC9	> 150	> 150	> 150
EC10	> 150	> 150	> 150
NL2	13.6 ± 0.9	11.6 ± 1.5	10.2 ± 1.2
NL3	> 150	> 150	> 150

Results are given as the lowest concentration causing 50% of cell growth inhibition (GI_{50}) after a continuous exposure to the compounds for 48 h, and are expressed as mean ± SEM of three independent experiments performed in duplicate. Doxorubicin was used as positive control, GI_{50}: MCF-7=60.3±1.2 nM; NCI-H460=19.6±1.9 nM; A375-C5=130.0±25 nM.

3.2.3. Antibacterial and Antibiofilm Activity Evaluation

Tryptoquivalines L (**NP2/NL4**), H (**NP3**), F (**NP6**) and T (**NL6**), 4(3*H*)-quinazolinone (**NP4**) and 3'-(4-oxoquinazolin-3-yl)spiro[1*H*-indole-3,5'-oxolane]-2, 2'-dione (**NP5/NL5**), together with meroditerpenes aszonapyrone A (**NL2**) and B (**NL3**), and the new meroditerpene sartorypyrone C (**NP1**) (Figure 78), were tested for their antibacterial activity against bacterial reference strains and environmental multidrug-resistant isolates. None of the quinazolinone alkaloids (**NP2/NL4, NP3, NP5/NL5, NP6, NL6**) exhibited relevant antibacterial activity (Table 30a). However, within the meroditerpene group, only aszonapyrone A (**NL2**) presented significant MIC values against Gram-positive bacteria, showing the MIC values of 8 µg/mL against *S. aureus* ATCC 25923 and *B. subtilis* ATCC 6633.

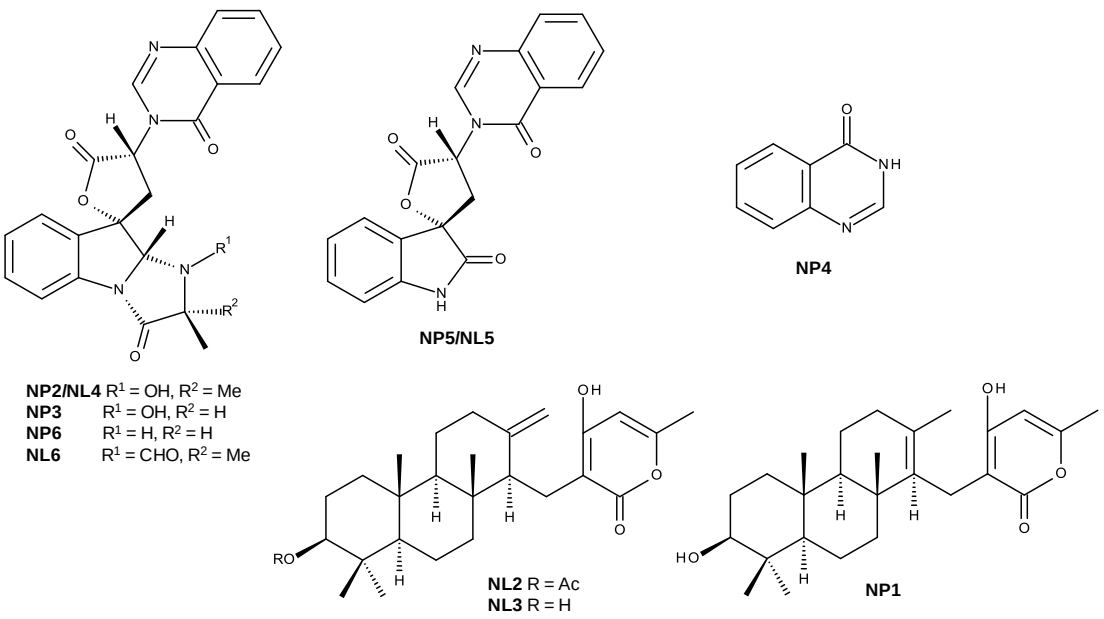

Figure 78. Structures of the compounds tested for antibacterial and antibiofilm activities.

Based on these results, the MIC values of aszonapyrone A (**NL2**) was further determined against Gram-positive multidrug-resistant strains, and it was found to be active against both *S. aureus* MRSA and *Enterococcus* spp. VRE isolates (Table 30b). MBC values were only achieved for aszonapyrone A (**NL2**) against Gram-positive reference strains.

Table 30. Antibacterial activity, expressed in µg/mL of compounds **NP1-NP6** and **NL2-NL6** against reference strains **(a)** and of **NL2** against multidrug-resistant isolates **(b)**.

a								
	S. aureus ATCC 25923		*P. aeruginosa* ATCC 27853		*B. subtilis* ATCC 6633		*E. coli* ATCC 25922	
Compounds	MIC	MIB	MIC	MIB	MIC	MIB	MIC	MIB
NP1	128	---	128	256	128	---	128	---
NP2/NL4	128	---	128	256	128	---	128	---
NP3	128	---	128	256	128	---	128	---
NP4	128	---	128	256	128	---	128	---
NP5/NL5	256	---	128	256	128	---	128	---
NP6	128	---	128	128	128	---	128	---
NL2	8	64	128	256	8	16	128	---
NL3	256	---	128	256	128	---	128	---
NL6	---	---	128	---	128	---	128	---

b

Compound	*S. aureus* B1		*S. aureus* B2		*E. faecalis* W1		*E. faecium* W5	
	MIC	MIB	MIC	MIB	MIC	MIB	MIC	MIB
NL2	8	---	8	---	16	---	16	---

(-) : > 256 µg/mL.

The disc diffusion method (Table 31) revealed a small synergistic association between all the compounds tested and the antibiotics to which *E. coli* G1 was resistant. Even though only a few compounds showed synergism against *S. aureus* B1 and *E. faecium* W5, association of aszonapyrone A (**NL2**) with the antibiotics was found to produce the biggest halos.

Table 31. Antibacterial efficacy (halos, mm) of combined effect of antibiotics with compounds **NP1-NP6** and **NL2-NL6** (15 µg/disc) against three multidrug-resistant isolates, using the disc diffusion method.

Compounds	*E. coli* G1			*S. aureus* B1			*E. faecium* W5		
	Antibiotics								
	CIP	AMP	CTX	S	OX	AMP	CTX	VA	AMP	E
NP1	7	7	=	7.5	=	=	=	=	=	=
NP2/NL4	7	7	=	7.5	=	=	=	=	=	=
NP3	7	7	=	7.5	=	=	=	=	=	=
NP4	7	7	=	7.5	=	=	=	=	=	=
NP5/NL5	7	7	=	7.5	=	=	=	=	=	=
NP6	7	7	=	7.5	=	=	=	=	=	=
NL2	8	8	=	8	12.5	13	13	11	12	13.5
NL3	7	7	=	7.5	11	10	10.5	11	12	13.5
NL6	7	7	=	7.5	=	=	=	=	=	=
Control	0	0	14	0	0	7	0	8	0	0

Control: Antibiotic with no compounds; **CIP:** Ciprofloxacin; **AMP:** Ampicillin; **CTX:** Cefotaxime; **S:** Streptomycin; **OX:** Oxacillin; **VA:** Vancomycin; **E:** Erythromycin.
(=): No influence of the compound / Same result as obtained with no compound.

The results of the Checkerboard method, represented by the FIC (Fractional Inhibitory Concentration) index, are shown in Table 32. The combination effect of aszonapyrone A (**NL2**) with oxacillin (OX) and ampicillin (AMP) against MRSA and VRE isolates, respectively, was found to be indifferent (ΣFIC > 0.5). However, aszonapyrone A (**NL2**) was found to lower the MIC of each

antibiotic tested, thus, it may be considered a partially synergist effect. The association of aszonapyrone A (**NL2**) with vancomycin (VA) showed a clear synergistic effect (ΣFIC < 0.5) against the two VRE isolates tested.

Table 32. FIC Index results obtained with aszonapyrone A (**NL2**) and antibiotic combinations by checkerboard method.

	OX		VA		AMP	
Bacterial Isolate	ΣFIC	Activity[a]	ΣFIC	Activity	ΣFIC	Activity
***S. aureus* B1**	0.562	**I**	---	---	2	**I**
***S. aureus* B2**	2	**I**	---	---	2	**I**
***E. faecalis* W1**	---	---	0.312	**S**	0.75	**I**
***E. faecium* W5**	---	---	0.312	**S**	0.75	**S**

AMP: Ampicillin; **OX:** Oxacillin; **VA:** Vancomycin
[a] **S** = Synergism; **I** = Indifference; **(-)**: Not determined

The effect of aszonapyrone A (**NL2**) at different concentrations (ranging from 2x MIC to 1/4x MIC), on the biofilm formation of *S. aureus* ATCC 25923, *B. subtilis* ATCC 6633, *S. aureus* B1 and *E. faecalis* W1 was also assessed using the biomass quantification, and the results are shown in Figure 73. All the strains tested showed no biofilm formation in the presence of 2x MIC and MIC of aszonapyrone A (**NL2**). However, *S. aureus* ATCC 25923 and *S. aureus* B1 formed more biofilm in the presence of a sub-inhibitory concentration (1/2x MIC) of aszonapyrone A (**NL2**) (Figure 79).

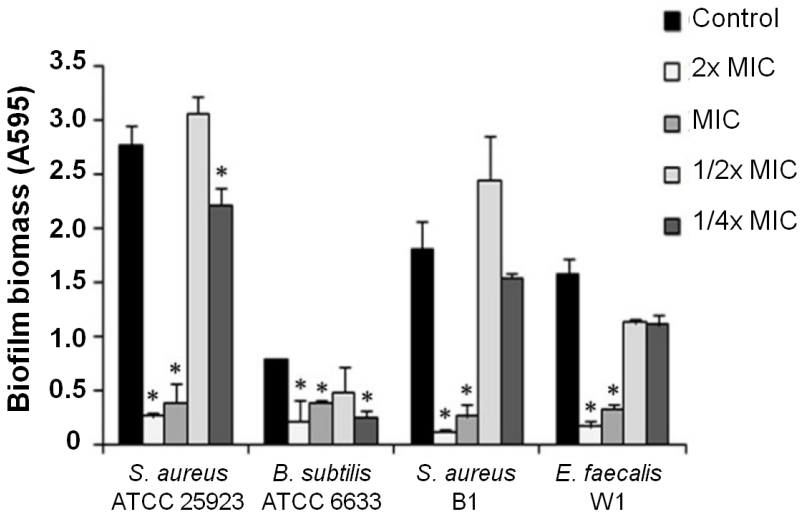

Figure 79. Biomass quantification of biofilms of Gram-positive bacteria formed in the presence of concentrations ranging from 2x MIC to 1/4x MIC of aszonapyrone A (**NL2**).

In order to confirm the effect of aszonapyrone A (**NL2**) on biofilm formation, the microscopic visualization of the biofilm produced by *S. aureus* ATCC 25923 was carried out using a Live/Dead staining. After 24 h, the majority of the cells within the biofilm were viable and large aggregates embedded in a matrix could be observed (Figure 80A). In the presence of aszonapyrone A (**NL2**), at a concentration equal to the MIC, no biofilm was formed and also no growth was observed (Figure 80B). However, at the concentration of 1/2x MIC, it was possible to observe more biofilm in comparison to the control (Figure 80C). These results are in agreement with those obtained in the biomass quantification for the same experimental conditions. However, this result is not unexpected since there are several reports of the increase in biofilm formation in both Gram-positive and Gram-negative bacteria in the presence of sub-inhibitory concentrations of antibiotics (Bessa *et al*., 2013; Hoffman *et al*., 2005; Kaplan *et al*., 2011).

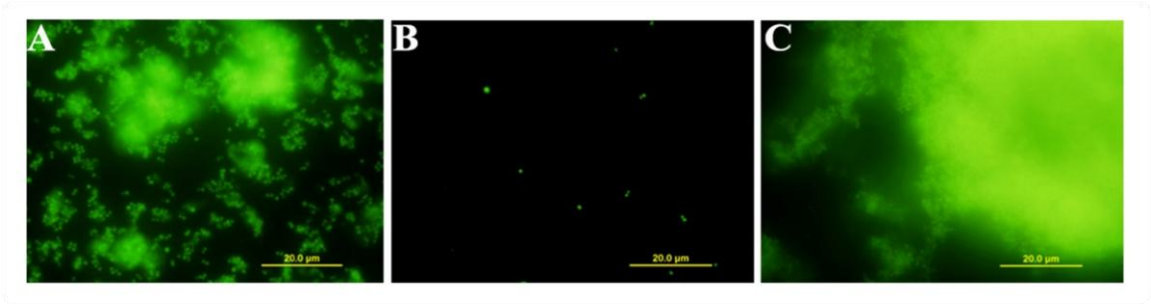

Figure 80. Evaluation of *S. aureus* ATCC 25953 biofilm formation. Live/dead viability staining images after 24 h. Control **(A)**; Biofilm formation in the presence of the MIC **(B)** and in the presence of 1/2 of the MIC **(C)** of aszonapyrone A (**NL2**).

Interestingly, the BIC value of aszonapyrone A (**NL2**) was found to be higher than 12× MIC against mature biofilms of both *S. aureus* B1 (BIC > 96 µg/mL) and *E. faecalis* W1 (BIC > 192 µg/mL). However, the exact BIC value could not be determined due to the limited quantity of this compound available to perform all these biological assays. These very high BIC values may reflect the difficulty of **NL2** in penetrating the extracellular biofilm matrix, thus hampering the eradication of the pre-established biofilm (Gomes *et al*., 2014).

Finally, the antibacterial activity evaluation of structurally related meroditerpenes isolated from our research group, could lead us to hypothesize some of the chemical requirements of this class of compounds for the antibacterial activity. Chevalones B (**140**) and C (**141**) and sartorypyrones A (**177**) and B (**196**) (Figure 81) were also tested for their antibacterial activity against the four reference strains (*S. aureus*, *B. subtilis*, *E. coli*, and *P. aeruginosa*, as well as the environmental multidrug-resistant isolates), however only sartorypyrone A exhibited moderate antibacterial activity as well as synergism with antibiotics against the Gram-positive multidrug-resistant strains.

Examination of the structures of the meroditerpenes tested (Figure 81) suggested the existence of some common features necessary for the antibacterial activity of this class of compounds.

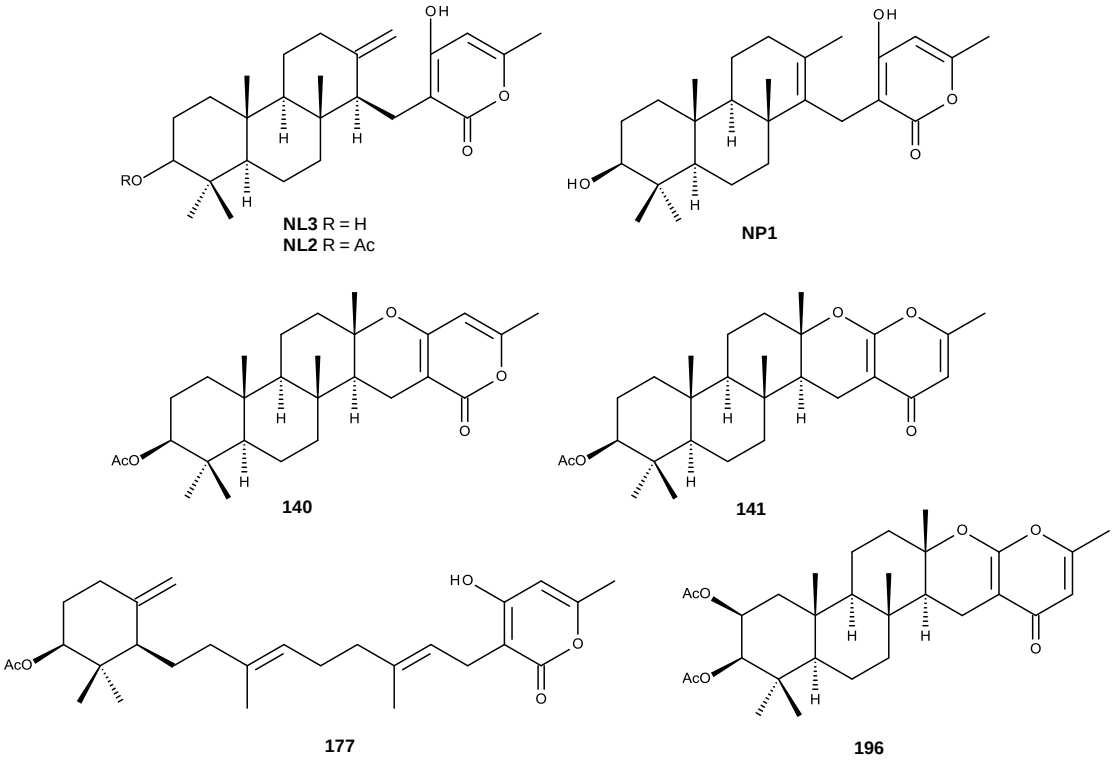

Figure 81. Structures of the meroditerpenes tested for antibacterial activity.

Although aszonapyrone A (**NL2**), aszonapyrone B (**NL3**), sartorypyrone C (**NP1**) and sartorypyrone A (**177**), all contain the 4-hydroxy-6-methyl-2*H*-pyran-2-one ring, only aszonapyrone A (**NL2**) and sartorypyrone A (**177**) have the β-acetoxyl group on C-3. On the other hand, while this 4-hydroxy-6-methyl-2*H*-pyran-2-one ring is connected to the perhydrophenanthrene portion by the ethereal bridge, forming a more rigid pentacyclic structure in chevalone B (**140**), both chevalone C (**141**) and sartorypyrone B (**196**) contain the 6-methyl-4*H*-pyran-4-one ring connected to the perhydrophenanthrene portion by an ethereal bridge. Therefore, it is apparent that the presence of a free 4-hydroxy-6-methyl-2*H*-pyran-2-one ring on C-15 and the β-acetoxyl group on C-3 of the perhydrophenanthrene portion are required for the antibacterial activity of this series of meroditerpenes.

CHAPTER IV
MATERIALS AND METHODS

4.1. General Experimental Procedures

Si gel 60 (0.2-0.5 mm; 70-230 mesh, Merck), LiChroPrep Si 60 (0.04-0.063 mm, Merck) and Sephadex LH-20 were used for column chromatography. Analytical TLC was performed on Si gel 60 (GF_{254}, Merck), 0.25 mm thickness (The plates were activated at 110 ºC in the oven Binder for 4 hours) and precoated silica gel sheets, GF_{254} (Macherey-Nagel), ALUGRAM®, Sil G/UV_{254}, 20 x 20 cm. TLC plates were visualized under UV_{254nm} and $_{365nm}$ or developed with iodine vapor.

^{1}H and ^{13}C NMR spectra were recorded at ambient temperature in $CDCl_3$ or DMSO-d_6 on a Bruker AMC instrument operating either at 300.13 and 75.47 MHz or 500.13 MHz and 125.77 MHz, respectively.

High resolution mass spectra were measured with a Waters Xevo QToF mass spectrometer coupled to a Waters Aquity UPLC system.

Ultraviolet and infrared spectra were recorded on a Shimadzu mini-1240UV-VIS spectrophotometer using 1.000 cm quartz cells, and on an ATT Mattson Genesis Series FTIR™ using WinFIRST Software, respectively.

Melting points were determined on a Bock monoscope and are uncorrected.

Optical rotations were determined on an ADP410 Polarimeter.

The weight was measured on the analytical balance AND GH-202.

The solvents used were from Merck and Fischer with analytical reagent grade. Solvents were evaporated at reduced pressure, using Büchi Heating Bath B-49, Büchi Rotavapor R-210, Büchi Vacuum Module V-801 EasyVac and Vacuum Pump V-700.

4.2. Isolation and Identification of the Biological Material

4.2.1. *Emericella variecolor* KUFC 7092

Emericella variecolor KUFC 7092 was isolated from the marine sponge *Clathria reinwardti* (Figure 82a), which was collected by scuba diving at 15 meters depth, from Koh Tarutao, Amphur Mueang, Satun Province, Southern Thailand. After rinsing three times with sterile sea water, the sponge was dried on sterile filter papers, cut into small pieces (5 x 5 mm) and placed on the plates containing malt extract agar (MEA, 30 g of malt extract, 15 g of bacto agar, distilled water 1000 mL, and adjusted to the final pH at 5.5) 70% sea water, and incubated at 28ºC under 12h light / 12h dark cycle for 7 days.

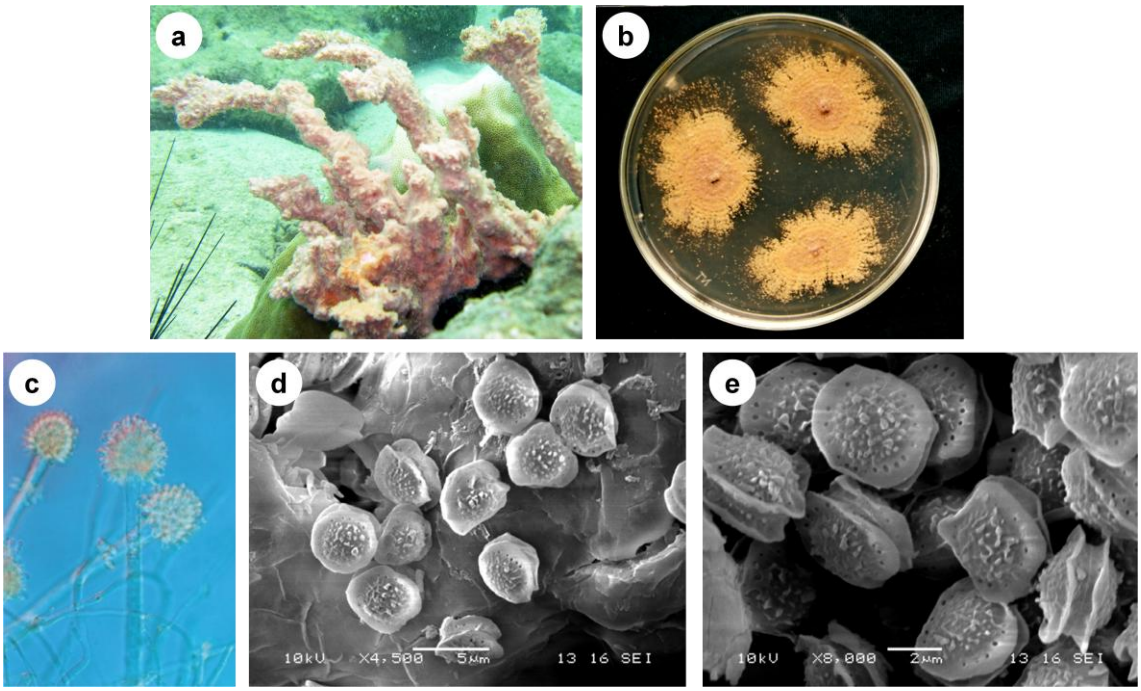

Figure 82. *Clathria reinwardti* (**a**)*. E. variecolor* KUFC 7092. Colony on MEA with 70 % sea water after 14 days (**b**). Conidiophores and conidia (**c**). SEM image of ascospores (**d**, **e**).

The fungus was identified by morphological features, including the characteristic of ascospores and colonies (Figure 82b-e). The pure cultures were deposited as KUFC 7092 at Kasetsart University Fungal Collection, Department of Plant Pathology, Faculty of Agriculture, Kasetsart University, Bangkok, Thailand.

4.2.2. *Eurotium cristatum* KUFC 7356

Eurotium cristatum KUFC 7356 was isolated from the marine sponge *Mycale* sp. (Figure 83a) which was collected from Wonnapa Beach, Bangsaen, Chonburi Province, Thailand. After rinsing with sterile sea water, the sponge was dried on sterile filter papers, cut into small pieces (5 x 5 mm) and placed on the plates containing MEA with 70% sea water. The plates were incubated at room temperature for one week and the fungus was transferred onto the MEA + 70% sea water slant.

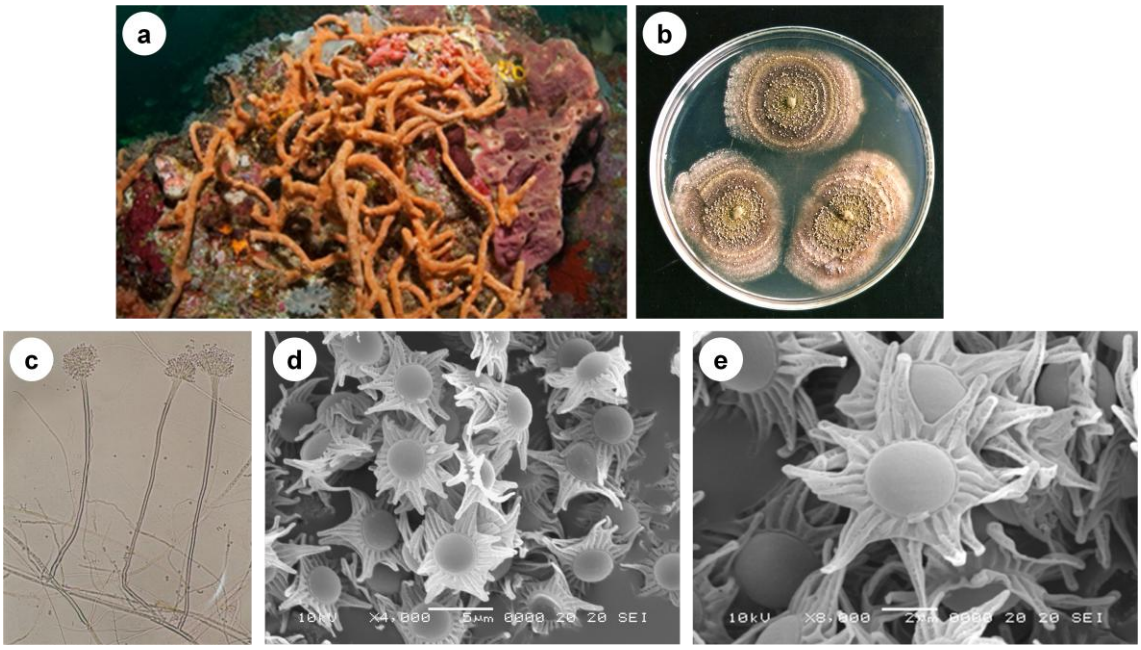

Figure 83. *Mycale* sp. (**a**). *E. cristatum* KUFC 7356. Colony on PDA with 70 % sea water after 14 days (**b**). Conidiophores and conidia (**c**). SEM image of ascospores (**d, e**).

The fungus was identified based on macro- and microscopic characteristics, observed under light and scanning electron microscopes (Figure 83b-e). The pure

cultures were deposited as KUFC 7356 at Kasetsart University Fungal Collection, Department of Plant Pathology, Faculty of Agriculture, Kasetsart University, Bangkok, Thailand.

4.2.3. *Neosartorya laciniosa* KUFC 7896

The strain KUFC 7896 was isolated from a diseased coral (*Porites lutea* ulcerative white spot) (Figure 84) which was collected by Jamrearn Buaruang at Ao Nuan Lan Island (altitude 12º 53’ 56.85’’ N, 100º 46’ 39.66’’ E), The Gulf of Thailand, Chonburi Province, in May 2010.

Figure 84. Diseased coral (*Porites lutea*).

The diseased coral was washed with 0.06% sodium hypochlorite for 1 min, followed by sterilized sea water for three times. The diseased coral was cut into 5 x.5 mm pieces and placed on MEA with 70% sea water, and incubated at 28 ºC for 5-7 days. The fungus was identified as *N. laciniosa* by morphological characteristics, such as colony growth rate and growth pattern on standard media namely Czapek’s agar (CZA), Czapek yeast autolysate agar (CYA) and MEA (Figure 85a-c). Microscopic characteristics including size, shape, ornamentation of ascospores and *Aspergillus laciniosus* anamorph were examined under light and scanning electron microscopes (Figure 85d-f). This identification was supported by sequence analysis of the β-tubulin gene (Glass and Donaldson, 1995) and the pure cultures were deposited as KUFC 7896 at Kasetsart University Fungal Collection, Department of Plant Pathology, Faculty of Agriculture, Kasetsart

University, Bangkok, Thailand, and as MMERU 01 at Microbes Marine Environment Research Unit, Division of Environmental Science, Faculty of Science, Ramkhamhaeng University, Bangkok, Thailand.

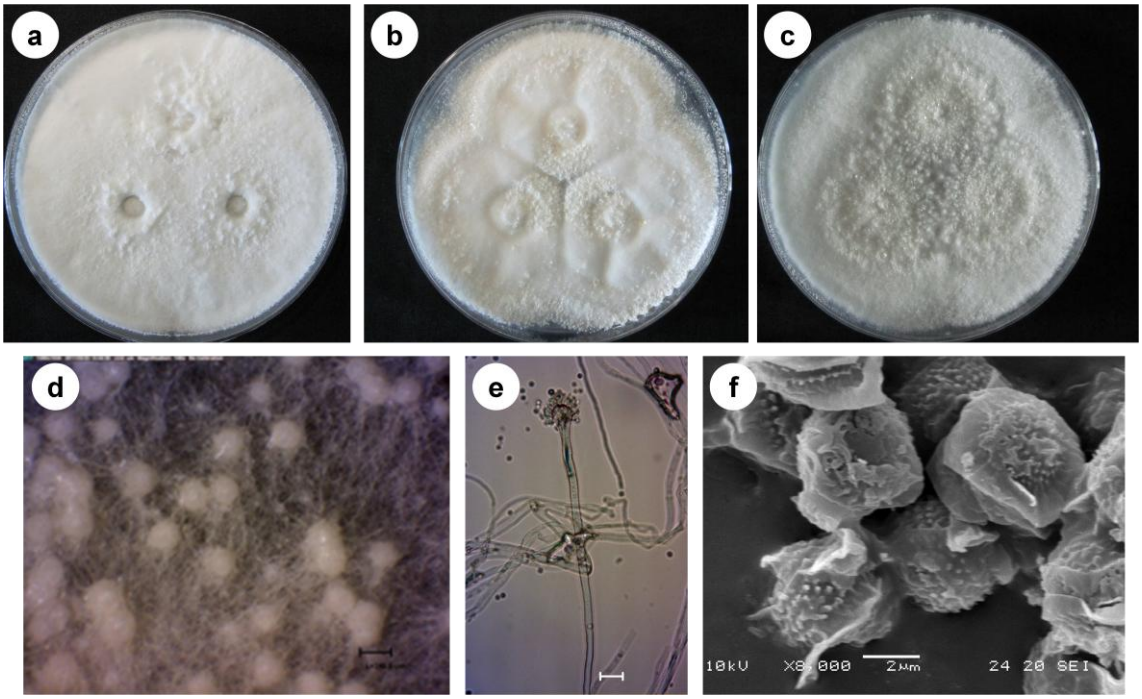

Figure 85. *N. laciniosa* KUFC 7896. Colonies incubated for 14 days at 28ºC on CZA (**a**), CYA (**b**) and MEA (**c**) media. Ascomata (**d**). Conidia (**e**). SEM image of ascospores (**f**).

4.2.4. *Neosartorya paulistensis* KUFC 7897

Neosartorya paulistensis KUFC 7897 was isolated from the marine sponge *Chondrilla australiensis* (Figure 86a) which was collected from Mu Kho Lan Beach, The Gulf of Thailand, Chonburi Province, in May 2010. The sponge was identified by Jamrearn Buaruang, Division of Environmental Science, Faculty of Science, Ramkhamhaeng University, Bangkok, Thailand. After rinsing with sterile sea water, the sponge was dried on sterile filter papers, cut into small pieces (5 x 5 mm) and placed on the plates containing MEA with 70% sea water and incubated at 28ºC for days. The fungus was identified by morphological features, including the characteristic of ascospores and colonies (Figure 86b-e). The identification

was supported by sequence analysis of the β-tubulin gene (Glass and Donaldson, 1995) and the pure cultures were deposited as KUFC 7897 at Kasetsart University Fungal Collection, Department of Plant Pathology, Faculty of Agriculture, Kasetsart University, Bangkok, Thailand, and as MMERU 02 at Microbes Marine Environment Research Unit, Division of Environmental Science, Faculty of Science, Ramkhamhaeng University, Bangkok, Thailand.

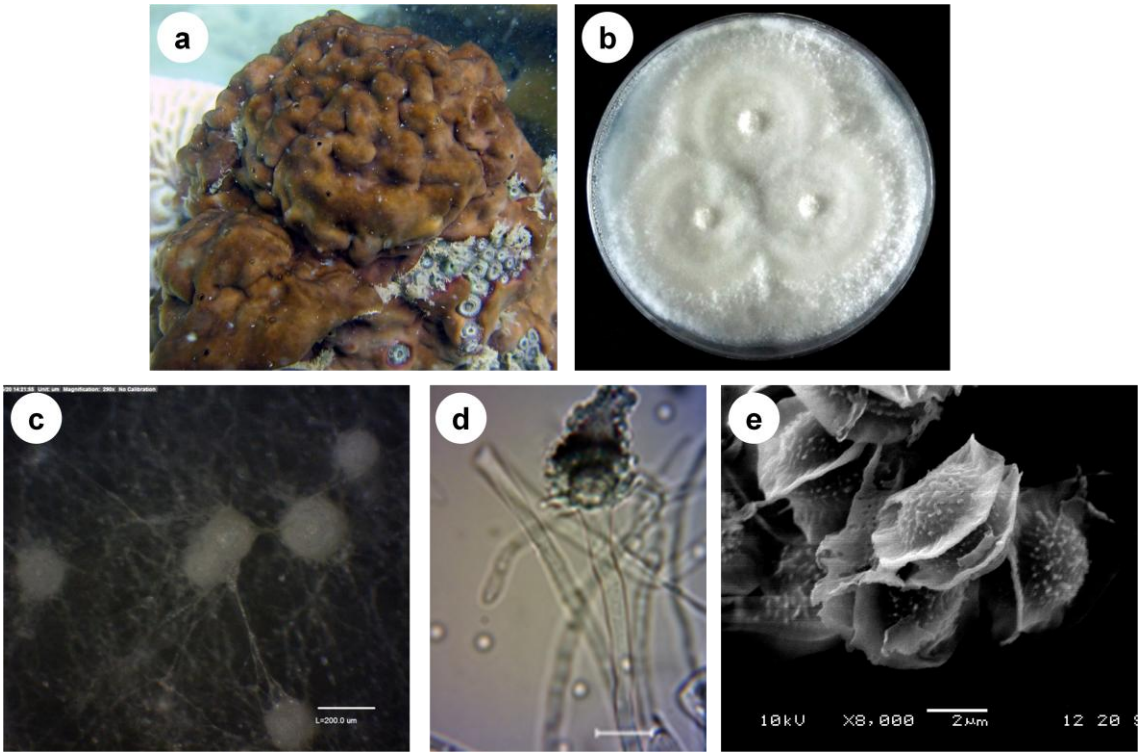

Figure 86. *Chondrilla australiensis* (**a**). *N. paulistensis* KUFC 7897. Colony on PDA with 70 % sea water after 14 days (**b**). Ascomata (**c**). Conidia (**d**). SEM image of ascospores (**d, e**).

4.3. Extraction and Isolation of Metabolites

4.3.1. *Emericella variecolor* KUFC 7356

The fungus was cultured for two weeks at 28ºC in 10 Petri dishes (i.d. 90 mm) containing 25 mL of MEA with 70% sea water per dish. Thirty five 1000 mL Erlenmeyer flasks, each containing 200 g of rice and 150 mL of water, were autoclaved, inoculated with five mycelial plugs of *E. variecolor* KUFC 7356 and incubated at 28ºC for 30 days, after which the mouldy rice was macerated in ethyl acetate (12 L total) for 7 days and then filtered. The two layers were separated using a separatory funnel, and the EtOAC solution was concentrated at a reduced pressure to yield 79.5 g of crude EtOAc extract which was washed with 5% of $NaHCO_3$ solution (2 x 500 mL) and H_2O (3 x 500 mL). The organic layer was dried with anhydrous Na_2SO_4, filtered and evaporated under reduced pressure to give 51 g of crude extract which was applied on a column chromatography over Si gel (0.2-0.5 mm Merck, 663 g) and eluted with mixtures of $CHCl_3$-petrol and $CHCl_3$-Me_2CO, wherein 250 mL fractions were collected as follows: fractions 1-60 ($CHCl_3$-petrol, 1:1), 61-122 ($CHCl_3$-petrol, 7:3), 123-167 ($CHCl_3$-petrol, 9:1), 168-196 ($CHCl_3$-Me_2CO, 9:1), 197-209 ($CHCl_3$-Me_2CO, 4:1), 210-272 ($CHCl_3$-Me_2CO, 7:3), 273-287 ($CHCl_3$-Me_2CO, 1:1).

Fractions 88-90 were combined (3.37 g) and recrystallized in a mixture of MeOH and $CHCl_3$ to give 47.7 mg of **EV1**.

Fractions 142-173 were combined (2.29 g) and applied on a column chromatography of LiChroPrep Si 60 (0.04–0.063 mm Merck, 45 g) and eluted with mixtures of $CHCl_3$-petrol and $CHCl_3$-Me_2CO, 100 mL sub-fractions were collected as follows: sub-fractions 1-46 ($CHCl_3$-petrol, 1:4), 47-138 ($CHCl_3$-petrol, 2:3), 139-174 ($CHCl_3$-petrol, 3:2), 175-205 ($CHCl_3$-petrol, 9:1), 206-246 ($CHCl_3$-Me_2CO, 9:1). Sub-fractions 58-98 were combined (218.4 mg) and recrystallized in MeOH to give 29 mg of **EV2**.

Fractions 175-182 were combined (1.76 g) and applied on a column chromatography of LiChroPrep Si 60 (0.04–0.063 mm Merck, 35 g) and eluted with mixtures of $CHCl_3$-petrol and $CHCl_3$-Me_2CO, 100 mL sub-fractions were collected as follows: sub-fractions 1-42 ($CHCl_3$-petrol, 3:2), 43-68 ($CHCl_3$-petrol,

4:1), 69-77 ($CHCl_3$), 78-89 ($CHCl_3$-Me_2CO, 9:1). Sub-fractions 17-34 were combined (159.6 mg) and purified by TLC (Si Gel, $CHCl_3$: petrol : EtOAc, HCO_2H, 7:1:2:0.1) to give 8 mg of **EV3**.

Fractions 203-217 were combined (1.35 g) and applied on a column chromatography of LiChroPrep Si 60 (0.04–0.063 mm Merck, 44 g) and eluted with mixtures of $CHCl_3$-petrol and $CHCl_3$-Me_2CO, 100 mL sub-fractions were collected as follows: sub-fractions 1-33 ($CHCl_3$-petrol, 1:1), 34-156 ($CHCl_3$-petrol, 7:3), 157-188 ($CHCl_3$-petrol, 9:1), 189-264 ($CHCl_3$), 265-287 ($CHCl_3$-Me_2CO, 9:1). Sub-fractions 81-110 were combined (81.9 mg) and recrystallized in MeOH to give 5 mg of **EV4**.

Fractions 238-247 were combined (338.1 mg) and recrystallized in a mixture of petrol and $CHCl_3$ to give 24.1 mg of **EV5**.

Acetylation of EV1: EV1 (27.2 mg) was dissolved in Ac_2O (1 mL) / Py (3 drops) and left to stand overnight in the dark. Elimination of acetic anhydride and pyridine yielded 11.8 mg of white solid of **EV1Ac**.

4.3.2. *Eurotium cristatum* KUFC 7356

E. cristatum KUFC 7356 was cultured for two weeks at 28ºC in 10 Petri dishes (i.d. 90 mm) containing 25 mL of MEA + 70% sea water per dish. Twenty five 1000 mL Erlenmeyer flasks, each containing rice (200 g), water (30 mL), and sea water (70 mL), were autoclaved, inoculated with five mycelia plugs of *E. cristatum* KUFC 7356, and incubated at 28ºC for 60 days, after which the mouldy rice was macerated in EtOAc (11 L total) for 10 days and filtered. The two layers were separated using separatory funnel and the EtOAc solution was concentrated at reduced pressure to give 25.3 g of crude EtOAc extract which was subject to column chromatography over a 0.2-0.5 mm Merck Si gel column (145 g) and eluted with mixtures of $CHCl_3$-petrol, $CHCl_3$-Me_2CO, $CHCl_3$-MeOH, 250 mL fractions being collected as follows: fractions 1-119 ($CHCl_3$-petrol, 1:4), 120-130 ($CHCl_3$-petrol, 3:7), 131-163 ($CHCl_3$-petrol, 2:3), 164-195 ($CHCl_3$-petrol, 1:1), 196-234 ($CHCl_3$-petrol, 3:2), 235-260 ($CHCl_3$-petrol, 7:3), 261-273 ($CHCl_3$-petrol, 4:1), 274-291 ($CHCl_3$-petrol, 9:1), 292-300 ($CHCl_3$), 301-348 ($CHCl_3$-Me_2CO, 9:1), 349-

376 ($CHCl_3$-Me_2CO, 4:1), 377-394 ($CHCl_3$-Me_2CO, 1:1), 395-402 ($CHCl_3$-MeOH, 1:1).

Fractions 13-20 were combined (154 mg) and recrystallized in a mixture of $CHCl_3$ and MeOH to give 14 mg of **EC1**. Fractions 21-29 were combined (259 mg) and recrystallized in a mixture of $CHCl_3$ and MeOH to give 6 mg of **EC2**. Fractions 91-119 were combined (493 mg) and purified by TLC (Si Gel, CH_2Cl_2 : Me_2CO : HCO_2H, 98:2:1) to give 5 mg of **EC3** and 5 mg of **EC4**. Fractions 178-201 were combined (162 mg) and purified by TLC (Si Gel, $CHCl_3$: Me_2CO : HCO_2H) to yield 9 mg of **EC5**. Fractions 202-208 were combined (306 mg) and recrystallized in Me_2CO to yield 53 mg of **EC6** and the mother liquor (247 mg) was combined with fractions 191-201 (201 mg) to give 5 mg of **EC7**. Fractions 209-216 were combined (216 mg) and recrystallized in Me_2CO to give 51 mg of **EC6** and the mother liquor (159 mg) was purified by TLC (Si Gel, $CHCl_3$: Me_2CO, HCO_2H, 95:5:1) to yield 13 mg of **EC8**. Fractions 217-234 were combined (228 mg) and recrystallized in Me_2CO to give 79 mg of **EC6**. Fractions 235-247 were combined (302 mg) and recrystallized in Me_2CO to give 26 mg of **EC6** and the mother liquor **(**272 mg**)** was recrystallized in a mixture of CH_2Cl_2 and petrol to give 17 mg of **EC9**. Fractions 303-321 were combined (338 mg) and recrystallized in MeOH to give 22 mg of **EC10**. The mother liquor of fractions 303-321 was then combined with fractions 277–301 (1.18 g), and applied on a column chromatography of LiChroPrep Si 60 (0.04–0.063 mm Merck, 45 g) and eluted with mixtures of $CHCl_3$-petrol, $CHCl_3$-Me_2CO, $CHCl_3$–MeOH, 100 mL sub-fractions were collected as follows: sub-fractions. 1-20 ($CHCl_3$-petrol, 1:4), 21-96 ($CHCl_3$-petrol, 3:7), 97-118 ($CHCl_3$-petrol, 2:3), 119-157 ($CHCl_3$-petrol, 1:1), 158-179 ($CHCl_3$-petrol, 3:2), 180-290 ($CHCl_3$-petrol, 7:3), 291-325 ($CHCl_3$-petrol, 4:1), 326-349 ($CHCl_3$-petrol, 9:1), 350-368 ($CHCl_3$), 369-379 ($CHCl_3$-Me_2CO, 9:1), 380-403 ($CHCl_3$-Me_2CO, 7:3), 404-413 ($CHCl_3$-Me_2CO, 1:1), 414-416 ($CHCl_3$–MeOH, 1:1). Sub-fractions 230-326 were combined (263 mg) and recrystallized in $CHCl_3$ to give additional 11 mg of **EC10**.

4.3.3. *Neosartorya laciniosa* KUFC 7896

N. laciniosa KUFC 7896 was cultured for one week in five 90 mm Petri dishes containing 25 ml of malt extract agar (MEA) with 70% sea water per dish. Thirty 1000 ml Erlenmeyer flasks, each containing 200 g rice and 200 ml water, were autoclaved, inoculated with ten mycelia plugs of the fungus and incubated at 28 ºC for 30 days. The moldy rice was macerated in EtOAc (12 L total) for five days and then filtered. The two layers were separated using a separatory funnel, and the EtOAc solution was concentrated at a reduced pressure to yield 72 g of crude EtOAc extract, which was applied on a column chromatography of Silica gel (800 g), and eluted with mixtures of $CHCl_3$-petrol and $CHCl_3$-Me_2CO, 250 ml fractions were collected as follows: fractions 1-19 ($CHCl_3$-petrol, 3:7), 20-114 ($CHCl_3$-petrol, 1:1), 115-188 ($CHCl_3$-petrol, 7:3), 189-340 ($CHCl_3$-petrol, 9:1), 341-484 ($CHCl_3$-Me_2CO, 9:1), 485-547 ($CHCl_3$-Me_2CO, 7:3), 548-603 ($CHCl_3$-Me_2CO, 1:1).

Fractions 348-364 were combined (7.73 g) and chromatographed over a column of LiChroPrep Si 60 (0.04–0.063 mm Merck, 114.01 g) and eluted with mixtures of $CHCl_3$-petrol and $CHCl_3$-Me_2CO, wherein 100 mL sub-fractions were collected as follows: sub-fractions 1-95 ($CHCl_3$-petrol, 7:3), 96-129 ($CHCl_3$-petrol, 9:1), 130-143 ($CHCl_3$-Me_2CO, 9:1), 144-165 ($CHCl_3$-Me_2CO, 4:1). Sub-fractions 39-51 were combined (825.3 mg) and chromatographed over a column of LiChroPrep Si 60 (0.04–0.063 mm Merck, 22.6 g) and eluted with mixtures of $CHCl_3$-petrol and $CHCl_3$-Me_2CO, wherein 100 mL sub-sub-fractions were collected as follows: sub-sub-fractions 1-52 ($CHCl_3$-petrol, 3:2), 53-66 ($CHCl_3$-petrol, 4:1), 67-80 ($CHCl_3$), 81-105 ($CHCl_3$-Me_2CO, 4:1). Sub-sub-fractions 15-49 were combined (271.1 mg) and purified by TLC (Si Gel, $CHCl_3$: Me_2CO : HCO_2H, 97:3:1) to give 37.9 mg of **NL1**.

Fractions 365-396 were combined (3.35 g) and recrystallized in Me_2CO to give 24.1 mg of **NL2**. The mother liquor of fractions 365-396 (3.32 g) and fractions 397-408 (465.7 mg) were combined and chromatographed over a column of LiChroPrep Si 60 (0.04–0.063 mm Merck, 43.4 g), and eluted with mixtures of $CHCl_3$-petrol and $CHCl_3$-Me_2CO, wherein 100 mL sub-fractions were collected as follows: sub-fractions 1-43 ($CHCl_3$-petrol, 7:3), 44-56 ($CHCl_3$-petrol, 9:1), 57-81

($CHCl_3$-Me_2CO, 9:1), 82-108 ($CHCl_3$-Me_2CO, 4:1). Sub-fractions 18-22 were combined (706.2 mg) and recrystallized in Me_2CO to give an additional 51.1 mg of **NL2**. Fractions 435-437 were combined (625.2 mg) and recrystallized in Me_2CO to give 12.8 mg of **NL3**. The mother liquor of fractions 435-437, fractions 409-434 and fractions 438-448 were combined (2.45 g) and chromatographed over a column of LiChroPrep Si 60 (0.04–0.063 mm Merck, 32.5 g) and eluted with mixtures of $CHCl_3$-petrol and $CHCl_3$-Me_2CO, wherein 100 ml sub-fractions were collected as follows: sub-fractions 1-45 ($CHCl_3$-petrol, 7:3), 46-62 ($CHCl_3$-petrol, 9:1). Sub-fractions 30-32 were combined (209.1 mg) and recrystallized in Me_2CO to give an additional 8.3 mg of **NL3**.

Fractions 449-465 were combined (826.0 mg) and recrystallized in Me_2CO to give 24.4 mg of **NL4**. Fractions 508-546 were combined (1.57 g) and recrystallized in Me_2CO to give 26.6 mg of **NL5**. The mother liquor of fractions 508-546 (1.57 g) was combined with fractions 498-507 (793 mg) and chromatographed over a LiChroPrep Si 60 column (0.04–0.063 mm Merck, 36 g) and eluted with mixtures of $CHCl_3$-petrol and $CHCl_3$-Me_2CO wherein 100 ml sub-fractions were collected as follows: sub-fractions 1-84 ($CHCl_3$-petrol, 9:1), 85-137 ($CHCl_3$-Me_2CO, 9:1), 138-162 ($CHCl_3$-Me_2CO, 4:1). Sub-fractions 43-50 were combined (214 mg) and recrystallized in Me_2CO to give 13 mg of **NL6**.

4.3.4. *Neosartorya paulistensis* KUFC 7897

The fungus was cultured for two weeks at 28ºC in 10 Petri dishes (i.d. 90 mm) containing 25 mL of MEA with 70% sea water per dish. Fifty 1000 mL Erlenmeyer flasks, each containing rice (200 g), water (30 mL), and sea water (70 mL), were autoclaved, inoculated with five mycelia plugs of *N. paulistensis* KUFC 7897 and incubated at 28ºC for 30 days, after which the mouldy rice was macerated in ethyl acetate (15 L total) for 10 days and then filtered. The two layers were separated using a separatory funnel and the ethyl acetate solution was concentrated at a reduced pressure to yield crude ethyl acetate extract, which was washed with 5% of $NaHCO_3$ solution (2 x 500 mL) and H_2O (3 x 500 mL). The organic layer was dried with anhydrous Na_2SO_4, filtered and evaporated under reduced pressure to give 51 g of crude extract which was applied on a column

chromatography over Si gel (0.2-0.5 mm Merck, 610 g) and eluted with mixtures of $CHCl_3$-petrol and $CHCl_3$-Me_2CO, wherein 250 mL fractions were collected as follows: fractions 1-25 ($CHCl_3$-petrol, 1:4), 26-149 ($CHCl_3$-petrol, 3:7), 150-177 ($CHCl_3$-petrol, 2:3), 178-278 ($CHCl_3$-petrol, 1:1), 279-399 ($CHCl_3$-petrol, 3:2), 400-534 ($CHCl_3$-petrol, 4:1), 535-549 ($CHCl_3$-petrol, 9:1), 550-592 ($CHCl_3$), 593- 837 ($CHCl_3$-Me_2CO, 9:1), 838-976 ($CHCl_3$-Me_2CO, 4:1), 977-1047 ($CHCl_3$-Me_2CO, 7:3), 1048-1090 ($CHCl_3$-Me_2CO, 1:1) and 1091-1112 ($CHCl_3$-Me_2CO, 1:4).

Fractions 299-307 (526 mg) were combined and recrystallized in petrol to give 12 mg of **NP1**. Fractions 627- 696 were combined (1.50 g) and crystallized in a mixture of $CHCl_3$ and Me_2CO to give 70 mg of **NP2**. Fractions 739-774 were combined (400 mg) and crystalized in Me_2CO to give 95 mg of **NP3**.

The mother liquor of fractions 739-774 and fractions 697-738 were combined (850 mg), applied on a column chromatography of LiChroPrep Si 60 (0.04–0.063 mm Merck, 46 g) and eluted with mixtures of $CHCl_3$-petrol and $CHCl_3$-Me_2CO, wherein 100 mL sub-fractions were collected as follows: sub-fractions 1-24 ($CHCl_3$-petrol, 4:1), 25-49 ($CHCl_3$-petrol, 9:1), 50-63 ($CHCl_3$), 64-142 ($CHCl_3$-Me_2CO, 9:1) and 143-163 ($CHCl_3$-Me_2CO, 4:1). Sub-fractions 82-86 were combined (31 mg) and purified by TLC (Si gel, $CHCl_3$: Me_2CO : EtOAc : HCO_2H, 7:2:1:0.1) to give 8.3 mg of **NP2** and 9.6 mg of **NP4**. Sub-fractions 87-102 were combined (250 mg) and purified by TLC (Si gel, $CHCl_3$: Me_2CO : EtOAc : HCO_2H, 7:2:1:0.1) to give additional 38 mg of **NP2** and 18 mg of **NP3**. Sub-fractions 103-130 were combined (157 mg) and crystallized in Me_2CO to give additional 27 mg of **NP3**.

Fractions 775 -832 were combined (690 mg) and crystalized in Me_2CO to give 95 mg of **NP5**, and the mother liquor was combined with fractions 833-860 were combined (902 mg), applied over a LiChroprep Si 60 column (0.04–0.063 mm Merck, 41 g) and eluted with mixtures of $CHCl_3$-petrol and $CHCl_3$-Me_2CO wherein 100 ml sub-fractions were collected as follows: sub-fractions 1-26 ($CHCl_3$-petrol, 4:1), 27-41 ($CHCl_3$), 42-108 ($CHCl_3$-Me_2CO, 9:1). Sub-fractions 61-68 were combined and purified by TLC (Si gel, $CHCl_3$: Me_2CO : EtOAc : HCO_2H, 7:2:1:0.1) to give 4.2 mg of **NP2** and 18 mg of **NP3**. Sub-fractions 69-86 were combined (176 mg) and recrystallized in Me_2CO to give 15 mg of **NP5**. Fractions 905-947 were combined (670 mg) and crystalized in Me_2CO to give 16.4 mg of **NP6**.

4.4. Physical Characteristics and Spectroscopic Data

Ergosterol (EV1): White amorphous solid (mp 157-159 ºC); ^{1}H and ^{13}C NMR (See Table 2).

Ergostel peroxide (EV2): Colorless needles; ^{1}H and ^{13}C NMR (See Table 3).

Orcinol (EV3): Colorless mass; ^{1}H and ^{13}C NMR (See Table 4).

1*H*-Indole-3-carboxylic acid (EV4): White amorphous solid; ^{1}H and ^{13}C NMR (See Table 5).

Cyclo-(L-Tryptophyl-L-phenylalanyl) (EV5): White solid; ^{1}H and ^{13}C NMR (See Table 11).

Erythroglaucin (EC1): Red needles (mp 204-206 ºC); ^{1}H and ^{13}C NMR (See Table 6).

Physcion (EC2): Orange needles (mp 202-203 ºC); ^{1}H and ^{13}C NMR (See Table 7).

Catenarin (EC3): Dark orange amorphous solid; ^{1}H and ^{13}C NMR (See Table 8).

Emodin (EC4): Light orange/yellow amorphous solid; ^{1}H and ^{13}C NMR (See Table 9).

Questin (EC5): Orange/yellow amorphous solid (mp 290-291 ºC); ^{1}H and ^{13}C NMR (See Table 10).

Echinulin (EC6): White amorphous solid; ^{1}H and ^{13}C NMR (See Table 16).

Neoechinulin (EC7): Purple solid; ^{1}H and ^{13}C NMR (See Table 14).

Neoechinulin A (EC8): Dark red amorphous solid (mp 262-264 ºC); ^{1}H and ^{13}C NMR (See Table 12).

Neoechinulin E (EC9): Orange-red amorphous solid; ^{1}H and ^{13}C NMR (See Table 13).

Eurocristatine (EC10): White crystals (mp 244-245 ºC); $[\alpha]^{20}_{D}$ = +300 (*c* 0.02, MeOH); UV (MeOH) λ_{max} (log *ε*) 212 (4.5), 241 (4.2), 302 (3.9) nm; IR (KBr) υ_{max} 3450, 3190, 2961, 1662, 1453, 1326 cm^{-1}; ^{1}H and ^{13}C NMR (See Table 17); (+)-HR-ESIMS *m/z* 569.2905 $[M+H]^{+}$ (calculated for $C_{32}H_{37}N_6O_4$, 569.2876).

Chevalone B (NL1): Colorless crystals (mp 161-163 ºC); $[\alpha]^{20}_{D}$ = +11 (*c* 0.12, $CHCl_3$); IR (KBr) υ_{max} 2937, 1702, 1585, 1378, 1240 cm^{-1}; ^{1}H and ^{13}C NMR (See Table 18); (+)-HR-ESIMS m/z 457.2949 [M+H]+ (calculated for $C_{28}H_{41}O_5$, 457.2954).

Aszonapyrone A (NL2): Colorless crystal (mp 242-244 ºC); $[\alpha]^{25}_{D}$ = -100 (*c* 0.02, $CHCl_3$); ^{1}H and ^{13}C NMR (See Table 19); (+)-HR-ESIMS *m/z* 457.2954 $[M+H]^{+}$ (calculated for $C_{28}H_{41}O_5$, 457.2954).

Aszonapyrone B (NL3): Colorless crystals (mp 171-173 ºC); ^{1}H and ^{13}C NMR (See Table 20).

Tryptoquivaline T (NL6): White solid (mp 258-260 ºC); $[\alpha]^{25}_{D}$ = -83.3 (*c* 0.04, MeOH); IR (KBr) υ_{max} 3010, 2930, 2852, 1701, 1582, 1450, 1402, 1269 cm^{-1}; ^{1}H and ^{13}C NMR (See Table 28); (+)-HR-ESIMS m/z 445.1512 $[M+H]^{+}$ (calculated for $C_{28}H_{41}O_5$, 445.1512).

Sartorypyrone C (NP1): White solid (mp 200-202 ºC); $[\alpha]^{25}_{D}$ = -73.5 (*c* 0.07, $CHCl_3$); IR (KBr) υ_{max} 3445, 2923, 2942, 2853, 1699, 1668, 1649, 1636, 1507, 1124 cm^{-1}; ^{1}H and ^{13}C NMR (See Table 22); (+)-HR-ESIMS *m/z* 415.2836 $[M+H]^{+}$ (calculated for $C_{26}H_{38}O_4$, 415.2848).

Tryptoquivaline L (NP2/NL4): Colorless crystal (mp 262-265 ºC); $[\alpha]^{20}_{D}$ = -30.5 (*c* 0.02, MeOH); UV ($CHCl_3$) λ_{max} (log ***ε***) 212 (4.69), 226 (4.53), 253 (sh 4.27), 275 (sh 3.72), 312 (3.17), 301 (3.26) nm; ^{1}H and ^{13}C NMR (See Table 25); (+)-HR-ESIMS *m/z* 433.1509 $[M+H]^+$ (calculated for $C_{23}H_{21}N_4O_5$, 433.1512).

Tryptoquivaline H (NP3): White solid (mp 246-248 ºC); $[\alpha]^{20}_{D}$ = -20.1 (*c* 0.03, MeOH); UV ($CHCl_3$) λ_{max} (log ***ε***) 210 (4.23), 226 (4.18), 253 (sh), 275 (sh), 312 (3.30), 301 (3.32) nm; ^{1}H and ^{13}C NMR (See Table 26); (+)-HR-ESIMS *m/z* 419.13496 $[M+H]^+$ (calculated for $C_{22}H_{19}N_4O_5$, 419.13500).

4(3*H*)-Quinazolinone (NP4): Colorless crystals (mp 216-218 ºC); ^{1}H and ^{13}C NMR (See Table 23).

3'- (4-Oxoquinazolin-3-yl) spiro [*1H*-indole-3,5'-oxolane] - 2,2' - dione (NP5/NL5): White solid (mp 267-269 ºC); $[\alpha]^{20}_{D}$ = +19.7 (*c* 0.02, MeOH); UV ($CHCl_3$) λ_{max} (log ***ε***) 212 (4.56), 263 (3.72), 301 (3.26), 312 (3.18) nm; ^{1}H and ^{13}C NMR (See Table 24); (+)-HR-ESIMS *m/z* 348.0968 $[M+H]^+$ (calculated for $C_{19}H_{14}N_3O_4$, 348.0984).

Tryptoquivaline F (NP6): White solid; $[\alpha]^{20}_{D}$ = -120.0 (*c* 0.05, MeOH); ^{1}H and ^{13}C NMR (See Table 27); (+)-HR-ESIMS m/z 403.1399 $[M+H]^+$ (calculated for $C_{22}H_{19}N_4O_4$, 403.1406).

4.5. X-Ray Crystallographic Analysis of EC10 and NL3

Crystals suitable for X-ray diffraction were obtained by slow evaporation of a solution in methanol (for **EC10**) and acetone (for **NL3**). Diffraction data were collected at 293 K with a Gemini PX Ultra equipped with CuKa radiation (λ = 1.54184 Å). The structures were solved by direct methods using SHELXS-97 (Sheldrick, 1997a) and refined with SHELXL-97 (Sheldrick, 1997b). Carbon, oxygen, and nitrogen atoms were refined anisotropically. Hydrogen atoms were

either refined freely with isotropic displacement parameters or were positioned with an idealized geometry and refined riding on their parent C atoms. For **EC10**, tables containing the final fractional coordinates, temperature parameters, bond distances, and bond angles were deposited with the Cambridge Crystallographic Data Centre: CCDC reference number 879091.

4.6. Biological Activity Assays

4.6.1. Cytotoxic Activity Bioassays

4.6.1.1. Samples: Stock solutions of the compounds were prepared in DMSO and kept at -20ºC. Appropriate dilutions of the compounds were freshly prepared just before the assays.

4.6.1.2. Cell cultures: Three human tumour cell lines were used in this study: MCF-7 (breast adenocarcinoma, a kind gift from NCI, Bethesda, USA), NCI-H460 (non-small cell lung cancer, NSCLC, a kind gift from NCI, Bethesda, USA) and A375-C5 (melanoma, ECACC, UK). Cells were routinely cultured in RPMI-1640 with Ultraglutamine (Lonza) supplemented with 10% FBS (PAA) and maintained in a humidified incubator at 37 ºC with 5% CO_2. Cell number and viability were determined with Trypan Blue exclusion assay. All experiments were performed with cells in exponential growth with viabilities over 90% and repeated at least three times.

4.6.1.3. Cell growth inhibitory assay: The screening of fungal metabolites was performed with the Sulforhodamine B (SRB) assay adopted from the National Cancer Institute, USA (Vichai and Kirtikara, 2006). Briefly, cells were plated in 96 well plates ($5x10^3$ cells/well for MCF-7 and NCI-H460 cells, and $7.5x10^3$ cells/well for the A375-C5 cell line) and incubated at 37 ºC for 24 h. Exponentially growing cells were then treated with five dilutions of each compound. After 48 h of treatment, cells were fixed with 10% ice-cold trichloroacetic acid, washed and stained with SRB. After washing with 1% acetic acid, the bound SRB was solubilized with 10 mM Tris Base, and the absorbance was measured at 515 nm in

a microplate reader (Biotek Instruments). Then, a dose-response curve was obtained for each compound and the corresponding GI_{50} (the concentration of compound that inhibited 50% of net cell growth) was determined. The effect of the vehicle solvent (DMSO) on the growth of these cell lines was evaluated by treating cells with the maximum concentration of DMSO used in each assay (0.25%).

4.6.2. Antifungal Activity Bioassays

Antifungal activity of fungal metabolites was evaluated against yeast (*Candida albicans*), filamentous fungus (*Aspergillus fumigatus*) and dermatophyte (*Trichophyton rubrum*) strains: one American Type Culture Collection (ATCC) type strain (*C. albicans* ATTC 10231), one *Aspergillus* ATCC type strain (*A. fumigatus* ATCC 46645), and one dermatophyte clinical strain (*T. rubrum* FF5).

The fungal isolates were identified by standard microbiology methods and stored on Sabouraud Dextrose broth with glycerol at -70ºC and subcultured in Sabouraud-Chloramphenicol agar. Minimal Inhibitory Concentration (MIC) was determined by a microdilution method according to the CLSI reference method M27-A2 for yeast (Wayne, 2002a), and M38-A for filamentous fungus (Wayne, 2002b). The test was performed in sterile 96 flat-bottom well microtitration plates and the medium used was MOPS buffered RPMI 1640. Briefly, MICs were determined for yeast strain with the adjusted final inoculum of $1\text{-}4x10^4$ CFU/mL, prepared from a 24-48 hours culture. With *A. fumigatus* ATCC 46645 the final inoculum used was $4\text{-}8x10^4$ CFU/mL, prepared from a sporulated culture. Two fold serial dilutions of compounds in DMSO, ranging from 250 to 0.25 µg/mL, were tested. Fungal growth controls, with and without DMSO, were included. The final DMSO concentration was 2%, and did not affect the fungal growth. In addition, reference antifungal compounds, fluconazole (Pfizer, United Kingdom) for *C. albicans* ATTC 10231 and *T. rubrum* FF5 or amphotericin B (Sigma) for *A. fumigatus* ATCC 46645, were used as the standard antifungal drugs. Two fold serial dilutions ranging from 128 to 0.25 µg/mL for fluconazole and 16 to 0.063 µg/mL for amphotericin B were used. Plates were incubated at 30ºC for 4-5 days for *A. fumigatus* ATCC 46645 and 8 days for *T. rubrum* FF5. All determinations

were performed in duplicate and three independent experiments lead to concordant results.

4.6.3. Antibacterial Activity Bioassays

4.6.3.1. Bacterial Strains: For the antibacterial bioassays, fungal metabolites were tested against reference strains, two Gram-positive (*Staphylococcus aureus* ATCC 25923 and *Bacillus subtilis* ATCC 6633) and two Gram-negative (*Escherichia coli* ATCC 25922 and *Pseudomonas aeruginosa* ATCC 27853) bacteria, and against multidrug-resistant isolates from the environment, *S. aureus* B1 and *S. aureus* B2 (isolated from public buses), *Enterococcus faecalis* W1 and *E. faecium* W5 (isolated from river water) and *E. coli* G1 (isolated from seagull feces). These bacteria were grown in Mueller-Hinton agar (MH – BioKar diagnostics, France) from stock cultures. MH plates were incubated at 37°C prior to obtain fresh cultures for each in vitro bioassay.

4.6.3.2. Determination of Minimum Inhibitory and Bactericidal Concentrations: The minimum inhibitory concentration (MIC) values of the compounds were determined by a broth microdilution technique, following the recommendations of the Clinical and Laboratory Standards Institute (Wayne, 2011). Stock solutions of 10 mg/mL (prepared by dissolving each metabolite in DMSO (Applichem GmbH, Germany) were serial diluted in Mueller-Hinton broth (MHB - BioKar diagnostics, France) to achieve in-test concentrations ranging from 2 to 256 µg/mL. Ciprofloxacin in the concentration range from 0.03125 to 16 µg/mL was used as control drug in the experiment. A bacterial inoculum was prepared in MHB and standardized in order obtain a concentration of 5×10^5 CFU/mL in each inoculated well of the microtiter plate. The concentration of DMSO in the highest in-test concentration did not affect the microbial growth. The MIC was defined as the lowest concentration of the compound that inhibited the visible growth. The minimum bactericidal concentration (MBC) was determined by spreading 10 µL on MH plates from the sample showing no visible growth and it was further incubated for 24 h at 37ºC; the lowest concentration at which no bacterial growth occurred on MB plates was defined as the MBC.

4.6.3.3. Synergistic Studies: A screening susceptibility test to assess combined effect between the compounds and antibiotics was conducted using the disc diffusion method on MH. Multidrug-resistant isolates were picked from overnight cultures in MH, and suspensions were prepared in buffered peptone water (Oxoid, England) by adjusting the turbidity to equal a 0.5 McFarland standard. A set of antibiotic discs (Oxoid, England) was selected based on the resistance of the isolates towards those antibiotics. Antibiotic discs alone (controls) and impregnated with 15 µL of a 1 mg/mL solution (in DMSO) of each metabolite were placed on the agar plate seeded with the respective bacteria. 15 µL of DMSO impregnated in a sterile filter paper disc (6 mm in diameter) (Oxoid, England) was used as the negative control. Inoculated MH plates were incubated overnight at 37°C. Each compound was tested in duplicate. Potential synergism was recorded when the halo of antibiotic discs impregnated with metabolites was greater than the halo of antibiotic discs or compound-impregnated blank discs alone.

Based on the results of the previous assay, potential synergism between the most promising compound **NL2** and antibiotics (oxacillin, vancomycin and ampicillin - Sigma-Aldrich, USA) was checked using a broth microdilution checkerboard method and tested against *S. aureus* MRSA and *Enterococcus* spp. VRE isolates. Briefly, the stock solutions and serial twofold dilutions of the compound and antibiotic to at least double the MIC were prepared according to the recommendations of CLSI (Wayne, 2011). The metabolite to be tested was serially diluted along the ordinate, while the antibiotic was diluted along the abscissa. A bacterial inoculum equal to a 0.5 McFarland turbidity standard was prepared in MHB. Each microtiter plate well was inoculated with 100 µL of a bacterial inoculum of 5×10^5 CFU/mL, and the plates were incubated overnight at 37ºC. The fractional inhibitory concentration (FIC) was calculated as follows: FIC of drug A (FIC A) = MIC of drug A in combination/MIC of drug A alone, and FIC of drug B (FIC B) = MIC of drug B in combination/MIC of drug B alone. The FIC index (ΣFIC), calculated as the sum of each FIC, was interpreted as follows: $\Sigma FIC \leq 0.5$, synergy; $0.5 < \Sigma FIC \leq 4$, no interaction; $4 < \Sigma FIC$, antagonism (Odds, 2003).

4.6.3.4. Antibiofilm Activity Assay: Giving the promising antibacterial activity of **NL2** against Gram-positive bacteria, the efficacy of the compound in interrupting the biofilm formation was assessed. The metabolite at concentrations of 2x MIC, MIC, 1/2x MIC and 1/4x MIC was added to bacterial suspensions of 1 x 10^6 CFU/ml in Tryptic Soy broth (TSB - BioKar diagnostics, France). Bacterial suspension without metabolite was used as the control. Each broth culture obtained was dispensed into a 96-well microtiter plate (200 µL/well) and incubated at 37ºC for 24 h. After that time, biofilm was stained with 0.5% crystal violet for 5 min, rinsed with water, air dried and eluted with acetic acid 33% (v/v). The optical density was measured at 595 nm (OD_{595}) using a microplate reader (iMark™ microplate absorbance reader**,** Bio-Rad Laboratories, USA). Two independent experiments were performed in triplicate for each experimental condition. The statistical significance of difference between biofilms of controls and biofilms in the presence of different concentrations of compound was evaluated using Student's t test. In both cases, probability levels < 0.05 were considered statistically significant. The efficacy of **NL2** on established biofilm of *S. aureus* B1 and *E. faecalis* W1 was also evaluated by determining the biofilm inhibitory concentration (BIC) according to the method described by Johnson et al., (2002). Briefly, bacterial suspensions in TSB at 1 x 10^6 CFU/mL, were used to grow the biofilms in 96-well microtiter plate. After 24 h of incubation at 37ºC, the planktonic cells were gently removed and the wells were rinsed once and filled with different dilutions ranging from the MIC values to 12 x MIC. The OD_{595} was measured at time 0 and after incubation for 24 h at 37ºC. The BIC was determined as the lowest concentration of the compound inhibiting growth in the supernatant fluid, confirmed by no increase in optical density compared with the initial reading.

Additionally, microscopic visualization of biofilms of *S. aureus* ATCC 25923 was performed using the Live/Dead BacLight viability kit (Molecular Probes, USA). Biofilms were formed in 35-mm diameter polystyrene plates using TSB (control) and TSB supplemented with MIC and 1/2 x MIC of **NL2**. After 24 h at 37ºC, the planktonic phase was removed from each plate, washed with PBS, stained with the appropriate mixture of SYTO 9 and propidium iodide stains and incubated for 20 minutes at room temperature in the dark; then, were rinsed and examined under a fluorescence microscope (BX41 Microscope, Olympus America Inc.,

USA). Images were recorded at an emission wavelength of 500 nm for SYTO 9 (green fluorescence) and of 635 nm for propidium iodide (red fluorescence).

CHAPTER V
CONCLUSIONS

This study aimed, mainly, to investigate the secondary metabolites produced by selected marine-derived fungi (*Emericella variecolor* KUFC 7092, *Eurotium cristatum* KUFC 7356, *Neosartorya laciniosa* KUFC 7896 and *Neosartorya paulistensis* KUFC 7897), collected from the Gulf of Thailand, as well as to evaluate their relevant biological activity.

A total of twenty-five compounds, including three new derivatives, were isolated comprising diverse structural groups of compounds including terpenes, alkaloids and polyketides. This chemical diversity clearly highlighted marine-derived fungi biosynthetic capabilities for the production of novel and diverse chemical structures.

However, despite the corresponding structural diversity, most of the isolated compounds have a terrestrial counterpart, or are structurally related to that of terrestrial fungi, which can be justified by two major reasons. In one hand, so far there is no evidence that marine fungi actively grow in the host macroorganims. Most reported species appear to be terrestrial species, washed into to the sea, or facultative marine fungi (Proksch *et al*., 2010). On the other hand, culture conditions mimicking the natural environment of this marine-derived fungal species is critical, not only to overcome the low culturability of some species, but also to activate the metabolic pathways that remain silent under standard culturing conditions (Kjer *et al*., 2010; Zengler *et al*., 2002).

This study, together with the latest research results from our research group, as well as literature reports dealing with the isolation of secondary metabolites from marine fungi, clearly support that the standard procedure of mere addition of sea water to the culture media is a limited approach for mimicking the marine natural environment, and subsequent production of metabolites with higher chemical diversity. To overcome this limitation, several studies point to different culturing approaches such as the OSMAC (One Strain, Many Compounds) concept (Bills *et al*., 2008; Bode *et al*., 2002) and co-culturing (Bertrand *et al*., 2013; Rateb *et al*., 2013; Røssland *et al*., 2006).

Despite the referred limitations, marine-derived fungal secondary metabolites already proved to be a promising source for the development of new therapeutic agents (Bugni and Ireland, 2004; Rateb and Ebel, 2011; Saleem *et al*., 2007). For the assessment of their biological properties, some of the isolated

compounds were screened for antibacterial, antibiofilm, antifungal and anticancer activities.

The burden of cancer is increasing largely being the leading cause of death in economically developed countries, and the second leading cause of death in developing countries (Jernal *et al*., 2011). The limited therapeutic arsenal of chemotherapeutic agents led to the urgency for more research in this area, with marine natural products playing a preponderant role as referred in Chapter I. Several compounds resulting from this study were tested against the three human cancer cell lines MCF-7 (breast adenocarcinoma), NCI-H460 (non-small cell lung cancer) and A375-C5 (melanoma). Among them, aszonapyrone A, the meroterpenoid isolated from the fungus *Neosartorya laciniosa* KUFC 7896, displayed strong *in vitro* growth inhibitory activity against the tested human cancer cell lines. Thus, aszonapyrone A represents a novel chemical scaffold with potential for the development of new anticancer derivatives.

Also infectious diseases are leading health problems with high morbidity and mortality in the developing countries. Since the mid-1970s, resistance to antimicrobial agents has become an escalating problem (Johnson *et al*., 2001). In the last thirty years, treatment of infections caused by Gram-positive bacteria has been more problematic than ever, with infections being caused by multidrug-resistant organisms, particularly methicillin-resistant staphylococci, penicillin- and erythromycin-resistant pneumococci, and vancomycin-resistant enterococci (Aksoy and Unal, 2008). Although there is a continuing effort in the pharmaceutical industry to develop new antimicrobial agents for the treatment of resistant infections, pursuing new antibiotic drugs is still a fair and necessary strategy to combat the multidrug-resistant bacteria that are spreading both in the community and clinical setting (Bassetti *et al*., 2013). Additionally, biofilm-related infections are extremely common nocosomial infectious (Donlan and Costerton, 2002) and account for significant morbidity and mortality. Biofilm formation at the surface of implants and prostheses are responsible for the failure of several antibiotics, with a limited number showing to be effective against biofilms (Gualtieri *et al*., 2006).

In light of the results presented in this study, we can conclude that the meroditerpene aszonapyrone A is a promising antibacterial agent, especially against Gram-positive bacteria, and its effect are comparable to those of standard antibiotics currently in use in therapeutics, with the advantage of being also active

against bacteria that already exhibit resistance towards these antibiotics. Additionally, aszonapyrone A was also found to inhibit the biofilm formation in both reference strains and multi-drug resistant isolates. To the best of our knowledge, none of the available antibiotics belongs to this class of compounds, which thereby may represent a novel and potential topic of investigation in the field of new antibacterial agents from the marine-derived fungi.

Despite the lack of activity of the new compounds, eurocristatine, sartorypyrone C and tryptoquivalines T, on the selected biological activity assays, they should be considered the starting point for other biological activity assays, against different diseases.

The isolation of twenty-one metabolites for the first time from the selected species contributed to a new insight, not only identifying new sources of fungal metabolites with relevant biological properties reported, but also due to their chemotaxonomic value. A single metabolite or metabolite pattern, frequently can point to a specific fungal taxon or series of taxa (Frisvad *et al*., 2008). Consequently, the isolation of some of the compounds during this study can be useful and classified as an additional tool for the purpose of taxonomic identification, in addition to the morphological and genomic classification.

The marine environment is a potential and tremendous source of biologically active metabolites, extremely valuable for the development of new drugs. This study confirms once more that marine-derived fungi are a prolific source for the discovery of new and interesting natural products, with potential for the development of new drugs, specifically antibiotic and anticancer agents.

Relevant cytotoxic and antibacterial properties of aszonapyrone A can be considered potential to provide a new alternative for the development of new anticancer and antibacterial agents in the future, and eurocristatine, sartorypyrone C and tryptoquivaline T chemical scaffolds can inspire the development of new derivatives that could be useful against other diseases.

REFERENCES

Absalon, M.J., Smith, F.O. **(2009)**. Treatment strategies for pediatric acute myeloid leukemia. *Expert Opinion in Pharmacotherapy* 10(1), 57-79.

Agarwal, S.K., Singh, S.S., Verma, S., Kumar, S. **(2000)**. Antifungal activity of anthraquinones derivatives from *Rheum emodi*. *Journal of Ethnopharmacology* 72, 43-46.

Akashi, S., Kimura, T., Takeuchi, T., Kuramochi, K., Kobayashi, S., Sugawara, F., Watanabe, N., Arai, T. **(2011)**. Neoechinulin A impedes the progression of rotenone-induced cytotoxicity in PC12 cells. *Biological & Pharmaceutical Bulletin* 34(2), 243-248.

Akashi, S., Shirai, K., Okada, T., Konishi, K., Takeuchi, T., Kuramochi, K., Takahashi, M., Nakagawa, T., Ogura, Y., Fujieda, S., Shibata, Y., Sugawara, F., Kobayashi, S., Watanabe, N., Arai, T. **(2012)**. Neoechinulin A imparts resistance to acute nitrosative stress in PC12 cells: A potential link of an elevated cellular reserve capacity for pyridine nucleotide redox turnover with cytoprotection. *Biological & Pharmaceutical Bulletin* 35(7), 1105-1117.

Aksoy, D.Y., Unal, S. **(2008)**. New antimicrobial agents for treatment of Gram-positive bacterial infections. *Clinical Microbiology and Infection* 14, 411-420.

Alcazar-Fuoli, L., Mellado, E., Garcia-Effron, G., Lopez, J.F., Grimalt, J.O., Cuenca-Estrella, J.M., Rodriguez-Tudela, J.L. **(2008)**. Ergosterol biosynthesis pathway in *Aspergillus fumigatus*. *Steroids* 73, 339-347.

Almeida, A.P., Dethoup, T., Singburaudom, N., Lima, R., Vasconcelos, M.H., Pinto, M., Kijjoa, A. **(2010)**. The *in vitro* anticancer activity of the crude extract of the sponge-associated fungus *Eurotium cristatum* and its secondary metabolites. *Journal of Natural Pharmaceuticals* 1(1), 25-29.

Aly, A.H., Debbab, A., Proksch, P. **(2011)**. Fifty years of drug discovery from fungi. *Fungal Diversity* 50, 3-19.

Amador, M.L., Jimeno, J., Paz-Ares, L., Cortes-Funes, H., Hidalgo, M. **(2003)**. Progress in the development and acquisition of anticancer agents from marine sources. *Annals of Oncology* 14, 1607-1615.

Amna, T., Puri, S.C., Verma, V., Sharma, J.P., Khajuria, R.K., Musarrat, J., Spiteller, M., Qazi, G.N. **(2006)**. Bioreactor studies on the endophytic fungus *Entrophospora infrequens* for the production of an anticancer alkaloid camptothecin. *Canadian Journal of Microbiology* 52, 189-196.

Andersen, B., Dongo, A., Pryor, B.M. **(2008)**. Secondary metabolite profiling of *Alternaria dauci*, *A. porri*, *A. solani*, and *A. tomatophila*. *Mycological Research* 112, 241-250.

Anke, H., Kolthoum, I., Zähner, H., Laatsch, H. **(1980)**. The Anthraquinones of the *Aspergillus glaucus* group. I. Occurrence, isolation, identification and antimicrobial activity. *Archives of Microbiology* 126, 223-230.

Aoki, T., Ohnishi, K., Kimoto, M., Fujieda, S., Kuramochi, K., Takeuchi, T., Nakazaki, A., Watanabe, N., Sugawara, F., Arai, T., Kobayashi, S. **(2010)**. Synthesis and neuroprotective action of optically pure neochinulin A and its analogs. *Pharmaceuticals* 3, 1063-1069.

Asami, Y., Kakeya, H., Komi, Y., Kojima, S., Nishikawa, K., Beebe, K., Neckers, L., Osada, H. **(2008)**. Azaspirene, a fungal product, inhibits angiogenesis by blocking Raf-1 activation. *Cancer Science* 99(9), 1853-1858.

Asami, Y., Kakeya, H., Onose, R., Chang, Y.-H., Toi, M., Osada, H. **(2004)**. RK-805, an endothelial-cell-growth inhibitor produced by *Neosartorya* sp., and a docking model with methionine aminopeptidase-2. *Tetrahedron* 60, 7085-7091.

Asami, Y., Kakeya, H., Onose, R., Yoshida, A., Matsuzaki, H., Osada, H. **(2002)**. Azaspirene: A novel angiogenesis inhibitor containing a 1-oxa-7-azaspiro[4.4]non-2-ene-4,6-dione skeleton produced by the fungus *Neosartorya* sp.. *Organic Letters* 4(17), 2845-2848.

Bačkorová, M., Jendželovský, R., Kello, M., Bačkor, M., Mikeš, J., Fedoročko, P. **(2012)**. Lichen secondary metabolites are responsible for induction of apoptosis in HT-29 and A2780 human cancer cell lines. *Toxicology in Vitro* 26, 462-468.

Bard, M., Lees, N.D., Turi, T., Craft, D., Cofrin, L., Barbuch, R., Koegel, C., Loper, J.C. **(1993)**. Sterol synthesis and viability of erf11 (cytochrome P450 lanosterol demethylase) mutations in *Saccharomyces cerevisiae* and *Candida albicans*. Lipids 28(11), 963-967.

Barrow, C.J., Cai, P., Snyder, J.K., Sedlock, D.M., Sung, H.H., Cooper, R. **(1993)**. WIN 64821 a new competitive antagonist to substance P, isolated from an *Aspergillus* species: structure determination and solution conformation. *The Journal of Organic Chemistry* 58, 6016-6021.

Barrow, C.J., Sedlock, D.M. **(1994)**. 1'-(2-Phenyl-ethylene)-ditryptophenaline, a new dimeric diketopiperazine from *Aspergillus flavus*. *Journal of Natural Products* 57, 1239-1244.

Bassetti, M., Merelli, M., Temperoni, C., Astilean, A. **(2013)**. New antibiotics for bad bugs: where are we? *Annals of Clinical Microbiology and Antimicrobials* 12, 22.

Bates, M.L., Reid, W.W., White, J.D. **(1976)**. Duality of pathways in the oxidation of ergosterol to its peroxide *in vivo*. *Journal of the Chemical Society, Chemical Communications* 44-45.

Beattie, K.D., Rouf, R., Gander, L., May, T.W., Ratkowsky, D., Donner, C.D., Gill, M., Grice, I.D., Tiralongo, E. **(2010)**. Antibacterial metabolites from Australian macrofungi from the genus *Cortinarius*. *Phytochemistry* 71, 948-955.

Bergmann, W., Feeney, R.J. **(1951)**. Contributions to the study of marine products. XXXII. The nucleosides of sponges I. *The Journal of Organic Chemistry* 16(6), 981-987.

Bertrand, S., Schumpp, O., Bohni, N., Monod, M., Gindro, K., Wolfender, J.-L. **(2013)**. *De novo* production of metabolites by fungal co-culture of *Trichophyton rubrum* and *Bionectria ochroleuca*. *Journal of Natural Products* 76(6), 1157-1165.

Bessa, L.J., Grande, R., Di Iorio, D., Di Giulio, M., Di Campli, E., Cellini, L. **(2013)**. *Helicobacter pylori* free-living and biofilm modes of growth: behavior in response to different culture media. *APMIS: Acta Pathologica, Microbiologica, et Immunologica Scandinavica* 121, 549-560.

Betina, V., Kuzela, S. **(1987)**. Uncoupling effect of fungal hydroxyanthraquinones on mitochondrial oxidative phosphorylation. *Chemico-Biological Interactions* 62(2), 179-189.

Bhadury, P., Mohammad, B.T., Wright, P.C. **(2006)**. The current status of natural products from marine fungi and their potential as anti-infective agents. *Journal of Industrial Microbiology and Biotechnology*. 33, 325-337.

Bhatnagar, I., Kim, S.-K. **(2010)**. Immense essence of excellence: marine microbial bioactive compounds. *Marine Drugs* 8, 2673-2701.

Biabani, M.A.F., Laatsch, H., **(1998)**. Advances in chemical studies on low-molecular weight metabolites of marine fungi. *Journal für Praktische Chemie* 340, 589-607.

Bills, G.F., Platas, G., Fillola, A., Jiménez, M.R., Collado, J., Vicente, F., Martín, J., González, A., Bur-Zimmermann, J., Tormo, J.R., Peláez, F. **(2008)**. Enhancement of antibiotic and secondary metabolite detection from filamentous fungi by growth on nutritional arrays. *Journal of Applied Microbiology* 104(6), 1644-1658.

Bingham, J.-P., Mitsunaga, E., Bergeron, Z.L. **(2010)**. Drugs from slugs – past, present and future perspectives of ω-conotoxin research. *Chemico-Biological Interactions* 183, 1-18.

Birch, A.J., Blance, G.E., David, S., Smith, H. **(1961)**. 600. Studies in relation to biosynthesis. Part XXIV. Some remarks on the structure of echinulin. *Journal of the Chemical Society* 3128-3131.

Blunt, J.W., Copp, B.R., Keyzers, R.A., Munro, M.H.G., Prinsep, M.R. **(2013)**. Marine natural products. *Natural Product Reports* 30, 237-323.

Bode, H.B., Bethe, B., Höfs, R., Zeeck, A. **(2002)**. Big effects from small changes: possible ways to explore Nature's chemical diversity. *ChemBioChem* 3, 619-627.

Bórrensen, T., Boyen, C., Dobson, A., Höfle, M., Ianora, A., Jaspars, M., Kijjoa, A., Olafsen, J., Querellou, J., Rigos, G., Wijffels, R. **(2010)**. Marine biotechnology: a new vision and strategy for Europe. *Marine Board-ESF Position Paper* 15, 1-91.

Brakhage, A.A., Schroeckh, V. **(2011)**. Fungal secondary metabolites – strategies to activate silent gene clusters. *Fungal Genetics and Biology* 48, 15-22.

Bringmann, G., Gulder, T.A.M., Lang, G., Schmitt, S., Stöhr, R., Wiese, J., Nagel, K., Imhoff, J.F. **(2007)**. Large-scale biotechnological production of the antileukemic marine natural product sorbicillactone A. *Marine Drugs* 5, 23-30.

Bringmann, G., Lang, G., Gulder, T.A.M., Tsuruta, H., Mühlbacher, J., Maksimenka, K., Steffens, S., Schaumann, K., Stöhr, R., Wiese, J., Imhoff, J.F., Perović-Ottstadt, S., Boreiko, O., Müller, W.E.G. **(2005)**. The first sorbicillinoid alkaloids, the antileukemic sorbicillactones A and B, from a sponge-derived *Penicillium chrysogenum* strain. *Tetrahedron* 61, 7252-7265.

Bringmann, G., Lang, G., Steffens, S., Günther, E., Schaumann, K. **(2003)**. Evariquinone, isoemericellin, and stromemycin from a sponge derived strain of the fungus *Emericella variecolor. Phytochemistry* 63, 437-443.

Büchi, G., Luk, K.C., Kobbe, B., Townsend, J.M. **(1977)**. Four new mycotoxins of *Aspergillus clavatus* related to tryptoquivaline. *The Journal of Organic Chemistry* 42(2), 244-246.

Buckland, B., Gbewonyo, K., Hallada, T., Kaplan, L., Masurekar, P. **(1989)**. Production of lovastatin, an inhibitor of cholesterol accumulation in humans. In: *Novel microbial product for medicine and agriculture, Topics in Industrial Microbiology* (ed. Demain, A.L.), Elsevier, Amsterdam 161-169.

Bugni, T.S., Ireland, C.M. **(2004)**. Marine-derived fungi: a chemically and biologically diverse group of microorganisms. *Natural Product Reports* 21, 143-163.

Butinar, L., Zalar, P., Frisvad, J.C., Gunde-Cimerman, N. **(2005)**. The genus *Eurotium* – members of indigenous fungal community in hypersaline waters of salterns. *FEMS Microbiology Ecology* 51, 155-166.

Buttachon, S., Chandrapatya, A., Manoch, L., Silva, A., Gales, L., Bruyère, C., Kiss, R., Kijjoa, A. **(2012)**. Sartorymensin, a new indole alkaloid, and new analogues of tryptoquivaline and fiscalins produced by *Neosartorya siamensis* (KUFC 6349). *Tetrahedron* 68, 3253-3262.

Cai, S., Kong, X., Wang, W., Zhou, H., Zhu, T., Li, D., Gu, Q. **(2012)**. Aspergilazine A, a diketopiperazine dimer with a rare N-1 to C-6 linkage, from a marine-derived fungus *Aspergillus taichungensis*. *Tetrahedron Letters* 53, 2615-1617.

Chan, T.M., Leung, J.K.-H., Tsang, R.C.-W., Liu, Z.H., Li, L.S., Yung, S. **(2003)**. Emodin ameliorates glucose-induced matrix synthesis in human peritoneal mesothelial cells. *Kidney International* 64, 519-533.

Chen, Y.-Y., Chiang, S.-Y., Lin, J.-G., Ma, Y.-S., Liao, C.-L., Weng, S.-W., Lai, T.-Y., Chung, J.-G. **(2010a)**. Emodin, aloe-emodin and rhein inhibit migration and invasion in human tongue cancer SCC-4 cells through the inhibition of gene expression of matrix metalloproteinase-9. *International Journal of Oncology* 36, 1113-1120.

Chen, Y.-Y., Chiang, S.-Y., Lin, J.-G., Yang, J.-S., Ma, Y.-S., Liao, C.-L., Lai, T.-Y., Tang, N.-Y., Chung, J.-G. **(2010b)**. Emodin, aloe-emodin and rhein induced DNA damage and inhibited DNA repair gene expression in SCC-4 human tongue cancer cells. *Anticancer Research* 30, 945-952.

Chen, Y.-K., Kuo, Y.-H., Chiang, B.-H., Lo, J.-M., Sheen, L.-Y. **(2009a)**. Cytotoxic activities of 9,11-dehydroergosterol peroxide and ergosterol peroxide from the fermentation mycelia of *Ganoderma lucidum* cultivated in the medium containing leguminous plants on Hep 3B cells. *Journal of Agricultural and Food Chemistry* 57, 5713-5719.

Chen, G., Qiu, H., Ke, S.-D., Hu, S.-M., Yu, S.-Y., Zou, S.-Q. **(2013)**. Emodin regulating excision repair cross-complementation group 1 through fibroblast growth factor receptor 2 signaling. *World Journal of Gastroenterology* 19(16), 2481-2491.

Chen, Y.-C., Shen, S.-C., Lee, W.-R., Hsu, F.-L., Lin, H.-Y., Ko, C.-H., Tseng, S.-W. **(2002)**. Emodin induces apoptosis in human promyeloleukemic HL-60 cells accompanied by activation of caspase 3 cascade but independent of reactive oxygen species production. *Biochemical Pharmacology* 64, 1713-1724.

Chen, J., Zhang, L., Zhang, Y., Zhang, H., Du, J., Ding, J., Guo, Y., Jiang, H., Shen, X. **(2009b)**. Emodin targets the β-hydroxyacyl-acyl carrier protein dehydratase from *Helicobacter pylori*: enzymatic inhibition assay with crystal structural and thermodynamic characterization. *BMC Microbiology* 9(91) 1-12.

Choi, S.-G., Kim, J., Sung, N.-D., Son, K.-H., Cheon, H.-G., Kim, K.-R., Kwon, B.-M. **(2007)**. Anthraquinones, Cdc25B phosphatase inhibitors, isolated from the roots of *Polygonum multiflorum* Thunb. *Natural Product Research* 21(6), 487-493.

Choi, R.J., Ngoc, T.M., Bae, K., Cho, H.-J., Kim, D.-D., Chun, J., Khan, S., Kim, Y.S. **(2013)**. Anti-inflammatory properties of anthraquinones and their relationship with the regulation of P-glycoprotein function and expression. *European Journal of Pharmaceutical Sciences* 48, 272-281.

Chooi, Y.-H., Fang, J., Liu, H., Filler, S.G., Wang, P., Tang, Y. **(2013)**. Genome mining of a prenylated and immunosuppressive polyketide from pathogenic fungi. *Organic Letters* 15(4), 780-783.

Chu, D., Peng, C., Ding, B., Liu, F., Zhang, F., Lin, H., Li, Z. **(2011)**. Biological active metabolite cyclo (L-Trp-L-Phe) produced by South China Sea sponge *Holoxea* sp. associated fungus *Aspergillus versicolor* strain TS08. *Bioprocess and Biosystems Engineering* 34, 223-229.

Chun, H.G., Davies, B., Hoth, D., Suffness, M., Plowman, J., Flora, K., Grieshaber, C., Leyland-Jones, B. **(1986)**. Didemnin B. The first marine compounds entering clinical trials as an antineoplastic agent. *Investigational New Drugs* 4(3), 279-284.

Chun-Guang, W., Jun-Qing, Y., Bei-Zhong, L., Dan-Ting, J., Chong, W., Liang, Z., Dan, Z., Yan, W. **(2010)**. Anti-tumor activity of emodin against human chronic myelocytic leukemia K562 cell lines *in vitro* and *in vivo*. *European Journal of Pharmacology* 627, 33-41.

Clardy, J., Springer, J.P., Büchi, G., Matsuo, K., Wightman, R. **(1975)**. Tryptoquivaline and tryptoquivalone, two tremorgenic metabolites of *Aspergillus clavatus*. *Journal of the American Chemical Society* 97(3), 663-665.

Colwell, R.R. **(2002)**. Fulfilling the promise of biotechnology. *Biotechnology Advances* 20, 215-228.

Cornacchia, C., Cacciatore, I., Baldassarre, L., Mollica, A., Feliciani, F., Pinnen, F. **(2012)**. 2,5-Diketopiperazines as neuroprotective agents. *Mini-Reviews in Medicinal Chemistry* 12, 2-12.

Cragg, G.M., Newman, D.J. **(2013)**. Natural products: a continuing source of novel drug leads. *Biochimica et Biophysica Acta* 1830, 3670-3695.

Cruz, M., Martín, J., González-Menéndez, V., Pérez-Victoria, I., Moreno, C., Tormo, J.R., Aouad, N.E., Guarro, J., Vicente, F., Reyes, F., Bills, G.F. **(2012)**. Chemical and physical modulation of antibiotic activity in *Emericella* species. *Chemistry & Biodiversity* 9, 1095-1113.

Cuevas, C., Pérez, M., Martin, M.J., Chicharro, J.L., Fernández-Rivas, C., Flores, M., Francesch, A., Gallego, P., Zarzuelo, M., de la Calle, F., García, J., Polanco, C., Rodríguez, I., Manzanares, I. **(2000)**. Synthesis of ecteinascidin ET-743 and phthalascidin Pt-650 from cyanosafracin B. *Organic Letters* 2(16), 2545-2548.

Debbab, A., Aly, A.H., Lin, W.H., Proksch, P. **(2010)**. Bioactive compounds from marine bacteria and fungi. *Microbial Biotechnology* 3, 544-563.

Debbab, A., Aly, A.H., Proksch, P. **(2012)**. Endophytes and associated marine derived fungi – ecological and chemical perspectives. *Fungal Diversity* 57(1), 45-83.

Demain, A.L. **(2000)**. Small bugs, big business: the economic power of the microbe. *Biotechnology Advances* 18, 499-514.

Dewapriya, P., Li, Y.-X., Himaya, S.W.A., Pangestuti, R., Kim, S.-K. **(2013)**. Neoechinulin A suppresses amyloid-β oligomer-induced microglia activation and

thereby protects PC-12 cells from inflammation-mediated toxicity. *NeuroToxicology* 35, 30-40.

Dewick, P.M. **(2009)**. The acetate pathway: fatty acids and polyketides. *Medicinal Natural Products: A Biosynthetic Approach* (ed. Dewick, P.M.), Wiley, ISBN 978-0-470-74168-9, 104-105.

Ding, G., Jiang, L., Guo, L., Chen, X., Zhang, H., Che, Y. **(2008)**. Pestalazines and pestalamides, bioactive metabolites from the plant pathogenic fungus *Pestalotiopsis theae*. *Journal of Natural Products* 71, 1861-1865.

Donlan, R.M., Costerton, J.W. **(2002)**. Biofilms: survival mechanisms of clinically relevant microorganisms. *Clinical Microbiology Reviews* 15(2), 167-193.

Dossena, A., Marchelli, R., Pochini, A. **(1974)**. New metabolites of *Aspergillus amstelodami* related to the biogenesis of neoechinulin. *Journal of the Chemical Society, Chemical Communications* 771-772.

Du, F.-Y., Li, X.-M., Li, C.-S., Shang, Z., Wang, B.-G. **(2012)**. Cristatumins A-D, new indole alkaloids from the marine-derived endophytic fungus *Eurotium cristatum* EN-220. *Bioorganic & Medicinal Chemistry* Letters 22, 4650-4653.

Du, L., Zhu, T., Liu, H., Fang, Y., Zhu, W., Gu, Q. **(2008)**. Cytotoxic polyketides from a marine-derived fungus *Aspergillus glaucus*. *Journal of Natural Products* 71, 1837-1842.

Duarte, N., Ferreira, M.-J.U., Martins, M., Viveiros, M., Amaral, L. **(2007)**. Antibacterial activity of ergosterol peroxide against *Mycobacterium tuberculosis*: dependence upon system and medium employed. *Phytotherapy Research* 21, 601-604.

Eamvijarn, A., Gomes, N.M., Dethoup, T., Buaruang, J., Manoch, L., Silva, A., Pedro, M., Marini, I., Roussis, V., Kijjoa, A. **(2013)**. Bioactive meroditerpenes and indole alkaloids from the soil fungus *Neosartorya fischeri* (KUFC 6344), and

the marine-derived fungi *Neosartorya laciniosa* (KUFC 7896) and *Neosartorya tsunodae* (KUFC 9213). *Tetrahedron* 69, 8583-8591.

Eamvijarn, A., Kijjoa, A., Bruyère, C., Mathieu, V., Manoch, L., Lefranc, F., Silva, A., Kiss, R., Herz, W. **(2012)**. Secondary metabolites from a culture of the fungus *Neosartorya pseudofischeri* and their *in vitro* cytostatic activity in human cancer cell lines. *Planta Medica* 78, 1767-1776.

Endo, A., Kuroda, M., Tsujita, Y. **(1976)**. New inhibitors of cholesterogenesis produced by *Penicillium citrinum*. *The Journal of Antibiotics (Tokyo)* 29, 1346-1348.

Engstrom, G.W., Stenkamp, R.E., McDorman, D.J., Jensen, L.H. **(1982)**. Spectral identification, X-ray structure determination, and iron-chelating capability of erythroglaucin, a red pigment from *Aspergillus ruber*. *Journal of Agricultural and Food Chemistry* 30(2), 304-307.

Eyberger, A.L., Dondapati, R., Porter, J.R. **(2006)** Endophyte fungal isolates from *Podophyllum peltatum* produce podophyllotoxin. *Journal of Natural Products* 69(8), 1121-1124.

Feling, R.H., Buchanan, G.O., Mincer, T.J., Kauffman, C.A., Jensen, P.R., Fenical, W. **(2003)**. Salinosporamide A: a highly cytotoxic proteasome inhibitor from a novel microbial source, a marine bacterium of the new genus *Salinospora*. *Angewandte Chemie International Edition (English)* 42(3), 355-357.

Feng, Y., Huang, S.-L., Dou, W., Zhang, S., Chen, J.-H., Shen, Y., Shen, J-H., Leng, Y. **(2010)**. Emodin, a natural product, selectively inhibits 11β-hydroxysteroid dehydrogenase type 1 and ameliorates metabolic disorder in diet-induced obese mice. *British Journal of Pharmacology* 161, 113-126.

Feng, S.-X., Li, J.-S., Qu, L.-B., Shi, Y.-M., Zhao, D. **(2013)**. Comparative pharmacokinetics of five Rhubard anthraquinones in normal and thrombotic focal cerebral ischemia-induced rats. *Phytotherapy Research* 27, 1489-1494.

Fenical, W. **(2013)**. Seriniquinoine, a marine microbial metabolite for the treatment of melanoma. *14th International Symposium on Marine Natural Products and the 8th European Congress on Marine Natural Products 2013, September*, 15-20, La Toja Island, Galicia, Spain

Fenical, W., Jensen, P.R. **(1993)**. Marine microorganisms: a new biomedical resource. In: *Marine Biotechnology, Volume 1, Pharmaceutical and Bioactive Natural Products, 1* (Eds. Attaway, D.H., Zaborsky, O.R.), 419-459, London: Plenum Press, New York, 419-459.

Fenical, W., Jensen, P.R. **(2006)**. Developing a new resource for drug discovery: marine actinomycete bacteria. *Nature Chemical Biology* 2(12), 666-673.

Figueroa, M., González, M.C., Rodríguez-Sotres, R., Sosa-Peinado, A., González-Andrade, M., Cerda-García-Rojas, C.M., Mata, R. **(2009)**. Calmodulin inhibitors from the fungus *Emericella* sp.. *Bioorganic & Medicinal Chemistry* 17, 2167-2174.

Firn, R.D., Jones, C.G. **(2000)**. The evolution of secondary metabolism – a unifying model. *Molecular Microbiology* 37(5), 989-994.

Fodstad, O, Breistøl, K., Pettit, G.R., Shoemaker, R.H., Boyd, M.R. **(1996)**. Comparative antitumor activities of halichondrins and vinblastine against human tumor xenografts. *Journal of Experimental Therapeutics and Oncology* 1(2), 119-125.

Fox, E.M., Howlett, B.J. **(2008)**. Secondary metabolism: regulation and role in fungal biology. *Current Opinion in Microbiology* 11, 481-487.

Frisvad, J.C., Andersen, B., Thrane, U. **(2008)**. The use of secondary metabolite profiling in chemotaxonomy of filamentous fungi. *Mycological Research* 112, 231-240.

Frisvad, J.C., Rank, C., Nielsen, K.F., Larsen, T.O. **(2009)**. Metabolomics of *Aspergillus fumigatus. Medical Mycology* 47, S53-S71.

Fujimoto, H., Asai, T., Kim, Y.-P., Ishibashi, M. **(2006)**. Nine constituents including six xanthone-related compounds isolated from two Ascomycetes, *Gelasinospora santi-florii* and *Emericella quadrilineata*, found in a screening study focused on immunomodulatory activity. *Chemical & Pharmaceutical Bulletin* 54(4), 550-553.

Fujimoto, H., Fujimaki, T., Okuyama, E., Yamazaki, M. **(1999)**. Immunomodulatory constituents from an Ascomycete, *Microascus tardifaciens*. *Chemical & Pharmaceutical Bulletin* 47(10), 1426-1432.

Fujimoto, H., Nakamura, E., Okuyama, E., Ishibashi, M. **(2000)**. Immunomodulatory constituents from an Ascomycete, *Emericella aurantio-brunnea. Chemical & Pharmaceutical Bulletin* 48(10), 1436-1441.

Fujimoto, H., Negishi, E., Yamaguchi, K., Nishi, N., Yamazaki, M. **(1996)**. Isolation of new tremorgenic metabolites from an Ascomycete, *Corynascus setosus*. *Chemical & Pharmaceutical Bulletin* 44(10), 1843-1848.

Gao, X., Chooi, Y.-H., Ames, B.D., Wang, P., Walsh, C.T., Tang, Y. **(2011b)**. Fungal indole alkaloid biosynthesis: genetic and biochemical investigation of the tryptoquialanine pathway in *Penicillium aethiopicum*. *Journal of the American Chemical Society* 133, 2729-2741.

Gao, J., León, F., Radwan, M.M., Dale, O.R., Husni, A.S., Manly, S.P., Lupien, S., Wang, X., Hill, R.A., Dugan, F.M., Cutler, H.G., Cutler, S.J. **(2011a)**. Benzyl derivatives with *in vitro* binding affinity for human opioid and cannabinoid receptors from the fungus *Eurotium repens. Journal of Natural Products* 74, 1636-1639.

Gao, J., Radwan, M.M., León, F., Wang, X., Jacob, M.R., Tekwani, B.L., Khan, S.I., Lupien, S., Hill, R.A., Dugan, F.M., Cutler, H.G., Cutler, S.J. **(2012)**.

Antimicrobial and antiprotozoal activities of secondary metabolites from the fungus *Eurotium repens. Medicinal Chemistry Research* 21, 3080-3086.

Gavin, J., Tabacchi, R. **(1975)**. Isolement et identification de composes phenoliques et monoterpeniques de la mousse de chene (*Evenia prunastri* (L.) Ach). *Helvetica Chimica Acta* 58, 190-194.

Geiser, D.M. **(2009)**. Sexual structures in *Aspergillus*: morphology, importance and genomics. *Medical Mycology* 47(Suppl.1), S21-S-26.

Geris, R., Simpson, T.J. **(2009)**. Meroterpenoids produced by fungi. *Natural Product Reports* 26, 1063-1094.

Gerwick, W.H., Fenner, A.M. **(2013)**. Drug discovery from marine microbes. *Microbial Ecology* 65, 800-806.

Gerwick, W.H., Moore, B.S. **(2012)**. Lessons from the past and charting the future of marine natural products drug discovery and chemical biology. *Chemistry & Biology* 19(1), 85-98.

Gibbons, J.G., Rokas, A. **(2013)**. The function and evolution of the *Aspergillus* genome. *Trends in Microbiology* 21(1), 14-22.

Glass, N.L., Donaldson, G.C. **(1995)**. Development of primer sets designed for use with the PCR to amplify conserved genes from filamentous ascomycetes. *Applied and Environmental Microbiology* 61, 1323-1330.

Gloer, J.B. **(1995)**. The chemistry of fungal antagonism and defense. *Canadian Journal of Botany* 73(1), S1265-S1274.

Gomes, N.M., Bessa, L.J., Buttachon, S., Costa, P.M., Buaruang, J., Dethoup, T., Silva, A.M.S., Kijjoa, A. **(2014)**. Antibacterial and antibiofilm activities of tryptoquivalines and meroditerpenes isolated from the marine-derived fungi

Neosartorya paulistensis, *N. laciniosa*, *N. tsunodae*, and the soil fungi *N. fischeri* and *N. siamensis*. *Marine Drugs* 12, 822-839.

Gomes, N.M., Dethoup, T., Singburaudom, N., Gales, L., Silva, A.M.S., Kijjoa, A. **(2012)**. Eurocristatine, a new diketopiperazine dimer from the marine sponge-associated fungus *Eurotium cristatum*. *Phytochemistry Letters* 5, 717-720.

Gosh, S., Sarma, M.D., Patra, A., Hazra, B. **(2010)**. Anti-inflammatory and anticancer compounds isolated from *Ventilago madraspatana* Gaertn., *Rubia cordifolia* Linn. and *Lantana camara* Linn.. *Journal of Pharmacy and Pharmacology* 62, 1158-1166.

Greve, H., Mohamed, I.E., Pontius, A., Kehraus, S., Gross, H., König G.M. **(2010)**. Fungal metabolites: structural diversity as incentive for anticancer drug development. *Phytochemistry Reviews* 9, 537-545.

Gualtieri, M., Bastide, L., Villain-Guillot, P., Michaux-Charachon, S., Latouche, J., Leonetti, J.-P. **(2006)**. *In vitro* activity of a new antibacterial rhodanine derivative against *Staphylococcus epidermidis* biofilms. *Journal of Antimicrobial Chemotherapy* 58(4), 778-783.

Haefner, B. **(2003)**. Drugs from the deep: marine natural products as drug candidates. *Drug Discovery Today* 8(12), 536-544.

Hamlin, P.A., Aghajanian, C., Younes, A., Hong, D.S., Palladino, M.A., Longenecker, A.M., Lloyd, G.K., Hannah, A.L., Spear, M.A., Kurzrock, R. **(2009)** First-in-human phase 1 study of the novel structure proteasome inhibitor NPI-0052. *Journal of Clinical Oncology* 27(15s), 3516.

Hart, J.B., Lill, R.E., Hickford, S.J.H., Blunt, J.W., Munro, M.H.G. **(2000)**. The halichondrins: Chemistry, biology, supply and delivery. In: *Drugs from the sea* (Ed. Fusetani, N). Krager: Basel, 134-153.

Hawksworth, D.L., Crous, P.W., Redhead, S.A., Reynolds, D.R., Samson, R.A., Seifert, K.A., Taylor, J.W., Wingfield, M.J., Abaci, Ö., Aime, C., Asan, A., Bai, F.-Y., de Beer, W., Begerow, D., Berikten, D., Boekhout, T., Buchanan, P.K., Burgess, T., Buzina, W., Cai, L., Cannon, P.F., Crane, J.L., Damm, U., Daniel, H.-D., van Diepeningen, A.D., Druzhinina, I., Dyer, P.S., Eberhardt, U., Fell, J.W., Frisvad, J.C., Geiser, D.M., Geml, J., Glienke, C., Gräfenham, T., Groenewald, J.Z., Groenewald, M., de Gruyter, D.M., Guého-Kellermann, E., Guo, L.-D., Hibbet, D.S., Hong, S.-B., de Hoog, G.S., Houbraken, J., Huhndorf, S.M., Hyde, K.D., Ismail, A., Johnston, P.R., Kadaifciler, D.G., Kirk, P.M., Kõljalg, U., Kurtzman, C.P., Lagneau, P.-E., Lévesque, C.A., Liu, X., Lombard, L., Meyer, W., Miller, A., Minter, D.W., Najafzadeh, M.J., Norvell, L., Ozerskaya, S.M., Öziç, R., Pennycook, S.R., Peterson, S.W., Pettersson, O.V., Quaedvlieg, W., Robert, V.A., Ruibal, C., Schnürer, J., Schroers, H.-J., Shivas, R., Slippers, B., Spierenburg, H., Takashima, M., Taşkin, E., Thines, M., Thrane, U., Uztan, A.H., van Raak, M., Varga, J., Vasco, A., Verkley, G., Videira, S.I.R., de Vries, R.P., Weir, B.S., Yilmaz, N., Yurkov, A., Zhang, N. **(2011a)**. The Amsterdam Declaration of Fungal Nomenclature. *IMA Fungus* 2(1), 105-112.

Hawksworth, D.L. **(2011b)**. A new dawn for the naming of fungi: impacts of decisions made in Melbourne in July 2011 on the future publication and regulation of fungal names. *MycoKeys* 1, 7-20.

Hentschel, U., Hopke, J., Horn, M., Friedrich, A.B., Wagner, M., Hacker, J., Moore, B.S. **(2002)**. Molecular evidence for a uniform microbial community in sponges from different oceans. *Applied and Environmental Microbiology* 68(9), 4431-4440.

Hertweck, C. **(2009)**. Hidden biosynthetic treasures brought to light. *Nature Chemical Biology* 5, 450-452.

Hill, R.A. **(2013)**. Marine natural products. *Annual Reports on the Progress of Chemistry Section B: Organic Chemistry* 109, 146-166.

Hirata, Y., Uemura, D. **(1986)**. Halichondrins – antitumor polyether macrolides from a marine sponge. *Pure and Applied Chemistry* 58(5), 701-710.

Hof, H., Dietz, A. **(2009)**. Antifungal activity of anidulafungin, a product of *Aspergillus nidulans*, against *Aspergillus nidulans*. *International Journal of Antimicrobial Agents* 33, 285-286.

Hoffman, L.R., D'Argenio, D.A., MacCoss, M.J., Zhang, Z., Jones, R.A., Miller, S.I. **(2005)**. Aminoglycoside antibiotics induce bacterial biofilm formation. *Nature* 436, 1171-1175.

Hölker, U., Höfer, M., Lenz, J. **(2004)**. Biotechnological advantages of laboratory-scale solid-state fermentation with fungi. *Applied Microbiology and Biotechnology* 64, 175-186.

Höller, U., Wright, A.D., Matthée, G.F., Konig., G.M., Draeger, S., Aust, H.-J., Schulz, B. **(2000)**. Fungi from marine sponges: diversity, biological activity and secondary metabolites. *Mycological Research* 104(11), 1354-1365.

Holick, M.F. **(2003)**. Vitamin D: a millennium perspective. *Journal of Cellular Biochemistry* 88(2), 296-307.

Hong, S.-B., Shin, H.-D., Hong, J., Frisvad, J.C., Nielsen, P.V., Varga, J., Samson, R.A. **(2008)**. New taxa of *Neosartorya* and *Aspergillus* in *Aspergillus* section *Fumigati. Antonie van Leeuwenhoek* 93, 87-98.

Hosoe, T., Itabashi, T., Kobayashi, N., Udagawa, S., Kawai, K. **(2006)**. Three new types of indoloditerpenes, emindole PA-PC, from *Emericella purpurea*. Revision of the structure of emindole PA. *Chemical & Pharmaceutical Bulletin* 54(2), 185-187.

Hsiang, C.-Y., Ho, T.-Y. **(2008)**. Emodin is a novel alkaline nuclease inhibitor that suppresses herpes simplex virus type 1 yields in cell cultures. *British Journal of Pharmacology* 155, 227-235.

Hsu, S.-C., Chung, J.-G. **(2012)**. Anticancer potential of emodin. *Biomedicine* 2, 108-116.

Hu, G.-P., Yuan, J., Sun, L., She, Z.-G., Wu, J.-H., Lan, X.-J., Zhu, X, Lin, Y.-C., Chen, S.-P. **(2011)**. Statistical research on marine natural products based on data obtained between 1985 and 2008. *Marine Drugs* 9, 514-525.

Huang, H.C., Chang, J.H., Tung, S.F., Wu, R.T., Foegh, M.L., Chu, S.H. **(1992)**. Immunosuppressive effect of emodin, a free radical generator. *European Journal of Pharmacology* 211, 359-364.

Huang, P.-H., Huang, C.-Y., Chen, M.-C., Lee, Y.-T., Yue, C.-H., Wang, H.-Y., Lin, H. **(2013)**. Emodin and aloe-emodin suppress breast cancer cell proliferation through ERα Inhibition. *Evidence-Based Complementary and Alternative Medicine*.

Hwang, J.-K., Noh, E.-M., Moon, S.-J., Kim, J.-M., Kwon, K.-B., Park, B.-H., You, Y.-O., Hwang, B.-M., Kim, H.-J., Kim, B.-S., Lee, S.-J., Kim, J.-S., Lee, Y.-R. **(2013)**. Emodin suppresses inflammatory responses and joint destruction in collagen-induced arthritic mice. *Rheumatology* 52, 1583-1591.

Hyun, S.K., Lee, H., Kang, S.S., Chung, H.Y., Choi, J.S. **(2009)**. Inhibitory activities of *Cassia tora* and its anthraquinone constituents on angiotensin-converting enzyme. *Phytotherapy Research* 23, 178-184.

Ishibashi, K., Nose, K., Shindo, T., Arai, M., Mishima, H. **(1968)**. Siccayne: a novel acetylenic metabolite of *Helminthosporium siccans*. *Annual Report Sankyo Research Laboratories* 20, 76-79.

Itabashi, T., Nozawa, K., Miyaji, M., Udagawa, S., Nakajima, S., Kawai, K. **(1992)**. Falconensins A, B, C, and D, new compounds related to azaphilone, from *Emericella falconensis. Chemical & Pharmaceutical Bulletin* 40(12), 3142-3144.

Itabashi, T., Nozawa, K., Nakajima, S., Kawai, K. **(1993)**. A new azaphilone, falconensin H, from *Emericella falconensis. Chemical & Pharmaceutical Bulletin* 41(11), 2040-2041.

Itabashi, T., Ogasawara, N., Nozawa, K., Kawai, K. **(1996)**. Isolation and structures of new azaphilone derivatives, falconensins E-G, from *Emericella falconensis* and absolute configurations of falconensins A-G. *Chemical & Pharmaceutical Bulletin* 44(12), 2213-2217.

Jain, N.K., Jain, S.C., Jain, R. **(2013)**. Two new compounds and other constituents from *Cassia fistula* root bark. *Chemistry of Natural Compounds* 49(2), 232-234.

Jayasuriya, H., Zink, D., Basilio, A., Vicente, F., Collado, J., Bills, G., Goldman, M.L., Motyl, M., Huber, J., Dezeny, G., Byrne, K., Singh, S.B. **(2009)**. Discovery and antibacterial activity of glabramycin A-C from *Neosartorya glabra* by an antisense strategy. *The Journal of Antibiotics* 62, 265-269.

Jernal, A., Bray, F., Center, M.M., Ferlay, J., Ward, E., Forman, D. **(2011)**. Global cancer statistics. *CA: A Cancer Journal for Clinicians* 61(2), 69-90.

Johnson, S.A., Goddard, P.A., Iliffe, C., Timmins, B., Rickard, A.H., Robson, G., Handley, P.S. **(2002)**. Comparative susceptibility of resident and transient hand bacteria to para-chloro-meta-xylenol and triclosan. *Journal of Applied Microbiology* 93, 336-344.

Johnson, A.P., Livermore, D.M., Tillotson, G.S. **(2001)**. Antimicrobial susceptibility of Gram-positive bacteria: what's current, what's anticipated ? *Journal of Hospital Infection* 49, S3-S11.

Jones, E.B.G. **(2011)**. Are there more marine fungi to be described? *Botanica Marina* 54, 343-354.

Kajimura, Y., Aoki, T., Kuramochi, K., Kobayashi, S., Sugawara, F., Watanabe, N., Arai, T. **(2008)**. Neoechinulin A protects PC12 cells against MPP^+-induced cytotoxicity. *The Journal of Antibiotics* 61(5), 330-333.

Kanoh, K., Kohno, S., Asari, T., Harada, T., Katada, J., Muramatsu, M., Kawashima, H., Sekiya, H., Uno, I. **(1997)**. (-)-Phenylahistin: a new mammalian cell cycle inhibitor produced by *Aspergillus ustus*. *Bioorganic & Medicinal Chemistry Letters* 7(22), 2847-2852.

Kanoh, K., Kohno, S., Katada, J., Hayashi, Y., Muramatsu, M., Uno, I. **(1999)**. Antitumor activity of phenylahistin *in vitro* and *in vivo*. *Bioscience, Biotechnology and Biochemistry* 63(6), 1130-1133.

Kanokmedhakul, K., Kanokmedhakul, S., Suwannatrai, R., Soytong, K., Prabpai, S., Kongsaeree, P. **(2011)**. Bioactive meroterpenoids and alkaloids from the fungus *Eurotium chevalieri. Tetrahedron* 67,5461-5468.

Kaplan, J.B., Jabbouri, S., Sadovskaya, I. **(2011)**. Extracellular DNA-dependent biofilm formation by *Staphylococcus epidermis* RP62A in response to subminimal inhibitory concentrations of antibiotics. *Research in Microbiology* 162, 535-541.

Kavitha, A., Prabhakar, P., Vijayalakshmi, M., Venkateswarlu, Y. **(2010)**. Purification and biological evaluation of the metabolites produced by *Streptomyces* sp. TK-VL_333. *Research in Microbiology* 161, 335-345.

Kawahara, N., Nakajima, S., Satoh, Y., Yamazaki, M., Kawai, K. **(1988c)**. Studies on fungal products. XVIII. Isolation and structures of a new fungal depsidone related to nidulin and a new phthalide from *Emericella unguis. Chemical & Pharmaceutical Bulletin* 36(6), 1970-1975.

Kawahara, N., Nakajima, S., Yamazaki, M., Kawai, K. **(1989b)**. Structure of a novel epidithiodioxopiperazine, emethallicin A, a potent inhibitor of histamine release, from *Emericella heterothallica. Chemical & Pharmaceutical Bulletin* 37(10), 2592-2595.

Kawahara, N., Nozawa, K., Nakajima, S., Kawai, K. **(1986)**. Aurantioemestrin from *Emericella striata* and silvathione from *Aspergillus silvaticus*, possible key intermediates from epidithiodioxopiperazines to trioxopiperazines. *Journal of the Chemical Society, Chemical Communications* 1495-1496.

Kawahara, N., Nozawa, K., Nakajima, S., Kawai, K. **(1988a)**. Emeheterone, a new pyrazinone derivative from *Emericella heterothallica*. *Phytochemistry* 27(9), 3022-3024.

Kawahara, N., Nozawa, K., Nakajima, S., Kawai, K. **(1988b)**. Studies on fungal products. Part 15. Isolation and structure determination of arugosin E from *Aspergillus silvaticus* and cycloisoemericellin from *Emericella striata*. *Journal of the Chemical Society Perkin Transactions 1* 907-911.

Kawahara, N., Nozawa, K., Nakajima, S., Kawai, K. **(1988d)**. Isolation and structures of novel fungal depsidones, emeguisins A, B, and C, from *Emericella unguis*. *Journal of the Chemical Society Perkin Transactions 1* 2611-2614.

Kawahara, N., Nozawa, K., Nakajima, S., Yamazaki, M., Kawai, K. **(1989a)**. Sulfur-containing dioxopiperazine derivatives from *Emericella heterothallica*. *Heterocycles* 29(2), 397-402.

Kawahara, N., Nozawa, K., Yamazaki, M., Nakajima, S., Kawai, K. **(1990)**. Structures of novel epipolythiodioxopiperazines, emethallicins B, C, and D, potent inhibitors of histamine release, from *Emericella heterothallica*. *Chemical & Pharmaceutical Bulletin* 38(1), 73-78.

Kijjoa, A., Santos, S., Dethoup, T., Manoch, L., Almeida, A.P., Vasconcelos, M.H., Silva, A., Gales, L., Herz, W. **(2011)**. Sartoryglabrins, analogs of ardeemins, from *Neosartorya glabra*. *Natural Product Communications* 6(6), 807-812.

Kijjoa, A., Sawangwong, P. **(2004)**. Drugs and cosmetics from the sea. *Marine Drugs* 2, 73-82.

Kim, J., Ashenhurst, J.A., Movassaghi, M. **(2009)**. Total synthesis of (+)-11,11'-dideoxyverticillin A. *Science* 324, 238-241.

Kim, D.S., Baek, N.-I., Oh, R.S., Jung, K.Y., Lee, I.S., Kim, J.H., Lee, H.-K. **(1997)**. Anticomplementary activity of ergosterol peroxide from *Naematoloma fasciculare* and reassignment of NMR data. *Archives of Pharmacal Research* 20(3), 201-205.

Kim, K.-S., Cui, X., Lee, D.-S., Sohn, J.H., Yim, J.H., Kim, Y.-C., Oh, H. **(2013)**. Anti-inflammatory effect of neoechinulin A from the marine fungus *Eurotium* sp. SF-5989 through the suppression of NF-κB and p38 MAPK pathways in lipopolysaccharide-stimulated RAW264.7 macrophages. *Molecules* 18, 13245-13259.

Kim, D.-H., Jung, S.J., Chung, I.-S., Lee, Y.-H., Kim, D.-K., Kim, S.-H., Kwon, B.-M., Jeong, T.-S., Park, M.-H., Seoung, N.-S., Baek, N.-I. **(2005)**. Ergosterol peroxide from flowers of *Erigeron annuus* L. as an anti-atherosclerosis agent. *Archives of Pharmacal Research* 28(5), 541-545.

Kim, Y.-M., Lee, C.-H., Kim, H.-G., Lee, H.-S. **(2004)**. Anthraquinones isolated from *Cassia tora* (Leguminosae) seed show an antifungal property against phytopathogenic fungi. *Journal of Agricultural and Food Chemistry* 52, 6096-6100.

Kimoto, K., Aoki, T., Shibata, Y., Kamisuki, S., Sugawara, F., Kuramochi, K., Nakazaki, A., Kobayashi, S., Kuroiwa, K., Watanabe, N., Arai, T. **(2007)**. Structure-activity relationships of neochinulin A analogues with cytoprotection against peroxynitrite-induced PC12 cell death. *The Journal of Antibiotics* 60(10), 614-621.

Kimura, Y., Hamasaki, T., Isogai, A., Nakajima, H. **(1982)**. Structure of aszonapyrone A, a new metabolite produced by *Aspergillus zonatus*. *Agricultural and Biological Chemistry* 46(7), 1963-1965.

Kimura, Y., Tani, K., Kojima, A. **(1996)**. Cyclo-(L-tryptophyl-L-phenylalanyl), a plant growth regulator produced by the fungus *Penicillium* sp.. *Phytochemistry* 41, 665-669.

Kjer, J., Debbab, A., Aly, A.H., Proksch, P. **(2010)**. Methods for isolation of marine-derived endophytic fungi and their bioactive secondary products. *Nature Protocols* 5, 479-490.

Kleinrock, M. **(2011)**. The use of medicines in the United States: review of 2010. *IMS Institute for Healthcare Informatics* Appendix 3, 32

Kobayashi, M., Uehara, H., Matsunami, K., Aoki, S., Kitagawa, I. **(1993)**. Trichoharzin, a new polyketide produced by the imperfect fungus *Trichoderma harzianum* separated from the marine sponge *Micale cecilia*. *Tetrahedron Letters* 34(49), 7925-7928.

Kobori, M., Yoshida, M., Ohnishi-Kameyama, M., Shinmoto, H. **(2007)**. Ergosterol peroxide from an edible mushroom suppresses inflammatory responses in RAW264.7 macrophages and growth of HT29 colon adenocarcinoma cells. *British Journal of Pharmacology* 150, 209-219.

Kohlmeyer, J., Kohlmeyer, E. **(1979)**. Marine mycology – the higher fungi. New York: Academic Press.

Kojima, H., Ogura, H. **(1989)**. Configurational studies on hydroxyl groups at C-2,3 and 23 or 24 of oleanene and ursine-type triterpenes by NMR spectroscopy. *Phytochemistry* 28(6), 1703-1710.

König, G.M., Kehraus, S., Seibert, S.F., Abdel-Lateff, A., Müller, D. **(2006)**. Natural products from marine organisms and their associated microbes. *ChemBioChem* 7, 229-238.

Koski, R.R. **(2008)**. Omega-3-acid ethyl esters (Lovaza) for severe hypertriglyceridemia. *Drug Forecast* 33(5), 271-273, 280-281, 303-303.

Kralj, A., Kehraus, S., Krick, A., Eguereva, E., Kelter, G., Maurer, M., Wortmann, A., Fiebig, H.-H., König, G.M. **(2006)**. Arugosins G and H: prenylated polyketides from the marine-derived fungus *Emericella nidulans* var. *acristata*. *Journal of Natural Products* 69, 995-1000.

Kremer, D., Kosalec, I., Locatelli, M., Epifano, F., Genovese, S., Carlucci, G., Končić, M.Z. **(2012)**. Anthraquinone profiles, antioxidant and antimicrobial properties of *Frangula ruprestris* (Scop.) Schur and *Frangula alnus* Mill. Bark. *Food Chemistry* 131(4), 1174-1180.

Kumar, S.N., Mohandas, C., Nambisan, B. **(2013)**. Purification, structural elucidation and bioactivity of tryptophan containing diketopiperazines, from *Comamonas testosteroni* associated with a rhabditid entomopathogenic nematode against major human-pathogenic bacteria. *Peptides* (In Press).

Kuo, C.-F., Hsieh, C.-H., Lin, W.-Y. **(2011)**. Proteomic response of LAP-activated RAW 264.7 macrophages to the anti-inflammatory property of fungal ergosterol. *Food Chemistry* 126, 207-212.

Kuo, Y.-C., Sun, C.-M., Ou, J.-C., Tsai, W.-J. **(1997)**. A tumor cell growth inhibitor from *Polygonum hypoleucum* Ohwi. *Life Sciences* 61(23), 2335-2344.

Kuo, T.-C., Yang, J.-S., Lin, M.-W., Hsu, S.-C., Lin, J.-J., Lin, H.-J., Hsia, T.-C., Liao, C.-H., Yang, M.-D., Fan, M.-J., Wood, W.G., Chung, J.-G. **(2009)**. Emodin has cytotoxic and protective effects in rat C6 glioma cells: roles of Mdr1a and nuclear factor κB in cell survival. *The Journal of Pharmacology and Experimental Therapeutics* 330(3), 736-744.

Kupka, J., Anke, T., Steglich, W., Zechlin, L. **(1981)**. Antibiotics from Basidiomycetes. XI The biological activity of siccayne, isolated from the marine fungus *Halocyphina villosa* J. & E. Kohlmeyer. *The Journal of Antibiotics* 34(3), 298-304.

Kuramochi, K., Ohnishi, K., Fujieda, S., Nakajima, M., Saitoh, Y., Watanabe, N., Takeuchi, T., Nakazaki, A., Sugawara, F., Arai, T., Kobayashi, S. **(2008)**. Synthesis and biological activities of neoechinulin A derivatives: new aspects of structure-activity relationships for neoechinulin A. *Chemical & Pharmaceutical Bulletin* 56(12), 1738-1743.

Kwak, H.-J., Park, M.-J., Park, C.-M., Moon, S.-I., Yoo, D.-H., Lee, H.-C., Lee, S.-H., Kim, M.-S., Lee, H.-W., Shin, W.-S., Park, I.-C., Rhee, C.H., Hong, S.-I. **(2006)**. Emodin inhibits vascular endothelial growth factor-A-induced angiogenesis by blocking receptor-2 (KDR/Flk-1) phosphorylation. *International Journal of Cancer* 118, 2711-2720.

Lee, S.J., Jeong, D., Park, W.-K., Kong, J.Y., Choi, G., Kim, H., Kang, S., Cho, H. **(2010)**. Screening of kit inhibitors: suppression of kit signaling and melanogenesis by emodin. *Phytotherapy Research* 24, 308-312.

Lee, Y.M., Kim, M.J., Li, H., Zhang, P., Bao, B., Lee, K.J., Jung, J.H. **(2013)**. Marine-derived *Aspergillus* species as a source of bioactive secondary metabolites. *Marine Biotechnology* 15, 499-519.

Leu, Y.-L., Hwang, T.-L., Hu, J.-W., Fang, J.-Y. **(2008)**. Anthraquinones from *Polygonum cuspidatum* as tyrosinase inhibitors for dermal use. *Phytotherapy Research* 22, 552-556.

Li, Y., Li, X., Kim, S.-K., Kang, J.S., Choi, H.D., Rho, J.R., Son, B.W. **(2004)**. Golmaenone, a new diketopiperazine alkaloid from the marine-derived fungus *Aspergillus* sp.. *Chemical & Pharmaceutical Bulletin* 52(3), 375-376.

Li, D.-L., Li, X.-M., Li, T.-G., Dang, H.-Y., Proksch, P., Wang, B.-G. **(2008a)**. Benzaldehyde derivatives from *Eurotium rubrum*, an endophytic fungus derived from the mangrove plant *Hibiscus tiliaceus*. *Chemical & Pharmaceutical Bulletin* 56(9), 1282-1285.

Li, D.-L., Li, X.-M., Li, T.-G., Dang, H.-Y., Wang, B.-G. **(2008b)**. Dioxopiperazine alkaloids produced by the marine mangrove derived endophytic fungus *Eurotium rubrum*. *Helvetica Chimica Acta* 91, 1888-1893.

Li, X., Li, X.-M., Xu, G.-M., Li, C.-S., Wang, B.-G. **(2014)**. Antioxidant metabolites from marine alga-derived fungus *Aspergillus wentii* EN-48. *Phytochemistry Letters* 7, 120-123.

Li, D.-L., Li, X.-M., Wang, B.-G. **(2009a)**. Natural anthraquinone derivatives from a marine mangrove plant-derived endophytic fungus *Eurotium rubrum*: structural elucidation and DPPH radical scavenging activity. *Journal of Microbiology and Biotechnology* 19(7), 675-680.

Li, J.-Y., Sidhu, R.S., Bollon, A., Strobel, G. **(1998)**. Stimulation of taxol production in liquid cultures of *Pestalotiopsis microspora*. *Mycological Research* 102(4), 461-464.

Li, Y., Sun, K.-L., Wang, Y., Fu, P., Liu, P.-P., Wang, C., Zhu, W.-M. **(2013a)**. A cytotoxic pyrrolidinoindoline diketopiperazine dimer from the algal fungus *Eurotium herbariorum* HT-2. *Chinese Chemical Letters* 24, 1049-1052.

Li, G.Y., Yang, T., Luo, Y.G., Chen, X.Z., Fang, D.M., Zhang, G.L. **(2009b)**. Brevianamide J, a new indole alkaloid dimer from the fungus *Aspergillus versicolor*. *Organic Letters* 11, 3714-3717.

Li, D., Zhang, N., Cao, Y., Zhang, W., Su, G., Sun, Y., Liu, Z., Li, F., Liang, D., Liu, B., Guo, M., Fu, Y., Zhang, X., Yang, Z. **(2013b)**. Emodin ameliorates lipopolysaccharide-induced mastitis in mice by inhibiting activation of NF-κB and MAPKs signal pathways. *European Journal of Pharmacology* 705, 79-85.

Liangsakul, J., Pornpakakul, S., Sangvichien, E., Muangsin, N., Sihanonth, P. **(2011)**. Emervaridione and varioxiranediol, two new metabolites from the endophytic fungus, *Emericella variecolor*. *Tetrahedron Letters* 52, 6427-6430.

Lin, L.-C., Chou, C.-J., Kuo, Y.-C. **(2001)**. Cytotoxic principles from *Ventilago leiocarpa*. *Journal of Natural Products* 64, 674-676.

Liu, A., Chen, H., Tong, H., Ye, S., Qiu, M., Wang, Z., Tan, W., Liu, J., Lin, S. **(2011b)**. Emodin potentiates the antitumor effects of gemcitabine in pancreatic cancer cells via inhibition of nuclear factor-κB. *Molecular Medicine Reports* 4, 221-227.

Liu, A., Chen, H., Wei, W., Ye, S., Liao, W., Gong, J., Jiang, Z., Wang, L., Lin, S. **(2011a)**. Antiproliferative and antimetastatic effects of emodin on human pancreatic cancer. *Oncology Reports* 26, 81-89.

Liu, Y., Jia, L., Liu, Z.C., Zhang, H., Zhang, P.J., Wan, Q., Wang, R. **(2009)**. Emodin ameliorates high-glucose induced mesangial p38 over-activation and hypocontractility via activation of PPARγ. *Experimental and Molecular Medicine* 41(9), 648-655.

Liu, J.-X., Zhang, J.-H., Li, H.-H., Lai, F.-J., Chen, K.-J., Chen, H., Luo, J., Guo, H.-C., Wang, Z.-H., Lin, S.-Z. **(2012)**. Emodin induces Panc-1 cell apoptosis via declining the mitochondrial membrane potential. *Oncology Reports* 28, 1991-1996.

Lu, Y., Yang, J.H., Li, X., Hwangbo, K., Hwang, S.-L., Taketomi, Y., Murakami, M., Chang, Y.-C., Kim, C.-H., Son, J.-K., Chang, H.W. **(2011)**. Emodin, a naturally occurring anthraquinone derivative, suppresses IgE-mediated anaphylactic reaction and mast cell activation. *Biochemical Pharmacology* 82, 1700-1708.

Luesch, H., Moore, R.E., Paul, V.J., Mooberry, S.L., Corbett, T.H. **(2001)**. Isolation of dolastatin 10 from the marine cyanobacterium *Symploca* species VP642 and total stereochemistry and biological evaluation of its analogue symplostatin 1. *Journal of Natural Products* 64(7), 907-910.

Maebaxashi, Y., Suzuki, S., Horie, Y., Murai, T., Yamazaki, M. **(1983)**. Isolation of a toxic metabolite, asteltoxin from *Emericella variecolor*. *Mycotoxins* 1(17), 47-49.

Mahato, S.B., Kundu, A.P. ^{13}C NMR spectra of pentacyclic triterpenoids – a compilation and some salient features. *Phytochemistry* 37(6), 1517-1575.

Malmström, J. **(1999)**. Unguisins A and B: New cyclic peptides from the marine-derived fungus *Emericella unguis*. *Journal of Natural Products* 62, 787-789.

Malmström, J., Christophersen, C., Barrero, A.F., Oltra, J.E., Justicia, J., Rosales, A. **(2002b)**. Bioactive metabolites from a marine-derived strain of the fungus *Emericella variecolor*. *Journal of Natural Products* 65, 364-367.

Malmström, J., Ryager, A., Anthoni, U., Nielsen, P.H. **(2002a)**. Unguisin C, a GABA-containing cyclic peptide from the fungus *Emericella unguis*. *Phytochemistry* 60, 869-872.

Manojlović, N.T., Solujić, S., Sukdolak, S., Krstić, L.J. **(2000)**. Isolation and antimicrobial activity of anthraquinones from some species of the lichen genus *Xanthoria*. *Journal of the Serbian Chemical Society* 65(8), 555-560.

Marchelli, R., Dossena, A., Pochini, A., Dradi, E. **(1977)**. The structures of five new didehydropeptides related to neoechinulin, isolated from *Aspergillus amstelodami*. *Journal of the Chemical Society Perkin Transactions 1* 7, 713-717.

MARTINDALE **(2012)** The Complete Drug Reference (database on the internet). Thomson MICROMEDEX Drug Information, 2012, Truven Health

Analytics. Available at: www.micromedex.com. Accessed December 1, 2013. Micromedex Health Care, Martindale-The Complete Drug Reference (www.micromedex.com).

Martins, M.B., Carvalho, I. **(2007)**. Diketopiperazines: biological activity and synthesis. *Tetrahedron* 63, 9923-9932.

Maruyama, K., Ohuchi, T., Yoshida, K., Shibata, Y., Sugawara, F., Arai, T. **(2004)**. Protective properties of neoechinulin A against SIN-1-induced neuronal cell death. *The Journal of Biochemistry* 136, 81-87.

Masaldan, S., Iyer, V.V. **(2014)**. Exploration of effects of emodin in selected cancer cell lines: enhanced growth inhibition by ascorbic acid and regulation of LRP1 and AR under hypoxia-like conditions. *Journal of Applied Toxicology* 34, 95-104.

Masi, M., Andolfi, A., Mathieu, V., Boari, A., Cimmino, A., Banuls, L.M.Y., Vurro, M., Kornienko, A., Kiss, R., Evidente, A. **(2013)**. Fischerindoline, a pyrroloindole sesquiterpenoid isolated from *Neosartorya pseudofischeri*, with *in vitro* growth inhibitory activity in human cancer cell lines. *Tetrahedron* 69, 7466-7470.

Mayer, A.M.S, Rodríguez, A.D., Taglialatela-Scafati, O., Fusetani, N. **(2013)**. Marine Pharmacology in 2009-2011: Marine compounds with antibacterial, antidiabetic, antifungal, anti-inflammatory, antiprotozoal, antituberculosis, and antiviral activities; affecting the immune and nervous Systems, and other miscellaneous mechanisms of action. *Marine Drugs* 11, 2510-2573.

McGivern, J.G. **(2006)**. Targeting N-type and T-type calcium channels for the treatment of pain. *Drug Discovery Today* 11(5/6), 245-253.

McNeill, J., Turland, N.J., Monro, A.M., Lepschi, B.J. **(2011)**. XVIII International Botanical Congress: preliminary mail vote and report of congress action of nomenclature proposals. *Taxon* 60(5), 1507-1520.

Mendola, D. **(2000)**. Aquacultural production of bryostatin 1 and ecteinascidin 743. In: *Drugs from the sea* (Ed. Fusetani, N), Karger: Basel, 120-133.

Millward, M., Mainwaring, P., Mita, A., Federico, K., Lloyd, G.K., Reddinger, N., Nawrocki, S., Mita, M., Spear, M.A. **(2012)**. Phase 1 study of the novel vascular disrupting agent plinabulin (NPI-2358) and docetaxel. *Investigational New Drugs* 30, 1065-1073.

Mita, M.M., Spear, M.A., Yee, L.K., Mita, A.C., Heath, E.I., Papadopoulos, K.P., Federico, K.C., Reich, S.D., Romero, O., Malburg, L., Pilat, M., Lloyd, G.K., Neuteboom, S.T.C., Cropp, G., Ashton, E., LoRusso, P.M. **(2010)**. Phase 1 first-in-human trial of the vascular disrupting agent plinabulin (NPI-2358) in patients with solid tumors or lymphomas. *Clinical Cancer Research* 16(23), 5892-5899.

Mhaske, S.B., Argade, N.P. **(2006)**. The chemistry of recently isolated naturally occurring quinazolinone alkaloids. *Tetrahedron* 62(42), 9787-9826.

Miyake, Y., Ito, C., Tokuda, H., Osawa, T., Itoigawa, M. **(2010)**. Evaluation of flavoglaucin, its derivatives and pyranonigrins produced by molds used in fermented foods for inhibiting tumor promotion. *Bioscience, Biotechnology and Biochemistry* 74(5), 1120-1122.

Mohamed, I.E., Gross, H., Pontius, A., Kehraus, S., Krick, A., Kelter, G., Maier, A., Fiebig, H.-H., König, G.M. **(2009)**. Epoxyphomalin A and B, prenylated polyketides with potent cytotoxicity from the marine-derived fungus *Phoma* sp.. *Organic Letters* 11(21), 5014-5017.

Mohamed, I.E., Kehraus, S., Krick, A., König, G.M., Kelter, G., Maier, A., Fiebeg, H.-H., Kalesse, M., Malek, N.P., Gross, H. **(2010)**. Mode of action of epoxyphomalins A and B and characterization of related metabolites from the marine-derived fungus *Paraconiothyrium* sp.. *Journal of Natural Products* 73, 2053-2056.

Molinski, T.F. **(2010)**. NMR of natural products at the “nanomole-scale”. *Natural Product Reports* 27, 321-329.

Moosophon, P., Kanokmedhakul, S., Kanokmedhakul, K., Soytong, K. **(2009)**. Prenylxanthones and a bicycle[3.3.1]nona-2,6-diene derivative from the fungus *Emericella rugulosa*. *Journal of Natural Products* 72, 1442-1446.

Mora, C., Tittensor, D.P., Adl, S., Simpson, A.G.B., Worm, B. **(2011)**. How many species are there on Earth and in the Ocean? *Public Library of Science, Biology* 9(8), 1-8.

Morino, T., Nishimoto, M., Itou, N., Nishikiori, T. **(1994)**. NK372135s, novel antifungal agents produced by *Neosartorya fischeri*. *The Journal of Antibiotics* 47(12), 1546-1548.

Nagasawa, H., Isogai, A., Ikeda, K., Sato, S., Murakoshi, S., Suzuki, A., Tamura, S. **(1975)**. Isolation and structure elucidation of a new indole metabolite from *Aspergillus ruber*. *Agricultural and Biological Chemistry* 39(9), 1901-1902.

Nakano, H., Schrader, K.K., Mamonov, L.K., Kustova, T.S., Mursaliyeva, V.K., Cantrell, C.L. **(2012)**. Isolation and identification of *Flavobacterium columnare* and *Streptococcus iniae* antibacterial compounds from the terrestrial plant *Atraphaxis laetevirens*. *Journal of Agricultural and Food Chemistry* 60, 10415-10419.

Nam, K.S., Jo, Y.S., Kim, Y.H., Hyun, J.W., Kim, H.W. **(2001)**. Cytotoxic activities of acetoxyscirpenediol and ergosterol peroxide from *Paecilomyces tenuipes*. *Life Sciences* 69, 229-237.

Negishi, S., Cai-Huang, Z., Hasumi, K., Murakawa, S., Endo, A. **(1986)**. Productivity of molacolin K (mevilonin) in the genus Monascus. *Hakko Kogaku Kaishi* 64, 509-512.

Newman, D.J., Cragg, G.M. **(2012)**. Natural products as sources of new drugs over the 30 years from 1981 to 2010. *Journal of Natural Products* 75(3), 311-335.

Newman, D.J., Hill, R.T. **(2006)**. New drugs from marine microbes: the tide is turning. *Journal of Industrial Microbiology and Biotechnology* 33, 539-544.

Nicolaou, K.C., Hale, C.R.H., Nilewski, Ioannidou, H.A. **(2012)**. Constructing molecular complexity and diversity: total synthesis of natural products of biological and medicinal importance. *Chemical Society Reviews* 41, 5185-5238.

Nielsen, J., Nielsen, P.H., Frisvad, J.C. **(1999)**. Fungal depside, guisinol, from a marine derived strain of *Emericella unguis*. *Phytochemistry* 50, 263-265.

Nomura, H., Isshiki, Y., Sakuda, K., Sakuma, K., Kondo, S. **(2012)**. The antibacterial activity of compounds isolated from Oakmoss against *Legionella pneumophila* and other *Legionella* spp.. *Biological & Pharmaceutical Bulletin* 35(9), 1560-1567.

Nozawa, K., Nakajima, S., Kawai, K. **(1988)**. Studies on fungal products. Part 17. Isolation and structures of novel indoloditerpenes, emindoles DA and DB, from *Emericella desertorum*: X-ray molecular structure of emindole DA acetate. *Journal of the Chemical Society Perkin Transactions 1*, 1689-1694.

Nozawa, K., Seyea, H., Nakajima, S., Udagawa, S., Kawai, K. **(1987a)**. Studies on fungal products. Part 10. Isolation and structures of novel bicoumarins, desertorins A, B, and C, from *Emericella desertorum*. *Journal of the Chemical Society Perkin Transactions 1*, 1735-1738.

Nozawa, K., Udagawa, S., Nakajima, S., Kawai, K. **(1987b)**. Studies on fungal products. XIV. Emestin B, a new epitrithiodioxopiperazine, from *Emericella striata*. *Chemical & Pharmaceutical Bulletin* 35(8), 3460-3463.

Nuijen, B., Bouma, M., Manada, C., Jimeno, J.M., Schellens, J.H.M., Bult, A., Beijnen, J.H. **(2000)**. Pharmaceutical development of anticancer agents derived from marine sources. *Anti-Cancer Drugs* 11, 793-811.

Nursid, M., Chasanah, E., Murwantoko, Wahyuono S. **(2011)**. Isolation and identification of emestrin from *Emericella nidulans* and investigation of its anticancer properties. *Microbiology Indonesia* 5(4), 160-169.

Odds, F.C. **(2003)**. Synergy, antagonism, and what the chequerboard puts between them. *Journal of Antimicrobial Chemotherapy* 52(1), 1.

Ogasawara, N., Kawai, K. **(1998)**. Hydrogenated azaphilones from *Emericella falconensins* and *E. fruticulosa*. *Phytochemistry* 47(6), 1131-1135.

Ogasawara, N., Mizuno, R., Kawai, K. **(1997)**. Structures of a new type of yellow pigments, falconensones A and B, from *Emericella falconensis*. *Journal of the Chemical Society Perkin Transactions 1*, 2527-2530.

Oh, D.-C., Kauffman, C.A., Jensen, P.R., Fenical, W. **(2007)**. Induced production of emericellamides A and B from the marine-derived fungus *Emericella* sp. in competing co-culture. *Journal of Natural Products* 70(4), 515-520.

Ok, S., Kim, S.-M., Kim, C., Nam, D., Shim, B.S., Kim, S.-H., Ahn, K.S., Choi, S.-H., Ahn, K.S. **(2012)**. Emodin inhibits invasion and migration of prostate and lung cancer cells by downregulation the expression of chemokine receptor CXCR4. *Immunopharmacology and Immunotoxicology* 34(5), 768-778.

Olivera, B.M. **(2000)**. ω-Conotoxin MVIIA: from marine snail venom to analgesic drug. In: *Drugs from the sea* (Ed. Fusetani, N.), Krager: Basel, 74-85.

Ooike, M., Nozawa, K., Kawai, K. **(1997)**. An epitetrathiodioxopiperazine related to emestrin from *Emericella foveolata*. *Phytochemistry* 46(1), 123-126.

Ovenden, S.P.B., Sberna, G., Tait, R.M., Wildman, H.G., Patel, R., Li, B., Steffy, K., Nguyen, N., Muerer-Grimes, B.M. **(2004)**. A diketopiperazine dimer from a marine-derived isolate *Aspergillus niger*. *Journal of Natural Products* 67, 2093-2095.

Ozoe, Y., Kuriyama, T., Tachibana, Y., Harimaya, K., Takahashi, N., Yaguchi, T., Suzuki, E., Imamura, K., Oyama, K. **(2004)**. Isocoumarin derivative as a novel GABA receptor ligand from *Neosartorya quadricincta*. *Journal of Pesticide Science* 29(4), 328-331.

Pan, C.-J., Wang, J., Huang, N. **(2010)**. Preparation, characterization and in vitro anticoagulation of emodin-eluting controlled biodegradable stent coatings. *Colloids and Surfaces B: Biointerfaces* 77, 155-160.

Pettit, G.R., Hogan, F., Xu, J.-P., Tan, R., Nogawa, T., Cichacz, Z., Pettit, R.K. **(2008)**. Antineoplastic agents. 536. New sources of naturally occurring cancer cell growth inhibitors from marine organisms, terrestrial plants, and microorganisms. *Journal of Natural Products* 71, 438-444.

Pettit, G.R., Kamano, Y., Herald, C.L., Tuinman, A.A., Boettner, F.E., Kizu, H., Schmidt, J.M., Baczynskyj, L., Tomer, K.B., Bontems, R.J. **(1987)**. The isolation and structure of a remarkable marine animal antineoplastic constituent: dolastatin 10. *Journal of the American Chemical Society* 109(22), 6883-6885.

Pettit, R.K. **(2011)**. Culturability and secondary metabolite diversity of extreme microbes: expanding contribution of deep sea and deep-sea vent microbes to natural product discovery. *Marine Biotechnology* 13, 1-11.

Podojil, M., Sedmera, P., Vokoun, J., Betina, V., Baráthová, H. Ďuračková, Z., Horáková, K., Nemec, P. **(1979)**. *Eurotium* (*Aspergillus*) *repens* metabolites and their biological activity. *Folia Microbiologica* 23, 438-443.

Pope, J.E., Deer, T.R. **(2013)**. Ziconotide: a clinical update and pharmacologic review. *Expert Opinion in Pharmacotherapy* 14(7), 957-966.

Potts, B.C., Albitar, M.X., Anderson, K.C., Baritaki, S., Berkers, C., Bonavida, B., Chandra, J., Chauhan, D., Cusack, J.C., Fenical, W., Ghobrial, I.M., Groll, M., Neuteboom, S.T.C., Oki, Y., Ovaa, H., Pajonk, F., Richardson, P.G., Roccaro, A.M., Sloss, C.M., Spear, M.A., Valashi, E., Younes, A., Palladino, M.A. **(2011)**. Marizomib, a proteasome inhibitor for all seasons: preclinical profile and a framework for clinical trials. *Current Cancer Drug Targets* 11(3), 254-284.

Proksa, B., Uhrín, D., Liptaj, T., Šturdíková, M. **(1998)**. Neosartorin, an ergochrome biosynthesized by *Neosartorya fischeri*. *Phytochemistry* 48(7), 1161-1164.

Proksch, P., Putz, A., Ortlepp, S., Kjer, J., Bayer, M. **(2010)**. Bioactive natural products from marine sponges and fungal endophytes. *Phytochemistry Reviews* 9, 475-489.

Puri, S.C., Verma, V., Amna, T., Qazi, G.N., Spiteller, M. **(2005)**. An endophytic fungus from *Nothapodytes foetida* that produces camptothecin. *Journal of Natural Products* 68(12), 1717-1719.

Qiu, X., Zhang, J., Huang, Z., Zhu, D., Xu, W. **(2013)**. Profiling of phenolic constituents in *Polygonum multiflorum* Thunb. by combination of ultra-high-pressure liquid chromatography with linear ion trap-orbitrap mass spectrometry. *Journal of Chromatography A* 1292, 121-131.

Rahbaek, L., Sperry, S., Piper, J.E., Crews, P. **(1998)**. Deoxynortichoharzin, a new polyketide from the saltwater culture of a sponge-derived *Paecilomyces* fungus. *Journal of Natural Products* 61, 1571-1573.

Raistrick, H., Robinson, R., Todd, A.R. **(1933)**. CLVII. Studies in The biochemistry of micro-organisms. XXXII. Cynodontin (1:4:5:8-Tetrahydroxy-2-methylanthraquinone), a metabolic product of *Helminthosporium cynodontis* Marignoni and *Helminthosporium euchlaenae* Zimmermann. *Biochemical Journal* 27(4), 1170-1175.

Raistrick, H., Robinson, R., Todd, A.R. **(1934)**. LXXIX. Studies in the biochemistry of micro-organisms. XXXVII. (a) On the production of hydroxyanthraquinones by species of *Helminthosporium*. (b) Isolation of tritisporin, a new metabolic product of *Helminthosporium tritici-vulgaris* Nisikado. (c) The molecular constitution of catenarin. *Biochemical Journal* 28(2), 559-572.

Rajendran, M., Gandhidasan, R., Murugesan R. **(2004)**. Photosensitisation and photoinduced DNA cleavage by four naturally occurring anthraquinones. *Journal of Photochemistry and Photobiology A: Chemistry* 168, 67-73.

Raju, R., Piggott, A.M., Conte, M., Aalbersberg, W.G.L., Feussner, K., Capon, R.J. **(2009)**. Naseseazines A and B: a new dimeric diketopiperazine framework from a marine-derived *Actinomycete*, *Streptomyces* sp.. *Organic Letters* 11, 3862-3865.

Ramos-Ligonio, A., López-Monteon, A., Trigos, Á. **(2012)**. Trypanocidal activity of ergosterol peroxide from *Pleurotus ostreatus*. *Phytotherapy Research* 26, 938-943.

Rateb, M.E., Ebel, R. **(2011)**. Secondary metabolites of fungi from marine habitats. *Natural Product Reports* 28, 290-344.

Rateb, M.E., Hallyburton, I., Houssen, W.E., Bull, A.T., Goodfellow, M., Santhanam, R., Jaspars, M., Ebel, R. **(2013)**. Induction of diverse secondary metabolites in *Aspergillus fumigatus* by microbial co-culture. *RSC Advances* 3, 14444-14450.

Rath, C.M., Janto, B., Earl, J., Ahmed, A., Hu, F.Z., Hiller, L., Dahlgren, M., Kreft, R., Yu, F., Wolff, J.J., Kweon, H.K., Christiansen, M.A., Håkansson, K., Williams, R.M., Ehrlich, G.D., Sherman, D.H. **(2011)**. Meta-omic characterization of the marine invertebrate microbial consortium that produces the chemotherapeutic natural product ET-743. *ACS Chemical Biology* 6, 1244-1256.

Rauck, R.L., Wallace, M.S., Burton, A.W., Kapural, L., North, J.M. **(2009)**. Intrathecal ziconotide for neuropathic pain: a review. *Pain Practice* 9(5), 327-337.

Rhee, Y.-H., Jeong, S.-J., Lee, H.-J., Lee, H.-J., Koh, W., Jung, J.H., Kim, S.-H., Sung-Hoon, K. **(2012)**. Inhibition of STAT3 signaling and induction of SHP1 mediate antiangiogenic and antitumor activities of ergosterol peroxide in U266 multiple myeloma cells. *BMC Cancer* 12, 28.

Rinehart Jr., K.L., Gloer, J.B., Hughes Jr., R.G., Renis, H.E., McGovren, J.P., Swynenberg, E.B., Stringfellow, D.A., Knentzel, S.L., Li, L.H. **(1981)**. Didemnins: antiviral and antitumor depsipeptides from a Caribbean tunicate. *Science* 212 (4497), 933-935.

Rinehart, K.L., Holt, T.G., Fregeau, N.L., Stroh, J.G., Keifer, P.A., Sun, F., Li, H.L., Martin, D.G. **(1990)**. Ecteinascidins 729, 743, 745, 759A, 759B, and 770: potent antitumor agents from the Caribbean tunicate *Ecteinascidia turbinata*. *The Journal of Organic Chemistry* 55(15), 4512-4515.

Rinehart, K.L., Holt, T.G., Fregeau, N.L., Stroh, J.G., Keifer, P.A., Sun, F., Li, H.L., Martin, D.G. **(1991)**. Ecteinascidins 729, 743, 745, 759A, 759B, and 770: potent antitumor agents from the Caribbean tunicate *Ecteinascidia turbinata* [Erratum to document cited in CA113(9):75189d]. *The Journal of Organic Chemistry* 56(4), 1676-1676.

Røssland, E., Langsrud, T., Granum, P.E., Sørhaug, T. **(2006)**. Production of antimicrobial metabolites by strains of *Lactobacillus* or *Lactococcus* co-cultured with *Bacillus cereus* in milk. *International Journal of Food Microbiology* 98(2), 193-200.

Rouhi, M. **(2003)**. Rediscovering natural products. *Chemical and Engineering News* 81(41), 77-91.

Russo, A., Cardile, V., Piovano, M., Caggia, S., Espinoza, C.L., Garbarino, J.A. **(2010)**. Pro-apoptotic activity of ergosterol peroxide and (22*E*)-ergosta-7,22-

dien-5α-hydroxy-3,6-dione in human prostate cancer cells. *Chemico-Biological Interactions* 184, 352-358.

Saleem, M., Ali., M.S., Hussain, S., Jabbar, A., Ashraf, M., Lee, Y.S. **(2007)**. Marine natural products of fungal origin. *Natural Product Reports* 24, 1142-1152.

Samson, R.A., Hong, S., Peterson, S.W., Frisvad, J.C., Varga, J. **(2007)**. Polyphasic taxonomy of *Aspergillus* section *Fumigati* and its teleomorph *Neosartorya*. *Studies in Mycology* 59, 147-203.

Schiff, P.B., Horwitz, S.B. **(1980)**. Taxol stabilizes microtubules in mouse fibroblast cells. *Proceeding of the National Academy of Sciences of the United States of America* 77, 1561-1565.

Seya, H., Nakajima, S., Kawai, K., Udagawa, S. **(1985)**. Structure and absolute configuration of emestrin, a new macrocyclic epidithiodioxopiperazine from *Emericella striata*. *Journal of the Chemical Society, Chemical Communications*. 117, 657-658.

Seya, H., Nozawa, K., Nakajima, S., Kawai, K., Udagawa, S. **(1986a)**. Studies on fungal products. Part 8. Isolation and structure of emestrin, a novel antifungal macrocyclic epidithiodioxopiperazine from *Emericella striata*. X-ray molecular structure of emestrin. *Journal of the Chemical Society Perkin Transactions 1* 109-116.

Seya, H., Nozawa, K., Udagawa, S., Nakajima, S., Kawai, K. **(1986b)**. Studies on fungal products IX. Dethiosecoemestrin, a new metabolite related to emestrin, from *Emericella striata*. *Chemical & Pharmaceutical Bulletin* 34(6), 2411-2416.

Sheldrick, G.M. **(1997a)**. *SHELXS-97*: program for the solution of crystal structures; University of Gottingen: Germany.

Sheldrick, G.M. **(1997b)**. *SHELXS-97*: program for the refinement of crystal structures; University of Gottingen: Germany.

Shaaban, K.A., Shaaban, M., Facey, P., Fotso, S., Frauendorf, H., Helmke, E., Maier, A., Fiebig, H.H., Laatsch, H. **(2008)**. Electrospray ionization mass spectra of piperazimycins A and B and *γ*-butyrolactones from a marine-derived *Streptomyces* sp.. *The Journal of Antibiotics* 61(12), 736-746.

Shen, M.-Y., Lin, Y.-P., Yang, B.-C., Jang, Y.-S., Chiang, C.-K., Mettling, C., Chen, Z.-W., Sheu, J.-R., Chang, C.L., Lin, Y.-L., Yang, W.-C. **(2012)**. Catenarin prevents type 1 diabetes in nonobese diabetic mice via inhibition of leukocyte migration involving the MEK6/p38 and MEK7/JNK pathways. *Evidence-Based Complementary and Alternative Medicine* 1-13.

Shieh, D.-E., Chen, Y.-Y., Yen, M.-H., Chiang, L.-C., Lin, C.-C. **(2004)**. Emodin-induced apoptosis through p53-dependent pathway in human hepatoma cells. *Life Sciences* 74, 2279-2290.

Simmons, T.L., Coates, R.C., Clark, B.R., Engene, N., Gonzalez, D., Esquenazi, E., Dorrestein, P.C., Gerwick, W.H. **(2008)**. Biosynthetic origin of natural products isolated from marine microorganism-invertebrate assemblages. *Proceedings of the National Academy of Sciences of the United States of America* 105(12), 4587-4594.

Skehan, P., Storeng, R., Scudiero, D., Monks, A., McMahon, J., Vistica, D., Warren, J.T., Bokesch, H., Kenney, S., Boyd, M.R. **(1990)**. New colorimetric cytotoxicity assay for anticancer-drug screening. *Journal of the National Cancer Institute* 82(13), 1107-1112.

Slack, G.J., Puniani, E., Frisvad, J.C., Samson, R.A., Miller, J.D. **(2009)**. Secondary metabolites from *Eurotium* species, *Aspergillus calidoustus* and *A. insuetus* common in Canadian homes with a review of their chemistry and biological activities. *Mycological Research* 113, 480-490.

Smetanina, O.F., Kalinovskii, A.I., Khudyakova, Y.V., Slinkina, N.N., Pivkin, M.V., Kuznetsova, T.A. **(2007)**. Metabolites from the marine fungus *Eurotium repens*. *Chemistry of Natural Compounds* 43(4), 395-398.

Sochting, U., Frödén, P. **(2002)**. Chemosyndromes in the lichen genus *Teloschistes* (Teloschistaceae, Lecanorales). *Mycological Progress* 1(3), 257-266.

Sohn, J.H., Lee, Y.-R., Lee, D.-S., Kim, Y.-C., Oh, H. **(2013)**. PTP1B Inhibitory secondary metabolites from marine-derived fungal strains *Penicillium* spp. and *Eurotium* sp.. *Journal of Microbiology and Biotechnology* 23(9), 1206-1211.

Son, B.W., Jensen, P.R., Kauffman, C.A., Fenical, W. **(1999)**. New cytotoxic epidithiodioxopiperazines related to verticillin A from a marine isolate of the fungus *Penicillium*. *Natural Product Letters* 13, 213-222.

Staats, P.S., Yearwood, T., Charapata, S.G., Presley, R.W., Wallace, M.S., Byas-Smith, M., Fisher, R., Bryce, D.A., Mangieri, E.A., Luther, R.R., Mayo, M., McGuire, D., Ellis, D. **(2004)**. Intrathecal ziconotide in the treatment of refractory pain in patients with cancer or AIDS: a randomized controlled trial. *The Journal of the American Medical Association* 291(1), 63-70.

Stierle, A., Strobel, G., Stierle, D. **(1993)**. Taxol and taxane production by *Taxomyces andreanae*, an endophytic fungus of Pacific yew. *Science* 260(5105), 214-216.

Suárez, Y., Fernández, C., Ledo, B., Ferruelo, A.J., Martín, M., Vega, M.A., Gómez-Coronado, D., Lasunción, M.A. **(2002)**. Differential effects of ergosterol and cholesterol in Cdk1 activation and SRE-driven transcription. *European Journal of Biochemistry* 269(6), 1761-1771.

Subbiah, R.M.T., Abplanalp, W. **(2003)**. Ergosterol (major sterol of baker's and brewer's yeast extracts) inhibits the growth of human breast cancer cells *in vitro* and the potential role of its oxidation products. *International Journal for Vitamin and Nutrition Research* 73(1), 19-23.

Suemitsu, R., Iwai, J., Kawaguchi, K., Haitani, N., Kitagawa, N. **(1977)**. Isolation and identification of erythroglaucin (1,4,5-Tryhydroxy-7-methoxy-2-methylanthraquinone) from the mycelium of *Alternaria porri* (Ellis) Ciferri. *Agricultural and Biological Chemistry* 41(11), 2289-2290.

Sun, F.-Y., Chen, G., Bai, J., Li, W., Pei, Y.-H. **(2012)**. Two new alkaloids from a marine-derived fungus *Neosartorya* sp. HN-M-3. *Journal of Asian Natural Products Research* 14(12), 1109-1115.

Takahashi, H., Hosoe, T., Nozawa, K., Kawai, K. **(1999)**. Two new sesterterpenes from the Ascomycetous fungus *Emericella purpurea*. *Journal of Natural Products* 62, 1712-1713.

Takahashi, N., Iwahori, A., Kawai, K., Fukui, T. **(1998)**. Induction of differentiation in human promyelocytic leukemia cell line HL60 by a new type of polyenes, falconensone A and its derivatives. *Archives of Biochemistry and Biophysics* 360(1), 113-120.

Takahashi, C., Minoura, K., Yamada, T., Numata, A., Kushida, K., Shingu, T., Hagishita, S., Nakai, H., Sato, T., Harada, H. **(1995b)**. Potent cytotoxic metabolites from a *Leptosphaeria* species. Structure determination an conformational analysis. *Tetrahedron* 51, 3483-3498.

Takahashi, H., Nozawa, K., Kawai, K. **(1996)**. Isolation and structures of dicyanide derivatives, epurpurins A to C, from *Emericella purpurea*. *Chemical & Pharmaceutical Bulletin* 44(12), 2227-2230.

Takahashi, C., Numata, A., Ito, Y., Matsumura, E., Araki, H., Iwaki, H., Kushida, K. **(1994)**. Leptosins, antitumour metabolites of a fungus isolated from a marine alga. *Journal of the Chemical Society Perkin Transictions 1*, 1859-1864.

Takahashi, C., Takai, Y., Kimura, Y., Numata, A., Shigematsu, N., Tanaka, H. **(1995a)**. Cytotoxic metabolites from a fungal adherent of a marine alga. *Phytochemistry* 38, 155-158.

Takahashi, N., Tamagawa, K., Kawai, K., Fukui, T. **(2000)**. Antioxidant properties of a new type of polyene, falconensone A and its derivatives. *Biological & Pharmaceutical Bulletin* 23(8), 989-994.

Talapatra, S.K., Mandal, S.K., Bhaumik, A., Mukhopadhyay, S., Kar, P., Patra, A., Talapatra, B. **(2001)**. Echinulin, a novel cyclic dipeptide carrying a triprenylated indole moiety from an Anacardiaceae, a Cucurbitaceae and two Orchidaceae plants: detailed high resolution 2D-NMR and mass spectral studies. *Journal – Indian Chemical Society* 78, 773-778.

Tan, J., Bednarek, P., Liu, J., Schneider, B., Svatoš, A., Hahlbrock, K. **(2004)**. Universally occurring phenylpropanoid and species-specific indolic metabolites in infected and uninfected *Arabidopsis thaliana* roots and leaves. *Phytochemistry* 65, 691-699.

Tan, Q.-W., Ouyang, M.-A., Shen, S., Li, W. **(2012)**. Bioactive metabolites from a marine-derived strain of the fungus *Neosartorya fischeri*. *Natural Product Research* 26(15), 1402-1407.

Taylor, M.W., Radax, R., Steger, D., Wagner, M. **(2007)**. Sponge-associated microorganisms: evolution, ecology, and biotechnological potential. *Microbiology and Molecular Biology Reviews* 71(2), 295-347.

Thadani, V.M., Choudhary, M.I., Ali, S., Omar, I., Siddique, H., Karunaratne, V. **(2011)**. Antioxidant activity of some lichen metabolites. *Natural Product Research* 25(19), 1827-1837.

Thomas, T.R.A., Kavlekar, D.P., LokaBharathi, P.A. **(2010)**. Marine drugs from sponge-microbe association – a review. *Marine Drugs* 8, 1417-1468.

Thomas, X. **(2009)**. Chemotherapy of acute leukemia in adults. *Expert Opinion in Pharmacotherapy* 10(2), 221-237.

Tong, H., Chen, K., Chen, H., Wu, H., Lin, H., Ni, Z., Lin, S. **(2011)**. Emodin prolongs recipient survival time after orthotopic liver transplantation in rats by polarizing the Th1/Th2 paradigm to Th2. *The Anatomical Record* 294, 445-452.

Tuckey, R.C., Nguyen, M.N., Chen, J., Slominski, A.T., Baldisseri, D.M., Tieu, E.W., Zjawiony J.K., Li, W. **(2012)**. Human cytochrome P450scc (CYP11A1) catalyzes epoxide formation with ergosterol. *Drug Metabolism and Disposition* 40(3), 436-444.

Unson, M.D., Holland, N.D., Faulkner, D.J. **(1994)**. A brominated secondary metabolite synthesized by the cyanobacterial symbionts of a marine sponge and accumulation of the crystalline metabolite in the sponge tissue. *Marine Biology* 119, 1-11.

van Eijk, G.W. **(1973)**. Anthraquinones in the fungus *Talaromyces stipitatus*. *Experentia* 29(5), 522-523.

Varoglu, M., Corbett, T.H., Valeriote, F.A., Crews, P. **(1997)**. Asperazine, a selective cytotoxic alkaloid from a sponge-derived culture of *Aspergillus niger*. *The Journal of Organic Chemistry* 62, 7078-7079.

Verweij, J. **(2009)**. Soft tissue sarcoma trials: one size no longer fits all. *Journal of Clinical Oncology* 27(19), 3085-3087.

Vichai, V., Kirtikara, K. **(2006)**. Sulforhodamine B colorimetric assay for cytotoxicity screening. *Nature Protocols* 1, 1112-1116.

Waites, M.J., Morgan, N.L., Rockey, J.S., Higton, G. **(2001)**. Fermentation systems. In: *Industrial microbiology: an introduction*. Blackwell Science Ltd, 94-108.

Wakana, D., Hosoe, T., Itabashi, T., Nozawa, K., Okada, K., Takaki, G.M.C., Yaguchi, T., Fukushima, K., Kawai, K. **(2006)**. Isolation of isoterrein from *Neosartorya fischeri*. *Mycotoxins* 56(1), 3-6.

Wakuliński, W., Kachlicki, P., Sobiczewski, P., Schollenberger, M., Zamorski, C., Lotocka, B, Šarova, J. **(2003)**. Catenarin production by isolates of *Pyrenophora tritici-repentis* (Died.) Drechsler and its antimicrobial activity. *Journal of Phytopathology* 151, 74-79.

Walsh, C. **(2004)**. Antibiotics: actions, origins, resistance. Protein Science 13(11), 3059-3060.

Wang, W., Brandt, D., Thakur, N.L., Wiens, M., Batel, R., Schröder, H.C., Müller, W.E.G. **(2013)**. Molecular cross-talk between sponge host and associated microbes. *Phytochemistry Reviews* 12, 369-390.

Wang, R.-P., Lin, H.-W., Li, L.-Z., Gao, P.-Y., Xu, Y., Song, S.-J. **(2012)**. Monoindole alkaloids from a marine sponge *Mycale fibrexilis*. *Biochemical Systematics and Ecology* 43, 210-13.

Wang, S., Li, X.-M., Teuscher, F., Li, D.-L., Diesel, A., Ebel, R., Proksch, P., Wang, B.-G. **(2006)**. Chaetopyranin, a benzaldehyde derivative, and other related metabolites from *Chaetomium globosum*, an endophytic fungus derived from the marine red alga *Polysiphonia urceolata*. *Journal of Natural Products* 69, 1622-1625.

Wang, R., Wan, Q., Zhang, Y., Huang, F., Yu, K., Xu, D., Wang, Q., Sun, J. **(2007)**. Emodin suppresses interleukin-1β induced mesangial cells proliferation and extracellular matrix production via inhibiting P38 MAPK. *Life Sciences* 80, 2481-2488.

Watanabe, J., Tsugitaka, N., Motohiro, K. **(2007)**. Comparison of the antivascular and cytotoxic activites of TZT-1027 (Soblidotin) with those of other anticancer agents. *Anti-Cancer Drugs* 18(8), 905-911.

Wattanadilok, R., Sawangwong, P., Rodrigues, C., Cidade, H., Pinto, M., Pinto, E., Silva, A., Kijjoa, A. **(2007)**. Antifungal activity evaluation of the constituents of *Haliclona baeri* and *Haliclona cymaeformis*, collected from the Gulf of Thailand. *Marine Drugs* 5, 40-51.

Way, T.-D., Huang, J.-T., Chou, C.-H., Huang, C.-H., Yang, M.-H., Ho, C.-T. **(2014)**. Emodin represses TWIST1-induced epithelial-mesenchymal transitions in head and neck squamous cell carcinoma cells by inhibiting the β-catenin and Akt pathways. *European Journal of Cancer* 50, 366-378.

Wayne, P.A. **(2002a)**. National Committee for Clinical Laboratory Standards. Reference method for broth dilution antifungal susceptibility testing for yeasts: approved standard Document. M27-A2: *National Committee for Clinical Laboratory Standards*.

Wayne, P.A. **(2002b)**. National Committee for Clinical Laboratory Standards. Reference method for broth dilution antifungal susceptibility testing of filamentous fungi: approved standard Document. M37-A: *National Committee for Clinical Laboratory Standards*.

Wayne, P.A. **(2011)**. Clinical and Laboratory Standards Institute (CLSI). Performance standards for antimicrobial susceptibility testing, *Twenty-First Informational Supplement M100-S-21*, USA.

Wei, H., Itoh, T., Kinoshita, M., Kotoku, N., Aoki, S., Kobayashi, M. **(2005)**. Shimalactone A, a novel polyketide, from marine-derived fungus *Emericella variecolor* GF10. *Tetrahedron* 61, 8054-8058.

Wei, H., Itoh, T., Kinoshita, M., Nakai, Y., Kurotaki, M., Kobayashi, M. **(2004)**. Cytotoxic sesterterpenes, 6-epi-ophiobolin G and 6-epi-ophiobolin N, from marine derived fungus *Emericella variecolor* GF10. *Tetrahedron* 60, 6015-6019.

Wijesekara, I., Zhang, C., Ta, Q.V., Vo, T.-S., Li, Y.-X., Kim, S.-K. **(2014)**. Physcion from marine-derived fungus *Microsporum* sp. induces apoptosis in human cervical carcinoma HeLa cells. *Medicinal Extracts in Microbiology* 169(4), 255-261.

Williamson, R.T., Chapin, E.L., Carr, A.W., Gilbert, J.R., Graupner, P.R., Lewer, P., McKamey, P., Carney, J.R., Gerwick, W.H. **(2000)**. New diffusion-edited NMR experiments to expedite the dereplication of known compounds from natural product mixtures. *Organic Letters* 2(3), 289-292.

Wong, S.-M., Musza, L.L., Kydd, G.C., Kullnig, R., Gillum, A.M., Cooper, R. **(1992)**. Fiscalins: New substance P inhibitors produced by the fungus *Neosartorya fischeri*. *The Journal of Antibiotics* 46(4), 545-553.

Wright, A.E., Forleo, D.A., Gunawardana, G.P., Gunasekera, S.P., Koehn, F.E., McConnel, O.J. **(1990)**. Antitumor tetrahydroisoquinoline alkaloids from the colonial ascidian *Ecteinascidia turbinata*. *The Journal of Organic Chemistry* 55(15), 4508-4512.

Wu, M.-D., Cheng, M.-J., Chen, I.-S., Su, Y.-S., Hsieh, S.-Y., Chang, H.-S., Chang, C.-W., Yuan, G.-F. **(2013)**. Phytochemical investigation of *Annulohypoxylon ilanense*, an endophytic fungus derived from *Cinnamomum* species. *Helvetica Chimica Acta* 10, 493-505.

Wu, Q.-P., Xie, Y.-Z., Deng, Z., Li, X.-M., Yang, W., Jiao, C.-W., Fang, L., Li, S.-Z., Pan, H.-H., Yee, A.J., Lee, D.Y., Li, C., Zhang, Z., Guo, J., Yang, B.B. **(2012)**. Ergosterol peroxide isolated from *Ganoderma lucidum* abolishes microRNA miR-378-mediated tumor cells on chemoresistance. *Public Library of Science One* 7(8), e44579.

Xiong, Z.-Q., Wang, J.-F., Hao, Y.-Y., Wang, Y. **(2013)**. Recent advances in the discovery and development of marine microbial natural products. *Marine Drugs* 11, 700-717.

Xu, N., Cao, Y., Wang, L., Chen, G., Pei, Y.-H. **(2013b)**. New alkaloids from a marine-derived fungus *Neosartorya* sp. HN-M-3. *Journal of Asian Natural Products Research* 15(7), 731-736.

Xu, Y., Espinosa-Artiles, P., Liu, M.X., Arnold, E., Gunatilaka, A.A.L. **(2013a)**. Secoemestrin D, a cytotoxic epitetrathiodioxopiperazine, and emericellenes A-E, five sesterterpenoids from *Emericella* sp. AST0036, a fungal endophyte of *Astragalus lentiginosus*. *Journal of Natural Products* 76, 2330-2336.

Yagi, R., Do, M. **(1999)**. Isolation of an antioxidative substance produced by *Aspergillus repens*. *Bioscience, Biotechnology and Biochemistry* 63(5), 932-933.

Yamada, T., Iwamoto, C., Yamagaki, N., Yamanouchi, T., Minoura, K., Yamori, T., Uehara, Y., Andoh, T., Umemura, K., Numata, A. **(2002)**. Leptosins M-N_1, cytotoxic metabolites from a *Leptosphaeria* species separated from a marine alga. Structure determination and biological activities. *Tetrahedron* 58, 479-487.

Yamazaki, M., Fujimoto, H., Okuyama, E. **(1976)**. Structure determination of six tryptoquivaline-related metabolites from *Aspergillus fumigatus*. *Tetrahedron Letters* 33, 2861-2864.

Yamazaki, M., Fujimoto, H., Okuyama, E. **(1977)**. Structure of Tryptoquivaline C (FTC) and D (FTD). Novel fungal metabolites from *Aspergillus fumigatus*. *Chemical & Pharmaceutical Bulletin* 25(10), 2554-2560.

Yamazaki, M., Fujimoto, H., Okuyama, E. **(1978)**. Structure determination of six fungal metabolites, tryptoquivaline E, F, G, H, I and J from *Aspergillus fumigatus*. *Chemical & Pharmaceutical Bulletin*. 26(1), 111-117.

Yamazaki, M., Okuyama, E., Maebayashi, Y. **(1979)**. Isolation of some new tryptoquivaline-related metabolites from *Aspergillus fumigatus*. *Chemical & Pharmaceutical Bulletin* 27(7), 1611-1617.

Yan, H.-J., Li, X.-M., Li, C.-S., Wang, B.-G. **(2012)**. Alkaloid and anthraquinone derivatives produced by the marine-derived endophytic fungus *Eurotium rubrum*. *Helvetica Chimica Acta* 95, 163-168.

Yang, S.-J., Liu, M.-C., Liang, N., Xiang, H.-M., Yang, S. **(2013b)**. Chemical constituents of *Cyrtomium fortumei* (J.) Smith. *Natural Product Research* 27(21), 2066-2068.

Yang, Y., Yan, Y.-M., Wei, W., Luo, J., Zhang, L.-S., Zhou, X.-J., Wang, P.-C., Yang, Y.-X., Cheng, Y.-X. **(2013a)**. Anthraquinone derivatives from *Rumex* plants and endophytic *Aspergillus fumigatus* and their effects on diabetic nephropathy. *Bioorganic & Medicinal Chemistry Letters* 23, 3905-3909.

Yap, T.A., Carden, C.P., Kaye, S.B. **(2009)**. Beyond chemotherapy: targeted therapies in ovarian cancer. *Nature Reviews Cancer* 9, 167-181.

Yasuhara, K., Takahashi, M., Natori, S., Kawai, K., Yamazaki, M., Takeuchi, M., Takido, M. **(1994)**. Azaphilones inhibit tumor promotion by 12-O-tetradecanoylphorbol-13-acetate in two-stage carcinogenesis in mice. *Oncology* 51(1), 108-112.

Yazawa, Y., Yokota, M., Sugiyama, K. **(2000)**. Antitumor promoting effect of an active component of *Polyporus,* ergosterol and related compounds on rat urinary bladder carcinogenesis in a short-term test with concanavalin A. *Biological & Pharmaceutical Bulletin* 23(11), 1298-1302.

Yoganathan, K., Rossant, C., Glover, R.P., Cao, S., Vittal, J.J., Ng, S., Huang, Y., Buss, A.D., Butler, M.S. **(2004)**. Inhibition of the human chemokine receptor CCR5 by variecolin and variecolol and isolation of four new variecolin analogues, emericolins A-D, from *Emericella aurantiobrunnea*. *Journal of Natural Products* 67, 1681-1684.

Yu, J.-Q., Bao, W., Lei, J.-C. **(2013)**. Emodin regulates apoptotic pathway in human liver cancer cells. *Phytotherapy Research* 27, 251-257.

Yu, J.-H., Keller, N. **(2005)**. Regulation of secondary metabolism in filamentous fungi. *Annual Review of Phytopathology* 43, 437-458.

Yu, Z., Lang, G., Kajahn, I., Schmaljohann, R., Imhoff, J.F. **(2008)**. Scopularides A and B, cyclodepsipeptides from a marine sponge-derived fungus, *Scopulariopsis brevicaulis*. *Journal of Natural Products* 71, 1052-1054. (Patents: DE10200800097 (2009), EP2229401 (2010)).

Zengler, K., Toledo, G., Rappe, M., Elkins, J., Mathur, E.J., Short, J.M., Keller, M. **(2002)**. Cultivating the uncultured. *Proceedings of the National Academy of Sciences of the United States of America* 99(24), 15681-15686.

Zewail-Foote, M., Hurley, L.H. **(2001)**. Differential rates of reversibility of ecteinascidin 743-DNA covalent adducts from different sequences lead to migration to favored bonding sites. *Journal of the American Chemical Society* 123, 6485-6495.

Zhang, L., Hung, M.C. **(1996)**. Sensitization of HER-2/neu-overexpressing non-small cell lung cancer cells to chemotherapeutic drugs by tyrosine kinase inhibitor emodin. *Oncogene* 12, 571-576.

Zhang, L., Lau, Y.K., Xia, W., Hortobagyi, G.N., Hung, M.C. **(1999)**. Tyrosine kinase inhibitor emodin suppresses growth of HER-2/neu-overexpressing breast cancer cells in athymic mice and sensitizes these cells to the inhibitory effect of paclitaxel. *Clinical Cancer Research* 5, 343-353.

Zhang, W., Li, H., Bu, H., Chen, H., Tong, H., Liu, D., Guo, H., Lin, S. **(2012)**. Emodin inhibits the differentiation and maturation of dendritic cells and increases the production of regulatory T cells. *International Journal of Molecular Medicine* 29, 159-164.

Zhang, P., Su, L.-K., Li, H.-M., Zhao, Y.-C., Yang, Z.-Q., Cui, X.-Y. **(2005)**. Protective effects of physcion against cerebral injury induced by ischemia-reperfusion in rats. *Chinese Journal of Pathophysiology* 21(9), 1829-1833.

Zhang, G., Sun, S., Zhu, T., Lin, Z., Gu, J., Li, D., Gu, Q. **(2011)**. Antiviral isoindolone derivatives from an endophytic fungus *Emericella* sp. associated with *Aegiceras corniculatum*. *Phytochemistry* 1436-1442.

Zhao, W.K., Guo, Y., Yasuhiro, T., Tohru, K. **(1991)**. Isolation and structure determination of echinuline from *Veratrum nigrum* L. var. *ussuriense* Nakai. *China Journal of Chinese Materia Medica* 16(7), 425-426.

Zhou, Y., Debbab, A., Mándi, A., Wray, V., Schulz, B., Müller, W.E.G., Kassack, M., Lin, W., Kurtán, T., Proksch, P., Aly, A.H. **(2013)**. Alkaloids from the sponge-associated fungus *Aspergillus* sp.. *European Journal of Organic Chemistry* 894-906.

Zhou, L.-N., Zhu, T.-J., Cai, S.-X., Gu, Q.-Q., Li, D.-H. **(2010)**. Three new indole-containing diketopiperazine alkaloids from a deep-ocean sediment derived fungus *Penicillium griseofulvum*. *Helvetica Chimica Acta* 93, 1758-1763.

Zhu, R., Zheng, R., Deng, Y., Chen, Y., Zhang, S. **(2013)**. Ergosterol peroxide from *Cordyceps cicadae* ameliorates TGF-β1-induced activation of kidney fibroblasts. *Phytomedicine* (in press).

APPENDICES

APPENDIX I. NMR SPECTRA OF THE ISOLATED COMPOUNDS

I.1. Ergosterol (EV1)

I.1.1. ^{1}H NMR spectrum (300.13 MHz)

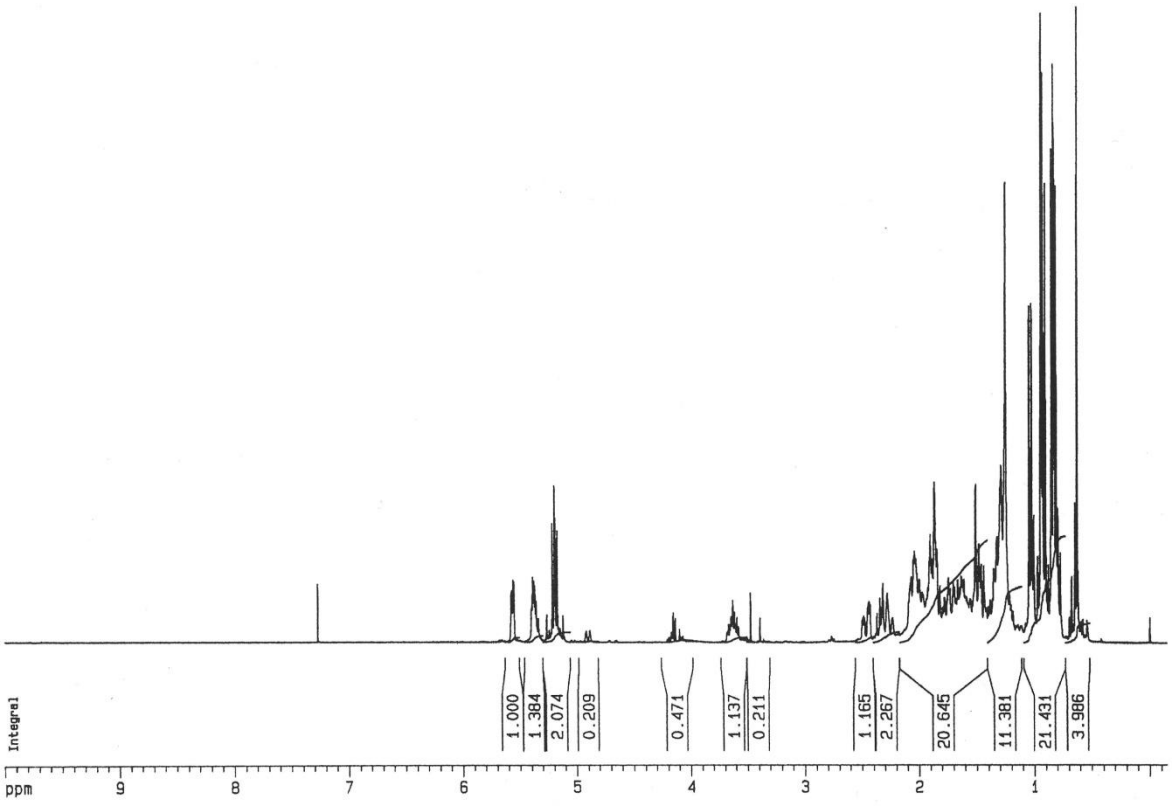

I.1.2. ^{13}C NMR spectrum (75.47 MHz)

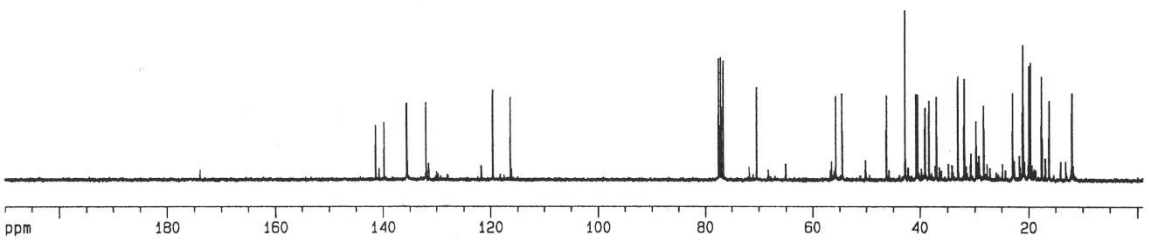

I.2. Ergosterol peroxide (EV2)

I.2.1. ^{1}H NMR spectrum (500.13 MHz)

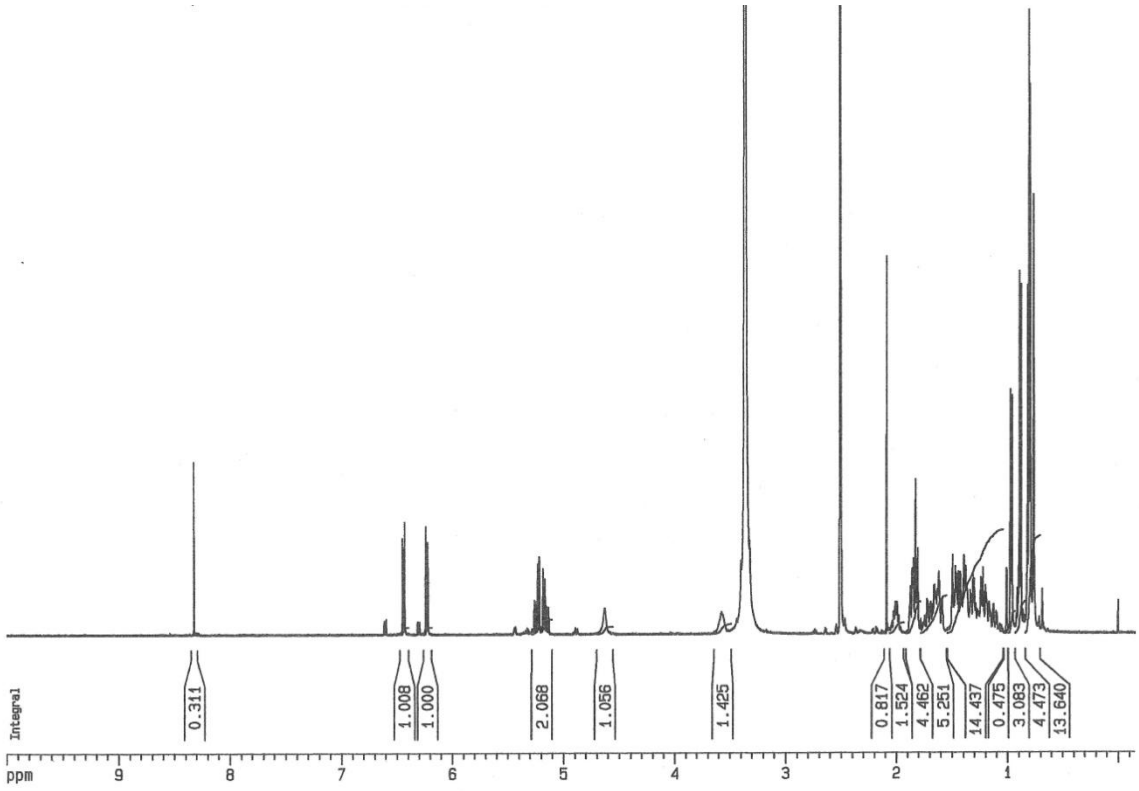

I.1.2. ^{13}C NMR spectrum (125.77 MHz)

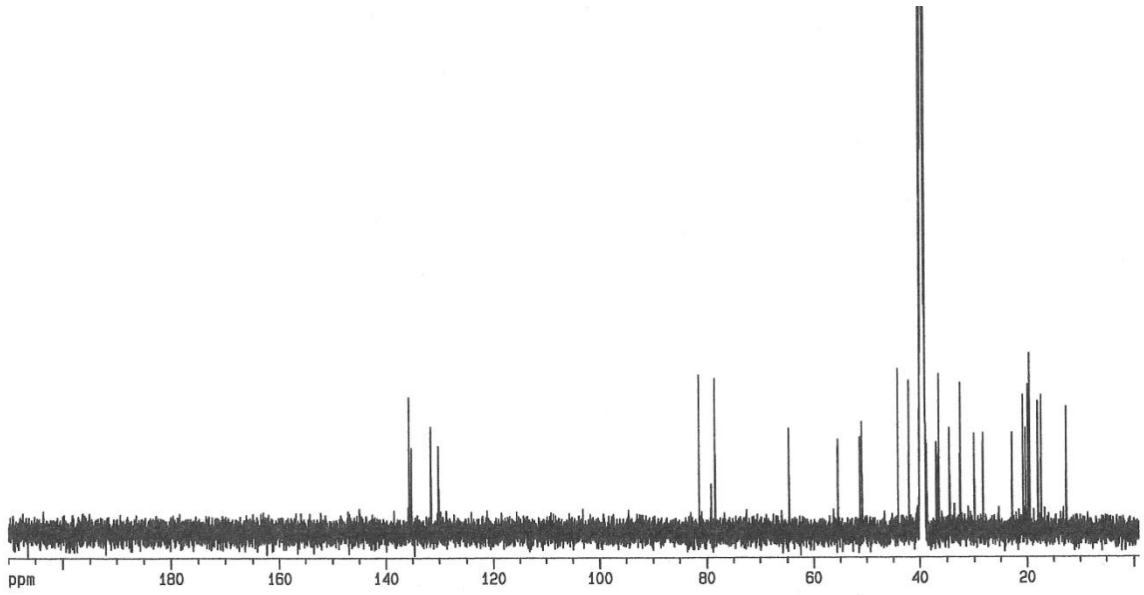

I.3. Orcinol (EV3)

I.3.1. ^{1}H NMR spectrum (300.13 MHz)

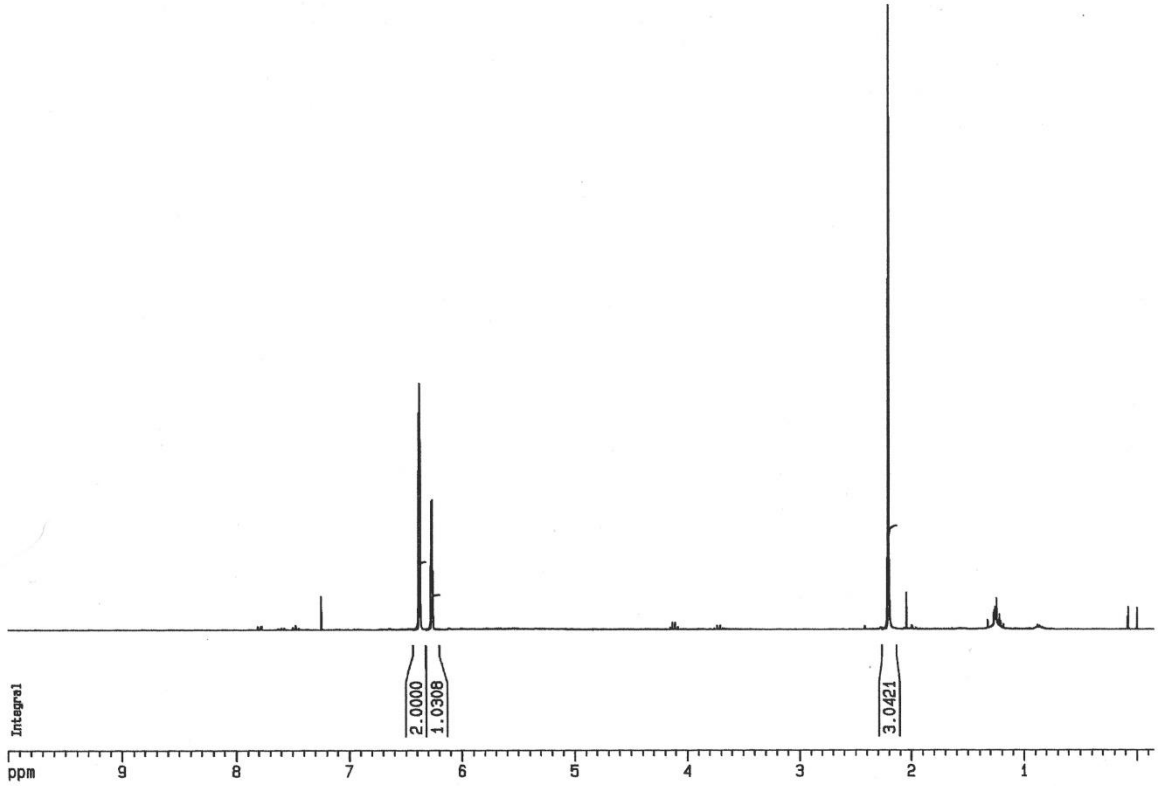

I.3.2. ^{13}C NMR spectrum (75.47 MHz)

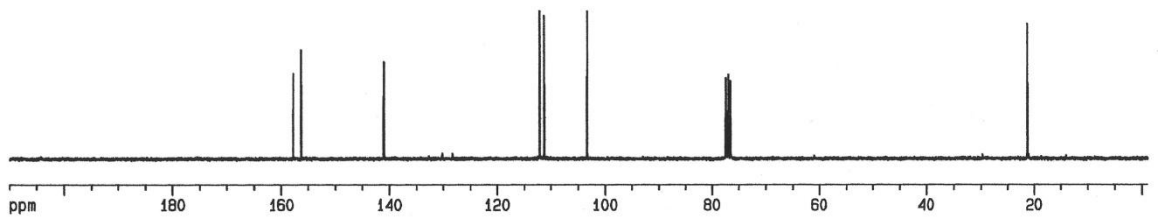

I.4. 1*H*-Indole-3-carboxylic acid (EV4)

I.4.1. ^{1}H NMR spectrum (500.13 MHz)

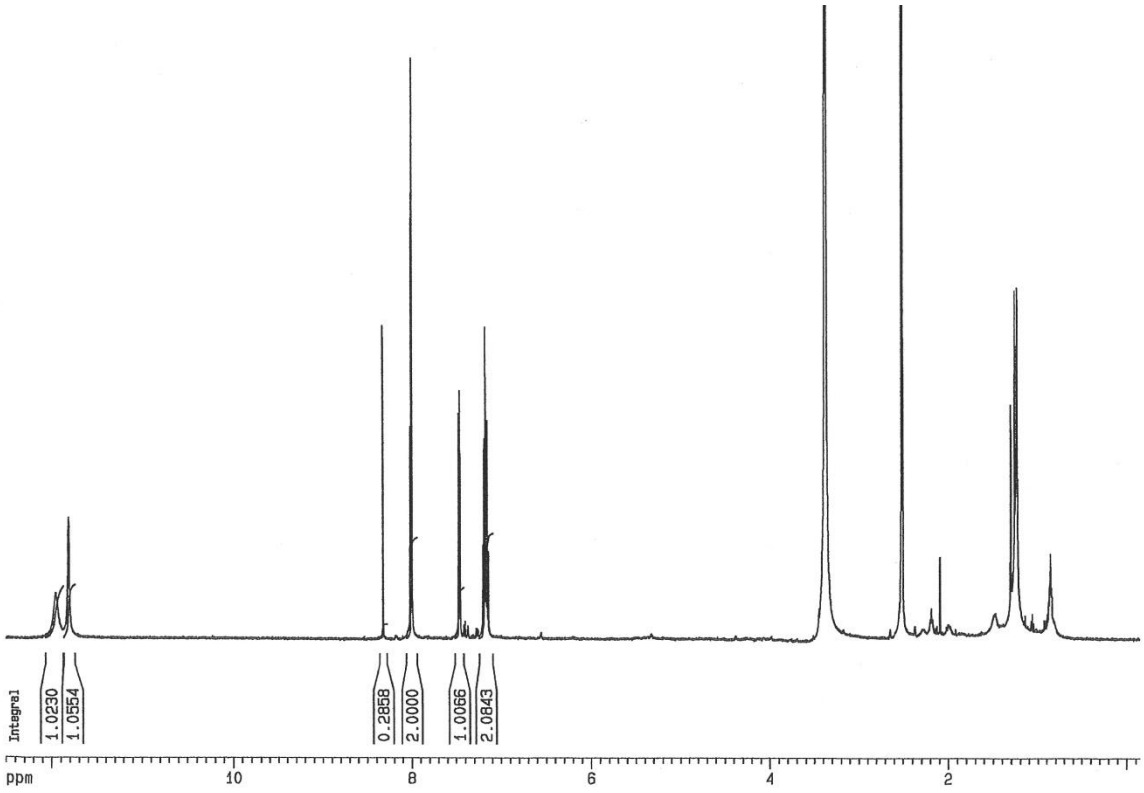

I.4.2. ^{13}C NMR spectrum (125.77 MHz)

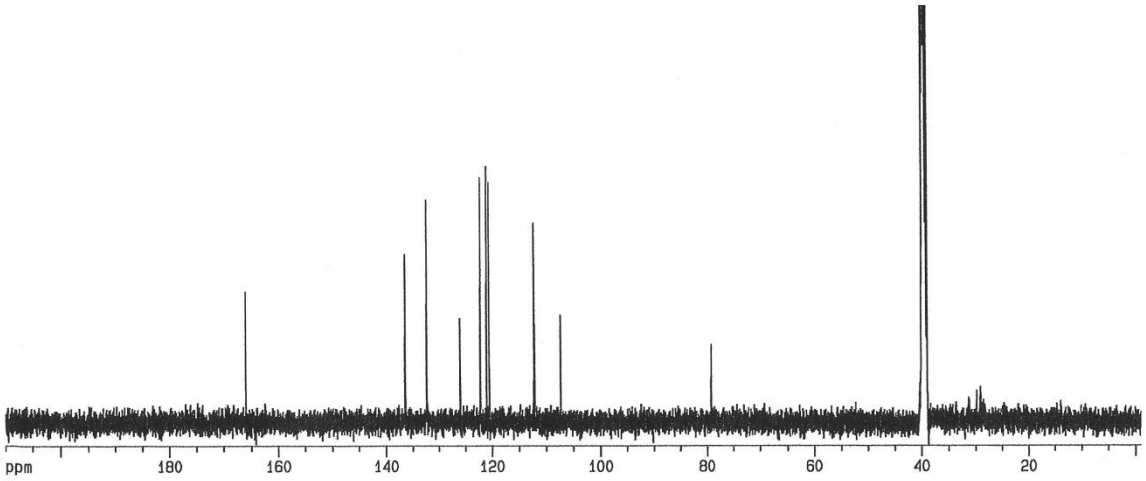

I.5. cyclo-(L-Tryptophyl-L-phenylalanyl) (EV5)

I.5.1. ^{1}H NMR spectrum (300.13 MHz)

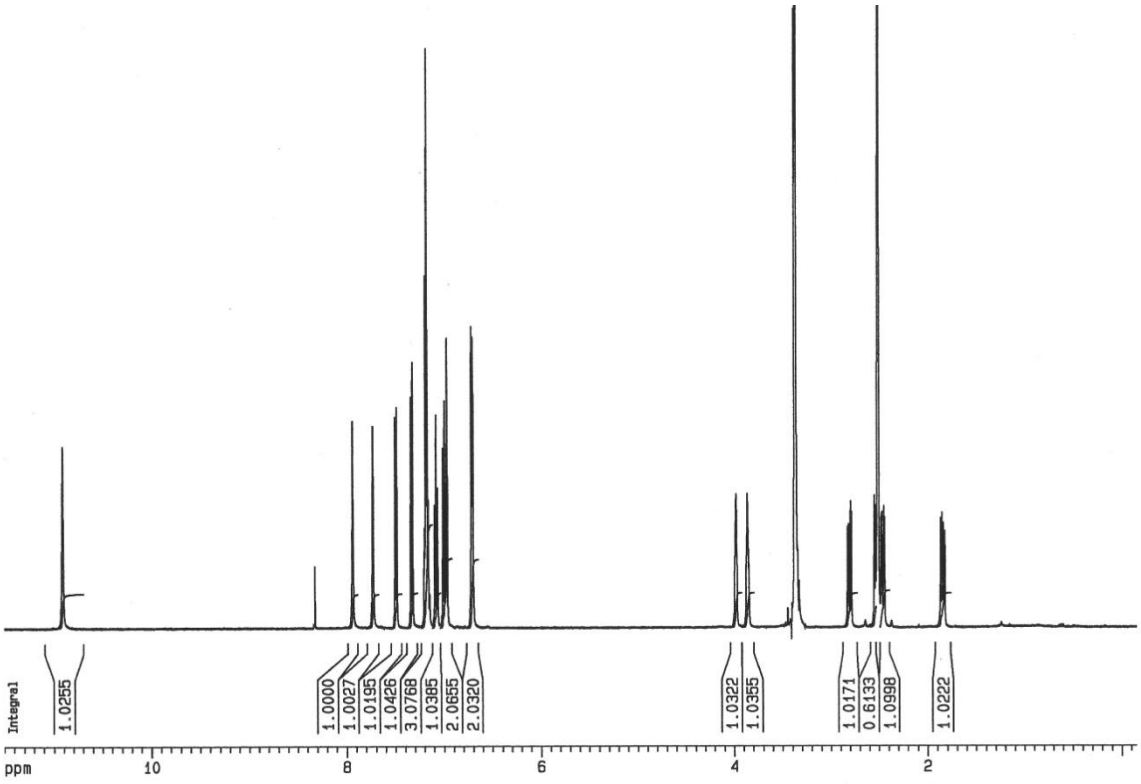

I.5.2. ^{13}C NMR spectrum (75.47 MHz)

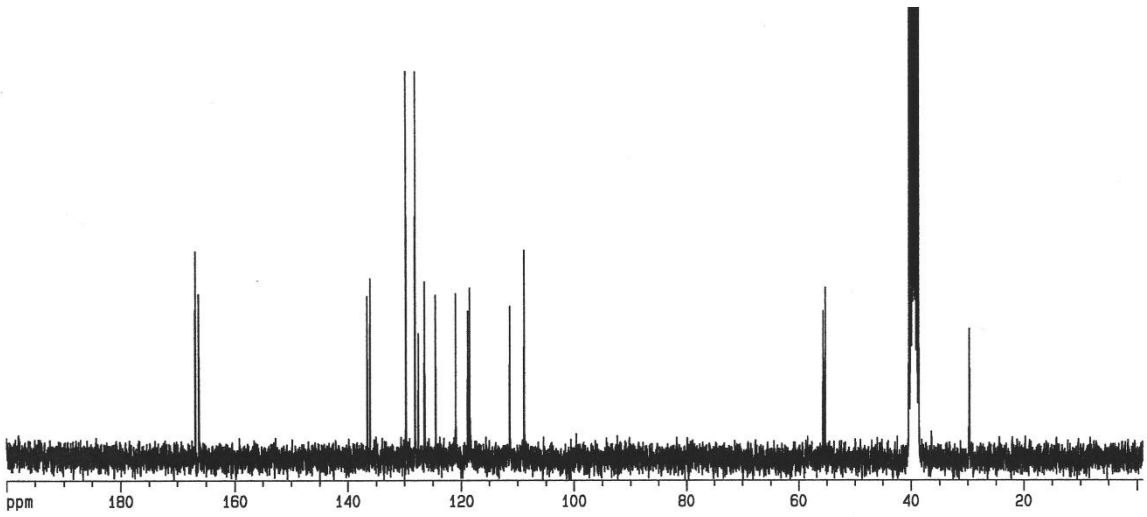

I.6. Erythroglaucin (EC1)

I.6.1. ^{1}H NMR spectrum (500.13 MHz)

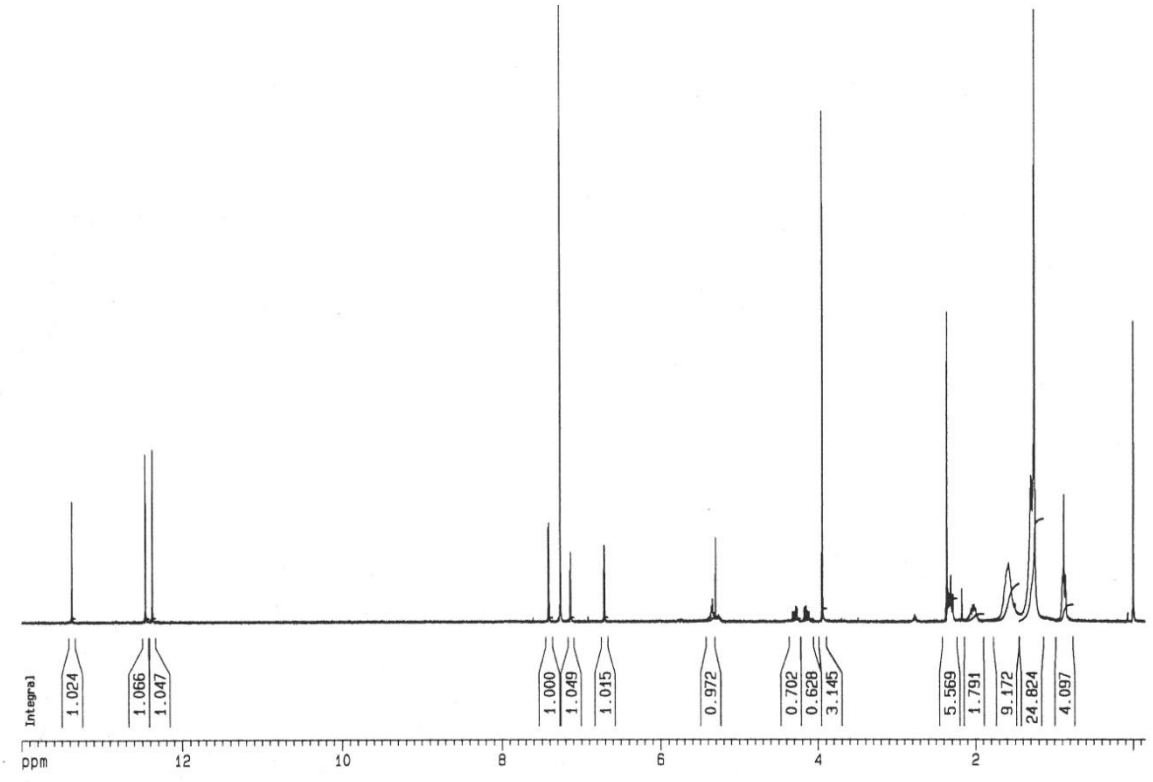

I.6.2. ^{13}C NMR spectrum (125.77 MHz)

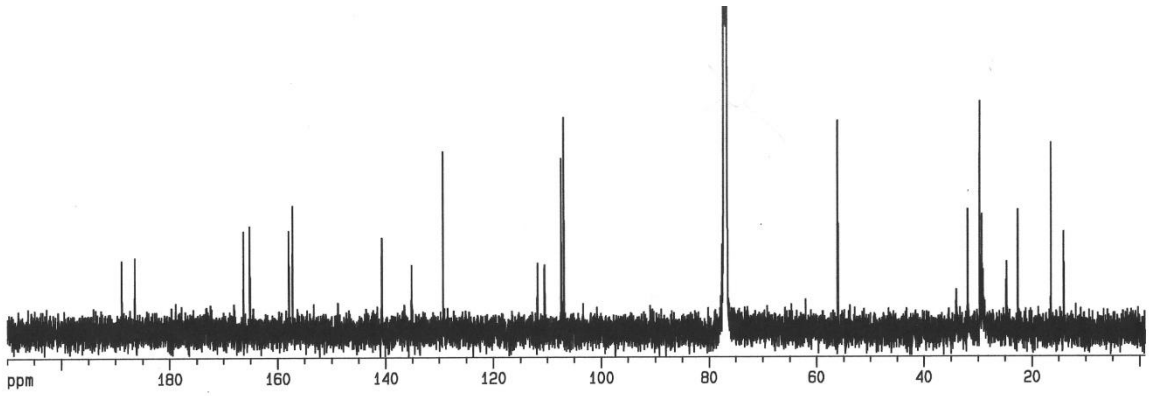

I.7. Physcion (EC2)

I.7.1. ^{1}H NMR spectrum (500.13 MHz)

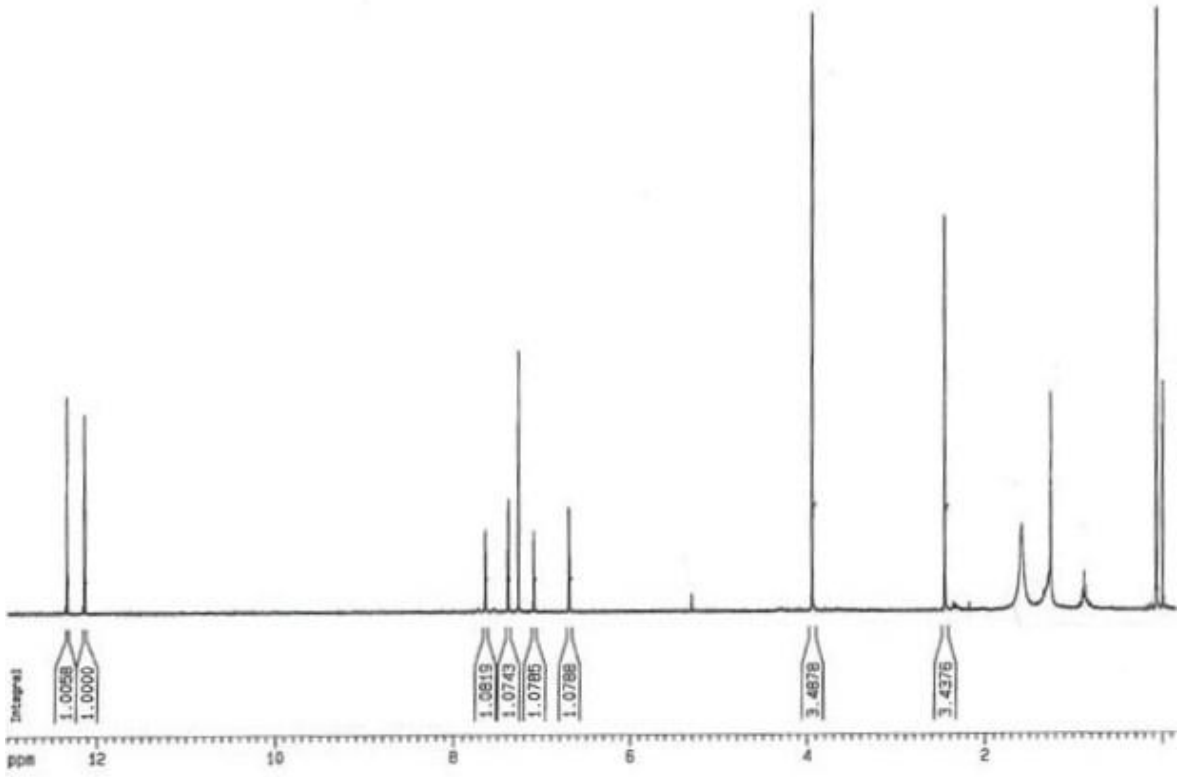

I.7.2. ^{13}C NMR spectrum (125.77 MHz)

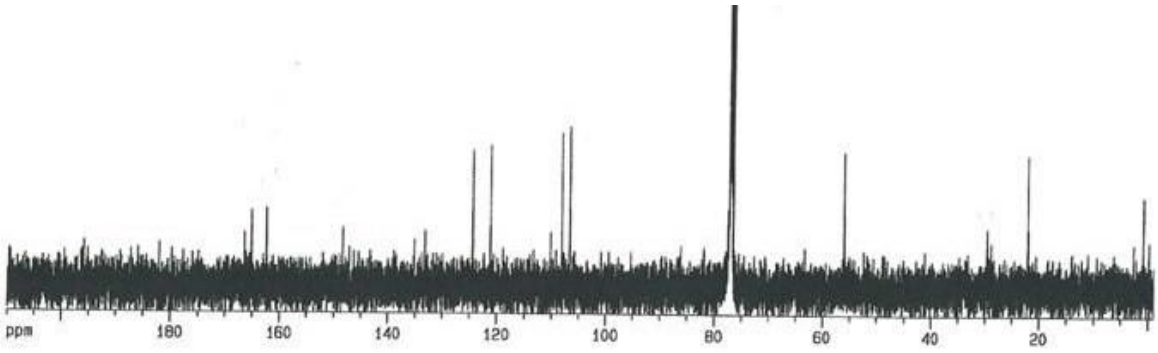

I.8. Catenarin (EC3)

I.8.1. ^{1}H NMR spectrum (300.13 MHz)

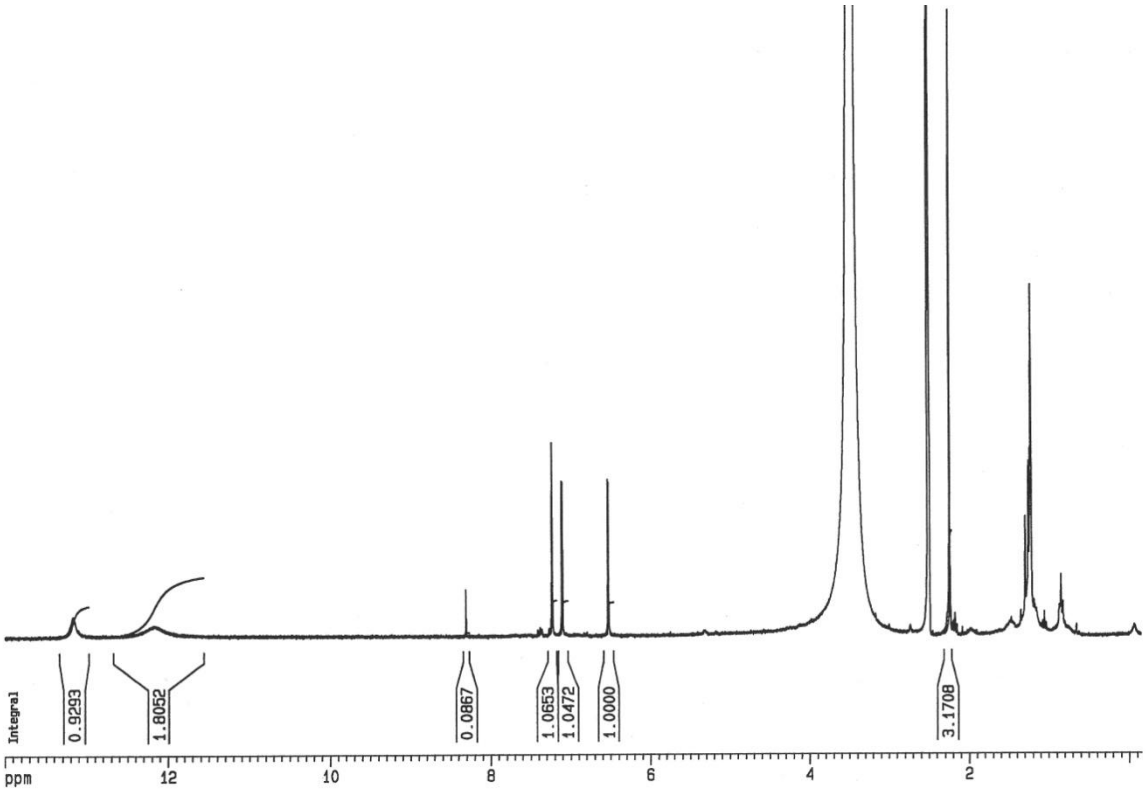

I.8.2. ^{13}C NMR spectrum (75.47 MHz)

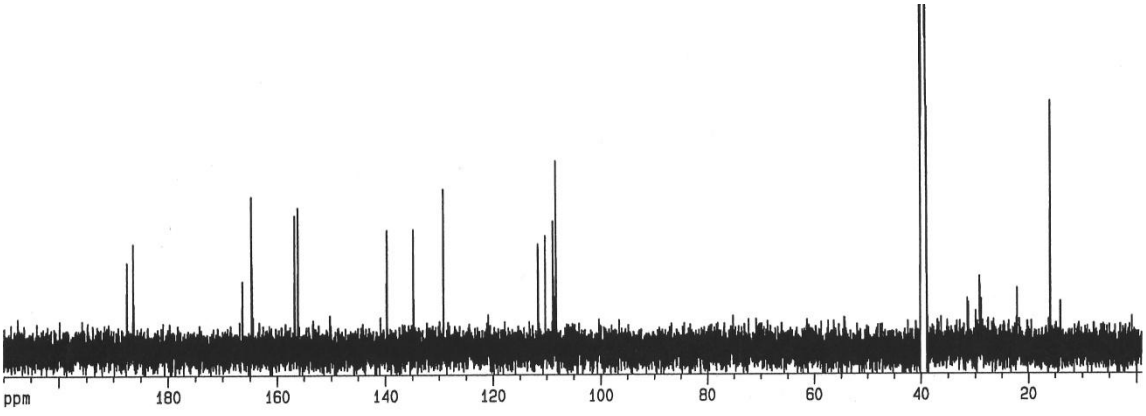

I.9. Emodin (EC4)

I.9.1. ^{1}H NMR spectrum (500.13 MHz)

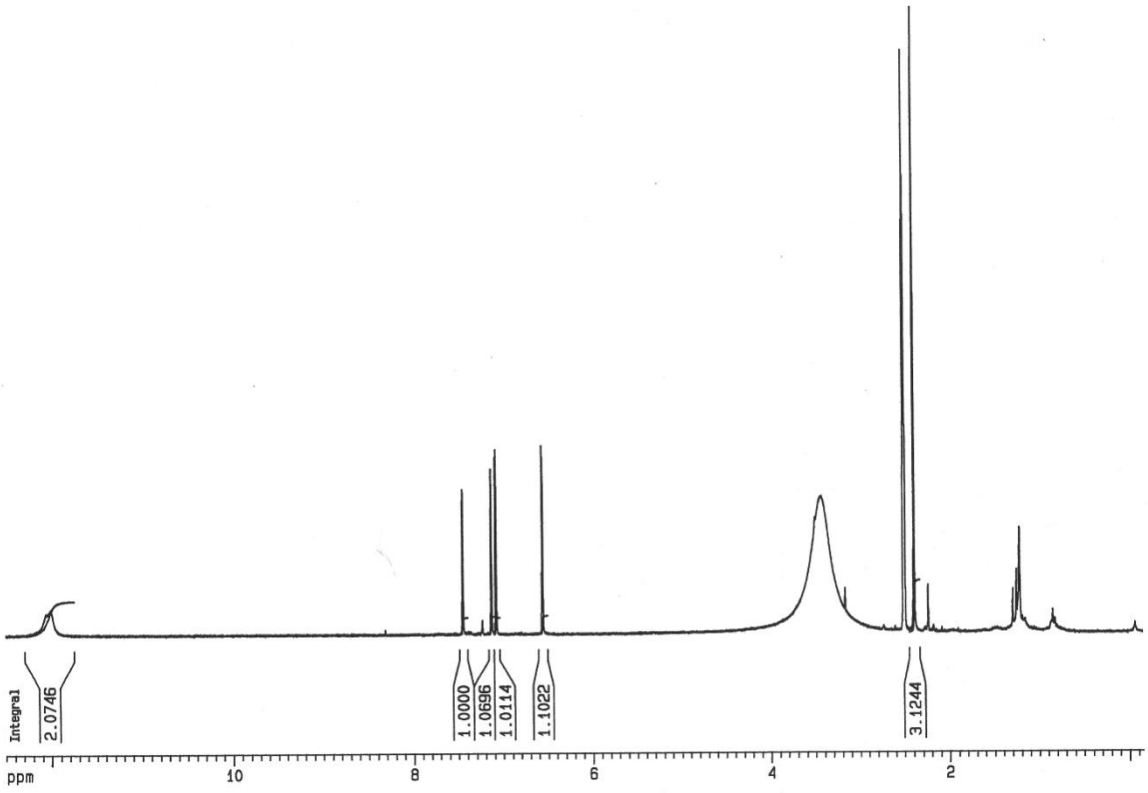

I.9.2. ^{13}C NMR spectrum (125.77 MHz)

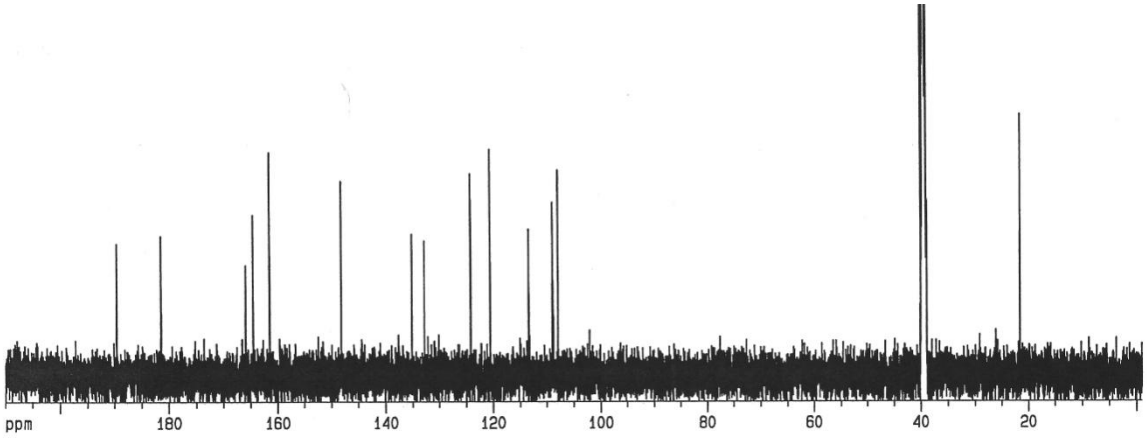

I.10. Questin (EC5)

I.10.1. ^{1}H NMR spectrum (300.13 MHz)

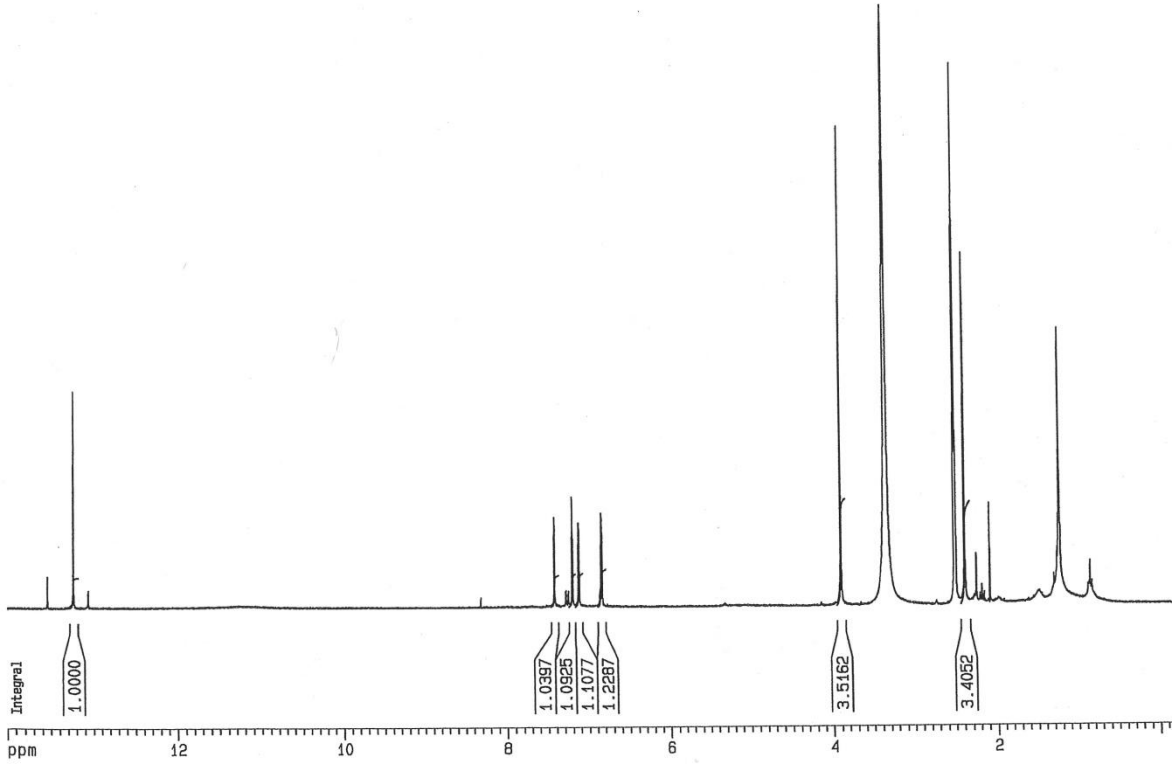

I.10.2. ^{13}C NMR spectrum (75.47 MHz)

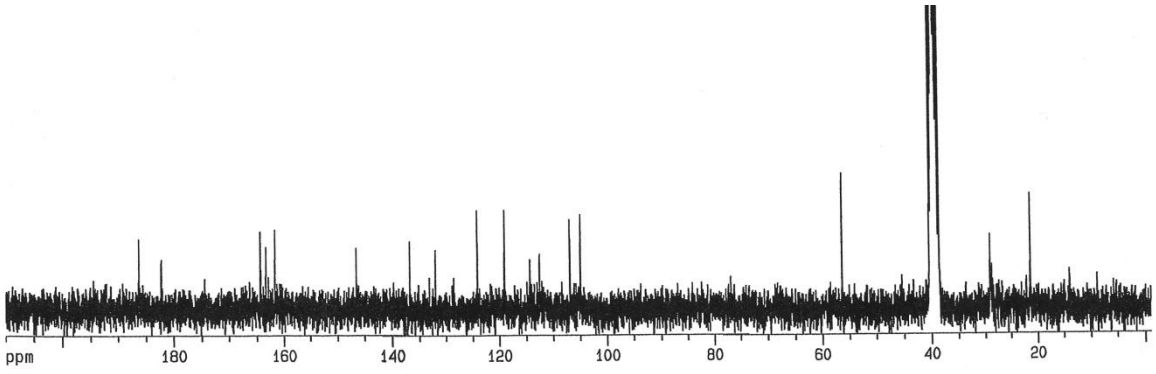

I.11. Echinulin (EC6)

I.11.1. ^{1}H NMR spectrum (300.13 MHz)

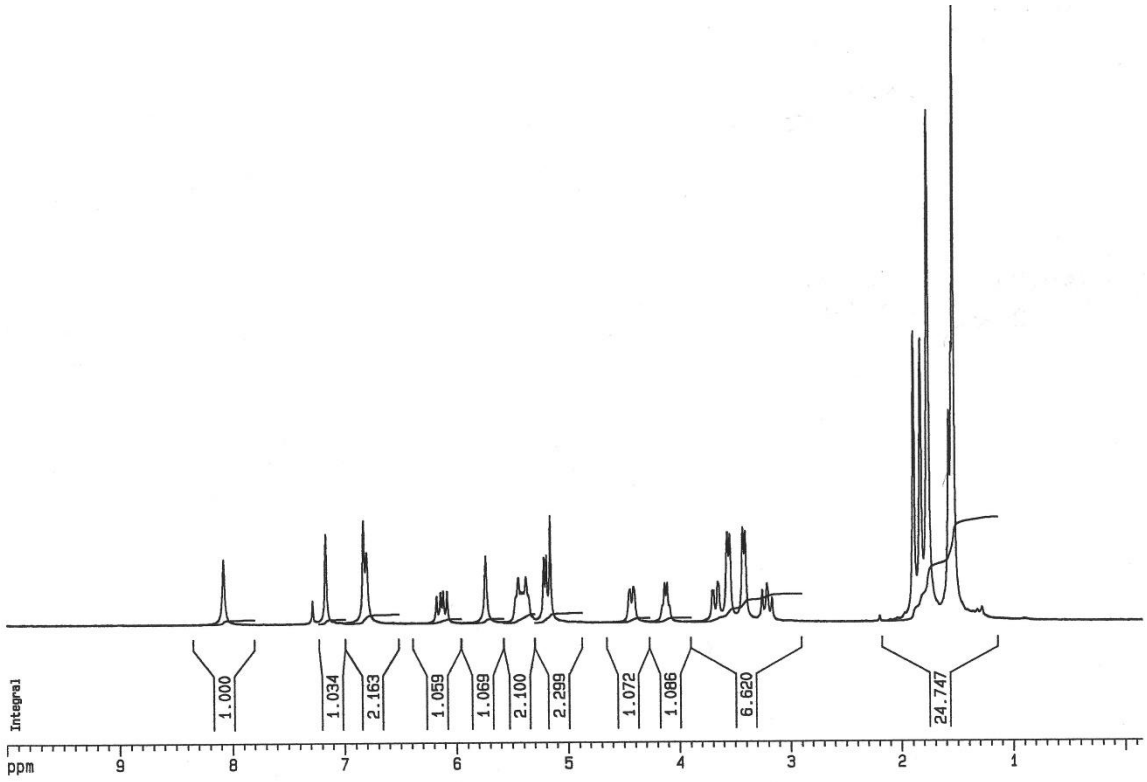

I.11.2. ^{13}C NMR spectrum (75.47 MHz)

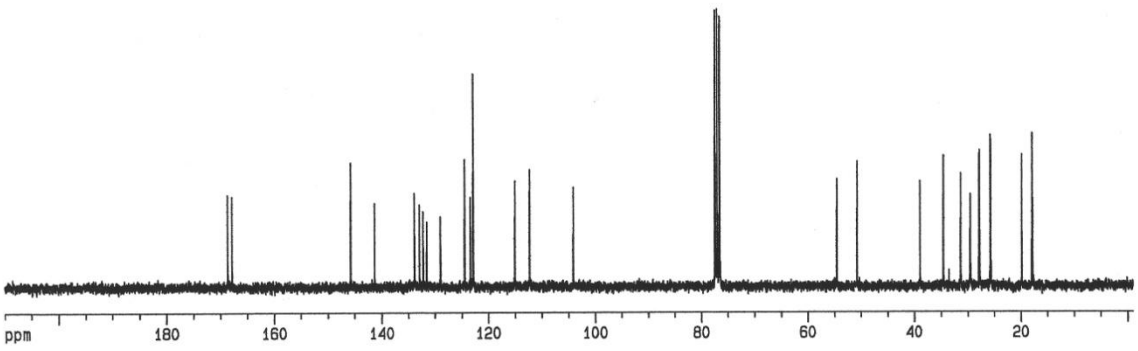

I.12. Neoechinulin (EC7)

I.12.1. ^{1}H NMR spectrum (300.13 MHz)

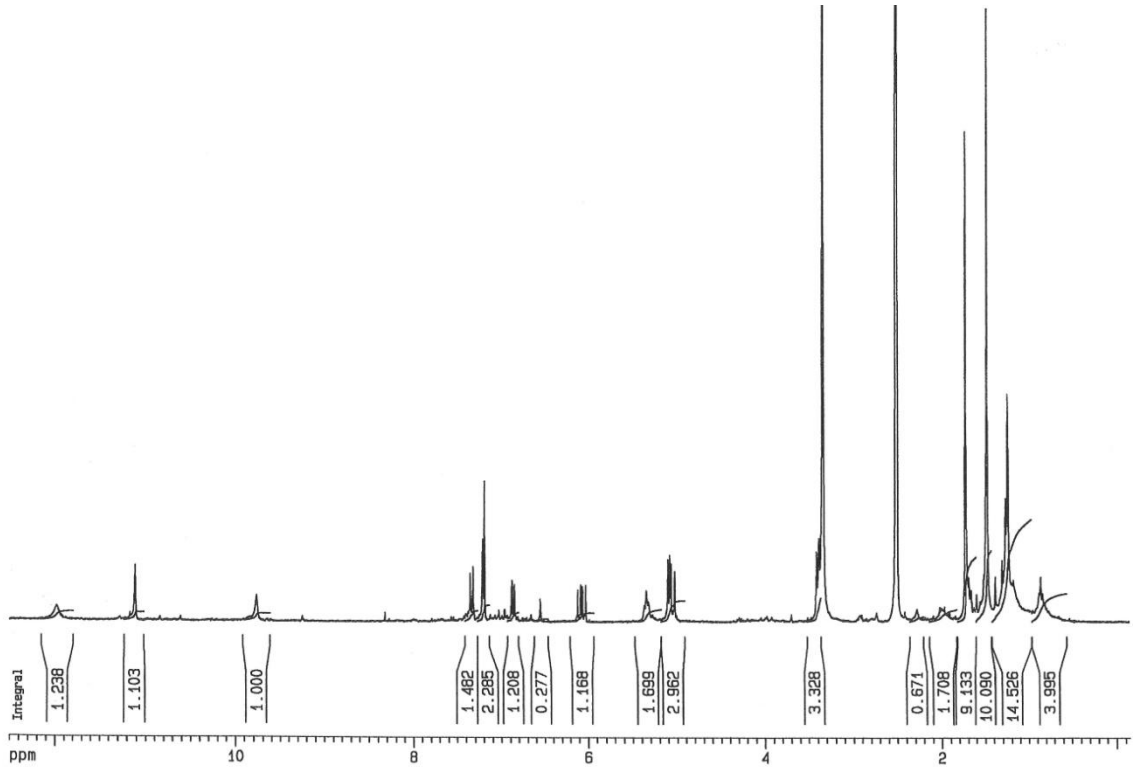

I.12.2. ^{13}C NMR spectrum (75.47 MHz)

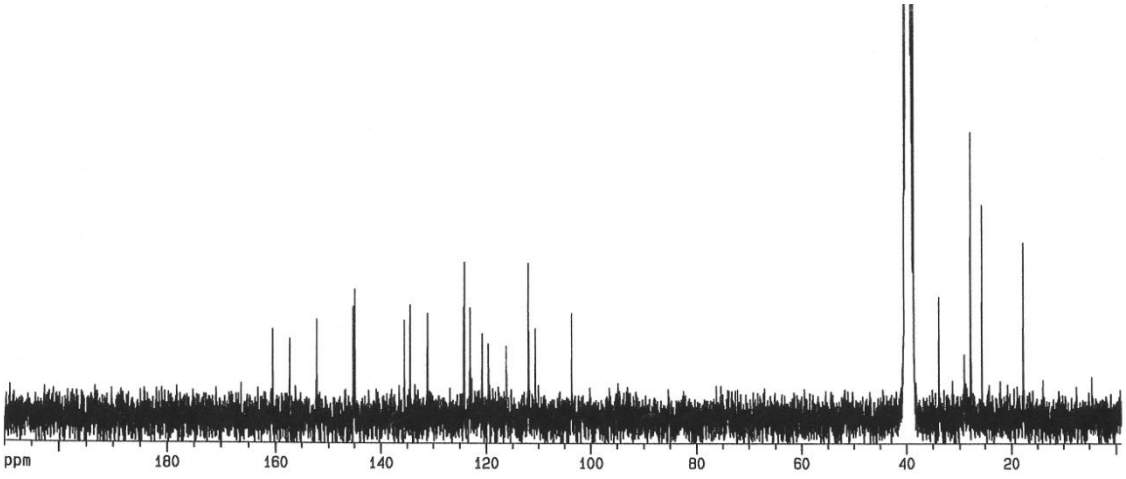

I.13. Neoechinulin A (EC8)

I.13.1. ^{1}H NMR spectrum (300.13 MHz)

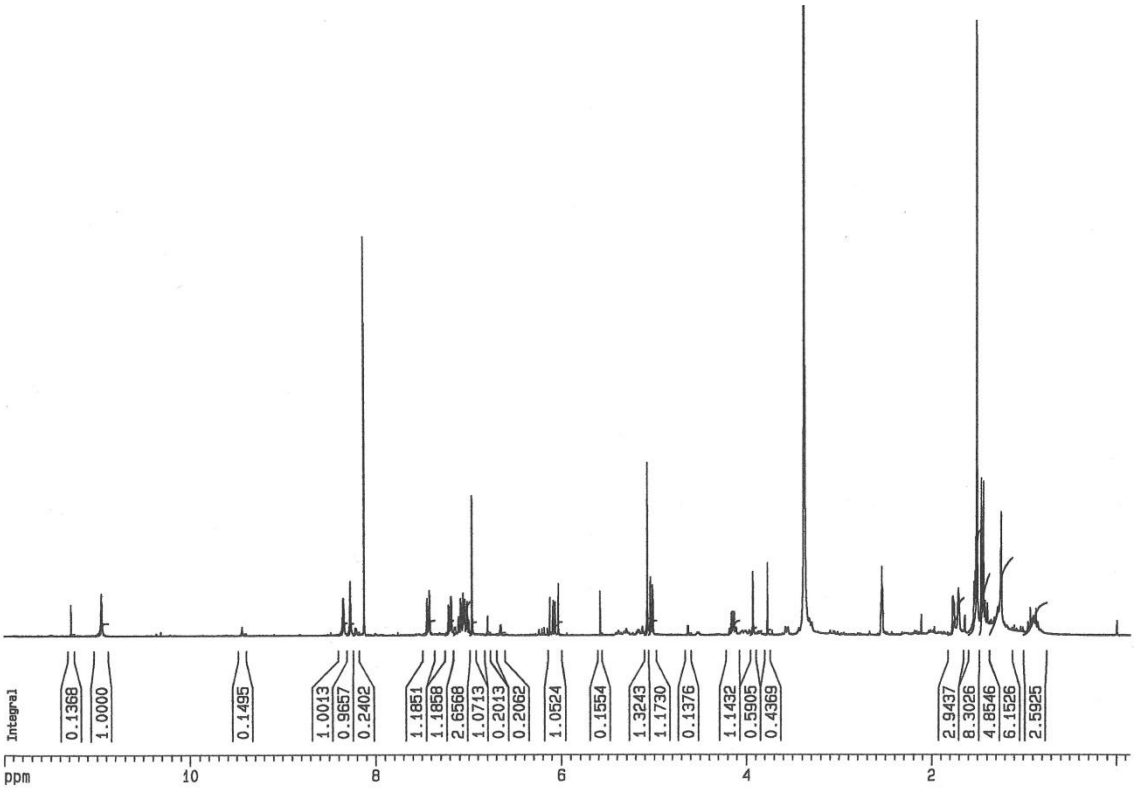

I.13.2. ^{13}C NMR spectrum (75.47 MHz)

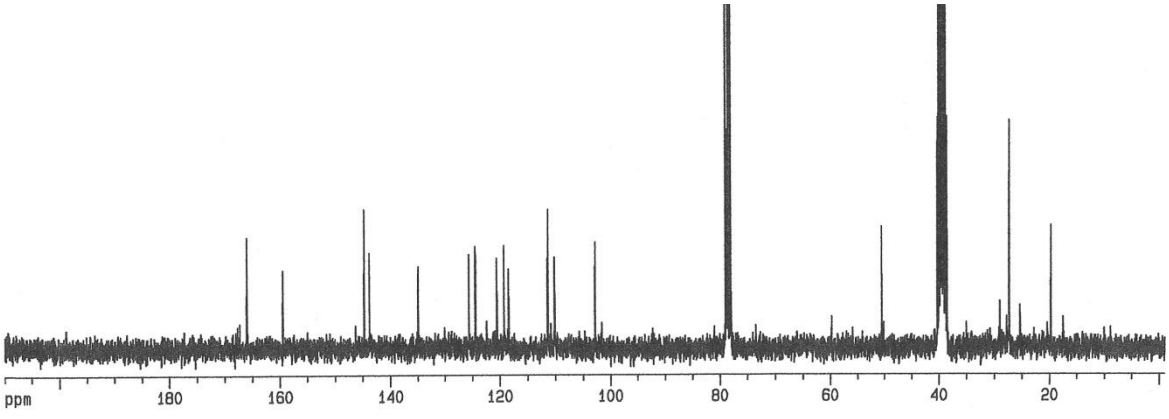

I.14. Neoechinulin E (EC9)

I.14.1. ^{1}H NMR spectrum (300.13 MHz)

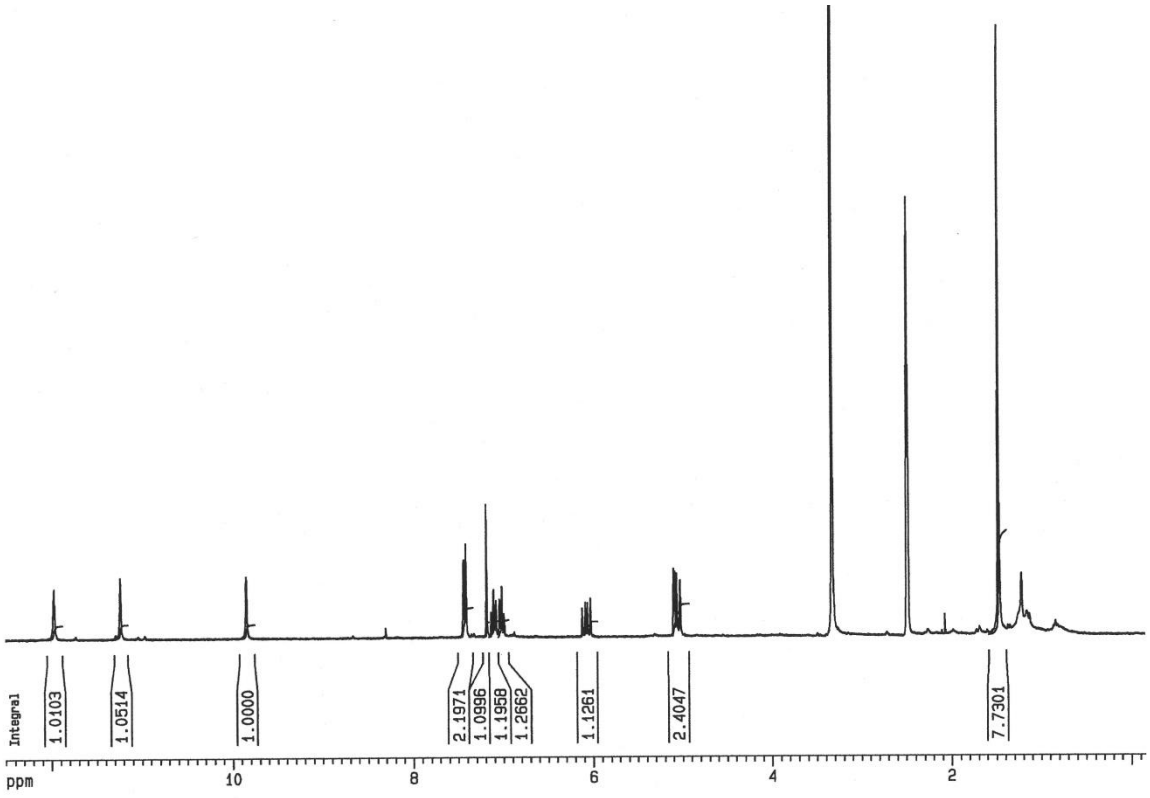

I.14.2. ^{13}C NMR spectrum (75.47 MHz)

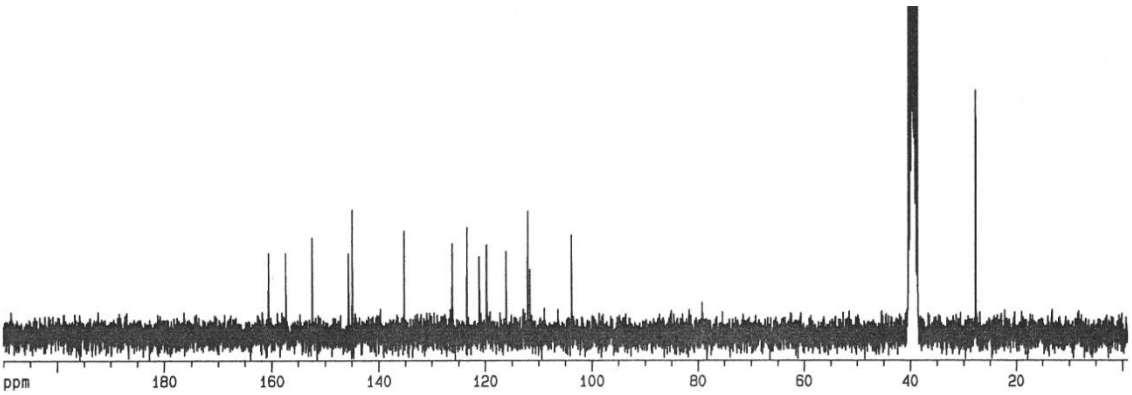

I.15. Eurocristatine (EC10)

I.15.1. ^{1}H NMR spectrum (300.13 MHz)

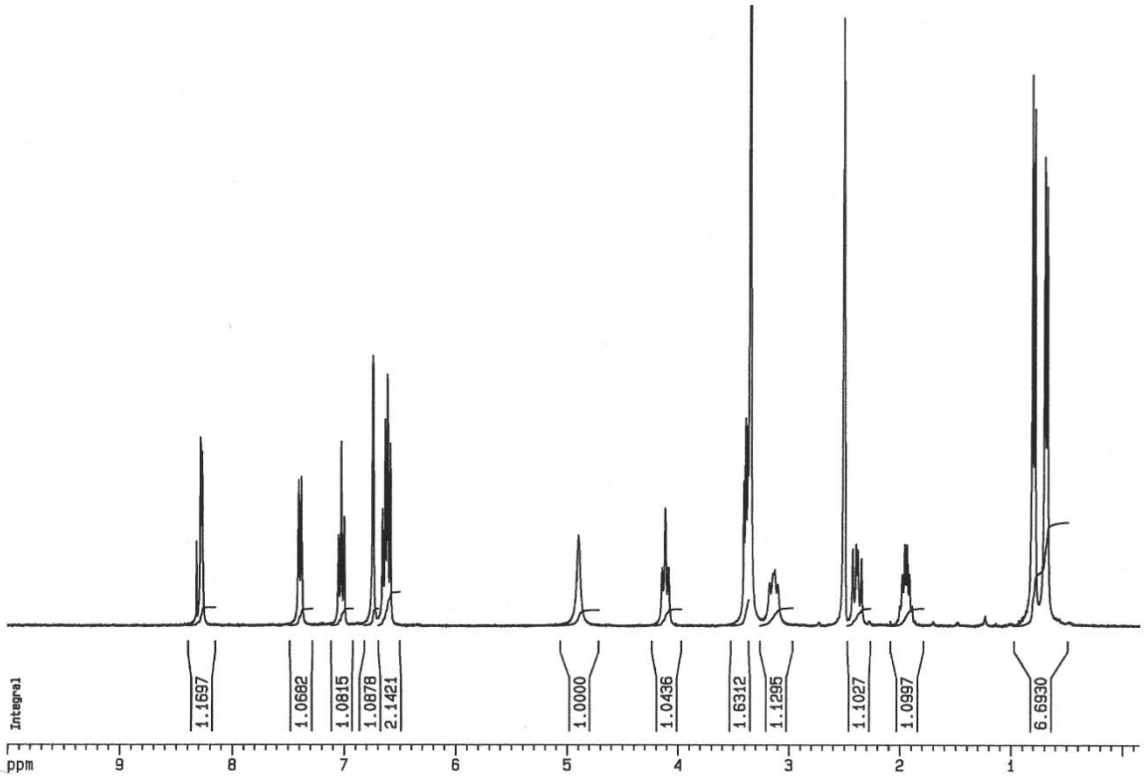

I.15.2. ^{13}C NMR spectrum (75.47 MHz)

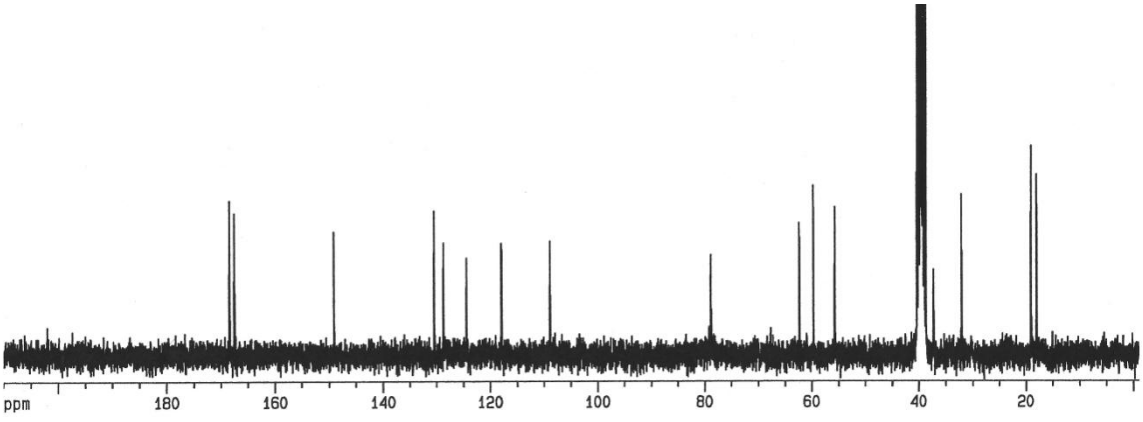

I.16. Chevalone B (NL1)

I.16.1. ^{1}H NMR spectrum (300.13 MHz)

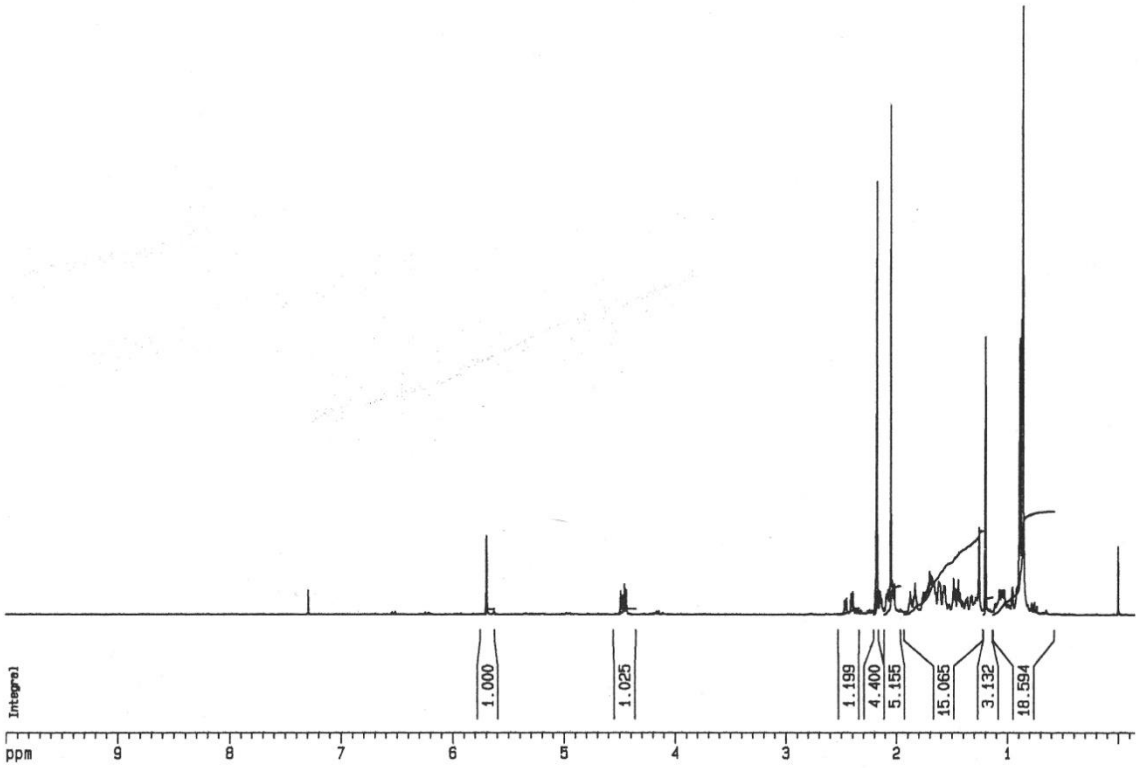

I.16.2. ^{13}C NMR spectrum (75.47 MHz)

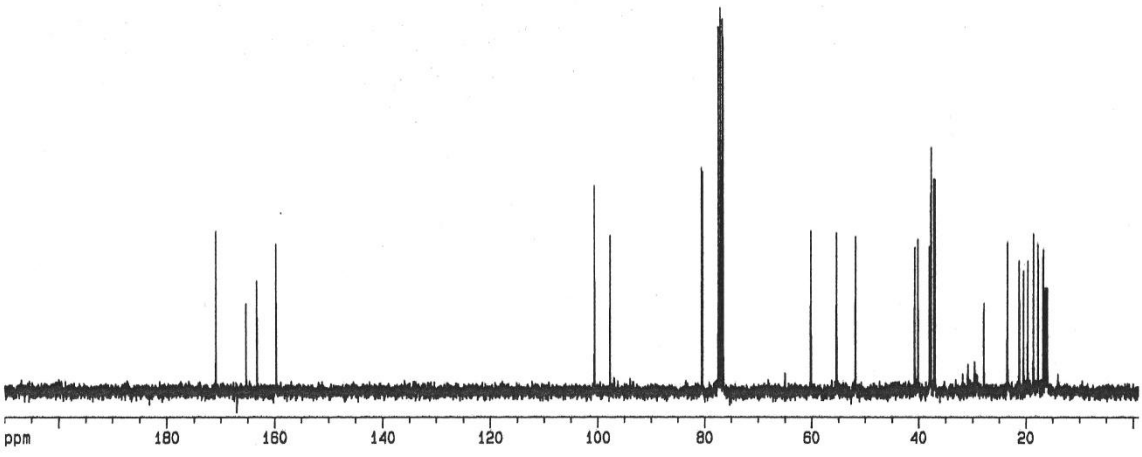

I.17. Aszonapyrone A (NL2)

I.17.1. ^{1}H NMR spectrum (300.13 MHz)

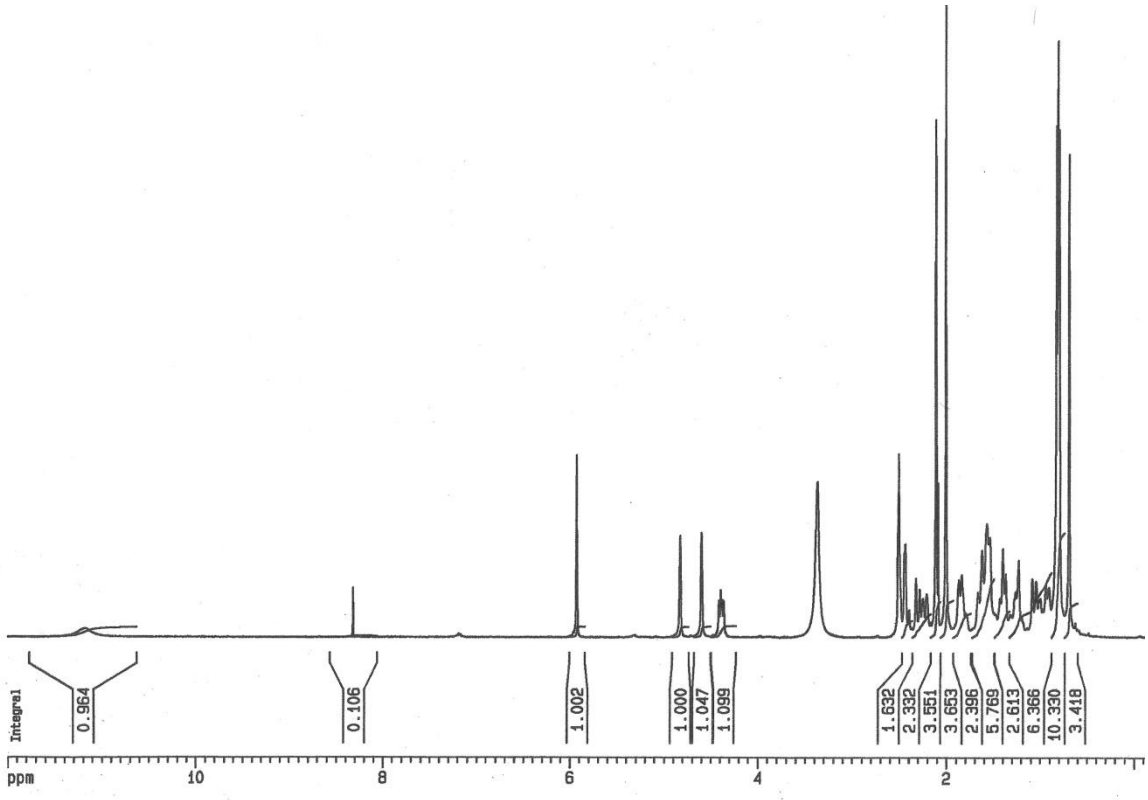

I.17.2. ^{13}C NMR spectrum (75.47 MHz)

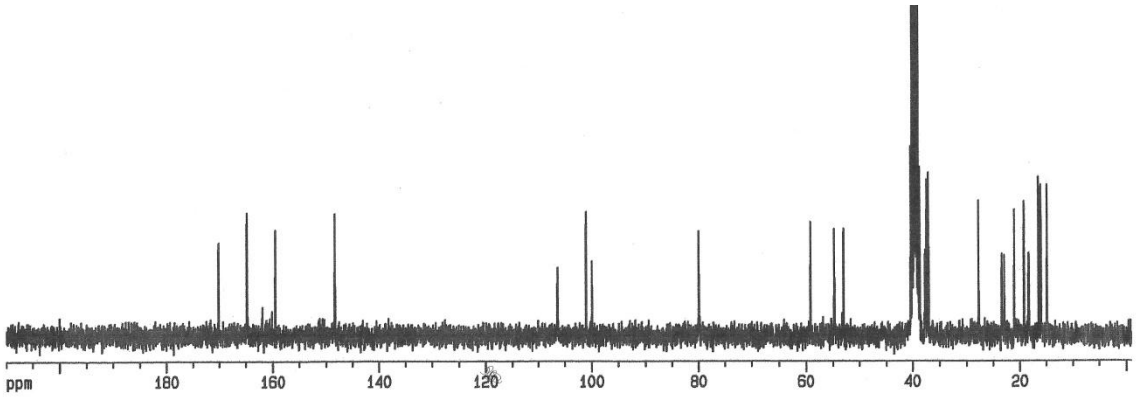

I.18. Aszonapyrone B (NL3)

I.18.1. ^{1}H NMR spectrum (300.13 MHz)

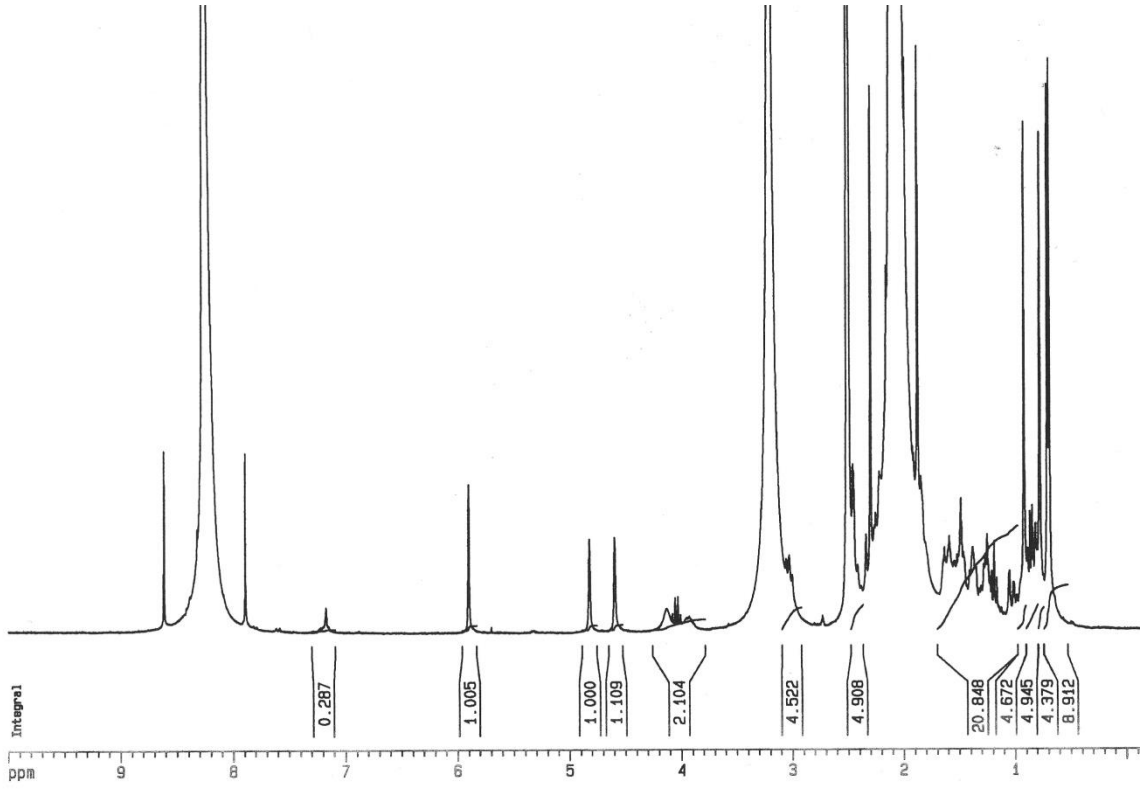

I.18.2. ^{13}C NMR spectrum (75.47 MHz)

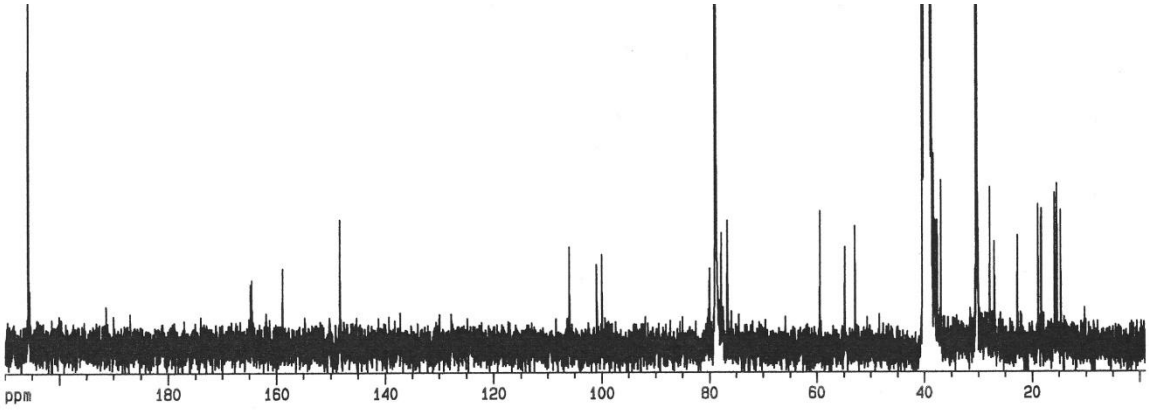

I.19. Tryptoquivaline L (NP2/NL4)

I.19.1. ^{1}H NMR spectrum (300.13 MHz)

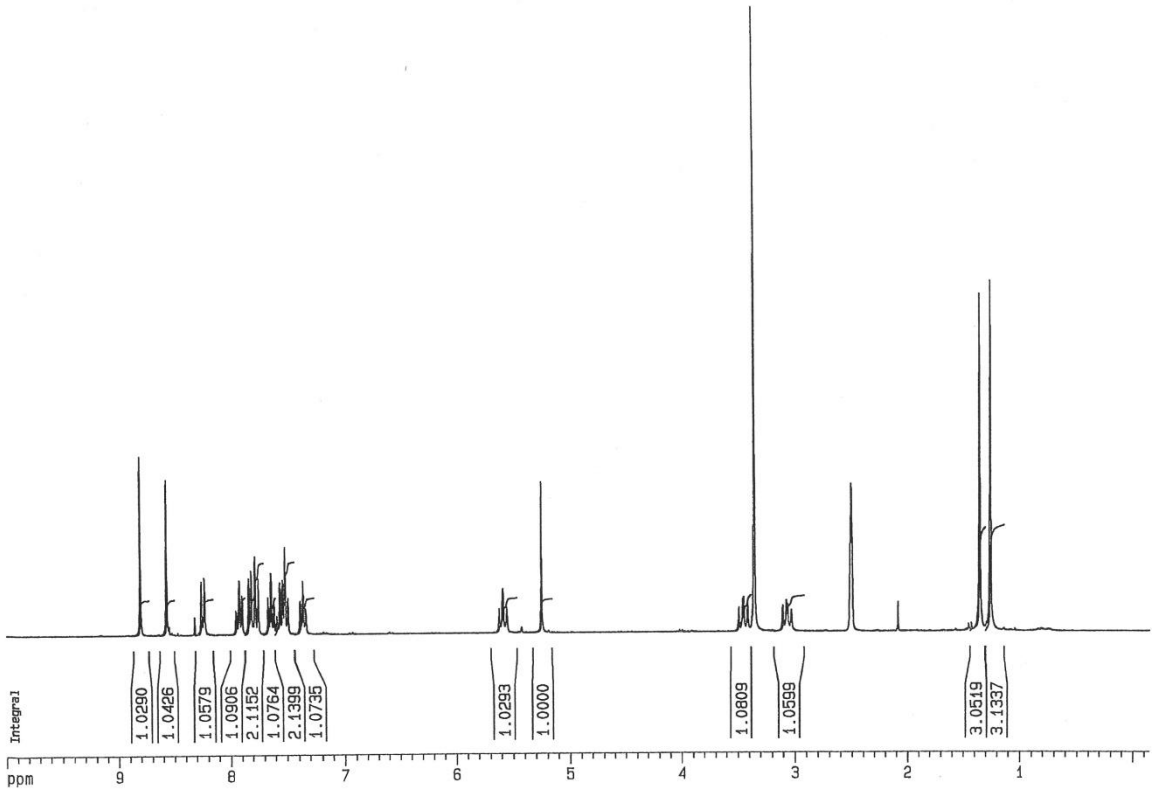

I.19.2. ^{13}C NMR spectrum (75.47 MHz)

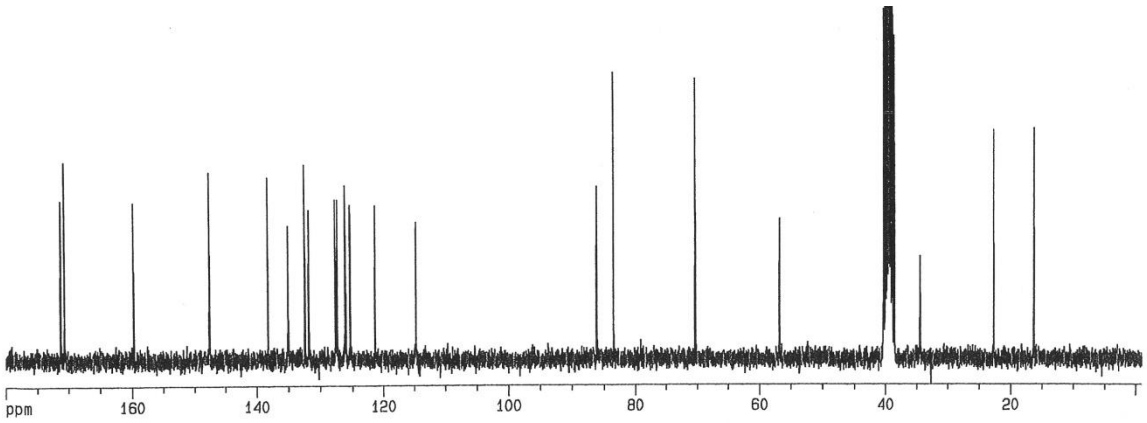

I.20. 3'-(4-Oxoquinazolin-3-yl)spiro[*1*H-indole-3,5'-oxolane]-2,2'-dione (NP5/NL5)

I.20.1. ^{1}H NMR spectrum (300.13 MHz)

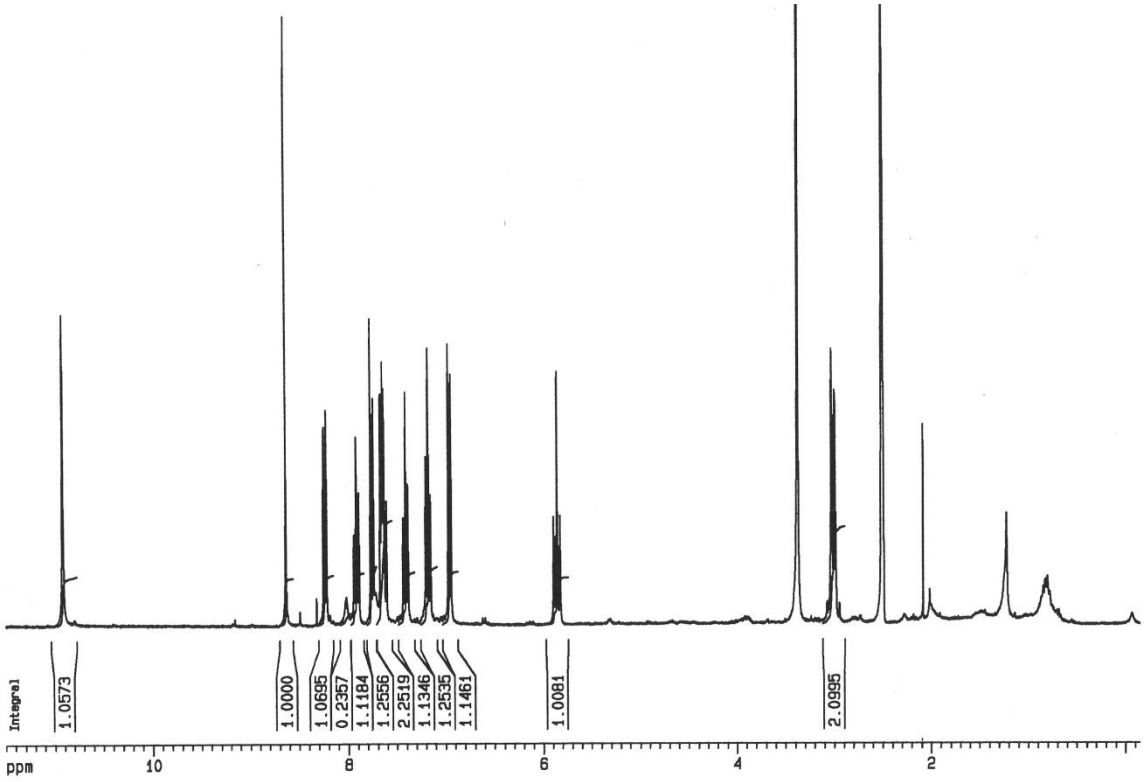

I.20.2. ^{13}C NMR spectrum (75.47 MHz)

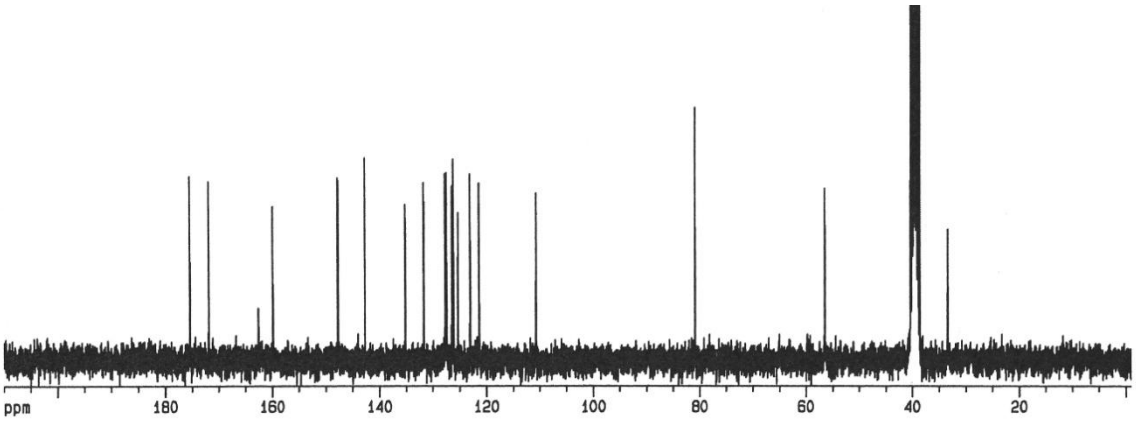

I.21. Tryptoquivaline T (NL6)

I.21.1. ^{1}H NMR spectrum (300.13 MHz)

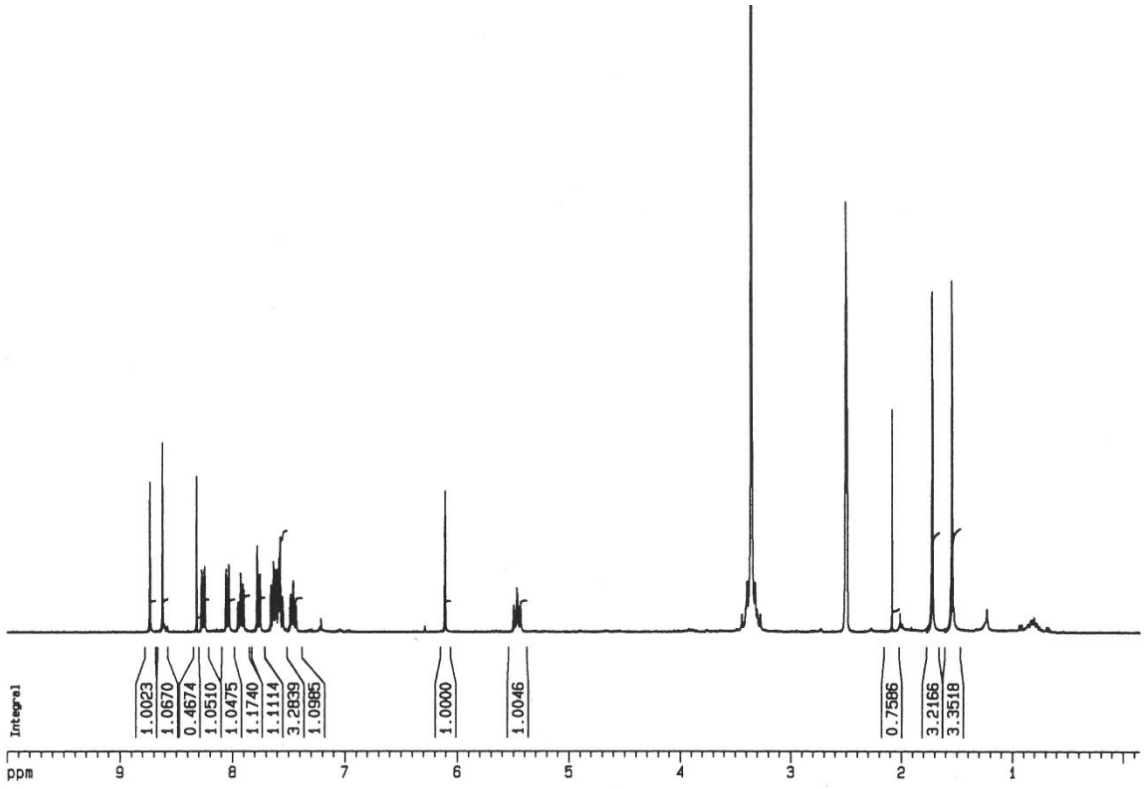

I.21.2. ^{13}C NMR spectrum (75.47 MHz)

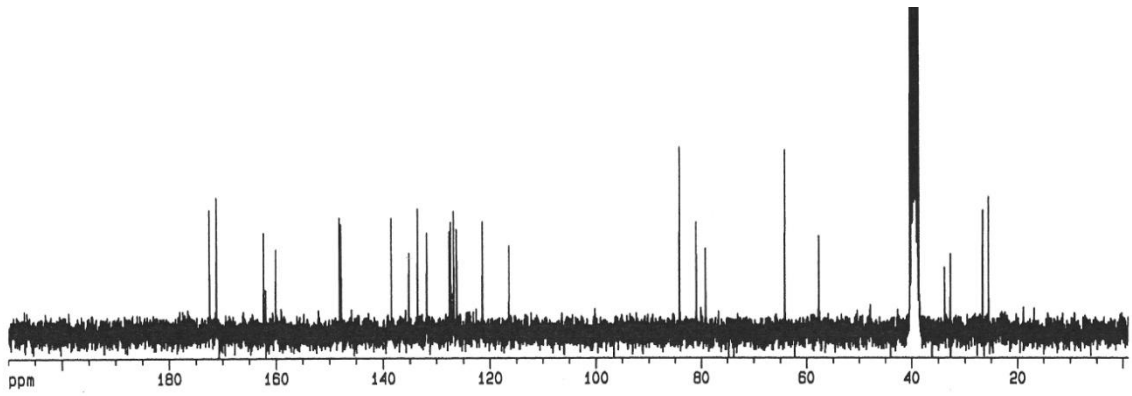

I.22. Sartorypyrone C (NP1)

I.22.1. ^{1}H NMR spectrum (300.13 MHz)

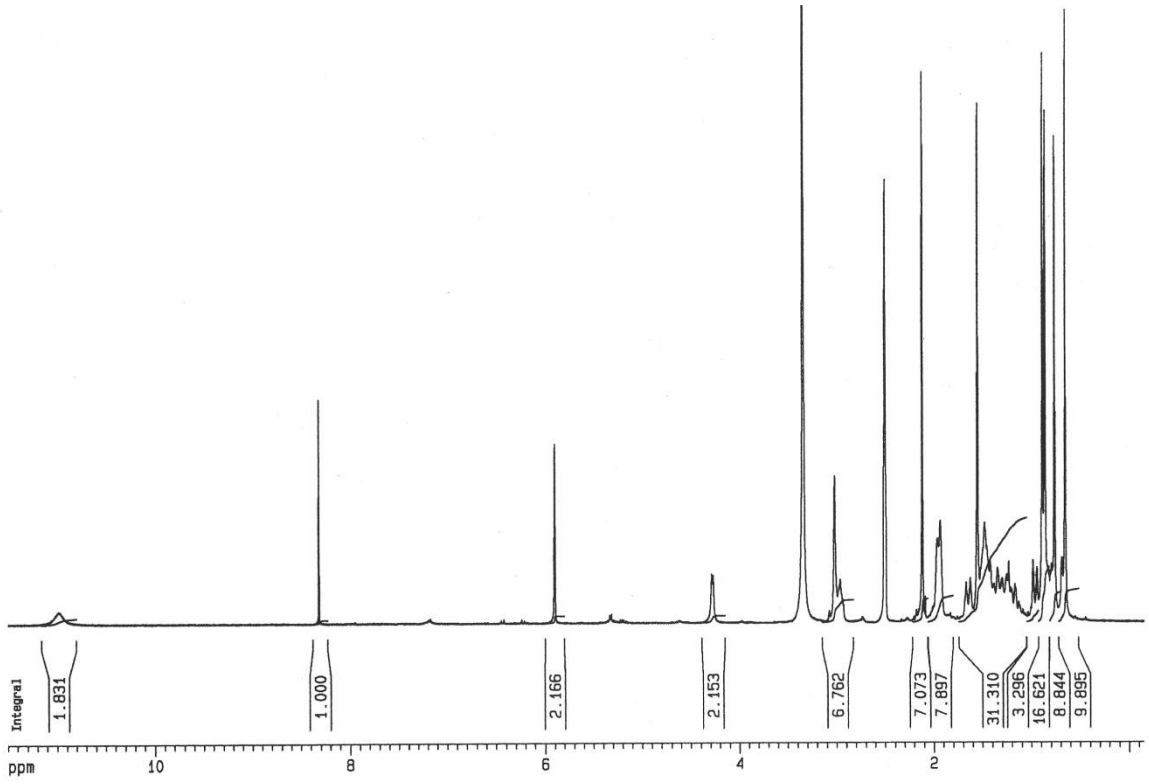

I.22.2. ^{13}C NMR spectrum (75.47 MHz)

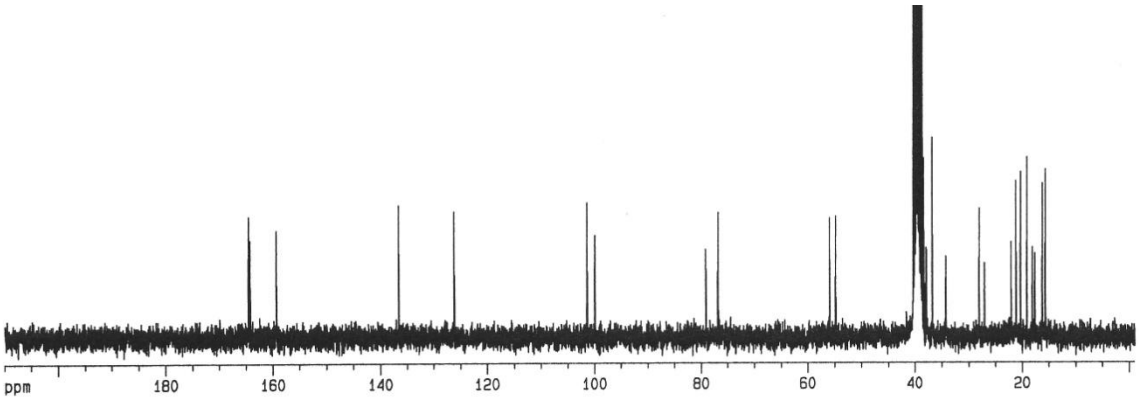

I.23. Tryptoquivaline H (NP3)

I.23.1. ^{1}H NMR spectrum (300.13 MHz)

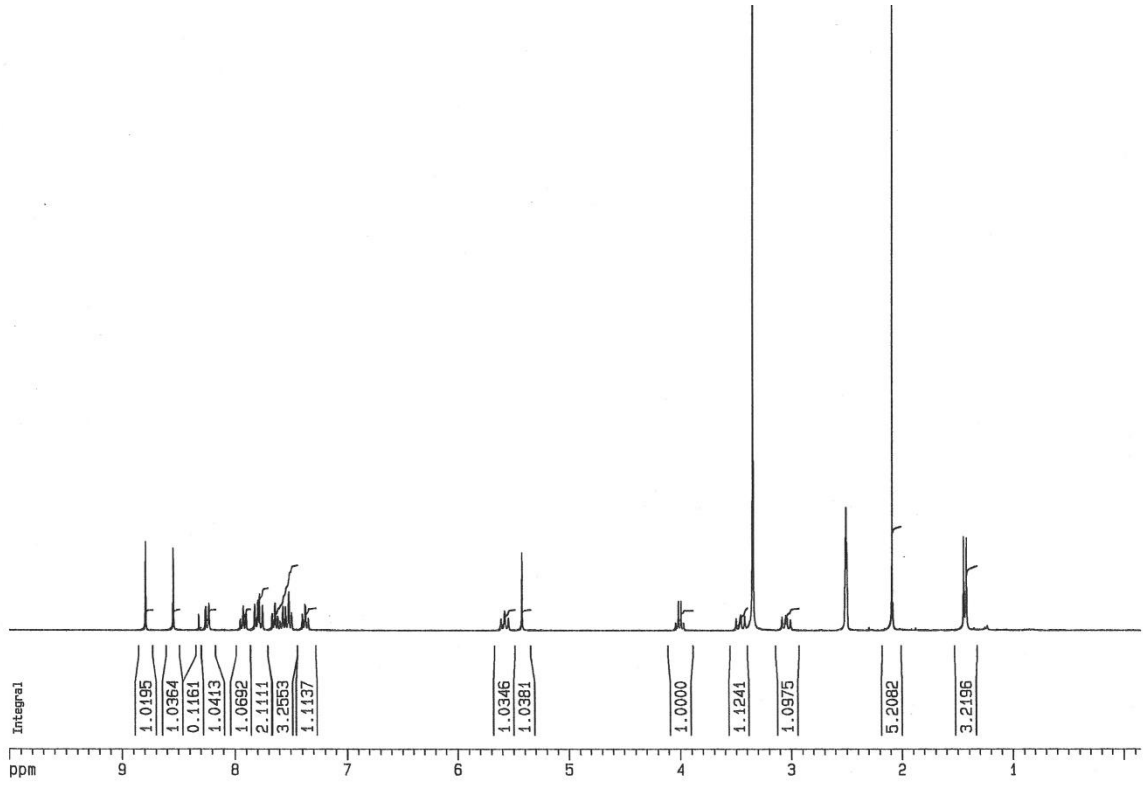

I.23.2. ^{13}C NMR spectrum (75.47 MHz)

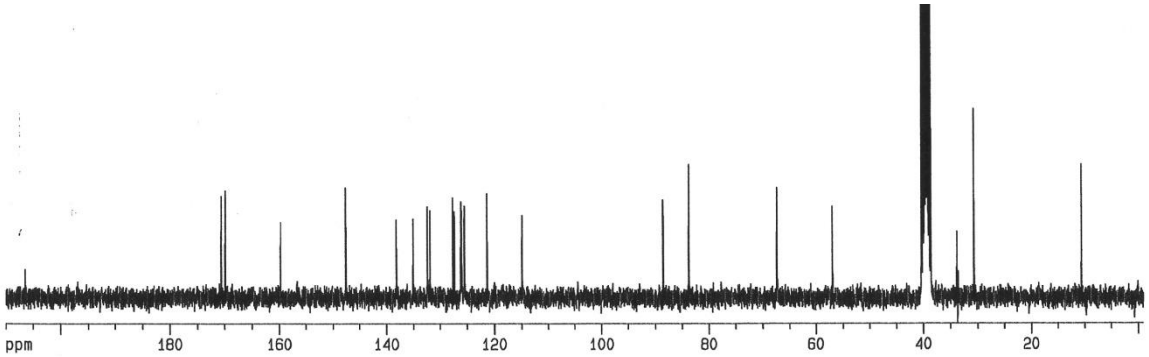

I.24. 4(3*H*)-Quinazolinone (NP4)

I.24.1. ^{1}H NMR spectrum (500.13 MHz)

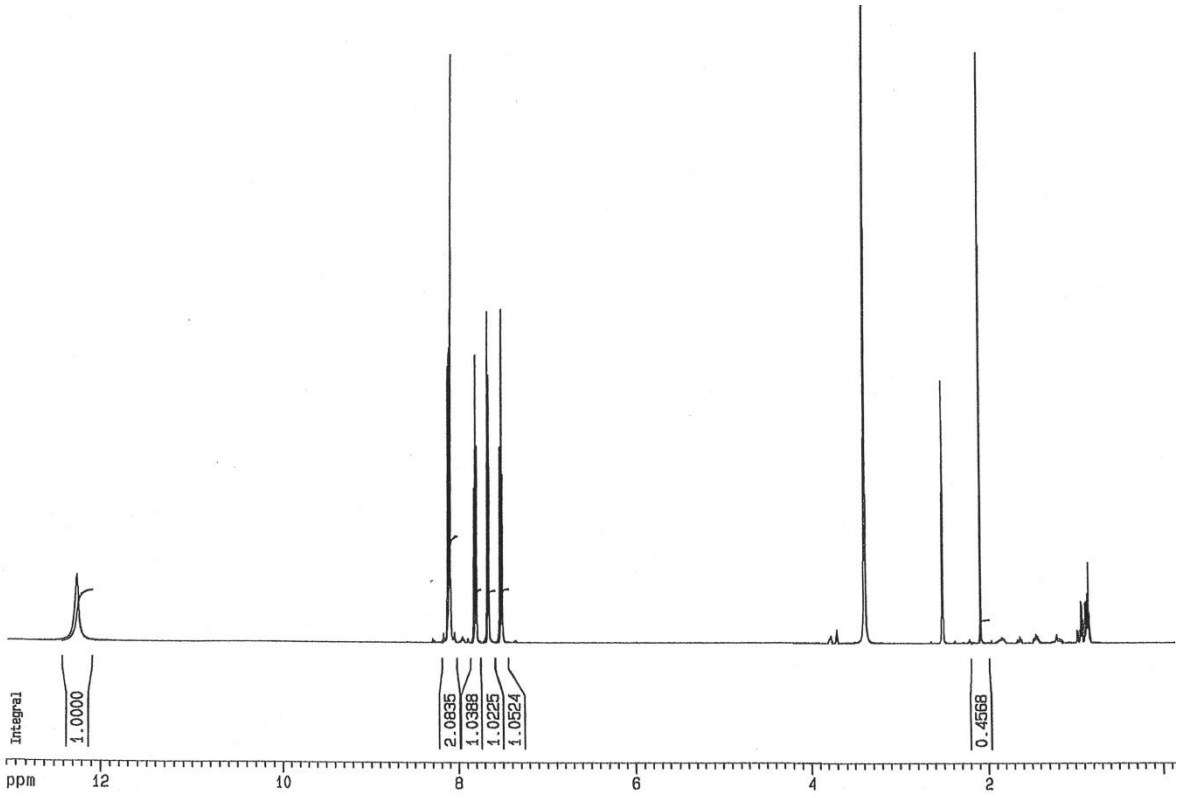

I.24.2. ^{13}C NMR spectrum (125.77 MHz)

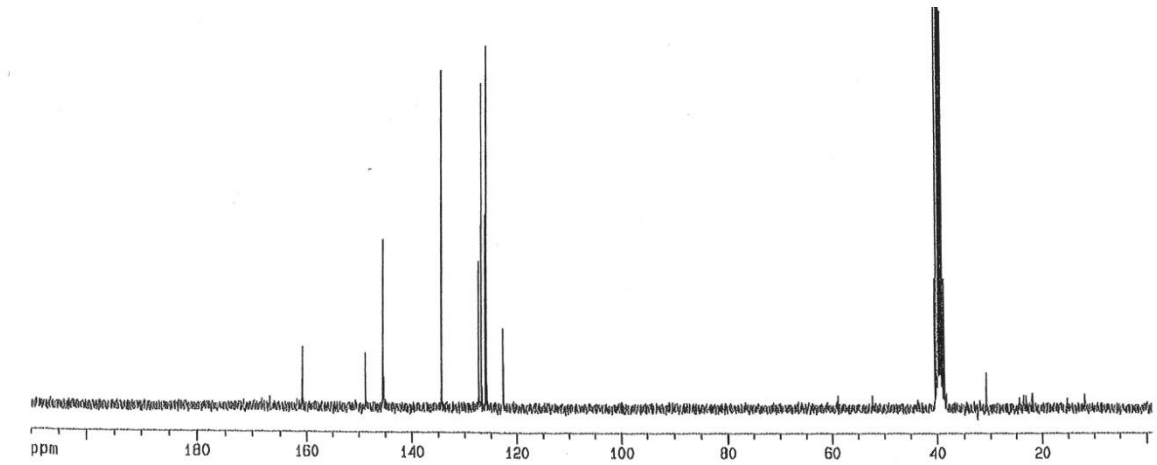

I.25. Tryptoquivaline F (NP6)

I.25.1. ^{1}H NMR spectrum (300.13 MHz)

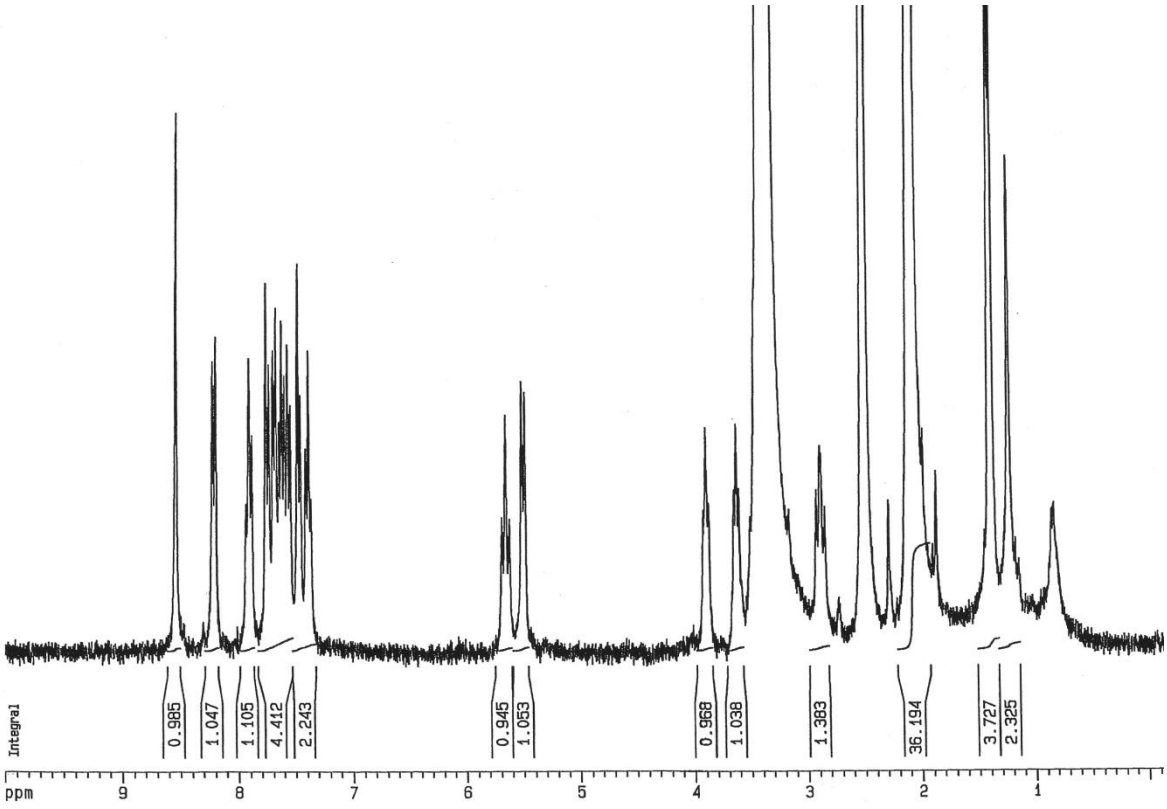

I.25.2. ^{13}C NMR spectrum (75.47 MHz)

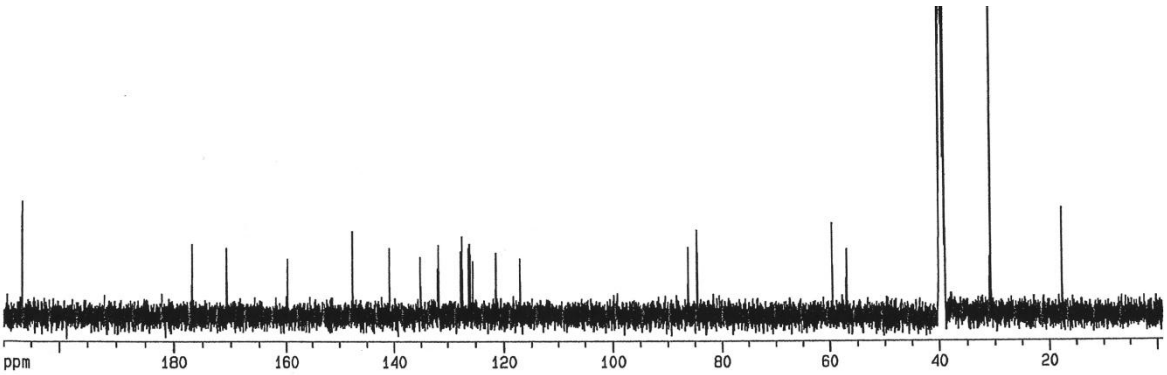

APPENDIX II

Gomes, N.M., Dethoup, T., Singburaudom, N., Gales, L., Silva, A.M.S., Kijjoa, A. **(2012).** Eurocristatine, a new diketopiperazine dimer from the marine sponge-associated fungus *Eurotium cristatum. Phytochemistry Letters* 5(4), 717-720.

Phytochemistry Letters 5 (2012) 717–720

Contents lists available at SciVerse ScienceDirect

Phytochemistry Letters

journal homepage: www.elsevier.com/locate/phytol

Eurocristatine, a new diketopiperazine dimer from the marine sponge-associated fungus *Eurotium cristatum*

Nelson M. Gomes [a], Tida Dethoup [a,b], Narong Singburaudom [b], Luís Gales [c], Artur M.S. Silva [d], Anake Kijjoa [a,*]

[a] *ICBAS - Instituto de Ciências Biomédicas de Abel Salazar and CIIMAR, Universidade do Porto, Rua de Jorge Viterbo Ferreira, 228, 4050-313 Porto, Portugal*
[b] *Department of Plant Pathology, Faculty of Agriculture, Kasetsart University, Bangkok, Thailand*
[c] *ICBAS - Instituto de Ciências Biomédicas de Abel Salazar and Instituto de Biologia Molecular e Celular (IBMC), Universidade do Porto, Rua de Jorge Viterbo Ferreira, 228, 4050-313 Porto, Portugal*
[d] *Departamento de Química, Universidade de Aveiro, 4810-1933 Aveiro, Portugal*

ARTICLE INFO

Article history:
Received 10 June 2012
Received in revised form 12 July 2012
Accepted 17 July 2012
Available online 31 July 2012

Keywords:
Eurotium cristatum
Marine-sponge associated fungus
Diketopiperazine dimer
Eurocristatine

ABSTRACT

A new diketopiperazine dimer, eurocristatine (**1**), was isolated, in addition to eight known metabolites including the anthraquinones erythroglaucin, physcion, catenarin, emodin and the dioxopiperazine alkaloids echinulin, neoechinulin A, neoechinulin E, variecolorin J, from the culture of the sponge-associated fungus *Eurotium cristatum* KUFC 7356. The structure of eurocristatine (**1**) was established based on 1D and 2D NMR spectral analysis as well as HRESIMS, and the absolute configuration of its stereogenic carbons was determined by an X-ray crystallographic analysis. Eurocristatine (**1**) did not exhibit cytotoxic, antibacterial or antifungal activity.

© 2012 Phytochemical Society of Europe. Published by Elsevier B.V. All rights reserved.

1. Introduction

Eurotium species are the sexual states of *Aspergillus* species, notably the *Aspergillus glaucus* group among others (Geiser, 2009). Contrary to *Aspergillus*, only few species of *Eurotium* have been investigated for their secondary metabolites. Smetanina *et al.* (2007) have reported isolation of the anthraquinone physcion, asperflavin, the prenyl benzaldehyde tetrahydroauroglaucin and the dioxopiperazine alkaloid echinulin from the ethyl acetate extract of the culture of *E. repens*, isolated from the marine sponge *Suberites domuncula*. Li et al. (2008a,b) reported isolation of a series of dioxopiperazine alkaloids and prenyl benzaldehyde derivatives from the culture of *E. rubrum*, an endophytic fungus isolated from the inner tissue of stems of the mangrove plant *Hibiscus tiliaceus*. In the process of investigation of the secondary metabolites from *Eurotium* and *Aspergillus* species, common in Canadian homes, Slack et al. (2009) have found that the dioxopiperazine derivatives neoechinulin A, neoechinulin B, and epiheveadride were present in the filtrate extracts of *E. rubrum* and *E. amstelodami*, while the filtrate extract of *E. herbariorum* contained cladosporin in addition to these three compounds; however, only the prenyl benzaldehydes flavoglaucin, auroglaucin and isotetrahydroauroglaucin were found in the mycelial extracts of the three species. Recently, Kanokmedhakul et al. (2011) have reported isolation of the meroterpenoids chevalones A–D, aszonapyrone A, aszonapyrone B, the sesquiterpene alkaloid eurochevalierine, and terpenoid pyrrolobenzoxazine CJ-12662 from the culture of *E. chevalieri*. In the course of our investigation on bioactive metabolites from the marine-derived fungi, we have recently found that the ethyl acetate extract of the culture of the marine sponge-associated *Eurotium cristatum* KUFC 7356 and some of its constituents exhibited the *in vitro* growth inhibitory activity on three cancer cell lines (Almeida et al., 2010). In order to discover more new bioactive metabolites, we have recultured this fungus to obtain more extract from which a new diketopiperazine dimer, eurocristatine (**1**) (Fig. 1) was isolated, in addition to eight known metabolites including the anthraquinones erythroglaucin (Anke et al., 1980), physcion (Anke et al., 1980), catenarin (Anke et al., 1980), emodin (Manojlović et al., 2000) and the dioxopiperazine alkaloids echinulin (Smetanina et al., 2007), neoechinulin A (Li et al., 2008a), neoechinulin E (Li et al., 2008a), variecolorin J (Wang et al., 2007).

2. Results and discussion

Eurocristatine (**1**) was isolated as white crystals and its IR spectrum showed absorption bands for amine (3450 cm^{-1}),

* Corresponding author. Tel.: +351 220428331; fax: +351 222062232.
E-mail addresses: ankijjoa@icbas.up.pt, anakekijjoa@yahoo.com (A. Kijjoa).

1874-3900/$ – see front matter © 2012 Phytochemical Society of Europe. Published by Elsevier B.V. All rights reserved.
http://dx.doi.org/10.1016/j.phytol.2012.07.010

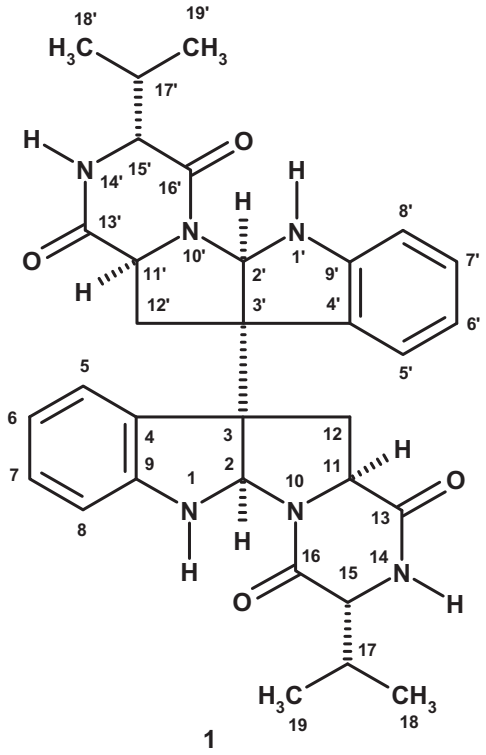

Fig. 1. Structure of eurocristatine (**1**).

aromatic (3190 cm^{-1}) and carbonyls (1662 cm^{-1}) groups. The ^{13}C NMR, DEPT and HSQC spectra (Table 1) revealed the presence of 16 carbon signals which can be categorized as 2 amide carbonyls (δ_C 168.4 and 167.5), 2 quaternary sp^2 (δ_C 149.1 and 130.4), 4 methine sp^2 (δ_C 128.7, 124.4, 117.9, 108.9), 1 quaternary sp^3 (δ_C 59.7), 4 methine sp^3 (δ_C 78.8, 62.3, 55.7, 32.0), 1 methylene sp^3 (δ_C 37.3) and 2 methyl (δ_C 19.0 and 18.0) carbons. However, the (+)-HRESIMS exhibited the *m/z* 569.2905 $[M+H]^+$, which corresponded to the molecular formula $C_{32}H_{36}N_6O_4$, implying that each carbon signal must correspond to two carbon atoms. The coupling system of the aromatic protons observed in the COSY spectrum (Table 1) revealed the presence of one 1,2-disubstituted benzene ring. The HMBC spectrum (Table 1 and Fig. 2) exhibited correlations of the proton signal at δ_H 6.74 brs (NH-1) to the

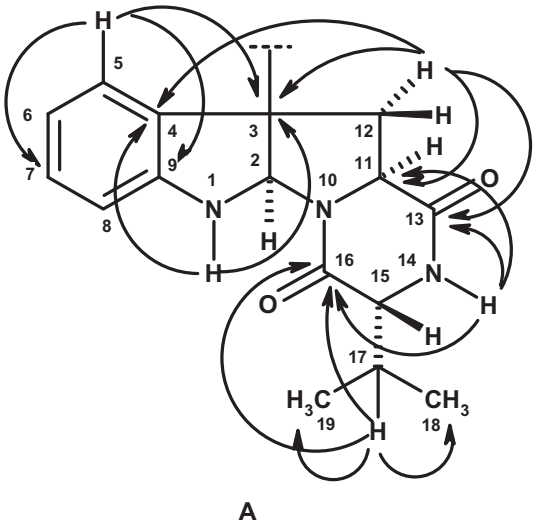

Fig. 2. Key HMBC correlations in the monomer (**A**).

carbon signals at δ_C 59.7 (C-3), 78.8 (C-2), 130.4 (C-4) and 149.1 (C-9), confirming that the 1,2-disubstituted benzene ring was part of the indole moiety of the molecule. The HMBC spectrum (Table 1 and Fig. 2) also showed cross peaks between the signal of NH-14 (δ_H 8.27d, *J* = 4.2 Hz) and the methine carbon signals at δ_C 55.7 (C-11), δ_C 62.3 (C-15); the carbonyl carbons at δ_C 167.5 (C-16), 168.4 (C-13), indicating that another portion of the molecule was a 1,4-diketopiperazine system. That the 1,4-diketopiperazine moiety was linked to the indole ring system through C-2 of the latter and N-10 of the former, and through the methylene group between C-3 of the latter and C-11 of the former, was evidenced by correlations between H-11 signal (δ_H 4.12, t, *J* = 9.0 Hz) and the signals of H-12 (δ_H 3.14, dd, *J* = 14.0, 9.5; 2.39, dd, *J* = 14.0, 9.5) in the COSY spectrum as well as the correlations of the signal of H-12α (δ_H 2.39, dd, *J* = 14.0, 9.5) to the signals of C-3 (δ_C 59.7), C-4 (δ_C 130.4), C-13 (168.4) (Table 1 and Fig. 2). Analysis of the COSY spectrum (Table 1) also revealed the presence of the isopropyl substituent [δ_H 1.94, m (1H), 0.80, d (3H, *J* = 6.7 Hz), 0.69, d (3H, *J* = 6.7 Hz); δ_C 32.0, 19.0, 18.0, respectively], which, through the correlations observed in the HMBC spectrum of the methyl proton signals at δ_H 0.80, d (3H, *J* = 6.7 Hz) and 0.69, d (3H, *J* = 6.7 Hz) to the methine carbon signal at δ_C 62.3 (C-15) and the correlation

Table 1
^1H and ^{13}C NMR data of eurocristatine (**1**) in DMSO-d_6 (^1H 300.13 MHz, ^{13}C 75.47 MHz).

Position	δ_C, type	δ_H (*J* in Hz)	COSY	HMBC[a]	NOESY
1	–	6.74, brs	H-2	C-2, 3, 4, 9	H-2
2	78.8, CH	4.90, brs	H-1		H-1, 11
3	59.7, C	–			
4	130.4, C	–			
5	124.4, CH	7.39, d (7.5)	H-2	C-3, 7, 9	H-6, 12β
6	117.9, CH	6.63, dd (7.5, 7.5)	H-5, 7	C-4, 8	
7	128.7, CH	7.02, dd, (7.5, 7.5)	H-6, 8	C-5, 9	
8	108.9, CH	6.60, d (7.5)	H-7		
9	149.1, C				
11	55.7, CH	4.12, t (9.0)	H-12α, 12β	C-12, 13	H-2, 17, 18, 19
12α	37.3, CH_2	2.39,dd (14.0, 9.5)	H-11, 12β	C-3, 4, 11, 13	12β
12β		3.14,dd (14.0, 9.5)	H-11, 12α	C-3, 4, 11, 13	H-5, 12α
13	168.4, CO				
14	–	8.27, d (4.2)	H-15	C-11, 13, 15, 16	H-17, 18, 19
15	62.3, CH	3.39, t (5.0)	H-14, 17	C-13, 16, 17, 18, 19	
16	167.5, CO	–			
17	32.0, CH	1.94, m	H-15, 18, 19	C-15, 16, 18, 19	H-11, 18, 19
18	19.0, CH_3	0.80, d (6.7)	H-17	C-15, 18, 19	H-17, 19
19	18.0, CH_3	0.69, d (6.7)	H-17	C-15, 18, 19	H-17, 18

[a] HMBC correlations are from proton(s) stated to the indicated carbon.

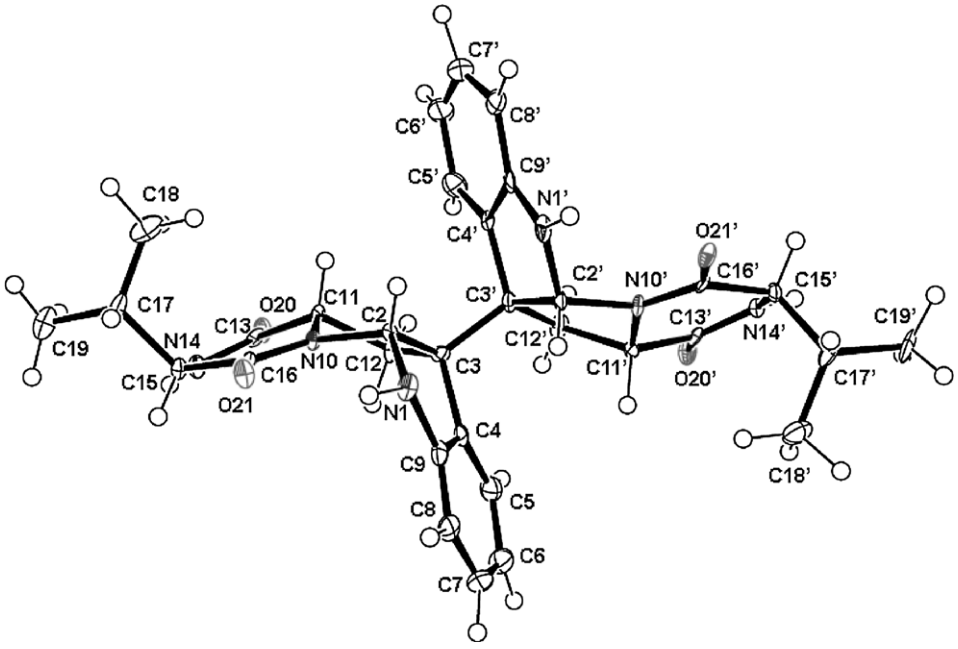

Fig. 3. ORTEP view of eurocristatine (**1**).

between the signals of NH-14 (δ_H 8.27, d, J = 4.2 Hz) and H-15 (δ_H 3.39, t, J = 5.0 Hz) in the COSY spectrum, was placed on C-15 of the 1,4-diketopiperazine ring. The cross peaks observed in the NOESY spectrum between the signals of H-2/H-11 and H-11/H-17, H-11/H_3-18, H-11/H_3-19, suggested that the isopropyl substituent was α oriented. Taking altogether the NMR data, the partial structure **A** ($C_{16}H_{18}N_3O_2$) was proposed (Fig. 2). Since the (+)-HRESIMS gave the molecular formula $C_{32}H_{36}N_6O_4$, the complete structure of eurocristatine (**1**) must comprise two **A** units connected to each other through C-3 (Fig. 1). Final proof of the structure and stereochemistry assigned to eurocristatine (**1**) was provided by an X-ray analysis which established the absolute configuration of C-2/2′, C-3/3′, C-11/11′and C-15/15′, respectively as 2/2′*R*, 3/3′*S*, 11/11′*S* and 15/15′*R*. The result depicted in the ORTEP view shown in Fig. 3 also revealed the symmetrical nature of eurocristatine (**1**). Although several diketopiperazine dimers have been previously reported from many fungal sources, and especially from *Aspergillus* species (Barrow et al., 1993; Barrow and Sedlock, 1994; Cai et al., 2012; Ding et al., 2008; Li et al., 2009; Ovenden et al., 2004; Ruju et al., 2009; Son et al., 1999; Takahashi et al., 1994, 1995a,b; Varoglu et al., 1997; Yamada et al., 2002), eurocristatine (**1**) represents the first diketopiperazine dimer isolated from the genus *Eurotium*. The structure of eurocristatine (**1**) closely resembles that of the diketopiperazine dimer isolated from a marine-derived *Aspergillus niger* by Ovenden et al. (2004) although eurocristatine is a symmetrical dimer whereas asperdimin is not.

Eurocristatine (**1**) was evaluated for its *in vitro* growth inhibitory activity against MCF-7 (breast adenocarcinoma), NCI-H-460 (non-small lung cancer) and A375-C5 (melanoma) cell lines using the protein binding dye SRB method (Kijjoa et al., 2011) and results showed that it was inactive against all the three cell lines at the highest concentration tested (150 μM). Eurocristatine (**1**) was also evaluated for its antifungal activity against yeast (*Candida albicans*), filamentous fungus (*Aspergillus fumigatus*) and dermatophyte (*Trichophyton rubrum*) as well as for its antibacterial activity against *Staphylococcus aureus*, *Escherichia coli* and *Pseudomonas aeruginosa*, according to the procedure described by Wattanadilok et al. (2007) and no antimicrobial activity was registered.

3. Experimental

3.1. General experimental procedures

Melting points were determined on a Bock monoscope and are uncorrected. Optical rotations were determined on an ADP410 Polarimeter. Ultraviolet and infrared spectra were recorded on a Shimadzu mini-1240UV-VIS spectrophotometer and on an ATT Mattson Genesis Series FTIR™ using WinFIRST Software, respectively. ^{1}H and ^{13}C NMR spectra were recorded at ambient temperature on a Bruker AMC instrument operating at 300.13 and 75.4 MHz, respectively. High resolution mass spectra were measured with a Waters Xevo QToF mass spectrometer coupled to a Waters Aquity UPLC system. A Merck silica gel GF 254 was used for preparative TLC, and a Merck Si gel 60 (0.2–0.5 mm) was used for analytical chromatography.

3.2. Extraction of the metabolites

The fungus was isolated, identified, cultured and extracted for its secondary metabolites according to the procedure described in our previous report (Almeida et al., 2010). The crude ethyl acetate extract was chromatographed over a 0.2–0.5 mm Merck Si gel column (145 g) and eluted with mixtures of $CHCl_3$–petrol, $CHCl_3$–Me_2CO, $CHCl_3$–MeOH, 250 mL fractions were collected as follows: frs. 1–119 ($CHCl_3$–petrol, 1:4), 120–130 ($CHCl_3$–petrol, 3:7), 131–163 ($CHCl_3$–petrol, 2:3), 164–195 ($CHCl_3$–petrol, 1:1), 196–234 ($CHCl_3$–petrol, 3:2), 235–260 ($CHCl_3$–petrol, 7:3), 261–273 ($CHCl_3$–petrol, 4:1), 274–291 ($CHCl_3$–petrol, 9:1), 292–300 ($CHCl_3$), 301–348 ($CHCl_3$–Me_2CO, 9:1), 349–376 ($CHCl_3$–Me_2CO, 4:1), 377–394 ($CHCl_3$–Me_2CO, 1:1), 395–402 ($CHCl_3$–MeOH, 1:1). Frs. 13–20 were combined (154 mg) and recrystallized in a mixture of MeOH and $CHCl_3$ to give 14 mg of erythroglaucin (Anke et al., 1980). Frs. 21–29 were combined (259 mg) and recrystallized in a mixture of MeOH and $CHCl_3$ to give 6 mg of physcion (Anke et al., 1980). Frs. 91–119 were combined (493 mg) and purified by TLC (Si Gel, CH_2Cl_2:Me_2CO:HCO_2H, 98:2:1) to give 5 mg of catenarin (Anke et al., 1980) and 5 mg of emodin (Manojlović et al., 2000). Frs. 202–208 were combined (306 mg) and recrystallized in Me_2CO

to yield 53 mg of echinulin (Smetanina et al., 2007) and the mother liquor (247 mg) was combined with frs. 191–201 (201 mg) and purified by TLC (Si Gel, $CHCl_3$:Me_2CO:HCO_2H, 95:5:1) to give 5 mg of variecolorin J (Wang et al., 2007). Frs. 209–216 were combined (216 mg) and recrystallized in Me_2CO to give 51 mg of echinulin and the mother liquor (159 mg) was purified by TLC (Si Gel, $CHCl_3$:Me_2CO:HCO_2H, 95:5:1) to yield 13 mg of neoechinulin A (Li et al., 2008a). Frs. 217–234 were combined (228 mg) and recrystallized in Me_2CO to give 79 mg of echinulin. Frs. 235–247 were combined (302 mg) and recrystallized in Me_2CO to give 26 mg of echinulin and the mother liquor (272 mg) was recrystallized in a mixture of CH_2Cl_2 and petrol to give 17 mg of neoechinulin E (Li et al., 2008a). Frs. 303–321 were combined (338 mg) and recrystallized in MeOH to give 22 mg of eurocristatine (**1**). The mother liquor of frs 303–321 was then combined with frs. 277–301 (1.18 g) and applied on a column chromatography of LiChroprep Si60 (0.04–0.063 mm Merck, 45 g) and eluted with mixtures of $CHCl_3$–petrol, $CHCl_3$–Me_2CO, $CHCl_3$–MeOH, 100 mL subfrs. were collected as follows: subfrs. 1–20 ($CHCl_3$–petrol, 1:4), 21–96 ($CHCl_3$–petrol, 3:7), 97–118 ($CHCl_3$–petrol, 2:3), 119–157 ($CHCl_3$–petrol, 1:1), 158–179 ($CHCl_3$–petrol, 3:2), 180–290 ($CHCl_3$–petrol, 7:3), 291–325 ($CHCl_3$–petrol, 4:1), 326–349 ($CHCl_3$–petrol, 9:1), 350–368 ($CHCl_3$), 369–379 ($CHCl_3$–Me_2CO, 9:1), 380–403 ($CHCl_3$–Me_2CO, 7:3), 404–413 ($CHCl_3$–Me_2CO, 1:1), 414–416 ($CHCl_3$–MeOH, 1:1). Subfrs. 230–326 were combined (263 mg) and recrystallized in $CHCl_3$ to give more 11 mg of eurocristatine (**1**).

3.3. Eurocristatine (*1*)

White crystals; mp 244–245 °C ($CHCl_3$/MeOH); $[\alpha]^{20}_D$ = +300 (*c* 0.02, MeOH); UV (MeOH) λ_{max} (log ε) 212 (4.5), 241 (4.2), 302 (3.9) nm; IR (KBr) υ_{max} 3450, 3190, 2961, 1662, 1453, 1326 cm^{-1}; ^1H and ^{13}C NMR see Table 1; HRESIMS *m*/*z* 569.2905 $[M+H]^+$ (calculated for $C_{32}H_{37}N_6O_4$, 569.2876).

3.4. X-ray crystal structure of eurocristatine (*1*)

Crystals suitable for X-ray diffraction were obtained by slow evaporation of a solution in $CHCl_3$/MeOH for eurocristatine (**1**). Diffraction data were collected at 100 K with a Gemini PX Ultra equipped with Cu Kα radiation (λ = 1.54184 Å). The structure was solved by direct methods using SHELXS-97 and refined with SHELXL-97. Crystals were monoclinic, space group $P2_1$, cell volume 2308.37(5) $Å^3$ and unit cell dimensions *a* = 10.3549(2) Å, *b* = 9.9862(2) Å and *c* = 22.7778(3) Å and β = 101.464(2)° (uncertainties in parenthesis). Carbon, oxygen and nitrogen atoms were refined anisotropically. Hydrogen atoms were refined freely with isotropic displacement parameters. The flack *x* parameter was refined with SHELXL-97 by means of TWIN and BASF to yield 0.031(18). Tables containing the final fractional coordinates, temperature parameters, bond distances, and bond angles were deposited with the Cambridge Crystallographic Data Centre: CCDC reference number 879091.

Acknowledgements

This work was partially supported by the project PEst-C/MAR/LA0015/2011 funded by Fundação para a Ciência e a Tecnologia (FCT) and the European Regional Development Fund (ERDF) through the COMPETE – Operational Competitiveness Programme as part of the National Strategic Reference Framework. NMG thanks Fundação para a Ciência e Tecnologia (FCT) for the scholarship (SFRH/BD/65671/2009) supported by the European Social Fund (ESF). We thank Mrs. Júlia Bessa, Ms. Sara Cravo for technical support and Dr. Mick Lee of the Department of Chemistry, Leicester University, UK for HRMS.

References

Almeida, A.P., Dethoup, T., Singburaudom, N., Lima, R., Vasconcelos, M.H., Pinto, M., Kijjoa, A., 2010. The in vitro anticancer activity of the crude extract of the sponge-associated fungus *Eurotium cristatum* and its secondary metabolites. J. Nat. Pharm. 1, 25–29.

Anke, H., Kolthoum, I., Zähner, H., Laatsch, H., 1980. Metabolic products of microorganisms 185. The anthraquinones of the *Aspergillus glaucus* group. I. Occurrence, isolation, identification and antimicrobial activity. Arch. Microbiol. 126, 223–230.

Barrow, C.J., Cai, P., Snyder, J.K., Sedlock, D.M., Sun, H.H., Cooper, R., 1993. WIN 64821 a new competitive antagonist to substance P, isolated from an *Aspergillus* species: structure determination and solution conformation. J. Org. Chem. 58, 6016–6021.

Barrow, C.J., Sedlock, D.M., 1994. 1′-(2-Phenyl-ethylene)-ditryptophenaline, a new dimeric diketopiperazine from *Aspergillus flavus*. J. Nat. Prod. 57, 1239–1244.

Cai, S., Kong, X., Wang, W., Zhou, H., Zhu, T., Li, D., Gu, Q., 2012. Aspergilazine A, a diketopiperazine dimer with a rare N-1 to C-6 linkage, from a marine-derived fungus *Aspergillus taichungensis*. Tetrahedron Lett. 53, 2615–2617.

Ding, G., Jiang, L., Guo, L., Chen, X., Zhang, H., Che, Y., 2008. Pestalazines and pestalamides, bioactive metabolites from the plant pathogenic fungus *Pestalotiopsis theae*. J. Nat. Prod. 71, 1861–1865.

Geiser, D.M., 2009. Sexual structures in *Aspergillus*: morphology, importance and genomics. Med. Mycol. 47 (Suppl. 1), S21–S26.

Kanokmedhakul, K., Kanokmedhakul, S., Suwannatrai, R., Soytong, K., Prabpai, S., Kongsaeree, P., 2011. Bioactive meroterpenoids and alkaloids from the fungus *Eurotium chevalieri*. Tetrahedron 67, 5461–5468.

Kijjoa, A., Santos, S., Dethoup, T., Manoch, L., Almeida, A.P., Vasconcelos, M.H., Silva, A., Gales, L., Herz, W., 2011. Sartoryglabrins, analog of ardeemins, from *Neosartorya glabra*. Nat. Prod. Commun. 6, 807–812.

Li, D.L., Li, X.M., Li, T.G., Dang, H.Y., Wang, B.G., 2008a. Dioxopiperazine alkaloids produced by the marine mangrove derived endophytic fungus *Eurotium rubrum*. Helv. Chim. Acta 91, 1888–1893.

Li, D.L., Li, X.M., Li, T.G., Dang, H.Y., Proksch, P., Wang, B.G., 2008b. Benzaldehyde derivatives from *Eurotium rubrum*, an endophytic fungus derived from the mangrove plant *Hibiscus tiliaceus*. Chem. Pharm. Bull. 56, 1282–1285.

Li, G.Y., Yang, T., Luo, Y.G., Chen, X.Z., Fang, D.M., Zhang, G.L., 2009. Brevianamide J, a new indole alkaloid dimer from fungus *Aspergillus versicolor*. Org. Lett. 11, 3714–3717.

Manojlović, N.T., Solujić, S., Sukdolak, S., Krstić, L.J., 2000. Isolation and antimicrobial activity of anthraquinones from some species of the lichen genus *Xanthoria*. J. Serb. Chem. Soc. 65, 555–560.

Ovenden, S.P.B., Sberna, G., Tait, R.M., Wildman, H.G., Patel, R., Li, B., Steffy, K., Nguyen, N., Muerer-Grimes, B.M., 2004. A diketopiperazine dimer from a marine-derived isolate *Aspergillus niger*. J. Nat. Prod. 67, 2093–2095.

Ruju, R., Piggott, A.M., Conte, M., Aalbersberg, W.G.L., Feussner, K., Capon, R.J., 2009. Naseseazines A and B: a new dimeric diketopiperazine framework from a marine-derived *Actinomycete*, *Streptomyces* sp. J. Org. Lett. 11, 3862–3865.

Slack, G.J., Puniani, E., Frisvad, J.C., Samson, R.A., Miller, J.D., 2009. Secondary metabolites from *Eurotium* species, *Aspergillus calidoustus* and *A. insuetus* common in Canadian homes with a review of their chemistry and biological activities. Mycol. Res. 113, 480–490.

Smetanina, O.F., Kalinovskii, A.I., Khudyakova, Y.V., Slinkina, N.N., Pivkin, M.V., Kuznetsova, T.A., 2007. Metabolites from the marine fungus *Eurotium repens*. Chem. Nat. Compd. 43, 395–398.

Son, B.W., Jensen, P.R., Kauffman, C.A., Fenical, W., 1999. New cytotoxic epidithiodioxopiperazines related to verticillin A from a marine isolate of the fungus *Penicillium*. Nat. Prod. Lett. 13, 213–222.

Takahashi, C., Numata, A., Ito, Y., Matsumura, E., Araki, H., Iwaki, H., Kushida, K., 1994. Leptosins, antitumour metabolites of a fungus isolated from a marine alga. J. Chem. Soc. Perkin Trans. 1, 1859–1864.

Takahashi, C., Takai, Y., Kimura, Y., Numata, A., Shigematsu, N., Tanaka, H., 1995a. Cytotoxic metabolites from a fungal adherent of a marine alga. Phytochemistry 38, 155–158.

Takahashi, C., Minoura, K., Yamada, T., Numata, A., Kushida, K., Shingu, T., Hagishita, S., Nakai, H., Sato, T., Harada, H., 1995b. Potent cytotoxic metabolites from a *Leptosphaeria* species. Structure determination and conformational analysis. Tetrahedron 51, 3483–3498.

Varoglu, M., Corbett, T.H., Valeriote, F.A., Crews, P., 1997. Asperazine, a selective cytotoxic alkaloid from a sponge-derived culture of *Aspergillus niger*. J. Org. Chem. 62, 7078–7079.

Wang, W.L., Lu, Z.Y., Tao, H.W., Zhu, T.J., Fang, Y.C., Gu, Q.Q., Zhu, W.M., 2007. Isoechinulin-type alkaloids, variecolorins A-L, from halotolerant *Aspergillus variecolor*. J. Nat. Prod. 70, 1558–1564.

Wattanadilok, R., Sawangwong, P., Rodrigues, C., Cidade, H., Pinto, M., Pinto, E., Silva, A., Kijjoa, A., 2007. Antifungal activity evaluation of the constituents of *Haliclona baeri* and *Haliclona cymaeformis*, collected from the Gulf of Thailand. Mar. Drugs 5, 40–51.

Yamada, T., Iwamoto, C., Yamagaki, N., Yamanouchi, T., Minoura, K., Yamori, T., Uehara, Y., Andoh, T., Umemura, K., Numata, A., 2002. Leptosins M-N_1, cytotoxic metabolites from a *Leptosphaeria* species separated from a marine alga. Structure determination and biological activities. Tetrahedron 58, 479–487.

APPENDIX III

Eamvijarn, A., **Gomes, N.M.,** Dethoup, T., Buaruang, J., Manoch, L., Silva, A., Pedro, M., Marini, I., Roussis, V., Kijjoa, A. **(2013)**. Bioactive meroditerpenes and indole alkaloids from the soil fungus *Neosartorya fischeri* (KUFC 6344), and the marine-derived fungi *Neosartorya laciniosa* (KUFC 7896) and *Neosartorya tsunodae* (KUFC 9213). *Tetrahedron* 69(40), 8583-8591.

Tetrahedron 69 (2013) 8583–8591

Contents lists available at SciVerse ScienceDirect

Tetrahedron

journal homepage: www.elsevier.com/locate/tet

Bioactive meroditerpenes and indole alkaloids from the soil fungus *Neosartorya fischeri* (KUFC 6344), and the marine-derived fungi *Neosartorya laciniosa* (KUFC 7896) and *Neosartorya tsunodae* (KUFC 9213)

Amnat Eamvijarn [a,b], Nelson M. Gomes [a], Tida Dethoup [a,b], Jamrearn Buaruang [c], Leka Manoch [b], Artur Silva [d], Madalena Pedro [e,f], Ioulia Marini [g], Vasilios Roussis [g], Anake Kijjoa [a,*]

[a] *ICBAS – Instituto de Ciências Biomédicas de Abel Salazar and CIIMAR, Universidade do Porto, Rua de Jorge Viterbo Ferreira 228, 4050-313 Porto, Portugal*
[b] *Department of Plant Pathology, Faculty of Agriculture, Kasetsart University, Bangkok, Thailand*
[c] *Division of Environmental Science, Faculty of Science, Ramkhamhaeng University, Bangkok 10240, Thailand*
[d] *Departamento de Química, Universidade de Aveiro, 4810-1933 Aveiro, Portugal*
[e] *CEQUIMED – Centro de Química Medicinal da Universidade do Porto, Rua de Jorge Viterbo Ferreira 228, 4050-313 Porto, Portugal*
[f] *Grupo de Biologia Molecular e Celular (GBMC), Centro de Investigação em Ciências da Saúde (CICS), Instituto Superior de Ciências da Saúde do Norte, CESPU, Rua Central de Gandra 1317, 4585-116 Gandra, Portugal*
[g] *Department of Pharmacognosy and Chemistry of Natural Products, School of Pharmacy, University of Athens, Panepistimiopolis Zografou, Athens 15771, Greece*

ARTICLE INFO

Article history:
Received 8 June 2013
Received in revised form 18 July 2013
Accepted 22 July 2013
Available online 31 July 2013

Keywords:
Neosartorya fischeri (KUFC 6344)
Neosartorya laciniosa (KUFC 7896)
Neosartorya tsunodae (KUFC 9213)
Meroditerpenes
Sartorypyrones
Aszonalenin

ABSTRACT

Two new metabolites including a new aszonalenin analogue (**1c**) and a new meroditerpene (**3**) were isolated, together with aszonalenin (**1a**), acetylaszonalenin (**1b**), 13-oxofumitremorgin B (**2**), aszonapyrone A (**4b**) and helvolic acid, from the culture of the soil fungus *Neosartorya fischeri* (KUFC 6344). While the ethyl acetate extract of the culture of the diseased coral-derived fungus *Neosartorya laciniosa* (KUFC 7896) furnished aszonapyrone B (**4a**), aszonapyrone A (**4b**), tryptoquivaline L and 3′-(4-oxoquinazolin-3-yl) spiro[1*H*-indole-3,5′-oxolane]-2,2′-dione, the ethyl acetate extract of the culture of the marine sponge-associated fungus *Neosartorya tsunodae* (KUFC 9213) yielded a new analogue of chevalone C (**5**) and helvolic acid. The structures of the new compounds were established based on 1D and 2D NMR spectral analysis as well as HR-ESIMS. Compounds **1a**–**c**, **2**, **3**, **4a**, **4b** and **5** were evaluated for their in vitro growth inhibitory activity on the MCF-7 (breast adenocarcinoma), NCI-H460 (non-small cell lung cancer) and A375-C5 (melanoma) cell lines by the protein binding dye SRB method.
© 2013 Elsevier Ltd. All rights reserved.

1. Introduction

Neosartorya species (Trichocomaceae) are sexual forms of the *Aspergillus* species, notably the section Fumigati. While the *Aspergillus* species only produce conidospores, *Neosartorya* species produce both a sexual state with ascospores and an asexual state with conidiospores.[1] Unlike *Aspergillus*, *Neosartorya* species have not been extensively investigated for their secondary metabolites. Consequently, we started to investigate the secondary metabolites of the fungi of this genus. We have previously reported isolation and structure elucidation of three new reverse prenylated indole derivatives sartoryglabrins A–C from the culture of a Thai collection of *Neosartorya glabra*.[2] We later reported isolation of cadenene sesquiterpene, the indole derivative eurochevalierine, brasiliaminde B, pyripyropene A and three new metabolites including 1,4-diacetyl-2,5-dibenzylpiperazine 3,7″-oxide, a quinazolinone-containing indole derivative and a phenyl ester of 2,4-dihydroxy-6-methylbenzoic acid from the culture of the soil fungus *Neosartorya pseudofisheri*, as well as the in vitro cytostatic activity of the cadenene sesquiterpene and eurochevalierine in human cancer cancer cells.[3] Recently, we reported isolation of a new indole alkaloid sartorymensin, and new analogues of tryptoquivaline and fiscalins, produced by a Thai collection of the soil fungus *Neosartorya siamensis* (KUFC 6349), as well as their in vitro growth

* Corresponding author. Tel.: +351 220428331; fax: +351 222062232; e-mail addresses: ankijjoa@icbas.up.pt, anakekijjoa@yahoo.com (A. Kijjoa).

0040-4020/$ – see front matter © 2013 Elsevier Ltd. All rights reserved.
http://dx.doi.org/10.1016/j.tet.2013.07.078

inhibitory activity on the human U373 and Hs683 glioblastoma, the A549 non-small cell lung cancer, the MCF-7 breast cancer and the SKMEL-28 melanoma cell lines by MTT colorimetric assay.[4]

In our ongoing search for bioactive compounds produced by soil and marine-derived fungi of the genus *Neosartorya*, we have investigated the cultures of the soil fungus *Neosartorya fischeri* and the marine-derived fungi *Neosartorya tsunodae* and *Neosartorya laciniosa*. Although *N. fischeri* has been extensively investigated for its secondary metabolites,[5–9] to the best of our knowledge, there is no report on the secondary metabolites produced by *N. tsunodae* and *N. laciniosa*. Examination of a collection of *N. fischeri* (KUFC 6344), isolated from the coastal forest soil in Thailand, resulted in isolation of a new aszonalenin analogue (**1c**) and a new meroditerpene sartorypyrone A (**3**), in addition to five known metabolites including aszonalenin (**1a**),[10] acetylaszonalenin (**1b**),[10] 13-oxofumitremorgin B (**2**),[11] aszonapyrone A (**4b**)[12] (Fig. 1) and helvolic acid,[13] from the ethyl acetate extract of its culture. In order to investigate the secondary metabolites profile of the marine-derived fungi of this genus, we also examined Thai collections of *N. laciniosa* (KUFC 7896), isolated from a diseased coral (*Porites lutea*) from the Gulf of Thailand, and *N. tsunodae* (KUFC 9213), isolated from the marine sponge *Aka coralliphaga*, collected from the coral reef of the Similan islands, Phagna province, southern Thailand. The ethyl acetate extract of the culture of *N. laciniosa* (KUFC 7896) furnished aszonapyrone B (**4a**),[14] aszonapyrone A (**4b**)[12] (Fig. 1), tryptoquivaline L[4] and 3′-(4-oxoquinazolin-3-yl) spiro[1*H*-indole-3,5′-oxolane]-2,2′-dione,[4] while the ethyl acetate extract of the culture of *N. tsunodae* (KUFC 9213) yielded, besides helvolic acid,[13] sartorypyrone B (**5**), a new analogue of chevalone C (Fig. 1). Additionally, we also evaluated the in vitro growth inhibitory activity of compounds **1a**–**c**, **2**, **3**, **4a**, **b** and **5** (Fig. 1) on MCF-7 (breast adenocarcinoma), NCI-H460 (non-small cell lung cancer) and A375-C5 (melanoma) cell lines by the protein binding dye SRB method.

2. Results and discussion

Compound **1c** was isolated as pale yellow semisolid, and its molecular formula $C_{24}H_{23}N_3O_4$ was established on the basis of the (+)-HR-ESIMS *m*/*z* 418.1767 $[M+H]^+$, indicating fifteen degrees of unsaturation. The general features of the ^1H and ^{13}C NMR spectra of **1c** closely resembled those of aszonalenin (**1a**) and acetylaszonalenin (**1b**). The IR spectrum showed absorption bands for hydroxyl (3377 cm^{-1}), amine (3242 cm^{-1}), aromatic (3089, 1485 cm^{-1}), amide carbonyl (1680, 1657 cm^{-1}) and olefin (1605 cm^{-1} g) groups. The ^{13}C NMR, DEPT and HSQC spectra (Table 1) revealed two amide carbonyls (δ_C 169.1 and 166.9), one *N*-formyl (δ_C 162.4), five quaternary sp^2 (δ_C 153.1, 136.1. 133.6, 133.1, 127.0), eight methine sp^2 (δ_C 142.6, 132.7, 131.3, 125.7, 120.5, 118.4, 115.5, 112.1), one methylene sp^2 (δ_C 115.0), two quaternary sp^3 (δ_C 59.4, 41.2), two methine sp^3 (δ_C 80.9, 57.1), one methylene sp^3 (δ_C 32.7) and two methyl (δ_C 22.8, 22.4) carbons. The coupling system of the aromatic protons observed in the COSY spectrum (Table 1) revealed the presence of one 1,2-disubstituted and one 1,2,4-trisubstituted benzene rings. Analysis of the HMBC spectrum (Table 1) indicated that the 1,2,4-

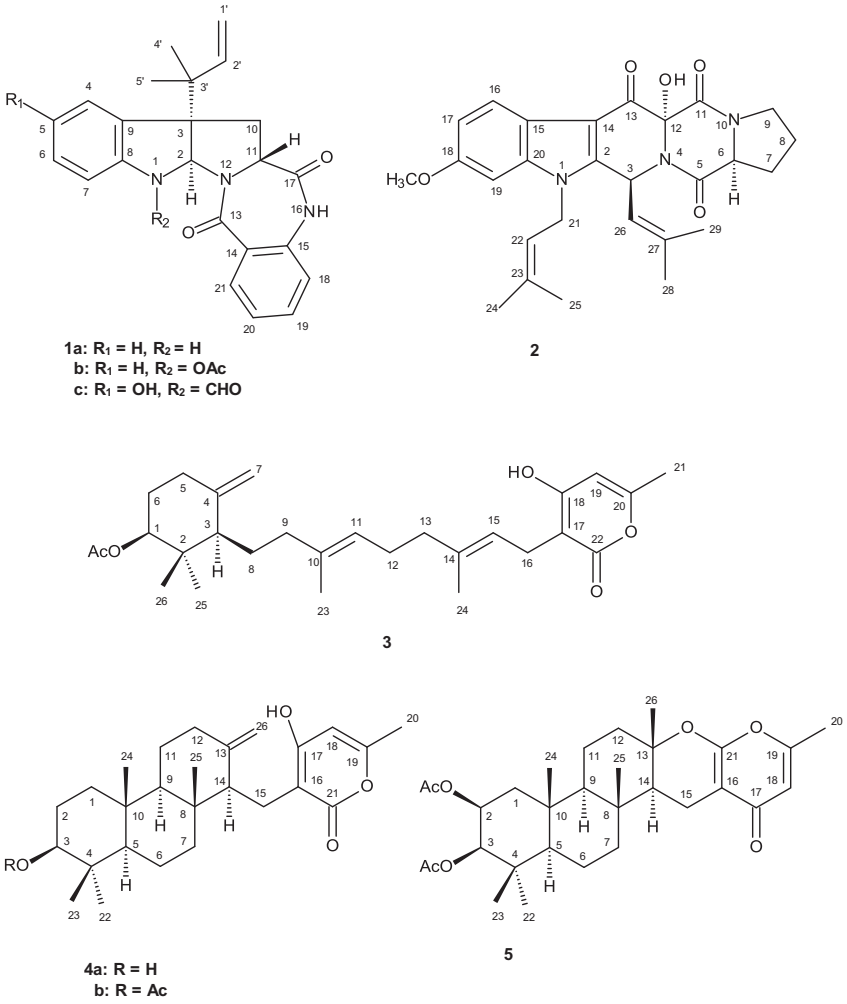

Fig. 1. Secondary metabolites of *Neosartorya fischeri* (KUFC 6344), *N. laciniosa* (KUFC 7896) and *N. tsunodae* (KUFC 9213).

Table 1
^{1}H and ^{13}C NMR ($CDCl_3$, 300.13 and 75.47 MHz) and HMBC assignments for **1c**

Position	δ_C, type	δ_H (J in Hz)	COSY	HMBC
2	80.9, CH	5.99, s		C-3′, 8, 9, 11, NCHO
3	59.4, C	—		
4	112.1, CH	6.79, d (2.5)	H-6	C-5, 6, 8
5	153.1, C	—		
6	115.5, CH	6.74, dd (8.5, 2.5)	H-4, 7	C-4, 8
7	118.4, CH	7.76, d, (8.5)	H-6	C-5, 9
8	133.6, C	—		
9	136.1, C	—		
10α	32.7, CH_2	3.38, dd (13.9, 8.6)	H-10β, 11	C-3, 3′, 9, 17
β		2.43, dd (13.9, 8.2)	H-10α, 11	C-2, 3′, 9
11	57.1, CH	4.04, t (8.4)	H-10α, 10β	C-10
13	166.9, CO	—		
14	127.0, C	—		
15	133.1, C	—		
16	—	8.27, s		C-11, 14
17	169.1, CO	—		
18	120.5, CH	6.92, d (7.7)	H-19	C-14, 20
19	132.7, CH	7.43, ddd (7.7, 7.7, 1.5)	H-18, 20	C-15, 21
20	125.7, CH	7.21, dd (7.7, 7.7)	H-19, 21	C-14, 18
21	131.3, CH	7.75, d (7.7)	H-20	C-13, 19
1′a	115.0, CH2	5.11, d (17.3)	H-2′	C-2′, 3′
b		5.15, d (10.8)	H-2′	
2′	142.6, CH	5.90, dd (17.3, 10.8)	H-1′a, 1′b	C-5′
3′	41.2, C	—		
4′	22.8, CH_3	1.02, s		C-2′, 3, 3′, 5′
5′	22.4, CH_3	1.15, s		C-2′, 3, 3′, 4′
NCHO	162.4, CO	8.95, s		C-8

trisubstituted benzene ring was part of a 2,3-dihydro-1*H*-indole moiety while the 1,2-disubstituted benzene ring was part of a 3,4-dihydro-1*H*-1,4-benzodiazepine-2,5-dione portion. That the 2,3-dihydro-1*H*-indole and the 3,4-dihydro-1*H*-1,4-benzodiazepine-2,5-dione portions were linked together through a pyrrolidine ring was corroborated by the HMBC cross peaks of H-2 (δ_H 5.99, s) to C-11 (δ_C 57.1); H-10α (δ_H 3.38, dd, J=13.9, 8.6 Hz) to C-3 (δ_C 59.4), C-9 (δ_C 136.1), C-17 (δ_C 169.1), as well as of N16-H (δ_H 8.27, s) to C-11 and C-14 (δ_C 127.0) (Fig. 2a). Additionally, the coupling system observed in the COSY spectrum (Table 1) also revealed the presence of a 2-methylbut-3-en-2-yl substituent, which was corroborated by the HMBC cross peaks (Table 1) of H_3-5′ (δ_H 1.15, s) to C-2′ (δ_C 142.6), C-3′ (δ_C 41.2), CH_3-4′(δ_C 22.8); H-4′ (δ_H 1.02, s) to C-2′, C-3′, CH_3-5′ (δ_C 22.4); H-2′ (δ_H 5.90, dd, J=17.3, 10.8 Hz) to CH_3-5′; H-1′a and H-1′b (δ_H 5.11, d, J=17.3 Hz and 5.15, d, J=10.8 Hz) to C-2′ and C-3′. That the 2-methylbut-3-en-2-yl substituent was on C-3 was substantiated by the HMBC cross peaks of H-2 to C-3′; H-10α to C-3′ as well as of H_3-4′ and H_3-5′ to C-3 (Fig. 2a). These ^{1}H and ^{13}C NMR data were very similar to those reported for aszonalenin,[5] and since the HMBC spectrum (Fig. 2a) also displayed cross peak between the proton signal at δ_H 8.95, s, to the signal of C-8 (δ_C 133.6), the formyl group was placed on N-1.

In order to verify the relative configuration of C-2, C-3 and C-11, the NOESY experiment was carried out. The NOESY spectrum (Fig. 2b) displayed correlations of H-2 to H_3-4′, H_3-5′, H-10α; and of H-11 (δ_H 4.04, t, J=8.4 Hz) to H-10β (δ_H 2.43, dd, J=13.9, 8.2 Hz); however no correlation between H-2 and H-11 was observed. Consequently, the relationship between H-2 and H-11 was *trans* whereas the relationship between H-2 and the 2-methylbut-3-en-2-yl substituent on C-3 was *cis*. Thus, the relative configuration of C-2, C-3 and C-11 of **1c** was the same as that of the corresponding carbons of aszonalenin.[5] Taking together the ^{1}H and ^{13}C NMR data, the HMBC and NOESY correlations and the molecular formula, the structure of **1c** was established as 1-formyl-5-hydroxyaszonalenin.

Although several analogues of aszonalenin have been previously isolated,[15] to our knowledge, this is the first report of isolation of the 5-hydroxyl analogue of aszonalenin.

Compound **3** was isolated as brown viscous mass and its molecular formula $C_{28}H_{40}O_5$ was established on the basis of the (+)-HR-ESIMS m/z 457.2954 $[M+H]^+$, indicating nine degrees of unsaturation. The IR spectrum showed absorption bands for hydroxyl (3434 cm^{-1}), olefinic (3080, 1585 cm^{-1}) and carbonyl (1730, 1684 cm^{-1}) groups. The ^{13}C NMR, DEPT and HSQC spectra (Table 2) revealed the presence of one ester carbonyl (δ_C 171.1), one conjugated ester carbonyl (δ_C 166.8), six quaternary sp^2 (δ_C 166.1, 159.9, 146.6, 138.2, 135.4, 101.7), three methine sp^2 (δ_C 124.1, 120.5, 101.1), one methylene sp^2 (δ_C 109.2), one quaternary sp^3 (δ_C 39.1), two methine sp^3 (δ_C 78.9, 51.0), seven methylene sp^3 (δ_C 39.7, 38.2, 31.7, 28.6, 26.3, 23.6, 22.4) and six methyl (δ_C 26.0, 21.3, 19.6, 17.5, 16.3, 15.9) carbons. The existence of a 4-hydroxy-6-methyl-2*H*-pyran-2-one moiety was supported not only by the cross peak between H-19 (δ_H 6.00, d, J=0.7 Hz) and H_3-21 (δ_H 2.19, s) in the COSY spectrum but also by HMBC cross peaks of H-19 to C-17 (δ_C 101.7), C-18 (δ_C 166.1), C-20 (δ_C 159.9), C-21 (δ_C 19.6) and H_3-21 to C-19 (δ_C 101.1) and C-20 (Fig. 3a). That another portion of the molecule 1-acetoxy-2,2-dimethyl-4-methylidenecyclohexyl derivative was evidenced by the correlations of H-1 (δ_H 4.66, dd, J=8.9, 4.1) to H-6β (δ_H 1.55, m) and H-6α (δ_H 1.85, m) in the COSY spectrum, as well as by HMBC cross peaks of H-1 to C-2 (δ_C 39.1), C-3 (δ_C 51.0), CH_3-26 (δ_C 17.5) and CO (δ_C 170.1); H-7a (δ_H 4.88, br s) and H-7b (δ_H 4.62, br s) to C-3 and C-5 (δ_C 31.7); H-5β (δ_H 2.31, dt, J=13.5, 5.6 Hz) to C-1 (δ_C 78.9), C-3, C-4 (δ_C 146.6) and C-7 (δ_C 109.2); H_3-25 (δ_H 0.94, s), and H_3-26 (δ_H 0.79, s) to C-1, C-2, C-3 (Fig. 3a). Since H-1 appeared as a double doublet with the coupling constants of 8.9 and 4.1 Hz, the position of the acetoxyl group on C-1 was β. Moreover, the COSY spectrum also exhibited correlations of H-11 (δ_H 5.05, dd, J=5.6, 6.5 Hz) to H_3-23 (δ_H 1.58, s) and H-12 (δ_H 2.08, m), as well as of H-15 (δ_H 5.29, ddd, J=7.2, 7.2, 1.0 Hz) to H_3-24 (δ_H 1.77,

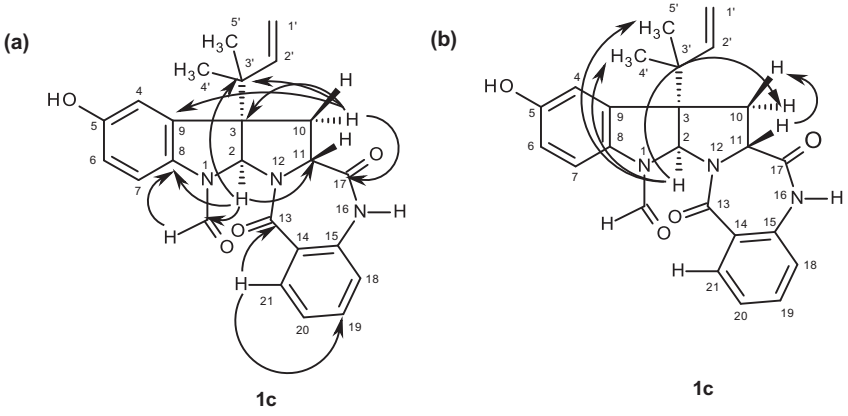

Fig. 2. Key HMBC (a) and NOESY (b) correlations of compound **1c**.

Table 2
^{1}H and ^{13}C NMR ($CDCl_3$, 300.13 and 75.47 MHz) and HMBC assignments for **3**

Position	δ_C, type	δ_H (J in Hz)	COSY	HBMC
1	78.9, CH	4.66, dd (8.9, 4.1)	H-6α, 6β	C-2, 3, 5, 26, CO (Ac)
2	39.1, C	—		
3	51.0, CH	1.72, dd (9.1, 3.1)	H-8	C-2, 4, 8
4	146.6, C	—		
5α	31.7, CH_2	2.03, m	H-5β, 6α, 6β	
β		2.31, dt, (13.5, 5.6)	H-5α, 6α, 6β	C-1, 3, 4, 7
6α	28.6, CH_2	1.85, m	H-5α, 5β, 6β	
β		1.55, m	H-5α, 5β, 6α	
7a	109.2, CH_2	4.88, br s	H-7b	C-3, 5
b		4.62, br s	H-7a	C-3, 5
8	23.6, CH_2	1.59, m	H-3, 9	
9	38.2, CH_2	1.80, m	H-8	
10	135.4, C	—		
11	124.1, CH	5.05, dd (5.6, 6.5)	H-12, 23	C-9, 23
12	26.3, CH_2	2.08, m	H-11, 13	
13	39.7, CH_2	2.04, m	H-12	
14	138.2, C	—		
15	120.5, CH	5.29, ddd (7.2, 7.2, 1.0)	H-16, 24	C-13, 24
16	22.4, CH_2	3.20, d (7.2)	H-15	C-14, 15, 17, 18, 22
17	101.7, C	—		
18	166.1, C	—		
19	101.1, CH	6.00, d (0.7)	H-21	C-17, 18, 20, 21
20	159.9, C	—		
21	19.6, CH_3	2.19, s	H-19	C-19, 20
22	166.8, CO	—		
23	15.9, CH_3	1.58, s		C-9, 10, 11
24	16.3, CH_3	1.77, s		C-13, 14, 15
25	26.0, CH_3	0.94, s		C-1, 2, 3, 26
26	17.5, CH_3	0.79, s		C-1, 2, 3, 25
OAc	171.1, CO	—		
	21.3, CH_3	2.07, s		CO (OAc)

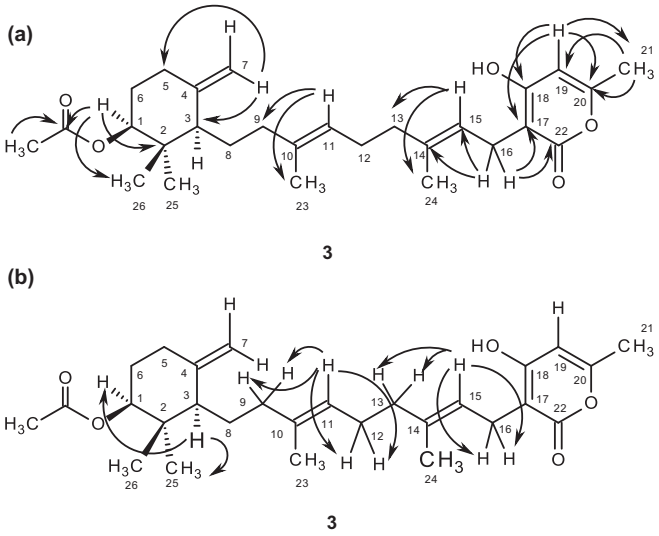

Fig. 3. Key HMBC (a) and NOESY (b) correlations of compound **3**.

s) and H-16 (δ_H 3.20, d, J=7.2 Hz), suggesting the presence of two trisubstituted double bonds in the molecule. These coupling systems were corroborated by HMBC cross peaks of H-11 signal to the signals of C-9 (δ_C 38.2) and C-23 (δ_C 15.9); and H_3-23 to C-9, C-10 (δ_C 135.4) and C-11 (δ_C 124.1), as well as cross peaks of H-15 signal to the signals of C-13 (δ_C 39.7) and C-24 (δ_C 16.3). Additionally, the HMBC spectrum also exhibited a cross peak between the signals of H-12 and C-14 (δ_C 138.2), suggesting that the two trisubstituted double bonds were connected through C-12 and C-13, thus another partial structure was a 3,7-dimethylnona-2,6-diene. That the 3,7-dimethylnona-2,6-diene portion and the 1-acetoxy-2,2-dimethyl-4-methylidenecyclohexyl derivative were connected through C-8 of the former and C-3 of the latter was substantiated by cross peaks observed between the signals of H-3 (δ_H 1.72, dd, J=9.1, 3.1) and H-8 (δ_H 1.59, m) in the COSY spectrum. Moreover, the HMBC cross peaks of H-16 signal to the signals of C-17, C-18 and C-22 (δ_C 166.8) provided evidence that another substituent of the 3,7-dimethylnona-2,6-diene portion was the 4-hydroxy-6-methyl-2*H*-pyran-2-one moiety, connected through C-16 of the former and C-17 of the latter. In order to determine the relative configuration of the stereogenic carbons and the configuration of the double bonds at C-10 and C-14, the NOESY experiment was carried out. As the NOESY spectrum (Fig. 3b) exhibited cross peaks of H-3 signal to the signals of H-1 and H_3-25, the relationship between H-1 and H-3 was *cis*. Consequently, the relative configuration of C-1 and C-3 was 1*S**, 3*S**. Furthermore, since the NOESY spectrum also exhibited cross peaks of H-11 to H-12 and H-9 (δ_H 1.80, m), as well as of H-15 to H-13 (δ_H 2.04, m) and H-16 (Fig. 3b), the configuration of the double bonds at C-10 and C-14 was 10*E*, 14*E*. Thus, compound **3** was a new monocyclic meroditerpene, which we have named sartorypyrone A.

Compound **5** was isolated as yellow viscous mass and its molecular formula $C_{30}H_{42}O_7$ was established on the basis of the (+)-HR-ESIMS m/z 515.3038 $[M+H]^+$(calculated 515.3009), indicating ten degrees of unsaturation. The IR spectrum showed absorption bands for ester (1734 cm^{-1}), conjugated ketone (1670 cm^{-1}) and olefinic (1631, 1596 cm^{-1}) groups. The ^{13}C NMR, DEPT and HSQC spectra (Table 3) revealed the presence of one carbonyl of a conjugated ketone (δ_C 180.8), two ester carbonyls (δ_C 170.7 and 170.2), three quaternary sp^2 (δ_C 162.7, 160.7, 98.5), one methine sp^2 (δ_C 111.8), four quaternary sp^3 (δ_C 84.2, 37.4, 37.3, 36.9), five methine sp^3 (δ_C 77.7,

Table 3
^{1}H and ^{13}C NMR ($CDCl_3$, 300.13 and 75.47 MHz) and HMBC assignments for **5**

Position	δ_C, type	δ_H (J in Hz)	COSY	HMBC
1α	41.8, CH_2	1.36, dd (14.8, 3.8)	H-2	
β		2.08, dd (14.8, 3.8)	H-2	
2	69.4, CH	5.36, ddd (4.0, 3.8, 3.8)	H-1, 3	C-3, 4, CO (Ac-2)
3	77.7, CH	4.61, d (4.0)	H-2	C-2, 4, 22, 23, CO (Ac-3)
4	37.4, C	—		
5	55.3, CH	1.04, m	H-6	
6	17.6, CH_2	1.59, m	H-5, 7α, β	
7α	40.8, CH_2	1.92, ddd (12.8, 3.0, 3.0)	H-6, 7β	
β		1.12, m	H-6, 7α	
8	37.3, C	—		
9	60.8, CH	0.95, m	H-11	
10	36.9, C	—		
11	18.9, CH_2	1.39, m	H-9, 12	
		1.42, m		
12	40.0, CH_2	1.68, m	H-11	
		2.03, m		
13	84.2, C	—		
14	52.4, CH	1.51, dd (12.7, 4.9)	H-15α, β	C-8, 13
15α	15.3, CH_2	2.55, dd (16.4, 4.9)	H-14, 15β	C-13, 14, 16, 17, 21
β		2.15, dd (16.4, 12.7)	H-14, 15α	
16	98.5, C	—		
17	180.8, CO	—		
18	111.8, CH	6.05, br s	H-20	C-16, 19, 20
19	160.7, C	—		
20	19.3, CH_3	2.22, s	H-18	C-18, 19
21	162.7, C	—		
22	29.0, CH_3	0.90, s		C-3, 4, 5, 23
23	17.4, CH_3	1.05, s		C-3, 4, 5, 22
24	17.0, CH_3	1.12, s		C-1, 5, 9, 10
25	16.3, CH_3	0.92, s		C-7, 8, 9, 14
26	20.5, CH_3	1.29, s		C-12, 13, 14, Ac-2
Ac-2	170.2, CO	—		
	21.3, CH_3	2.06, s		CO (Ac-2)
Ac-3	170.7, CO	—		
	20.9, CH_3	2.03, s		CO (Ac-3)

69.4, 60.8, 55.3, 52.4), six methylene sp^3 (δ_C 41.8, 40.8, 40.0, 18.9, 17.6, 15.3) and eight methyl (δ_C 29.0, 21.3, 20.9, 20.5, 19.3, 17.4, 17.0, 16.3) groups. Except for the presence of an additional acetoxyl group, the ^1H and ^{13}C NMR data (Table 3), revealed the existence of a perhydrophenanthrene moiety connected to the 2-methyl-4*H*-pyran-4-one portion through the methylene group and the ethereal bridge, similar to those of chevalone C, a meroditerpenoid isolated from *Eurotium chevalieri*.[14] The COSY spectrum (Table 3) revealed the coupling of the oxymethine proton (δ_H 5.36, ddd, J=4.0, 3.8, 3.8, H-2) to another oxymethine proton (δ_H 4.61, d, J=4.0, H-3) and to the methylene protons at δ_H 1.36, dd, J=14.8, 3.8 and δ_H 2.08, dd, J=14.8, 3.8 (δ_C 41.8). That the acetoxyl groups were on C-2 (δ_C 69.4) and C-3 (δ_C 77.7) were corroborated by the HMBC cross peaks of H-2 signal and the methyl protons signal at δ_H 2.06, s (δ_C 21.3) to the carbonyl signal at δ_C 170.2, as well as of the HMBC cross peaks of H-3 signal and the signal of the methyl protons at δ_H 2.03, s (δ_C 20.9) to the carbonyl signal at δ_C 170.7, respectively (Fig. 4a). The HMBC spectrum also exhibited cross peaks of H-3 signal to the signals of CH_3-23 (δ_C 17.4) and CH_3-22 (δ_C 29.0), C-4 (δ_C 37.4) and C-2, as well as cross peaks of H-2 to the signals of C-3 and C-4 (Fig. 4a). Since H-3 and H-2, respectively, appeared as a doublet at δ_H 4.61 (J=4.0 Hz) and a double of double doublet at δ_H 5 0.36 (J=4.0, 3.8, 3.8), the positions of the acetoxyl groups on C-2 and C-3 were both β oriented.[16]

intermediate (II). Enolization of II leads to the formation of the intermediate III, which can undergo different modes of cyclization. Cyclization via pathway *a* would yield the monocyclic diterpene intermediate (IV), which upon acetylation, produces sartorypyrone A (**3**), while cyclization via pathway *b* would lead to the formation of aszonapyrone B (**4a**); and after acetylation of the β-hydroxyl group on C-3, yields aszonapyrone A (**4b**). On the other hand, formation of the pyran ring (pathway *c*) would lead to the hexacyclic derivative (VI), which gives chevalone C upon acetylation of the β-hydroxyl group on C-3. Hydroxylation of C-2 of chevalone C, followed by acetylation of this β-hydroxyl group would finally form sartorypyrone B (**5**). Isolation of sartorypyrone A (**3**), together with aszonapyrone B (**4a**), aszonapyrone A (**4b**) and sartorypyrone B (**5**) provides evidence that extension of the diterpene unit by the triketide moiety occurs prior to cyclization of GPP, and that different modes of cyclization of GPP can operate to produce these meroditerpenoids (Fig. 5).

Aszonalenin derivatives (**1a**–**c**), 13-oxofumitremorgin B (**2**), sartorypyrone A (**3**), aszonapyrone B (**4a**), aszonapyrone A (**4b**) and sartorypyrone B (**5**) were evaluated for their capacity to inhibit the in vitro growth of MCF-7 (breast adenocarcinoma), NCI-H460 (non-small cell lung cancer) and A375-C5 (melanoma) cell lines, using the protein binding dye SRB method. Results (Table 4) showed that, among the meroditerpenes tested, aszonapyrone A (**4b**) was the most

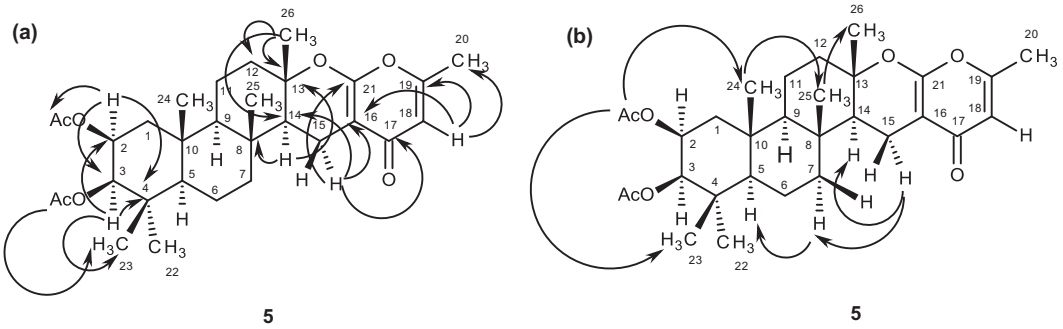

Fig. 4. Key HMBC (a) and NOESY (b) correlations of compound **5**.

The positions of the methyl groups on C-8, C-10 and C-13 were determined by a NOESY experiment. The NOESY spectrum (Fig. 4b) exhibited cross peaks of the methyl protons signal of the β-acetoxyl group on C-2 (δ_H 2.06, s) to the signals of CH_3-23 (δ_H 1.05, s) and CH_3-24 (δ_H 1.12, s), implying that CH_3-24 was β oriented. That CH_3-25 and CH_3-26 were both β oriented was evidenced by the cross peaks between the signals of CH_3-24 and CH_3-25 (δ_H 0.92, s), as well as between the signals of CH_3-25 and CH_3-26 (δ_H 1.29, s). The NOESY spectrum also displayed cross peaks of the signal of H-15α (δ_H 2.55, dd, J=16.4, 4.9) to the signals of H-14 (δ_H 1.51, dd, J=12.7, 4.9) and H-7α (δ_H 1.92, ddd, J=12.8, 3.0, 3.0), suggesting that the latters were α oriented. In turn, the signal of H-7α also exhibited cross peaks to H-5 signal (δ_H 1.04, m), implying that it was also α oriented. Since H-3 signal was found to exhibit cross peak with the proton signal at δ_H 1.36, dd, J=14.8, 3.8, the latter was assigned for H-1α. Thus, compound **5** is a 2β-acetoxyl analogue of chevalone C, and since it is a new compound, we have named it sartorypyrone B.

To our knowledge, this is the first report of isolation of meroditerpenes from *N. fischeri*, even though xanthone derivatives including ergochrome and indole alkaloids, such as aszonalenin derivatives, tryptoquivalines, fiscalins and fumitremorgins, have been previously reported from this fungus.[5–9]

The biosynthetic pathways leading to the formation of sartorypyrone A (**3**), aszonapyrone B (**4a**), aszonapyrone A (**4b**) and sartorypyrone B (**5**) can be hypothesized to originate from the reaction of the triketide derivative (I) with GPP to form the meroditerpene

active, showing strong growth inhibitory activity against the three cell lines, with GI_{50}=13.6±0.9 μM, 11.6±1.5 μM and 10.2±1.2 μM, for MCF-7, NCI-H460 and A375-C5, respectively, while aszonapyrone B (**4a**), whose structure corresponds to 3-deacetyl aszonapyrone A (**4b**), was inactive at the highest concentration tested (150 μM). Sartorypyrone B (**5**) also exhibited strong growth inhibitory activity, although less active than aszonapyrone A (**4b**), having GI_{50}=17.8±7.4 μM, 20.5±2.4 μM and 25.0±4.4, respectively, for MCF-7, NCI-H460 A375-C5. Interestingly, sartorypyrone A (**3**), which possesses a monocyclic diterpene core, was more selective, exhibiting similar inhibitory activity to sartorypyrone B (**5**) against A375-C5 (GI_{50}=21.5±1.9 μM), but less active against MCF-7 (GI_{50}=46.3±7.6 μM) and NCI-H460 (GI_{50}=37.3±4.0 μM) cell lines. On the contrary, all the three aszonalenin derivatives (**1a**–**c**) were found to be inactive against all the three cell lines at the highest concentration tested (150 μM), whereas 13-oxofumitremorgin B (**2**) exhibited only weak inhibitory activity against all the three cell lines (GI_{50}=115.0±20.0 μM, 123.3±11.5 μM and 68.6±12.9 μM, respectively, for MCF-7, NCI-H460 and A375-C5).

3. Experimental section

3.1. General experimental procedures

Melting points were determined on a Bock monoscope and are uncorrected. Optical rotations were determined on an ADP410 Polarimeter. Infrared spectra were recorded on an ATT Mattson

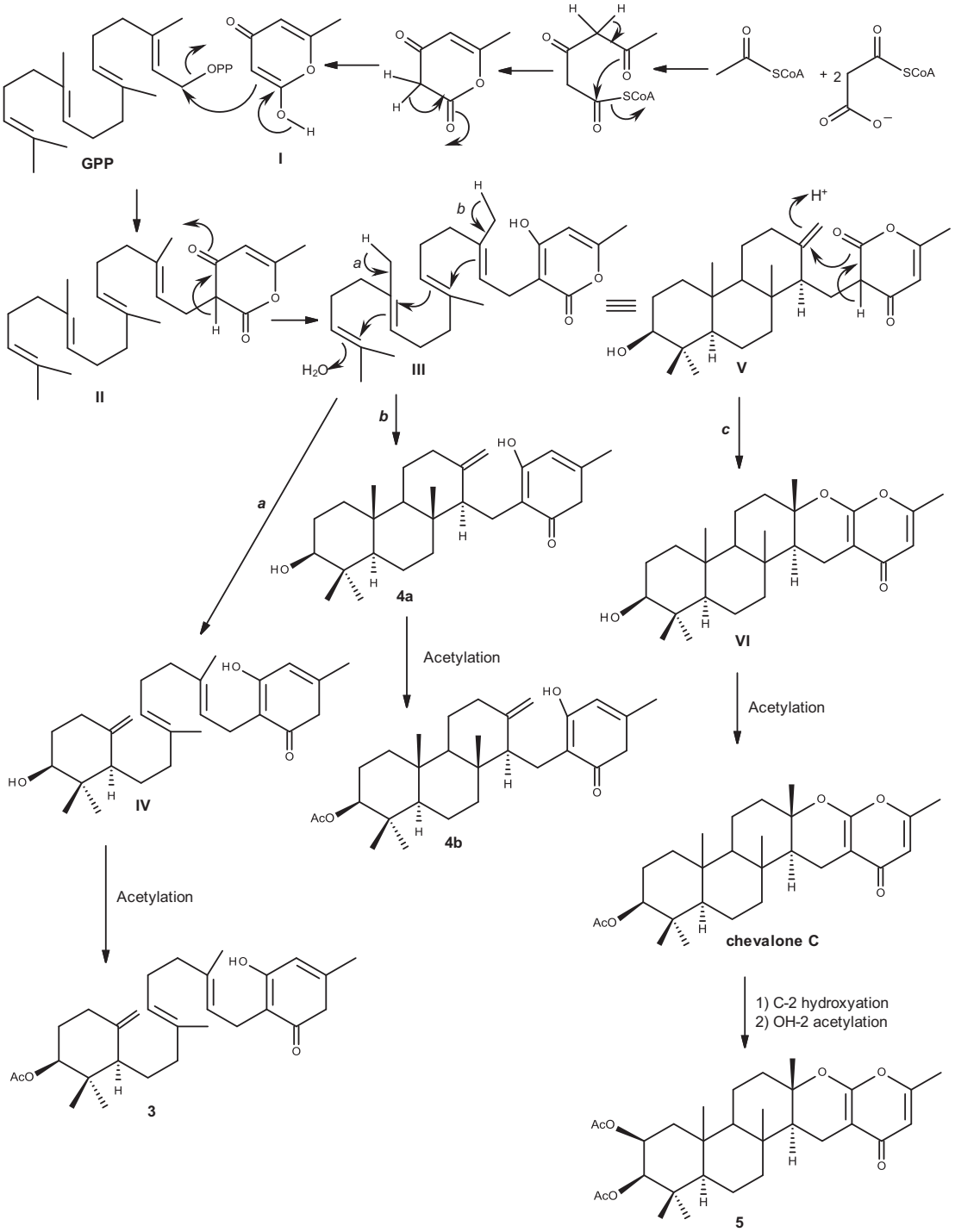

Fig. 5. Proposed biogenesis of meroditerpenes sartorypyrone A (**3**), aszonapyrone B (**4a**), aszonapyrone A (**4b**) and sartorypyrone B (**5**).

Genesis Series FTIR™ using WinFIRST Software. ^{1}H and ^{13}C NMR spectra were recorded at ambient temperature on a Bruker AMC instrument operating at 300.13 and 75.4 MHz, respectively. High resolution mass spectra were measured with a Waters Xevo QToF mass spectrometer coupled to a Waters Aquity UPLC system. A Merck silica gel GF_{254} was used for preparative TLC, and a Merck Si gel 60 (0.2–0.5 mm) was used for analytical chromatography.

3.2. Fungal material

The strain KUFC 6344 was isolated from coastal forest soil at Samaersarn island (altitude 12° 34′ 23″ N, 100° 57′ 23″ E), Chonburi Province, Thailand, in November 2008. Briefly, 1 g of the soil (collected from the surface) was placed in 65% ethanol for 10–20 min, after which the liquid was drained off. The soil particles were placed into sterile Petri dishes, mixed with GAN and streptomycin sulfate and incubated at 28 °C. The fungus was identified as *N. fischeri* by the morphological features, including characteristic of ascospores, conidiogenesis and colonies. The identification was supported by sequence analysis of the β-tubulin, calmodulin and actin genes and homologies of those gene sequences between the strain and *N. fischeri* NRRL 181^{T} were 100%, 100% and 99.7% (GeneBank accession No.; EF669796, EF669865 and DQ094863), respectively. The pure cultures were deposited as KUFC 6344 at the

Table 4
Growth inhibitory effect of aszonalenin derivatives (**1a**–**c**), 13-oxofumitremorgin B (**2**), sartorypyrone A (**3**), aszonapyrone B (**4a**), aszonapyrone A (**4b**) and sartorypyrone B (**5**) in three human tumour cell lines

Compounds	GI_{50} (μM)		
	MCF-7	NCI-H460	A375-C5
1a	>150	>150	>150
1b	>150	>150	>150
1c	>150	>150	>150
2	115.2±20.0	123.3±11.5	68.6±12.9
3	46.3±7.6	37.3±4.0	21.5±1.9
4a	>150	>150	>150
4b	13.6±0.9	11.6±1.5	10.2±1.2
5	17.8±7.4	20.5±2.4	25.0±4.4

Results are given as the lowest concentration causing 50% of cell growth inhibition (GI_{50}) after a continuous exposure to the compounds for 48 h, and are expressed as mean±SEM of three independent experiments performed in duplicate. Doxorubicin was used as positive control, GI_{50}: MCF-7=60.3±1.2 nM; NCI-H460=19.6±1.9 nM; A375-C5=130.0±25.2 nM.

Mycology Laboratory, Department of Plant Pathology, Faculty of Agriculture, Kasetsart University, Bangkok, Thailand, and as IFM 59696 at the Medical Mycology Research Center, Chiba University, Japan.

The strain KUFC 7896 was isolated from a diseased coral (*P. lutea* ulcerative white spot) at Ao Nuan Lan island (altitude 12° 53′ 56.85″ N, 100° 46′ 39.66″ E), Chonburi Province, in the Gulf of Thailand, in May 2010. The diseased coral was washed with 0.06% sodium hypochlorite for 1 min, followed by sterilized sea water for three times. The diseased coral was cut into 0.5×0.5 cm pieces and placed on malt extract agar (MEA) with 70% sea water and incubated at 28 °C for 5–7 days. The fungus was identified as *N. laciniosa* by morphological characteristics, such as colony growth rate and growth pattern on standard media namely Czapek's agar (CZA), Czapek yeast autolysate agar (CYA) and malt extract agar (MEA). Microscopic characteristics including size, shape, ornamentation of ascospores and *Aspergillus laciniosus* anamorph were examined under light and scanning electron microscopes. This identification was supported by sequence analysis of the β-tubulin gene as described in the previous report[17] and the pure cultures were deposited as KUFC 7896 at Kasetsart University Fungal Collection, Department of Plant Pathology, Faculty of Agriculture, Kasetsart University, Bangkok, Thailand, and as MMERU 01 at Microbes Marine Environment Research Unit, Division of Environmental Science, Faculty of Science, Ramkhamhaeng University, Bangkok, Thailand.

N. tsunodae Yaguchi, Abliz & Y. Horie was isolated from the marine sponge *A. coralliphaga*, which was collected from the coral reef of the Similan islands, Phagna province, Thailand, by scuba diving at 10 m depth, in April 2010 and the sponge was identified by J. Buaruang. Briefly, the sponge tissue was cut into a piece of 0.5×0.5 cm, placed on the malt extract agar (MEA) with 70% sea water and incubated for 28 °C for 7 days. The fungus was identified by one of us (T.D.), by morphological features, including the characteristic of ascospores and colonies. The identification was supported by sequence analysis of the β-tubulin gene described in the previous report[18] and the pure cultures were deposited as KUFC 9213 at Kasetsart University Fungal Collection, Department of Plant Pathology, Faculty of Agriculture, Kasetsart University, Bangkok, Thailand.

3.3. Extraction of the metabolites

N. fischeri (KUFC 6344) was cultured for one week in five 90 mm Petri dishes with 25 ml of potato dextrose agar per dish. Twenty five 1000 ml Erlenmeyer flasks each containing cooked rice (300 g), were autoclaved, incubated with two mycelia plugs of *N. fischeri* (KUFC 6344) and incubated at 28 °C for 30 days. The moldy rice was macerated in ethyl acetate (20 L total) for three days and then filtered. The two layers were separated using a separatory funnel and the ethyl acetate solution was concentrated at a reduced pressure to yield 62.5 g of crude ethyl acetate extract, which was dissolved in 500 ml of a 4:1 mixture of $CHCl_3$ and EtOAc and then washed with H_2O (3×500 ml). The organic layer was dried with anhydrous Na_2SO_4, filtered and evaporated under reduced pressure to give 50 g of the crude extract, which was applied on a column chromatography of Silica gel (350 g) and eluted with mixtures of petrol–$CHCl_3$ and $CHCl_3$–Me_2CO, 250 ml fractions were collected as follows: Frs 1–89 (petrol–$CHCl_3$, 1:1), 90–179 (petrol–$CHCl_3$, 3:7), 180–288 (petrol–$CHCl_3$, 1:9), 289–358 ($CHCl_3$), 359–430 ($CHCl_3$–Me_2CO, 9:1), 431–451 ($CHCl_3$–Me_2CO, 7:3). Frs 107–131 were combined (2.8 g) and applied on a Silica gel column (30 g) and eluted with mixtures of $CHCl_3$–petrol, 100 ml fractions were collected as follows: sfrs 1–38 (petrol–$CHCl_3$, 7:3), 39–64 (petrol–$CHCl_3$, 1:1). Sfr 41 (286 mg) was crystallized in a mixture of petrol and $CHCl_3$ to give 39.4 mg of aszonalenin (**1a**). Sfrs 46–64 were combined (50.9 mg) and purified by TLC (Si Gel, $CHCl_3$/petrol, 9:1) to give 24 mg of sartorypyrone A (**3**). Frs 132–159 were combined (1.86 g) and applied on a Silica gel column (30 g) and eluted with mixtures of $CHCl_3$–petrol, 100 ml fractions were collected as follows: sfrs 1–66 (petrol–$CHCl_3$, 7:3), 67–112 (petrol–$CHCl_3$, 1:1). Sfrs 49–64 were combined (188 mg) and purified by TLC (Si Gel, $CHCl_3$/Me_2CO/HCO_2H, 9:1:0.1) to give an additional 18 mg of sartorypyrone A (**3**). Sfrs 65–80 were combined (530 mg) and purified by TLC (Si Gel, $CHCl_3$/EtOAc/petrol/HCO_2H, 8:1:1:0.1) to give 40 mg of 13-oxofumitremorgin B (**2**). Frs 175–189 were combined (890.9 mg) and crystallized in a mixture of petrol and $CHCl_3$ to give 320 mg of aszonapyrone A (**4b**). Frs 190–225 were combined (975 mg) and crystallized in a mixture of petrol and $CHCl_3$ to give 140 mg of aszonapyrone A (**4b**) and the mother liquor was applied on a Silica gel column (28 g) and eluted with mixtures of $CHCl_3$–petrol, 100 ml fractions were collected as follows: sfrs 1–8 (petrol–$CHCl_3$, 1:1), 9–43 (petrol–$CHCl_3$, 3:7), 44–53 (petrol–$CHCl_3$, 1:9). Sfrs 9–16 were combined and crystallized in a mixture of petrol and $CHCl_3$ to give an additional 53 mg aszonapyrone A (**4b**). Frs 226–236 were combined (1.75 g) and crystallized in a mixture of petrol and $CHCl_3$ to give 214.4 mg of acetylaszonalenin (**1b**). Frs 237–293 were combined and crystallized in a mixture of petrol and $CHCl_3$ to give helvolic acid (153 mg). Frs 294–332 were combined (1.15 g) and applied on a Silica gel column (30 g) and eluted with mixtures of petrol–$CHCl_3$, 100 ml fractions were collected as follows: sfrs 1–7 (petrol–$CHCl_3$, 1:1), 8–66 (petrol–$CHCl_3$, 3:7), 67–81 (petrol–$CHCl_3$, 1:9). Sfrs 35–40 were combined (70.9 mg) and purified by TLC (Si Gel, $CHCl_3$/EtOAc/Me_2CO/HCO_2H, 15:6:1:0.1) to give 34 mg of 1-formyl-5-hydroxyaszonalenin (**1c**).

N. laciniosa (KUFC 7896) was cultured for one week in five 90 mm Petri dishes with 25 ml of malt extract agar (MEA) with 70% sea water per dish. Thirty 1000 ml Erlenmeyer flasks, each containing 200 g rice and 200 ml water, were autoclaved, inoculated with ten mycelia plugs of the fungus and incubated at 28 °C for 30 days. The moldy rice was macerated in ethyl acetate (12 L) for five days and then filtered. The two layers were separated using a separatory funnel, and the ethyl acetate solution was concentrated at a reduced pressure to yield 72 g of crude ethyl acetate extract, which was applied on a column chromatography of Silica gel (800 g) and eluted with mixtures of petrol–$CHCl_3$ and $CHCl_3$–Me_2CO, 250 ml fractions were collected as follows: frs 1–19 ($CHCl_3$–petrol, 3:7), 20–114 ($CHCl_3$–petrol, 1:1), 115–188 ($CHCl_3$–petrol, 7:3), 189–340 ($CHCl_3$–petrol, 9:1), 341–484 ($CHCl_3$–Me_2CO, 9:1), 485–547 ($CHCl_3$–Me_2CO, 7:3), 548–603 ($CHCl_3$–Me_2CO, 1:1). Frs 365–396 were combined (3.35 g) and recrystallized in Me_2CO to give 24.1 mg

of aszonapyrone A (**4b**). The mother liquor of frs 365–396 (3.32 g) and frs 397–408 (465.7 mg) were combined and chromatographed over a column of LiChroprep Si 60 (40–63 μm, 43.4 g) and eluted with mixtures of $CHCl_3$–petrol and $CHCl_3$–Me_2CO, wherein 100 ml sub-fractions were collected as follows: sfrs 1–43 ($CHCl_3$–petrol, 7:3), 44–56 ($CHCl_3$–petrol, 9:1), 57–81 ($CHCl_3$–Me_2CO, 9:1), 82–108 ($CHCl_3$–Me_2CO, 4:1). Sfrs 18–22 were combined (706.2 mg) and recrystallized in Me_2CO to give an additional 51.1 mg of aszonapyrone A (**4b**). Frs 435–437 were combined (625.2 mg) and recrystallized in Me_2CO to give 12.8 mg of aszonapyrone B (**4a**). The mother liquor of frs 435–437, frs 409–434 and frs 438–448 were combined (2.45 g) and chromatographed over a column of LiChroprep Si 60 (40–63 μm, 32.5 g) and eluted with mixtures of $CHCl_3$–petrol and $CHCl_3$–Me_2CO, wherein 100 ml sub-fractions were collected as follows: sfrs 1–45 ($CHCl_3$–petrol, 7:3), 46–62 ($CHCl_3$–petrol, 9:1). Sfr 30–32 were combined (209.1 mg) and recrystallized in Me_2CO to give an additional 8.3 mg of aszonapyrone B (**4a**). Frs 449–465 were combined (826.0 mg) and recrystallized in Me_2CO to give 24.4 mg of tryptoquivaline L. Frs 508–546 were combined (1.57 g) and recrystallized in Me_2CO to give 26.6 mg of 3′-(4-oxoquinazolin-3-yl) spiro[1*H*-indole-3,5′-oxolane]-2,2′-dione.

N. tsunodae (KUFC 9213), was cultured for one week in five 90 mm Petri dishes with 25 ml of malt extract agar (MEA) with 70% sea water per dish. Fifty 1000 ml Erlenmeyer flasks, each containing 200 g rice and 150 ml water, were autoclaved, inoculated with ten mycelia plugs of the fungus and incubated at 28 °C for 30 days. The moldy rice was macerated in ethyl acetate (10 L total) for seven days and then filtered. The two layers were separated using a separatory funnel, and the ethyl acetate solution was concentrated at a reduced pressure to yield 40 g of crude ethyl acetate extract, which was chromatographed over a 0.2–0.5 mm Merck Silica gel column (400 g) and eluted with mixtures of $CHCl_3$–petrol and $CHCl_3$–Me_2CO, wherein 250 ml fractions were collected as follows: frs 1–14 ($CHCl_3$–petrol, 1:9), 15–43 ($CHCl_3$–petrol, 3:7), 44–78 ($CHCl_3$–petrol, 1:1), 79–140 ($CHCl_3$–petrol, 7:3), 141–181 ($CHCl_3$–petrol, 9:1), 182–253 ($CHCl_3$–Me_2CO, 9:1), 254–314 ($CHCl_3$–Me_2CO, 7:3). Frs 193–208 were combined (980 g) and purified by TLC (Si Gel, $CHCl_3$/Me_2CO/HCO_2H, 9.5:0.5:0.1) to yield 92 mg of sartorypryrone B (**5**). Frs 220–243 were combined (920 mg) and chromatographed over a LiChroprep Si 60 column (40–63 μm, 25 g) and eluted with $CHCl_3$–Me_2CO, 9:1; 50 ml fractions were being collected. Sfrs 5–8 were combined and purified by TLC (Si Gel, $CHCl_3$/Me_2CO/HCO_2H, 9:1:0.1) to yield 130 mg of sartorypryrone B (**5**). Frs 283–298 were combined (507 mg) and applied over a Silica gel column (10 g) and eluted with mixtures of $CHCl_3$–Me_2CO; 50 ml fractions were collected as follows: sfrs 1–10 ($CHCl_3$–Me_2CO, 9:1), 11–25 ($CHCl_3$–Me_2CO, 7:3). Sfrs 5–10 were combined and recrystallized in a mixture of petrol–$CHCl_3$ to give 31.4 mg of helvolic acid. Frs 299–315 were combined (140.8 mg) and purified by TLC (Si Gel, $CHCl_3$/Me_2CO/HCO_2H, 9.5:0.5:0.1) to give an additional 10 mg of sartorypryrone B (**5**).

*3.3.1. 1-Formyl-5-hydroxyaszonalenin (**1c**).* Pale yellow semisolid. $[\alpha]_D^{25}$ −18 (*c* 0.056, $CHCl_3$); IR (KBr) ν_{max} 3377, 3242, 3089, 2966, 2923, 2852, 1680, 1657, 1605, 1496, 1485, 1465, 1384 cm^{-1}. ^1H and ^{13}C see Table 1. HR-ESIMS *m*/*z* 418.1777 $[M+H]^+$ (calculated for $C_{24}H_{24}N_3O_4$, 418.1767).

*3.3.2. Sartorypyrone A (**3**).* Brown viscous mass. $[\alpha]_D^{25}$ +74.8 (*c* 0.02, $CHCl_3$); IR (KBr) ν_{max} 3434, 3080, 2964, 2942, 2872, 1730, 1684, 1667, 1585, 1448, 1245 cm^{-1}. ^1H and ^{13}C see Table 2. HR-ESIMS *m*/*z* 457.2967 $(M+H)^+$ (calculated for $C_{28}H_{41}O_5$, 457.2954).

*3.3.3. Sartorypyrone B (**5**).* Yellow viscous mass; $[\alpha]_D^{20}$ −59.0 (*c* 0.07, $CHCl_3$); IR (KBR) ν_{max} 2939, 1734, 1670, 1631, 1596, 1426, 1238 cm^{-1}; ^1H and ^{13}C see Table 3. HR-ESIMS *m*/*z* 515.3038 $[M+H]^+$ (calculated for $C_{30}H_{43}O_7$, 515.3009).

3.4. Bioassay

3.4.1. Cell cultures. Three human tumour cell lines were used in this study: MCF-7 (breast adenocarcinoma, a kind gift from NCI, Bethesda, USA), NCI-H460 (non-small cell lung cancer, NSCLC, a kind gift from NCI, Bethesda, USA) and A375-C5 (melanoma, ECACC, UK). Cells were routinely cultured in RPMI-1640 with Ultraglutamine (Lonza) supplemented with 10% FBS (Fetal Bovine Serum, PAA) and maintained in a humidified incubator at 37 °C with 5% CO_2. Cell number and viability were determined with Trypan Blue exclusion assay. All experiments were performed with cells in exponential growth with viabilities over 90% and repeated at least three times.

3.4.2. Cell growth inhibitory assay. The screening of compounds was performed with the Sulforhodamine B (SRB) assay adopted from the National Cancer Institute, USA.[19] Briefly, cells were plated in 96 well plates (5×10^3 cells/well for MCF-7 and NCI-H460 cells, and 7.5×10^3 cells/well for the A375-C5 cell line) and incubated at 37 °C for 24 h. Exponentially growing cells were then treated with five dilutions of each compound. After 48 h of treatment, cells were fixed with 10% ice-cold trichloroacetic acid, washed and stained with SRB. After washing with 1% acetic acid, the bound SRB was solubilized with 10 mM Tris Base, and the absorbance was measured at 515 nm in a microplate reader (Biotek Instruments). Then, a dose–response curve was obtained for each compound and the corresponding GI_{50} (the concentration of compound that inhibited 50% of net cell growth) was determined. The effect of the vehicle solvent (DMSO) on the growth of these cell lines was evaluated by treating cells with the maximum concentration of DMSO used in each assay (0.25%).

Acknowledgements

This work was partially supported by the Project MARBIOTECH (reference NORTE-07-0124-FEDER-000047) within the SR&TD Integrated Program MARVALOR – Building research and innovation capacity for improved management and valorization of marine resources, supported by the Programa Operacional Regional do Norte (ON.2 – O Novo Norte) and by the European Regional Development Fund, and also by FCT – Fundação para a Ciência e a Tecnologia under the project CEQUIMED-PEst-OE/SAU/UI4040/2011, FEDER funds through the COMPETE program under the project FCOMP-01-0124-FEDER-011057. We thank Dr. Mick Lee of the Department of Chemistry, Leicester University (UK), for providing the HR-ESIMS. A.E. thanks the Royal Golden Jubilee Ph.D. program of Thailand for his scholarship to the University of Porto. N.M.G. thanks Fundação para a Ciência e Tecnologia (FCT) for the scholarship (SFRH/BD/65671/2009) supported by the European Social Fund (ESF). We thank Mrs. Júlia Bessa and Ms. Sara Cravo for technical support, and Dr. John Bulger for checking the English language.

Supplementary data

Supplementary data associated with this article can be found in the online version, at http://dx.doi.org/10.1016/j.tet.2013.07.078.

References and notes

1. Frisvad, J. C.; Rank, C.; Nielsen, K. F.; Larsen, T. O. *Med. Mycol.* **2009**, *47*, S53–S71.
2. Kijjoa, A.; Santos, S.; Dethoup, T.; Manoch, L.; Almeida, A. P.; Vasconcelos, M. H.; Silva, A.; Gales, L.; Herz, W. *Nat. Prod. Commun.* **2011**, *6*, 807–812.

3. Eamvijarn, A.; Kijjoa, A.; Bruyère, C.; Mathieu, V.; Manoch, L.; Lefranc, F.; Silva, A.; Kiss, R.; Herz, W. *Planta Med.* **2012**, *78*, 1767–1776.
4. Buttachon, S.; Chandrapatya, A.; Manoch, L.; Silva, A.; Gales, L.; Bruyère, C.; Kiss, R.; Kijjoa, A. *Tetrahedron* **2012**, *68*, 3253–3262.
5. Fujimoto, H.; Ikeda, M.; Yamamoto, K.; Yamazaki, M. *J. Nat. Prod.* **1993**, *56*, 1268–1275.
6. Wong, S.-M.; Laszlo, L.; Musza, L. L.; Kydd, G. C.; Kullnig, R. ;M.; Gillum, A. M.; Cooper, R. *J. Antibiot.* **1993**, *46*, 545–553.
7. Proksa, B.; Uhrín, D.; Liptaj, T.; Šturdíková, M. *Phytochemisty* **1998**, *48*, 1161–1164.
8. Wakana, D.; Hosoe, T.; Itabashi, T.; Nozawa, K.; Okada, K.; Takaki, G. M. C.; Yaguchi, T.; Fukushima, K.; Kawai, K. *Mycotoxins* **2006**, *56*, 3–6.
9. Tan, Q.-W.; Ouyang, M.-A.; Shen, S.; Li, W. *Nat. Prod. Res.* **2012**, *26*, 1402–1407.
10. Yin, W.-B.; Grundmann, A.; Cheng, J.; Li, S.-M. *J. Biol. Chem.* **2009**, *284*, 100–109.
11. Wang, F.; Fang, Y.; Zhu, T.; Zhang, M.; Lin, A.; Gu, Q.; Zhu, W. *Tetrahedron* **2008**, *64*, 7986–7991.
12. Kimura, Y.; Hamasaki, T.; Isogai, A.; Nakajima, H. *Agric. Biol. Chem.* **1982**, *46*, 1963–1965.
13. Fujimoto, H.; Negishi, E.; Yamaguchi, K.; Nishi, N.; Yamazaki, M. *Chem. Pharm. Bull.* **1996**, *44*, 1843–1848.
14. Kanokmedhakul, K.; Kanokmedhakul, S.; Suwannatrai, R.; Soytong, K.; Prabpai, S.; Kongsaeree, P. *Tetrahedron* **2011**, *67*, 5461–5468.
15. Li, S.-M. *Nat. Prod. Rep.* **2010**, *27*, 57–78.
16. Kojima, H.; Ogura, H. *Phytochemistry* **1989**, *28*, 1703–1710.
17. Hong, S. B.; Cho, H. S.; Shin, H. D.; Frisvad, J. C.; Samson, R. A. *Int. J. Syst. Evol. Microbiol.* **2006**, *56*, 477–486.
18. Glass, N. L.; Donaldson, G. C. *Appl. Environ. Microbiol.* **1995**, *61*, 1323–1330.
19. Vichai, V.; Kirtikara, K. *Nat. Protoc.* **2006**, *1*, 1112–1116.

APPENDIX IV

Gomes, N.M., Bessa, L.J, Buttachon, S., Costa, P.M., Buaruang, J., Dethoup, T., Silva, A.M.S., Kijjoa, A. **(2014)**. Antibacterial and Antibiofilm Activities of Tryptoquivalines and Meroditerpenes Isolated from the Marine-Derived Fungi *Neosartorya paulistensis*, *N. laciniosa*, *N. tsunodae*, and the Soil Fungi *N. fischeri* and *N. siamensis*. *Marine Drugs* 12(2), 822-839.

Mar. Drugs **2014**, *12*, 822-839; doi:10.3390/md12020822

OPEN ACCESS

marine drugs

ISSN 1660-3397

www.mdpi.com/journal/marinedrugs

Article

Antibacterial and Antibiofilm Activities of Tryptoquivalines and Meroditerpenes Isolated from the Marine-Derived Fungi *Neosartorya paulistensis*, *N. laciniosa*, *N. tsunodae*, and the Soil Fungi *N. fischeri* and *N. siamensis*

Nelson M. Gomes [1,2,†], Lucinda J. Bessa [1,2,†], Suradet Buttachon [1,2], Paulo M. Costa [1,2], Jamrearn Buaruang [3], Tida Dethoup [4], Artur M. S. Silva [5] and Anake Kijjoa [1,2,*]

[1] ICBAS—Instituto de Ciências Biomédicas de Abel Salazar, Rua de Jorge Viterbo Ferreira, 228, Porto 4050-313, Portugal; E-Mails: ngomes@ciimar.up.pt (N.M.G.); lbessa@ciimar.up.pt (L.J.B.); nokrari_209@hotmail.com (S.B.); pmcosta@icbas.up.pt (P.M.C.)

[2] Interdisciplinary Centre of Marine and Environmental Research (CIIMAR), Universidade do Porto, Rua dos Bragas 289, Porto 4050-123, Portugal

[3] Division of Environmental Science, Faculty of Science, Ramkhamhaeng University, Bangkok 10240, Thailand; E-Mail: jbuaruang@ru.mail.go.th

[4] Department of Plant Pathology, Faculty of Agriculture, Kasetsart University, Bangkok 10240, Thailand; E-Mail: agrtdd@ku.ac.th

[5] Departamento de Química, Universidade de Aveiro, Aveiro 4810-1933, Portugal; E-Mail: artur.silva@ua.pt

† These authors contributed equally to this work.

* Author to whom correspondence should be addressed; E-Mail: ankijjoa@icbas.up.pt; Tel.: +351-220428331.

Received: 25 December 2013; in revised form: 17 January 2014 / Accepted: 20 January 2014 / Published: 28 January 2014

Abstract: A new meroditerpene, sartorypyrone C (**5**), was isolated, together with the known tryptoquivalines L (**1a**), H (**1b**), F (**1c**), 3′-(4-oxoquinazolin-3-yl) spiro [1*H*-indole-3,5′]-2,2′-dione (**2**) and 4(3*H*)-quinazolinone (**3**), from the culture of the marine sponge-associated fungus *Neosartorya paulistensis* (KUFC 7897), while reexamination of the fractions remaining from a previous study of the culture of the diseased coral-derived fungus *N. laciniosa* (KUFC 7896) led to isolation of a new tryptoquivaline derivative tryptoquivaline T (**1d**). Compounds **1a**–**d**, **2**, **3**, and **5**, together with aszonapyrones A (**4a**) and B (**4b**), chevalones B (**6**) and C (**7a**), sartorypyrones B (**7b**) and A (**8**), were tested for

their antibacterial activity against four reference strains (*Staphylococcus aureus*, *Bacillus subtilis*, *Escherichia coli*, and *Pseudomonas aeruginosa*), as well as the environmental multidrug-resistant isolates. Only aszonapyrone A (**4a**) and sartorypyrone A (**8**) exhibited significant antibacterial activity as well as synergism with antibiotics against the Gram-positive multidrug-resistant strains. Antibiofilm assays of aszonapyrone A (**4a**) and sartorypyrone A (**8**) showed that practically no biofilm was formed in the presence of their 2× MIC and MIC. However, the presence of a sub-inhibitory concentration of ½ MIC of **4a** and **8** was found to increase the biofilm production in both reference strain and the multidrug-resistant isolates of *S. aureus.*

Keywords: antibacterial; antibiofilm; multidrug-resistant; tryptoquivalines; meroditerpenes; *Neosartorya*; marine-derived fungi

1. Introduction

Infectious diseases are leading health problems with high morbidity and mortality in the developing countries. Although the introduction of penicillin and other antibiotics ushered in an era of effective treatment of microbial infection, their overuse has caused acquired resistance of pathogens to antimicrobial agents. Since the mid-1970s, resistance to antimicrobial agents has become an escalating problem [1]. In the last 30 years, treatment of infections caused by Gram-positive bacteria has been more problematic than ever, with infections being caused by multidrug-resistant organisms, particularly methicillin-resistant staphylococci, penicillin- and erythromycin-resistant pneumococci, and vancomycin-resistant enterococci [2]. The development of resistance to multiple drugs is therefore a worldwide problem in the treatment of these infectious diseases caused by clinically relevant pathogenic microorganisms and must be approached in a large variety of strategies [3]. Although there is a continuing effort in the pharmaceutical industry to develop new antimicrobial agents for the treatment of resistant infections, pursuing new antibiotic drugs is still a fair and necessary strategy to combat the multidrug-resistant bacteria that are spreading both in the community and clinical setting [4]. Since the marine environment is a prolific source of bioactive compounds with extraordinary chemical and biological diversity [5–7], it has become a potential target in the search for new antibiotics. Specifically, the marine-derived fungi which have been reported as producers of bioactive metabolites with antiviral [8,9], antitumor [10,11] and antibacterial [12–14] activities. In the pursuit for bioactive secondary metabolites produced by marine and soil fungi of the genus *Neosartorya*, we have recently reported isolation and structure elucidation of sartorypyrone A (**8**), aszonapyrone A (**4a**), aszonalenin, acetylaszonalenin, 1-formyl-5-hydroxyaszonalenin and 13-oxofumitremorgin B, from the culture of the soil fungus *Neosartorya fischeri* (KUFC 6344), sartorypyrone B (**7b**) from the marine sponge-associated fungus *N. tsunodae*, as well as aszonapyrone A (**4a**), aszonapyrone B (**4b**), tryptoquivaline L (**1a**) and 3′-(4-oxoquinazolin-3-yl) spiro[1*H*-indole-3,5′-oxolane]-2,2′-dione (**2**) from *N. laciniosa* isolated from a diseased coral [15].

Figure 1. Secondary metabolites from *Neosartorya paulistensis*, *N. laciniosa*, *N. siamensis*, *N. tsunodae* and *N. fischeri*.

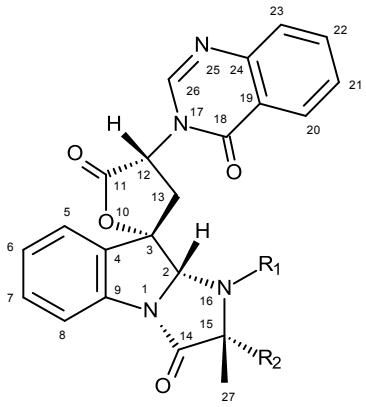

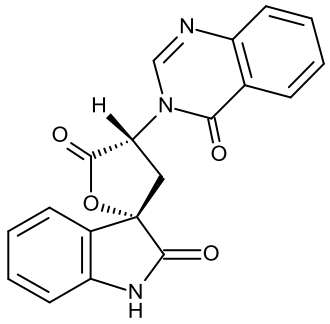

2

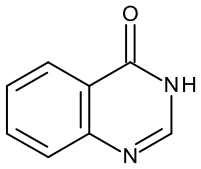

3

1a: R_1 = OH, R_2 = Me
1b: R_1 = OH, R_2 = H
1c: R_1 =H, R_2 = H
1d: R_1 = CHO, R_2 = Me

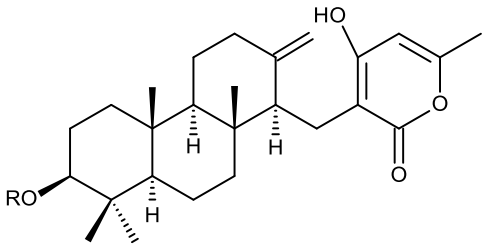

4a: R = Ac
4b: R = H

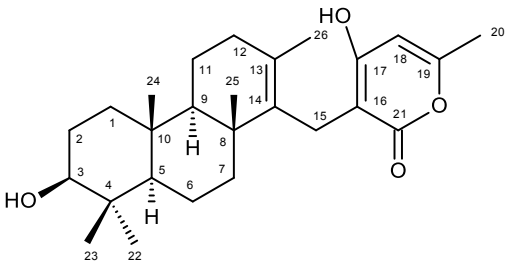

5

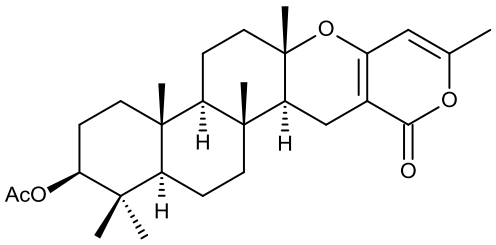

6

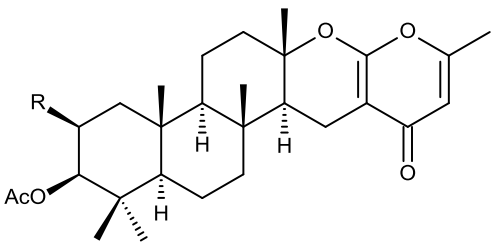

7a: R = H
7b: R = OAc

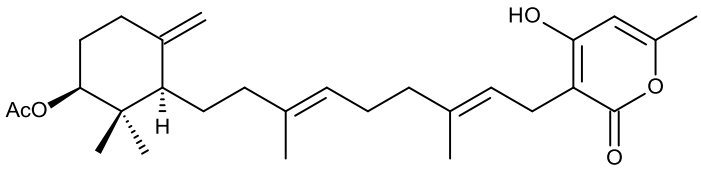

8

Examination of a collection of *N. paulistensis* (KUFC 7897), isolated from the marine sponge *Chondrilla australiensis*, collected from the Gulf of Thailand, resulted in isolation of a new aszonapyrone analogue which we have named sartorypyrone C (**5**), in addition to five known metabolites including tryptoquivalines L (**1a**), H (**1b**), F (**1c**), 3′-(4-oxoquinazolin-3-yl) spiro [1*H*-indole-3,5′-oxolane]-2, 2′-dione (**2**) and 4(3*H*)-quinazolinone (**3**) (Figure 1). Reexamination of the

column fractions left over from our previous work of *N. laciniosa* (KUFC 7896) [15] led to isolation of a new tryptoquivaline analogue, tryptoquivaline T (**1d**), whereas reexamination of the nonpolar fractions from the column chromatography of *N. siamensis* (KUFC 6349) [16] furnished chevalone B (**6**) and chevalone C (**7a**) (Figure 1). The isolated compounds were evaluated, together with sartorypyrone B (**7b**) previously isolated from *N. tsunodae* and sartorypyrone A (**8**) (Figure 1) previously isolated from *N. fischeri*, for antibacterial activity against the Gram-positive (*Staphylococcus aureus* ATCC 25923 and *Bacillus subtilis* ATCC 6633) and Gram-negative (*Escherichia coli* ATCC 25922 and *Pseudomonas aeruginosa* ATCC 27853) bacteria, as well as multidrug-resistant isolates from the environment. The potential synergism between these fungal metabolites and antibiotics was evaluated against multidrug-resistant bacteria, methicillin-resistant *S. aureus* (MRSA) and vancomycin-resistant Enterococci (VRE). Since aszonapyrone A (**4a**) and sartorypyrone A (**8**) exhibited interesting antibacterial activity against both Gram-negative reference strains and the environmental multidrug-resistant isolates, their capacity to inhibit biofilm formation was also studied.

Table 1. ^{1}H and ^{13}C NMR (DMSO, 300.13 and 75.47 MHz) and HMBC assignment for tryptoquivaline T (**1d**).

Position	δ_C, Type	δ_H, (*J* in Hz)	COSY	HMBC
1	---	---		
2	81.0, CH	6.10, s	H-29	C-3, 13, 14
3	84.2, C	---		
4	133.5,C	---		
5	126.8, CH	8.04, dd (8.0, 1.0)	H-6	C-3, 7, 9
6	126.7, CH	7.46, ddd (8.0, 8.0, 1.0)	H-5	C-4, 8
7	131.8, CH	7.61, ddd (8.0, 8.0, 1.0)	H-6, 8	C-5, 9
8	116.4, CH	7.56, ddd (8.0, 1.0)	H-7	C-4, 6
9	138.4, C	---		
11	171.1, CO	---		
12	57.7, CH	5.47, dd (10.7, 8.6)	H-13	C-11, 18
13a	33.8, CH_2	3.30, dd (14.0, 8.6)	H-12, 13b	C-2, 3, 4
b		3.40, dd (14.0, 10.7)	H-12, 13a	C-2, 3, 4
14	172.5, CO	---		
15	64.1, C	---		
18	160.0, CO	---		
19	121.4, C	---		
20	126.2, CH	8.26, d (8.0, 1.0)	H-21	C-18, 22, 24
21	127.6, CH	7.63, ddd (8.0, 8.0, 1.0)	H-20, 22	C-19, 23
22	135.1, CH	7.93, ddd (8.0, 8.0, 1.0)	H-21, 23	C-20, 24
23	127.4, CH	7.76, d (8.0)	H-22	C-19, 21
24	147.8, C	---		
26	148.1, CH	8.62, s		C-12, 18, 24
27	26.6, CH_3	1.72, s		C-14, 15, 28
28	25.5, CH_3	1.55, s		C-14, 15, 27
29	162.3, CHO	8.73, d (0.9)	H-2	C-2

2. Results and Discussion

Compound **1d** was isolated as white solid, and its molecular formula $C_{24}H_{20}N_4O_5$ was established on the basis of the (+)-HRESIMS *m/z* 445.1512 $[M + H]^+$, indicating 17 degrees of unsaturation. The IR spectrum showed absorption bands for aromatic (3010, 1582, 1450 cm^{-1}) and carbonyls of ester/amide groups (1700 cm^{-1}). The general features of the ^1H and ^{13}C spectra of **1d** (Supplementary Information, Figures S1 and S2) closely resembled those of tryptoquivaline L (**1a**). The ^{13}C NMR, DEPT and HSQC spectra (Table 1) revealed three amide/ester carbonyls (δ_C 172.5, 171.1 and 160.0), one *N*-formyl (δ_C 162.3), four quaternary sp^2 (δ_C 147.8, 138.4, 133.5, 121.4), nine methine sp^2 (δ_C 148.1, 135.1, 131.8, 127.6, 127.4, 126.8, 126.7, 126.2, 116.4), two quaternary sp^3 (δ_C 84.2 and 64.1), two methine sp^3 (δ_C 81.0 and 57.7), one methylene sp^3 (δ_C 33.8) and two methyl (δ_C 26.6 and 25.5) carbons.

Analysis of the ^1H, ^{13}C NMR, HSQC, COSY and HMBC (Table 1) revealed the presence of the *N*-substituted quinazolin-4-one and the 6-5-5 *gem*-dimethyl imidazoindole ring systems which were connected via a five membered spirolactone as in tryptoquivaline L [16]. However, the only difference between **1d** and tryptoquivaline L (**1a**) is the presence of the formyl group on N-16 of the *gem*-dimethyl imidazoindole moiety in the former and a hydroxyl group in the latter. On the other hand, the structure of **1d** differs from that of tryptoquivaline O, previously reported from *N. siamensis* by Buttachon *et al.* [16], in that there are two methyl groups on C-15 of the imidazoindole ring in the former instead of one methyl group in the latter. The assignments of the proton and carbon chemical shifts for CH_3-27 and CH_3-28 were based on the NOESY correlation between the signals of H-2 (δ_H 6.10, s) and CH_3-27(δ_H 1.72, s). Thus, **1d** is a new tryptoquivaline analogue which we have named tryptoquivaline T. Since the chemical shift values of H-2 and H-12 of tryptoquivaline T (**1d**) are similar of those of the corresponding protons of tryptoquivaline O, we assume that the stereochemistry of tryptoquivaline T (**1d**) is the same as that of tryptoquivaline O, *i.e.*, C-2*S*, C-3*S* and C-12*R*. This assumption was also supported by the negative value of the rotation tryptoquivaline T (**1d**).

Compound **5** was also isolated as white solid (mp, 200–202 °C) and its molecular formula $C_{26}H_{38}O_4$ was established on the basis of the (+)-HRESIMS *m/z* 415.2836 $[M + H]^+$ (calculated 415.2848), indicating eight degrees of unsaturation. The IR spectrum showed absorption bands for hydroxyl (3445 cm^{-1}), conjugated ester carbonyl (1668 cm^{-1}) and olefin (1649, 1636 cm^{-1}) groups. The ^{13}C NMR, DEPT and HSQC spectra (Table 2) exhibited the signals of one conjugated ester carbonyl (δ_C 164.6), five quaternary sp^2 (δ_C 164.3, 159.3, 136.6, 126.2. 101.4), one methine sp^2 (δ_C 99.9), three quaternary sp^3 (δ_C 38.8, 38.4 and 36.8), one oxymethine sp^3 (δ_C 76.9), two methine sp^3 (δ_C 56.0, 54.8), seven methylene sp^3 (δ_C 38.0, 37.9, 34.2, 27.1, 22.1, 18.2, 17.7), and six methyl (δ_C 28.1, 21.2, 20.3, 19.2, 16.3 and 15.7) carbons. Except for the presence of one more methyl group instead of an exocyclic methylene group, and a tetra-substituted double bond (δ_C 126.2 and 136.6), the ^1H and ^{13}C data (Table 2, Supplementary Information, Figures S3 and S4) revealed the existence of the perhydrophenanthrene moiety connected to the 4-hydroxy-6-methyl-2*H*-pyran-2-one portion through the methylene group, similar to those of aszonapyrone B (**4b**) [15]. That the double bond in the perhydrophenanthrene moiety was on C-13 and C-14 was supported by the HMBC correlations of H_3-26 (δ_H 1.55) to C-12 (δ_C 34.2), C-13 (δ_C 126.2), C-14 (δ_C 136.6); H-15 (δ_H 3.02, brs) to C-8 (δ_C 38.8), C-13, C-14, C-16 (δ_C 101.4), C-17 (δ_C 164.3) and C-21 (δ_C 164.6). That the hydroxyl group on C-3 was β is supported by the chemical shift value (δ_C 15.7) of the C-4 axial methyl (CH_3-23) which suffered a γ-*gauche* interaction [17]. Thus, compound **5** is a new analogue of aszonapyrones which we have named sartorypyrone C.

Table 2. ^{1}H and ^{13}C NMR (DMSO, 300.13 and 75.47 MHz) and HMBC assignment for sartorypyrone C (**5**).

Position	δ_C, Type	δ_H, (*J* in Hz)	COSY	HMBC
1	37.9, CH_2	1.65, m	H-2	
2	27.1, CH_2	1.46, m	H-1, 3	
3	76.9, CH	2.97, m	H-2	
4	38.4, C	---	---	
5	54.8, CH	0.67, brd (9.6)	H-6	
6	17.7, CH_2	1.35, m	H-5, 7	
7	38.0, CH_2	1.96, m	H-6	
8	38.8, C	--		
9	56.0, CH	0.97, brd (11.4)	H-11	CH_3-24
10	36.8, C	---		
11	18.2, CH_2	1.46, m	H-9, 12	
12	34.2, CH_2	1.94, m	H-11	
13	126.2, C	---	---	
14	136.6, C	---	---	
15	22.1, CH2	3.02, brs	---	C-8, 13, 14, 16, 17, 21
16	101.4, C	---	---	
17	164.3, C	---	---	
18	99.9, CH	5.90, s		CH_3-20, C-1617, 19, 20
19	159.3, C	---	---	
20	19.2, CH_3	2.12, s	H-18	C-18, 19
21	164.6, C	---	---	C-3, 4, 5, 23
22	28.1, CH_3	0.86, s	---	C-3, 4, 5, 22
23	15.7, CH_3	0.66, s	---	
24	16.3, CH_3	0.77, s	---	C-1, 5, 9, 10
25	21.2, CH_3	0.89, s	---	C-8, 9, 14
26	20.3, CH_3	1.55, s	---	C-12, 13, 14

Compounds **1**–**8** (Figure 1) were tested for their antibacterial activity against bacterial reference strains and environmental multidrug-resistant isolates, and their MIC and MBC (when determined) values are shown in Table 3A. It is interesting to note that neither of the indole alkaloids (**1a**–**d**, **2**) exhibited relevant antibacterial activity. However, within the meroditerpene group, only aszonapyrone A (**4a**) and sartorypyrone A (**8**) presented significant MIC values against Gram-positive bacteria. Aszonapyrone A (**4a**) showed the MIC values of 8 μg/mL against *S. aureus* ATCC 25923 and *B. subtilis* ATCC 6633, while sartorypyrone A (**8**) showed the MIC values of 32 and 64 μg/mL, respectively, against the same reference strains. Based on these results, the MIC values of these two compounds were further determined against Gram-positive multidrug-resistant strains. While aszonapyrone A (**4a**) was found to be active against both *S. aureus* MRSA and *Enterococcus* spp. VRE isolates, sartorypyrone A (**8**) did not show any inhibition on the growth of *Enterococcus* spp. VRE isolates in the range of concentrations tested (Table 3B). MBC values were only achieved for aszonapyrone A (**4a**) against Gram-positive reference strains, and since sartorypyrone A (**8**) did not exhibit any bactericidal effect against any strain, its MBC values could not be determined.

Table 3. Antimicrobial activity, expressed in μg/mL of **1**–**8** against references strains (**A**) and of **4a** and **8** against multidrug-resistant isolates (**B**).

(A)								
Compounds	***S. aureus* ATCC 25923**		***P. aeruginosa* ATCC 27853**		***B. subtilis* ATCC 6633**		***E. coli* ATCC 25922**	
	MIC	**MBC**	**MIC**	**MBC**	**MIC**	**MBC**	**MIC**	**MBC**
1a	128	−	128	256	128	−	128	−
1b	128	−	128	256	128	−	128	−
1c	128	−	128	128	128	−	128	−
1d	−	−	128	−	128	−	128	−
2	256	−	128	256	128	−	128	−
3	128	−	128	256	128	−	128	−
4a	8	64	128	256	8	16	128	−
4b	256	−	128	256	128	−	128	−
5	128	−	128	256	128	−	128	−
6	−	−	−	−	−	−	−	−
7a	−	−	−	−	−	−	−	−
7b	−	−	−	−	−	−	−	−
8	32	−	−	−	64	−	−	−
(B)								
Compounds	***S. aureus* B1**		***S. aureus* B1**		***E. faecalis* W1**		***E. faecium* W5**	
	MIC	**MBC**	**MIC**	**MBC**	**MIC**	**MBC**	**MIC**	**MBC**
4a	8	−	8	−	16	−	16	−
8	32	−	32	−	−	−	−	−

(−): >256 μg/mL.

Table 4. Antibacterial efficacy (halos, mm) of combined effect of antibiotics with compounds **1**–**8** (15 μg/disc) against three multidrug-resistant isolates, using the disc diffusion method.

	***E. coli* G1**			***S. aureus* B1**				***E. faecium* W5**		
	Antibiotics									
Compounds	**CIP**	**AMP**	**CTX**	**S**	**OX**	**AMP**	**CTX**	**VA**	**AMP**	**E**
1a	7	7	=	7.5	=	=	=	=	=	=
1b	7	7	=	7.5	=	=	=	=	=	=
1c	7	7	=	7.5	=	=	=	=	=	=
1d	7	7	=	7.5	=	=	=	=	=	=
2	7	7	=	7.5	=	=	=	=	=	=
3	7	7	=	7.5	=	=	=	=	=	=
4a	8	8	=	8	12.5	13	13	11	12	13.5
4b	7	7	=	7.5	11	10	10.5	11	12	13.5
5	7	7	=	7.5	=	=	=	=	=	=
6	7	7	=	7.5	=	9	=	=	=	=
7a	8	8	=	8	9.5	10	9.5	8.5	9	8
7b	7	7.5	=	7.5	8.5	9.5	8.5	=	=	=
8	7.5	7.5	=	7.5	10	10	10	8.5	7	7
Control	0	0	14	0	0	7	0	8	0	0

Control: Antibiotic with no compounds; CIP: Ciprofloxacin; AMP: Ampicillin; CTX: Cefotaxime; S: Streptomycin; OX: Oxacillin; VA: Vancomycin; E: Erythromycin. (=): Indicates no influence of the compound; same result as obtained with no compound.

Table 5. Fractional inhibitory concentration (FIC) index results obtained with **4a**/**8** and antibiotic combinations by checkerboard method.

Bacterial Isolate	**4a-OX**		**8-OX**		**4a-VA**		**8-Va**		**4a-AMP**		**8-AMP**	
	ΣFIC	**Activity** [a]	**ΣFIC**	**Activity**	**ΣFIC**	**Activity**	**ΣFIC**	**Activity**	**ΣFIC**	**Activity**	**ΣFIC**	**Activity**
***S. aureus* B1**	0.562	**I**	0.516	**I**	−	−	−	−	2	**I**	0.516	**I**
***S. aureus* B2**	2	**I**	0.625	**I**	−	−	−	−	2	**I**	0.625	**I**
***E. faecalis* W1**	−	−	−	−	0.312	S	−	−	0.75	**I**	−	−
***E. faecium* W5**	−	−	−	−	0.312	S	−	−	0.75	S	−	−

AMP: Ampicillin; OX: Oxacillin; VA: Vancomycin; [a] S = synergism; I = indifference; (−): Not determined.

The disc diffusion method (Table 4) revealed a small synergistic association between all the compounds tested and the antibiotics to which *E. coli* G1 was resistant. Even though only a few compounds showed synergism against *S. aureus* B1 and *E. faecium* W5, association of aszonapyrone A (**4a**) with the antibiotics was found to produce the biggest halos, whereas sartorypyrone A (**8**) increased the antibiotic inhibition halos against *S. aureus* B1 and, to a lesser extent, against *E. faecium* W5. Interestingly, although chevalone C (**7a**) alone did not show antibacterial activity at the highest concentration tested (MIC > 256 mg/mL), it demonstrated a synergistic effect with antibiotics against all three multidrug-resistant isolates. The results of the Checkerboard method, represented by the FIC index, are shown in Table 5. The combination effect of aszonapyrone A (**4a**) with oxacillin (OX) and ampicillin (AMP) against MRSA and VRE isolates, respectively, was found to be indifferent ($\Sigma FIC > 0.5$); however, aszonapyrone A (**4a**) was found to lower the MIC of each antibiotic tested, thus, it may be considered a partially synergist effect. The association of aszonapyrone A (**4a**) with vancomycin (VA) showed a clear synergistic effect ($\Sigma FIC < 0.5$) against the two VRE isolates tested. The combination of sartorypyrone A (**8**) with OX and AMP against MRSA isolates was found to be also indifferent. Since the MIC of sartorypyrone A (**8**) against VRE was higher than 256 μg/mL, no checkerboard method was performed for this compound against VRE isolates.

The effect of aszonapyrone A (**4a**) and sartorypyrone A (**8**), at different concentrations (ranging from 2× MIC to 1/4× MIC), on the biofilm formation of *S. aureus* ATCC 25923, *B. subtilis* ATCC 6633 and *S. aureus* B1, and also *E. faecalis* W1 (in the case of **4a**) was also assessed using the biomass quantification, and the results are shown in Figure 2. All the strains tested showed no biofilm formation in the presence of 2xMIC and MIC of aszonapyrone A (**4a**) and sartorypyrone A (**8**). However, *S. aureus* ATCC 25923 and *S. aureus* B1 formed more biofilm in the presence of a sub-inhibitory concentration (1/2× MIC) of aszonapyrone A (**4a**) (Figure 2A). Moreover, *S. aureus* ATCC 25923 was found to produce a significantly ($P < 0.05$) higher amount of biomass in the presence of 1/2× MIC of sartorypyrone A (**8**), when compared to the control (Figure 2B). In order to confirm the effect of these compounds on biofilm formation, the microscopic visualization of the biofilm produced by *S. aureus* ATCC 25923 was carried out using a Live/Dead staining. After 24 h, the majority of the cells within the biofilm were viable and large aggregates embedded in a matrix could be observed (Figure 3A). In the presence of aszonapyrone A (**4a**), at a concentration equal to the MIC, no biofilm was formed and also no growth was observed (Figure 3B). However, at the concentration of 1/2× MIC, it was possible to observe more biofilm in comparison to the control (Figure 3C). These results are in agreement with those obtained in the biomass quantification for the same experimental conditions. However, this result is not unexpected since there are several reports of the increase in biofilm formation in both Gram-positive and Gram-negative bacteria in the presence of sub-inhibitory concentrations of antibiotics [18–20]. Interestingly, the BIC value of aszonapyrone A (**4a**) was found to be higher than 12× MIC against mature biofilms of both *S. aureus* B1 (BIC > 96 μg/mL) and *E. faecalis* W1 (BIC > 192 μg/mL). However, the exact BIC value could not be determined due to the limited quantity of this compound available to perform all these biological assays. These very high BIC values may reflect the difficulty of **4a** in penetrating the extracellular biofilm matrix, thus hampering the eradication of the pre-established biofilm.

Examination of the structures of the meroditerpenes tested (Figure 1) suggested the existence of some common features necessary for the antibacterial activity of this class of compounds. Although

aszonapyrone A (**4a**), aszonapyrone B (**4b**), sartorypyrone C (**5**) and sartorypyrone A (**8**), all contain the 4-hydroxy-6-methyl-2*H*-pyran-2-one ring, only aszonapyrone A (**4a**) and sartorypyrone A (**8**) have the β-acetoxyl group on C-3. On the other hand, this 4-hydroxy-6-methyl-2*H*-pyran-2-one ring is connected to the perhydrophenanthrene portion by the ethereal bridge, forming a more rigid pentacyclic structure in chevalone B (**6**). On the other contrary, both chevalone C (**7a**) and sartorypyrone B (**7b**) contain the 6-methyl-4*H*-pyran-4-one ring connected to the perhydrophenanthrene portion by an ethereal bridge. Therefore, it is apparent that the presence of a free 4-hydroxy-6-methyl-2*H*-pyran-2-one ring on C-15 and the β-acetoxyl group on C-4 of the perhydrophenanthrene portion are required for the antibacterial activity of this series of meroditerpenes.

Figure 2. Biomass quantification of biofilms of Gram-positive bacteria formed in the presence of different concentrations (ranging from 2× MIC to 1/4× MIC) of **4a** (**A**) and **8** (**B**).

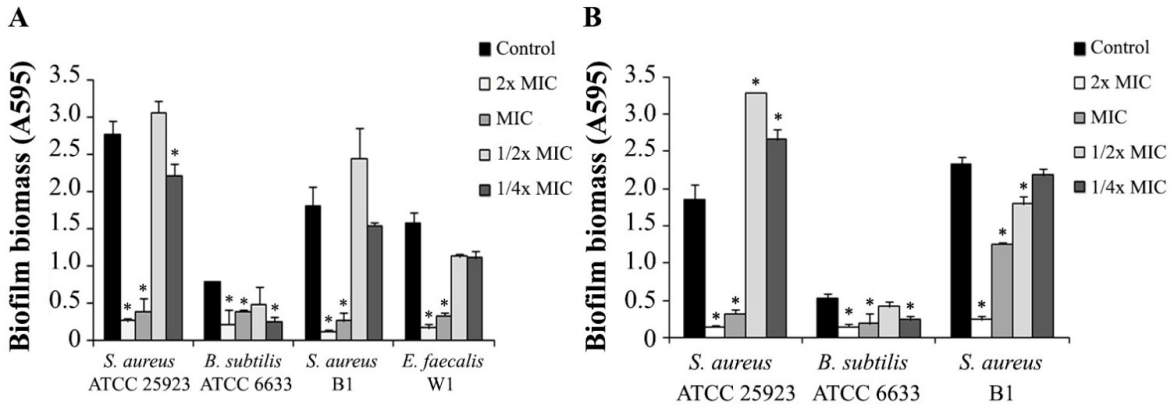

Figure 3. Evaluation of *S. aureus* ATCC 25953 biofilm formation. Live/dead viability staining images after 24 h. Control (**A**); Biofilm formation in the presence of the MIC (**B**) and in the presence of ½ of the MIC (**C**) of **4a**.

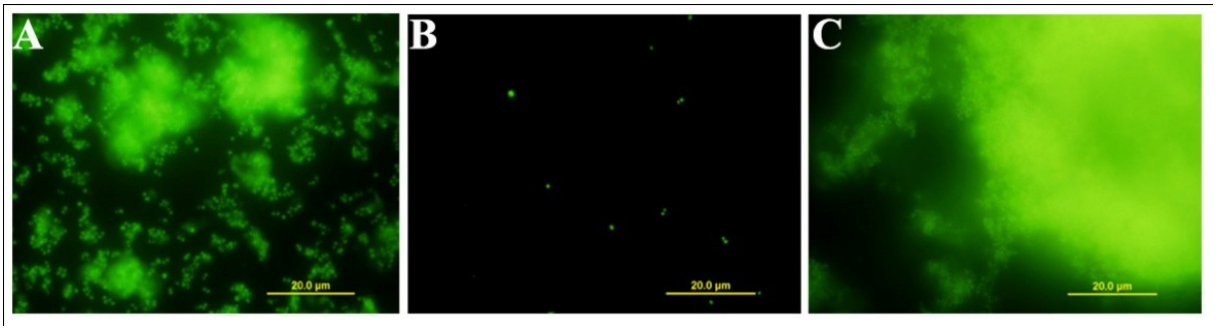

3. Experimental Section

3.1. General Experimentation Procedures

Melting points were determined on a Bock monoscope and are uncorrected. Optical rotations were determined on an ADP410 Polarimeter (Bellingham+Stanley Ltd., Tunbridge Wells, Kent, UK) Infrared spectra were recorded on an ATT Mattson Genesis Series FTIR™ using WinFIRST Software. ^{1}H and ^{13}C NMR spectra were recorded at ambient temperature on a Bruker AMC instrument (Bruker

Biosciences Corporation, Billerica, MA, USA) operating at 300.13 and 75.4 MHz, respectively. High resolution mass spectra were measured with a Xevo QToF mass spectrometer (Waters Corporations, Milford, MA, USA) coupled to the Aquity UPLC system (Waters Corporations, Milford, MA, USA). A Merck silica gel GF_{254} was used for preparative TLC, and a Merck Si gel 60 (0.2–0.5 mm) was used for analytical chromatography.

3.2. Extraction and Isolation

Extraction and Isolation of Secondary Metabolites from the Culture of *Neosartorya paulistensis* (KUFC 7897)

Neosartorya paulistensis (KUFC 7897) was isolated from the marine sponge *Chondrilla australiensis* which was collected from Mu Kho Lan Beach, Chonburi Province, Thailand in May 2010. After rinsing with sterile sea water, the sponge was dried on sterile filter papers and cut into small pieces (5 × 5 mm) and placed on the plates containing malt extract agar (MEA, 30 g of malt extract, 15 g of bacto agar, distilled water 1000 mL and adjusted to the final pH at 5.5) with 70% sea water and incubated at 28 °C under 12 h light/12 h dark cycle for 7 days. The fungus was identified by Prof. Dr. Leka Manoch (Department of Plant Pathology, Kasetsart University, Bangkok, Thailand), by morphological features, including the characteristic of ascospores and colonies. The identification was supported by sequence analysis of the β-tubulin gene described in the previous report [21] and the pure cultures were deposited as KUFC 7897 at Kasetsart University Fungal Collection, Department of Plant Pathology, Faculty of Agriculture, Kasetsart University, Bangkok, Thailand, and as MMERU 02 at Microbes Marine Environment Research Unit, Division of Environmental Science, Faculty of Science, Ramkhamhaeng University, Bangkok, Thailand. The fungus was cultured for two weeks at 28 °C in 10 Petri dishes (i.d. 90 mm) containing 25 mL of MEA with 70% sea water per dish. Fifty 1000 mL Erlenmeyer flasks each containing rice (200 g), water (30 mL), and sea water (70 mL), were autoclaved, inoculated with five mycelia plugs of *N. paulistensis* and incubated at 28 °C for 30 days, after which the mouldy rice was macerated in ethyl acetate (15 L total) for 10 days and then filtered. The two layers were separated using a separatory funnel and the ethyl acetate solution was concentrated at a reduced pressure to yield crude ethyl acetate extract, which was washed with 5% of $NaHCO_3$ solution (2 × 500 mL) and H_2O (3 × 500 mL). The organic layer was dried with anhydrous Na_2SO_4, filtered and evaporated under reduced pressure to give 51 g of crude extract which was applied on a column chromatography over 610 g of Si gel (0.2–0.5 mm, Merck KGaA, Darmstadt, Germany) and eluted with mixtures of $CHCl_3$–petrol and $CHCl_3$–Me_2CO, wherein 250 mL fractions were collected as follows: fractions 1–25 ($CHCl_3$–petrol, 1:4), 26–149 ($CHCl_3$–petrol, 3:7), 150–177 ($CHCl_3$–petrol, 2:3), 178–278 ($CHCl_3$–petrol, 1:1), 279-399 ($CHCl_3$–petrol, 3:2), 400–534 ($CHCl_3$–petrol, 4:1), 535–549 ($CHCl_3$–petrol, 9:1), 550–592 ($CHCl_3$), 593–837 ($CHCl_3$–Me_2CO, 9:1), 838–976 ($CHCl_3$–Me_2CO, 8:2), 977–1047 ($CHCl_3$–Me_2CO, 7:3), 1048–1090 ($CHCl_3$–Me_2CO, 1:1) and 1091–1112 ($CHCl_3$–Me_2CO, 1:4). Frs 299–307 (526 mg) were combined and recrystallized in petrol to give 12 mg of sartorypyrone C (**5**). Frs 627–696 were combined (1.50 g) and crystallized in a mixture of $CHCl_3$ and acetone to give 70 mg of tryptoquivaline L (**1a**). Frs 739–774 were combined (400 mg) and crystalized in Me_2CO to give 95 mg of tryptoquivaline H (**1b**). The mother liquor of

frs 739–774 and frs 697–774 were combined (850 mg), applied on a column chromatography of LiChroprep Si 60 (40–63 mm, 46 g) and eluted with mixtures of $CHCl_3$–petrol and $CHCl_3$–Me_2CO wherein 100 mL sub-fractions were collected as follows: subfrs 1–24 ($CHCl_3$–petrol, 4:1), 25–49 ($CHCl_3$–petrol, 9:1), 50–63 ($CHCl_3$), 64–142 ($CHCl_3$–Me_2CO, 9:1) and 143–163 ($CHCl_3$–Me_2CO, 4:1). Subfrs 82–86 were combined (31 mg) and purified by TLC (Si gel, $CHCl_3$–Me_2CO–EtOAc–HCO_2H, 7:2:1:0.1) to give 8.3 mg of tryptoquivaline L (**1a**) and 9.6 mg of 4(3*H*)-quinazolinone (**3**) [22]. Subfrs 87–102 were combined (250 mg) and purified by TLC (Si gel, $CHCl_3$–Me_2CO–EtOAc–HCO_2H, 7:2:1:0.1) to give 38 mg of tryptoquivaline L (**1a**) and 18 mg of tryptoquivaline H (**1b**). Subfrs 103–130 were combined (157 mg) and crystallized in Me_2CO to give 27 mg of tryptoquivaline H (**1b**). Frs 775–832 were combined (690 mg) and crystalized in Me_2CO to give 95 mg of 3′-(4-oxoquinazolin-3-yl)spiro[1*H*-indole-3,5′]-2,2′-dione (**2**). The mother liquor of frs 775–832 and frs 833-860 were combined (902 mg) and applied over a LiChroprep Si 60 column (40–63 μm, 41 g, Merck KGaA, Darmstadt, Germany) and eluted with mixtures of $CHCl_3$–petrol and $CHCl_3$–Me_2CO wherein 100 ml sub-fractions were collected as follows: subfrs 1–26 ($CHCl_3$–petrol, 4:1), 27–41 ($CHCl_3$), 42–108 ($CHCl_3$–Me_2CO, 9:1). Subfrs 61–68 were combined and purified by TLC (Si gel, $CHCl_3$–Me_2CO–EtOAc–HCO_2H, 7:2:1:0.1) to give 4.2 mg of tryptoquivaline L (**1a**) and 18 mg of tryptoquivaline H (**1b**). Subfrs 69-86 were combined (176 mg) and recrystallized in Me_2CO to give 15 mg of 3′-(4-oxoquinazolin-3-yl)spiro[1*H*-indole-3,5′]-2,2′-dione (**2**). Frs 905–947 were combined (670 mg) and crystalized in Me_2CO to give 16.4 mg of tryptoquivaline F (**1c**). The structures of the compounds were established by comparison their NMR spectral data with those in the literature [16] as well as with authentic samples.

3.2.1. Sartorypyrone C (**5**)

White solid, Mp = 200–202 °C. $[\alpha]_D^{25}$ = −73.5° (*c* 0.07, $CHCl_3$); IR (KBr) ν_{max} 3445, 2923, 2942, 2853, 1699, 1668, 1649, 1636, 1507, 1124 cm^{-1}. ^1H and ^{13}C see Table 1. HR-ESIMS *m/z* 415.2836 $(M + H)^+$ (calculated for $C_{28}H_{41}O_5$, 415.2848).

3.2.2. Isolation of Tryptoquivaline T (**1d**) from the Culture of *Neosartorya laciniosa* (KUFC 7896)

Extraction and isolation of tryptoquivaline L (**1a**) 3′-(4-oxoquinazolin-3-yl) spiro[1*H*-indole-3, 5′]-2,2′-dione (**2**), aszonapyrone A (**4a**) and aszonapyrone B (**4b**) from the culture of the diseased coral derived fungus *Neosartorya laciniosa* (KUFC 7896) have been previously described by us [15]. The column fractions 498–507 (793 mg) and mother liquor of the combined frs 508–546 (1.57 g) were combined and chromatographed over a LiChroprep Si 60 column (40–63 μm, 36 g, Merck KGaA, Darmstadt, Germany) and eluted with mixtures of $CHCl_3$–petrol and $CHCl_3$–Me_2CO wherein 100 mL sub-fractions were collected as follows: Subfrs 1–84 ($CHCl_3$–petrol, 9:1), 85–137 ($CHCl_3$–Me_2CO, 9:1), 138–162 ($CHCl_3$–Me_2CO, 4:1). Subfrs 43–50 were combined (214 mg) and recrystallized in Me_2CO to give 13 mg of tryptoquivaline T (**1d**).

Tryptoquivaline T (**1d**)

White solid, Mp = 258–260 °C. $[\alpha]_D^{25}$ = −83.3 (*c* 0.04, MeOH); IR (KBr) ν_{max} 3010, 2930, 2852, 1701, 1582, 1450, 1402, 1269 cm^{-1}. ^1H and ^{13}C see Table 2. HR-ESIMS *m/z* 445.1512 $(M + H)^+$ (calculated for $C_{28}H_{41}O_5$, 445.1512).

3.2.3. Isolation of Chevalone B (**6**) and Chevalone C (**7a**) from the Culture of *Neosartorya siamensis* (KUFC 6349)

Isolation and identification of the fungus as well as fractionation of the crude extract and isolation of other constituents from the culture of *Neosartorya siamensis* (KUFC 6349) have been previously described by us [16]. Fr 34 (1.02 g) was applied on a column chromatography of Si gel (35 g) and eluted with mixtures of petrol–$CHCl_3$ and $CHCl_3$–Me_2CO, 100 mL fractions were collected as follows: Subfrs 1–32 ($CHCl_3$–petrol 3:7), 33–54 ($CHCl_3$–petrol, 1:1), 55–58 ($CHCl_3$–petrol, 7:3). Subfrs 15–17 were combined (0.28 g) and crystallized in mixture of petrol and $CHCl_3$ to give 137.5 mg of chevalone B (**6**). Frs 35 (630 g) was applied on a column chromatography of Si gel (35 g) and eluted with mixtures of petrol–$CHCl_3$, 100 mL fractions were collected as follows: Frs 1–52 ($CHCl_3$–petrol, 3:7), 53–64 ($CHCl_3$–petrol, 1:1). Subfrs 33–52 were combined (63.6 mg) and purified by TLC (Si Gel, $CHCl_3$–Me_2CO–HCO_2H, 95:0.5:0.1) to give 12 mg of chevalone C (**7a**). Subfrs 53–56 were combined (300 mg) and crystallized in petrol to give 40.3 mg of chevalone C (**7a**). Frs 36–53 were combined (1.80 g) and crystallized in a mixture of petrol and $CHCl_3$ to give 375 mg of chevalone C (**7a**). Frs 83–100 were combined (300 mg) and crystallized in a mixture petrol and $CHCl_3$ to give 112.5 mg of chevalone C (**7a**).

3.3. Antibacterial Activity Bioassays

3.3.1. Bacterial Strains

For the antibacterial bioassays, fungal metabolites were tested against reference strains, two Gram-positive (*Staphylococcus aureus* ATCC 25923 and *Bacillus subtilis* ATCC 6633) and two Gram-negative (*Escherichia coli* ATCC 25922 and *Pseudomonas aeruginosa* ATCC 27853) bacteria, and against multidrug-resistant isolates from the environment, *S. aureus* B1 and *S. aureus* B2 (isolated from public buses), *Enterococcus faecalis* W1 and *E. faecium* W5 (isolated from river water) and *E. coli* G1 (isolated from seagull feces). These bacteria were grown in Mueller-Hinton agar (MH—BioKar diagnostics, Allonne, France) from stock cultures. MH plates were incubated at 37 °C prior to obtain fresh cultures for each *in vitro* bioassay.

3.3.2. Determination of Minimum Inhibitory and Bactericidal Concentrations

The minimum inhibitory concentration (MIC) values of the 13 compounds were determined by a broth microdilution technique, following the recommendations of the Clinical and Laboratory Standards Institute [23]. Stock solutions of 10 mg/mL prepared by dissolving each metabolite in dimethylsulfoxide (DMSO—Applichem GmbH, Darmstadt, Germany) were serial diluted in Mueller-Hinton broth (MHB—BioKar diagnostics, Allonne, France) to achieve in-test concentrations

ranging from 2 to 256 μg/mL. Ciprofloxacin in the concentration range from 0.03125 to 16 μg/mL was used as control drug in the experiment. A bacterial inoculum was prepared in MHB and standardized in order obtain a concentration of 5×10^5 CFU/mL in each inoculated well of the microtiter plate. The concentration of DMSO in the highest in-test concentration did not affect the microbial growth. The MIC was defined as the lowest concentration of the compound that inhibited the visible growth. The minimum bactericidal concentration (MBC) was determined by spreading 10 μL on MH plates from the sample showing no visible growth and it was further incubated for 24 h at 37 °C; the lowest concentration at which no bacterial growth occurred on MB plates was defined as the MBC.

3.3.3. Synergistic Studies

A screening susceptibility test to assess combined effect between compounds **1**–**8** and antibiotics was conducted using the disc diffusion method on MH. Multidrug-resistant isolates were picked from overnight cultures in MH, and suspensions were prepared in buffered peptone water (Oxoid, Basingstoke, England) by adjusting the turbidity to equal a 0.5 McFarland standard. A set of antibiotic discs (Oxoid, Basingstoke, England) was selected based on the resistance of the isolates towards those antibiotics. Antibiotic discs alone (controls) and impregnated with 15 μL of a 1 mg/mL solution (in DMSO) of each metabolite were placed on the agar plate seeded with the respective bacteria. Fifteen μL of DMSO impregnated in a sterile filter paper disc (6 mm in diameter) (Oxoid, Basingstoke, England) was used as the negative control. Inoculated MH plates were incubated overnight at 37 °C. Each compound was tested in duplicate. Potential synergism was recorded when the halo of antibiotic discs impregnated with metabolites was greater than the halo of antibiotic discs or compound-impregnated blank discs alone.

Based on the results of the previous assay, potential synergism between the most promising compounds (**4a** and **8**) and antibiotics (oxacillin, vancomycin and ampicillin—Sigma-Aldrich, St. Louis, MO, USA) was checked using a broth microdilution checkerboard method and tested against *S. aureus* MRSA and *Enterococcus* spp. VRE isolates. Briefly, the stock solutions and serial twofold dilutions of each compound and antibiotic to at least double the MIC were prepared according to the recommendations of CLSI [23]. The metabolite to be tested was serially diluted along the ordinate, while the antibiotic was diluted along the abscissa. A bacterial inoculum equal to a 0.5 McFarland turbidity standard was prepared in MHB. Each microtiter plate well was inoculated with 100 μL of a bacterial inoculum of 5×10^5 CFU/mL, and the plates were incubated overnight at 37 °C. The fractional inhibitory concentration (FIC) was calculated as follows: FIC of drug A (FIC A) = MIC of drug A in combination/MIC of drug A alone, and FIC of drug B (FIC B) = MIC of drug B in combination/MIC of drug B alone. The FIC index (ΣFIC), calculated as the sum of each FIC, was interpreted as follows: $\Sigma FIC \leq 0.5$, synergy; $0.5 < \Sigma FIC \leq 4$, no interaction; $4 < \Sigma FIC$, antagonism [24].

3.3.4. Antibiofilm Activity Assay

Given the promising antibacterial activity of **4a** and **8** against Gram-positive bacteria, the efficacy of those two compounds in interrupting the biofilm formation was assessed. The metabolites at concentrations of 2× MIC, MIC, 1/2× MIC and 1/4× MIC were added to bacterial suspensions of 1×10^6 CFU/ml in Tryptic Soy broth (TSB—BioKar diagnostics, Allonne, France). Bacterial

suspension without metabolites was used as the control. Each broth culture obtained was dispensed into a 96-well microtiter plate (200 µL/well) and incubated at 37 °C for 24 h. After that time, biofilm was stained with 0.5% crystal violet for 5 min, rinsed with water, air dried and eluted with acetic acid 33% (v/v). The optical density was measured at 595 nm (OD_{595}) using a microplate reader (iMark™ microplate absorbance reader, Bio-Rad Laboratories, Hercules, CA, USA). Two independent experiments were performed in triplicate for each experimental condition. The statistical significance of difference between biofilms of controls and biofilms in the presence of different concentrations of compounds was evaluated using Student's t test. In both cases, probability levels <0.05 were considered statistically significant. The efficacy of **4a** on established biofilm of *S. aureus* B1 and *E. faecalis* W1 was also evaluated by determining the biofilm inhibitory concentration (BIC) according to the method described by Johnson *et al.* [25]. Briefly, bacterial suspensions in TSB at 1×10^6 CFU/mL were used to grow the biofilms in 96-well microtiter plate. After 24 h of incubation at 37 °C, the planktonic cells were gently removed and the wells were rinsed once and filled with different dilutions ranging from the MIC values to 12× MIC. The OD_{595} was measured at time 0 and after incubation for 24 h at 37 °C. The BIC was determined as the lowest concentration of the compound inhibiting growth in the supernatant fluid, confirmed by no increase in optical density compared with the initial reading.

Additionally, microscopic visualization of biofilms of *S. aureus* ATCC 25923 was performed using the Live/Dead BacLight viability kit (Life Technologies—Molecular Probes, Carlsbad, CA, USA). Biofilms were formed in 35-mm diameter polystyrene plates using TSB (control) and TSB supplemented with MIC and 1/2× MIC of **4a**. After 24 h at 37 °C. The planktonic phase was removed from each plate, washed with PBS, stained with the appropriate mixture of SYTO 9 and propidium iodide stains and incubated for 20 minutes at room temperature in the dark; then, were rinsed and examined under a fluorescence microscope (BX41 Microscope, Olympus America Inc., Center Valley, PA, USA). Images were recorded at an emission wavelength of 500 nm for SYTO 9 (green fluorescence) and of 635 nm for propidium iodide (red fluorescence).

4. Conclusions

We reported the isolation and structure elucidation of a new meroditerpene, sartorypyrone C (**5**), together with the previously described tryptoquivalines L (**1a**), H (**1b**), F (**1c**), 3′-(4-oxoquinazolin-3-yl) spiro[1*H*-indole-3,5′]-2,2′-dione (**2**) and 4(3*H*)-quinazolinone (**3**), from the culture of the marine sponge-associated fungus *N. paulistensis* (KUFC 7897), as well as a new tryptoquivaline derivative which we have named tryptoquivaline T (**1d**), from the culture of the diseased coral-derived fungus *N. laciniosa* (KUFC 7896). Antibacterial activity evaluation of the isolated compounds, together with the previously described meroditerpenes aszonapyrones A (**4a**) and B (**4b**), chevalones B (**6**) and C (**7a**), sartorypyrones B (**7b**) and A (**8**), against four reference strains (*S. aureus*, *B. subtilis*, *E. coli*, and *P. aeruginosa*), as well as the environmental multidrug-resistant isolates, showed that only the meroditerpenes aszonapyrone A (**4a**) and sartorypyrone A (**8**) were active against both Gram-negative reference strains and the environmental multidrug-resistant isolates. Aszonapyrone A (**4a**) also exhibited a clear synergistic effect with vancomycin against the two VRE isolates, while it showed only partially synergist effect with oxacillin and ampicillin against MRSA and VRE isolates. Both

aszonapyrone A (**4a**) and sartorypyrone A (**8**) were found to inhibit the biofilm formation in both reference strains (*S. aureus* ATCC 25923 and *B. subtilis* ATCC 6633) and the multi-drug resistant isolates (*S. aureus* B1 and *E. faecalis* W1), at the 2× MIC and MIC.

In light of the results presented in this work, we can conclude that the meroditerpenes aszonapyrone A (**4a**) and sartorypyrone A (**8**) are two promising antibacterial agents, especially against Gram-positive bacteria, and their effects are comparable to those of standard antibiotics currently in use in therapeutics, with the advantage of being also active against bacteria that already exhibit resistance towards these antibiotics. To the best of our knowledge, none of the available antibiotics belongs to this class of compounds, which thereby may represent a novel and potential topic of investigation in the field of new antibacterial agents from the marine-derived fungi.

Acknowledgements

This work was partially funded by the Project MARBIOTECH (reference NORTE-07-0124-FED ER-000047) within the SR&TD Integrated Program MARVALOR—Building research and innovation capacity for improved management and valorization of marine resources, supported by the Programa Operacional Regional do Norte (ON.2—O Novo Norte) and by the European Regional Development Fund. N. M. G. thanks Fundação para a Ciência e Tecnologia (FCT) for the scholarship (SFRH/BD/65671/2009) supported by the European Social Fund (ESF). We thank Mick Lee of the Department of Chemistry, Leicester University (UK), for providing the HR-ESIMS and Sara Cravo, Laboratório de Química Orgânica e Farmacêutica, Faculdade de Farmácia do Porto for technical support.

Conflicts of Interest

The authors declare no conflict of interest.

References

1. Johnson, A.P.; Livermore, D.M.; Tillotson, G.S. Antimicrobial susceptibility of Gram-positive bacteria: What's current, what's anticipated? *J. Hosp. Infect.* **2001**, *49*, S3–S11.
2. Aksoy, D.Y.; Unal, S. New antimicrobial agents for treatment of Gram-positive bacterial infections. *Clin. Microbiol. Infect.* **2008**, *14*, 411–420.
3. Aziz, A.M. The role of healthcare strategies in controlling antibiotic resistance. *Br. J. Nurs.* **2013**, *22*, 1066–1074.
4. Bassetti, M.; Merelli, M.; Temperoni, C.; Astilean, A. New antibiotics for bad bugs: Where are we? *Ann. Clin. Microbiol. Antimicrob.* **2013**, *12*, doi:10.1186/1476-0711-12-22.
5. Kijjoa, A.; Sawangwong, P. Drugs and Cosmetics from the Sea. *Mar. Drugs* **2004**, *2*, 73–82.
6. Newman, D.J.; Cragg, G.M. Natural Products as Sources of New Drugs over the 30 Years from 1981 to 2010. *J. Nat. Prod.* **2012**, *75*, 311–335.
7. Blunt, J.W.; Copp, B.R.; Keyzers, R.A.; Munro, M.H.G.; Prinsep, M.R. Marine natural products. *Nat. Prod. Rep.* **2013**, *30*, 237–323.

8. Rowley, D.C.; Kelly, S.; Kauffman, C.A.; Jensen P.R.; Fenical, W. Halovirs A–E, new antiviral agents from a marine-derived fungus of the genus *Scytalidium*. *Bioorg. Med. Chem.* **2003**, *11*, 4263–4274.
9. Shen, S.; Li, W.; Ouyang, M.A.; Wu, Z.J.; Lin, Q.Y.; Xie, L.H. Identification of two marine fungi and evaluation of their antivirus and antitumor activities. *Acta Microbiol. Sin.* **2009**, *49*, 1240–1246.
10. Bugni, T.S.; Ireland, C.M. Marine-derived fungi: A chemically and biologically diverse group of microorganisms. *Nat. Prod. Rep.* **2004**, *21*, 143–163.
11. Pejin, B.; Jovanović, K.K.; Mojović, M.; Savić, A.G. New and highly potent antitumor natural products from marine-derived fungi: Covering the period from 2003 to 2012. *Curr. Top. Med. Chem.* **2013**, *13*, 2745–2766.
12. Christophersen, C.; Crescente, C.; Frisvad, J.C.; Gram, L.; Nielsen, J.; Nielsen, P.H.; Rahbæk, L. Antibacterial activity of marine-derived fungi. *Mycopathologia* **1999**, *143*, 135–138.
13. Arasu, M.V.; Duraipandiyan, V.; Ignacimuthu, S. Antibacterial and antifungal activities of polyketide metabolite from marine *Streptomyces* sp. AP-123 and its cytotoxic effect. *Chemosphere* **2013**, *90*, 479–487.
14. Manimegalai, K.; Devi, N.K.A.; Padmavathy, S. Marine fungi as a source of secondary metabolites of antibiotics. *Int. J. Biotechnol. Bioeng. Res.* **2013**, *4*, 275–282.
15. Eamvijarn, A.; Gomes, N.M.; Dethoup, T.; Buaruang, J.; Manoch, L.; Silva, A.; Pedro, M.; Marini, I.; Roussis, V.; Kijjoa, A. Bioactive meroditerpenes and indole alkaloids from the soil fungus *Neosartorya fischeri* (KUFC 6344), and the marine-derived fungi *Neosartorya laciniosa* (KUFC 7896) and *Neosartorya tsunodae* (KUFC 9213). *Tetrahedron* **2013**, *69*, 8583–8591.
16. Buttachon, S.; Chandrapatya, A.; Manoch, L.; Silva, A.; Gales, L.; Bruyére, C.; Kiss, R.; Kijjoa, A. Sartorymensin, a new indole alkaloid, and new analogues of tryptoquivaline and fiscalins produced by *Neosartorya siamensis* (KUFC 6349). *Tetrahedron* **2012**, *68*, 3253–3262.
17. Mahato, S.B.; Kundu, A.P. 13C NMR spectra of pentacyclic triterpenoids—a compilation and some salient feature. *Phytochemistry* **1994**, *37*, 1517–1575.
18. Hoffman, L.R.; D'Argenio, D.A.; MacCoss, M.J.; Zhang, Z.; Jones, R.A.; Miller, S.I. Aminoglycoside antibiotics induce bacterial biofilm formation. *Nature* **2005**, *436*, 1171–1175.
19. Kaplan, J.B.; Jabbouri, S.; Sadovskaya, I. Extracellular DNA-dependent biofilm formation by *Staphylococcus epidermidis* RP62A in response to subminimal inhibitory concentrations of antibiotics. *Res. Microbiol.* **2011**, *162*, 535–541.
20. Bessa, L.J.; Grande, R.; Di Iorio, D.; Di Giulio, M.; Di Campli, E.; Cellini, L. *Helicobacter pylori* free-living and biofilm modes of growth: Behavior in response to different culture media. *APMIS* **2013**, *121*, 549–560.
21. Glass, N.L., Donaldson, G.C. Development of primer sets designed for use with the PCR to amplify conserved genes from filamentous ascomycetes. *Appl. Environ. Microbiol.* **1995**, *61*, 1323–1330.
22. Kulkarni, S.S.; Singh, S.; Shah, J.R.; Low, W. K.; Talele, T.T. Synthesis and SAR optimization of quinazolin-4(3*H*)-ones as poly(ADP-ribose)polymerase-1 inhibitors. *Eur. J. Med. Chem.* **2012**, *50*, 264–273.

23. Franklin, R.; Cockerill, M.D., III. *Performance Standards for Antimicrobial Susceptibility Testing, Twenty-First Informational Supplement M100-S21*; Clinical and Laboratory Standards Institute (CLSI): Wayne, PA, USA, 2011.
24. Odds, F.C. Synergy, antagonism, and what the chequerboard puts between them. *J. Antimicrob. Chemother.* **2003**, *52*, doi:10.1093/jac/dkg301.
25. Johnson, S.A.; Goddard, P.A.; Iliffe, C.; Timmins, B.; Rickard, A.H.; Robson, G.; Handley, P.S. Comparative susceptibility of resident and transient hand bacteria to para-chloro-meta-xylenol and triclosan. *J. Appl. Microbiol.* **2002**, *93*, 336–344.

© 2014 by the authors; licensee MDPI, Basel, Switzerland. This article is an open access article distributed under the terms and conditions of the Creative Commons Attribution license (http://creativecommons.org/licenses/by/3.0/).

APPENDIX V

Gomes, N.M., Buttachon, S., Kijjoa, A. Meroterpenoids from Marine Microorganisms: Potential Scaffolds for New Chemotherapy Leads. In: *Anticancer Drugs from Marine Origins* (Ed. Kim, S.-K.) *(Accepted)*.

MBPRC Marine Bioprocess Research Center

Tel: +82 -620-6375
Fax: + 82-51-628-8147
Email: sknkim@pknu.ac.kr

Prof. Se-Kwon Kim,
Director,
Marine Bioprocess Research Center,
Department of Chemistry,
Pukyong National University,
Busan, 608-737
South Korea

From

Se-Kwon Kim, PhD
Professor, Department of Chemistry
Director, Marine Bioprocess Research Center
Pukyong National University
599-1 Daeyeon 3-dong, Nam-gu, Busan, 608-737, South Korea
Tel.:+82-51-629-7094
Fax:+82-51-629-7099

To

Anake Kijjoa
Professor of Chemistry
Instituto de Ciências Biomédicas de Abel Salazar
Universidade do Porto
4050-313 Porto
Portugal

SUB: Acceptance Letter,

This is confirming you that you submitted book chapters entitled as

1. Pyridoacridine Alkaloids from Marine Origin: Sources and Anticancer Activity

2. Meroterpenoids from Marine Microorganisms: Potential Scaffolds for New Chemotherapy Leads

has been accepted in Anticancer Drugs from Marine Origins" books. Further proof copy of your article will sent you as soon as possible.

Thank you

Best regards

Prof. Se-Kwon Kim

1